

**Expression and characterisation of a novel  
cyclic nucleotide phosphodiesterase Type 1A from dog heart**

A thesis submitted in partial fulfilment of the requirements  
for the degree of Doctor of Philosophy  
2002

**RAVINDER SIDHU**

School of Pharmacy  
University of London  
Department of Pharmaceutical and Biological Chemistry  
29-39 Brunswick Square  
London  
WC1N 1AX



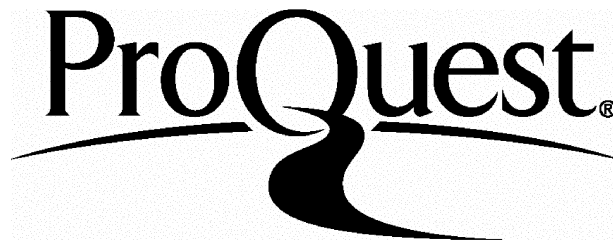
ProQuest Number: 10104896

All rights reserved

INFORMATION TO ALL USERS

The quality of this reproduction is dependent upon the quality of the copy submitted.

In the unlikely event that the author did not send a complete manuscript and there are missing pages, these will be noted. Also, if material had to be removed, a note will indicate the deletion.



ProQuest 10104896

Published by ProQuest LLC(2016). Copyright of the Dissertation is held by the Author.

All rights reserved.

This work is protected against unauthorized copying under Title 17, United States Code.  
Microform Edition © ProQuest LLC.

ProQuest LLC  
789 East Eisenhower Parkway  
P.O. Box 1346  
Ann Arbor, MI 48106-1346

## Abstract

Cyclic nucleotide phosphodiesterase Type 1A belongs to a family of intracellular enzymes involved in the modulation of the key second messengers cAMP and cGMP. There are eleven members in the superfamily of PDE enzymes (PDE1 - PDE11), all exhibiting tissue-specific distribution. The PDE1 enzymes are found mainly in the brain, lungs, heart and vascular smooth muscle with smaller amounts present in inflammatory B lymphocytes and macrophages.

In this study, the expression of dog heart PDE1A1 was investigated using cDNA previously produced by Clapham and Wilderspin (2001). This cDNA had not been explored for the expression of a functional protein so it formed the starting point of the present work. The experimental work comprised of expression studies to identify suitable host/vector combinations followed by detailed biochemical characterisation of the recombinant enzyme for comparison with the native enzyme. The dog has been used extensively as a model for the investigation of cardiovascular function in the pharmacological analysis of PDE inhibitors but there is little information regarding the characterisation of PDE enzymes in this species so the present study extends the information regarding characterisation of PDE1A enzymes in the dog.

For the first part of the work, the full-length dog heart PDE1A1 cDNA was cloned into pPICZ $\alpha$ C for secreted expression in the *Pichia pastoris* expression system. Culture media from *P. pastoris* cells transformed with the construct pPICZ $\alpha$ C-PDE1A1 showed no PDE activity. Full-length and N-terminal truncated PDE1A1 enzymes were then expressed in *E. coli* using the expression vectors pGEX-3X and pTrcHisA to generate the enzymes GST-PDE1A1 and His<sub>6</sub>-PDE1A1<sub>N-trunc</sub> respectively. The majority of the recombinant protein was sequestered into insoluble inclusion bodies and exhibited extensive proteolytic degradation in both cases. The full-length as well as the N- and/or C-terminal truncated dog heart PDE1A1 enzymes were then produced using the Semliki Forest virus (SFV) system.

Recombinant dog heart PDE1A1 was successfully produced in a soluble, active form using the SFV system. The results of the present study revealed that only the full-length and the N-terminal truncated constructs had PDE activity. The successful expression of dog heart PDE1A1 enzymes in the SFV system represents the first report of the expression of PDE1 enzymes in this expression system. The  $K_m$  (1.99  $\mu$ M) for the full length enzyme, for cAMP, was comparable to the native enzyme (1.2  $\mu$ M), while the  $K_m$  for cGMP was higher for the recombinant enzyme (12.55  $\mu$ M) compared to the native enzyme (0.53  $\mu$ M). Inhibitor studies on the recombinant enzymes showed that the enzymes were sensitive to the PDE1-selective inhibitor vinpocetine as well as the PDE1/5-selective inhibitor zaprinast while being insensitive to the PDE2- and PDE3-inhibitors EHNA and amrinone respectively. However, the sensitivity of the recombinant enzymes to the selective inhibitors, vinpocetine and zaprinast, was reduced compared to the native enzyme with sensitivity to zaprinast reduced by approximately 18-fold. There was also a particularly notable difference between the recombinant enzymes produced in the present study and the native enzyme. This was the unexpected sensitivity that the recombinant enzymes had to the archetypical PDE4 inhibitor, rolipram, with the full-length PDE1A1 having an IC<sub>50</sub> of 0.2  $\mu$ M. The findings of the present study have implications in the interpretation of data obtained for recombinant PDE1 enzymes particularly with regards to evaluation of PDE1 as well as PDE4 inhibitors for clinical use since PDE1 enzymes are often found in tissues having PDE4 enzymes. The results also indicate that rolipram may not be as selective as first reported.

**Dedicated to J. S.**

## Abbreviations

AKAP	A-kinase anchoring protein	DMF	Dimethylfluoride
Amp	Ampicillin	DMSO	Dimethylsulfoxide
ANP	Atrial natriuretic peptide	DNA	Deoxyribonucleic Acid
AOX	Alcohol oxidase	dNTP	Deoxynucleotide triphosphate
<i>AOX1</i>	Alcohol oxidase gene	DPM	Disintegrations per minute
APS	Ammonium persulphate	DSS	Disuccinimidyl suberate
ATP	Adenosine triphosphate	EDTA	Ethylenediaminetetracetic acid
$\beta$ -Gal	Beta galactosidase	EGTA	Ethyleneglycol- <i>O,O'</i> bis(2-aminoethyl)- <i>N, N, N', N'</i> -tetraacetic acid
BHK-21	Baby Hamster Kidney - 21 cells	End6	Amino-terminal truncated PDE1A1 construct
BNP	Brain natriuretic peptide	FDA	Food and Drug Administration
bp	Base pair	FL4	Full-length PDE1A1 construct
BSA	Bovine serum albumin	FT (1 or 2)	Flow-through sample (1 or 2)
BT	<i>Bos taurus</i> (Cow)	G2	Carboxy-terminal truncated PDE1A1 construct
c1	PDE1A1 construct pTrcHisA-PDE1A1 <sub>N-trunc</sub>	GMEM	Glasgow minimum essential medium
c12	PDE1A1 construct pGEX-3X-PDE1A1	GST	Glutathione S-transferase
Ca <sup>2+</sup>	Calcium ions	H	Histidine residue
Ca <sup>2+</sup> /CaM	Calcium ions and calmodulin	H(1-16)	Helices (1 - 16)
CaM-PDE	Calmodulin cyclic nucleotide phosphodiesterase	HEPES	<i>N</i> -2-hydroxyethylpiperazine- <i>N</i> -2-ethane-sulphonic acid
cAMP	3', 5' cyclic adenosine monophosphate	<sup>1</sup> H NMR	Proton nuclear magnetic resonance
Cat9	Amino- and carboxy-terminal truncated PDE1A1 construct	HS	<i>Homo sapiens</i> (Human)
cDNA	Complementary DNA	HX <sub>3</sub> HX <sub>n</sub> E	Metal binding motif: Histidine (H), any amino acid (X), glutamic acid (E)
CF	<i>Canis familiaris</i> (dog)	IC <sub>50</sub>	Inhibitory concentration 50%
cGMP	3', 5' cyclic guanosine monophosphate	IBMX	3-Isobutyl-1-methylxanthine
CIAP	Calf Intestinal Alkaline Phosphatase	IPTG	Isopropyl- $\beta$ -D-1-thiogalactopyranoside
CK-11	Casein kinase 11	kb	Kilo base
CM	Complete media	kDa	Kilo Daltons
CPM	Counts Per Minute	<i>K<sub>m</sub></i>	Michaelis-Menten constant
CREB	cAMP response element binding protein	LB	Luria Broth
CREM	cAMP response element modulator	M	Moles per 1000ml
DAB	Diaminobenzidine	mA	Milliamperes
DEAE	Diethylaminoethyl	MAP	Mitogen-Activated Protein
DEPC	Diethylpyrocarbonate	MAPK	Mitogen-Activated Protein Kinase
dH <sub>2</sub> O	Water	MDH	Minimal Dextrose Medium with Histidine

Me/ME	Metal ion	w/v	Weight per volume
MES	2-(N-Morpholino)ethanesulfonic acid	YPD	Yeast Extract Peptone Dextrose Medium
MGYH	Minimal Glycerol Medium with Histidine	YPDS	Yeast Extract Peptone Dextrose Sorbitol Medium
μF	MicroFaraday	X	Any amino acid residue
MLCK	Myosin Light Chain Kinase	X-Gal	5-bromo-4-chloro-3-indolyl-β-D-galactoside
MM	<i>Mus musculus</i> (Mouse)		
MMH	Minimal Methanol Medium with Histidine		
8-MOMX	8-methoxy methyl-3-isobutyl xanthine		
NP40	Nonidet P 40 (non-ionic detergent)		
NT	Not tested		
OD	Optical Density		
Ω	Ohm		
ORF	Open reading frame		
PEST	Proline Glutamate Serine Threonine		
PBS	Phosphate buffered saline		
PCR	Polymerase chain reaction		
PDE(s)	Cyclic nucleotide phosphodiesterase(s)		
PDE1A1	Cyclic nucleotide phosphodiesterase Type 1A1		
PKA	Protein Kinase A		
PMSF	Phenylmethylsulfonyl fluoride		
Psi	Pounds per square inch		
PTA/pT	plasmid pTrcHisA		
PYP	Photoactive Yellow Protein		
RN	<i>Rattus norvegicus</i> (Rat)		
RNA	Ribonucleic acid		
sAC	Soluble adenylate cyclase		
SDS PAGE	Sodium Dodecyl Sulphate Polyacrylamide Gel Electrophoresis		
SFV	Semliki Forest virus		
TAE	Tris-Acetate EDTA		
TEMED	N, N, N', N' Tetramethylethylenediamine		
TLCK	Nα-p-Tosyl-L-Lysine Chloromethyl Ketone		
TPCK	N-Tosyl-L-Phenylalanine Chloromethyl Ketone		
UV/Vis	Ultra violet/Visible spectrophotometer		
V	Volt		
V <sub>max</sub>	Maximum velocity		
v/v	Volume per volume		

### Amino acid abbreviations

<b>Amino acid</b>	<b>Three letter code</b>	<b>Single letter code</b>
Alanine	Ala	A
Arginine	Arg	R
Asparagine	Asn	N
Aspartic acid	Asp	D
Cysteine	Cys	C
Glutamic acid	Glu	E
Glutamine	Gln	Q
Glycine	Gly	G
Histidine	His	H
Isoleucine	Ile	I
Leucine	Leu	L
Lysine	Lys	K
Methionine	Met	M
Phenylalanine	Phe	F
Proline	Pro	P
Serine	Ser	S
Threonine	Thr	T
Tryptophan	Trp	W
Tyrosine	Tyr	Y
Valine	Val	V

## Contents

Abstract		2
Abbreviations		4
Contents		7
List of Figures		20
List of Tables		26
<b>Chapter 1</b>	<b>Introduction</b>	<b>28</b>
1.1	Cellular signalling	28
1.2	cAMP and adenylyl cyclase	28
1.2.1	Discovery of cAMP and adenylyl cyclase	28
1.2.2	Particulate and soluble adenylyl cyclase enzymes	29
1.2.2.1	Particular adenylyl cyclase enzymes	29
1.2.2.2	Soluble adenylyl cyclase enzymes	30
1.2.3	Signal transduction mechanism for the G-protein coupled receptors involving cAMP	31
1.3	cGMP and guanylyl cyclases	33
1.3.1	Discovery of cGMP and guanylyl cyclase	33
1.3.2	Particulate and soluble guanylyl cyclase enzymes	33
1.3.2.1	Particulate guanylyl cyclase enzymes	33
1.3.2.2	Soluble guanylyl cyclase enzymes	34
1.3.3	Signal transduction mechanism involving cGMP	34
1.4	Cyclic nucleotide phosphodiesterase enzymes	35
1.4.1	Background to cyclic nucleotide phosphodiesterase enzymes	35
1.4.2	Nomenclature	37
1.4.3	Classification of the PDEs	39
1.4.4	General domain organisation	40
1.4.5	Amino-terminal regulatory domain	41
1.4.6	Carboxy-terminal region	43
1.4.7	Catalytic domain	43
1.4.7.1	General domain organisation	43
1.4.7.2	Cyclic nucleotide specificity	43
1.4.7.3	Metal binding residues in the catalytic domain	47
1.4.7.4	Structural features of the HSPDE4B2B catalytic domain	49
1.4.7.4.1	Amino terminal subdomain	54
1.4.7.4.2	Middle subdomain	54
1.4.7.4.3	Carboxy terminal subdomain	54
1.4.7.4.4	Substrate-binding pocket	55



1.4.7.5	Amino acid sequence alignment to compare PDE4B2B and PDE1A1 catalytic domains	56
1.5	Role of PDEs in health and disease	57
1.6	Cyclic nucleotide phosphodiesterase families in detail	61
1.6.1	cAMP hydrolysing PDEs	62
1.6.1.1	cAMP-specific, PDE4 family	62
1.6.1.1.1	Background to the PDE4 enzymes	62
1.6.1.1.2	Domain organisation of PDE4 enzymes	63
1.6.1.1.3	Regulation of PDE4 enzymes	65
1.6.1.1.4	PDE4D interactions with scaffold or anchoring proteins	66
1.6.1.2	cAMP-specific, rolipram-insensitive PDE7 family	67
1.6.1.3	High affinity cAMP-specific, IBMX-insensitive PDE8 family	68
1.6.2	cGMP modulated/hydrolysing PDE enzymes containing GAF domains	69
1.6.2.1	Derivation of the term 'GAF'	69
1.6.2.2	cGMP-stimulated PDE2 family	70
1.6.2.3	cGMP-specific PDE5 family	71
1.6.2.4	cGMP-specific photoreceptor PDE6 family	71
1.6.3	cGMP-specific PDE9 family	73
1.6.4	Dual substrate PDE families	73
1.6.4.1	cGMP-inhibited PDE3 family	73
1.6.4.2	cAMP and cGMP-specific PDE10 family	75
1.6.4.3	cAMP and cGMP-specific PDE11 family	76
1.7	Calcium/calmodulin-stimulated PDE1 Family	77
1.7.1	Discovery of PDE1 enzymes	77
1.7.2	Domain organisation of the PDE1 enzymes	79
1.7.3	Regulation of the PDE1 enzymes by phosphorylation	81
1.7.3.1	Regulation by phosphorylation	81
1.7.3.2	Regulation by proteolytic degradation	82
1.7.4	PDE1 splice variants	85
1.7.4.1	PDE1A splice variants	85
1.7.4.2	PDE1B splice variants	88
1.7.4.3	PDE1C splice variants	89
1.7.5	Tissue distribution of PDE1 enzymes	90
1.8	Background to the present work	92
1.8.1	Characterisation of purified native dog heart PDE1A enzyme	92

1.8.2	Sequence analysis of dog heart PDE1A cDNA	92
1.8.2.1	Putative amino acid sequence of the dog heart PDE1A	92
1.8.2.2	PEST sequence in the dog heart PDE1A	96
1.9	Overview of the present work	97
1.9.1	Cloning and expression of dog heart PDE1A	98
1.9.1.1	Yeast expression system	98
1.9.1.2	Bacterial expression system	99
1.9.1.3	Mammalian expression system	99
1.9.2	Characterisation of the soluble recombinant dog heart PDE1A1	100
<b>Chapter 2</b>	<b>General Materials and Methods</b>	101
2.1	Materials	101
2.1.1	Chemical reagents	101
2.1.2	DNA reagents	101
2.1.3	Bacterial reagents and strains	101
2.1.4	Protein reagents	102
2.1.5	Phosphodiesterase assay reagents	103
2.2	Methods	103
2.2.1	Bacterial growth media	103
2.2.1.1	Minimal media	103
2.2.1.2	LB media	104
2.2.2	40% Glycerol Stock preparation	105
2.2.3	Preparation of Calcium-Chloride Competent <i>E. coli</i> cells	105
2.2.4	Transformation of Competent <i>E. coli</i> cells by the heat-shock method	105
2.2.5	Growth of bacterial cultures for plasmid DNA purification	106
2.2.5.1	Small scale plasmid DNA purification	106
2.2.5.2	Large scale plasmid DNA purification	106
2.2.6	Quantitation of purified plasmid DNA	107
2.2.7	Restriction Enzyme Analysis	107
2.2.8	Agarose gel electrophoresis	108
2.2.8.1	Reagents for agarose gel electrophoresis	108
2.2.8.2	Preparation of 0.4 - 1.0% Agarose gels	108
2.2.8.3	Sample preparation	109
2.2.8.4	Flat-bed agarose gel electrophoresis	109
2.2.8.5	Visualisation of samples	109
2.2.9	DNA extraction and purification from agarose gels	110
2.2.10	Automated DNA sequence analysis	110
2.2.10.1	Sample preparation for DNA sequence analysis	110
2.2.10.2	Ethanol precipitation	111

2.2.11	Phosphodiesterase activity assay	111
2.2.11.1	Dowex slurry preparation (1:4 slurry)	111
2.2.11.2	PDE assay buffer	111
2.2.11.3	PDE bioassay	112
2.2.12	Sodium dodecyl sulphate polyacrylamide gel electrophoresis(SDS PAGE)	113
2.2.12.1	Reagents for SDS PAGE	113
2.2.12.2	Preparation of the gels for SDS PAGE	115
2.2.12.3	Sample preparation and SDS PAGE	115
2.2.13	Silver staining of SDS PAGE gels	116
2.2.13.1	Reagents for silver staining of SDS PAGE gels	116
2.2.13.2	Silver staining procedure	117
2.2.14	Western blotting	117
2.2.14.1	Reagents for Western blotting	117
2.2.14.2	Western blot procedure	118
2.2.15	Determination of protein concentration	119
2.2.16	Buffers used in bacteria and mammalian cell work	120
<b>Chapter 3</b>	<b>Cloning and expression of PDE1A1 in pPICZ<math>\alpha</math>C for secreted expression in <i>Pichia pastoris</i></b>	<b>122</b>
3.1	Introduction	122
3.1.1	Foreign gene expression in <i>Saccharomyces cerevisiae</i>	122
3.1.2	Expression in non- <i>Saccharomyces</i> yeasts	124
3.1.3	<i>Pichia pastoris</i> expression system	125
3.1.3.1	The alcohol oxidase promoter	125
3.1.3.2	Expression vectors for <i>Pichia pastoris</i>	125
3.1.3.3	Strains of <i>Pichia pastoris</i>	126
3.1.3.4	Expression of foreign proteins in <i>Pichia pastoris</i>	127
3.2	Background and aims for the present study	127
3.2.1	Background	127
3.2.2	Aims	131
3.3	Materials	132
3.4	Methods	133
3.4.1	Preparation of stocks and media	133
3.4.1.1	pPICZ $\alpha$ C and <i>Pichia pastoris</i> stocks	133
3.4.1.2	Protein expression media	133
3.4.2	Cloning the full-length PDE1A1cDNA in pPICZ $\alpha$ C	135
3.4.2.1	Purification of PDE1A1 cDNA from pCR-Script-PDE1A1 construct	135

3.4.2.2	Restriction enzyme digestion of the vector pPICZ $\alpha$ C	135
3.4.2.3	Ligation of PDE1A1 ORF into pPICZ $\alpha$ C	136
3.4.2.4	Automated DNA sequence analysis	136
3.4.3	Transformation of <i>Pichia pastoris</i> cells with construct DNA	137
3.4.3.1	Preparation of competent <i>Pichia pastoris</i> cells	137
3.4.3.2	<i>PmeI</i> -Linearisation of the construct DNA	137
3.4.3.3	Transformation of <i>Pichia pastoris</i> with linearised construct	138
3.4.3.4	Determination of the methanol phenotype of transformant colonies	138
3.4.4	Expression of the GS115/Mut <sup>s</sup> Albumin (Mut <sup>s</sup> ) and transformant <i>Pichia pastoris</i> cells	139
3.4.4.1	Secreted expression of albumin	139
3.4.4.2	Expression studies on <i>Pichia pastoris</i> transformant colonies	140
3.5	Results	140
3.5.1	Cloning of PDE1A1 into pPICZ $\alpha$ C	140
3.5.1.1	Screening transformant colonies	140
3.5.1.2	Automated DNA sequence analysis	143
3.5.2	Methanol phenotype determination for the transformant <i>Pichia pastoris</i> strains	143
3.5.3	Secreted expression of GS115/Mut <sup>s</sup> -Albumin (Mut <sup>s</sup> )	144
3.5.4	Expression studies on pPICZ $\alpha$ C-PDE1A1 constructs	145
3.6	Discussion	147
<b>Chapter 4</b>	<b>Cloning and expression of PDE1A1 in pGEX-3X and pTrcHisA for protein expression in <i>E. coli</i></b>	<b>151</b>
4.1	Introduction	151
4.1.1	Background to prokaryotic expression systems	151
4.1.2	Foreign gene expression using prokaryotic expression systems	152
4.2	Background and aims of the present study using the bacterial expression system for the cloning and expression of dog heart PDE1A1	157
4.2.1	Overview	157
4.2.2	Cloning the full-length and N-terminal truncated PDE1A1 into prokaryotic expression vectors	157
4.2.2.1	pGEX-3X expression vector	157
4.2.2.2	pTrcHisA expression vector	159
4.2.3	Aims	161
4.3	Materials	162

4.4	Methods	163
4.4.1	Cloning of the full length PDE1A1 ORF into pGEX-3X	163
4.4.1.1	PDE1A1 ORF purification from pCR-Script-PDE1A1	163
4.4.1.2	Cloning purified PDE1A1 ORF into pGEX-3X	163
4.4.1.3	Screening transformant colonies using <i>Bam</i> HI	164
4.4.1.4	Filling-in the <i>Bam</i> HI overhang in pGEX-3X-PDE1A1 constructs	164
4.4.1.5	Screening transformant colonies using <i>Bam</i> HI and <i>Hind</i> III	164
4.4.2	Expression studies on pGEX-PDE1A1 (c12) in <i>E. coli</i> JM109(DE3)	164
4.4.2.1	The effect of temperature on recombinant protein expression	165
4.4.2.1.1	Protein expression at 37°C	165
4.4.2.1.2	Protein expression at 24°C	165
4.4.2.2	Protein expression in media supplemented with sorbitol	165
4.4.3	Processing bacterial cells following protein expression	166
4.4.3.1	Timed bacterial samples	166
4.4.3.2	Bacterial cultures grown to the end of the expression period	166
4.4.4	Washing and refolding of GST-PDE1A1 (c12) from inclusion bodies	167
4.4.4.1	Washing of the inclusion bodies	167
4.4.4.2	Denaturing inclusion bodies for extraction of the recombinant protein	167
4.4.4.3	Renaturation of the recombinant protein	167
4.4.5	Cloning of the PDE1A1 ORF into pTrcHisA	168
4.4.5.1	PDE1A1 purification from pCR-Script-PDE1A1	168
4.4.5.2	Cloning the purified truncated PDE1A1 into pTrcHisA	168
4.4.5.3	Screening transformant colonies	169
4.4.6	Expression studies on pTrcHisA-PDE1A1 <sub>N-trunc</sub> clone 1 (c1)	170
4.4.6.1	Small-scale expression studies on pTrcHisA-PDE1A1 <sub>N-trunc</sub> clone 1 (c1)	170
4.4.6.1.1	Expression of pTrcHisA and pTrcHisA-PDE1A1 <sub>N-trunc</sub> (c1) in <i>E. coli</i> JM109	170
4.4.6.1.2	Expression of pTrcHisA and pTrcHisA-PDE1A1 <sub>N-trunc</sub> (c1) in <i>E. coli</i> JM109(DE3)	170

4.4.6.2	Large-scale expression and purification of pTrcHisA-PDE1A1 <sub>N-trunc</sub> clone 1	171
4.4.6.2.1	Expression of pTrcHisA-PDE1A1 <sub>N-trunc</sub> (c1) in <i>E. coli</i> JM109 using a 10-litre fermenter vessel	171
4.4.6.2.2	Purification of pTrcHisA-PDE1A1 <sub>N-trunc</sub> clone 1 expressed in <i>E. coli</i> JM109	171
4.4.6.2.2.1	Denaturing and Elution Buffers	172
4.4.6.2.2.2	Equilibration of the nickel resin	172
4.4.6.2.2.3	Sample preparation	173
4.4.6.2.2.4	Sample application and elution	173
4.5	Results and Discussion	174
4.5.1	Cloning of PDE1A1 in pGEX-3X	174
4.5.1.1	Screening transformant <i>E. coli</i> colonies	174
4.5.1.2	Automated DNA sequence analysis	175
4.5.2	Expression studies on pGEX-3X-PDE1A1	175
4.5.2.1	Effect of temperature on protein expression	175
4.5.2.2	Protein expression in media supplemented with sorbitol	180
4.5.3	Refolding of GST-PDE1A1 from inclusion bodies	185
4.5.4	Cloning of the N-terminal truncated PDE1A1 in pTrcHisA	189
4.5.4.1	Screening transformant <i>E. coli</i> colonies	189
4.5.4.2	Automated DNA sequence analysis	190
4.5.5	Small-scale expression of pTrcHisA-PDE1A1 <sub>N-trunc</sub> in <i>E. coli</i>	191
4.5.5.1	pTrcHisA-PDE1A1 <sub>N-trunc</sub> (c1 and c3) in <i>E. coli</i> JM109 cells	191
4.5.5.2	pTrcHisA-PDE1A1 <sub>N-trunc</sub> (c1) in <i>E. coli</i> JM109(DE3) cells	193
4.5.6	Large-scale expression of pTrcHisA-PDE1A1 <sub>N-trunc</sub> in <i>E. coli</i> JM109 cells	198
4.5.7	Purification of His <sub>6</sub> -PDE1A1 <sub>N-trunc</sub> using nickel chelate affinity chromatography	200
4.7	Conclusion	202
<b>Chapter 5</b>	<b>Semliki Forest virus for the cloning and expression of full-length and truncated PDE1A1</b>	<b>205</b>
5.1	Introduction	205
5.1.2	Virus vectors for heterologous protein expression	205
5.1.2.1	Insect cells for the expression for heterologous proteins	205
5.1.2.2	Mammalian cells for the expression of heterologous proteins	207
5.1.2.2.1	<i>Vaccinia</i> virus vectors	207
5.1.2.2.2	Adenovirus vectors	207

	5.1.2.2.3	Alphavirus vectors	207
5.2		Semliki Forest virus vectors	208
	5.2.1	Lifecycle of the Semliki Forest virus	208
	5.2.2	Semliki Forest virus expression vectors	210
	5.2.2.1	Background to the construction of the Semliki Forest virus vectors	210
	5.2.2.2	Semliki Forest virus vectors for the production of foreign protein	214
	5.2.3	Background and aims of the present study using the Semliki Forest virus expression system	215
	5.2.3.1	Semliki Forest virus vectors used in the present study	215
	5.2.3.1.1	pSFV3 <i>lacZ</i> vector	215
	5.2.3.1.2	pSFV1 and pSFV-Helper 2 vectors	216
	5.2.3.2	Generation of full-length and truncated dog heart PDE1A1 constructs	216
	5.2.3.3	Expression of full-length and truncated dog heart PDE1A1	217
	5.2.4	Aims	219
5.3		Materials	220
	5.3.1	Chemical reagents	220
	5.3.2	Vectors	220
	5.3.3	Bacterial strains	220
	5.3.4	DNA reagents	221
	5.3.5	RNA reagents	221
	5.3.6	Tissue culture reagents	221
	5.3.7	Protein reagents	222
	5.3.8	Protein purification resins and columns	222
5.4		Methods	223
	5.4.1	Polymerase Chain Reaction	223
	5.4.1.1	Primer design and preparation	223
	5.4.1.2	DNA template used for the generation of full-length and truncated PDE1A1 fragments by PCR	224
	5.4.1.3	Optimisation of the PCR	225
	5.4.2	Cloning the PDE1A1 PCR products into pSFV1	226
	5.4.2.1	<i>Bam</i> HI and <i>Sma</i> I restriction digestion of the PCR product	226
	5.4.2.2	<i>Bam</i> HI and <i>Sma</i> I restriction digestion of pSFV1	226
	5.4.2.3	Dephosphorylation of pSFV1	226
	5.4.2.4	Ligation of digested PDE1A1 PCR fragments and pSFV1	226

5.4.3	Transformation of <i>E. coli</i> DH5 $\alpha$ competent cells with ligation mixtures	227
5.4.4	Screening transformant colonies for the correct construct	227
5.4.4.1	DNA purification for screening of transformant colonies	227
5.4.4.2	<i>Bam</i> HI, <i>Sma</i> I and <i>Eco</i> RV Enzyme Restriction Analysis for selection of constructs	227
5.4.5	<i>In vitro</i> RNA synthesis	228
5.4.5.1	Linearisation of the construct	228
5.4.5.2	Phenol/Chloroform Clean-up of linearised construct, pSFV3 <i>lacZ</i> and pSFV-H2 DNA	228
5.4.5.3	Salt/ethanol precipitation	229
5.4.5.4	<i>In vitro</i> RNA synthesis	229
5.4.5.5	Analysis of RNA transcripts	229
5.4.6	Growth and maintenance of Baby Hamster Kidney-21 cells(BHK21)	230
5.4.6.1	Preparation of Complete Media used for the maintenance of BHK-21 cells	230
5.4.6.2	Resuscitation of BHK-21 cells	230
5.4.6.3	BHK-21 Cell Passage	231
5.4.6.4	Freezing BHK-21 cells	231
5.4.7	Direct transfection of BHK-21 cells with pSFV3 <i>lacZ</i> RNA transcripts	231
5.4.7.1	BHK-21 cell preparation and electroporation	231
5.4.7.2	In-situ $\beta$ -Galactosidase ( $\beta$ -Gal) staining with X-Gal	232
5.4.8	Direct transfection of BHK-21 cells with pSFV1-PDE1A1 RNA transcripts	233
5.4.9	Co-transfection of BHK-21 cells with pSFV1-PDE1A1/ pSFV3 <i>lacZ</i> RNA and Helper-2 virus RNA	233
5.4.10	Harvesting recombinant virus	233
5.4.11	Infection of BHK-21 cells with recombinant virus particles	234
5.4.11.1	BHK-21 cell preparation for infection with recombinant virus	234
5.4.11.2	Recombinant virus activation	234
5.4.11.3	Determination of transfection efficiency and virus titer	234
5.4.11.3.1	Infection of BHK-21 cells with pSFV3 <i>lacZ</i> virus stocks	234
5.4.11.3.2	Transfection efficiency and viral titer determination	235
5.4.11.4	Infection of BHK-21 cells with the recombinant pSFV1-PDE1A1 virus stocks	235



5.4.12	Optimisation of the conditions for the expression of recombinant enzyme following pSFV1-PDE1A1 virus infection	236
5.4.13	Harvesting BHK-21 cells following direct transfection with pSFV1-PDE1A1 RNA transcripts or co-transfection with pSFV1-PDE1A1 and pSFV-H2 RNA transcripts	236
5.4.13.1	BHK-21 cell harvesting following direct transfection with pSFV1- PDE1A1 RNA transcripts	236
5.4.13.2	BHK-21 cell harvesting following co-transfection of pSFV1-PDE1A1 and pSFV-H2 RNA transcripts	237
5.4.14	Concentration of samples	237
5.4.14.1	Methanol/chloroform concentration of samples	237
5.4.14.2	Centricon 10/30 concentration of samples	238
5.4.15	Stability studies on the full-length PDE1A1 enzyme	238
5.4.15.1	Storage of FL4 at 4°C	238
5.4.15.2	Effect of pH on FL4 PDE activity	239
5.4.15.3	Effect of glycerol on FL4 and End6 PDE activity	239
5.4.16	Studies to determine the native state of the recombinant PDE1A1 enzyme (FL4 and End6 constructs)	240
5.4.16.1	Cross-linking studies on End6	240
5.4.16.1.1	DSS stock preparation	240
5.4.16.1.2	Cross-linking reaction using DSS	240
5.4.16.2	Sephadex G100 size exclusion chromatography on FL4	241
5.4.16.2.1	Sephadex G100 resin equilibration	241
5.4.16.2.2	Standards for Sephadex G100 gel filtration chromatography	241
5.4.16.2.3	Preparation and loading of the FL4 sample for gel filtration	242
5.4.17	PDE1A1 purification	243
5.4.17.1	Q Sepharose Fast Flow ion exchange chromatography	243
5.4.17.1.1	Column packing and equilibration	243
5.4.17.1.2	Protein binding and elution	243
5.4.17.2	Vivapure-Q Spin Columns for ion exchange chromatography	244
5.4.17.2.1	Equilibration of the Vivapure-Q Spin Columns	244
5.4.17.2.2	Sample application and elution from the Q Spin Columns	244

5.4.17.3	Calmodulin-agarose affinity chromatography on pSFV1-PDE1A1 (FL4)	245
5.4.17.3.1	Calmodulin-agarose resin equilibration	245
5.4.17.3.2	Sample application and elution	245
5.4.18	Preliminary PDE assays on the full-length (FL4) and N-terminal truncated (End6) enzymes	246
5.5	Results	247
5.5.1	Generation of Full-length and truncated PDE1A1 for cloning in pSFV1	247
5.5.1.1	PCR products	247
5.5.1.2	pSFV1-PDE1A1 constructs	248
5.5.2	Automated DNA sequence analysis	250
5.5.3	<i>In vitro</i> RNA synthesis of the four recombinant pSFV1-PDE1A1 constructs	251
5.5.4	BHK-21 cells transfected by electroporation directly with pSFV3 <i>lacZ</i> RNA or pSFV1-PDE1A1 construct RNA	251
5.5.4.1	<i>In-situ</i> $\beta$ -galactosidase staining of BHK-21 cells transfected with pSFV3 <i>lacZ</i> RNA	252
5.5.4.2	PDE assay results for cells harvested following direct transfection with pSFV1-PDE1A1 RNA	252
5.5.4.3	SDS PAGE and Western blot analysis of cells harvested following direct transfection with pSFV1-PDE1A1 RNA	254
5.5.5	Virus titer determination and optimisation of BHK-21 cell infection with recombinant FL4 virus	256
5.5.5.1	Transfection efficiency and virus titer determination	256
5.5.5.2	Optimisation of the conditions for the infection of BHK-21 cells with pSFV1-PDE1A1 virus particles	257
5.5.6	Stability studies on FL4	259
5.5.6.1	Storage of FL4 at 4°C	259
5.5.6.2	Effect of pH on FL4 PDE activity	260
5.5.6.3	The effect of glycerol on basal FL4 PDE activity	261
5.5.7	Determination of the native state of the recombinant enzymes End6 and FL4	262
5.5.7.1	DSS cross-linking studies on End6	262
5.5.7.2	Gel filtration chromatography on FL4	263
5.5.8	PDE1A1 purification	266
5.5.8.1	Q Sepharose ion exchange chromatography on End6	266
5.5.8.2	Vivaspin-Q ion exchange chromatography on FL4	268

	5.5.8.3	Calmodulin-agarose affinity chromatography on FL4	270
	5.5.9	Preliminary kinetic analysis on FL4 and End6	271
5.6		Discussion	274
	5.6.1	Cloning and expression of the full-length and truncated PDE1A1 in pSFV1	274
	5.6.2	Preliminary PDE activity analysis of the full-length and truncated PDE1A1 enzymes	275
	5.6.3	Stability studies on FL4	280
	5.6.4	Determination of the native state of the recombinant enzymes	281
	5.6.5	Purification studies on FL4 and End6	283
	5.6.6	Summary of the preliminary analysis of full-length and truncated PDE1A1 proteins	285
5.7		Conclusion	285
<b>Chapter 6</b>		<b>Biochemical analysis of the recombinant full-length (FL4) and N-terminal truncated (End6) PDE1A enzymes</b>	287
6.1		Introduction	287
	6.1.1	Cyclic nucleotide specificity for PDE1 family members	287
	6.1.2	Inhibition of PDE1 enzymes by PDE inhibitors	288
6.2		Background and aims of the present work	292
	6.2.1	Background	292
	6.2.2	Aims	293
6.3		Materials	294
6.4		Methods	294
	6.4.1	Determination of the linear range of reaction of cAMP and cGMP hydrolysis by FL4 and End6	294
	6.4.2	Determination of the kinetic parameters of FL4 and End6	294
	6.4.3	Estimation of PDE1A1 protein concentration in total cell lysate samples	295
6.5		Results	296
	6.5.1	Time-course study on FL4 and End6	296
	6.5.2	Determination of the $K_m$ and $V_{max}$ values for the full-length (FL4) and N-terminal truncated (End6) enzymes	297
	6.5.3	Inhibitor studies on the full-length (FL4) and N-terminal truncated (End6) enzymes	300
	6.5.4	Focus on the FL4 and End6 sensitivity to rolipram	304
	6.5.4.1	PDE activity assays	304
	6.5.4.2	Immunoblot to demonstrate the absence of PDE4 in FL4 and End6 samples	307

6.6	Discussion	310
6.6.1	Kinetic analysis of FL4 and End6 for the determination of $K_m$ and $V_{max}$	310
6.6.2	Inhibitor studies on FL4 and End6	313
6.7	Conclusion	317
<b>Chapter 7</b>	<b>General discussion</b>	<b>318</b>
7.1	Introduction	318
7.2	Expression of dog heart PDE1A1	324
7.3	Biochemical characterisation of dog heart PDE1A1	325
<b>References</b>		<b>328</b>

## List of Figures

<b>Figure 1.1</b>	Simple schematic of the intracellular events following the binding of ligands to receptors to $\alpha$ - and $\beta$ -adrenoreceptors.	32
<b>Figure 1.2</b>	Simple schematic of the intracellular events following the binding of ligands to guanylyl cyclases.	35
<b>Figure 1.3</b>	Structures of the non-selective PDE inhibitors.	36
<b>Figure 1.4</b>	The hydrolysis of cAMP to the corresponding inactive monophosphate.	37
<b>Figure 1.5</b>	The hydrolysis of cGMP to the corresponding inactive monophosphate.	37
<b>Figure 1.6</b>	Nomenclature of PDE1 as proposed by Beavo and co-workers (1994).	39
<b>Figure 1.7</b>	Human Genome Project Nomenclature of PDE1.	39
<b>Figure 1.8</b>	General domain organisation of the PDE families.	40
<b>Figure 1.9</b>	Schematic showing divergent amino terminal domains in the PDE family of enzymes.	42
<b>Figure 1.10</b>	Amino acid sequence alignment for PDE5, PDE4 and PDE1 enzymes showing conserved residues (shown coloured) around the invariant glutamic acid (shown underlined).	45
<b>Figure 1.11.1</b>	Amino acid sequence alignment for thermolysin, PDE5, PDE1, PDE4 and PDE3 showing the metal binding residues.	48
<b>Figure 1.11.2</b>	Signature motif in the catalytic domain of PDE enzymes.	49
<b>Figure 1.12</b>	PDE domains indicating the metal binding motifs within the catalytic domain, the conserved dyad together with the sequence surrounding the invariant glutamic acid residue for PDE5.	49
<b>Figure 1.13.1</b>	Schematic of the subdomain organisation of the catalytic domain of the PDE4B2B.	51
<b>Figure 1.13.2(a)</b>	Ribbon diagram of the catalytic domain of PDE4B2B with cAMP in the substrate binding pocket.	52
<b>Figure 1.13.2(b)</b>	Ribbon diagram showing detail of the catalytic domain of PDE4B2B with cAMP in the substrate binding pocket	53
<b>Figure 1.14.1</b>	Amino acid residues associated with cAMP binding for PDE4B2B catalytic pocket.	55
<b>Figure 1.14.2</b>	Amino acid sequence alignment for PDE4B2B and PDE1A1.	57
<b>Figure 1.15.1</b>	Structures of selective PDE inhibitors.	59
<b>Figure 1.15.2</b>	Structures of PDE4-selective inhibitors undergoing clinical development	60
<b>Figure 1.16</b>	Schematic of the domain organisation of the PDE4 enzymes.	64
<b>Figure 1.17</b>	Schematic showing the PEST motif and m-calpain cleavage site in bovine PDE1A2.	84

<b>Figure 1.18.1</b>	Amino terminal residues for the PDE1 family.	87
<b>Figure 1.18.2</b>	Carboxy terminal residues for the PDE1 family.	87
<b>Figure 1.19.1</b>	Nucleotide and amino acid sequence for the dog heart PDE1A (GenBank Accession AF252536) together with the putative single letter amino acid polypeptide sequence.	95
<b>Figure 1.19.2</b>	Schematic of the four PDE1A1 fragments used for cloning into pSFV1.	96
<b>Figure 1.20</b>	PEST sequences in the bovine PDE1A2 and the dog heart PDE1A.	97
<b>Figure 1.21</b>	Calpain cleavage sequences in the bovine PDE1A2 and the dog heart PDE1A.	97
<b>Figure 2.1</b>	Apparatus used for the Western blot procedure.	119
<b>Figure 3.1.1</b>	Schematic of pPICZ $\alpha$ C-PDE1A1 construct.	129
<b>Figure 3.1.2</b>	Expression cassette containing the PDE1A1 insert.	129
<b>Figure 3.2.1</b>	DNA fragments expected following enzyme restriction analysis of the insert in the correct orientation in the pPICZ $\alpha$ C-PDE1A1 construct.	130
<b>Figure 3.2.2</b>	DNA fragments expected following enzyme restriction analysis of the insert in the reverse orientation in the pPICZ $\alpha$ C-PDE1A1 construct.	130
<b>Figure 3.3</b>	Schematic of the PDE1A1 ORF showing the position of the sequencing primers.	137
<b>Figure 3.4</b>	Grid template used for streaking <i>Pichia pastoris</i> transformant strains.	139
<b>Figure 3.5</b>	Screening transformant colonies for the presence of the construct (s) containing the PDE1A1 insert using <i>Hind</i> III enzyme restriction analysis.	142
<b>Figure 3.6.1</b>	Confirmation of the PDE1A1 orientation in the construct pPICZ $\alpha$ C-PDE1A1 using enzyme restriction analysis.	142
<b>Figure 3.6.2</b>	DNA sequence analysis of pPICZ $\alpha$ C-PDE1A1.	143
<b>Figure 3.7</b>	Analysis of cleared media following secreted expression of albumin from GS115/Mut <sup>s</sup> -Albumin (Mut <sup>s</sup> ).	145
<b>Figure 3.8.1</b>	Analysis of GS115-PDE1 samples using PDE activity assays.	146
<b>Figure 3.8.2</b>	Analysis of KM71-PDE1 samples using PDE activity assays.	146
<b>Figure 3.8.3</b>	Analysis of X-33-PDE1 samples using PDE activity assays.	146
<b>Figure 4.1</b>	Cloning strategy for the full-length PDE1A1 in pGEX-3X.	158
<b>Figure 4.2</b>	Schematic map of the pGEX-3X-PDE1A1 construct.	159
<b>Figure 4.3</b>	Schematic showing the coding sequence for the full-length dog heart PDE1A1 cDNA.	160
<b>Figure 4.4</b>	Schematic map of the pTrcHisA-PDE1A1 <sub>N-trunc</sub> construct.	160

<b>Figure 4.5.1</b>	Agarose gel analysis of pGEX-3X-PDE1A1 constructs showing clones 12 and 17 (i) and the vector pGEX-3X (ii).	174
<b>Figure 4.5.2</b>	DNA sequence analysis of the construct pGEX-3X-PDE1A1 (c12).	175
<b>Figure 4.6</b>	Effect of IPTG on recombinant protein expression carried out at 37°C.	176
<b>Figure 4.7.1a</b>	SDS PAGE analysis of c12 expressed at 24°C in the presence and absence of IPTG.	177
<b>Figure 4.7.1b</b>	SDS PAGE analysis on pGEX-3X expressed at 24°C in the presence and absence of IPTG.	178
<b>Figure 4.7.2</b>	Western blot analysis on c12 and the vector using GST and CaM-PDE antibodies for expression carried out at 24°C.	179
<b>Figure 4.8</b>	SDS PAGE analysis of c12 and the vector for expression carried out at 30°C with media supplemented with sorbitol.	180
<b>Figure 4.9.1</b>	PDE activity analysis of c12 and pGEX-3X cleared total cell lysate samples for expression carried out at 30°C with media supplemented with sorbitol.	181
<b>Figure 4.9.2</b>	SDS PAGE analysis of c12 and pGEX-3X samples expressed at 30°C in media supplemented with sorbitol.	182
<b>Figure 4.10.1</b>	SDS PAGE analysis of clone 12 and the vector for expression carried out at 30°C in media supplemented with sorbitol.	183
<b>Figure 4.10.2</b>	Western blot analysis of clone 12 and the vector for expression carried out at 30°C in media supplemented with sorbitol.	183
<b>Figure 4.11</b>	Analysis of c12 proteins refolded from inclusion bodies.	188
<b>Figure 4.12</b>	Western blot analysis of c12 proteins purified from inclusion bodies.	188
<b>Figure 4.13.1</b>	Agarose gel analysis of pTrcHisA-PDE1A1 <sub>N-trunc</sub> clones 1 and 3.	190
<b>Figure 4.13.2</b>	DNA sequence analysis for construct pTrcHisA-PDE1A1 <sub>N-trunc</sub> , c1.	191
<b>Figure 4.14.1</b>	SDS PAGE and Western blot analysis of c1 and c3 expressed in <i>E. coli</i> JM109 cells.	192
<b>Figure 4.14.2</b>	PDE activity analysis of c1 and PTA supernatant samples harvested at 3 hours post-induction.	192
<b>Figure 4.15.1</b>	Western blot analysis of total cell lysates of c1 and the empty vector using CaM-PDE antibody for the expression carried out in <i>E. coli</i> JM109 (DE3) cells.	194
<b>Figure 4.15.2</b>	PDE activity analysis of c1 and PTA supernatant samples.	195
<b>Figure 4.16.1</b>	SDS PAGE and Western blot analysis of c1 and PTA particulate fractions.	197
<b>Figure 4.16.2</b>	SDS PAGE and Western blot analysis of c1 and PTA supernatant samples.	197
<b>Figure 4.17.1</b>	SDS PAGE and Western blot analysis of c1 from large-scale protein expression.	199

<b>Figure 4.17.2</b>	Western blot analysis on c1 from large-scale protein expression.	199
<b>Figure 4.17.3</b>	PDE activity results for the supernatant sample from the large-scale expression of pTrcHisA-PDE1A1 <sub>N-trunc</sub> (c1).	200
<b>Figure 4.18.1</b>	Analysis of the c1 fractions following nickel chelate affinity purification.	201
<b>Figure 4.18.2</b>	SDS PAGE and Western blot analysis on purified His <sub>6</sub> -PDE1A1 <sub>N-trunc</sub> (c1) protein.	201
<b>Figure 5.1</b>	Overview of the Semliki Forest virus replication cycle.	210
<b>Figure 5.2</b>	Recombinant pSFV1 and pSFV-Helper for the production of foreign proteins.	212
<b>Figure 5.3</b>	Wild type and variant amino acid sequences surrounding the p62 cleavage site in the SFV Helper virus.	213
<b>Figure 5.4</b>	Sequence of the multiple cloning site in pSFV1.	216
<b>Figure 5.5</b>	Analysis of the PDE1A1 PCR products generated using the full-length dog heart PDE1A1 cDNA.	247
<b>Figure 5.6</b>	Analysis of the full-length pSFV1-PDE1A1 constructs (FL4 and FL28) following <i>Bam</i> HI, <i>Sma</i> I and <i>Eco</i> RV restriction analysis.	249
<b>Figure 5.7.1</b>	Analysis of the C-terminal truncated pSFV1-PDE1A1 (G2) construct following <i>Bam</i> HI and <i>Sma</i> I restriction analysis.	249
<b>Figure 5.7.2</b>	Analysis of the N-terminal truncated (End6) and the catalytic (Cat9) pSFV1-PDE1A1 constructs following <i>Bam</i> HI and <i>Sma</i> I digestion.	250
<b>Figure 5.8</b>	DNA sequence analysis of FL4.	250
<b>Figure 5.9</b>	Analysis of the RNA transcripts for all four PDE1A1 constructs.	251
<b>Figure 5.10</b>	PDE activity analysis of truncated PDE1A1 constructs (G2, End6 and Cat9) as well as BHK-21 cells for background PDE activity.	253
<b>Figure 5.11</b>	PDE activity analysis of the full-length construct (FL4) diluted a hundred fold.	253
<b>Figure 5.12</b>	PDE activity analysis of the supernatant and particulate fraction samples for G2, End6, Cat9 and pSFV1.	254
<b>Figure 5.13</b>	Western blot analysis of full-length and truncated PDE1A1 constructs together with the pSFV1 vector and no-vector-BHK-21 cells.	255
<b>Figure 5.14</b>	Western blot analysis of FL4 and G2 enzymes concentrated ten fold.	255
<b>Figure 5.15</b>	Western blot analysis of End6 and Cat9 enzymes concentrated ten fold.	256
<b>Figure 5.16.1</b>	Optimisation of the infection of BHK-21 cells with recombinant FL4 virus.	257
<b>Figure 5.16.2</b>	PDE activity analysis for the optimisation of the infection of BHK-21 cells with recombinant FL4 virus carried out in the presence of Ca <sup>2+</sup> /CaM.	258



<b>Figure 5.17</b>	Total protein concentration for BHK-21 cells infected with the recombinant FL4 virus.	259
<b>Figure 5.18</b>	PDE activity analysis of FL4 stored at 4°C for up to five days.	260
<b>Figure 5.19</b>	PDE activity analysis of FL4 stored in different pH buffers at 4°C for up to four days.	261
<b>Figure 5.20</b>	The effect of glycerol on FL4 and End6 PDE activity.	262
<b>Figure 5.21</b>	Western blot analysis of the DSS cross-linking of End6 (N-terminal truncated) enzyme.	263
<b>Figure 5.22.1</b>	PDE activity analysis of FL4 purified using Vivaspin Q ion exchange chromatography.	264
<b>Figure 5.22.2</b>	SDS PAGE analysis of FL4 purified following Vivaspin Q ion exchange chromatography.	265
<b>Figure 5.23.1</b>	Absorbance ( $A_{280}$ ) profile for the gel filtration standards.	265
<b>Figure 5.23.2</b>	PDE activity (DPM) profile for FL4 sample analysed by gel filtration chromatography.	266
<b>Figure 5.24.1</b>	PDE activity analysis of End6 purified using Q Sepharose ion exchange chromatography.	267
<b>Figure 5.24.2</b>	SDS PAGE analysis of End6 purified using Q Sepharose ion exchange chromatography.	268
<b>Figure 5.25.1</b>	PDE activity profile for FL4 fractions obtained from the Vivaspin Q ion exchange units.	269
<b>Figure 5.25.2</b>	SDS PAGE analysis of FL4 purified using Vivaspin Q ion exchange units.	269
<b>Figure 5.26.1</b>	Purification profile of FL4 purified by Vivaspin Q ion exchange chromatography followed by calmodulin-agarose chromatography.	270
<b>Figure 5.26.2</b>	SDS PAGE analysis of FL4 purified using Vivaspin Q ion exchange followed by calmodulin agarose affinity chromatography.	271
<b>Figure 5.27.1</b>	Cyclic nucleotide substrate specificity of FL4.	272
<b>Figure 5.27.2</b>	Cyclic nucleotide substrate specificity of End6.	272
<b>Figure 5.28.1</b>	Response of FL4 to $Ca^{2+}$ /CaM using cAMP and cGMP as substrates.	273
<b>Figure 5.28.2</b>	Response of End6 to $Ca^{2+}$ /CaM using cAMP and cGMP as substrates.	273
<b>Figure 5.29</b>	Schematic showing possible PDE1A1 fragments generated following proteolysis.	276
<b>Figure 6.1.1</b>	Time course study on FL4.	296
<b>Figure 6.1.2</b>	Time course study on End6.	297

<b>Figure 6.2.1</b>	Determination of $K_m$ value for FL4 using cAMP as the substrate.	298
<b>Figure 6.2.2</b>	Determination of $K_m$ value for FL4 using cGMP as the substrate.	298
<b>Figure 6.3.1</b>	Determination of $K_m$ value for End6 using cAMP as the substrate.	299
<b>Figure 6.3.2</b>	Determination of $K_m$ value for End6 using cGMP as the substrate.	299
<b>Figure 6.4</b>	The effect of inhibitors on FL4 activity using cAMP and cGMP as substrates.	301
<b>Figure 6.5</b>	The effect of inhibitors on End6 activity using cAMP and cGMP as substrates.	302
<b>Figure 6.6</b>	Effect of DMSO on recombinant PDE activity.	304
<b>Figure 6.7</b>	Schematic of the PDE assay mechanism.	305
<b>Figure 6.8.1</b>	Rolipram inhibition of FL4 using the two-step PDE assay.	307
<b>Figure 6.8.2</b>	Rolipram inhibition of End6 using the two-step PDE assay.	307
<b>Figure 6.9.1</b>	Western blot analysis of FL4 and End6 using polyclonal PDE4 antibody.	309
<b>Figure 6.9.2</b>	Western blot analysis of FL4 and End6 using polyclonal CaM-PDE antibody.	309
<b>Figure 7.1</b>	Conserved cGMP-binding motif.	321
<b>Figure 7.2</b>	Structure of the PDE2A GAF domains ( <u>a</u> and <u>b</u> ), YKG9 and PYP proteins.	322

## List of Tables

<b>Table 1.1</b>	Nomenclature of cyclic nucleotide phosphodiesterase Type 1 as proposed by Beavo and Reifsnnyder (1990).	38
<b>Table 1.2</b>	Nomenclature of cyclic nucleotide phosphodiesterase Type 1 as proposed by Beavo and co-workers (1994).	39
<b>Table 1.3</b>	cGMP selectivity of PDE5A1 following site-directed mutagenesis (Turko <i>et al.</i> , 1998a, 1998b).	46
<b>Table 1.4</b>	PDE Family-specific inhibitors.	59
<b>Table 1.5</b>	Overview of the PDE families.	61
<b>Table 1.6</b>	PDE1 enzymes identified by early studies named according to the nomenclature proposed by Beavo (1990) together with the new PDE name (Beavo <i>et al.</i> , 1994).	79
<b>Table 1.7</b>	PDE1 family splice variants.	85
<b>Table 1.8</b>	PDE1A splice variants generated by the combination of the different amino- and carboxy-termini sequences as reported by Michibata and co-workers (2001).	87
<b>Table 1.9</b>	Summary of biochemical analysis carried out on PDE1C splice variants.	90
<b>Table 2.1</b>	M-9 Minimal media preparation.	104
<b>Table 2.2</b>	Composition of the separating and stacking gels for SDS PAGE.	115
<b>Table 2.3</b>	Composition of buffers used for the bacteria and mammalian work.	121
<b>Table 3.1</b>	Proteins expressed using the <i>Pichia pastoris</i> expression system.	127
<b>Table 3.2</b>	DNA fragment sizes for pPICZ $\alpha$ C-PDE1A1 constructs with the insert in the correct (PDE1) and reverse (PDE1R) orientation.	141
<b>Table 3.3</b>	Methanol phenotype determination of transformant <i>P. pastoris</i> strains.	144
<b>Table 4.1</b>	Foreign genes expressed using <i>E. coli</i> as the host.	153
<b>Table 4.2</b>	GST-PDE1A1 fragments predicted following proteolytic cleavage.	185
<b>Table 4.3</b>	Summary of PDE1A1 expression using the pGEX-3X and pTrcHisA expression vectors in <i>E. coli</i> .	203
<b>Table 5.1</b>	Proteins expressed using the SFV expression system.	215
<b>Table 5.2</b>	PCR primer combinations used for the generation of full-length and truncated PDE1A1 constructs for the present study.	217
<b>Table 5.3</b>	Sequences of the PCR primers designed for the generation of full-length and truncated PDE1A1 enzymes.	224
<b>Table 5.4</b>	Optimised PCR conditions for the generation of full-length and truncated PDE1A1 fragments.	225
<b>Table 5.5</b>	Composition of the Complete Media used for BHK-21 cells.	230

<b>Table 5.6</b>	Standards used for Sephadex G100 gel filtration chromatography.	242
<b>Table 5.7</b>	pSFV1- PDE1A1 DNA fragments following digestion with <i>Bam</i> HI and <i>Sma</i> I restriction enzymes.	248
<b>Table 5.8</b>	Transfection efficiency and virus titer for pSFV3 <i>lacZ</i> virus particles.	256
<b>Table 5.9</b>	Summary of the PDE activity results for the full-length and truncated constructs in the present study.	278
<b>Table 5.10</b>	Summary of results for the native state of FL4 and End6.	283
<b>Table 5.11</b>	Summary of the analysis of the full-length and truncated PDE1A1 recombinant enzymes.	285
<b>Table 6.1</b>	$K_m$ values for PDE1 isoenzymes.	288
<b>Table 6.2</b>	IC <sub>50</sub> values for PDE1 isoenzymes.	290
<b>Table 6.3</b>	IC <sub>50</sub> values for PDE2 through to PDE11 families.	291
<b>Table 6.4.1</b>	Summary of the $K_m$ and $V_{max}$ values for the full-length (FL4) and N-terminal truncated (End6) PDE1A1 enzymes obtained in the present study.	300
<b>Table 6.4.2</b>	$K_m$ and $V_{max}$ values for the full-length native dog heart PDE1A obtained by Clapham and Wilderpsin (2001).	300
<b>Table 6.5.1</b>	Summary of the IC <sub>50</sub> values for the full-length (FL4) and N-terminal truncated (End6) PDE1A1 enzymes.	303
<b>Table 6.5.2</b>	IC <sub>50</sub> values obtained for the native dog heart PDE1A by Clapham and Wilderspin (2001).	303
<b>Table 6.6</b>	Comparison of the kinetic parameters of PDE enzymes.	311
<b>Table 6.7</b>	PDE inhibitor sensitivity of full-length and truncated PDE enzymes.	315

## Chapter One

### 1 Introduction

#### 1.1 The intracellular signalling process

Intracellular processes are coordinated by a series of events which are initiated by the interaction of extracellular molecules (first messengers) with cell surface receptors. Extracellular signalling molecules include hormones, neurotransmitters, growth factors, odour and light. Cell surface receptors include G-protein coupled receptors (e.g.  $\alpha$ - and  $\beta$ -adrenergic receptors, rhodopsin receptors), ion-channel receptors (e.g. nicotinic acetylcholine receptors) and enzyme receptors (e.g. tyrosine kinase receptors). The triggering of receptors by first messengers causes a cascade of reactions within the cell involving a number of intracellular molecules such as the second messengers cAMP, cGMP and calcium ions which in turn lead to a chain of events culminating in the cellular response. This particular response is terminated by a combination of the removal of the extracellular signal from the receptor and degradation of intracellular messengers by enzymes, specifically cyclic nucleotide phosphodiesterases. Termination of the signal is crucial for the proper functioning of a cell.

#### 1.2 cAMP and adenylyl cyclase

##### 1.2.1 Discovery of cAMP and adenylyl cyclase

The best studied example of a first messenger response is that of the hormone adrenaline which interacts with a G-protein coupled cell surface receptor. The interaction of adrenaline with the receptor leads to a cascade of intracellular reactions resulting in the breakdown of glycogen to glucose. This happens to a larger extent in the muscle than the liver. Early experiments carried out in the 1950s by Sutherland and Rall showed that there was an increase in the formation of the enzyme phosphorylase in liver homogenates caused by the presence of adrenaline, and mediated by a heat-stable factor identified as cyclic adenosine monophosphate or cAMP (Rall and Sutherland, 1958).

The cellular response to adrenaline was thought to occur in two stages. In the first stage, the particulate fraction of the liver homogenates produced the heat-stable factor (cAMP) in the presence of adrenaline while in the second stage, this heat-stable factor stimulated the formation of active phosphorylase in the supernatant fractions in which the hormone itself did not have any effect. In a key experiment, Rall and co-workers (Rall *et al.*, 1957) carried out phosphorylase activity assays on whole liver homogenates as well as centrifuged homogenates which removed the particulate fractions. These workers showed that when whole liver homogenates were incubated for ten minutes at 30°C with ATP plus the hormone, there was an increase in the phosphorylase activity in the homogenate preparation. However, when the centrifuged homogenates were incubated under the same conditions there was virtually no phosphorylase activity in the supernatant sample. When they added the particulate fraction remaining after centrifugation to the supernatant sample, the response to the hormone was restored. These results indicated that there was a particulate component involved in the formation of active phosphorylase. This particulate component was later identified as the enzyme adenylyl cyclase.

## **1.2.2 Particulate and soluble adenylyl cyclase enzymes**

### **1.2.2.1 Particulate adenylyl cyclase enzymes**

Membrane-bound adenylyl cyclases are considered to be the main generators of intracellular cAMP in mammals. There are thought to be nine isoforms of adenylyl cyclase enzymes which show tissue-specific expression, and while all isoforms are expressed in the brain, there are substantial differences in the isoforms present in the peripheral tissues (Taussig and Gilman, 1995). These are further characterised into those that are calmodulin-sensitive and those that are calmodulin-insensitive (Brostrom *et al.*, 1977; Westcott *et al.*, 1979; Rosenberg and Storm, 1987). Rosenberg and Storm (1987) showed that 40-60% of the rat brain, and 15% of the rat heart and lung adenylyl cyclases were calmodulin-sensitive. The rat liver and testes showed no detectable calmodulin-sensitive adenylyl cyclase. Adenylyl cyclase purified from the bovine brain was shown to be stimulated by the addition of forskolin and also calcium-calmodulin (Smigel, 1986)

Particulate adenylyl cyclases are sensitive to regulation by the heterotrimeric G-proteins and

the non-physiological compound forskolin (Pfeuffer and Metzger, 1982; Seamon *et al.*, 1981). The enzymes are characterised by the presence of six tandem repeat membrane-spanning domains. There is a short amino-terminal cytoplasmic domain followed by six-transmembrane domains ( $M_1$ ), then a large cytoplasmic domain ( $C_1$ ). This motif is then repeated with a second set of six-transmembrane domains ( $M_2$ ) followed by a carboxy-terminal cytoplasmic domain ( $C_2$ ). The cytoplasmic domains ( $C_1$  and  $C_2$ ) are highly conserved and show a high degree of homology with the catalytic domains of the membrane-bound guanylyl cyclase enzymes so are considered to be the catalytic sites involved in the generation of cyclic nucleotides (Taussig and Gilman, 1995).

### **1.2.2.2 Soluble adenylyl cyclase enzymes**

A manganese ion-sensitive soluble form of adenylyl cyclase (sAC) was first shown to be present in cytosolic fractions of rat testis and it was said to be present in the cytoplasm either unattached or loosely bound to intracellular membranes before it became firmly attached to sperm membranes in later development (Braun and Dods, 1975). Soluble adenylyl cyclase has been detected subsequently and shown to be preferentially expressed in mammalian germ cells (Buck *et al.*, 1999; Jaiswal and Conti, 2001). The sACs are thought to be involved in completing a bicarbonate-induced process involving cAMP and leading to fertilisation of an egg (Okamura *et al.*, 1985, 1991; Garty *et al.*, 1987). Chen and co-workers (2000) used anti-sera raised against the sAC to show the presence of sACs in rat testes, sperm and kidney.

The soluble adenylyl cyclase is structurally and biochemically distinct from the particulate form. The sAC has no membrane domains, is not regulated by G-proteins and is insensitive to forskolin (Forte *et al.*, 1983; Buck *et al.*, 1999; Wuttke *et al.*, 2001). Structurally, the enzyme has two catalytic domains located at the amino terminal, followed by a P-loop and then a Leucine Zipper sequence (Buck *et al.*, 1999). Buck and co-workers (1999) produced the full-length and C-terminal truncated (comprising mainly the catalytic domains) recombinant sAC enzymes and showed that the truncated enzyme exhibited 10-20 fold higher activity compared to the full-length construct suggesting possible autoregulatory processes present in the full-length enzyme. The truncated enzyme was stimulated by bicarbonate suggesting modulation occurs directly via the two catalytic domains. This

sensitivity to bicarbonate has been shown to be present in sAC enzymes of several mammalian species (Garber *et al.*, 1982; Okamura *et al.*, 1985; Chen *et al.*, 2000). The catalytic domains of mammalian sAC are homologous to the catalytic domains of cyanobacterial cyclases and are evolutionarily conserved indicating their importance. Cyanobacterial adenylyl cyclases are stimulated by carbon dioxide to generate cAMP which is involved in processes leading to cell growth and metabolism. Cyanobacteria are thought to have been the predominant life forms present in the pre-Cambrian environment and it has been hypothesised that these bacteria transformed the carbon dioxide-rich atmosphere into an oxygen atmosphere before the emergence of the animal phyla (Ohno, 1997; Kasahara *et al.*, 2001).

### **1.2.3 Signal transduction mechanism for the G-protein coupled receptors involving cAMP**

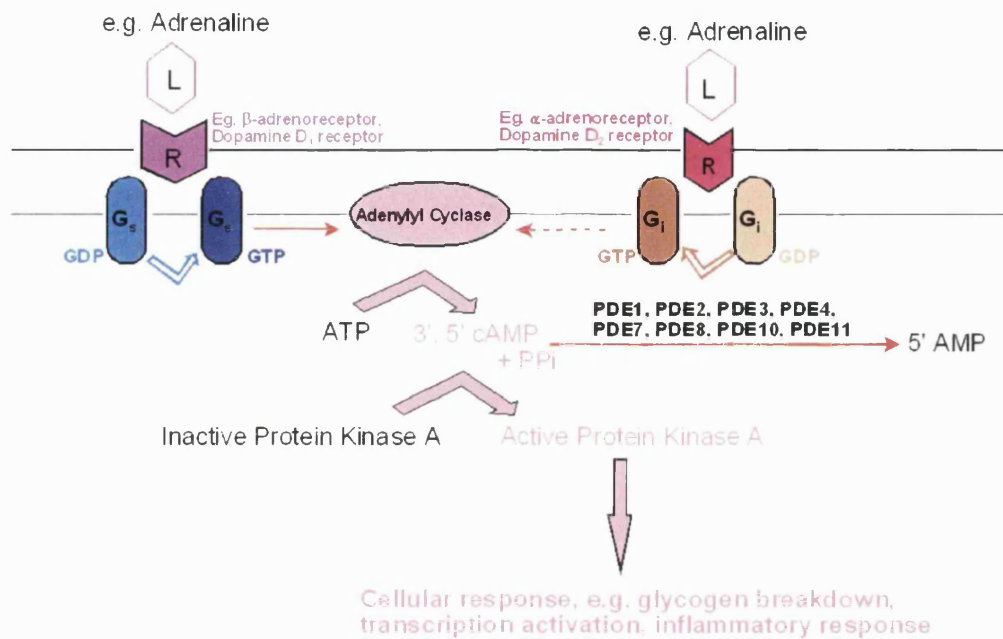
G-protein coupled receptors belong to a family of membrane receptor proteins characterised by the presence of a seven-helix transmembrane motif together with an extracellular amino-terminal portion and an intracellular carboxy-terminal portion. Members of the G-protein coupled receptors include the  $\alpha$ - and  $\beta$ -adrenergic receptors.

The G-proteins are heterotrimeric membrane proteins which bind guanosine diphosphate (GDP) in the unstimulated state. These proteins can be stimulatory ( $G_s$  for  $\beta$ -adrenergic receptors) so that when they are stimulated they go on to activate adenylyl cyclase, or inhibitory G-proteins ( $G_i$  for  $\alpha$ -adrenergic receptors) which will inhibit adenylyl cyclase.

Hormones such as adrenaline bind to the  $\beta$ -adrenergic receptor triggering events leading to the formation of cAMP and the target cellular response. Stimulation of the receptor leads to a conformation change in the receptor which then interacts with the G-protein ( $G_s$ ) located nearby. This stimulates the G-protein leading to the bound GDP to be replaced with GTP giving the active  $G_s$ -GTP complex which in turn activates adenylyl cyclase. Activated adenylyl cyclase forms cAMP from ATP, which activates protein kinase A (PKA) initiating a cascade of intracellular events involving the phosphorylation of proteins leading to the ultimate cellular response (Figure 1.1). G-proteins contain inherent GTPase activity which will slowly hydrolyse the bound GTP thus regulating the hormonal response. The hormonal



response is however mainly regulated by the hydrolysis of cAMP by the cyclic nucleotide phosphodiesterases. Regulation of cAMP levels by the PDEs will be discussed in detail later (see section 1.4).



**Figure 1.1** Simple schematic of the intracellular events following the binding of ligands to  $\alpha$ - and  $\beta$ -adrenoreceptors. Abbreviations: R = Receptor (e.g.  $\beta$ -adrenergic receptor,  $\alpha$ -adrenergic receptor, dopamine receptor or insulin receptor); L = Ligand (e.g. adrenaline or insulin);  $G_s$  = G-stimulatory protein;  $G_i$  = G-inhibitory protein; PDEs = cyclic nucleotide phosphodiesterase enzymes.

(Figure adapted from Matthews and Van Holde, 1990)

The enzyme protein kinase was originally discovered by Fischer and Krebs (1955) and was thought to be the only molecule known to specifically interact with cAMP. Protein kinase A (PKA) is anchored to different regions of the cytosol by A kinase anchoring proteins (AKAPs) where it is thought to be involved with phosphorylating intracellular proteins to initiate cellular processes. Targets for PKA include enzymes as well as transcription factors such as the cAMP response element binding protein (CREB) and cAMP response element modulator (CREM) (Dwarki *et al.*, 1990). Dwarki and co-workers (1990) have shown that the formation of CREB homodimers as well as phosphorylation of CREB by PKA is necessary for the transcriptional activation of a gene. The transcription factor NF- $\kappa$ B is thought to be controlled by cAMP as well as PKA and is involved in the inflammatory response (Carter *et al.*, 1996; Ollivier *et al.*, 1996). cAMP and PKA are also thought to be involved with a variety of nuclear receptors including the steroid hormones. However, the

mechanism involved with these nuclear receptors is unclear (Daniel *et al.*, 1998).

### **1.3 cGMP and guanylyl cyclases**

#### **1.3.1 Discovery of cGMP and guanylyl cyclase**

The molecule guanosine 3', 5' monophosphate (GMP) was detected in the urine sample of rats in the late 1960s (Hardman *et al.*, 1966 and 1969; Ishikawa, 1969). Hardman and Sutherland (1969) then reported the existence of an enzyme system which catalysed the formation of cGMP from GTP in rat tissues. This enzyme system was distinct from the adenylate cyclase system and was called the guanyl cyclase system. These workers showed that although the guanylyl cyclase was found largely in the soluble component of the cell it was also found in the particulate fraction. It differed in tissue distribution from adenylyl cyclase and it was heat-labile. The membrane form of guanylyl cyclase is a single, transmembrane polypeptide chain. The predicted amino acid sequences of the membrane forms of guanylyl cyclase proteins from sea urchin, rat brain and human kidney revealed that the intracellular (catalytic) domains are highly conserved among these species while the extracellular (ligand binding) domain is highly divergent (Singh *et al.*, 1988; Garbers, 1989; Chinkers *et al.*, 1989). Ligands binding to the extracellular domain of these membrane cyclases activate the cyclase directly to form the second messenger cGMP, a process quite distinct from the activation of the particulate forms of adenylyl cyclases which are activated indirectly via G-proteins.

#### **1.3.2 Particulate and soluble guanylyl cyclase enzymes**

##### **1.3.2.1 Particulate guanylyl cyclase enzymes**

The particulate form of guanylyl cyclase belongs to a family of enzymes which comprise of at least four different monomeric isoenzymes: Type A, B, C and P (Bentley and Beavo, 1992). Type A is activated by atrial natriuretic peptide (ANP) (Winqvist *et al.*, 1984; Chinkers *et al.*, 1989, 1991) while type B is activated by ANP and brain natriuretic protein (BNP) but at nonphysiologically high concentrations (Schulz *et al.*, 1989). Type C is found almost exclusively in the epithelium of the gut and is known to be stimulated by the *E. coli*

enterotoxin (Bentley and Beavo, 1992). Type P is a photoreceptor-specific isoform involved in the visual transduction pathway and is activated by the protein recoverin which is a calcium-sensitive protein (Koch and Stryer, 1988; Koch, 1991; Dizhoor *et al.*, 1991).

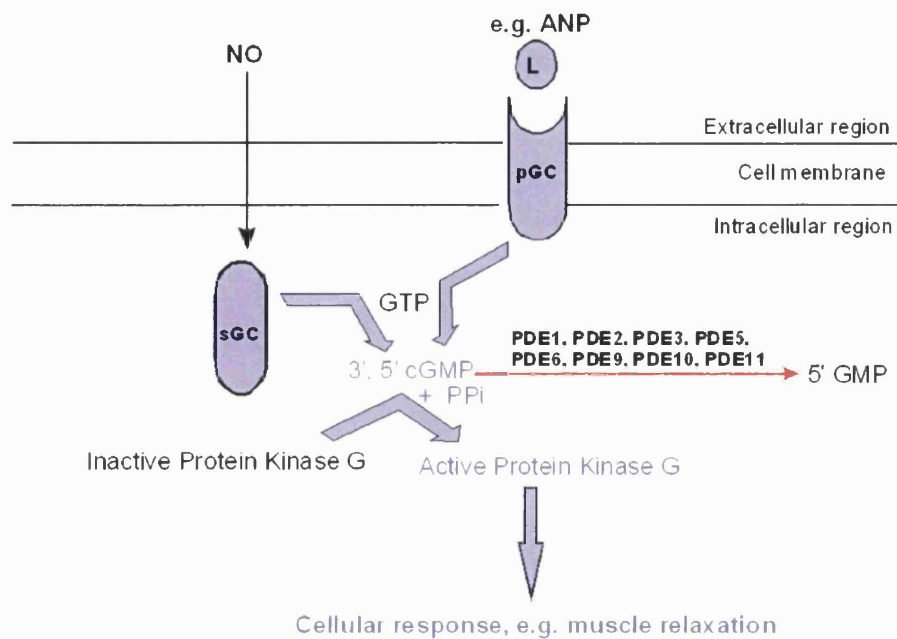
### **1.3.2.2 Soluble guanylyl cyclase enzymes**

Soluble guanylyl cyclases are responsible for the endothelium mediated production of cGMP in the vascular smooth muscle. The enzyme itself is composed of two subunits (a and b) with at least one heme group associated with the enzyme (Stone and Marletta, 1995). The carboxy-terminals of the subunits show considerable homology with the known cytoplasmic catalytic domain of the particulate guanylyl cyclases. The main activator of the soluble guanylyl cyclase is nitric oxide (NO) which is released from nerve endings as a neurotransmitter as well as from vascular endothelial cells (Ignarro *et al.*, 1984, 1989; Maggi *et al.*, 2000).

### **1.3.3 Signal transduction mechanism involving cGMP**

The guanylyl cyclase enzymes are stimulated by a variety of compounds including atrial natriuretic peptides (ANP) and nitrovasodilators such as nitric oxide. The natriuretic peptides bind to the extracellular domain of the membrane forms of monomeric guanylyl cyclases to initiate events leading to natriuresis, diuresis, vasodilation and inhibition of aldosterone secretion (Seidah *et al.*, 1984; Waldman *et al.*, 1984). Nitric oxide released from nerve endings as a neurotransmitter, or vascular endothelial cells, diffuses into smooth muscle cells where it binds to soluble heterodimeric guanylyl cyclases thereby activating these enzymes to ultimately cause muscle relaxation (Figure 1.2). The activated soluble guanylyl cyclases synthesise cGMP from GTP which in turn bind and activate cGMP-dependent protein kinases. These activated kinases then play a key regulatory role leading to muscle relaxation. This action is regulated by the breakdown of cGMP by cGMP-hydrolysing cyclic nucleotide phosphodiesterases (e.g. PDE5). Inhibition of PDE5, for example, will give rise to a prolongation of the muscle relaxation. The much publicised drug sildenafil is thought to act by this mechanism, inhibiting PDE5 in erectile tissue to give the desired effect (Boolell *et al.*, 1996). Other targets for the cGMP-dependent protein kinases include the K<sup>+</sup>- and Ca<sup>2+</sup>- ion channels, myosin light-chain phosphatase and the

inositol triphosphate receptor.



**Figure 1.2** Simple schematic of the intracellular events following the binding of ligands to guanylyl cyclases. Abbreviations used: L = ligand; ANP = Atrial natriuretic protein; NO = nitric oxide; pGC = particulate guanylyl cyclase; sGC = soluble guanylyl cyclase; PDE = cyclic nucleotide phosphodiesterase enzymes

(Figure adapted from Matthews and Van Holde, 1990)

## 1.4 Cyclic nucleotide phosphodiesterase enzymes

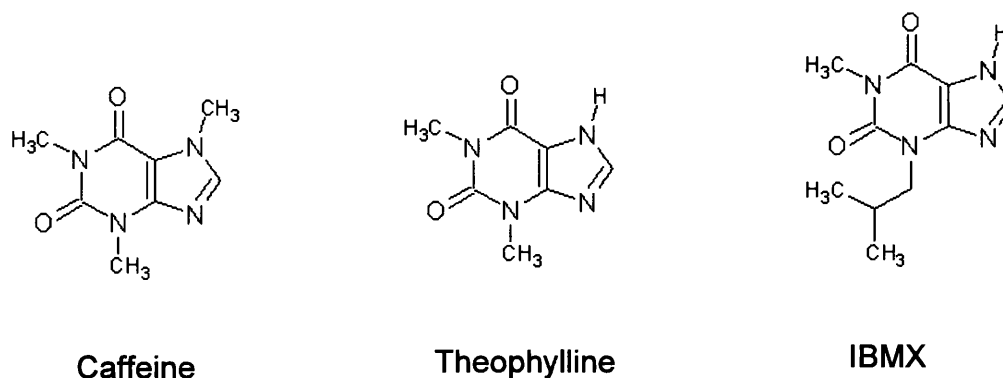
A general introduction to the PDEs will be given in this section which will include the discovery of the enzymes, nomenclature and the general domain organisation of the enzymes. The important features of the amino terminal domain and the catalytic domain will also be discussed which will include a discussion on the recently elucidated atomic structure of the catalytic domain of PDE4B2B by Xu and co-workers (2000). Individual PDE families will be discussed in detail in section 1.6. The PDE1 family will be discussed separately in section 1.7 since this family forms the subject of the present work.

### 1.4.1 Background to cyclic nucleotide phosphodiesterase enzymes

Shortly after the discovery of cAMP and the involvement of adenylyl cyclase enzymes in the generation of cAMP, Sutherland and Rall (1958) showed the presence of cAMP-

hydrolysing activity in the liver. The enzyme involved was designated as cyclic nucleotide phosphodiesterase (PDE). This PDE activity was also shown to be present in the dog heart, brain and liver (Sutherland and Rall, 1958; Butcher and Sutherland, 1962).

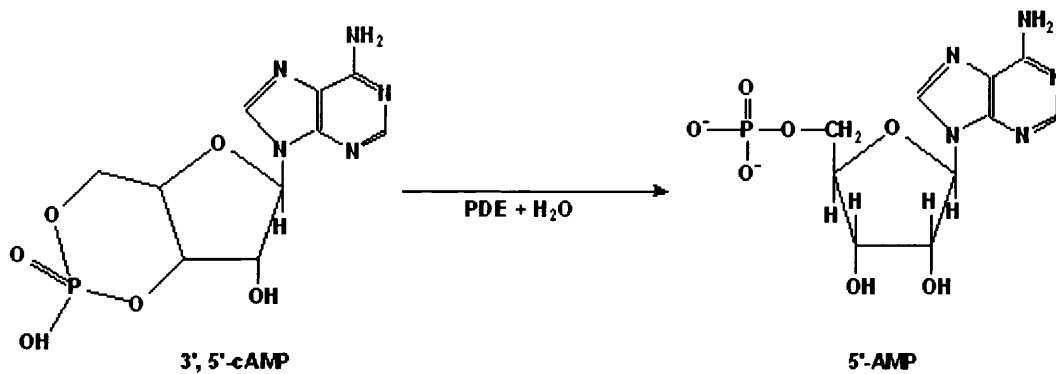
Early purification and characterisation studies showed that cAMP-hydrolysing activity identified by Sutherland and Rall (1958) was inhibited in the presence of caffeine and theophylline, and later by another methylxanthine inhibitor IBMX (Sutherland and Rall, 1958; Butcher and Sutherland, 1962; Hardman and Sutherland, 1969; Ishikawa *et al.*, 1969). This was followed by the discovery that PDE activity from some tissues was stimulated in the presence of calcium and calmodulin. Figure 1.3 shows the structures of the inhibitors used for these early experiments. These xanthine inhibitors are non-selective PDE inhibitors but were the only ones available until the development of more selective inhibitors such as vinpocetine for PDE1 (Hagiwara, 1984) and rolipram for PDE4 (Schwabe *et al.*, 1976).



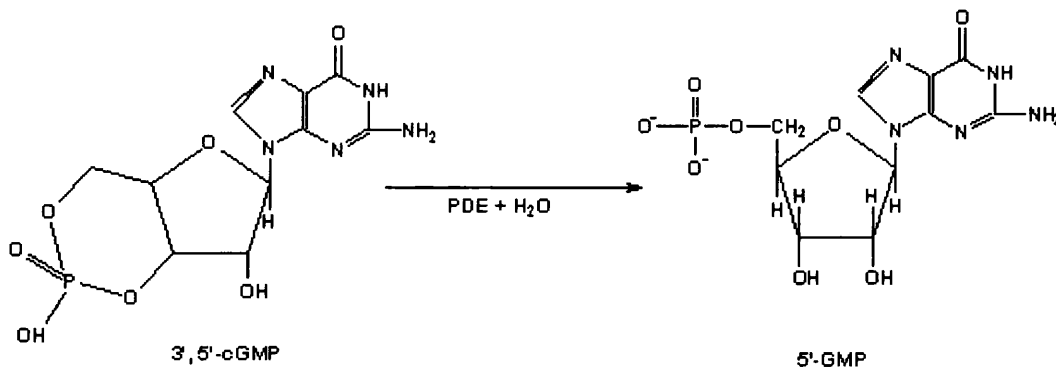
**Figure 1.3** Structures of the non-selective PDE inhibitors. IBMX was used in the present study.

Since the initial observations of cyclic nucleotide hydrolysing activities from mammalian tissues, 11 PDE families have been described so far. These differ in kinetic properties, substrate and inhibitor specificity, tissue distribution as well as primary structure. Cyclic nucleotide phosphodiesterases (PDEs) are a superfamily of intracellular enzymes involved in the hydrolysis of second messengers 3':5'- cyclic nucleotide adenosine monophosphate (cAMP), 3':5'- cyclic nucleotide guanosine monophosphate (cGMP), or both (Figures 1.4 and 1.5 respectively). These second messengers are inactivated by conversion to their corresponding 5'- nucleotide monophosphate products by PDEs which are the sole enzymes

involved in the breakdown of these second messengers. cAMP and cGMP are found in most tissues throughout the body. As discussed earlier (section 1.2 and 1.3), extracellular signals arising from hormones and neurotransmitters modify physiological processes by causing changes in the steady state levels of the second messengers. These intracellular processes are regulated by the rate of production of the second messengers from adenosine triphosphate (ATP) or guanosine triphosphate (GTP) via adenylyl and guanylyl cyclases as well as the degradation of the second messengers by PDEs. PDEs are important in the degradation of the intracellular messengers, and hence the termination of the signalling response.



**Figure 1.4** The hydrolysis of cAMP to the corresponding inactive monophosphate.



**Figure 1.5** The hydrolysis of cGMP to the corresponding inactive monophosphate.

### 1.4.2 Nomenclature

PDEs were initially classified according to their elution profiles from DEAE-cellulose column chromatography using names such as peak I, II, III and IV. Apparent molecular mass on sodium dodecyl sulphate-polyacrylamide gel electrophoresis, substrate preference,

inhibitor specificity and tissue distribution were also used to identify these peaks. A nomenclature system was proposed by Strada in the 1980s (Strada *et al.*, 1984) but it was not widely accepted. Also, regulatory studies and kinetic properties soon revealed that many of the peaks of activity contained multiple isoenzymes and also that the elution profiles from DEAE resins varied with pH and salt concentration used. An alternative nomenclature system was then proposed by Beavo and Reifsnyder (1990) which took into consideration the primary amino acid and cDNA sequence information as well as substrate specificity and any regulatory properties known at the time. Five PDE families were known at that time and these were renamed according to the proposed nomenclature. A descriptive name and a Roman numeral were assigned to each of the five families. The Roman numeral was arbitrary and did not correspond to the DEAE chromatography peaks. This was followed by the subfamily designated by a capital letter followed by the splice variant, assigned an Arabic numeral. Table 1.1 gives an example of this nomenclature for the PDE1 family.

**Table 1.1** Nomenclature of cyclic nucleotide phosphodiesterase Type 1 as proposed by Beavo and Reifsnyder (1990).

FamilySubfamilySplice variant	Description
<b>Ca<sup>2+</sup>-calmodulin-dependent family:</b>	
PDE1A1	59 kDa heart isoenzyme
PDE1A2	61 kDa brain isoenzyme
PDE1B1	63 kDa brain isoenzyme
PDE1C1	67 kDa smooth muscle form
PDE1D1	67 kDa 'Low $K_m$ ' form
PDE1E1	75 kDa brain cGMP-selective form
PDE1F1	75 kDa lung form

As the number of new PDEs discovered increased there was a further need for rationalisation of the nomenclature and classification of the PDE families. This involved the introduction of the identity of the species from which the PDE was isolated and the use of a short name for the PDE enzymes (Beavo *et al.*, 1994). Figure 1.6 shows an example of the proposed new nomenclature scheme. This was the format used for GenBank entries and is the format used to date. Furthermore, entries to the Human Genome Nomenclature

missed out the species since entries were presumed to be of human origin (Figure 1.7).

## HSPDE1A1

Species Gene Family Gene Splice variant

**Figure 1.6** Nomenclature of PDE1 as proposed by Beavo and co-workers (1994).

## PDE1A1

Gene Family Gene Splice variant

**Figure 1.7** Human Genome Project Nomenclature of PDE1.

Table 1.2 summarises the nomenclature of the PDE1 family of enzymes according to the proposal by Beavo and co-workers (1994).

**Table 1.2** Nomenclature of cyclic nucleotide phosphodiesterase Type 1 as proposed by Beavo and co-workers (1994).

New Name	Early Name(s)	Old GenBank Locus
BTPDE1A1	59kDa CaM-PDE	BOVBTPDE1A
BTPDE1A2	61kDa CaM-PDE	BOVCNPA
BTPDE1B1A	63kDa CaM-PDE	BOVCALPHOS
RNPDE1B1B	63kDa CaM-PDE	RATCAMPDE
MMPDE1B1C	63kDa CaM-PDE	MUSPDE1B1
HSPDE1C	70kDa CaM-PDE	HSPDE1C
MMPDE1C	70kDa CaM-PDE	RATPDE12M

BT = *Bos taurus*

RN = *Rattus norvegicus*

MM = *Mus musculus*

HS = *Homo sapiens*

CF = *Canis familiaris*

### 1.4.3 Classification of the PDEs

The superfamily of PDE enzymes are divided into two major classes based on the differences of the primary structure: Class I and Class II. Class I is by far the largest and

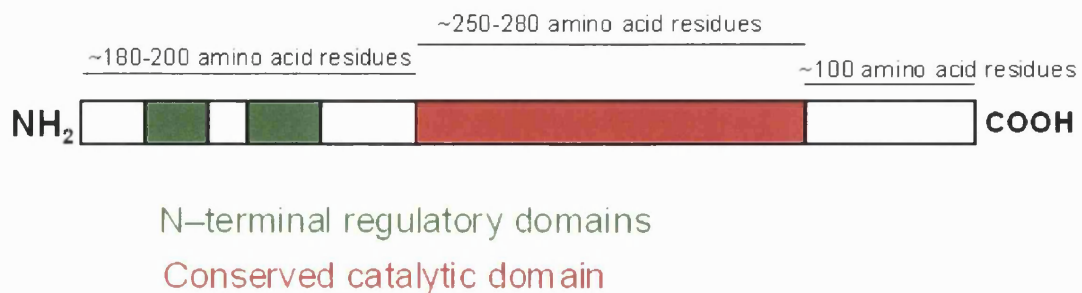


includes all known mammalian PDEs, four freshwater sponge PDEs (PDEs 1 - 4), *Drosophila* PDE, two nematode PDEs (PDE1 and PDE4) and *Saccharomyces cerevisiae* PDE2 gene product. These enzymes all contain a conserved segment of amino acids (~250-300) at the carboxy-terminal corresponding to the catalytic domain. The Class I PDEs are intracellular and can be found in the particulate fraction or the cytoplasmic fraction of the cell.

The second major class of PDE enzymes, Class II, contains only three members. These include *Saccharomyces cerevisiae* PDE1 gene product, a periplasmic PDE from *Vibrio fischeri* and a *Dictyostelium discoideum* PDE found as an extracellular enzyme as well as being associated with the cell membrane. No mammalian PDEs are included in this class. The Class II PDEs do not contain a conserved catalytic domain and also do not show any sequence similarities with Class I PDEs.

#### 1.4.4 General domain organisation

Mammalian PDEs have a common general structure in that they all contain a conserved C-terminal domain comprising of ~270 amino acids corresponding to the catalytic unit, a C-terminal region and a divergent N-terminal region (Figure 1.8). These N-terminal regions form the regulatory domains of the enzymes. For example, in the PDE1 family of enzymes, there are two calmodulin binding domains together with a phosphorylation site within the second calmodulin binding domain located at the N-terminal.



**Figure 1.8** General domain organisation of the PDE families.

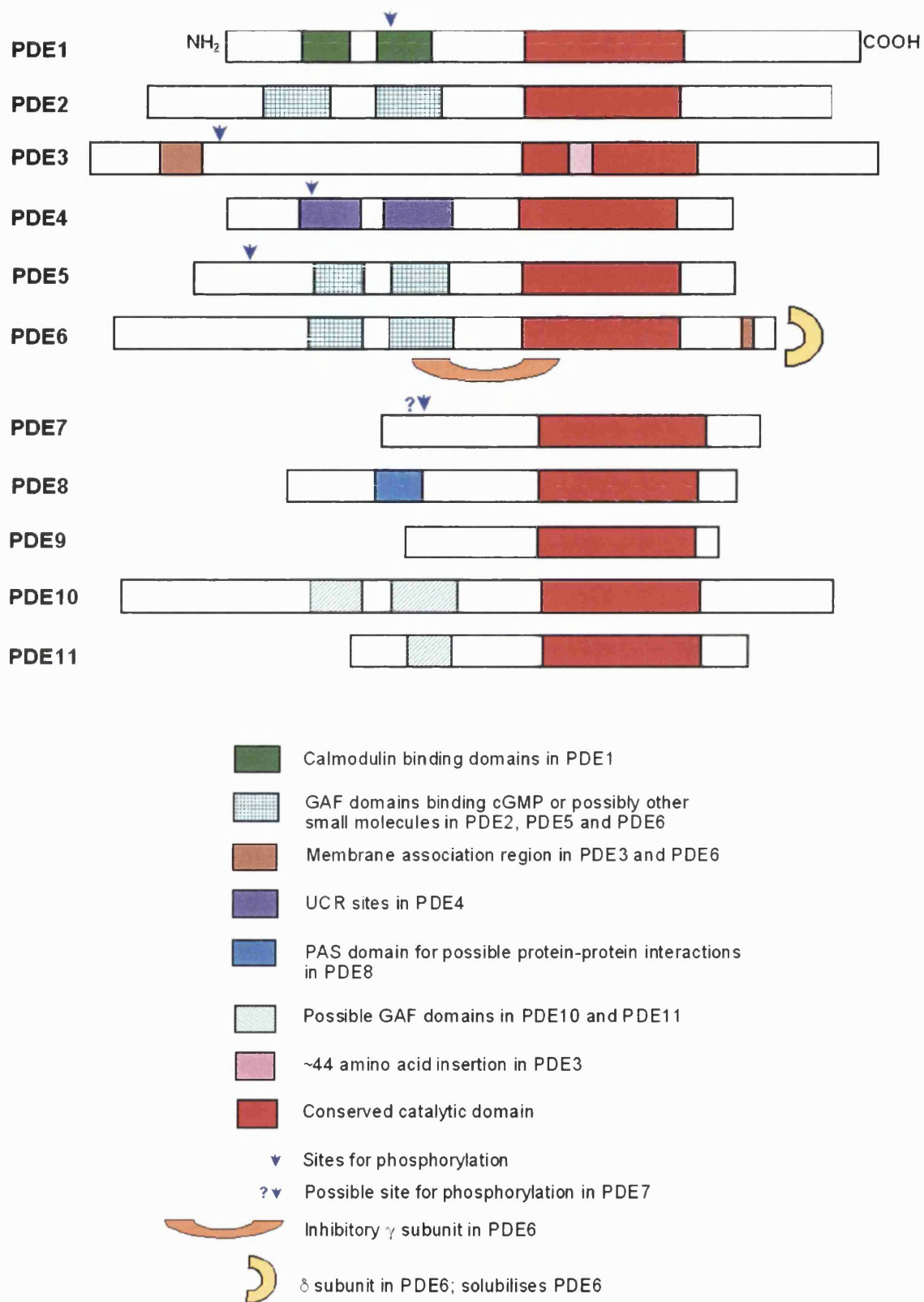
An analysis of the phylogenetic tree constructed for the Class I PDEs has shown that the vertebrate PDEs diverged from a common ancestral gene and that the catalytic domain, the

calmodulin-binding domain, the upstream conserved regions (UCR1 and UCR2 in PDE4) and the allosteric cGMP-binding domains are ancient in origin and this may be an indication as to the importance of these domains (Koyanagi *et al.*, 1998).

#### 1.4.5 N-terminal regulatory domain

The amino terminal of the PDEs is highly divergent and varies in length. Figure 1.9 shows a simplified schematic of the divergent amino-terminals of the eleven PDE families discovered so far. These include distinct domains for calmodulin-binding in the PDE1 family, cGMP-binding in the PDE2, PDE5, PDE6, PDE10 and PDE11 families, upstream conserved regulatory regions (UCR1 and UCR2) in the PDE4 family, phosphorylation sites in the PDE1, PDE3, PDE4 and PDE5 families, and a membrane association region in the PDE3 family. The amino terminals have also been thought to be involved in the sensitivity of the PDEs to certain well known inhibitors like IBMX and rolipram. For example, PDE7 is a rolipram-insensitive isoenzyme while PDE8 and PDE9 are IBMX-insensitive (Fisher *et al.*, 1998a, 1998b; Soderling *et al.*, 1998). All of these PDE families have shortened amino-terminals (Figure 1.9). However, PDE11, also having a shortened amino terminal, is IBMX-sensitive (Fawcett *et al.*, 2000).

There is some data available on the structure of the N-terminal region of the PDE4A1 enzyme. Smith and co-workers (1996) produced a 25-residue peptide representing the membrane targeting N-terminal domain of PDE4A1 and determined its structure using <sup>1</sup>H NMR. Their studies indicated that the peptide formed two independently folding, helical regions separated by a mobile hinge.



**Figure 1.9** Schematic showing divergent amino terminal domains in the PDE family of enzymes. PDE enzymes are not drawn to scale.

Figure adapted from Soderling and Beavo, 2000; Francis *et al.*, 2000a, 2000b; Gardner *et al.*, 2000.

## 1.4.6 Carboxy-terminal region

The carboxy-terminal region immediately follows the catalytic domain. This is a hydrophilic region with several stretches of acidic residues. MAP kinases have been shown to phosphorylate a serine residue located at the C-terminus for PDE4B but this did not show any change in activity so the role of this phosphorylation is unclear (Lenhard *et al.*, 1996). There has been some evidence for the involvement of the C-terminal region in dimerisation and aggregation (Richter *et al.*, 2000). In this report, *in vitro* studies on full-length and truncated constructs of PDE4A indicated that the C-terminal truncated construct formed dimers while the full-length enzyme tended to form larger aggregates of the enzyme.

## 1.4.7 Catalytic domain

### 1.4.7.1 General domain organisation

The region of 250-300 amino acids located at the C-terminal comprises the catalytic domain. Greatest sequence similarity is seen in this region with ~40% homology between the gene families and ~80% homology within a gene family. Experiments carried out using partial proteolysis of PDEs 1, 2 and 3, as well as expression of truncated PDEs 3, 4 and 5, demonstrated that the catalytic activity was indeed located in this region (Kincaid *et al.*, 1985; Charbonneau *et al.*, 1991; Novack *et al.*, 1991; Jin *et al.*, 1992; Jacobitz *et al.*, 1996; Fink *et al.*, 1999).

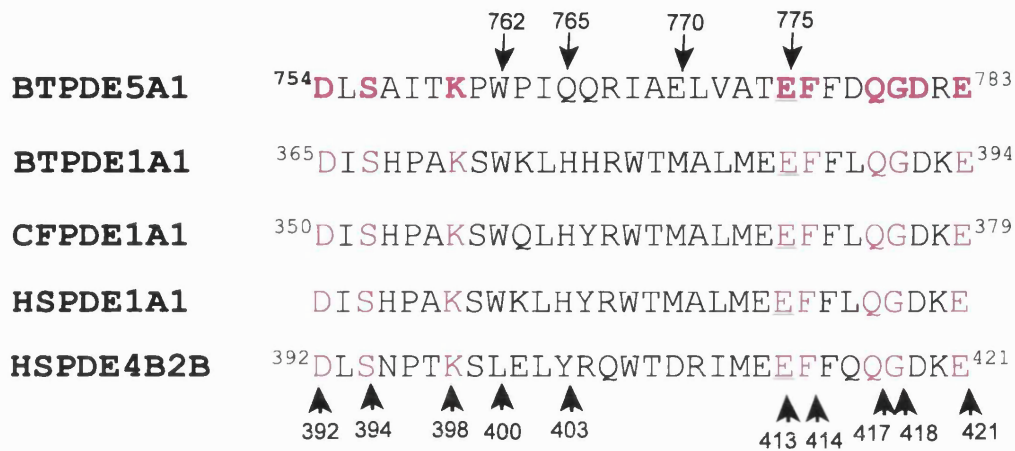
Mammalian PDEs are all thought to be either dimeric or oligomeric proteins. However, studies carried out on monomeric PDE5 gave  $K_m$  and  $IC_{50}$  values close to those of the native PDE5 (Fink *et al.*, 1999). These results therefore indicate that interactions between the two catalytic domains or with the regulatory domains of the dimer are not a pre-requisite for the catalytic process.

### 1.4.7.2 Cyclic nucleotide specificity

The six member phosphodiester ring and the purine moiety of cAMP and cGMP are critical for interaction with the PDEs as other nucleotides (ATP, ADP, GTP, GDP) do not interact

with PDEs. cAMP and cGMP are also resistant to other phosphodiesterases such as intestinal phosphatases. PDEs can be very selective for one or the other of the cyclic nucleotides as with cAMP-specific PDE4, PDE7 and PDE8 which have  $K_m$  values of 1 - 4 $\mu$ M for cAMP while having  $K_m$  values greater than 1000 $\mu$ M for cGMP. PDE5, PDE6 and PDE9 have a preference for cGMP while PDE1, PDE2, PDE3, PDE10 and PDE11 have comparable  $K_m$  values for both cyclic nucleotides. This cyclic nucleotide selectivity of the catalytic domains is determined by interactions between residues or sequence of residues within the catalytic domain and the substrate (Turko *et al.*, 1996; Turko *et al.*, 1998a). Site-directed mutagenesis studies on cGMP-specific PDE5 have revealed a short sequence of ~30 amino acid residues around an invariant glutamic acid (Glu<sup>775</sup>) as being important for substrate specificity (Turko *et al.*, 1996; Turko *et al.*, 1998a). Turko and co-workers (1998a) showed that by replacing residues around this Glu<sup>775</sup> with conserved residues in the corresponding positions of cAMP-specific PDEs, the substrate affinity of the enzyme could be altered (amino acid residues shown in colour in Figure 1.10). They found that when particular residues were mutated, there was a lowering of the PDE5 affinity for cGMP. The most significant effect seen was a substantial reduction in substrate affinity when Glu(E)<sup>775</sup> and Tyr(Y)<sup>602</sup> were replaced with alanine (A). This increased the  $K_m$  for cGMP from 2 $\mu$ M for the wild-type to 70 $\mu$ M for E775A mutation, and 65 $\mu$ M for the Y602A mutation. Their experiments also revealed that by substituting just two residues of the PDE5 enzyme (Trp<sup>762</sup> and Gln<sup>765</sup>) with the residues in the corresponding position of PDE4 (Leu and Tyr respectively), the cGMP/cAMP selectivity could be shifted by ~80-fold in favour of cAMP hydrolysis (Table 1.3, Turko *et al.*, 1998b). Figure 1.10 shows the sequence alignment of the amino acid residues for PDE5A1, PDE4 and PDE1 enzymes corresponding to the section around the invariant Glu<sup>775</sup> for PDE5. It includes the corresponding sequence for the dog heart PDE1A1 (AF252536) used in the present study for comparison. Since this portion of ~30 amino acids is conserved to a large extent between the PDE families, it is possible that site-directed mutagenesis experiments on other PDEs would give similar shifts in substrate affinities. However, further experiments by Francis and co-workers (2000b) revealed that catalytic activity in some of the mutants could be restored by the addition of divalent metal ions and that the results obtained in the mutagenesis experiments apply under the conditions used for these studies (Francis *et al.*, 2000b). Despite this dependence on assay conditions for the mutagenesis experiment results, the importance of the residues shown to be involved in catalysis has been confirmed by the data obtained by Xu and co-

workers following their elucidation of the crystal structure of PDE4B2B catalytic domain (2000). Residues interacting with cAMP are discussed in section 1.4.7.4.4 and are highlighted in Figure 1.14.1.



**Figure 1.10** Amino acid sequence alignment for PDE5, PDE4 and PDE1 enzymes showing conserved residues (shown coloured) around the invariant glutamic acid (shown underlined). The coloured residues in bovine PDE5A1 (bold) represent the residues mutated by Turko and co-workers (1996, 1998a) and shown to be important in cGMP specificity. Positions of the specific amino acids referred to in the text with reference to PDE5 are indicated by the arrows above the PDE5 sequence (W<sup>762</sup>, Q<sup>765</sup>, E<sup>775</sup>). Residues highlighted for HSPDE4B2B (arrow-heads below the sequence) are also highlighted in the ribbon diagram (Figure 1.13.2) of the catalytic domain of PDE4B2B. Sequences shown are BTPDE1A5 (McAllister-Lucas *et al.*, 1993), BTPDE1A1 (Sonnenburg *et al.* 1995), CFPDE1A1 (GenBank Accession number AF252536), HSPDE1A1 (GenBank Accession number AL110263) and HSPDE4B2B (GenBank Accession number L20971).

**Table 1.3** cGMP selectivity of PDE5A1 following site-directed mutagenesis (Turko *et al.*, 1998a, 1998b).

PDE5A1	$K_m$ ( $\mu$ M)	
	cGMP	cAMP
Wild type	2	330
Y602A	65	NT
Y602F	2	NT
T713A	30	NT
D714A	5	NT
E775A	70	NT
E775D	6	NT
A769T/L771R (double mutant)	8	84
W762L/Q765Y (double mutant)	36	77
W762L/Q765Y/A769T/L771R (multiple mutant)	43	67

Simplistic classification of amino acid residues:

Hydrophobic amino acid residues:	Ala, A	Ile, I	Leu, L	Phe, F (aromatic)		
Hydrophilic amino acid residues:	Arg, R	Asp, D	Glu, E	Gln, Q	Lys, K	Tyr, Y (aromatic)
	Thr, T	Trp, W (aromatic)				

Hydropathy analysis was also carried out by Turko and co-workers (1998b) on selected PDEs to compare selected sequences around the invariant Glu<sup>775</sup>. These revealed that the amino acid residues around this Glu<sup>775</sup> in the cGMP-specific PDE enzymes (PDE5 and PDE6) were predominantly hydrophobic while those in the cAMP-specific PDE enzymes (PDE4 and PDE7) were predominantly hydrophilic. PDE enzymes with a dual substrate specificity (PDE1, PDE2 and PDE3) had a mixture of hydrophobic and hydrophilic residues around the invariant Glu. The site directed mutagenesis carried out by Turko and co-workers on PDE5 enzyme altered the hydrophathy profiles such that while the wild-type enzyme contained predominantly hydrophobic residues around the invariant Glu<sup>775</sup>, the mutated enzymes were made progressively more hydrophilic resembling the hydropathy profile of the cAMP-specific PDE4 enzymes. This reflected in the substrate affinities as a shift from cGMP-specificity to equal affinity for both cAMP and cGMP as seen by the  $K_m$  values (Table 1.3).

The recent publication by Xu and co-workers (2000) describing the atomic structure of the catalytic domain of PDE4B2B has provided vital information on the involvement of key

amino acids interacting with cAMP. This will be discussed in a separate section but it is worth noting that the importance of the amino acid residues described as being vital in substrate interactions by Turko and co-workers in their mutagenesis experiments (1998a, 1998b) have been said to be involved with cAMP binding by Xu and co-workers (2000). The stretch of ~30 amino acids around the invariant Glu<sup>413</sup> in PDE4 (equivalent to the invariant Glu<sup>775</sup> in PDE5) are contained within helix 14 of the catalytic domain of the PDE4 structure described. Helix 14 forms part of the deep pocket in the carboxy-subdomain of the catalytic domain and is where the substrate cAMP is accommodated for subsequent hydrolysis by the enzyme. Figure 1.13.1 shows a simple schematic of the subdomain organisation of the catalytic structure described by Xu and co-workers (2000) while Figure 1.13.2 shows the ribbon diagram of the subdomain organisation of the catalytic domain. The position of the amino acids for PDE4B corresponding to the residues mutated in the PDE5 mutagenesis experiments are also highlighted in Figure 1.13.2.

#### 1.4.7.3 Metal binding residues in the catalytic domain

Francis and Corbin (1988) had already shown that bovine PDE5 could be purified using zinc chelate chromatography as part of the purification procedure. Later experiments by these workers showed that zinc bound to PDE5 with a binding coefficient  $K_d$  of ~0.5 $\mu$ M (Francis *et al.*, 1994). This binding of zinc ions, or the PDE5 catalysis in the presence of zinc ions, was not diminished by the presence of high concentrations of other divalent cations - copper, cadmium, calcium or iron. Manganese, cobalt and magnesium were also shown to support catalysis but at much higher concentrations. However, high concentrations (>1.5 $\mu$ M) of zinc ions was inhibitory to the PDE5 activity, a phenomenon noted for other Zn<sup>2+</sup>-dependent enzymes (Murakami *et al.*, 1987; Wang and Cooper, 1993). Divalent metal ions have also been shown to be necessary in the re-folding of denatured, purified recombinant PDE enzymes from *E. coli* inclusion bodies (Richter *et al.*, 2000). In these experiments, the presence of zinc ions was found to be important for the re-folding process allowing PDE4A activity to be dramatically increased. The presence of magnesium ions was found to have a much smaller effect on the PDE activity.

The primary structure of the bovine PDE5, PDE1, PDE2 and *Drosophila* cAMP-specific duncce PDE has been examined for the presence of a zinc-binding motif seen in other zinc



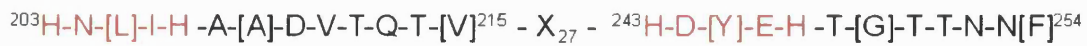
hydrolase enzymes such as bacterial thermolysin enzymes which contain one zinc binding motif (**HX<sub>3</sub>HX<sub>n</sub>E**) (McAllister-Lucas *et al.*, 1993; Vallee and Auld, 1990a, 1990b; Francis *et al.*, 1994). PDEs were found to contain two zinc binding motifs in the catalytic domain with six conserved histidines that are invariant all Class I PDEs. Figure 1.11.1 shows an amino acid alignment of the metal binding motif for the enzyme thermolysin together with the metal binding region for bovine PDE5, bovine PDE1, dog heart PDE1A1, human PDE1A1, human PDE4B2B and human PDE3A enzymes. This particular sequence in the PDEs is followed by a dyad of conserved residues, threonine (T) and aspartic acid (D) (Francis *et al.*, 1994; Turko *et al.*, 1996). Site-directed mutagenesis studies replacing threonine with alanine in PDE5 dramatically alters the cGMP affinity with the  $K_m$  changing from 2 $\mu$ M to 30 $\mu$ M indicating their importance in the catalytic process (Turko *et al.*, 1998a). There is then a stretch of conserved amino acids at the carboxy-terminal of the catalytic domain which are important in substrate binding and catalysis (Figure 1.12). The importance of this stretch of amino acids has already been discussed in section 1.4.7.2 since the invariant Glu is located within this region.

<b>Bacterial Thermolysin</b>		VVAHELTHAVT-X <sub>17</sub> -EISD
<b>BTPDE5A1</b>	<sup>602</sup> <b>YHNWRHX<sub>24</sub></b> EILALLIAALS <b>HDLDH</b> RGVNNX <sub>19</sub> <b>EH<sup>675</sup>HH</b>	
<b>BTPDE1A1</b>	<sup>217</sup> <b>YHNLIHX<sub>24</sub></b> EILAMVFAAAI <b>HDYEH</b> TGTTNX <sub>20</sub> <b>EN<sup>291</sup>HH</b>	
<b>CFPDE1A1</b>	<sup>202</sup> <b>YHNLIHX<sub>24</sub></b> EILAMVFAAAI <b>HDYEH</b> TGTTNX <sub>20</sub> <b>EN<sup>276</sup>HH</b>	
<b>HSPDE1A1</b>	<sup>751</sup> <b>YHNLIHX<sub>24</sub></b> EILAMVFAAAI <b>HDYEH</b> TGTTNX <sub>20</sub> <b>EN<sup>825</sup>HH</b>	
<b>HSPDE4B2B</b>	<sup>233</sup> <b>YHNSLHX<sub>24</sub></b> EILAAIFAAAI <b>HDVDH</b> PGVSNX <sub>20</sub> <b>EN<sup>307</sup>HH</b>	
<b>HSPDE3A</b>	<b>YHNRIHX<sub>x</sub></b> ELMALYVAAAM <b>HDYDH</b> -X <sub>24</sub> - <b>EN<sup>669</sup>HH</b>	

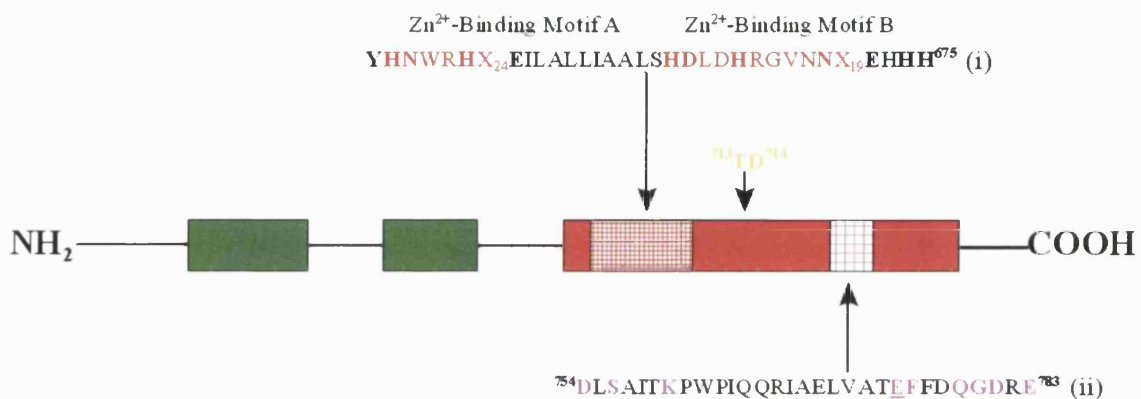
**Figure 1.11.1** Amino acid sequence alignment for thermolysin, PDE5, PDE1, PDE4 and PDE3 enzymes showing the metal binding residues. Residues shown in bold represent the amino acids conserved in all the PDEs. Residues shown in red represent the amino acids involved in metal-binding. Sequences shown are for thermolysin (Vallee and Auld, 1990), BTPDE5A1 (L16545; McAllister-Lucas *et al.*, 1993), BTPDE1A1 (L34069; Sonnenburg *et al.*, 1995), CFPDE1A1 (AF252536; Clapham and Wilderspin, 2001), HSPDE1A1 (AL110263), HSPDE4B2B (AL110263) and HSPDE3A (M91667).

The region of amino acids involved in metal binding represents the signature motif present in all PDE enzymes identified to date (Houslay, 2001). This motif is present in the catalytic domain of the PDE enzymes and is shown in Figure 1.11.2 (upper panel) which also shows

the motif as present in the PDE1A1 enzyme used in the present study (also see Figure 1.14.2).



**Figure 1.11.2** Signature motif in the catalytic domain of PDE enzymes. The upper panel shows the signature motif present in all PDE enzymes while the lower panel shows the motif present in the dog heart PDE1A1 used in the present study.



**Figure 1.12** PDE domains indicating the metal binding motifs within the catalytic domain, the conserved dyad together with the sequence surrounding the invariant glutamic acid residue for PDE5.

**(i) Metal binding domains**

Coloured (red) residues represent the  $Zn^{2+}$ -binding motifs in the PDE family. Bold residues represent the amino acids that are identical in all the PDEs

**(ii) Sequence surrounding the invariant glutamic acid**

Coloured (magenta) residues represent amino acids mutated in the mutagenesis experiments carried out by Turko and co-workers (1998a, 1998b). Underlined glutamic acid represents the invariant Glu<sup>775</sup> in BTPDE5A1 shown to be critical in cGMP binding.

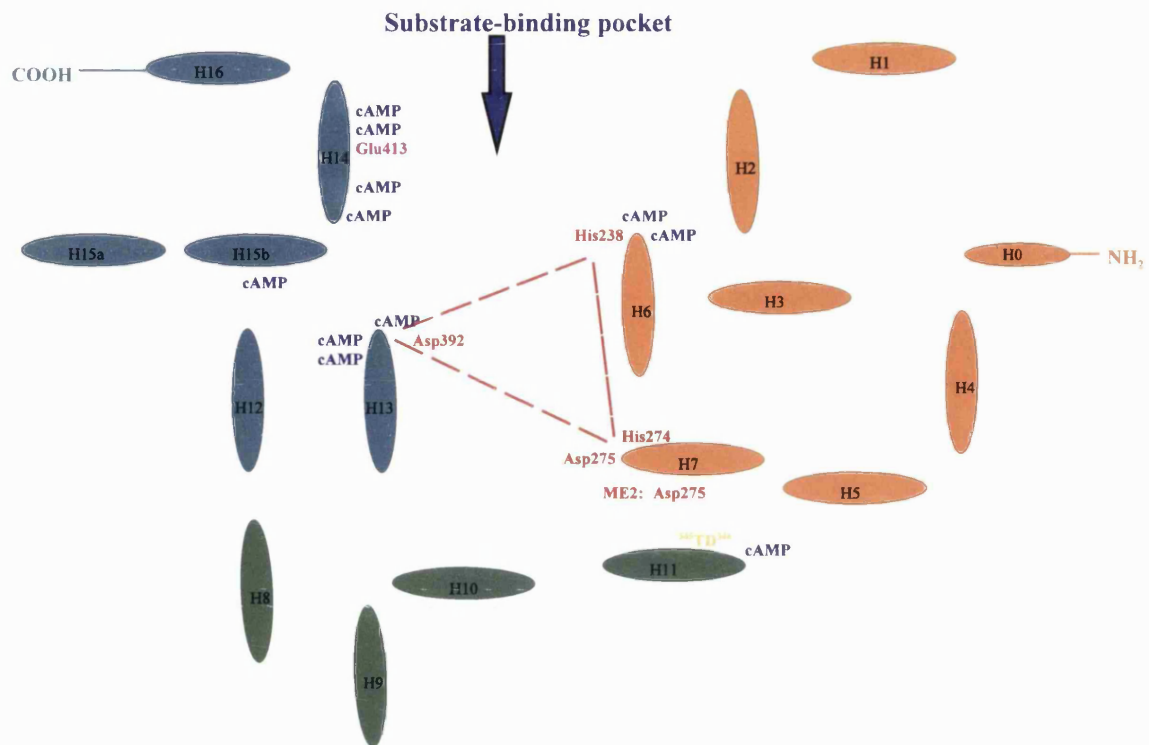
#### 1.4.7.4 Structural features of the HSPDE4B2B catalytic domain




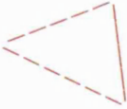
The recent elucidation of the crystal structure of the catalytic domain of HSPDE4B2B (residues 152 to 489) has been important in the understanding of the catalytic process of the hydrolysis of cAMP (Xu *et al.*, 2000). As already stated, it has provided critical

information of the involvement of conserved residues deep in the catalytic pocket which interact with metal ions as well as cAMP. Electron density maps indicated that ME1 (metal ion one) has high occupancy and interacts with His<sup>238</sup>, His<sup>274</sup>, Asp<sup>275</sup> and Asp<sup>392</sup> in a trigonal bipyramid configuration. A solvent molecule acts as a bridging ligand to ME2 (metal ion two) which interacts with Asp<sup>275</sup> (see Figure 1.13.2 (b)).

The identity of the first metal ion (ME1) is thought to be zinc while that of the second metal ion (ME2) as magnesium. The importance of zinc ions for catalytic activity had already been suggested as being crucial (Francis and Corbin, 1988) and shown to be important for PDE4 enzymes (Londesborough, 1985) and PDE5 enzymes (Richter *et al.*, 2000).

The structure of PDE4B2B catalytic domain comprises of 17  $\alpha$ -helices which form three distinct subdomains: amino terminal subdomain (residues 152-274), middle subdomain (residues 275-347) and carboxy terminal subdomain (residues 348- 489). Salient features of these domains are discussed separately in the next section. Figure 1.13.1 shows a very simplistic overview of the subdomains while Figure 1.13.2 (a) shows a ribbon diagram of the catalytic domain of PDE4B2B (Xu *et al.*, 2000) with cAMP located within the substrate binding pocket. The position of the two metal ions (ME1, Zn<sup>2+</sup> and ME2, Mg<sup>2+</sup>) together with the amino acid residues thought to interact with the substrate are also highlighted in the figure. Figure 1.13.2 (b) shows the substrate binding pocket in detail.



- H0 to H16**  $\alpha$  Helices 0 to 16
-  Amino-terminal domain (residues 152 - 274)
-  Middle subdomain (residues 275 - 347)
-  Carboxy-terminal subdomain (residues 348 - 489)
-  Metal ion (ME1) co-ordination triangle
- cAMP** cAMP substrate contacts with amino acid residues within the catalytic pocket.
- Glu413** Glutamic acid residue 413 (equivalent to the invariant Glu<sup>775</sup> of PDE5)
- <sup>345</sup>TD<sup>346</sup>** Conserved diad, threonine and aspartic acid

**Figure 1.13.1** Schematic of the subdomain organisation of the catalytic domain of the PDE4B2B.

Diagram adapted from Xu *et al.*, 2000.

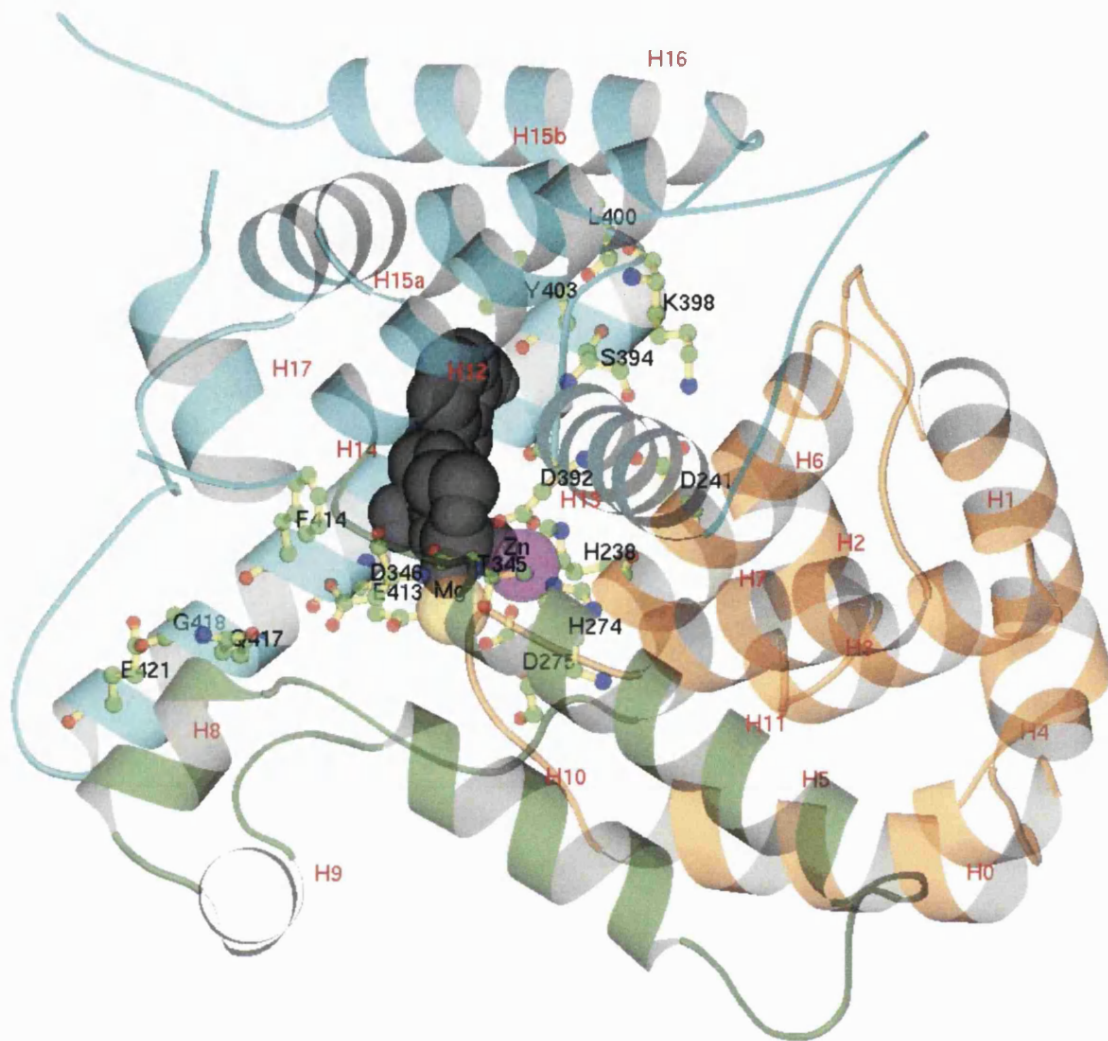
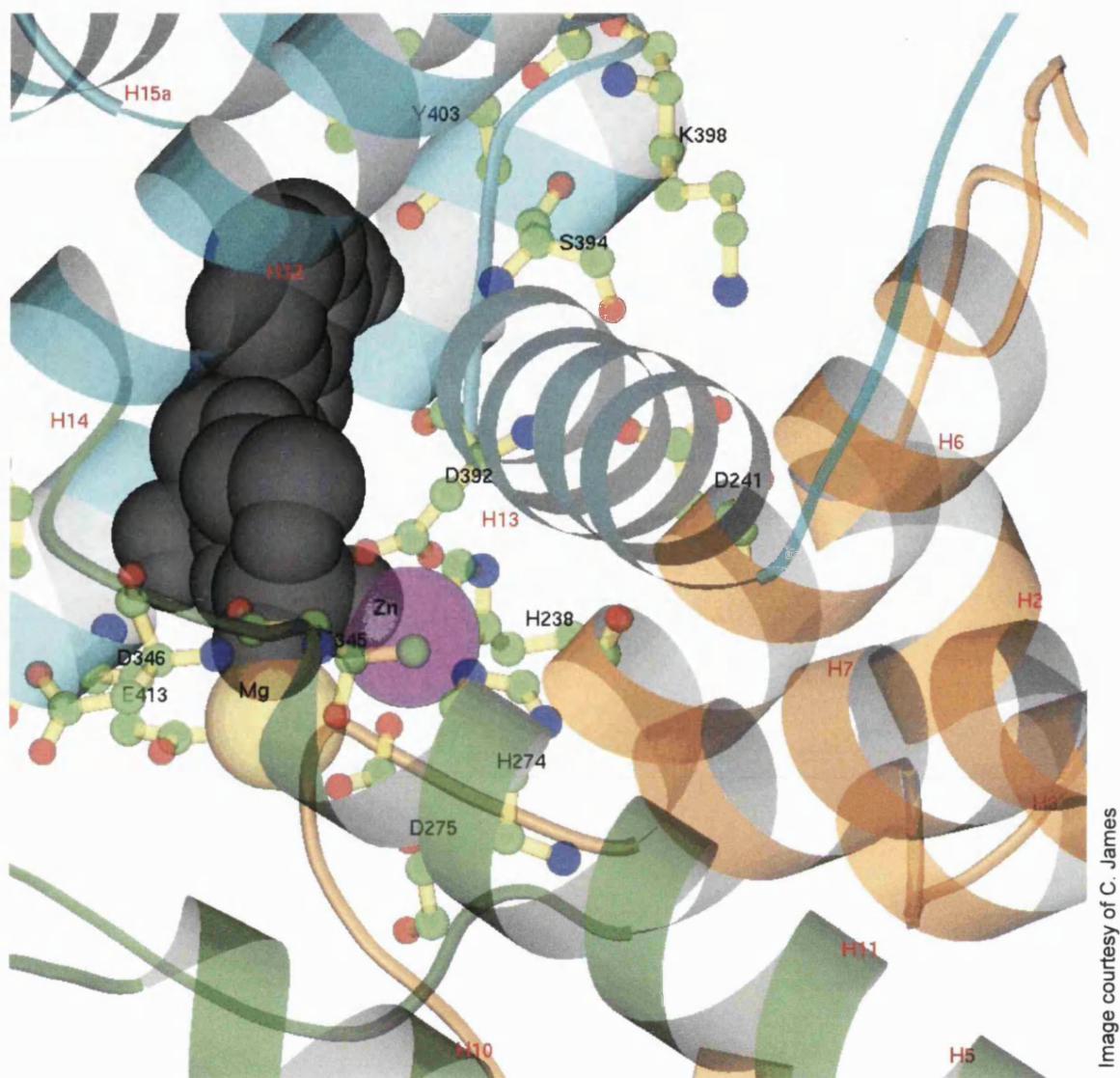


Image courtesy of C. James

**Figure 1.13.2 (a)** Ribbon diagram of the catalytic domain of PDE4B2B with cAMP in the substrate binding pocket. cAMP is shown in grey within the substrate binding pocket. The position of the amino acids shown to be important in substrate binding in PDE5 by Turko and co-workers (1998a, 1998b) are indicated in the equivalent positions for PDE4 (see Figure 1.10). Amino acid residues involved with interactions with the two metal ions are also highlighted (see Figure 1.11.1). See section 1.4.7.3 for details on these interactions.

Figure adapted from Xu *et al.*, 2000.



**Figure 1.13.2 (b)** Ribbon diagram showing detail of the catalytic domain of PDE4B2B with cAMP in the substrate binding pocket.

#### 1.4.7.4.1 Amino terminal subdomain

The amino terminal subdomain (NH<sub>2</sub>-subdomain) comprises of four  $\alpha$  helices (H3, H5, H6 and H7) with smaller interconnecting  $\alpha$  helices (H2 and H4). This subdomain also contains two additional  $\alpha$  helices (H0 and H1) which are not considered to be an essential part of the catalytic domain and the residues are poorly conserved across the PDE family.

The first of the two zinc-binding motifs (**HNSLH**) is located in H6 of the NH<sub>2</sub>-subdomain (residues 234- 238) while the second zinc-binding motif (**HDVDH**) is located between H7 and H8 (residues 274-278). Zinc ion (corresponding to the first metal ion, ME1) is thought to co-ordinate the residues histidine<sup>238</sup> (in H6), histidine<sup>274</sup> (in H7), aspartic acid<sup>275</sup> (in H7) and aspartic acid<sup>392</sup> (in H13) in a trigonal bipyramid fashion. A solvent ion is thought to act as a bridging ligand to the second metal ion (ME2). The identity of ME2 is less certain but is thought to be either manganese or magnesium ion. ME2 makes only one direct contact within the catalytic domain and this is with aspartic acid (Asp<sup>275</sup>).

#### 1.4.7.4.2 Middle subdomain

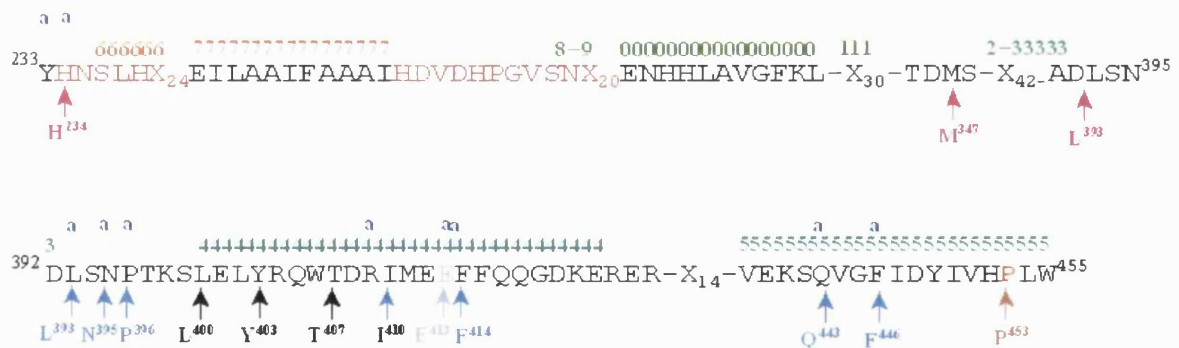
The middle subdomain comprises of two short  $\alpha$  helices (H8 and H9) which sit perpendicular to a pair of antiparallel  $\alpha$  helices (H10 and H11). H11 contains the conserved diad, threonine (Thr<sup>345</sup>) and aspartic acid (Asp<sup>346</sup>) shown to be important in substrate binding for PDE5 (<sup>713</sup>TD<sup>714</sup>) (Francis *et al.*, 1994; Turko *et al.*, 1996).

#### 1.4.7.4.3 Carboxy terminal subdomain

The third subdomain, carboxy terminal subdomain, is formed by five  $\alpha$  helices (H12 to H16) together with an extended loop forming a  $\beta$  hairpin between H12 and H13. Helix 15 contains a proline residue (Pro<sup>453</sup>) thought to give this region a kink so that this helix is designated H15a and H15b. It has been postulated that without this Pro<sup>453</sup>, H15 would be a continuous helix. ME1 is thought to co-ordinate with an aspartic acid residue (Asp<sup>392</sup>) in H13 as part of the trigonal bipyramid association. H14 contains the invariant glutamic acid (Glu<sup>413</sup> corresponding to the invariant Glu<sup>775</sup> in PDE5) residue conserved in the PDE family.

#### 1.4.7.4.4 Substrate-binding pocket

Xu and co-workers (2000) have proposed a model for the binding of cAMP within the catalytic site based on their data derived from the crystal structure. There is a deep pocket within the carboxy terminal subdomain big enough to house cAMP as well as the 5' AMP product. Metal ions also form a co-ordination triangle across this region (see Figure 1.13.1). Several key and conserved amino acid residues shown to be important for the catalytic process by mutagenesis studies are contained within subdomains lining this pocket (see sections 1.4.7.2 and 1.4.7.3). Figure 1.14.1 shows the residues involved in substrate binding and metal ion co-ordination for PDE4B2B. Molecular docking procedures used by Xu and co-workers (2000) showed that cAMP preferred the anti conformation with the adenine base docking in the lipophilic pocket lined with the residues Leu<sup>393</sup>, Pro<sup>396</sup>, Ile<sup>410</sup>, Phe<sup>414</sup> and Phe<sup>446</sup>. The cyclic phosphate group binds to the two metal ions (ME1 and ME2) while the ribose ring loosely interacts with Met<sup>347</sup>, Leu<sup>393</sup> and His<sup>234</sup>. All of these interactions are with amino acid residues located in the helices H6, H7, H12, H13, H14 and H15 which line the catalytic pocket with the most interactions occurring with residues located within H14 (see Figures 1.14.1 and 1.14.2).



**Figure 1.14.1** Amino acid residues associated with cAMP binding for PDE4B2B catalytic pocket. Amino terminal subdomain helices (H0 to H7); Middle subdomain helices (H8 to H11); Carboxy terminal subdomain helices (H12 to H16); Metal-binding motifs; a = cAMP; Residues thought to be important for cAMP binding (shown in black, ↑); Residues involved with interactions with the adenine base (↑), cyclic phosphate group (↑) and the ribose ring (↑) of cAMP; Proline residue thought to be responsible for the kink in H5 (P<sup>453</sup>); Invariant glutamic acid (E<sup>413</sup>).

Figure adapted from Xu *et al.*, 2000.



#### **1.4.7.5 Amino acid sequence alignment to compare PDE4B2B and PDE1A1 catalytic domains**

The catalytic domains of the PDE family are approximately 40 - 80% homologous and there are several key residues within this region which are conserved in all the PDE families (see section 1.4.7). A comparison of the amino acid residues for PDE4B2B and PDE1A1 (used in the present study) was carried out by generating a sequence alignment to show overlapping catalytic domain residues for both enzymes using the ClustalX program. The sequence alignment generated is shown in Figure 1.14.2. The subdomain helices (H0 to H17) for PDE4B2B, as determined by Xu and co-workers (2000), are marked above the PDE4B2B sequence. Amino acid residues thought to interact with cAMP and the metal ions are also indicated on this alignment (below the sequence alignment). The alignment highlights the regions of conserved amino acids involved in substrate binding and metal ion interactions discussed in sections 1.4.7.2 and 1.4.7.3 respectively.



secretion is thought to be mediated by PDE3B and leptin (Snyder, 1999; Kitamura *et al.*, 1999). The PDE7 family of enzymes are thought to be involved in the regulation of T-cells whereby induction of T-cells have been shown to up-regulate PDE7 which is thought to be a prerequisite for T-cell proliferation (Li *et al.*, 1999). PDE3A in platelets and PDE4 in the lungs are also involved in the regulatory processes of the inflammatory cells.

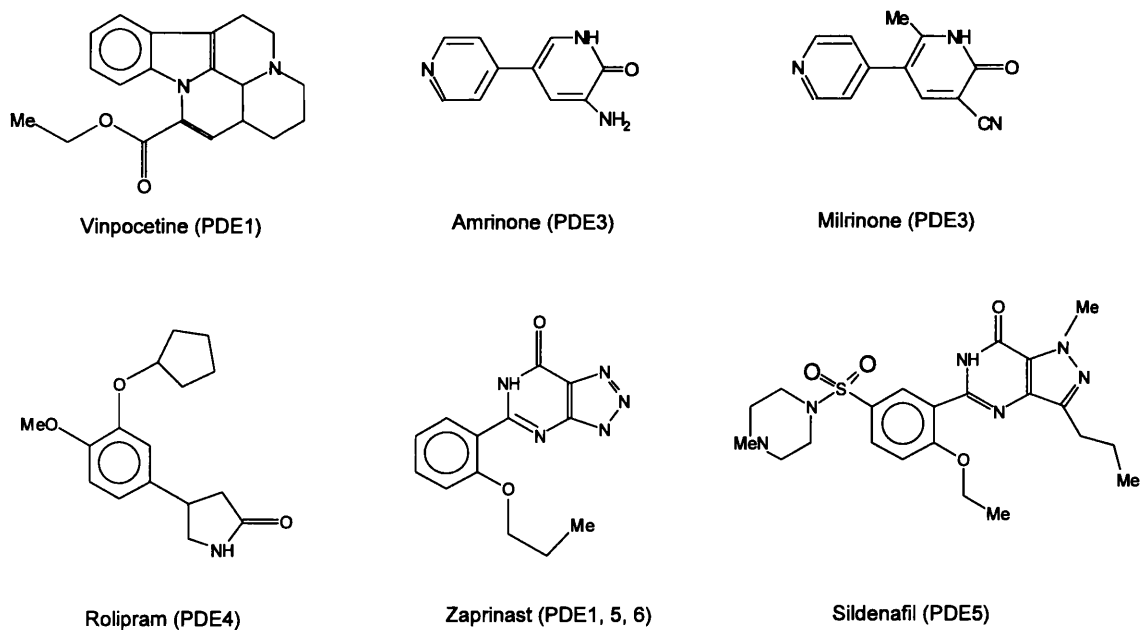
PDEs have been implicated in diseases such as leukemia, Alzheimer's, asthma and erectile dysfunction. For example, PDE1B1 and PDE4 were both shown to be present in the cytosolic extracts of human lymphoblastoid B-cell line established from a patient with acute lymphocytic leukemia (ALL) (Jiang *et al.*, 1996; Ogawa *et al.*, 2002). In these lymphocytes, cAMP has been shown to induce apoptotic cell death. Inhibition of PDE1 by vinpocetine, and PDE4 by rolipram were shown to induce apoptosis in the lymphoblastoid B-cells at concentrations of  $\geq 40\mu\text{M}$  and  $\geq 10\mu\text{M}$  respectively (Jiang *et al.*, 1996). Targeting PDEs is therefore a novel therapeutic strategy for the treatment of leukemia. The success of the PDE5 inhibitor, sildenafil, in the treatment of male erectile dysfunction is well known (Boolell *et al.*, 1996). Another area of intense research has been the investigation of potential PDE4 inhibitors in the treatment of asthma and chronic obstructive airway disease (COAD). Inflammation is thought to be the underlying factor in both these diseases. PDE4 inhibitors have been shown to be effective in the inhibition of the release of inflammatory mediators from inflammatory cells and hence arrest the inflammatory progression in both asthma and COAD. They also cause bronchodilation so their dual action is of benefit in diseases such as asthma for which long term use of inhaled and oral steroids, together with  $\beta$ -agonists, are usually necessary to control the shortness of breath seen in asthma sufferers. Although there are no PDE4 inhibitors for the treatment of asthma or COAD in clinical use at present, there are promising clinical trial results for the drugs roflumilast and cilomilast which are PDE4 inhibitors investigated for use in asthma (Bundschuh *et al.*, 2001; Compton *et al.*, 2001). Figure 1.15.2 shows the structures of some of the PDE4-selective inhibitors for which clinical efficacy data in inflammatory diseases has been reported.

PDE inhibitors have been used as one of the features in the classification of PDEs into their respective families. Table 1.4 shows a summary of some of the PDE family-specific inhibitors used in the assignment of PDEs to their families while Figure 1.15.1 shows the

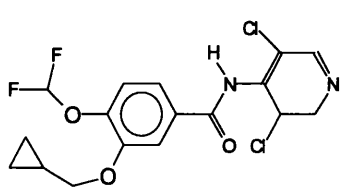
structures of some of these inhibitors. These inhibitors were also used in the present study as part of the characterisation of the recombinant dog heart PDE1A1. Specific inhibitors for the newly discovered PDEs (PDE7 -PDE11) have not yet been reported.

**Table 1.4** PDE Family-specific inhibitors.

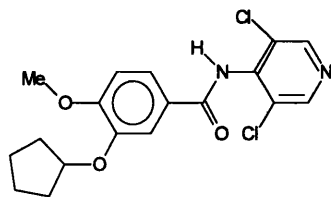
PDE Family	Inhibitor(s)
PDE1	Vinpocetine, zaprinast, 8-MOMX
PDE2	EHNA
PDE3	Amrinone, milrinone
PDE4	Rolipram
PDE5	Zaprinast, sildenafil
PDE6	Zaprinast



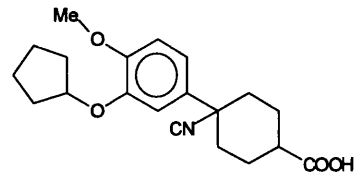
**Figure 1.15.1** Structures of selective PDE inhibitors. Vinpocetine, amrinone, rolipram and zaprinast were used in the present study.



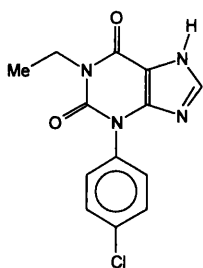
Roflumilast (Byk Gulden)



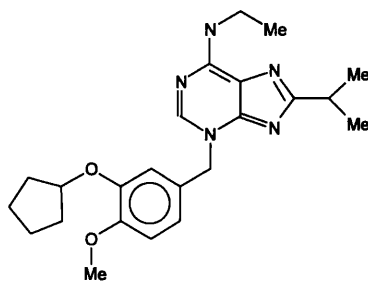
Piclamilast (RPR)



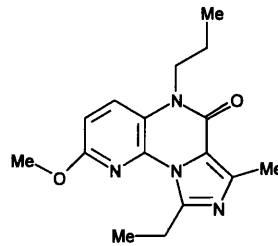
Ariflo (SKB)



Arofyline (Almirall)



V-11294A (Napp/Purdue Pharma)



D-22888 (AstraZeneca)

Figure 1.15.2 Structures of PDE4-selective inhibitors undergoing clinical development.

## 1.6 Cyclic nucleotide phosphodiesterase families in detail

The 11 PDE families known to date will be discussed in detail in this section. These families have been grouped into three main sections for ease of discussion: cAMP hydrolysing, cGMP hydrolysing/modulated and the dual substrate hydrolysing PDEs. The PDE1 family, however, will be discussed separately in section 1.7. Table 1.5 provides an overview of the PDE families together with any known unique N-terminal domain features (see Figure 1.9).

**Table 1.5** Overview of the PDE families.

<b>PDE family</b>	<b>Description</b>	<b>Genes</b>	<b>Unique N-terminal features</b>
<b>cAMP hydrolysing PDEs</b>			
PDE4	cAMP-specific PDE	4A, B, C, D	UCR
PDE7	cAMP-specific, rolipram-insensitive PDE	7A, B	
PDE8	cAMP-specific, IBMX-insensitive PDE	8A, B	PAS
<b>cGMP modulated/hydrolysing PDE enzymes containing GAF domains</b>			
PDE2	cGMP-stimulated PDE	2A	GAF
PDE5	cGMP-specific PDE	5A	GAF
PDE6	cGMP-specific photoreceptor PDE	6A, B, C	GAF
<b>cGMP-specific PDE enzymes without GAF domains</b>			
PDE9	cGMP-specific PDE	9A	
<b>cAMP and cGMP hydrolysing PDEs</b>			
PDE1	Calcium/calmodulin stimulated PDE	1A, B, C	CaM
PDE3	cGMP-inhibited PDE	3A, B	Membrane association
PDE10	cAMP and cGMP-specific PDE	10A	GAF
PDE11	cAMP and cGMP-specific PDE	11A	GAF

Abbreviations: GAF = cGMP binding sites  
 UCR = Upstream conserved regions  
 PAS = Protein-protein interaction sites  
 CaM = Ca<sup>2+</sup>/calmodulin binding site

Table adapted from Houslay, 2001; Francis *et al.*, 2000a.

## 1.6.1 cAMP hydrolysing PDEs

This family of enzymes is characterised by their high affinity for cAMP with  $K_m$  values ranging from 0.06 $\mu$ M to 3 $\mu$ M. It includes the families PDE4, PDE7 and PDE8 which are discussed below. The PDE4 family has been the focus of interest as a potential therapeutic target for inflammatory diseases such as asthma, and there is a wealth of information regarding regulation of this family of enzymes. As such, this family will be discussed in detail.

### 1.6.1.1 cAMP-specific, PDE4 family

#### 1.6.1.1.1 Background to the PDE4 enzymes

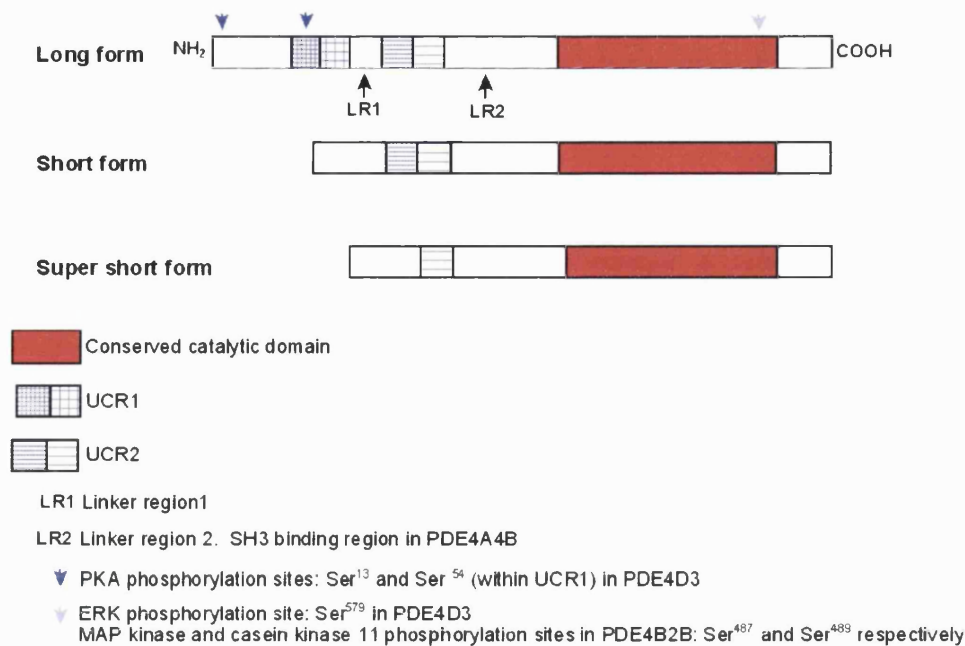
The fruit fly *Drosophila melanogaster* has been used as a model for many years to study the processes involved in learning and memory. Mutant flies defective in these processes were generated in the early studies and the mutant dunce was one of the first to be isolated and studied in detail (Dudai *et al.*, 1976). These dunce mutants showed a defective memory of the learned information and the female flies also exhibited sterility (Byers, 1981). The latter phenotype of sterility was not studied in as much detail but there has been one recent study where PDE4 gene knockout mice were created and the female mice lacking the PDE4D isoform exhibited fertility impairments (Jin *et al.*, 1999). In the case of the defective memory phenotype displayed in the dunce mutants, it was postulated that the dunce<sup>+</sup> (*dnc*<sup>+</sup>) gene product played a central role in the biochemical processes underlying conditioned behaviour in the flies, particularly the involvement of cAMP (Dudai, 1983; Tempel *et al.*, 1983). Molecular analysis of the *dnc*<sup>+</sup> gene revealed that the gene encoded the cAMP phosphodiesterases (PDE4) (Chen *et al.*, 1986). Davis and co-workers (1989) used a probe representing the *Drosophila dnc*<sup>+</sup> gene to explore homologous sequences in mammals and identified a sequence in the rat naming it ratdnc-1 (RD1). Since these early studies, several PDE4 isoforms have been identified in mammalian species (Houslay, 2001).

### 1.6.1.1.2 Domain organisation of PDE4 enzymes

The PDE4 family is described as the cAMP-specific PDE having  $K_m$  for cAMP hydrolysis of  $\sim 1\mu\text{M}$  while having a  $K_m$  for cGMP of  $>50\mu\text{M}$ . It is potently inhibited by the antidepressant rolipram. The enzymes are encoded for by four different genes: PDE4A, PDE4B, PDE4C and PDE4D. Each of these genes also encode more than one splice variant giving rise to at least 15 proteins or PDE4 isoforms with different molecular weights and properties. These isoenzymes arise from alternate 5' mRNA splicing or alternative transcription start sites such that there are differences in the N-terminal portions of the enzymes which determine, for example, cellular localisation (Burns *et al.*, 1996).

PDE4A1 was the first PDE4 isoenzyme to be cloned (Davis *et al.*, 1989). Shortly after this, Bolger and co-workers (1993, 1996) showed the presence of two regions of homology located at the N-terminal portion of the enzymes designated as UCR1 and UCR2 for upstream conserved regions 1 and 2. The presence of these UCRs allowed further classification of the PDE4 enzymes into long, short and super short forms of PDE4 enzymes. UCR1 is linked to UCR2 by a linker region (LR1), and UCR2 is linked to the catalytic domain by a second linker region (LR2) (Lim *et al.*, 1999; Beard *et al.*, 2000). Figure 1.16 shows a schematic of the PDE4 isoforms. Mutagenesis studies by Beard and co-workers (2000) have shown that the carboxy terminal of UCR1 interacts with the amino terminal region of UCR2. UCR1 is divided into two domains with the N-terminal portion containing a protein kinase A (PKA) phosphorylation site (**RRES**<sup>54</sup> motif) and the C-terminal portion interacting with UCR2. UCR2 itself is also thought to be divided into domains with the N-terminal domain being important for interactions with UCR1 (Sette and Conti, 1996; Houslay *et al.*, 1998). The long and short isoforms have also been associated with different subcellular compartments (Jin *et al.*, 1998). Jin and co-workers (1998) recovered PDE4D4 (long isoform) mostly from the particulate fraction, PDE4D3 (long isoform) from both the soluble and particulate fractions while PDE4D2 (super short isoform) was only recovered from the soluble fraction suggesting a role for the N-terminal domains in cellular targeting.





**Figure 1.16** Schematic of the domain organisation of the PDE4 enzymes.

Diagram adapted from Houslay (2001).

McPhee and co-workers (1999) have identified a proline- and arginine-rich stretch of amino acids located within LR2 of PDE4A4B (long isoform) corresponding to an SH3 binding domain which allows for interactions with proteins containing SH3 domains. SH3 domains are found in many proteins including cytoskeletal proteins and signal transducing proteins such as SRC family tyrosyl kinases (Pawson and Scott, 1997). The interaction between LR2 of PDE4A4B and SH3 domain of tyrosyl kinase was shown to cause a marked change in the sensitivity of the PDE4 enzyme to rolipram such that it mimicked the enhanced rolipram inhibition seen for the particulate enzyme (McPhee *et al.*, 1999). Interaction between PDE4 SH3-binding domain with tyrosyl kinase has also been shown to occur with PDE4A5 which is also a long PDE4 isoform (Huston *et al.*, 2000).

The rat PDE4A5 is usually found in both the particulate and cytosol fractions of a cell. This isoform has been shown to interact with SH3-domain expressing proteins by virtue of its unique N-terminal region which is rich in proline and arginine residues (PxxPxxR motif). The presence of these residues is thought to be characteristic of proteins able to interact with SH3 domains (O'Connell *et al.*, 1996; Beard *et al.*, 1999). PDE4A5 was shown to interact with the SH3 domain of v-Src which then targets the complex to particular subcellular compartments. Beard and co-workers (1999) have shown that there

is a preference for the rat PDE4D4 interaction with SH3 over PDE4A5. This has been attributed to the presence of stretches of proline residues in PDE4D4, which contains at least two proline-rich stretches at its N-terminal portion, as opposed to the proline-arginine motif present in PDE4A5.

#### 1.6.1.1.3 Regulation of PDE4 enzymes

Phosphorylation has been shown to be important for PDE4 enzyme regulation. Studies carried out on PDE4D3 isoenzyme, which is a commonly expressed long isoform, have revealed the presence of at least two protein kinase (PKA) phosphorylation sites (**RRXS**) located at the N-terminal portion of the enzyme (Ser<sup>13</sup> and Ser<sup>54</sup>) and an extracellular signal-related kinase 2 (ERK2 or p42-44<sup>MAP</sup> kinase) phosphorylation site (**PQSP**) at the C-terminal portion of the conserved catalytic domain (Ser<sup>579</sup>) (Sette and Conti, 1996; Hoffman *et al.*, 1999) (Figure 1.16). It is the PKA phosphorylation of Ser<sup>54</sup>, located within UCR1, which caused activation of PDE4D3 which in turn attenuated the ability of UCR1 to interact with UCR2 leading to activation of the enzyme (Sette and Conti, 1996; Beard *et al.*, 2000).

UCR2 is thought to contain an inhibitory domain retaining the PDE4 enzymes in a less active state, analagous to the calcium, calmodulin-binding domains found in the PDE1 family. Jin and co-workers (1992) carried out deletion experiments involving the removal of the region corresponding to UCR2 in PDE4D1 which is a short PDE4 isoenzyme lacking UCR1 but having the entire UCR2 region. On removal of UCR2, an enzyme with increased catalytic activity was observed. The two regions, UCR1 and UCR2, are also thought to amplify the small inhibitory effect on the PDE4D3 catalytic unit which follows the ERK2 phosphorylation of Ser<sup>579</sup> (PQS<sup>579</sup>P consensus motif) located at the C-terminal portion of the catalytic domain. However, this inhibition could be reversed by subsequent phosphorylation by PKA (Hoffman *et al.*, 1999).

Phosphorylation has also been observed in the isoform PDE4B2B which has the consensus motif for phosphorylation by MAP kinase (ERK2) and casein kinase 11 (Lenhard *et al.*, 1996). The targets for phosphorylation are Ser<sup>487</sup> and Ser<sup>489</sup> for MAP kinase (PQS<sup>487</sup>P consensus motif) and casein kinase 11 respectively. These residues lie at the C-terminal

end of the catalytic domain of PDE4B2B (see Figure 1.14.2). Experiments by Lenhard and co-workers (1996) showed that phosphorylation by MAP kinase did not affect the  $K_m$  or  $V_{max}$  of the enzyme for cAMP nor affect the  $IC_{50}$  for rolipram. The secondary structure of the phosphorylated enzyme also remained unaffected. However, the phosphorylated enzyme was less susceptible to proteolysis suggesting a role for phosphorylation in the stability of the enzyme. Lenhard and co-workers (1996) have suggested that the phosphorylation of PDE4B2B by MAP kinase could link the cAMP and Ras signalling pathways, which are activated by growth factors, in the regulation of PDE4B2B.

PDE4 variants have also been shown to be regulated by transcriptional control through a mechanism involving co-ordination between PKA and ERK2-mediated phosphorylation (Liu and Maurice, 1999; MacKenzie *et al.*, 2000). Studies carried out on vascular smooth muscle cells revealed that cells incubated with agents causing an increase in intracellular cAMP showed a marked increase in the short isoforms, PDE4D1 and PDE4D2 mRNA, while untreated cells expressed the long isoforms, PDE4D3 and PDE4D5 (Liu *et al.*, 2000).

#### **1.6.1.1.4 PDE4D interactions with scaffold or anchoring proteins**

A PDE4 isoform was shown to interact with the protein receptor for activated C-kinase (RACK1) (Yarwood *et al.*, 1999). RACK1 is thought to act as a “scaffold” or “anchor” protein for certain protein kinase C isoforms (PKC) as well as with Src tyrosyl kinase (Chang *et al.*, 1998). Yarwood and co-workers (1999) used a yeast two-hybrid system to show that RACK1 interacted with the PDE4D5 (long) isoform. RACK1 did not interact with PDE4D1 (short) or PDE4D2 (supershort) isoforms. These workers had already isolated the PDE4D5 isoform and shown it to contain a unique 88-amino acid sequence at the N-terminal portion of the enzyme (Yarwood *et al.*, 1999). Residues located within this sequence were shown to be important for the RACK1 interaction.

Verde and co-workers (2001) observed the co-precipitation of PDE4D3 (long) isoform with a protein called myomegalin which is found mainly in the cardiac and skeletal muscles (Verde *et al.*, 2001). This is a scaffold protein associated with the sarcoplasmic reticulum. These workers have shown that a region within the C-terminal portion of the UCR2 of PDE4D3 interacts with myomegalin. Co-precipitation was also possible with PDE4D1,

which is a short isoform with an intact UCR2 region, but was not possible with PDE4D2, which is a super short isoform with a truncated UCR2 region. An anchoring protein, protein kinase A anchoring protein (AKAP) has also been shown to interact with the first 15 amino acid residues at the amino terminal portion of PDE4D3 as part of a molecular complex that includes PKA such that there is an enhanced cAMP breakdown (Tasken *et al.*, 2001; Dodge *et al.*, 2001).

It is apparent from the above discussion that PDE4 isoforms interact with a number of intracellular proteins which provides for compartmentalisation of the complex cAMP-signalling pathway involving PDE4 and cAMP. An increasingly common theme is that of the involvement of scaffold proteins which serve to bring together different elements of the signalling process for activation of the signalling cascade. It is possible that revelations regarding PDE4 isoforms and scaffold proteins may also apply to the other members of the PDE families.

#### **1.6.1.2 cAMP-specific, rolipram-insensitive PDE7 family**

The PDE7 family comprises of two genes: PDE7A and PDE7B. The enzymes in this family are cAMP-specific with  $K_m$  values ranging from  $0.1\mu\text{M}$  to  $0.2\mu\text{M}$  (Wang *et al.*, 2000; Gardner *et al.*, 2000), but are insensitive to rolipram having  $\text{IC}_{50}$  values of greater than  $100\mu\text{M}$  (Bloom *et al.*, 1996; Hetman *et al.*, 2000). Three splice variants have been identified for PDE7A: PDE7A1, PDE7A2 and PDE7A3. These differ in their tissue distribution with PDE7A1 and PDE7A3 expressed in the immune system, specifically T cells but not B cells, (Li *et al.*, 1999a; Glavas *et al.*, 2001) thus suggesting a role for this isoform in inflammatory diseases such as asthma and rheumatoid arthritis (Wang *et al.*, 2000). PDE7A2 on the other hand is highly expressed in the skeletal muscle and to a lesser extent in the heart (Bloom *et al.*, 1996; Hetman *et al.*, 2000). There are thought to be differences in the N-terminal sequences of the two splice variants which dictate cellular localisation (Han *et al.*, 1997). Human PDE7A2 contain sites for myristoylation (Gly<sup>2</sup>) and palmitoylation (Cys<sup>8</sup>) which allow for membrane association. Hydrophobicity studies on PDE7A1 and PDE7A2 have shown that the N-terminal region of PDE7A1 is significantly more hydrophilic than PDE7A2 which is reflected on the cellular localisation of the enzymes with the more hydrophilic enzyme (PDE7A1) being found in the soluble fraction

of the cell (Wang *et al.*, 2000) while the more hydrophobic enzyme (PDE7A2) is found in the particulate fractions (Han *et al.*, 1997). PDE7A1 has also been shown to contain a PKA pseudosubstrate sequence (RRGAIS) but the significance of this finding is unclear (Wang *et al.*, 2000; Michaeli *et al.*, 1993).

The PDE7B enzymes are highly expressed in the brain, heart and skeletal muscle (Hetman *et al.*, 2000). The enzyme has been cloned from mouse and human, and these show 95% identity (Sasaki *et al.*, 2000). There are differences in the C-terminal portions of the enzymes from the two species and this has been suggested as evidence for a C-terminal splice variant. Enzymes from both species contain two metal-binding motifs important for the PDE catalytic process: **HNAVH-X<sub>35</sub>-HDVDH** where residues in bold are conserved in all the PDE families (see section 1.4.7.3). A putative PKA phosphorylation site (RRGSY) has also been shown to be present in both species of PDE7B enzymes (Gardner *et al.*, 2000).

### 1.6.1.3 High affinity cAMP-specific, IBMX-insensitive PDE8 family

The enzymes in the PDE8 family are high-affinity cAMP-specific, IBMX-insensitive PDEs (Soderling *et al.*, 1998; Fisher *et al.*, 1998a, 1998b). PDE8 has a very low  $K_m$  (0.15 $\mu$ M) for the hydrolysis of cAMP and is insensitive to the commonly used PDE inhibitors which include IBMX, zaprinast and rolipram ( $IC_{50} >100\mu$ M). However, it is sensitive to dipyrindamole ( $IC_{50} = 4.5\mu$ M and 40 $\mu$ M for PDE8A and PDE8B respectively) which is an inhibitor generally considered to be specific for cGMP-hydrolysing PDEs. There are two gene products for the PDE8 family: PDE8A and PDE8B. These two enzymes differ in their tissue distribution. In the mouse, PDE8A is most highly expressed in the testes followed by the eye, liver, skeletal muscle as well as the brain (Soderling *et al.*, 1998). It has been shown to have a similar distribution in humans (Fisher *et al.*, 1998). Human PDE8B has been shown to be found mainly in the thyroid gland followed by the brain (Hayashi *et al.*, 1998).

The PDE8 enzymes contain a unique N-terminal region called the PAS domain (Soderling *et al.*, 1998). PAS stands for Period, ARNT and Sim proteins and the domain usually comprises of about 100 residues (Huang *et al.*, 1993). A motif of unknown function, the

PAS domain, is found in the protein PER. *Drosophila melanogaster* has the *period* gene and its product is the protein period (PER). PER is involved in the circadian rhythms of the fly. The PAS domain has been shown to be present in a number of proteins involved in cellular signalling but the exact function remains uncertain.

In the PDE8 enzymes, the PAS domain is thought to be involved in protein-protein interactions allowing subcellular localisation but the exact role remains elusive. There is also a consensus sequence present in the PDE8 enzyme which allows nuclear localisation (Soderling *et al.*, 1998; Nigg, 1997).

### **1.6.2 cGMP modulated/hydrolysing PDE enzymes containing GAF domains**

The enzymes belonging to the families PDE2, PDE5, PDE6, PDE10 and PDE11 all contain allosteric cGMP-binding regulatory domains called GAF domains at their N-terminals. PDE2, PDE5, PDE6 and PDE9 families of enzymes will be discussed in this section as these are either modulated by cGMP or hydrolyse cGMP. The PDE3, PDE10 and PDE11 families, which are dual substrate PDEs, will be discussed in the next section of dual substrate PDEs but PDE1 will be discussed in a separate section (section 1.7).

#### **1.6.2.1 Derivation of the term ‘GAF’**

The name GAF is derived from three very diverse proteins which contain these conserved domains: cGMP-specific phosphodiesterases, cyanobacterial *Anabaena* adenylyl cyclase, and *Escherichia coli* transcriptional regulator *fhlA* (Aravind and Ponting, 1997; Shabb and Corbin, 1992). The functional role of these domains is not clear in most instances, but in the case of the PDEs, these GAF domains bind cGMP thereby increasing the enzyme affinity for cGMP. Multiple sequence alignment of three cGMP-binding PDEs (PDE2, PDE5 and PDE6) has shown the presence of two homologous tandem repeat sequences, a and b, within the N-terminal cGMP-binding region (Trong *et al.*, 1990). Site-directed mutagenesis of the cGMP-binding region of PDE5 revealed an essential aspartic acid at each of the two tandem repeats within this region (McAllister-Lucas *et al.*, 1995). An Asp→Ala mutation within region a (Asp<sup>289</sup>) caused a decrease in the enzyme affinity for cGMP ( $K_d > 10\mu\text{M}$ ) while the same mutation carried out in region b (Asp<sup>478</sup>) showed an

increased affinity for cGMP ( $K_d \sim 0.5\mu\text{M}$ ).

### 1.6.2.2 cGMP-stimulated PDE2 family

The PDE2 enzymes are cGMP-stimulated PDEs hydrolysing both cAMP and cGMP. There are three isoforms of PDE2 derived from one gene: PDE2A1, PDE2A2, PDE2A3 (Sonnenburg *et al.*, 1991; Yan *et al.*, 1994; Rosman *et al.*, 1997). These differ in their N-terminal sequence which is thought to be the determining factor in the cellular localisation of the isoenzymes to either the particulate or cytosolic compartments of a cell. The tissue distribution pattern of PDE2 enzymes show that it is highly expressed in the brain (mainly particulate form) followed by the heart (mainly soluble forms) (Rosman *et al.*, 1997; Sonnenberg *et al.*, 1991; Repaske *et al.*, 1993). PDE2 is also particularly abundant in the adrenal glands where hormones such as adrenocorticotrophic hormones (ACTH) induce increases in cAMP leading to increased synthesis and secretion of aldosterone which causes an expansion in blood volume (MacFarland *et al.*, 1991). Atrial natriuretic protein (ANP), which is sensitive to blood volume, also binds to the cells in the adrenal glands and activates the guanylyl cyclase enzymes to cause an increase in cGMP levels. This is then thought to stimulate PDE2 to hydrolyse cAMP, diminishing levels of cAMP and leading to a decrease in the secretion of aldosterone and hence a decrease in the blood volume. A  $G_i$ -dependent inhibition of adenylyl cyclase has also been proposed as the mechanism by which ANP acts to reduce cAMP levels (MacFarland *et al.*, 1991). There is thus an interplay between the cGMP and cAMP pathways in the control of blood volume and blood pressure.

Kinetic analysis of the PDE2 isoforms revealed that the enzyme exhibited positive cooperativity (Sonnenberg *et al.*, 1991). The reported  $K_m$  for the hydrolysis of cAMP is approximately  $30\mu\text{M}$  while that for cGMP is approximately  $10\mu\text{M}$  but the hydrolysis of cAMP can be stimulated up to 30-fold by the binding of cGMP to the GAF domains (Murashima *et al.*, 1990). It has also been shown that low levels of IBMX can stimulate PDE2 catalytic activity by binding to the GAF regions (Butt *et al.*, 1995; Beltman *et al.*, 1995).

### 1.6.2.3 cGMP-specific PDE5 family

PDE5 was first purified and characterised from bovine and rat lung tissues (Francis and Corbin, 1988; Thomas *et al.*, 1990a). PDE5A1 and PDE5A2 have since been isolated from human aortic smooth muscle cells (Loughney *et al.*, 1998) and canine lung (Kotera *et al.*, 1998). The enzymes from the different species differ at their amino-terminal regions with the rat PDE5 differing from the bovine and human PDE5 enzymes (Kotera *et al.*, 1997, 1998). All the PDE5 enzymes have a high affinity for cGMP having a  $K_m$  for cGMP hydrolysis of between 1 $\mu$ M to 5 $\mu$ M (Thomas *et al.*, 1990a; Turko *et al.*, 1998a; Kotera *et al.*, 1998) and are potently inhibited by zaprinast ( $IC_{50}$  of 0.3 $\mu$ M to 0.5 $\mu$ M) (Turko *et al.*, 1998b; Loughney *et al.*, 1998; Kotera *et al.*, 1998).

The amino-terminal portion of PDE5 enzymes contain two allosteric cGMP-binding domains (GAF domains) which are distinct from the site of cGMP hydrolysis (Thomas *et al.*, 1990b; McAllister-Lucas *et al.*, 1993; Kotera *et al.*, 1998). The binding of cGMP to both of these sites has been shown to enhance phosphorylation of a single serine located upstream of the cGMP-binding regions by both cGMP-dependent and cAMP-dependent protein kinases (Thomas *et al.*, 1990b; Turko *et al.*, 1998b). Phosphorylation leads to an increase in enzyme activity as well as increasing the affinity of allosteric cGMP binding of the enzyme (Corbin *et al.*, 2000). The GAF domains, or regions adjacent to these, have been thought to be involved in the dimerisation of the enzyme (Thomas *et al.*, 1990b).

### 1.6.2.4 cGMP-specific photoreceptor PDE6 family

The PDE6 family of enzymes are highly specific for cGMP and contain high-affinity non-catalytic cGMP-binding sites (GAF domains). These enzymes are present in the rod and cone cells of the retina playing a pivotal role in the visual signalling cascade. There are three gene products described for the PDE6 family: PDE6A1, PDE6B1 and PDE6C1. As with other members of the GAF domain-containing PDE enzymes, the GAF domains are located at the N-terminal portion of the catalytic  $\alpha$  subunits, with the C-terminal portion being involved in the catalytic process as well as membrane association.

PDE6 enzymes are heterotetrameric enzymes composed of  $\alpha\beta\gamma$  subunits with distinct



forms present in the rod and cone cells (Deterre *et al.*, 1988; Lipkin *et al.*, 1990; Li *et al.*, 1990). Bovine rod cell PDE6 has been shown to be composed of two large catalytic  $\alpha$  (88kDa) and  $\beta$  (84kDa) subunits and two small inhibitory  $\gamma$  subunits (13kDa). Bovine cone cell PDE6 on the other hand is composed of two identical catalytic  $\alpha'$  subunits (90kDa) as well as three smaller polypeptides (11, 13 and 15kDa) (Gillespie and Beavo, 1988). The majority of the rod and cone PDE6 is associated with the membrane but soluble PDE6 is also present. Gillespie and Beavo (1988) have also reported the presence of a delta ( $\delta$ ) subunit (17kDa) which co-purified with the soluble rod and cone PDEs. This  $\delta$  subunit is thought to be involved in the solubilisation of particulate PDE6 by interactions with the C-terminal portion of the enzyme (Florio *et al.*, 1996; Conti and Jin, 1999). The  $\delta$  subunit mRNA has also shown to be present in non-retinal tissue such as the bovine brain and adrenal gland indicating that it may interact with other PDEs or proteins in these tissues (Florio *et al.*, 1996).

In the 'resting' or dark-adapted rods and cones, intracellular cGMP is mainly found bound to the allosteric GAF domains of PDE6 but there is still enough unbound cGMP occupying the cGMP-gated cation channels which remain in the open-state. Under these conditions, there is an influx of calcium ions through the cGMP-gated channel matched by an efflux of sodium, potassium, calcium-exchanger and the membrane is relatively depolarised. The initiation of the visual transduction pathway involves the activation of the photoreceptor rhodopsin which is a member of the seven-helix transmembrane receptor proteins. This in turn will activate the associated heterotrimeric G-protein, transducin (GDP- $\alpha\beta\gamma$ ), so that there is an exchange of the bound GDP with GTP on the  $\alpha$ -subunit of transducin. The  $\alpha$ -GTP dissociates from the complex and interacts with the inhibitory  $\gamma$ -subunits of PDE6 thereby activating PDE6 enzymes. PDE6 rapidly decreases the intracellular level of cGMP such that receptor occupation by cGMP is reduced which leads to the closure of the cGMP-gated channel which blocks calcium ion entry but does not block the efflux of calcium ions. The membrane becomes increasingly hyperpolarised which provides the signal to the higher centers of the brain to perceive light (Dizhoor *et al.*, 1991; Francis *et al.*, 2000a). cGMP levels are restored by the activation of guanylate cyclase and a calcium-sensitive protein, recoverin, which responds to low calcium ion levels to restore the dark state (Koch and Stryer, 1988; Dizhoor *et al.*, 1991).

### 1.6.3 cGMP-specific PDE9 family

The PDE9A enzymes have a high affinity for cGMP hydrolysis having a  $K_m$  of 0.07 $\mu$ M and 0.17 $\mu$ M for the mouse and human PDE9A respectively (Soderling *et al.*, 1998; Fisher *et al.*, 1998b). The enzymes do not contain the GAF domains shown to be present in the cGMP hydrolysing PDE2, PDE5 and PDE6 families and are also not inhibited by dipyridamole which is usually selective for cGMP-hydrolysing PDEs. The human PDE9A mRNA has been shown to be most abundant in the spleen, small intestine and the brain while mouse PDE9A mRNA showed the highest levels in the kidney with lower levels seen in the liver, lung and the brain (Soderling *et al.*, 1998; Fisher *et al.*, 1998b). There have been four PDE9A transcripts described to date: PDE9A1, PDE9A2, PDE9A3 and PDE9A4. However, the functional significance of these is not known. The physiological role of the PDE9A enzymes also remains elusive but as it has such a high affinity for cGMP, it is possible that it is involved in the control of the basal level of cGMP in the cells.

### 1.6.4 Dual substrate PDE families

PDE families that hydrolyse both cAMP and cGMP include the PDE1, PDE3, PDE10 and PDE11 families. The PDE1 family will be discussed in a separate section (1.7) as it forms the focus of the present work.

#### 1.6.4.1 cGMP-inhibited PDE3 family

The PDE3 family of enzymes are referred to as the cGMP-inhibited PDE enzymes. They hydrolyse both cAMP and cGMP with high affinity having  $K_m$  values in the range 0.1-0.8 $\mu$ M (Degerman *et al.*, 1997) while low levels of cGMP inhibit the hydrolysis of cAMP by these enzymes (Meacci *et al.*, 1992). The inhibition of cAMP hydrolysis by the presence of cGMP is thought to occur by a competitive inhibition where the cGMP binds within the catalytic domain as opposed to regions outside the catalytic domain as occurs for the GAF domain-containing enzymes. There are unique features present in the PDE3 family that clearly distinguish them from the other PDE families. Firstly, they contain a 44 amino acid insertion in the catalytic domain situated within the amino-terminal zinc-binding motif (Francis *et al.*, 2000a, 2000b; Meacci *et al.*, 1992). Tang and co-workers (1997) carried out

mutagenesis studies to remove a portion of the N-terminal region, and also the 44 amino acid insert in a separate mutant. These workers found that the cGMP hydrolysis by the N-terminal mutant was increased relative to cAMP suggesting an involvement of this region of the enzyme for cGMP selectivity. Removal of the 44 amino acid insertion showed no detectable cyclic nucleotide hydrolysis implicating the importance of this insertion in the PDE3 catalytic activity. Secondly, PDE3 enzymes have been shown to contain six membrane-association hydrophobic segments located at the amino-terminal region of the enzymes (Leroy *et al.*, 1996; Shakur *et al.*, 2000; Meacci *et al.*, 1992). These regions are followed by consensus sites for phosphorylation by protein kinase A and protein kinase B which are thought to activate the enzyme (Wijkander *et al.*, 1997; Kitamura *et al.*, 1999).

There have been two isoforms of PDE3 described to date: PDE3A and PDE3B. These are products of two different genes (Manganiello *et al.*, 1995). Both isoforms are found in the cytosolic as well as particulate fractions of the cell. Tissue distribution of these isoforms differs in that the PDE3A enzymes, mainly found in the cytosolic fractions, are abundant in the platelets and the cardiovascular system (Meacci *et al.*, 1992; Cheung *et al.*, 1996; Conti and Jin, 1999), while the PDE3B enzymes are mainly found in the adipose tissues, hepatocytes and T-lymphocytes (Snyder, 1999; Reinhardt *et al.*, 1995; Liu and Maurice, 1998). However, both PDE3A and PDE3B have also been shown to be expressed in human vascular smooth muscle (Palmer and Maurice, 2000).

PDE3A enzymes have historically been the target for cardiotonic drugs such as milrinone and amrinone for use in heart failure. Early clinical evidence on the short term use of these drugs in patients with heart failure showed that there was an improved cardiac function in these patients (Andrews and Cowley, 1993; Movsesian, 1999). However, repeated oral doses of milrinone were shown to increase mortality by heart failure so development of this drug was curtailed (Packer *et al.*, 1991).

PDE3B inhibitors have recently been considered for the treatment of obesity (Snyder, 1999). Adipocytes contain both  $\beta$ -adrenoreceptors and tyrosine kinase receptors. In general, stimulation of  $\beta$ -adrenoreceptors will promote lipolysis by increasing cAMP levels and activating cAMP-dependent protein kinases which in turn activate hormone sensitive

lipase (HSL). Insulin stimulation of the tyrosine kinase receptor on the other hand will cause phosphorylation of PDE3B, via lipid phosphatidylinositol-3-kinase (PI-3K) and protein kinase B (*Akt*), thereby activating the PDE3B (Snyder, 1999; Kitamura *et al.*, 1999). Activated PDE3B reduces cAMP levels leading to a down-regulation of the lipolytic pathway. Based on this, PDE3B inhibitors are proposed to behave as lipolytic agents in the treatment of obesity (Snyder, 1999). PDE3B has also been implicated in the pathway involving receptor activation by leptin (White and Tartaglia, 1996; Zhao *et al.*, 2000). Leptin is a hormone secreted by adipocytes, and is thought to activate receptors that are structurally similar to the cytokine receptors which signal through the JAK enzymes (name derived from Janus). Activation of JAK enzymes initiates a sequence of phosphorylation events involving PI-3-K and protein kinase B which leads to activation of PDE3B and a decrease in cAMP-mediated lipolytic pathway as with insulin (Conti, 2000; Zhao *et al.*, 2000).

#### **1.6.4.2 cAMP and cGMP-specific PDE10 family**

The PDE10 enzymes have a dual substrate specificity having a  $K_m$  of 0.05 $\mu$ M for cAMP and 3 $\mu$ M for cGMP hydrolysis for the mouse PDE10A (Soderling *et al.*, 1999) while the human PDE10A have  $K_m$  values of 0.26 $\mu$ M and 7.2 $\mu$ M for cAMP and cGMP respectively (Fujishige *et al.*, 1999). Low levels of cAMP were also shown to inhibit the cGMP hydrolysing activity of PDE10 while higher levels of cGMP were shown to inhibit cAMP hydrolysis by the enzyme (Fujishige *et al.*, 1999). Human PDE10 enzymes contain two GAF domains homologous to those seen in PDE2, PDE5 and PDE6 enzymes (Soderling *et al.*, 1999; Kotera *et al.*, 1999; Fujishige *et al.*, 1999). However, these GAF domains have not been shown to bind cGMP in the PDE10A enzymes.

Two variants of PDE10A have been described so far, PDE10A1 and PDE10A2, which differ at their N-terminal regions (Kotera *et al.*, 1999). Kotera and co-workers (1999) have shown human PDE10A2, but not PDE10A1, to contain a putative phosphorylation site for cAMP-dependent protein kinase A. However, Fujishige and co-workers (1999) have suggested that human PDE10A1 lacked phosphorylation sites for cAMP- and cGMP-dependent protein kinase but were instead regulated by protein kinase C phosphorylation.

#### 1.6.4.3 cAMP and cGMP-specific PDE11 family

The PDE11 family is the most recently identified PDE family. Human PDE11A was shown to hydrolyse both cAMP and cGMP having  $K_m$  values of  $1.04\mu\text{M}$  and  $0.52\mu\text{M}$  respectively (Fawcett *et al.*, 2000). Variants of PDE11A with differences in their N-terminal regions have been described (Fawcett *et al.*, 2000; Yuasa *et al.*, 2000, 2001). For example, the N-terminal of PDE11A1 contains a single GAF domain as opposed to the double GAF domains found in the PDE2, PDE5, PDE6 and PDE10 families. Furthermore, PDE11A3 has been shown to contain one complete and one incomplete GAF domain, while PDE11A4 contains two complete GAF domains as well as putative phosphorylation sites for cAMP- and cGMP-protein kinases at their N-terminal portions (RRXS and RKXS/T respectively) (Yuasa *et al.*, 2000). It is not clear whether phosphorylation plays a role *in vivo*. PDE11A4 enzymes also contain the motif “NKX<sub>n</sub>FX<sub>3</sub>D” which is found in the GAF domain of PDE5 and shown to be important for cGMP binding. However, kinetic studies examining the effect of cGMP on PDE11A4 catalytic activity did not show any modulation of the catalytic activity so it is possible that this may be a site for interaction with other proteins (Fawcett *et al.*, 2000). The physiological role of the PDE11 enzymes has yet to be established.

## 1.7 Calcium/calmodulin-stimulated PDE1 Family

The PDE1 family of enzymes are characterised by their stimulation by calmodulin (CaM) in the presence of calcium ions and are hence known as calmodulin-phosphodiesterases (CaM-PDEs). Calmodulin is a 17 kDa calcium-binding protein involved in a wide range of calcium ion dependent signalling pathways. It binds four calcium ions which is followed by a conformational change in the molecule exposing hydrophobic regions present within the molecule (Babu *et al.*, 1985). It is these hydrophobic regions which are thought to bind the calmodulin-binding domains of target enzymes which include the PDE1 molecule as well protein kinases and protein phosphatases (Head, 1992; Vaillancourt *et al.*, 1992; Crivici and Ikura, 1995). Calmodulin itself has been shown to be phosphorylated by casein kinase 11 (CK-11) and myosin light-chain kinase (MLCK) which alters the ability of the phosphorylated calmodulin to modulate its target enzymes (Quadroni *et al.*, 1998; Leclerc *et al.*, 1999). In general, phosphorylation of calmodulin reduces its ability to activate its target enzymes (Quadroni *et al.*, 1998; Leclerc *et al.*, 1999; Corti *et al.*, 1999).

CaM-PDEs hydrolyse both cAMP and cGMP but they do differ in their affinity for these substrates. For example, the PDE1A enzymes show a higher affinity for cAMP than for cGMP while PDE1C enzymes have an equal affinity for both substrates. There are also differences between the splice variants. For example, PDE1A1 enzymes are stimulated at a much lower calmodulin concentration ( $K_{CaM} \sim 0.3nM$ ) compared to PDE1A2 ( $K_{CaM} \sim 4nM$ ) (Sonnenburg *et al.*, 1995).

### 1.7.1 Discovery of PDE1 enzymes

The existence of a PDE activated by calcium ions in the presence of an endogenous regulatory protein was first demonstrated in the rat brain and bovine heart in the early 1970s (Kakiuchi and Yamzaki, 1970; Goren and Rosen, 1970; Teo *et al.*, 1973; Waisman *et al.*, 1975). The regulatory protein, calmodulin, was originally discovered as an activator protein, present in snake venom, by Cheung (1967, 1970, 1971). Ho and co-workers (1977) then purified the first calmodulin-dependent phosphodiesterase from the bovine heart. This was followed by reports of the purification of calmodulin-dependent PDEs from bovine brain, heart and lungs by other workers (Klee *et al.*, 1979; Morrill *et al.*, 1979; Sharma *et*

*al.*, 1980, 1986a, 1986b; Kincaid *et al.*, 1984). PDE1 enzymes from these tissues exhibited different molecular masses as determined by SDS PAGE analysis as well as displaying differing biochemical properties. For example, a feature of the rabbit and bovine lung CaM-PDE was the tight association these enzymes retained with calmodulin in the form of a stable CaM\*PDE complex (Sharma and Wirch, 1979; Sharma and Wang, 1986b). Purification of the lung 58 kDa enzyme showed that it retained its calcium ion activation in the absence of exogenous calmodulin and that it contained calmodulin activity despite successive chromatographic purification procedures carried out (Sharma and Wang, 1986b). This calmodulin was only dissociated from the CaM\*PDE complex by 2.5M magnesium chloride. Sharma and Wang (1986b) showed that the lung CaM-PDE activity increased as the Ca<sup>2+</sup> concentration was increased, and that there was no change in this increased activity when either 1µM or 10µM calmodulin was added together with the Ca<sup>2+</sup>. When the calmodulin antagonist, fluphenazine was added to the bovine lung PDE, there was no effect on the lung phosphodiesterase activity. Similarly, calcineurin had little or no effect on the bovine lung PDE. In contrast to this, the bovine brain PDE activity was dramatically reduced in the presence of both fluphenazine and calcineurin. These results indicated that the tightly bound CaM in the bovine lung PDE was not subject to competition by other CaM-binding proteins such as calcineurin.

Further PDE1 enzymes isolated from bovine tissues included a PDE1 enzyme isolated from the bovine brain which had a subunit molecular mass of 74 kDa and showed an increased affinity for cGMP relative to cAMP (Shenolikar *et al.*, 1985). A 70 kDa PDE1 which dimerises in the presence of Ca<sup>2+</sup>/CaM to form a 180 kDa protein was isolated from the mouse testis (Rossi *et al.*, 1988).

Characterisation of the early CaM-PDEs showed that the enzymes were stimulated up to four-fold by calmodulin in the presence of calcium ions and that this activation was lost when the enzyme preparations were subjected to repeated freeze-thaw cycles. CaM-PDEs were thought to be dimeric molecules with subunit molecular weights of between 58 - 63 kDa. SDS PAGE analysis on the CaM-PDE enzymes showed the bovine brain to contain not only a single 60 kDa protein (Sharma *et al.*, 1980) but two distinct bands with masses of 60 kDa and 63 kDa (Sharma *et al.*, 1984) suggesting the presence of different isoforms with different regulatory properties in the bovine brain. A comparison of the amino acid

sequences for the bovine heart (59 kDa) and bovine brain (61 kDa and 63 kDa) enzymes revealed that the 59 kDa and 61 kDa enzymes differed only at their amino-terminal regions by 34 residues (Novack *et al.*, 1991; Charbonneau *et al.*, 1991). These were therefore thought to be products of a single gene resulting from alternate RNA splicing. These correspond to the PDE1A1 and PDE1A2 enzymes respectively according to the presently accepted nomenclature for the PDE enzymes (Beavo *et al.*, 1995). In contrast, the 63 kDa bovine brain CaM-PDE displayed only 67% identity with the 61 kDa enzyme with differences in the sequence dispersed throughout the sequence. Therefore, the 63 kDa enzyme was suggested as being a product of a separate but homologous gene. This 63 kDa enzyme corresponds to the PDE1B enzyme.

Table 1.6 shows some of the early CaM-PDEs identified and named according to the nomenclature proposed by Beavo and Reifsnnyder (1990) together with the presently accepted new name for the PDEs (Beavo *et al.*, 1994).

**Table 1.6** PDE1 enzymes identified by early studies named according to the nomenclature proposed by Beavo (1990) together with the new PDE name (Beavo *et al.*, 1994).

New PDE Name	PDE1 Name	kDa (estimated by SDS PAGE)	Reference
PDE1A1	58 kDa lung CaM-PDE	58	Sharma and Wang, 1986b
PDE1A1	59 kDa heart CaM-PDE	59 - 60	Novack <i>et al.</i> , 1991
PDE1A2	61 kDa brain CaM-PDE	60 - 61	Charbonneau <i>et al.</i> , 1991
PDE1B1	63 kDa brain CaM-PDE	63	Bentley and Bentley, 1992; Repaske <i>et al.</i> , 1992
	67 kDa low $k_m$ rat testes CaM-PDE	67 - 68	Purvis and Rui, 1988
PDE1C	75 kDa brain CaM-PDE	75	Shenolikar <i>et al.</i> , 1985

### 1.7.2 Domain organisation of the PDE1 enzymes

In common with other PDE families, PDE1 enzymes share a region of approximately 270 amino acid at the carboxy-terminal portion of the enzymes corresponding to the conserved catalytic domain with divergence seen at the N- and C- terminal regions of the enzymes



(Figure 1.9). Early studies on the comparison of segments of amino acid sequence of the bovine brain 61 kDa CaM-PDE (PDE1A2), bovine heart cGMP-stimulated PDE (PDE3) and the product of a *dnc*<sup>+</sup> gene of *Drosophila melanogaster*, which is a cAMP-specific PDE (PDE4), revealed the region of about 270 residues which displayed structural homology between the sequences corresponding to the catalytic portions of the enzymes described in section 1.4.7 (Charbonneau *et al.*, 1986). The presence of a fully active catalytic unit has been confirmed by experiments carried out using trypsin digestion on the native bovine brain CaM-PDE (Tucker *et al.*, 1981; Charbonneau *et al.*, 1991; Sonnenburg *et al.*, 1995).

PDE1 enzymes uniquely contain two calmodulin-binding domains at their amino-terminal portions which are involved in the regulation of the PDE1 enzymes. Charbonneau and co-workers (1991) first predicted the presence of a calmodulin-binding region present at the N-terminal of the bovine brain 61 kDa enzyme (PDE1A2). These workers determined the complete amino acid sequence of the enzyme and investigated the structural organisation of the CaM-PDE using limited proteolysis. The position of the first CaM-binding region was indicated as being between the residues 23 and 41 of the native enzyme. Sonnenburg and co-workers (1995) then carried out deletion mutation experiments on the bovine brain 61 kDa enzyme to remove the amino acid residues 4 to 46. This truncated fragment, however, produced an enzyme which was still activated three-fold by calmodulin in the presence of calcium ions. Residues 4 to 98 were then removed and this gave a calmodulin-independent enzyme. These results provided evidence for the presence of a second CaM-binding region within the N-terminal portion of the PDE1 enzymes. This second CaM-binding region was mapped to a region approximately 90 residues from the first putative CaM-binding region. Furthermore, the region separating the two CaM-binding domains was thought to be important for retaining the PDE1 enzymes in a less active state at low calcium ion levels. This inhibitory region comprised of 11 amino acid residues (see Figure 1.19.1) and its removal together with the first calmodulin-binding region was necessary for a Ca<sup>2+</sup>/CaM-independent enzyme (Sonnenburg *et al.*, 1995).

### 1.7.3 Regulation of the PDE1 enzymes

#### 1.7.3.1 Regulation by phosphorylation

Phosphorylation of the CaM-PDE enzymes was demonstrated in the early studies of CaM-PDE enzymes purified from bovine tissues. Sharma and co-workers (1980) showed that the bovine brain 58 kDa CaM-PDE (PDE1A) could be phosphorylated by cAMP-dependent protein kinase (PKA) but this phosphorylation did not appear to affect the catalytic activity of the enzyme in this study. Studies by Sharma and Wang (1985) on the bovine brain CaM-PDE showed that the 61 kDa enzyme (PDE1A2), and not the 63 kDa (PDE1B) enzyme, was phosphorylated by PKA and that this caused a decrease in the affinity of the enzyme for calmodulin. The phosphorylated enzyme could be dephosphorylated by the calmodulin-dependent phosphatase, calcineurin, which was followed by an increase in the enzyme affinity for calmodulin (Sharma and Wang, 1985). Moreover, the same workers later showed that the 63 kDa bovine brain CaM-PDE could be phosphorylated by a preparation of bovine brain in the presence of calcium ions (Sharma and Wang, 1986a). As with phosphorylation of the 61 kDa CaM-PDE, phosphorylated 63 kDa CaM-PDE also showed a reduced affinity for calmodulin. The enzyme involved in the phosphorylation of the 63 kDa CaM-PDE was proposed as being the autophosphorylated calcium and calmodulin-dependent protein kinase II (CaM-kinase II) which is particularly abundant in the brain (Sharma and Wang, 1986a; Hashimoto *et al.*, 1989). Bovine brain 63 kDa CaM-PDE is thought to have multiple phosphorylation sites for CaMKII since tryptic digestions carried out on the phosphorylated enzyme revealed two major and two minor phosphorylated peptide fragments (Hashimoto *et al.*, 1989).

In general, phosphorylation of the CaM-PDEs is blocked by the binding of calmodulin to the enzyme and phosphorylation of CaM-PDEs results in the reduction of the affinity of the enzymes for calmodulin. Although different kinases are involved in the phosphorylation process (Sharma and Wang, 1985; Sharma, 1991) all the CaM-PDEs can be dephosphorylated by the calmodulin-dependent phosphatase, calcineurin (Sharma and Wang, 1986a), which is accompanied by an increase in the affinity of the enzymes for calmodulin.

The consensus sequences for the two kinases involved in the phosphorylation of PDE1 enzymes are **RRXS** and **RXXS/P(T)** (Payne *et al.*, 1983; Pearson *et al.*, 1985) for cAMP-dependent protein kinase (PKA) and calmodulin-dependent protein kinase (CaMKII) respectively. There is a strong requirement for the presence of an arginine residue (R) at the -3 position to the serine residue. The presence of a second arginine at -2 is usually a positive determinant for PKA (**RRXS**) and a relatively strong negative determinant for CaMKII (Soderling *et al.*, 1986).

The phosphorylation of PDE1A1 and PDE1A2 was demonstrated in the early studies on CaM-PDEs (Sharma, 1991; Sharma and Wang, 1985). Sonnenburg and co-workers (1995) identified a potential PKA recognition sequence (**RGRS<sup>104</sup>**) at the N-terminal portion of the bovine lung PDE1A1 which is within the second calmodulin-binding domain of the enzyme. Florio and co-workers (1994) identified serine 120 as well as serine 138 in bovine brain PDE1A2 as being targets for phosphorylation by PKA (**RFRS<sup>120</sup>**). PDE1B1 has two potential phosphorylation sites at the carboxy-terminal portion (**RQPS<sup>466</sup>**; **RAAS<sup>502</sup>**) (Yu *et al.*, 1997). PDE1B1 has been shown to be phosphorylated *in vitro* by CaMKII but the location of these sites of phosphorylation have not been identified (Sharma and Wang, 1986a). CaMKII is known to phosphorylate target serine residues located at the C-terminal portion of at least one of its other target proteins - a Na<sup>+</sup>/H<sup>+</sup> exchanger (Fliegel *et al.*, 1992). This exchanger was also found not to be a substrate for phosphorylation by PKA or PKC.

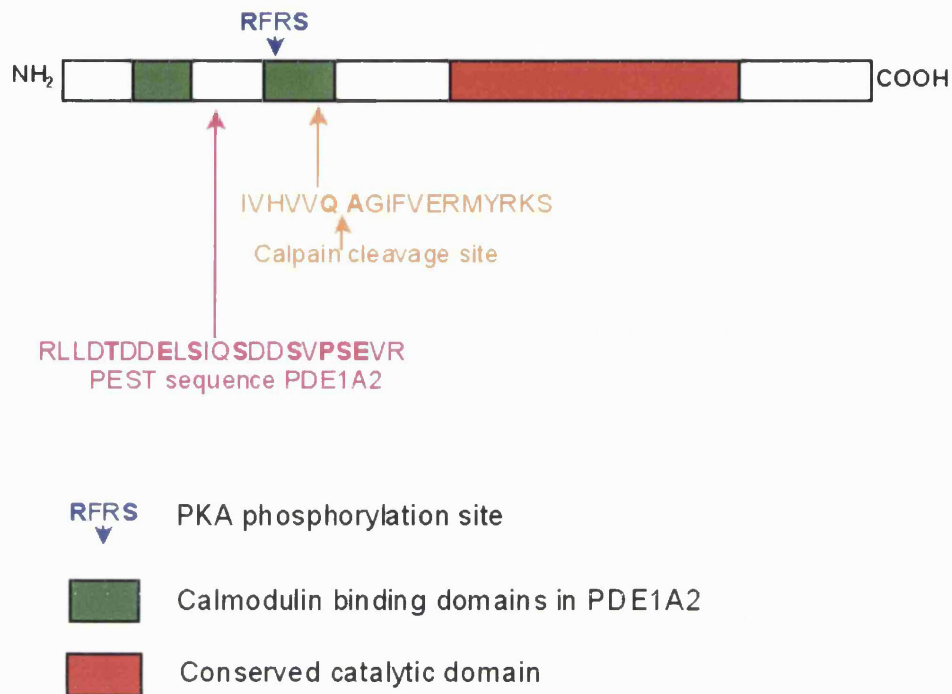
### **1.7.3.2 Regulation by proteolytic degradation**

The PDE1A1 enzymes have been shown to be regulated through proteolytic cleavage by m-calpain (Kakkar *et al.*, 1998). Calpains are Ca<sup>2+</sup>-dependent cysteine proteases that are widely distributed in the animal kingdom, from mammals to invertebrates but have not been described in plants or bacteria (Murachi, 1983; Mykles and Skinner, 1986; Carafoli and Molinari, 1998). They are sensitive to the inhibitor calpastatin as well as leupeptin (Carafoli and Molinari, 1998). Calpains are thought to be major mediators for calcium signalling in many tissues including the brain, lung and the liver (Murachi, 1983; Croall and Demartino, 1991; Sorimachi *et al.*, 1997; Carafoli and Molinari, 1998). Substrates of calpains include myelin basic protein and tubulin as well as enzymes such as myosin light chain kinase, calcineurin and phospholipase C (Croall and Demartino, 1991). The two

forms that exist, m-calpains and  $\mu$ -calpains, differ in their sensitivity to  $\text{Ca}^{2+}$  with the former requiring millimolar concentrations of  $\text{Ca}^{2+}$  and the latter requiring micromolar  $\text{Ca}^{2+}$  concentrations for activation. Target proteins with sequences enriched with the residues proline (P), glutamate (E), serine (S) and threonine (T), known as PEST motifs, are thought to be the signal for proteolytic cleavage by calpains (Rogers *et al.*, 1986). Calpains target many different proteins and include transcription factors (c-Jun, c-Fos and nuclear factor  $\kappa\text{B}$ ) as well as plasma membrane  $\text{Ca}^{2+}$ -ATPase (Hirai *et al.*, 1991; Molinari *et al.*, 1995; Liu *et al.*, 1996). The strength of the PEST sequence is determined by the PEST score which has a range of -45 (weak) to +50 (strong). Generally, a PEST score between -5 and 0 denotes a weak strength, a score  $>0$  denotes a possible PEST sequence and a value  $>5$  indicates the strong presence of a PEST sequence (Rogers *et al.*, 1986).

Kakkar and co-workers (1999) used a PEST-FIND program to identify the presence of a PEST sequence in the bovine PDE1A2 enzyme sequenced by Sonnenburg and co-workers (1996). Their analysis revealed a PEST sequence with a score of 7.36 located at the amino terminal portion of the enzyme (Figure 1.17). Cleavage by calpains does not usually occur within the PEST motifs but at a distant site. Kakkar and co-workers (1998) have demonstrated that the proteolytic cleavage of PDE1A2 by m-calpain was at a site approximately 30 amino acid residues away and that this cleavage yielded an enzymatically active calmodulin-independent 45 kDa fragment. N-terminal sequence analysis of the 45 kDa fragment, together with the fact that the activity of the fragment was no longer affected by  $\text{Ca}^{2+}$ /CaM, indicated that the calpain cleavage occurred at residues located between 120 and 138 (Figure 1.17). Biochemical analysis of the cleavage process showed that the presence of CaM did not interfere with substrate recognition by calpain, and phosphorylation of PDE1A2 also did not affect the cleavage process. The exact significance of this cleavage is not known but the proteolysis of PDE1A2 to a CaM-independent enzyme in neural tissues has been postulated as being important in decreasing cAMP levels in these tissues. In diseases such as Parkinson's disease there is a significant decrease in the cAMP levels and since PDE1A2 has been shown to be co-localised with calpains in the same region as the dopamine receptors, it is possible that PDE1A2 plays a role in the decreased cAMP levels in this region. Kakkar and co-workers (2002) have recently reported the calpain cleavage of rat heart PDE1A1 by both m- and  $\mu$ -calpains during hypoxic injury to the heart. As with PDE1A2, a CaM-independent fragment was

generated following calpain cleavage. Since increased cAMP has been associated with cell death (Jiang *et al.*, 1996), it is possible that the generation of a CaM-independent species in damaged cells limit further cell damage or death.



**Figure 1.17** Schematic showing the PEST motif and m-calpain cleavage site in bovine PDE1A2. Figure adapted from Kakkar *et al.*, 1998, 1999; Sonnenburg *et al.*, 1993.

#### 1.7.4 PDE1 splice variants

The PDE1 family of enzymes is encoded for by three different genes: PDE1A, PDE1B and PDE1C. These give rise to multiple splice variants generated by both 5' as well as 3' mRNA splicing to give proteins that differ at their amino and carboxy terminal regions. Table 1.7 summarises the PDE1 splice variants described to date.

**Table 1.7** PDE1 family splice variants.

PDE1 gene	Splice variant	Reference
PDE1A	PDE1A1	Sharma and Wang, 1986b; Novack <i>et al.</i> , 1991; Snyder <i>et al.</i> , 1999
	PDE1A2	Charbonneau <i>et al.</i> , 1991; Snyder <i>et al.</i> , 1999
	PDE1A3	Loughney <i>et al.</i> , 1996
	PDE1A5	Fidock <i>et al.</i> , 2002
	PDE1A4, 1A5, 1A6, 1A8, 1A9, 1A10, 1A11, 1A12	Michibata <i>et al.</i> , 2001
PDE1B	PDE1B1	Yu <i>et al.</i> , 1997
	PDE1B2	Fidock <i>et al.</i> , 2002
PDE1C	PDE1C1	Loughney <i>et al.</i> , 1996; Yan <i>et al.</i> , 1996
	PDE1C2	Yan <i>et al.</i> , 1995
	PDE1C3	Loughney <i>et al.</i> , 1996
	PDE1C4	Yan <i>et al.</i> , 1996
	PDE1C5	Yan <i>et al.</i> , 1996

##### 1.7.4.1 PDE1A splice variants

The PDE1A1 and PDE1A2 enzymes have been extensively characterised biochemically since these were the first PDE1 enzymes to be isolated and purified in the early studies on PDEs (Sharma and Wang, 1986b; Novack *et al.*, 1991; Charbonneau *et al.*, 1991). Comparisons of the nucleotide and amino acid sequences of the two enzymes revealed that they differ only at the N-terminal regions within the first putative calmodulin-binding region which is thought to account for the differences in their relative affinities for calmodulin. The calmodulin concentration required for half-maximal activation ( $K_{CaM}$ ) of PDE1A1 is 0.3nM while that for PDE1A2 is 4nM (Sonnenburg *et al.*, 1995). The different affinities of the PDE1 enzymes for calmodulin are thought to be important in the regulation

of different CaM-PDEs as an adaptation to the calcium/calmodulin levels in various cell types or compartments (Novack *et al.*, 1991). For example, PDE1A2 was shown to be present mainly in the bovine brain and calmodulin concentration in the brain is ten times higher than the concentration in the heart (Sonnenburg *et al.*, 1998; Kakkar *et al.*, 1999). This may explain the relatively low calmodulin affinity of PDE1A2 enzyme compared to PDE1A1.

A third splice variant for the human PDE1A gene, PDE1A3, was identified by Loughney and co-workers (1996). PDE1A3 is highly homologous to PDE1A2 but differs in amino acid residues located at the carboxy-terminal region of the enzyme. The isolation of the cDNA for human PDE1A5 was reported by Fidock and co-workers (2002) and this is said to be most similar to the bovine PDE1A1. However, there are differences in the amino acid residues located at the carboxy terminal between the two enzymes which have been suggested as being species-related differences.

Michibata and co-workers (2001) identified a further five new human PDE1A splice variants using cDNA library screening. These workers also reported the localisation of the human PDE1A gene as being on chromosome 2q32. The new splice variants were said to be generated through combinations of different N- and C-termini regions which they named N1, N2, N3 and C1, C2, C3 for the amino and carboxy termini respectively. Splice variants containing the regions corresponding to N3 and C3 were the novel sequences identified while the others matched reported sequences for the PDE1A splice variants already reported (Loughney *et al.*, 1996). Figure 1.18 shows the sequences of the N- and C-termini regions identified by Michibata and co-workers (2001) while Table 1.8 gives a summary of the PDE1A splice variants generated by the combination of the different N- and C-termini. The significance of the divergent N-terminal regions has been said to play a role in the tissue distribution of the PDE1A splice variants. For example, splice variants containing the N2 (PDE1A1 and PDE1A4) amino terminal show a wide tissue distribution pattern with the highest expression in the kidney, liver and pancreas but little or no expression in the brain (Michibata *et al.*, 2001). Splice variants with the N1 (PDE1A2, PDE1A5 and PDE1A6) amino terminal were found to be highly expressed in the brain only while those with the N3 terminal (PDE1A10) were shown to be expressed only in the testis. The dog heart PDE1A1 used in the present study has the N- and C-termini regions

corresponding to the N2/C2 sequences.

MGS SATEIEELENT TFKY **LTGEQTEKMWQRLKGILRCLVKQL** ERGDVNVVDLKKNI EYAA SVLEAVYIDET **RRLLDTEDE**.....N1  
 MD **DHVTIRKKHLQRPIFRLRCLVKQL** ERGDVNVVDLKKNI EYAA SVLEAVYIDET **RRLLDTEDE**.....N2  
 MGKKINKLFCFNFLVQCFRGKSKPSKCOIRKKVKNHI **ERLLDTEDE**.....N3

**Figure 1.18.1** Amino terminal residues for the PDE1 family. The residues shown boxed represent the first calmodulin-binding region in the PDE1 enzymes while the residues in bold represent identical residues.

**C1**.....**DIIQQNKERWKELAAQ**EARTSSQFCEFIHQ\*  
**C2**.....**DIIQQNKERWKELAAQ**GESDLHKNSEDLVNAEEKHDETHS\*  
**C3**.....**DIIQQNKERWKELAAQ**GSVVYEALLPSLSVFTSPLRVWITSSRFLLL\*

**Figure 1.18.2** Carboxy terminal residues for the PDE1 family. Residues shown in bold represent identical residues while the asterisk marks the end of the sequence. The dog heart PDE1A used in the present study contains the N2C2 sequences.

**Table 1.8** PDE1A splice variants generated by the combination of the different amino- and carboxy-termini sequences as reported by Michibata and co-workers (2001).

PDE1A enzyme	kDa	Regions	
		N-terminal	C-terminal
PDE1A1	61	N2	C2
PDE1A4	60	N2	C1
PDE1A5	62	N1	C2
PDE1A6	61	N1	C1
PDE1A8	61	N2	C3
PDE1A9	63	N1	C3
PDE1A10	57	N3	C1
PDE1A11	59	N3	C2
PDE1A12	59	N3	C2



### 1.7.4.2 PDE1B splice variants

Two splice variants have been reported for the PDE1B: PDE1B1 and PDE1B2. Yu and co-workers (1997) reported the isolation of the human cDNA for PDE1B1 as well as the mapping of PDE1B1 to chromosome 12. The human PDE1B1 shares approximately 96% amino acid homology with the bovine, rat and mouse isoforms. Comparisons with other human PDE1 isoforms showed that the PDE1B1 amino terminal portion shares up to approximately 60% homology with PDE1A3 and PDE1C1 while showing up to approximately 75% homology with the catalytic domains of these isoforms. PDE1B1 showed greatest divergence from other members of the PDE1 family at its C-terminal region. Two potential phosphorylation sites (RXXS/T) are present at the carboxy-terminal of PDE1B1. Biochemical analysis of human PDE1B1 also showed it to be most similar to the bovine PDE1B1 (63 kDa isoform) as expected in that it is stimulated approximately 2-fold by calmodulin with cAMP as substrate but having greater than 2-fold stimulation when cGMP was used as the substrate (Yu *et al.*, 1997). Examination of the tissue distribution of PDE1B1 showed that it was highly expressed in the heart, brain and skeletal muscle. Detailed analysis of the distribution of PDE1B1 in the brain showed it to be localised in specific regions of the brain. These regions corresponded to the areas of the brain which are rich in G-protein coupled dopamine receptors (D1 and D2) which allow for signalling to proceed in these cells through  $\text{Ca}^{2+}$  oscillations (Bofill-Cardona *et al.*, 2000). Activation of these receptors leads to a complex interplay between cAMP,  $\text{Ca}^{2+}$ , calmodulin, and PDPE1B1. Another point of cross-talk in these cells is the involvement of DARPP-32 (dopamine- and cAMP-regulated phosphoprotein; molecular weight 32,000) which is an inhibitor of protein phosphatase 1. On activation of the dopamine receptors, DARPP-32 is dephosphorylated and becomes active. This event is enhanced by the  $\text{Ca}^{2+}$ /CaM activation of calcineurin which is CaM-dependent protein phosphatase (Nishi *et al.*, 1997).

The second splice variant for human PDE1B, PDE1B2, has only recently been reported by Fidock and co-workers (2002). PDE1B2 differs from PDE1B1 at its N-terminal region by replacement of the first 38 residues with an alternative 18 residues. PDE1B2 also shows a variant tissue distribution pattern compared to PDE1B1 which corroborates the findings by Michibata and co-workers (2001) who proposed that the divergent amino terminals (N1 - N3) identified for the PDE1A enzymes was reflected in the tissue distribution of these

enzymes. Whereas PDE1B1 was found mainly in the brain, PDE1B2 is abundantly expressed in the spinal cord (Fidock *et al.*, 2002).

### 1.7.4.3 PDE1C splice variants

Diversity within the PDE1C family is brought about by alternate 5' as well as 3' mRNA splicing resulting in isoforms that differ at their amino and carboxy terminal regions which is reflected in their biochemical properties and tissue distributions (Loughney *et al.*, 1996; Yan *et al.*, 1995, 1996). Loughney and co-workers (1996) isolated the cDNA for human PDE1C1 and PDE1C3 as well as cDNA for human PDE1A3 which corresponds to the bovine 61 kDa PDE1A2 enzyme. Biochemical analysis of PDE1C3 enzymes showed that PDE1C3 had a high affinity for both cAMP ( $K_m$  0.33 $\mu$ M) and cGMP ( $K_m$  0.57 $\mu$ M) while the PDE1A3 enzymes showed a higher affinity for cGMP ( $K_m$  3.5 $\mu$ M) than for cAMP ( $K_m$  51 $\mu$ M).

The cDNAs for the mouse and rat PDE1C3 (Yan *et al.*, 1995) and mouse PDE1C1, PDE1C4 and PDE1C5 (Yan *et al.*, 1996) have also been reported. The amino acid sequences for PDE1C1, PDE1C4 and PDE1C5 are the same except in the C-terminal regions but they differ from the PDE1C2 at both the N- and C-terminal regions (Yan *et al.*, 1996). Moreover, PDE1C4 and PDE1C5 are thought to be products of 3' splicing. The divergence at the N-terminal occurs in the middle of the region which corresponds to the first calmodulin-binding site identified in the PDE1A1 and PDE1A2 enzymes (Novack *et al.*, 1991; Charbonneau *et al.*, 1991). The calcium ion and calmodulin sensitivity of the newly identified PDE1C splice variants were compared with those for PDE1A1 and PDE1A2 enzymes by Yan and co-workers (1996). As already discussed, PDE1A1 is much more sensitive to stimulation by calmodulin in the presence of calcium compared to PDE1A2, a difference attributed to the variant N-terminal regions of the two enzymes (Sonnenburg *et al.*, 1995). The half-maximal stimulation of the PDE1C enzymes was determined using increasing concentrations of calcium ions. These results are summarised in Table 1.9. Generally, these show that PDE1C1, PDE1C4 and PDE1C5 are less sensitive to calcium ions compared to the PDE1C2 splice variant. Comparison of the amino acid sequences of the splice variants show that PDE1C2 has a unique N-terminal sequence compared to the other PDE1C splice variants which may account for the difference in

calcium sensitivity.

**Table 1.9** Summary of biochemical analysis carried out on PDE1C splice variants.

PDE splice variant	Km ( $\mu\text{M}$ )		[Ca <sup>2+</sup> ] for half-maximal activity ( $\mu\text{M}$ )	Reference
	cAMP	cGMP		
Bovine PDE1A1	42	3	0.27	Sharma and Kalra, 1994; Yan <i>et al.</i> , 1996
Bovine PDE1A2	112.7	5.1	1.99	Yan <i>et al.</i> , 1996
Bovine PDE1B1	24.3	2.7	1.25	Yan <i>et al.</i> , 1996
Mouse PDE1C1	3.5	2.2	3.01	Yan <i>et al.</i> , 1996
Rat PDE1C2	1.2	1.1	0.83	Yan <i>et al.</i> , 1996
Mouse PDE1C4/5	1.1	1.0	2.43	Yan <i>et al.</i> , 1996
Human PDE1C3	0.33	0.57	-	Loughney <i>et al.</i> , 1996
Human PDE1A3	51	3.5	-	Loughney <i>et al.</i> , 1996

### 1.7.5 Tissue distribution of PDE1 enzymes

Substantial levels of PDE1 enzymes have been identified in bovine brain tissues (Kincaid *et al.*, 1981a, 1984; Sharma *et al.*, 1980, 1984; Charbonneau *et al.*, 1991; Novack *et al.*, 1991; Sonnenburg *et al.*, 1993); bovine heart tissues (Sharma, 1991; Novack *et al.*, 1991), bovine lung tissues (Sharma and Kalra, 1994) as well as mouse testes (Rossi *et al.*, 1988). These early studies did not differentiate the CaM-PDEs into the many isoforms now identified but it was known that different isoforms did exist. For example, Sonnenburg and co-workers (1991) identified two different mRNA species (3.8 kb and 4.4 kb) from bovine cerebral cortex and the heart. Northern blots of these tissues using a 61 kDa CaM-PDE cDNA probe showed that this probe hybridised with just one of the mRNA species (4.4 kb) in both tissues indicating the presence of a separate PDE1 isoform corresponding to the 3.8 kb mRNA.

As mentioned earlier, the different splice variants have also been shown to be preferentially expressed in certain tissues as well as showing cell type specific distribution. For example, PDE1B1 mRNA was located primarily in the bovine brain while lower levels were found in the heart (Yu *et al.*, 1997). Molecular techniques have been used to map the PDE1

enzymes present in the mouse CNS (Yan *et al.*, 1994). The PDE1A mRNA showed the highest signal in the cerebral cortex and the pyramidal cells of the hippocampal CA1 to CA4 regions; PDE1B gave the strongest signal in the caudate-putamen, olfactory tubercle and Purkinje cells; and, PDE1C was limited to the granule and Purkinje cells of the cerebellum and the olfactory bulb. PDE1C is thought to play a major role in the regulation of nitric oxide-modulated (NO) cGMP in the cerebellum as it has been shown that CaM-PDE strongly modulates cGMP responses elicited by NO (Yu *et al.*, 1997; Mayer *et al.*, 1992). This distribution pattern in the CNS is thought to represent the different physiological roles of the PDE1 enzyme in the regulation of cAMP in these cells.

The involvement of CaM-PDE activity in the olfactory sensory neurons was proposed by several workers (Anhold and Rivers, 1990; Firestein *et al.*, 1991) shortly after the demonstration of the presence of odorant-stimulated calcium/calmodulin-dependent adenylyl cyclases in the olfactory cilia (Pace *et al.*, 1985; Sklar *et al.*, 1986). Yan and co-workers (1995, 1996) have since shown that PDE1C2 is found in abundance in the olfactory sensory neurons with PDE1C1 showing a lower level of expression. Odorants are thought to activate olfactory sensory neurons by activating G-protein coupled receptors giving a transient intracellular cAMP pulse leading to the activation of a cyclic nucleotide gated (CNG) channel to allow influx to sodium and calcium ions (Nakamura and Gold, 1987). The transient nature of this signal is particularly important in order that the neurons can be repeatedly stimulated. PDE1C2 is thought to be important in the hydrolysis of the cAMP generated by an odorant molecule as this isoform is found in abundance in the olfactory cilia (Yan *et al.*, 1995). The second messenger molecule inositol 1,4,5-triphosphate (InsP3) is also thought to be involved in the odorant process as receptors for this molecule have been shown to be localised in the ciliary surface membrane (Cunningham *et al.*, 1993; Restrepo *et al.*, 1990). The InsP3 receptor is thought to play a role in the regulation of Ca<sup>2+</sup> flux at the ciliary surface. Since CNG channels are also involved in the Ca<sup>2+</sup> flux, there is the possibility of cross-talk between the pathways involving cAMP, InsP3 and PDE1C2.

## **1.8 Background to the present work**

### **1.8.1 Characterisation of purified native dog heart PDE1A enzyme**

The dog heart PDE1A enzyme forms the focus of the present study. The dog has been used extensively as a model for the investigation of cardiac function in the testing of pharmacological agents but there have been very few reports on the isolation of PDE enzymes from this species. The main PDE families represented in the heart are PDE1A, PDE3A and PDE4 families. PDE1A has been isolated from the heart tissues of a number of mammalian species including the bovine heart (Sharma, 1991; Novack *et al.*, 1991) and guinea pig heart (Weishaar *et al.*, 1986; Reeves *et al.*, 1987). There has been only one report on the isolation and purification to homogeneity of PDE1A enzymes from the dog heart (Clapham and Wilderspin, 2001). In this study, PDE1A enzyme was purified using a combination of dye affinity, Mono-Q and calmodulin affinity chromatography to yield a single protein of 68 kDa size as judged by SDS PAGE analysis. Size exclusion chromatography indicated that the protein existed as a dimer. Biochemical analysis revealed that it had a slightly higher affinity for cGMP, with the  $K_m$  for cAMP being  $1.2\mu\text{M}$  and that for cGMP as being  $0.53\mu\text{M}$ . The enzyme was stimulated 3-4 fold by calmodulin in the presence of  $\text{Ca}^{2+}$ . Inhibitor analysis revealed that the purified enzyme was inhibited by the PDE1/5 inhibitors vinpocetine ( $\text{IC}_{50} = 1.38\mu\text{M}$ ) and zaprinast ( $\text{IC}_{50} = 1.93\mu\text{M}$ ) as well as the non-specific PDE inhibitor IBMX ( $\text{IC}_{50} = 16.37\mu\text{M}$ ). It was not inhibited by PDE3 and PDE4 inhibitors amrinone and rolipram respectively.

### **1.8.2 Sequence analysis of dog heart PDE1A cDNA**

#### **1.8.2.1 Putative amino acid sequence of the dog heart PDE1A**

The full-length cDNA for PDE1A1 used in the present study was produced using total RNA from dog heart tissue (Clapham and Wilderspin, 2001). The calculated molecular mass of the translated protein, comprising 515 amino acid residues, was 59373 daltons. A comparison of the amino acid sequence of this enzyme and that of the bovine and human PDE1A1 enzymes revealed that the dog heart PDE1A was 95% identical to the bovine enzyme and 91% identical to the human PDE1A1. Figure 1.19.1 shows the amino acid

sequence of the dog heart PDE1A1 together with the putative calmodulin-binding domains at the amino terminal portion of the enzyme. It also indicates the 30 amino acid residues identified as being important in the catalytic specificity for PDE5 enzymes by Turko and co-workers (1998a, 1998b) together with the Zn<sup>2+</sup>-binding motifs (HX<sub>3</sub>HX<sub>n</sub>E) identified by McAllister-Lucas and co-workers (1993), and Francis and co-workers (1994) (see Figure 1.10). The importance of these regions has already been discussed in section 1.4.7. Salient features regarding the dog heart PDE1A1 amino acid sequence are highlighted in Figure 1.19.1 and include the following:

- ▶ Two calmodulin-binding domains located at the amino terminal region between residues 5 - 27 (shown green and single underlined) and 98 - 121 (shown in green and double underlined).
- ▶ Catalytic domain located between residues 178 - 431 (shown red).
- ▶ Metal-binding regions between residues 203 - 276 including the two Zn<sup>2+</sup>-binding motifs A and B: HX<sub>3</sub>HX<sub>n</sub>E (shaded yellow).
- ▶ Sequence identified by Sonnenburg and co-workers (1995) as being important in bovine PDE1A for maintaining the enzyme in a less active state in the absence of Ca<sup>2+</sup>/CaM located between residues 73 - 83 (shown in lavender).
- ▶ A conserved diad of threonine (T<sup>314</sup>) and aspartic acid (D<sup>315</sup>) located within the catalytic domain (indicated by the double blue arrow-heads) said to be important for cGMP substrate specificity and the catalytic process in PDE5 by Francis and co-workers (1994), and Turko and co-workers (1997) (see Figure 1.12).
- ▶ Presence of the conserved amino acid sequence (30 amino acid residues; shown in red and underlined) shown by site-directed mutagenesis studies on PDE5 as being important in the catalytic process (Turko *et al.*, 1996, 1998a), located between residues 350 - 379 which include the invariant glutamic acid (E<sup>271</sup> - indicated by the single blue arrow-head) again shown to be important for cGMP specificity and the catalytic process in PDE5 (invariant E<sup>775</sup> in PDE5) (see Figure 1.10).
- ▶ Location of the PEST sequence identified by the PESTFIND program in the present work as being between the residues 57 - 78 (indicated by the dashed

underlining) (see section 1.8.2.2).

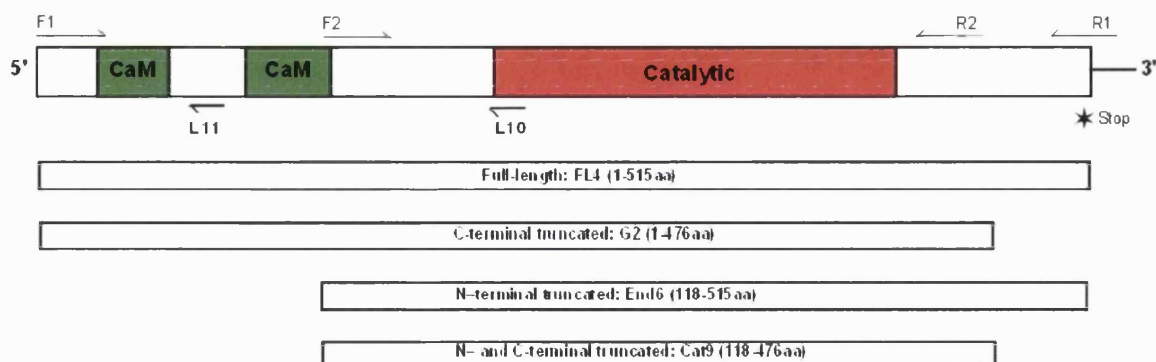
- ▶ The probable calpain cleavage point between residues Q<sup>110</sup> and A<sup>111</sup> (indicated by the double blue arrow) located within the calpain recognition sequence (residues 105 - 121) 32 residues away from the actual PEST sequence (see section 1.8.2.2).
- ▶ Position of the four PCR primers used in Chapter 5 to generate the full-length and truncated PDE1A1 enzymes are shown as arrows above the relevant sequence: F1 and F2 for the forward primers, R1 and R2 for the reverse primers. See section 5.2.3 for details.

Figure 1.19.2 shows a schematic of the four PDE1A1 fragments generated by PCR using combinations of the four primers (F1, F2, R1 and R2) in Chapter 5.

ATGGATGACCATGTCACAATCAGGAAGAAACATCTCCAAAGACCCATCTTTAGACTAAGA	60
M D H V T I E K K H L Q R P I F R L E	20
TGCTTAGTGAAGCAGCTGGAGAGAGGTGATGTTAACGTCGTAGACTTAAAGAAGAATATT	120
Q L V K Q L E E G D V N V V D L K K N I	40
GAATATGCAGCATCTGTATTGGAAGCTGTTTACATTGACGAAACAAGAAGACTGCTGGAT	180
E Y A A S V L E A V Y I D E T R R L L D	60
ACTGAAGATGAGCTCAGTGACATTCAGACAGACTCAGTCCCATCAGAAGTACGGGACTGG	240
T E D E L S D I Q T D S Y P R A V R D W	80
TTGGCGTCCACCTTCACGCGGAAAATGGGGATGATGAAAAAATAATCTGAGGAAAAACCC	300
L A S T F T R K M G M M K K K S E E K P	100
AAATTCGAAGCATTGTGCATGCTGTTCAAGCTGGAATTTTGTGGAAAGGATGTACAGA	360
K F R S I V H A V Q A G I F V E R M Y R	120
AAGTCTATCACATGTTGGTTGGTATATCCAGAAGCTGTCATAGTAAAGTTAAAGGAC	420
E S Y H M V G L V Y P E A V I V T L K D	140
GTTGATAAATGGTCTTTTGACGTATTGTCCTTAAATGAAGCAAGTGGAGAACACAGTCTG	480
V D K W S F D V F A L N E A S G E H S L	160
AAGTTTATGATTTGAACTGTTTACCAGATATGATCTTATCAATCGTTTCAAGATTCTT	540
K F M I Y E L F T R Y D L I N R F K I P	180
GTTTCTGCTAATTTCCTTGCAGAAGCTTTAGAAAGTGGTTACAGCAAGTACAAAAAT	600
V S C L I S F A E A L E V G Y S K Y K N	200
CCTTATCACAATTTGATTCATGCAGCTGATGTCACGCAAACTGTGCACTACATAATGCTT	660
P Y H N L I H A A D V T Q T V H Y I M L	220
CATACAGGTATCATGCACTGGCTCACTGAACTGGAATTTTAGCAATGGTCTTTCGCCGT	720
H T G I M H W L T E L E I L A M V F A A	240
GCCATTCATGATTATGAGCATACAGGAACTACAAACAACCTTTCATATTCAGACAAGGTCA	780
A I H D Y E H T G T T N N F H I Q T R S	260
GATGTTGCCCTTTTGATAATGATCGCTCTGTCC TAGAGAATCACCATGTGAGTGCAGCT	840
D V A L L Y N D R S V L E N H H V S A A	280
TATCGACTATGCAAGAAGAAGAAATGAATGTTTGTATAAATTTATCCAAAGATGACTGG	900
Y R L M Q E E E M N V L I N L S K D D W	300
AGGGATCTCGGAACCTAGTGATTGAAATGGTTTTATCTACAGACATGTCAGGTCACTTC	960
R D L R N L V I E M V L S T D M S G H F	320
CAGCAAATATAAATATAAGAAACAGTTTGCAGCAGCCTGAAGGATGACAAAGCCAAA	1020
Q Q I K N I R N S L Q Q P E G I D K A K	340
ACTATGTCCTGATTCTTCATGCAGCAGACATCAGCCACCCGGCCAAGTCTGGCAGCTG	1080
T M S L I L H A A D I S H P A K S W Q L	360
CACTACCGGTGGACCATGGCCCTGATGGAGGAGT TTTTCTACAGGGAGATAAAGAAGCC	1140
H Y R W T M A L M E E F F L Q G D K E A	380
GAGTTAGGACTTCCATTTTCTCCACTTTGTGATCGGAAGTCAACGATGGTGGCCAGTCA	1200
E L G L P F S P L C D R K S T M V A Q S	400
CAAATAGGTTTCATTGATTTTCATAGTAGGCCAAATTTTCTTCTGACAGACTCGACA	1260
Q I G F I D F I V E P T F S L L T D S T	420
GAGAAAATATTATTCTCTTATAGAGGAAGCCTCAAAAACAGACACTTCTTCCATATGGG	1320
E K I I I P L I E E A S K T D T S S Y G	440
GCAAGCAGACGATCAAAATATGAAAGGCACCTGAACGATGGAACCTATCCCCAGACTAC	1380
A S R R S N M K G T M N D G T Y S P D Y	460
TCCCTTGCAAGCGTGACCTAAAGAGCTTCAAAAACAACCTGGTGGACATCATCCAGCAG	1440
S L A S V D L K S F K N N L V D I I Q Q	480
AACAAAGAGAGGTGGAAAGAGTTGGCTGCTCAAGGTGAACCAGATCTTCATAAGAAGTCA	1500
N K E R W K E L A A Q G E P D L H K N S	500
GAAGATCTAGTAAACGCTGAAGAAAACATGTGATACACATTCATAGGTTTGAATACC	1548
E D L V N A E E K H V D T H S *	515

**Figure 1.19.1** Nucleotide and amino acid sequence for the dog heart PDE1A1 (GenBank Accession AF252536) together with the putative single letter amino acid polypeptide sequence. See text for explanatory features regarding the amino acid sequence.





**Figure 1.19.2** Schematic of the four PDE1A1 fragments used for cloning into pSFV1. The full-length PDE1A1 is shown together with the two calmodulin-binding domains (CaM), the catalytic domain and the positions of the four PCR primers (Forward, F, and Reverse, R) used to generate the full-length (FL4), C-terminal truncated (G2), N-terminal truncated (End6) and the N- and C-terminal truncated (Cat9) products. The position of the two sequencing primers (L10 and L11) are also shown.

### 1.8.2.2 PEST sequence in the dog heart PDE1A1

For the present work, the PEST-FIND program was used on the dog heart PDE1A1 amino acid sequence to identify possible PEST sequences. This program identified one such sequence with a PEST score of +7.77 located at the amino terminal region. The PEST sequence identified by Kakkar and co-workers (1998) in the bovine PDE1A2 had a PEST score of +7.36. The position of the PEST sequence identified for the dog heart PDE1A1 is located between residues 57 to 78 (Figures 1.19.1 and 1.20). The probable calpain cleavage sequence for PDE1A1 is located between the sequences 105 - 122 with the cleavage point within this sequence between the glutamine (Q<sup>110</sup>) and alanine (A<sup>111</sup>). Figure 1.20 shows an amino acid alignment of the PEST sequences for PDE1A2 (Kakkar *et al.*, 1998) and the PDE1A1 used in the present work. Figure 1.21 shows the calpain cleavage sequence for both these enzymes. Although calpain cleavage studies have not been performed on the dog heart PDE1A1, a comparison of the pertinent sequences involved indicate that calpains are very likely to cleave the dog heart PDE1A1.

BTPDE1A2    <sup>73</sup>RLLD**T**DDELSIQSDD**SVPSEVR**<sup>94</sup>  
 CFPDE1A1    <sup>57</sup>RLLD**TE**DELSDIQ**TDSVPSEVR**<sup>78</sup>

**Figure 1.20** PEST sequences in the bovine PDE1A2 and the dog heart PDE1A. Sequence identified by the PESTFIND program as having a PEST score of +7.77 for the PDE1A1 used in the present study is shown together with the sequence from the calpain-cleavage studies carried out by Kakkar and co-workers (1998). See text for details. Figure adapted from Kakkar *et al.*, 1998; Clapham and Wilderspin, 2001.

BTPDE1A2    <sup>121</sup>IVHVV**Q** **AGIFVERMYRKS**<sup>138</sup>  
 CFPDE1A1    <sup>105</sup>IVHAV**Q** **AGIFVERMYRKS**<sup>122</sup>

↑  
Calpain cleavage site

**Figure 1.21** Calpain cleavage sequences in the bovine PDE1A2 and the dog heart PDE1A. Figure adapted from Kakkar *et al.*, 1998; Clapham and Wilderspin, 2001.

## 1.9 Overview of the present work

The main aim and focus of the present work was to devise a system capable of producing milligram amounts of active PDE1A1 for structural studies, to establish methods for purification of recombinant PDE1A1 and relate the biological activity of the recombinant enzyme with the native dog heart PDE1A enzyme. Evidence suggesting that the dog heart PDE1A1 cDNA encoded a functional gene was given by sequence alignment studies of the translated putative polypeptide amino acid sequence compared to the bovine and human PDE1A1 sequences. This alignment study showed a strong homology (as discussed in section 1.8.2.1) suggesting that dog heart PDE1A1 cDNA encoded for a functional gene.

The present work was divided into two main sections. The first comprised of the cloning and expression studies on the dog heart PDE1A1 to find the most suitable host for the expression of soluble recombinant PDE1A1. The second part concentrated on the biochemical characterisation of the recombinant enzyme. These goals are introduced below.

## 1.9.1 Cloning and expression of dog heart PDE1A1

The cloning and expression work involved the cloning of the PDE1A1 cDNA into different expression vectors and analysis of subsequent expression in these expression systems to discover the most suitable system. Three different expression systems, spanning prokaryotic to eukaryotic, were explored and these are discussed briefly below. They will be discussed in more detail in the individual chapters dedicated to each system.

### 1.9.1.1 Yeast expression system

The yeast expression system chosen was that employing *Pichia pastoris* as the host. *P. pastoris* is a methylotrophic yeast which means that it utilises methanol as its sole carbon and energy source (Ogata *et al.*, 1969). It offers two main advantages over the traditional *Saccharomyces cerevisiae* host. Firstly, the promoter used by *P. pastoris* to transcribe foreign genes is an alcohol oxidase promoter (AOX1) which is highly repressed under non-methanol growing conditions maintaining an “expression-off” state minimising expression of foreign proteins during cell growth phase. This is a distinct advantage if the protein is toxic, and the over-expression of PDE may cause adverse effects. The second advantage that *P. pastoris* has over *S. cerevisiae* is that the former does not have a tendency to ferment. A product of fermentation is ethanol which can rapidly build up to toxic levels in high-density cultures and cause cell death. Another advantage of the *P. pastoris* system is the option to export the recombinant protein out of the cell into the culture media. Therefore, *P. pastoris* offers itself as a useful host for the expression of foreign proteins allowing scale-up of the expression system from shake-flasks to large-volume fermenter vessels. The major drawback of the *P. pastoris* expression system is the requirement for different media needed during the cell-growth phase and the protein expression phase.

In the present work, the *P. pastoris* expression system was set up for the first time in this laboratory and optimised so that it could be used for the expression of PDE1A1. The dog heart PDE1A1 cDNA was cloned into the yeast vector pPICZ $\alpha$ C. This vector had the signal sequence,  $\alpha$ -Factor, for targeting expressed proteins towards a secretory pathway resulting in the secretion of proteins into the growth media. The advantage of secreted expression is in the ease of purification of the target protein. Expression of PDE1A1 in this

part of the study was monitored by carrying out PDE activity assays on the culture media.

### **1.9.1.2 Bacterial expression system**

Historically, *Eschericia coli* has been extensively used as a host for the expression of foreign proteins. It was the first organism to be used as a host for the production of foreign proteins. Many proteins have been successfully expressed using this host including PDEs, in particular PDE4 (Kovalala *et al.*, 1997). *E. coli* requires relatively little manipulation for the expression of foreign proteins and is a relatively inexpensive host to use in terms of culture media required which are considerations when scale-up of the expression system is required. However, *E. coli* is unable to perform post-translational modifications such as glycosylation and phosphorylation, which are possible in a eukaryotic host, and also necessary for many eukaryotic proteins. The production of co-factors and proteins important for assembly or stability may also be absent.

For the present work, dog heart PDE1A1 cDNA was cloned into two different vectors. Firstly, it was cloned into the expression vector pGEX-3X. In this case, PDE1A1 was produced as a fusion protein with the protein being N-terminal tagged with glutathione-S-transferase (GST), a protein derived from the blood fluke *Schistosoma japonicum*. The expression of soluble fusion protein was monitored using PDE activity assays as well as Western blot analysis using a commercial primary antibody raised against the GST. Since *E. coli* are well known for producing inclusion bodies, especially when expressing foreign genes toxic to the bacteria, Western blot analysis was also carried out on the insoluble material remaining following lysis of the bacteria. The second vector used for cloning the PDE1A1 cDNA was pTrcHisA which produced an N-terminal histidine (His<sub>6</sub>) tagged PDE1A1 protein. As before, detection of soluble PDE1A1 was by carrying out PDE activity assays. For both expression vectors, different strains of *E. coli* were explored to determine the effect, if any, of these strains on the expression of soluble PDE1A1.

### **1.9.1.3 Mammalian expression system**

The final expression system explored was that using the Semliki Forest virus system. This system has been successfully used for the expression of many mammalian proteins

including thyroid peroxidase, dopamine receptor 3 and interleukin-4 (Blasey *et al.*, 2000). There are no reports of its use for the expression of PDE1 enzymes. The advantage that it offers over the bacterial system is that it will process the target protein in terms of post-translational modifications as well as correctly fold the PDE1A1 protein being expressed - both of which are necessary for the biological activity of the enzyme. However, protein expression using this system does require attention to biosafety considerations since there is a reported fatality from wild type SFV infection (Willems *et al.*, 1979). *In vitro* synthesis of PDE1A1 mRNA transcripts for transfection of the host cells (BHK-21) involves the use of commercially available biochemicals. The preparation of BHK-21 cells also requires training in the handling and processing of these cells in readiness for the transfection procedure. The details of the expression system are discussed later in the relevant chapter on this system (Chapter 5).

For the purposes of the cloning work for the Semliki Forest virus system, the full-length as well as N- and/or C-terminal truncated PDE1A1 constructs were generated using PCR and then cloned into the vector pSFV1 for expression in the Semliki Forest virus system. As before, expression of PDE1A1 was monitored using PDE activity assays as well as Western blot analysis using a commercial CaM-PDE antibody.

### **1.9.2 Characterisation of the soluble recombinant dog heart PDE1A1**

The second part of the study involved the biochemical characterisation of the biologically active recombinant PDE1A1 enzyme to ascertain the  $K_m$ ,  $V_{max}$  and  $IC_{50}$  values for comparison with the native dog heart PDE1A purified by Clapham and Wilderspin (2001). The data obtained for the recombinant enzyme was also compared to published information regarding PDE1 enzymes isolated from other tissues as well as other PDEs.

The native state of the recombinant PDE1A1 enzyme produced in the present study was also investigated using a combination of size exclusion chromatography and covalent cross-linking studies.

## Chapter Two

### 2 General Materials and Methods

The reagents and methods common to the three expression systems explored (*P. pastoris*, *E. coli* and Semliki Forest virus) are discussed below. Reagents and methods unique to the individual expression system are discussed in the relevant chapters.

#### 2.1 Materials

##### 2.1.1 Chemical reagents

Tris Base, HEPES (N-(2-Hydroxyethyl)piperazine-N'-(2-ethanesulfonic acid), MES (2-(N-Morpholino)ethanesulfonic acid), EDTA, sucrose, sodium chloride, magnesium chloride, calcium chloride, glycerol, hydrochloric acid, sodium hydroxide pellets, sodium azide, methanol, isopropanol and concentrated acetic acid were obtained from BDH and Sigma. These were all either AnalaR or molecular biology grade reagents. Stock buffer solutions were routinely prepared as 1M solutions unless otherwise stated using milli Q water ( $\geq 18\Omega$  purity) and then autoclaved for 20 minutes, 15 Psi at 121°C. All the solutions were stored at room temperature unless otherwise stated. Dimethylsulfoxide (DMSO) was purchased from Sigma.

##### 2.1.2 DNA reagents

Low-melting agarose, standard agarose and ethidium bromide were from Sigma. The 1 kb and 1 kb plus DNA ladders were from GibcoBRL. Restriction enzymes were purchased from either Biolabs or GibcoBRL: *Bam*HI, *Sma*I, *Dra*I, *Hind*III, *Eco*RV. Wizard Mini-Prep and Qiagen Maxi-Prep kits were purchased from Promega for the small-scale and large-scale isolation of plasmid DNA respectively.

##### 2.1.3 Bacterial reagents and strains

Millers LB Broth Base (pancreatic digest of casein (SELECT Peptone 140) 10g/L, low

sodium yeast extract 5g/L, NaCl 10g/L) were purchased from GibcoBRL. Ampicillin and IPTG were from Melfords. The strains of *E. coli* used included TOP10F' from Invitrogen; DH5 $\alpha$ , JM109 and JM109(DE3) from Promega.

#### 2.1.4 Protein reagents

The Hoeffler Mini-gel apparatus for SDS PAGE was from BioRad. Ultra Pure Protogel 30% (w/v) Acrylamide was from National Diagnostics. TEMED (N, N, N', N' Tetramethylethylenediamine) and ammonium persulphate were from Sigma. Glycine, silver nitrate, glutaraldehyde solution (50%) and Coomassie Brilliant Blue dye were from BDH. Dithiothreitol was from Melford Laboratories. Pre-stained protein markers were purchased from New England Biolabs as a mixture containing MBP- $\beta$ -Galactosidase (175 kDa), MBP-Paramyosin (83 kDa), Glutamic dehydrogenase (62 kDa), Aldolase (47.5 kDa), Triosephosphate isomerase (32.5 kDa),  $\beta$ -Lactoglobulin A (25 kDa), Lysozyme (16.5 kDa) and Aprotinin (6.5 kDa) all at 0.1-0.2mg/ml. Individual proteins were also obtained from Sigma for the size exclusion chromatography and included  $\beta$ -Amylase (200 kDa), Bovine serum albumin (66 kDa), Carbonic anhydrase (29 kDa) and Vitamin B<sub>12</sub> (1.4 kDa). Bovine serum albumin for Western blotting was purchased from Fluka.

The primary antibody routinely used for Western blotting was a commercial polyclonal rabbit anti-CaM-PDE from Chemicon International. This recognised the 61 kDa PDE1A2, the 63 kDa PDE1B1 as well as the 75 kDa isoforms. Two other commercial primary PDE1 antibodies, also from Chemicon International, were the peptide antibody corresponding to the PDE1A2 only (rabbit CaM-PDE1A2) and the peptide antibody specific for PDE1B1 only (CaM-PDE1B1). Both of these peptide antibodies recognised a short stretch of amino acid residues located at the carboxy-terminal portion of the enzymes. The secondary antibody, Horseradish peroxidase labelled Sheep or Donkey anti-rabbit CaM-PDE, was from DAKO or Amersham Life Science. The nitrocellulose membrane was purchased from Amersham Life Science. 3,3'-Diaminobenzidine Tablet Sets (DAB Peroxidase Substrate) were from Sigma.

Protease inhibitors used were all purchased from Sigma: PMSF (Phenylmethanesulfonyl fluoride), TLCK (N $\alpha$ -p-Tosyl-L-lysine chloromethyl ketone), TPCK (N-p-Tosyl-L-

phenylalanine chloromethyl ketone), Leupeptin and Aprotinin. Stock solutions of these inhibitors were prepared using DMSO.

### **2.1.5 Phosphodiesterase assay reagents**

Tritiated cAMP (8-<sup>3</sup>H adenosine 3' 5' cyclic phosphate ammonium salt) and tritiated cGMP (8-<sup>3</sup>H guanosine 3' 5' cyclic phosphate ammonium salt) were from Amersham. cAMP, cGMP, Western Diamondback Rattlesnake venom (*Crotalus atrox*), sodium dodecyl sulphate, Calmodulin (Phosphodiesterase 3':5'-Cyclic Nucleotide-Activator), Dowex 1 Strongly Basic Anion Exchanger and β-mercaptoethanol were from Sigma. Optiphase Scintillation Liquid was obtained from Wallac UK.

The PDE inhibitors were all purchased from Sigma: Vinpocetine, EHNA (Erythro-9-(2-Hydroxy-3-nonyl)-adenine hydrochloride), Amrinone, Rolipram, Zaprinast and IBMX (3-Isobutyl-1-methylxanthine).

## **2.2 Methods**

### **2.2.1 Bacterial growth media**

Sterile reagents and equipment, as well as aseptic techniques, were used for all manipulations involving bacteria. Heat-labile ampicillin was prepared as a stock of 50mg/ml using sterile Milli Q water and then filter-sterilised using a 0.22μ membrane filter unit. These were prepared in advance and stored in 1ml aliquots at -20°C until needed.

#### **2.2.1.1 Minimal media**

Minimal media containing agarose (1.5% w/v) was prepared for the growth of *E. coli* in the preparation of calcium-chloride competent cells. M-9 minimal media was prepared as shown in Table 2.1.



**Table 2.1** M-9 Minimal media preparation

<b>grams per 1000ml</b>	<b>Reagent</b>
6.0	Na <sub>2</sub> HPO <sub>4</sub>
3.0	KH <sub>2</sub> PO <sub>4</sub>
0.5	NaCl
1.0	NH <sub>4</sub> Cl
15.0	Agarose

Above reagents were mixed and sterilised by autoclaving for 20 minutes, 15 Psi and 121°C. When cooled to ~40°C, the following were added pre-sterilised:

2.0ml	1M MgSO <sub>4</sub>
0.1ml	1M CaCl <sub>2</sub>
10.0ml	20% Glucose
1.0ml	1M thiamine

Once all the above reagents were mixed, the molten solution was poured into sterile, round petri dishes (~15ml per plate) and allowed to set fully (~1 hour). Unused plates were stored, lid down, at 4°C. To grow *E. coli* for the preparation of competent cells, a sterile loop was used to take a sample of the required strain from a 40% glycerol stock (see 2.2.2) and streaked across the minimal media to allow for single bacterial colonies to grow. Plates were incubated at 37°C overnight.

### 2.2.1.2 LB media

Millers LB media was routinely used for the growth of *E. coli* transformed with the required plasmid for small-scale and large-scale DNA purification. 25g of the media were mixed with 1L of Milli Q water and sterilised by autoclaving. Filter-sterilised ampicillin was added when the media cooled to ~40°C to a final concentration of 100µg/ml. LB media with agar (1.5%) was also routinely prepared and for these agar was added to the LB media before autoclaving the media. Once this had cooled, ampicillin was added (100µg/ml) to the molten mixture, mixed and the media poured into sterile petri dishes as before. These plates were stored at 4°C for up to two weeks. Plates containing antibiotic were used to select for transformant colonies containing plasmids (with or without PDE1A1 ORF) which

possessed ampicillin-resistance.

### **2.2.2 40% Glycerol Stock preparation**

0.6ml of an overnight bacterial culture were mixed with 0.4ml of sterile 100% glycerol, to give a 40% stock, and vortex mixed. These were stored at -70°C for approximately six months after which fresh glycerol stocks were prepared.

### **2.2.3 Preparation of Calcium-Chloride Competent *E. coli* cells**

A minimal agar plate was streaked with the required strain of *E. coli* cells from a 40% glycerol stock and incubated at 37°C for 16-18 hours (overnight). A single colony was selected for inoculation into 5ml of sterile LB media and incubated in a shaking 37°C incubator for a further 16-18 hours. The 5ml overnight culture was added to 500ml of sterile media and allowed to grow to an OD<sub>600</sub> of 0.6. Once this target OD<sub>600</sub> had been reached, the culture was placed on ice for 1 ½ hours and then centrifuged at 3,600rpm at 4°C for 25 minutes. The supernatant was discarded and the cells resuspended in 500ml of ice cold 100mM calcium chloride. The resuspended cells were left on ice for a further 45 minutes and then centrifuged as before. The supernatant was discarded and the cells finally resuspended in a solution containing 5ml of ice cold 100mM calcium chloride and 20% glycerol. The competent cells were aliquoted in 200µl volumes into sterile pre-cooled 1.5ml eppendorf tubes and snap-frozen in liquid nitrogen before being stored at -70°C for approximately six months. Storing competent cells in this manner will have tended to reduce the transformation efficiency to a small extent but this did not affect the experiments for which they were used.

### **2.2.4 Transformation of Competent *E. coli* cells by the heat-shock method**

50µl of competent cells were placed in the required number of chilled 1.5ml eppendorf tubes. 10µl (1 - 50ng) of the required plasmid DNA were then added to the cells and mixed gently but thoroughly. The tubes were left on ice for 45 minutes and then placed into a 42°C waterbath for exactly 90 seconds followed by chilling on ice for 30 seconds. 50µl of LB media were added to all the tubes and the cells allowed to recover in a 37°C shaking

incubator for 45 minutes. All of the mixture (110 $\mu$ l) was plated out onto LB agar plates containing 100 $\mu$ g/ml ampicillin. Plates were left in a 37°C incubator overnight.

### **2.2.5 Growth of bacterial cultures for plasmid DNA purification**

For small scale DNA purification, a single transformant colony or 10 $\mu$ l of a 40% glycerol stock (usually stored at -70°C) of the required *E. coli* strain were inoculated into 5ml LB(ampicillin) and allowed to grow for 16 hours (overnight) at 37°C in a shaking incubator (200 rpm).

For large scale DNA purification, a single transformant colony or 10 $\mu$ l of a 40% glycerol stock were inoculated into 5ml LB with ampicillin and allowed to grow for 6 hours. This 6-hour culture was added to 500ml of LB(ampicillin) and left to grow overnight.

#### **2.2.5.1 Small scale plasmid DNA purification**

Samples prepared using the small scale DNA purification procedure were used to screen 10 - 20 transformant colonies to look for the desired clone using enzyme restriction analysis (2.2.7). Single bacterial colonies obtained from the transformation procedure were inoculated into 5ml LB containing ampicillin. These were incubated in a 37°C shaking incubator overnight (~16 hours). The following day 40% glycerol stocks were made of all the samples and stored at -70°C. 1.5ml of the remaining cultures were centrifuged at maximum speed (14000 rpm) in a bench top centrifuge. The bacterial cell pellets were processed using the Wizard Mini-Prep kit according to the manufacturer's instructions. The final purified plasmid DNA was routinely resuspended in 50 $\mu$ l of sterile Milli Q water. A 1/100 dilution of the DNA was made using water and the sample scanned in a UV/Vis spectrophotometer to ascertain the DNA concentration (2.2.6).

#### **2.2.5.2 Large scale plasmid DNA purification**

This was carried out once the required construct had been identified. Large scale overnight cultures were grown (2.2.5) and plasmid DNA purified using the Qiagen Maxi-Prep kit according to the manufacturers instructions. Purified plasmid DNA was resuspended in

250µl of sterile Milli Q water. The DNA concentration was calculated by scanning a diluted (1/100) sample using a UV/Vis spectrophotometer (2.2.6).

### **2.2.6 Quantitation of purified plasmid DNA**

A 1 in 100 dilution was made of the purified DNA (5µl in 495µl of dH<sub>2</sub>O) and the sample scanned over a wavelength range of 200nm to 350nm in a UV/Vis spectrophotometer (Cecil 2021/2000 Series) using a quartz cuvette with a path length of 1cm. The concentration of the DNA was calculated using the formula:

$$50 \times \text{Dilution factor (100)} \times \text{OD}_{260} = [\text{DNA}] \mu\text{g/ml}$$

where, at OD<sub>260</sub> one absorbance unit is equivalent to 50µg/ml of double stranded DNA (40µg/ml of single stranded RNA and 20µg/ml of oligonucleotides).

The ratio of OD readings at OD<sub>260</sub> and OD<sub>280</sub> determines the purity of the purified DNA and this ratio should be in the range 1.8 - 2.0 with lower ratios obtained for less pure DNA samples (Sambrook *et al.*, 1989).

### **2.2.7 Restriction Enzyme Analysis**

This was routinely carried out on DNA purified from the small scale DNA purification procedure to screen for the required clone(s) before proceeding to large scale DNA purification of the construct(s). Once the clone had been identified and large scale DNA purification carried out, enzyme restriction analysis using a combination of restriction enzymes was carried out for the confirmation of the clone. Where more than one restriction enzyme was used, the volume of the mixture was adjusted by adjusting the amount of water added. In most cases, when DNA from the Mini-Prep procedure was used, the enzyme digestion mixture comprised only of the DNA, restriction enzyme and the restriction buffer with no added water as the yield from these procedures tended to be lower than those obtained from the Maxi-prep procedures. DNA samples of higher concentration usually required diluting for the digestion process. In general, ten units of enzyme were used for each reaction where one unit is defined as the amount of enzyme required to completely

digest 1µg of DNA in one hour at the optimum temperature.

A mixture comprising of 8µl (500ng - 1µg) of purified DNA, 1µl (10 enzyme units) of the restriction enzyme and 1µl of 10x Restriction Buffer was prepared and incubated at 37°C (optimum temperature for the enzyme) for approximately 2 hours and then subjected to agarose gel electrophoresis (2.2.8). When a digestion required the use of two different enzymes with different optimum working temperatures - as with *Sma*I (30°C) and *Bam*HI (37°C) - the mixture was incubated at the lower temperature first followed by incubation at the higher temperature.

## **2.2.8 Agarose gel electrophoresis**

### **2.2.8.1 Reagents for agarose gel electrophoresis**

<b>50x TAE Buffer (1L)</b>	242g Tris base 57.1ml glacial acetic acid 100ml 0.5M EDTA Made up to 1L with Milli Q water and autoclaved.
<b>6x DNA gel loading buffer</b>	10mM Tris pH6.8 1mM EDTA 40% sucrose 0.25% Bromophenol Blue dye
<b>Ethidium Bromide</b>	10mg/ml stock solution (0.5µg/ml working strength)
<b>1 kb and 1 kb Plus DNA ladders</b>	1mg/ml stock (50ng/µl working strength) (1 kb Plus ladder had more markers <0.5 Kb)

### **2.2.8.2 Preparation of 0.4 - 1.0% Agarose gels**

Agarose gel electrophoresis allowed the separation of the DNA fragments obtained following enzyme restriction analysis. Lower percentage gels (0.4% - 0.6%) were used to

separate larger DNA fragments (>1 kb) while higher percentage gels (1%) were used to separate smaller DNA fragments (<1 kb). A Biorad flat-bed horizontal mini-gel system was used for the agarose gel electrophoresis.

0.4g or 1.0g of agarose were added to 100ml of 1x TAE buffer for the preparation of 0.4% and 1% gels respectively. The mixture was heated to boiling point (~ 2 minutes) in a microwave to completely dissolve the agar. Once this had cooled to ~40°C, ethidium bromide was added to give a final concentration of 0.5µg/ml. This was mixed into the molten agar thoroughly and the molten mixture poured into a horizontal gel mould. A shark's tooth comb (either 8- or 15-well) was inserted into the gel about a 1/3rd of the way down the gel. This was allowed to set fully (~1 hour) before the comb was firmly pulled out of the gel which was then placed into an electrophoresis tank filled with 1x TAE buffer containing ethidium bromide (0.5µg/ml) so that the gel was completely immersed in the buffer.

#### **2.2.8.3 Sample preparation**

2µl of 6x DNA gel loading buffer were added to the 10µl (250-500ng) of the DNA sample to be analysed, mixed, then briefly pulse-centrifuged before loading into the wells of the gel. 5 - 7µl of the diluted DNA marker ladder (1 kb or 1 kb plus) were also loaded into one of the wells of the gel.

#### **2.2.8.4 Flat-bed agarose gel electrophoresis**

Once the DNA samples and the marker had been loaded into the gel, electrophoresis was carried out at 60V for ~1 hour or until the dye front had reached the bottom of the gel.

#### **2.2.8.5 Visualisation of samples**

Gels were removed from the electrophoresis tank and placed onto a UV Transilluminator (LKB 2011 Macrovue) platform for visualisation of the DNA fragments. A polaroid photograph was taken of the gel.

## **2.2.9 DNA extraction and purification from agarose gels**

In some instances, it was necessary to purify DNA fragments from agarose gels following enzyme restriction analysis of the plasmid containing the desired ORF. This extracted and purified ORF was then used for cloning into another plasmid. The Wizard DNA Clean-up kit was used for purification of DNA fragments from gels. Enzyme restriction analysis digestions prior to cloning were also cleaned using the Wizard DNA Clean-up kit.

The desired DNA fragment was located using a UV Transilluminator and the band excised from the gel using a clean scalpel. Exposure to the UV was kept to a minimum in order to minimise chances of mutations occurring in the ORF. The excised DNA bands were placed in a 1.5ml eppendorf tube and frozen at -20°C overnight. These were then allowed to thaw briefly and a sterile spatula used to break up the agarose to release the DNA. DNA was purified from the agarose using the Wizard DNA Clean-up kit according to manufacturers instructions. Bound DNA was eluted from the Minicolumn using 50µl of warm sterile Milli Q water. In most cases, the amount of DNA retrieved by this method was quite poor so no attempt was made to quantify the DNA. For the cloning experiments, the maximum amount of the purified DNA was used.

## **2.2.10 Automated DNA sequence analysis**

### **2.2.10.1 Sample preparation for DNA sequence analysis**

A reaction mixture consisting of 4µl of construct DNA (50ng/µl), 1.6µl of either forward or reverse primer (1pmol/µl), 2µl each of 5x sequencing buffer and Dye Terminator, made up to 10µl with water, was subjected to a cycling reaction (90°C for 10 seconds, 50°C for 5 seconds, 60°C for 4 minutes; repeated for 25 cycles). The Dye Terminator method was used whereby growing chains of DNA were labelled with four different dyes attached to chain terminators (ddATP, ddCTP, ddGTP, ddATP). Ethanol precipitation of the resulting DNA was then carried out as described in section 2.2.10.2. Precipitated DNA was resuspended in 20µl of Template Suppression Reagent and the sample then loaded onto an Applied Biosystems ABI Prism DNA Analyzer machine which analysed the labelled DNA.

### **2.2.10.2 Ethanol precipitation**

Ethanol precipitation was carried out following the cycling reaction of the construct DNA. A tenth of the volume (1µl) of the total sample volume (10µl) of 3M sodium acetate pH 5.2 was added to the sample, followed by two and half volumes of ice cold 100% ethanol. This was mixed and left on ice for approximately 20 minutes then centrifuged at maximum speed (14,000 rpm) in a bench top centrifuge at 4°C for 10 minutes. The supernatant was discarded and the pellet washed twice with 500µl of ice cold 70% ethanol. This was vortex mixed and centrifuged as before. The final pellet was air-dried for about an hour and then resuspended in 20µl of the Template Suppression Reagent. Automated DNA sequence analysis was performed on this sample using the ABI Automated Sequencer.

### **2.2.11 Phosphodiesterase activity assay**

#### **2.2.11.1 Dowex slurry preparation (1:4 slurry)**

100g of the Dowex resin were placed in a 1L duran bottle and approximately 800ml of 0.5M hydrochloric acid added to the resin. The resin was mixed gently and left to stand for approximately 20 minutes after which the acid was poured away. The resin was washed three times with 800ml deionised water and then left in ~800ml of 0.5M sodium hydroxide for ~20 minutes. The alkali was then discarded and the resin washed with water as before and then left in 0.5M hydrochloric acid for ~20 minutes. The resin was finally washed 4 - 5 times before being made up to 500ml volume using deionised water to provide a 1:4 slurry. The pH of the resin was adjusted to ~pH 7.5 with 10M sodium hydroxide. Sodium azide (0.01%) was added to the slurry which was stored in a sealed bottle at room temperature. The pH of the slurry was usually checked prior to use.

#### **2.2.11.2 PDE assay buffer**

A 10x stock of the assay buffer was prepared and stored in 1ml aliquots at -80°C. 20ml of stock consisting of 40mM Tris pH 8.0, 20mM magnesium chloride, 43mM β-mercaptoethanol and 100mg Rattlesnake venom were mixed and aliquoted into 1.5ml eppendorf tubes for storage at -70°C.



### 2.2.11.3 PDE bioassay

This was carried out according to the method of Thompson and Appleman (1971). A One-step procedure was adopted throughout the present work. In this case, two consecutive reactions were performed in a single reaction mixture with the first part of the reaction involving the conversion of 3', 5' cAMP to 5'-AMP product by PDE and the second part involving the conversion of the 5'-AMP product to adenine (uncharged) and inorganic phosphate by the action of nucleotidase contained in the snake venom. The uncharged adenine ( $^3\text{H}$  - labelled and unlabelled) was separated by the anion exchange resin Dowex which was removed from the reaction mixture by centrifugation. The cleared supernatant was mixed with scintillation fluid for analysis.

A master reaction mixture was prepared comprising for both the cAMP and cGMP assays as follows:

**cAMP master mixture**      1ml 10x PDE assay buffer  
   217 $\mu\text{l}$  10 $\mu\text{M}$  cAMP (217nM)  
   5 $\mu\text{l}$   $^3\text{H}$ -cAMP (33nM)

**cGMP master mixture**      1ml 10x PDE assay buffer  
   178 $\mu\text{l}$  10 $\mu\text{M}$  cGMP (178nm)  
   10 $\mu\text{l}$   $^3\text{H}$ -cGMP (72nM)

Reactions comprised of either 24.44 $\mu\text{l}$  of the cAMP master mixture or 23.76 $\mu\text{l}$  of the cGMP master mixture together with 165.56 $\mu\text{l}$  or 166.24 $\mu\text{l}$  of Milli Q water respectively. These were pre-warmed to 30°C before starting the reactions by adding 10 $\mu\text{l}$  of the supernatant sample to be analysed to the mixture and incubated at 30°C for exactly 15 minutes. The reaction was stopped by adding 20 $\mu\text{l}$  of 10% SDS. 1ml of the mixed Dowex slurry was added to the sample tubes and mixed gently for 10 minutes. Samples were then centrifuged in a benchtop centrifuge at maximum speed for 5 minutes. 0.5ml of the supernatant sample were transferred into scintillation tubes containing 4.5ml Optiphase scintillation liquid. These were vortex-mixed briefly and loaded onto a Beckman Scintillation Counter.

Analysis of supernatant samples in the presence of calcium (10-100 $\mu$ M), calmodulin (2-10 units per reaction), with and without the presence of PDE inhibitors (0 - 800 $\mu$ M) was also carried out. In this case, the master mixture was prepared as before and the volume of water adjusted to allow for the calcium, calmodulin and inhibitors added. To determine IC<sub>50</sub> values for the PDE inhibitors used (0 - 800 $\mu$ M inhibitor range), a constant substrate concentration of 0.25 $\mu$ M was used for both cAMP and cGMP.

For the analysis of the samples to determine the  $K_m$  values for each of the substrates, master mixtures were prepared without the substrates so that individual tubes had a range of substrate concentrations for both cAMP and cGMP (0.1 $\mu$ M - 10 $\mu$ M).

## **2.2.12 Sodium dodecyl sulphate polyacrylamide gel electrophoresis (SDS PAGE)**

### **2.2.12.1 Reagents for SDS PAGE**

Solutions were all prepared in sterile Milli Q water and stored at room temperature unless otherwise stated.

<b>5x Tris-Glycine Buffer (500ml)</b>	7.55g Tris-HCl
	47g Glycine
	25ml 10% SDS
	Dissolved in ~400ml Milli Q water then made up 500ml with water.

<b>1M Dithiothreitol (DTT) stock</b>	154mg
	1ml water

This was stored in 50 $\mu$ l aliquots at -20°C. A single aliquot was thawed when needed and any remaining was discarded.

<b>10% Ammonium Persulphate (APS)</b>	0.1g APS
	1ml water

This was stored in 200 $\mu$ l aliquots at -20°C. Once thawed, any remaining solution was discarded.

**2x SDS Gel Loading Buffer**            100mM Tris-HCl pH 6.8  
(10ml)                                    4% SDS  
   20% Glycerol  
   0.2% Bromophenol Blue dye

**6x SDS Gel Loading Buffer**            350mM Tris-HCl pH 6.8  
(10ml)                                    10% SDS  
   30% Glycerol  
   1.2% Bromophenol Blue dye

Both the 2x and 6x gel loading buffers were filtered using a 0.22 $\mu$ m filter to remove any undissolved dye.

**Ultra Pure Protogel**                    30% Acrylamide (w/v), 0.8% (w/v) Bis-acrylamide  
   (37.5:1). This was purchased ready-mixed from  
   National Diagnostics.

**Destaining Solution (1L)**            300ml Methanol  
   100ml Glacial Acetic Acid  
   Made up to 1L with Milli Q water and stored in an  
   air-tight container.

**Coomassie Blue R-250 stain**        0.2g Coomassie Blue dye  
   Dissolved in 100ml Destaining solution.

The Coomassie stain was filtered before use to remove any undissolved dye particles and then stored at 4°C in an air-tight container when not in use. This stain was routinely re-used for staining up to 10 -15 gels before being replaced.

### 2.2.12.2 Preparation of the gels for SDS PAGE

Gels were prepared according to the method of Laemmli (1970). Table 2.2 gives the composition of the resolving and stacking gels for 10% and 12% resolving gels. The volumes given in this table were enough to prepare two mini-gels.

**Table 2.2** Composition of the separating and stacking gels for SDS PAGE.

Reagent	Separating (resolving) gel		Stacking gel
	10%	12%	(5%)
dH <sub>2</sub> O	3.75ml	2.75ml	3.551ml
30% Protogel	5.0ml	6.0ml	867μl
1M Tris pH 8.0/8.8 (400mM)	6.0ml	6.0ml	-
1M Tris pH 6.8 (130mM)	-	-	676μl
10% SDS	120μl	120μl	52μl
10% APS	120μl	120μl	52μl
TEMED	12μl	12μl	5.2μl
<i>Total volume</i>	<i>15.002ml</i>	<i>15.002ml</i>	<i>5.203ml</i>

The separating gel was prepared in a 20ml universal container placed on ice. The mixed solution was poured between the two glass plates of the gel assembly apparatus up to 3cm from the top of the inner glass plate. This was allowed to polymerise for ~1 hour. The stacking gel was then prepared and poured over the top of the separating gel. A comb (10- or 15-well) was immediately inserted into the stacking gel. This was left for a further 1 hour to fully polymerise. Gels were transferred and positioned vertically into the electrophoresis tank containing 1x tris-glycine tank buffer. The comb was removed from the stacking gel and the wells gently rinsed with the tank buffer.

### 2.2.12.3 Sample preparation and SDS PAGE

Samples to be analysed were mixed with either 2x SDS protein gel loading buffer or 6x SDS protein gel loading buffer. DTT was added to the samples to give a final concentration of 200mM. These were then boiled for 10 minutes, pulse-centrifuged before

loading into wells of the stacking gel. 6µl of pre-stained protein marker (Biolabs) was also boiled for 10 minutes before loading onto the gel. Electrophoresis was carried out at 70V, 20mA for approximately 1 hour or until samples had crossed the stacking gel. Voltage was then increased to 110V, 30mA and the electrophoresis carried out for a further 2-2 ½ hours or until the dye front had reached the base of the resolving gel. The glass plates, together with the gels, were then removed from the tank and gently separated to release the gel which was carefully lifted from the glass plates. The gel was either further processed for Western blot analysis (section 2.2.14) or placed into Coomassie staining solution for up to 1 hour. Gels were destained using the destaining solution with at least 2 - 3 changes of the destaining solution before being left overnight to destain fully. Destained gels were either preserved by drying or processed further for silver staining (section 2.2.13). Coomassie staining of gels to visualise the separated proteins was routinely carried out but the sensitivity of this stain meant that the protein had to be present in up to microgram amounts for it to be visualised by this method. So if very little protein was seen using Coomassie stain, completely destained gels were then processed for silver staining of the proteins. Silver staining allowed the visualisation of proteins present in the nanogram range.

## **2.2.13 Silver staining of SDS PAGE gels**

### **2.2.13.1 Reagents for silver staining of SDS PAGE gels**

<b>Fixing Solution</b>	8ml 50% Glutaraldehyde solution Made up to 100ml with Milli Q water (8% v/v).
<b>Silver staining solution</b>	0.5g silver nitrate Made up to 100ml with Milli Q water (0.5% w/v).
<b>Developer Solution</b>	3g Na <sub>2</sub> CO <sub>3</sub> dissolved in 100ml water 50µl 37% formaldehyde solution Made up to 100 with Milli Q water (3% w/v and 0.02% v/v respectively).

**Gel Storage Solution**                      5ml Acetic acid  
Made up to 100ml with Milli Q water (5% v/v)

### **2.2.13.2 Silver staining procedure**

Coomassie stained gels were completely destained to clear the background as the presence of any Coomassie would have a detrimental effect on the silver staining. Destained gels were completely submerged into the glutaraldehyde fixing solution and left on a rocking platform for one hour. The fixing solution was then discarded and the gels rinsed with Milli Q water several times before being left in water overnight to remove any excess glutaraldehyde from the gel. These were then left in the silver staining solution for one hour on a rocking platform followed by submersion in water for half an hour to remove any excess silver. The protein bands were developed using the developer solution by pouring this solution on to the gel and gently rocking the gels in the solution. Appearance of protein bands usually required about 2 - 5 minutes. When the bands were visible, the reaction was stopped by rinsing the gels with water then finally submerging in a 5% acetic acid solution. Gels could be stored in this solution at 4°C for up to a month but they were usually preserved by drying either the same day (at least one hour after storage in 5% acetic acid) or the following day.

### **2.2.14 Western blotting**

#### **2.2.14.1 Reagents for Western blotting**

**Tris-Glycine Transfer Buffer**            2.424g Tris base  
    11.52g Glycine  
    160ml Methanol  
Made up to 800ml with Milli Q water.

**Tris-Saline Buffer**                            10ml 1M Tris pH 7.0 (10mM)  
(TS Buffer)                                      30ml 5M NaCl (150mM)  
Made up to 1L with Milli Q water

**Blocking Solution**

1g Bovine Serum Albumin

Dissolved in 100ml TS Buffer (1% w/v).

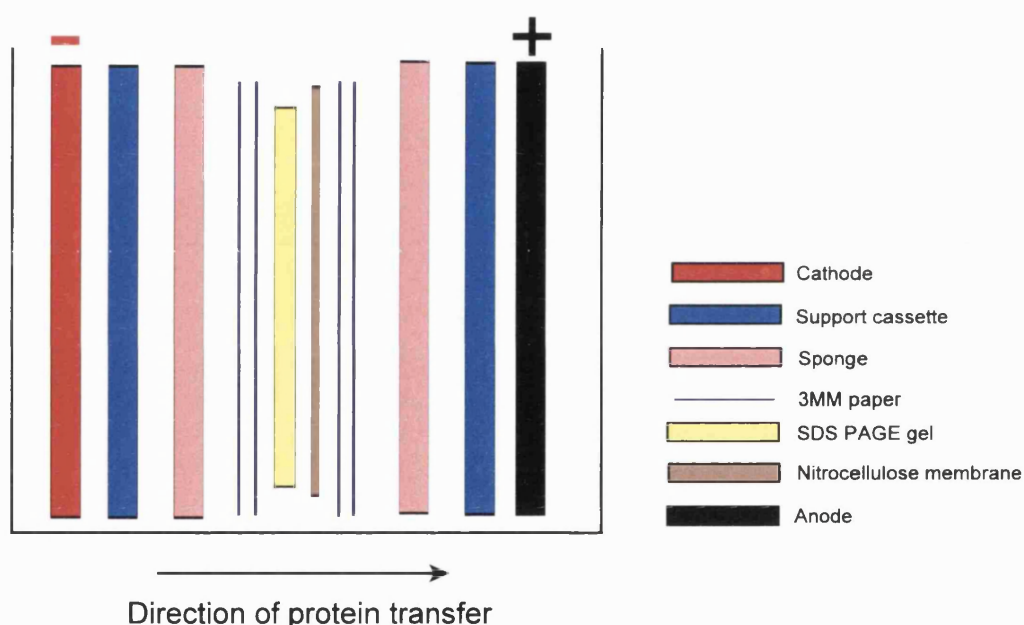
**DAB Peroxidase Substrate**

DAB (3, 3'-Diaminobenzidine) substrate and Urea H<sub>2</sub>O<sub>2</sub> tablets were bought from Sigma. One each of the tablets were dissolved in 20ml of Milli Q water just before use.

**2.2.14.2 Western blot procedure**

SDS PAGE gels run to completion were left to soak in the transfer buffer for about 15-20 minutes before transferring onto a piece of pre-cut nitrocellulose membrane also pre-soaked in transfer buffer. A 'sandwich' was assembled in a support cassette and consisted of a piece of pre-soaked sponge (slightly larger than the gel) overlaid with two pieces of pre-soaked 3MM paper followed by the SDS PAGE gel then the nitrocellulose membrane. A further 2 pieces of pre-soaked 3MM paper were carefully placed over this without disturbing the nitrocellulose membrane and then finally another piece of sponge. This 'sandwich' was placed into the electroblotting tank containing transfer buffer so that the nitrocellulose face forward towards the anode, i.e. direction of the protein transfer (Figure 2.1). Gels were electroblotted at 100V, 150mA for 1 - 1 ½ hours with an ice block placed in the tank to prevent over-heating occurring. The support cassette was then removed from the tank and disassembled. The nitrocellulose membrane containing the proteins was submerged into the blocking solution for approximately one hour on a rocking platform while the gel itself was stained with Coomassie dye to check for untransferred proteins. The membrane was then placed into primary antibody diluted 1/1000 using blocking solution containing 0.05% NP-40 and left at 4°C on a rocking platform overnight. The following day, the primary antibody was carefully removed and retained for further use (stored at 4°C) while the nitrocellulose membrane was washed once in TS buffer, twice in TS buffer containing 0.05% NP-40 and then finally in TS buffer again. Each of these washes were for 10 minutes on a rocking platform at room temperature. The membrane was then placed into a horseradish peroxidase labelled secondary antibody, diluted 1/1000, for two hours on a rocking platform at room temperature. At the end of this period, the secondary antibody was removed and the nitrocellulose membrane washed as before. For

the visualisation of the protein bands, DAB peroxidase substrate was prepared by placing one tablet each of the DAB substrate and Urea H<sub>2</sub>O<sub>2</sub> into 20ml of Milli Q water. When these were completely dissolved, the solution was poured over the nitrocellulose membrane and the time taken for protein bands to appear noted as this gave an indication to the amount of protein present. Generally, signals appeared within the first 10 seconds where a large amount of protein was present but blots were left to develop for up to ten minutes where the protein signal was very faint. The reaction was stopped by discarding the substrate solution and rinsing the membrane in Milli Q water before leaving the blot to dry between two pieces of 3MM paper.



**Figure 2.1** Apparatus used for the Western blot procedure.

### 2.2.15 Determination of protein concentration

Protein concentration was ascertained by using the Bradford Assay (1976). Total protein concentration in crude samples as well as semi/purified samples was measured by this method. The assay involved the use of an acidic solution of Coomassie Blue dye (brown in colour) which changed colour when it was bound to protein. This was reflected in the shift of the absorbance from 465nm to 595nm. The absorbance of the samples, mixed with the acidic Coomassie solution, was measured at 595nm. The reagents for the assay were purchased from Biorad and the recommended protocol was followed. Briefly, a standard



curve using Bovine serum albumin (BSA) was constructed using a range of BSA concentrations (0 - 40 $\mu$ g/ml). Samples to be analysed were diluted 1/10 and 1/100 in water. A 100 $\mu$ l each of the standards and the samples, run in duplicate, were transferred into designated wells of a 96-well microtitre tray. 100 $\mu$ l of the diluted (1/5 in water) Coomassie Blue dye solution were added to all the wells and gently mixed. The absorbance of the reaction mixture was measured using a plate reader (Dynex Technologies - Prior Laboratory Supplies) programmed with the values for the standard curve. Absorbance at 595nm was measured and the protein concentration in samples estimated using the BSA standard curve graph.

#### **2.2.16 Buffers used in bacteria and mammalian cell work**

Buffers common to both bacteria and tissue culture experiments are shown in Table 2.3. Detergents were added to the appropriate buffers where required: 0.01% NP-40 or Triton X-100. Protease inhibitor stocks were prepared using sterile water or DMSO at 20mM stock concentration (1mM for pepstatin) and then added to the buffers to give final working concentrations of 20 $\mu$ M for TPCK, TLCK, Leupeptin and Chymostatin, and 1 $\mu$ M for Pepstatin (Beynon and Salvesen, 1996). PMSF was initially used at a concentration of 1mM with a 100mM stock prepared in isopropanol and stored at -20°C. However, due to the instability of PMSF and the presence of isopropanol (which may have been detrimental to PDE activity), a small amount of PMSF powder was carefully added directly to the resuspended cells.

**Table 2.3** Composition of buffers used for the bacteria and mammalian work.

<b>Buffer Name</b>	<b>Composition</b>
Lysis Buffer 1	50mM Tris-HCl pH8.0 20mM MgCl <sub>2</sub> 1mM DTT 1mM EDTA* 20-30% Glycerol
Lysis Buffer 2	50mM Tris-HCl pH8.0 20mM MgCl <sub>2</sub> 1mM DTT 1mM EDTA*
Lysis Buffer 3	50mM HEPES, pH7.5 20mM MgCl <sub>2</sub> 1mM DTT 1mM EDTA*
Purification Buffer 1	50mM Tris-HCl pH8.0 20mM MgCl <sub>2</sub> 20-30% Glycerol
Purification Buffer 2	50mM HEPES, pH7.5 20mM MgCl <sub>2</sub>
Gel Filtration Buffer 1	15mM HEPES, pH7.5
Gel Filtration Buffer 2	50mM HEPES, pH7.5
Gel Filtration Buffer 3	50mM HEPES, pH7.5 20mM MgCl <sub>2</sub> 200mM NaCl

\* EDTA was omitted from buffers for histidine-tagged proteins which were to be purified using nickel resin.

## Chapter Three

### 3 Cloning and expression of PDE1A1 in pPICZ $\alpha$ C for secreted expression in *Pichia pastoris*

#### 3.1 Introduction

##### 3.1.1 Foreign gene expression in *Saccharomyces cerevisiae*

Early successes on the expression of foreign proteins were achieved with *Escherichia coli* as the host but the use of yeast as a host became more attractive as the nature of the recombinant proteins being expressed became more complex. Yeasts are able to carry out post-translational processing and modifications necessary for many mammalian proteins. The baker's yeast *Saccharomyces cerevisiae* has been well-characterised and used for the expression of the majority of recombinant proteins. The choice of this organism was largely based on its familiarity and the accumulated knowledge about its genetics and physiology. Also, the fact that it had a long history of use in the brewing and baking industries meant that its growth properties at large-scale had been well-studied (Buckholz and Gleeson, 1991). Recombinant protein expression using *S. cerevisiae* was first described in 1981 when Hitzeman and co-workers expressed the human interferon protein as a secreted protein. This was followed by the first genetically engineered vaccine (hepatitis B, HBsAg), expressed intracellularly in yeast, to be licensed by the FDA for administration to human (Valenzuela *et al.*, 1982).

*Saccharomyces cerevisiae* has a well-defined secretory pathway during which proteins undergo post-translational modifications. The secretory pathway enables the localisation of products outside the cell in a soluble, active form which eases the recovery and purification procedures. *S. cerevisiae* secretes very few of its own proteins. The enzymes invertase and acid phosphatase are secreted into the periplasmic space and do not pass into the culture medium. On the other hand, the sex pheromone  $\alpha$ -factor and yeast killer toxin are secreted into the culture medium (Duntze *et al.*, 1970; Esmon *et al.*, 1987). The signal sequence required for the secretion of protein either into the periplasmic space or the culture medium has been used to direct secretion of heterologous proteins (King *et al.*,

1989). The most extensively used signal sequence is that using the prepro region of the mating factor gene (*Mfa1*) which yields the peptide  $\alpha$ -factor (Kurjan and Herskowitz, 1982). The product of this gene is produced as a 165-amino acid precursor molecule containing four copies of the  $\alpha$ -factor, separated by spacer sequences, which is processed in the endoplasmic reticulum and the Golgi apparatus before being released as the mature 13-amino acid  $\alpha$ -factor (Julius *et al.*, 1983, 1984; King *et al.*, 1989). The leader and spacer amino acids appear to contain the signals necessary for proteolytic processing and secretion (Brake *et al.*, 1984). Brake and co-workers (1984) constructed plasmids in which genes coding foreign proteins had been fused to the yeast  $\alpha$ -factor gene. They were able to show the successful expression and secretion of the human epidermal growth factor using this system. The epidermal growth factor (6 kDa) was expressed and secreted to high levels, with over >90% of the material present in the medium (Brake *et al.*, 1984). Proteins such as  $\beta$ -Endorphin (~40 kDa) and calcitonin (~36 kDa), both small proteins, were found to be efficiently secreted using the  $\alpha$ -factor signal sequence (Zsebo *et al.*, 1986). However, secretion of larger proteins such as  $\gamma$ -interferon (~187 kDa) has proven to be difficult with ~95% of the protein remaining trapped in the periplasmic space (Zsebo *et al.*, 1986; King *et al.*, 1989). This trapped protein was released from the cells using oxalyticase and glass beads. However, the secretion of heterologous proteins is not only dependent on the size of the protein but factors such as the charge of the protein and its glycosylation also determine its secretion from the host cell into the medium (De Nobel and Barnett, 1991).

Limitations of *S. cerevisiae* as a host for heterologous protein expression include low yield if the foreign protein is toxic to the host as well as hyperglycosylation of proteins which can affect activity of expressed enzymes (Buckholz and Gleeson, 1991). Most of the promoters used to express heterologous proteins must also be present on multi-copy plasmids for high levels of expression. When these systems are scaled-up to fermenter levels, plasmid stability can become a significant problem. Also, the increased number of generations to accumulate cell mass in a fermenter may allow for the succession of non-expressing strains over the desired strains. To overcome some of these problems, alternative yeast systems have been explored and these are discussed in section 3.1.2.

### 3.1.2 Expression in non-*Saccharomyces* yeasts

Yeast expression systems that have been used as alternatives to *S. cerevisiae* include *Schizosaccharomyces pombe*, containing alcohol dehydrogenase (*ADH*) promoter, as well as *Kluyveromyces lactis* and *Kluyveromyces fragilis* which are able to utilise lactose as the sole carbon source (Reiser *et al.*, 1990). Non-*Saccharomyces* yeasts that have received most attention are the methylotrophic yeasts belonging to the genera *Pichia*, *Hansenula*, *Candida* and *Torulopsis*. These yeasts are able to utilise methanol as the sole carbon source. The initial steps of this utilisation occurs in membrane-enclosed organelles called peroxisomes which contain the key enzymes, alcohol oxidase, catalase and dihydroxyacetone synthase. Peroxisomes proliferate during growth on methanol and can constitute up to 80% of the cytoplasmic volume of the cell (Hagenson, 1991). Alcohol oxidase is the first enzyme in the pathway of methanol utilisation and it oxidises methanol to formaldehyde, generating hydrogen peroxide in the process. Since this occurs in peroxisomes, the toxic hydrogen peroxide is sequestered away from the rest of the cell.

The ability of certain yeast species to grow on methanol as the sole carbon source was first described in the 1960s by Ogata and co-workers (1969) prior to which methanol utilisation was known to occur only in bacteria such as *Pseudomonas methanica*. Subsequent biochemical studies have revealed that methanol utilization occurs via a novel metabolic pathway involving several unique enzymes, and some of these enzymes are present at substantial levels only when the cells are grown on methanol. The most tightly regulated of these enzymes is alcohol oxidase (*AOX*), first enzyme in the methanol-utilisation pathway. This enzyme is absent in the presence of even a small amount of glucose, glycerol or ethanol. Based on this observation, it was predicted that the *AOX* promoter would be suitable for the expression of foreign genes and thus a substantial body of work followed on this yeast. The enzyme has a poor affinity for oxygen and the methylotrophic yeasts compensate for this deficiency by synthesising large amounts of the enzyme (Higgins and Cregg, 1998).

The first industrial application of the methylotrophic yeasts was for the production of single-cell protein (SCP) for marketing as a high protein animal feed by the Phillips Petroleum company (Wegner, 1990; Hagenson, 1991). *Pichia pastoris* was selected from

the yeasts screened for the production of SCP on the basis of higher cell mass yield from methanol, higher protein content and stable fermentation characteristics. The yeast *Hansenula polymorpha* has also been developed commercially for the production of foreign proteins (Faber *et al.*, 1995; Hagenon, 1991).

### **3.1.3 *Pichia pastoris* expression system**

#### **3.1.3.1 The alcohol oxidase promoter**

The development of the *P. pastoris* expression system has been based around the use of the methanol-inducible promoter for alcohol oxidase (*AOX*) (Hagenon, 1991). There are two genes in *P. pastoris* coding alcohol oxidase : *AOX1* and *AOX2*. *AOX1* is responsible for the vast majority of alcohol oxidase activity in the cell (Cregg *et al.*, 1989). Expression of *AOX* enzyme is controlled at the level of transcription. In methanol-grown cells, ~5% of polyA+ RNA is from the *AOX1* gene, whereas in cells grown on other carbon sources, the *AOX1* message is undetectable. *AOX2* is about 97% homologous to *AOX1* and has approximately the same specific activity as that of *AOX1*. However, growth on methanol is much slower than with *AOX1*. Loss of the *AOX1* gene, and thus a loss of most of the cell's alcohol oxidase activity, results in a strain of *P. pastoris* that is phenotypically **Methanol Utilization Slow (Mut<sup>s</sup>)**. These cells exhibit slower growth on methanol medium requiring approximately 30 hours per generation. **Methanol Utilization Positive (Mut<sup>+</sup>)** refers to the wild-type ability of strains to metabolize methanol and these strains have a generation time of approximately 5 hours (Cregg *et al.*, 1989).

#### **3.1.3.2 Expression vectors for *Pichia pastoris***

Expression vectors developed for the expression of foreign proteins in *P. pastoris* contain DNA sequences for growth and selection in *E. coli* and *P. pastoris* strains. They also contain a foreign gene expression cassette which is composed of DNA sequences containing the *P. pastoris AOX1* promoter, followed by one or more unique restriction sites for insertion of foreign gene as well as a gene conferring antibiotic resistance (Higgins and Cregg, 1998). The vectors pPIC3K and pPIC9K contain the bacterial kanamycin resistance gene while the pPICZ series of vectors contain the *Sh ble* gene from *Streptoalloteichus*

*hindustanus* which confers resistance to zeocin in *E. coli* as well as *P. pastoris*. Sequences encoding affinity tags such as polyhistidine tags are also used to tag foreign proteins to allow for ease of purification using affinity chromatography.

Vectors containing the gene of interest are linearised to generate stable transformants of *P. pastoris* strains through homologous recombination between sequences shared by the vector and host genome. Cleavage of the vector within a sequence shared by the host genome stimulates homologous recombination leading to target integration of the vector (containing the expression cassette) to the genomic locus (Cregg and Higgins, 1994). In the present work, the vector pPICZ $\alpha$ C was used and this contained a *PmeI* enzyme restriction site located within the *AOX1* promoter region (see Figure 3.1.1). Cleavage at this restriction site was carried out to linearise the vector and stimulate homologous recombination of the vector with the host genome. However, the frequency of the homologous recombination process occurs at a lower frequency than with *S. cerevisiae* (Cregg and Higgins, 1994).

The *P. pastoris* expression vectors have been designed to allow either intracellular or secreted expression of foreign proteins. Secretion of foreign protein requires the presence of a signal sequence on the protein to target it to the secretory pathway. The secretion signal sequence from *S. cerevisiae*,  $\alpha$ -Factor peptide, has been used with most success as already discussed (3.1.1). The vector series pPICZ $\alpha$  and pGAPZ $\alpha$  contain the secretory signal sequence allowing expression of foreign proteins secreted into the growth media. The pPICZ vectors contain the *AOX1* promoter while pGAPZ series of vectors contain a constitutive *P. pastoris* promoter derived from the glyceraldehyde-3-phosphate dehydrogenase gene (GAP). The pGAP vectors offer an alternative to the pPICZ vectors when the foreign gene expression product is not toxic to the host cell.

### 3.1.3.3 Strains of *Pichia pastoris*

There are three main strains of *Pichia pastoris*:

- 1 X-33 which is a wild-type Mut<sup>+</sup> strain (fast utiliser of methanol).
- 2 GS115 which has a disrupted histidine gene (*his4*) and is Mut<sup>+</sup>.
- 3 KM71 which has a disrupted *AOX1* gene (*aox1*) and is therefore Mut<sup>s</sup> (slow utiliser of methanol). This strain is wild-type for the *AOX2* gene.

The advantage of using X-33 and GS115 is the shorter generation time needed during cell growth in methanol-containing medium. However, these strains need to be screened for the methanol phenotype to ensure foreign gene insertion does not disrupt the *AOX1* gene which would make these cells Mut<sup>s</sup>. Although KM71 are slower growing in methanol medium, some foreign proteins are better expressed in this strain. Also, these transformants do not need to be screened for methanol phenotype.

### 3.1.3.4 Expression of foreign proteins in *Pichia pastoris*

Many heterologous proteins have been expressed as intracellular and secreted proteins using the *P. pastoris* expression system. Some of these are shown in Table 3.1.

**Table 3.1** Proteins expressed using the *Pichia pastoris* expression system.

<b>Protein</b>	<b><i>P. pastoris</i> vector/strain</b>	<b>Reference</b>
<b>Intracellular expression:</b>		
β-galactosidase	pSOAH, pT76H4/GS115	Tschopp <i>et al.</i> , 1987a
Hepatitis B surface antigen (HbsAg)	pBSAG151/GS115	Cregg <i>et al.</i> , 1987
Tumour necrosis factor	pHIL3/KM71	Sreekrishna <i>et al.</i> , 1988
Tetanus toxin	pPIC3/KM71	Clare <i>et al.</i> , 1991
<b>Secreted expression:</b>		
Invertase	pGS102/GS115	Tschopp <i>et al.</i> , 1987b
Insect Venum Antigen 5	pPICZαA/KM71	Monsalve <i>et al.</i> , 1999
Pokeweed antiviral protein	pPICZαC/GS115	Rajamohan <i>et al.</i> , 2000
Mammalian calreticulin	pPIC/KM71	Andrin <i>et al.</i> , 2000
<i>T. cruzi</i> sialidase	pHILD2/GS115	Laroy and Contreras, 2000
Equistatin	pPIC9/GS115 & KM71	Rogelj <i>et al.</i> , 2000

## 3.2 Background and aims of the present study

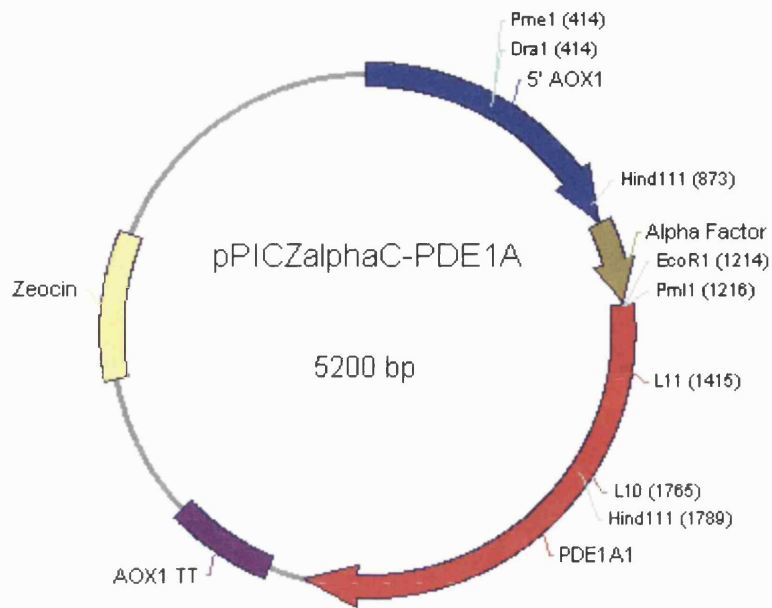
### 3.2.1 Background

The *Pichia pastoris* expression system was set up for the first time in this laboratory for the present work. The system was optimised for the expression of secreted proteins. A control

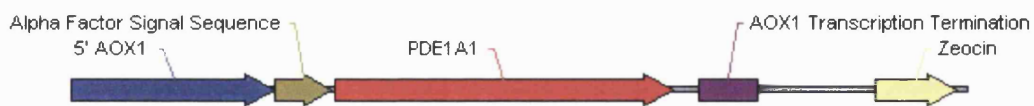


strain was used to check for efficient secretion of proteins using the *P. pastoris* system. Once this had been established, the system was used for the secreted expression of dog heart PDE1A1.

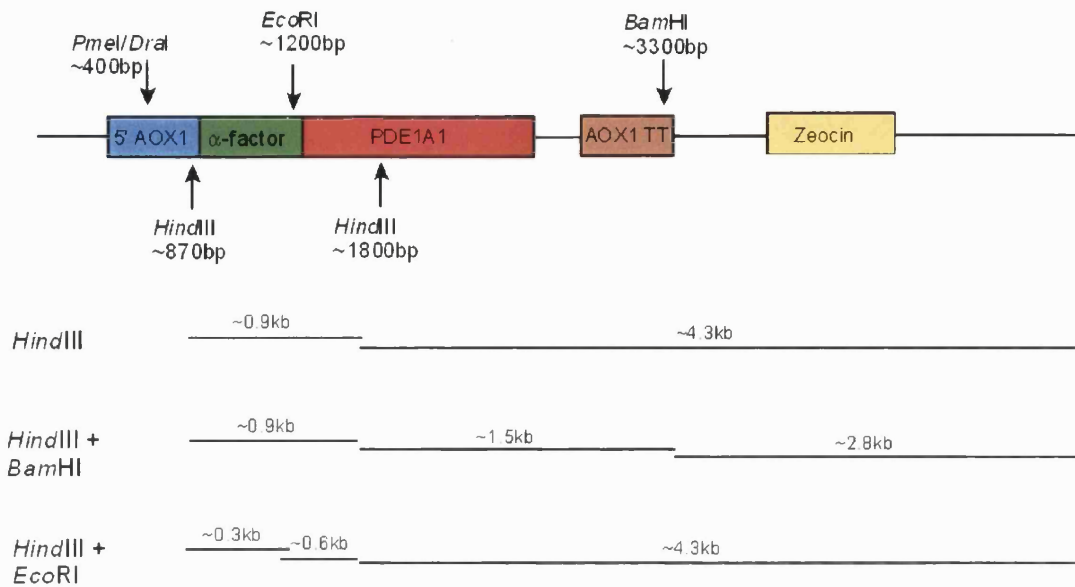
The dog heart PDE1A1 was the focus of the present study. The full-length cDNA for PDE1A1 used was produced using total RNA from dog heart tissue by Clapham and Wilderspin (2001) as already discussed in section 1.8. This cDNA had been cloned into the vector pCR-Script and used as the starting point for the cloning and expression studies using the *Pichia pastoris* expression vector. The full-length open reading frame (~1.6 kb) was excised from this vector using the enzyme *DraI*, as the ORF was flanked by *DraI* restriction sites. The vector pPICZ $\alpha$ C was cut with the enzyme *PmlI* (located within the multiple cloning site) which also produced blunt-ends so the purified ORF was cloned into this site. The vector used for the cloning, pPICZ $\alpha$ C, contained the  $\alpha$ -factor signal sequence for secreted expression in the host *Pichia pastoris*. The ORF was cloned so that it was in-frame with the signal sequence. Figure 3.1.1 shows a schematic map of the vector together with the insert while Figure 3.1.2 shows the linearised expression cassette. Since directional cloning was not carried out in the present work, it was possible that the PDE1A1 ORF would be cloned into the vector in the reverse orientation. A combination of three different restriction enzymes was therefore used to confirm the orientation of the cloned insert. Figure 3.2 shows a schematic for the pPICZ $\alpha$ C-PDE1A1 in the correct (Figure 3.2.1) and the reverse orientation (Figure 3.2.2) together with the DNA fragments expected following restriction enzyme analysis with *HindIII*, *BamHI* and *EcoRI*.



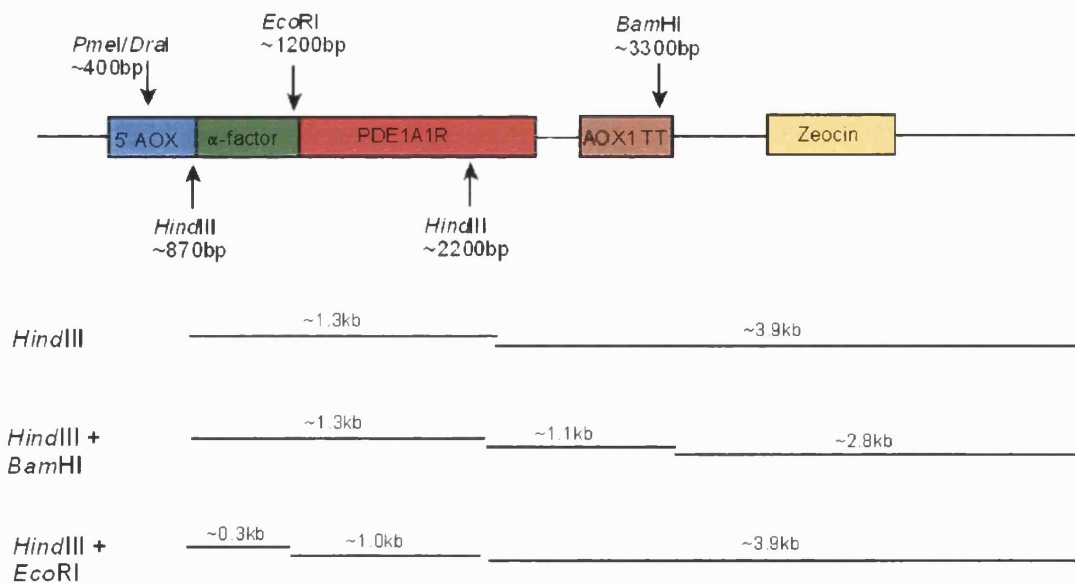
**Figure 3.1.1** Schematic of pPICZ $\alpha$ C-PDE1A1 construct. The position of the PDE1A1 insert together with the enzyme restriction sites in the construct are labelled. The position of the two reverse primers (L10 and L11) used to confirm cloning of the insert in the vector are also indicated. *PmeI* restriction site used to linearise the vector prior to transformation into *Pichia pastoris* cells is shown within the 5' AOX1 region. Abbreviations: AOX1 TT = Alcohol oxidase transcription termination.



**Figure 3.1.2** Expression cassette containing the PDE1A1 insert.



**Figure 3.2.1** DNA fragments expected following enzyme restriction analysis of the insert in the correct orientation in the pPICZ $\alpha$ C-PDE1A1 construct. A schematic of the construct is shown indicating positions of the restriction sites. DNA fragment sizes expected following enzyme restriction analysis with *HindIII*, *BamHI* and *EcoRI* are shown in the lower panel.



**Figure 3.2.2** DNA fragments expected following enzyme restriction analysis of the insert in the reverse orientation in the pPICZ $\alpha$ C-PDE1A1 construct. A schematic of the construct is shown indicating positions of the restriction sites. DNA fragment sizes expected following enzyme restriction analysis with *HindIII*, *BamHI* and *EcoRI* are shown in the lower panel.

### 3.2.2 Aims

- ▶ Establish the *Pichia pastoris* expression system for the secreted expression of heterologous proteins.
- ▶ Cloning and expression of the full-length dog heart PDE1A1 cDNA in pPICZ $\alpha$ C for secreted expression in *Pichia pastoris*.
- ▶ Small-scale expression and purification studies on the recombinant PDE1A1 protein.
- ▶ Scale-up to 10L fermenter for the large-scale expression and purification of recombinant PDE1A1.
- ▶ Purification and biochemical characterisation of the recombinant protein.

### 3.3 Materials

The chemical and DNA reagents were as described in section 2.1. Only those reagents not described before will be described in this section.

Restriction enzymes *DraI*, *HindIII* and *EcoRI*, were from GibcoBRL while *PmeI* and *PmII* were from New England Biolabs. L-Histidine, d-Biotin, Sorbitol, Lennox L Broth Base (low-salt LB) and glass beads (425-600 microns) were from Sigma. Yeast Nitrogen Base (YNB) was purchased from Invitrogen as ready-mixed media for reconstitution according to manufacturers instructions. Potassium phosphate, sodium phosphate, Yeast extract, Peptone, glucose and Select Agar were from BDH. 2mm electroporation cuvettes (sterile, individually wrapped) were from Equibio. Zeocin (100mg/ml) was purchased from Invitrogen.

Freeze-dried supercoiled vector pPICZ $\alpha$ C was purchased from Invitrogen together with stab vials containing three *Pichia pastoris* strains (GS115, KM71 and X-33), and the strain GS115-albumin as the control for the secreted expression of albumin.

## 3.4 Methods

### 3.4.1 Preparation of stocks and media

#### 3.4.1.1 pPICZ $\alpha$ C and *Pichia pastoris* stocks

The supercoiled vector, pPICZ $\alpha$ C, was received freeze-dried (20 $\mu$ g) and was reconstituted with 20 $\mu$ l of sterile, Milli Q water to give a final concentration of 1 $\mu$ g/ $\mu$ l. This was further diluted 1 in 100 to give a working DNA concentration of 10ng/ $\mu$ l. Reconstituted vector was stored at -20°C, and the diluted vector used to transform calcium-chloride competent DH5 $\alpha$  *E. coli* cells as described in section 2.2.4 but grown on low salt LB containing zeocin (25 $\mu$ g/ml), and purified as in section 2.2.5. Confirmation of the purified vector was carried out using enzyme restriction analysis (2.2.7) followed by analysis on agarose gel electrophoresis (2.2.8). 40% glycerol stocks were then prepared for storage at -70°C as already described (section 2.2.2).

The three strains of *Pichia pastoris* used were GS115, KM71 and X33. These were received as stab vials and a sample of each was inoculated into YPD media (see section 3.4.1.2), and allowed to grow in a shaking incubator (200 rpm) at 30°C overnight. 40% glycerol stocks of the cultures were made for long-term storage as described in section 2.2.2. Glycerol stocks for the control strains, GS115/Mut<sup>s</sup> Albumin and GS115/pPICZ/lacZ/Mut<sup>t</sup>, were also prepared in the same way.

#### 3.4.1.2 Protein expression media

Media was prepared using Milli Q water followed by sterilisation by autoclaving. The antibiotic, zeocin, was added once the media had cooled.

#### 10X YNB

13.4% Yeast Nitrogen Base

With ammonium sulphate

Without amino acids

This was bought as a ready-mixed powder which was dissolved in 1L of sterile Milli Q water, filter-sterilised using a 0.2 $\mu$ m filter and stored at 4°C.

<b>Yeast Extract Peptone Dextrose Medium (YPD)</b>	1% Yeast extract 2% Peptone 2% Dextrose ± 1.5% agar for plates ± 100µg/ml zeocin
<b>YPDS</b>	1% Yeast extract 2% Peptone 2% Dextrose 1M Sorbitol ± 1.5% agar for plates ± 100µg/ml zeocin
<b>Minimal dextrose media (MDH)</b>	1.34% YNB 4 x 10 <sup>-5</sup> %w/v Biotin 2% Dextrose ± 1.5% agar
<b>Minimal methanol histidine media (MMH)</b>	1.34% v/v YNB 4 x 10 <sup>-5</sup> %w/v Biotin 0.004% w/v Histidine 0.5% v/v Methanol
<b>Buffered minimal glycerol-complex media (BMGY);</b>	1% Yeast extract 2% Peptone
<b>Buffered minimal methanol-complex media (BMMY)</b>	100mM potassium phosphate, pH 6.0 1.34% YNB 4 x 10 <sup>-5</sup> %w/v Biotin 1% Glycerol or 0.5% methanol

<b>Breaking buffer</b>	50mM sodium phosphate, pH 7.4
	1mM PMSF
	1mM EDTA
	5% glycerol

### **3.4.2 Cloning the full-length PDE1A1 cDNA in pPICZ $\alpha$ C**

#### **3.4.2.1 Purification of PDE1A1 cDNA from pCR-Script-PDE1A1 construct**

As already stated in section 3.2.1, the full-length PDE1A1 ORF had been cloned into the vector pCR-Script by Clapham and Wilderspin (2001). The ORF was flanked by *DraI* restriction sites and the vector contained a single *DraI* restriction site. Restriction digestion with this enzyme would therefore give four DNA fragments including the ORF. Reactions comprising of 1400ng construct DNA (pCR-Script-PDE1A1), 10 units of the enzyme *DraI*, 10x enzyme buffer in a total volume of 10 $\mu$ l were set up in quadruplicate. These were incubated at 37°C for one hour and the products analysed on 1% agarose gels as before (section 2.2.8). The fragments were visualised on a UV Transilluminator and the fragment corresponding to the ORF (~1.6 kb) purified from the gel for subsequent cloning (section 2.2.9).

#### **3.4.2.2 Restriction enzyme digestion of the vector pPICZ $\alpha$ C**

The vector pPICZ $\alpha$ C was digested using *PmII* in a reaction mixture containing 1 $\mu$ g of the vector, 10 units of *PmII*, 10x enzyme buffer in a total volume of 10 $\mu$ l. Sterile milli Q water was used to make up the volume. This was incubated at 37°C for one hour and then the mixture cleaned using Wizard DNA Clean-up kit to remove the restriction enzymes and buffer as before (2.2.9). The cleaned, cut vector was subjected to a dephosphorylating reaction to prevent religation of the vector during the cloning procedure. Reaction mixture comprised of the cleaned vector, 1 unit of calf intestinal alkaline phosphatase (CIAP), 10x CIAP enzyme buffer in a total volume of 50 $\mu$ l, made up to volume with milli Q water as before. The mixture was incubated at 37°C for 15 minutes followed by incubation at 56°C for another 15 minutes before being cleaned using the Wizard DNA Clean-up kit as before.

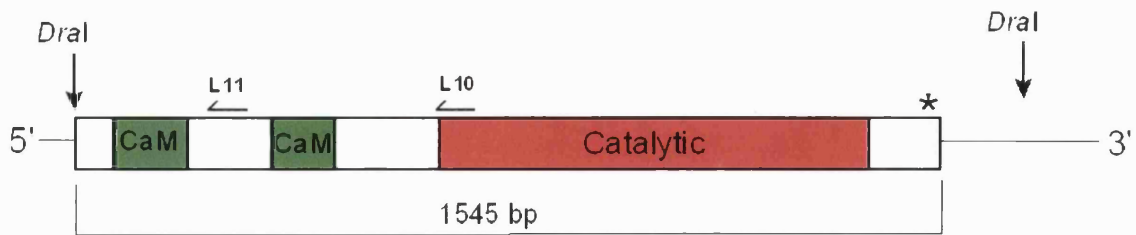


### 3.4.2.3 Ligation of PDE1A1 ORF into pPICZ $\alpha$ C

The purified PDE1A1 ORF and the dephosphorylated vector were mixed in a reaction mixture containing equal volumes of the insert and vector, 1.5 units of T4 DNA ligase and 10x ligation buffer in a total volume of 10 $\mu$ l. This was incubated at 4°C for 8 hours followed by incubation at 15°C for at 24 hours. The ligation mixture was then used to transform calcium-chloride competent *E.coli* DH5 $\alpha$  cells (section 2.2.4). Cells were plated on low salt LB agar plates containing 100 $\mu$ g/ml zeocin and incubated at 37°C overnight. Colonies were inoculated into 5ml low salt LB containing zeocin and grown overnight. Small-scale DNA purification was carried out as described in section 2.2.5.1 and a combination of the restriction enzymes *Hind*III, *Bam*HI and *Eco*RI used to confirm the identity of the correct clone. As already discussed (see section 3.2.1), non-directional (blunt-ended) cloning was carried out so there was a possibility of the insert being cloned in the reverse orientation. Enzymes restriction analysis was used to confirm the orientation of the insert in the vector. Digestion reactions comprised of ~500ng of the purified construct DNA, 10 units of the restriction enzyme (s), 10x enzyme buffer with the total volume made up to 10 $\mu$ l using sterile Milli Q water. These samples were incubated at 37°C for one hour and the products analysed on 1% agarose gels as before (section 2.2.8). Once the construct with the insert in the correct orientation (PDE1) was identified, large-scale DNA purification was carried out as described in section 2.2.5.2.

### 3.4.2.4 Automated DNA sequence analysis

Automated DNA sequence analysis was carried out to confirm presence of the insert in the correct orientation, as described in Chapter two (2.2.10), using two reverse primer, L10 (5'-GGCAAGAAACAGGAATCTTG) and L11 (5'-CTGAGCTCATCTTCAGTATCCAAG). Figure 3.3 shows the hybridisation positions of these primers on the PDE1A1 cDNA.



**Figure 3.3** Schematic of the PDE1A1 ORF showing the position of the sequencing primers. The positions of the two primers, L10 and L11 are shown together with the *DraI* restriction sites used for the cloning of the cDNA. The asterisk marks the position of the stop codon.

### 3.4.3 Transformation of *Pichia pastoris* cells with construct DNA

#### 3.4.3.1 Preparation of competent *Pichia pastoris* cells

10  $\mu$ l of the 40% glycerol stocks of the three *Pichia pastoris* strains (GS115, KM71 and X-33) were inoculated into 5ml YPD media and incubated in a 30°C shaking incubator (200 rpm) overnight. 0.5ml of this were then transferred into 500ml of YPD media a 2-litre flask and left to grow in a 30°C shaking incubator overnight. The OD<sub>600</sub> of the culture was measured using a UV/Vis spectrophotometer to check if the culture had reached the required OD<sub>260</sub> of 1.5 which would be equivalent to approximately  $7.5 \times 10^7$  cells per ml. Cells were harvested by centrifugation at 1500g, 4°C for five minutes then resuspended in 500ml of ice cold H<sub>2</sub>O. Cells were centrifuged as before and resuspended in 20ml of ice cold 1M sorbitol. Cells were centrifuged as before and resuspended in 1ml of ice cold 1M sorbitol. Competent cells were stored on ice and used the same day.

#### 3.4.3.2 *PmeI*-Linearisation of the construct DNA

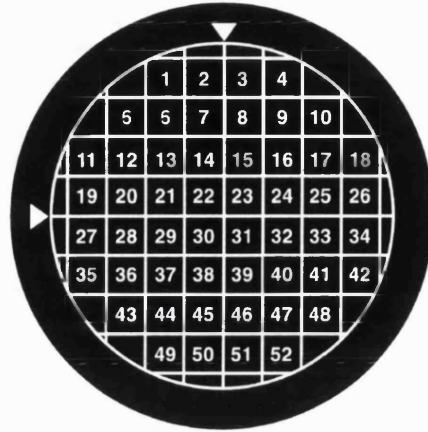
Linearisation of constructs was necessary prior to transformation into *Pichia pastoris* cells to stimulate homologous recombination with the host genome as discussed in section 3.1.3.2. This reaction was carried out in a mixture consisting of  $\sim 15 \mu$ g of construct DNA, 20 units of *PmeI*, 10x restriction enzyme buffer and Milli Q water in a total reaction volume of 10  $\mu$ l. The mixture was incubated at 37°C for one hour then cleaned using the Wizard DNA Clean-up kit as described in section 2.2.9.

### 3.4.3.3 Transformation of *Pichia pastoris* with linearised construct

The linearised construct DNA was used to transform competent *Pichia pastoris* cells (GS115, KM71 and X-33) using the method of electroporation. All reagents used for the electroporation procedure were kept cold on ice. Approximately 7µg of construct DNA were mixed with 100µl of competent *Pichia pastoris* cells in a 1.5ml eppendorf tube before transferring the mixture to a 2mm electroporation cuvette. The mixture was electroporated using a charging voltage of 1500V, capacitance of 25µF and resistance of 200Ω. 1ml of ice cold 1M sorbitol was added immediately to the electroporated cells and the mixture plated out onto YPDS agar plates with 100µg/ml zeocin. Plates were incubated at 30°C for up to three days or until colonies had formed. Glycerol stocks of the control *Pichia pastoris* strains, GS115/Mut<sup>s</sup> Albumin (Mut<sup>s</sup>) and GS115/pPICZ/lacZ/Mut<sup>+</sup> (Mut<sup>+</sup>), were also streaked onto YPDS agar plates containing zeocin. The Mut<sup>s</sup> control was a negative control for growth on zeocin medium while the Mut<sup>+</sup> was a positive control for growth on this medium.

### 3.4.3.4 Determination of the methanol phenotype of transformant colonies

This was carried out to ensure that GS115 and X-33 transformants were still Mut<sup>+</sup> phenotype when grown on methanol-containing medium. Zeocin resistant colonies for all three transformant strains of *Pichia pastoris* (GS115, KM71 and X-33), with the insert in the correct orientation, were selected for methanol phenotype screening. Colonies were picked with a sterile loop and resuspended in 200µl of 1M sorbitol in a 96-well microtitre tray. A template grid was used to draw a grid on the MDH and MMH agar plates (Figure 3.4). Resuspended colonies were then streaked in a regular pattern onto a dedicated grid ensuring MMH plate was streaked before the MDH plate. A sterile toothpick was used for each colony. Control strains for both Mut<sup>+</sup> and Mut<sup>s</sup> were also streaked on both plates. These were the GS115/Mut<sup>s</sup> Albumin and GS115/pPICZ/lacZ/Mut<sup>+</sup> control strains. The plates were incubated at 30°C for up to four days but were examined for growth at day 2 and day 4.



**Figure 3.4** Grid template used for streaking *Pichia pastoris* transformant strains. This template was used to mark both the MDH and MMH plates for methanol phenotype determination.

### 3.4.4 Expression of the GS115/Mut<sup>s</sup> Albumin (Mut<sup>s</sup>) and transformant *Pichia pastoris* cells

#### 3.4.4.1 Secreted expression of albumin

A single colony for the GS115/Mut<sup>s</sup> Albumin (Mut<sup>s</sup>) was inoculated into 25ml of BMGY media and incubated at 30°C shaking incubator until growth of the yeast gave an absorbance of between 2 - 6 units when measured at 600nm using a UV/Vis spectrophotometer. The cells would be in log phase of growth at this stage. Once the cells had reached the required OD<sub>600</sub>, they were centrifuged at 2000g at room temperature for five minutes. The supernatant was discarded and the cell pellet resuspended in BMMY to an OD<sub>600</sub> of 1.0. The flasks were returned to the 30°C shaking incubator to allow expression to occur in the presence of the methanol. These cultures were allowed to grow for up to 5 days and 100% methanol (0.5%v/v) was added every 24 hours to maintain induction. 1ml samples of the cultures were taken at the time points: 0, 24, 96 and 120 hours after induction, i.e. switching of media from BMGY to BMMY. These were centrifuged at maximum speed in a bench top centrifuge and the supernatant separated from the cell pellet. Both were retained and stored at -70°C for analysis by SDS PAGE.

#### **3.4.4.2 Expression studies on *Pichia pastoris* transformant colonies**

GS115/KM71/X-33-PDE1A1 transformant colonies, as well as cells not containing the insert, were treated in the same way as the expression of the GS115/Mut<sup>s</sup>-Albumin for the secreted expression of recombinant PDE1A1. Expression was carried out for up to 5 days and 1ml samples of the culture media removed every 24 hours for monitoring protein expression. These were centrifuged as before and both the cleared media and cell pellet samples retained for analysis; both were stored at -70°C until needed. The cells were lysed using breaking buffer containing PMSF and glass beads (425-600 microns). This mixture was vortex mixed for 4 - 5 times to break up the yeast cells and then centrifuged at maximum speed (14,000 rpm) in a benchtop centrifuge. Cleared total cell lysate (supernatant) was separated from the cell debris and retained for analysis by PDE activity assays as described in section 2.2.11. Western blot analysis using CaM-PDE antibody was carried out on both the cleared culture media as well as the cleared total cell lysate samples as described in section 2.2.14.

### **3.5 Results**

#### **3.5.1 Cloning of PDE1A1 in pPICZ $\alpha$ C**

The PDE1A1 ORF was subcloned into pPICZ $\alpha$ C as detailed in section 3.4.2 and the product used to transform *Pichia pastoris* cells as described in section 3.4.3. Transformed cells were grown on YPDS agar containing zeocin.

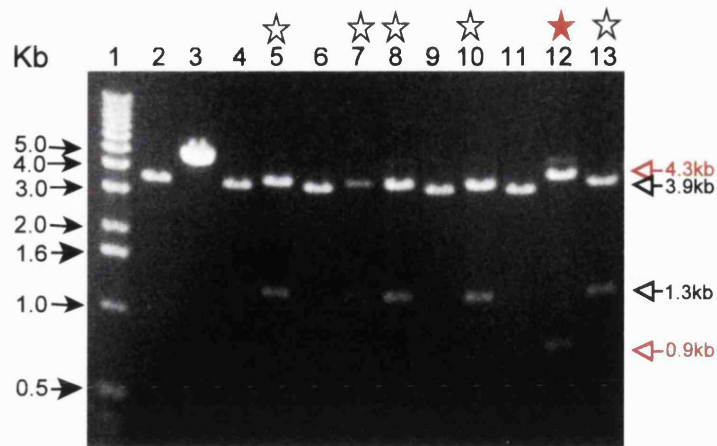
##### **3.5.1.1 Screening transformant colonies**

*Pichia pastoris* transformant colonies were selected on YPDS agar containing zeocin. Twelve single colonies were selected for DNA purification followed by enzyme restriction analysis using *Hind*III. Digestion with this single enzyme was expected to give two DNA fragments of sizes 0.9 and 4.3 kb for the PDE1A1 insert cloned into pPICZ $\alpha$ C in the correct orientation (Table 3.2). Where the insert was cloned in the reverse orientation, 1.3 and 3.9 kb fragments were expected following digestion with *Hind*III (Table 3.2). Figure 3.5 shows the results for the restriction analysis on the twelve transformant colonies. There were five

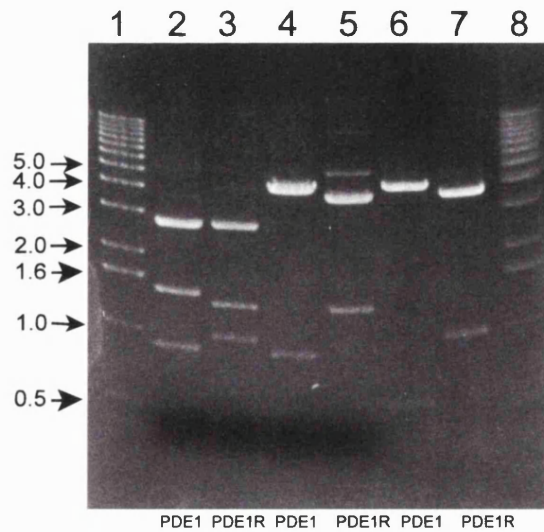
constructs with the insert in the reverse orientation (indicated by the black stars in Figure 3.5) and one construct with the insert in the correct orientation (indicated by the solid red star in Figure 3.5). Figure 3.6.1 shows the enzyme restriction analysis carried out on the single construct with the insert in the correct orientation using a combination of *HindIII*, *BamHI* and *EcoRI* restriction enzymes. This was also carried out for a construct with the insert in the reverse orientation for comparison. Table 3.2 summarises the DNA fragments expected following enzyme restriction analysis of the construct with the insert in the correct and reverse orientation. A schematic showing the constructs with the insert in the correct and reverse orientation together with the DNA fragments sizes following restriction enzyme digestion has already been described in Figures 3.2.1 and 3.2.2.

**Table 3.2** DNA fragment sizes for pPICZ $\alpha$ C-PDE1A1 constructs with the insert in the correct (PDE1) and reverse (PDE1R) orientation.

<b>Construct</b>	<b>Restriction enzyme (s)</b>	<b>DNA fragment sizes (kb)</b>
PDE1 (correct orientation)	<i>BamHI + HindIII</i>	0.9 + 1.5 + 2.8
	<i>HindIII</i>	0.9 + 4.3
	<i>EcoRI + HindIII</i>	0.3 + 0.6 + 4.3
PDE1R (reverse orientation)	<i>BamHI + HindIII</i>	1.3 + 1.1 + 2.8
	<i>HindIII</i>	1.3 + 3.9
	<i>EcoRI + HindIII</i>	0.3 + 1.0 + 3.9



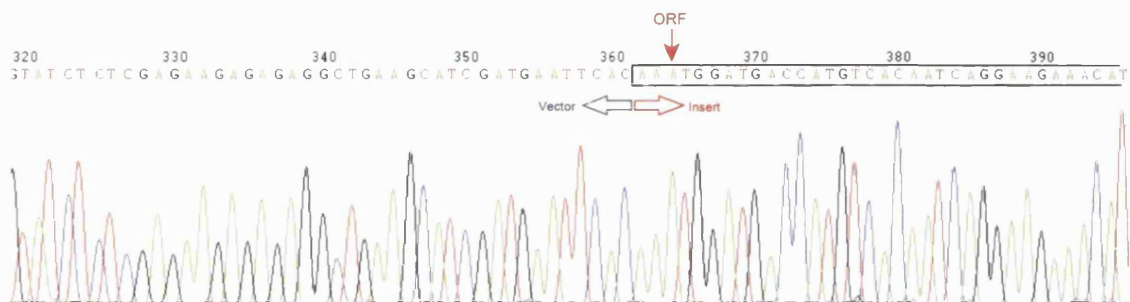
**Figure 3.5** Screening transformant colonies for the presence of the construct(s) containing the PDE1A1 insert using *Hind*III enzyme restriction analysis. Digestion samples were analysed on 1% agarose gels. Lane 1 = 1 kb DNA Marker lane with sizes indicated on the left; Lanes 5, 7, 8, 10 and 13 = construct DNA with the insert in the reverse orientation (PDE1R; indicated by the black stars), fragment sizes indicated by the open black arrows; Lane 12 = construct DNA with PDE1A1 insert in the correct orientation (PDE1; indicated by the solid red star), fragment sizes indicated by the open red arrows.



**Figure 3.6.1** Confirmation of the PDE1A1 orientation in the construct pPICZ $\alpha$ C-PDE1A1 using enzyme restriction analysis. Samples were analysed on 1% agarose gels following restriction analysis with a combination of *Hind*III, *Bam*HI and *Eco*RI restriction enzymes. Lanes 1 and 8 = 1 kb DNA Markers with sizes indicated on the left; Lanes 2 and 3 = PDE1 and PDE1R respectively following digestion with *Bam*HI and *Hind*III; Lanes 4 and 5 = PDE1 and PDE1R respectively following digestion with *Hind*III; Lanes 6 and 7 = PDE1 and PDE1R respectively following digestion with *Eco*RI and *Hind*III.

### 3.5.1.2 Automated DNA sequence analysis

DNA sequence analysis was carried out on the construct with the insert in correct orientation using the reverse primer L11 as described in section 3.4.2.4. The sequence analysed included the sequence at the N-terminal portion of the ORF and encompasses the region between the two calmodulin-binding domains, the first calmodulin-binding domain and the cloning junction between the N-terminal ORF and the vector. Figure 3.6.2 shows a portion of the sequence at the cloning junction between the N-terminal ORF and the vector.



**Figure 3.6.2** DNA sequence analysis of pPICZ $\alpha$ C-PDE1A1. PDE1A1 insert is shown in the open box with the red arrow marking the position of the ORF.

The sequence analysed showed no deviations from the sequence obtained by Clapham and Wilderspin (2001).

### 3.5.2 Methanol phenotype determination for the transformant *Pichia pastoris* strains

The methanol phenotype of the transformant strains (*P. pastoris*-PDE1) was carried out to ensure that the *AOX1* gene was not disrupted following integration of the expression cassette. There were two GS115, twenty X-33 and one KM71 transformant colonies which were screened for methanol phenotype. Both GS115 and X-33 strains have an intact *AOX1* gene so are able to grow on methanol-containing media (MMH) with a generation time of approximately 5 hours. Transformation of the KM71 strain of *P. pastoris* with construct DNA produced only one transformant colony so this was also screened for methanol phenotype. This strain was expected to show a slower growth on MMH media since it has



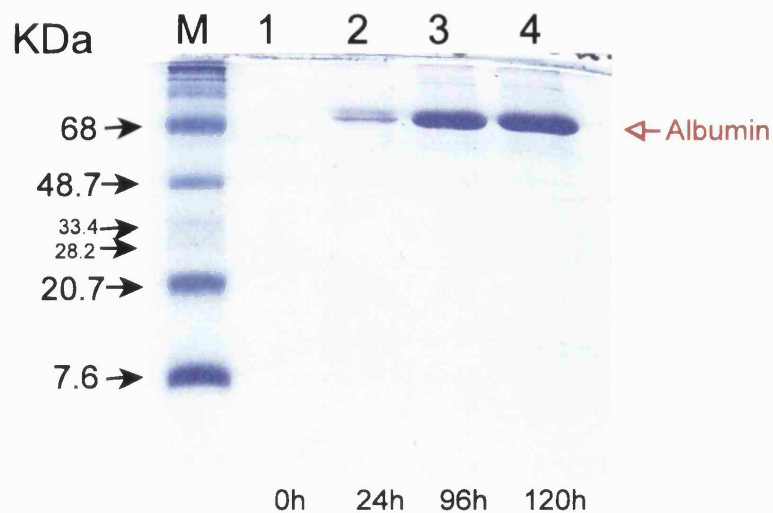
a disrupted *AOX1* gene and has a generation time of approximately 30 hours. Table 3.3 summarises the results for the methanol phenotype screening. Growth is denoted as “+” symbols and represent an estimation of the cell growth at days 2 and 4. All three transformant strains showed growth on dextrose media (MDH). GS115 and X-33 transformant strains showed a faster growth than the KM71 transformant strain on methanol media (MMH) as expected since the KM71 strain has a disrupted *AOX1* gene as discussed earlier (3.1.3.1 and 3.1.3.3). The faster growth rate of the GS115 and X-33 transformant colonies confirmed that the *AOX1* gene was intact. Both GS115 transformant colonies, twenty X-33 transformant colonies as well as the single KM71 transformant colony were selected for expression studies. Strains of *P. pastoris* not containing construct DNA were used as controls for expression of background proteins, including any endogenous PDE activity.

**Table 3.3** Methanol phenotype determination of transformant *P. pastoris* strains.

Transformant strain	Grid /colony number	MDH		MMH	
		Day 2	Day 4	Day 2	Day 4
X-33-PDE1	1 - 20	++	+++	-	+++
KM71-PDE1	21	++	+++	-	+
GS115-PDE1	22 - 23	++	+++	-	+++

### 3.5.3 Secreted expression of GS115/Mut<sup>s</sup>-Albumin (Mut<sup>s</sup>)

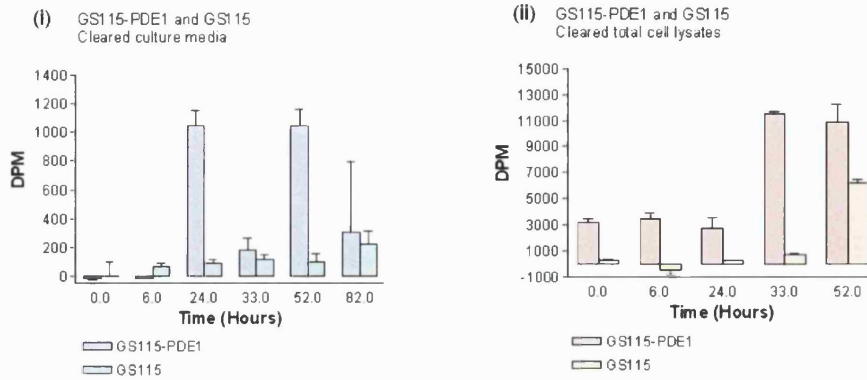
The strain GS115/Mut<sup>s</sup> contained an expression cassette comprising of the gene for albumin, in frame with the  $\alpha$ -factor signal sequence, together with the zeocin resistance gene. Expression was carried out using this strain to establish the *Pichia pastoris* expression system for the expression of secreted proteins. 1ml samples of the culture were removed at the time points 0, 24, 96 and 120 hours, following the switch of media from BMGY to the expression media, BMMY. These samples were centrifuged to remove the cells and the cleared media analysed on 20% SDS PAGE. Figure 3.7 shows the results for these samples.



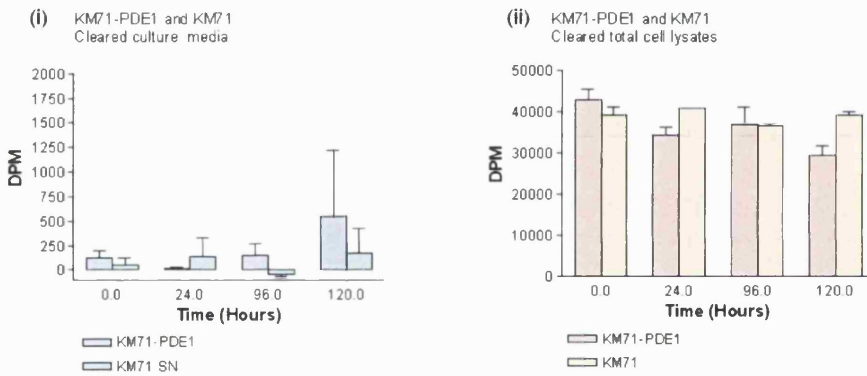
**Figure 3.7** Analysis of cleared media following secreted expression of albumin from GS115/*Mut<sup>s</sup>*-Albumin (*Mut<sup>s</sup>*). Coomassie stained supernatant samples separated from the growth media and analysed on 20% SDS PAGE. Lane 1 = pre-stained protein mixture with sizes indicated on the left; Lanes 1, 2, 3 and 4 = samples at time points 0, 24, 96 and 120 hours respectively; M = Pre-stained protein marker mixture.

#### 3.5.4 Expression studies on pPICZ $\alpha$ C-PDE1A1 constructs

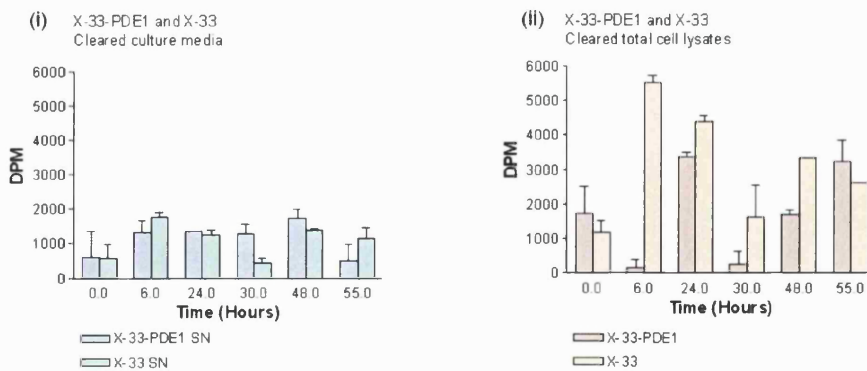
Expression studies were carried out on the three transformant *P. pastoris* strains plus the empty, untransformed strains for background PDE activity. Samples of the expression media for GS115 and X-33 strains were removed for up to 3 - 4 days of growth while cultures of the slow-growing KM71 strain were removed for up to 5 - 7 days. These samples were centrifuged and the cleared culture samples (cleared media) analysed for PDE activity. The cells remaining were lysed using glass beads as described in section 3.4.4.2, and cleared total cell lysate samples (supernatants) also analysed for PDE activity using cAMP as the substrate. Figures 3.8 show the PDE activity results for both the cleared media and the supernatant samples for all three transformant strains of *P. pastoris* together with background PDE activity observed for *P. pastoris* cells not containing construct DNA.



**Figure 3.8.1** Analysis of GS115-PDE1 samples using PDE activity assays. Samples of the culture media (cleared culture media) removed at the time points indicated were analysed by PDE activity assays using cAMP as the substrate (i). The cells remaining were lysed and the cleared total cell lysates also analysed (ii).



**Figure 3.8.2** Analysis of KM71-PDE1 samples using PDE activity assays. Cleared culture media (i) and total cell lysate samples (ii) were analysed by PDE activity assays using cAMP the substrate.



**Figure 3.8.3** Analysis of X-33-PDE1 samples using PDE activity assays. Cleared culture media (i) and total cell lysate samples (ii) were analysed by PDE activity assays using cAMP the substrate.

### 3.6 Discussion

The *Pichia pastoris* expression system for the secreted expression of heterologous proteins was successfully set up for the first time in this laboratory. This was demonstrated by the successful expression of albumin into the culture media by the control strain, GS115-albumin, as shown by the Coomassie-stained SDS PAGE gel on cleared culture media (Figure 3.7). This showed the presence of albumin in the culture media from 24 hours up to 120 hours (5 days).

Cloning of the full-length dog heart PDE1A1 cDNA in pPICZ $\alpha$ C was successfully carried out as demonstrated by the enzyme restriction analysis on the single transformant colony which contained the insert in the correct orientation (see Figures 3.5 and 3.6.1). DNA sequence analysis carried out on this construct further confirmed the presence of the insert in the correct orientation (Figure 3.6.2). This construct, together with a construct with the insert in the reverse orientation, were used to transform all three strains of *Pichia pastoris* competent cells as described in section 3.4.3.3.

Expression studies were carried out on all the transformant colonies obtained for the three strains of *Pichia pastoris* transformed with the pPICZ $\alpha$ C-PDE1A1 construct DNA (see Table 3.3), as well as *P. pastoris* strains not containing construct DNA. The two transformant GS115-PDE1 colonies were analysed for the secreted expression of the recombinant enzyme. Only one of the transformant colonies showed PDE activity above the background activity in the culture media (Figure 3.8.1 (i)). Cleared total cell lysate samples for this transformant also showed PDE activity above the background (Figure 3.8.1 (ii)). However, Western blot analysis carried out on both the cleared culture media and the cleared total cell lysate samples of GS115-PDE1 did not reveal a positive signal for the presence of PDE1 (data not shown). Further transformant GS115-PDE1 strains were analysed for the secreted expression of the recombinant enzyme but none of these revealed significant PDE activity above the background in the cleared culture media or in the cleared total cell lysate samples (data not shown).

The single transformant strain of KM71 (KM71-PDE1) analysed for the secreted expression of PDE1A1 showed very little PDE activity above background for the cleared culture media

(Figure 3.8.2 (i)). Cleared total cell lysate samples of KM71-PDE1 and KM71 revealed only the presence of endogenous PDE activity (Figure 3.8.2 (ii)). In fact, the endogenous PDE activity in KM71 was found to be very high in this strain of cells compared to GS115 and X-33 cells. Western blot analysis on the transformant KM71-PDE1 samples did not show the presence of the recombinant enzyme in the culture media or the cleared total cell lysate sample.

Expression studies were carried out on the twenty X-33-PDE1 transformant colonies. PDE activity analysis carried out on the cleared culture media showed that there was no significant PDE activity above the background activity in these transformants. Figure 3.8.3 shows the PDE activity results for one of the transformant strains. As with the transformant GS115-PDE1 and KM71-PDE1 colonies, Western blot analysis of the transformant X-33-PDE1 samples did not show the presence of PDE1 enzyme in the culture media or in the cleared total cell lysate samples.

PDE activity and Western blot analysis using CaM-PDE antibody had shown the absence of the recombinant PDE1A1 protein in the expression media for all three *P. pastoris* strains. There have been reports of foreign proteins remaining in the periplasmic space using the *P. pastoris* expression system for the secreted expression of foreign proteins where the host cell has not been able to efficiently utilize the secretory signal sequence (Tschopp *et al.*, 1987b). However, analysis of the cleared total cell lysate samples in the present study did not show the presence of the PDE1A1 protein. These results indicated that the recombinant protein was not being expressed or that it was being expressed at very low levels. DNA sequence analysis of the construct pPICZ $\alpha$ C-PDE1A1 had confirmed the presence of the ORF in the correct reading frame (see Figure 3.6.2) so this was not thought to be the problem in the absence of the recombinant enzyme activity in the expression medium. The expression studies were carried out at small-scale levels using shake-flasks (100ml cultures) so it was possible that scale-up to a large-scale fermenter level may have produced more protein but this was not pursued since small-scale expression studies did not yield positive results. Another method to improve levels of heterologous protein expression is to construct *P. pastoris* strains containing multiple copies of the heterologous gene expression cassette (Cregg *et al.*, 1993). Multi-copy strains do exist naturally but at a very low frequency so the introduction of multiple expression cassette copies is favoured over the

screening of a large number of transformant colonies. Multicopy transformants have been used successfully for the high level expression of tetanus toxin (Clare *et al.*, 1991).

One of the advantages of using *Pichia pastoris* for the expression of foreign proteins is the generation of stable transformants through homologous recombination with the host genome. However, the recombination process occurs at a low frequency (1-10%) and can also result in the excision of the expression cassette leaving behind the marker gene (Romanos *et al.*, 1992; Cregg and Higgins, 1995). The transformant colonies screened in the present study were all selected on YPDS agar plates containing zeocin as described in section 3.4.3.3, as only transformants containing the expression cassette (see Figure 3.1.2) would be selected on this media. The fact that none of the transformant colonies produced the recombinant enzyme may suggest the absence of the expression cassette, containing the PDE1A1 ORF, from the transformant colonies but the presence of the antibiotic resistance gene in the host genome.

Although the *Pichia pastoris* system did not produce the recombinant PDE1A1 protein in the present study, the objective of establishing the *Pichia pastoris* expression system for the secreted expression of proteins was established for the first time in this laboratory, as proven by the successful expression of albumin into the medium from the control strain (see Figure 3.7). Furthermore, the full-length dog heart PDE1A1 gene was successfully cloned into the pPICZ $\alpha$ C vector as shown by the enzyme restriction analysis (Figure 3.6.1) and DNA sequence analysis (Figure 3.6.2). This construct can be used for further expression studies for the large-scale expression of recombinant enzyme and also for the generation of multi-copy transformants for high-level expression of the recombinant protein. Also, while it is well known that the yeast *Saccharomyces cerevisiae* contains endogenous high-affinity and low-affinity cAMP phosphodiesterase activity (Sass *et al.*, 1986), there have been no reports on the determination of endogenous PDE activity in the *Pichia pastoris* cells. The present work does provide experimental data on the presence of PDE activity in this yeast. Figures 3.8.1 to 3.8.3 show the cAMP-hydrolysing PDE activity present in the cleared total cell lysate samples of the three strains of *Pichia pastoris* used in the present work. While the strains GS115 and X-33 reveal relatively low levels of PDE activity, the strain KM71 does have a very high cAMP-hydrolysing activity (Figure 3.8.2). However, expression studies using the *Pichia pastoris* system for the secreted expression

of PDE1A1 protein were not pursued further, but the prokaryotic expression system using *E. coli* as the host cell investigated as this system had been used successfully for the expression of soluble PDE4 protein (Kovalá *et al.*, 1997). Chapter four describes the work carried out using the prokaryotic expression system.

## Chapter Four

### 4 Cloning and expression of PDE1A1 in pGEX-3X and pTrcHisA for protein expression in *E. coli*

#### 4.1 Introduction

##### 4.1.1 Background to prokaryotic expression systems

Prokaryotic expressions systems have been the most widely used systems for the expression of recombinant proteins. The gram-negative bacteria, *Escherichia coli*, is the most commonly used host for the expression of both prokaryotic and eukaryotic recombinant proteins. There are several features about *E. coli* that make it an attractive host. These include the ability of the bacteria to grow rapidly and at high density on relatively inexpensive substrates which means that it readily offers itself to large scale production of foreign proteins. Cultures grown in shake flasks in up to 1L cultures can provide milligram amounts of protein within 1 - 2 weeks (Appelbaum and Shatzman, 1999). Scale-up to fermenter vessels with up to 10L cultures produces enough protein for purification purposes for ultimate structural studies on the protein. *E. coli* has also been well-characterised and there is a wealth of information regarding the genetics and physiology of the bacteria.

There are a large number of cloning vectors that have been developed for foreign protein expression in *E. coli*. These vectors have been designed to allow the cloning of foreign genes with relative ease into enzyme restriction sites located within regions called the multiple cloning sites (MCS). They also contain genes for antibiotic resistance which is a feature used for the selection of transformant colonies. The use of strong promoters allows efficient transcription of heterologous genes. The lactose utilisation by *E. coli*, *lac* operon system, has been used as the model of prokaryotic regulation. This is a relatively tightly regulated system since only minute amounts of the repressor protein have been shown to be present in *E. coli* cells and in the uninduced state, the repressor protein is tightly bound to the downstream operator region. The non-hydrolysable lactose analog isopropyl- $\beta$ -D-1-thiogalactopyranoside (IPTG) is used to induce transcription in these cells. Synthetic *tac* and *trc* promoters have been produced and consist of the *trp* (tryptophan) and



the *lac* promoter regions. Both of the synthetic promoters are strong promoters and allow the routine accumulation of proteins to about 30% of the total cell protein with the addition of IPTG (Baneyx, 1999). These promoters are repressed by the *lac* repressor protein which is usually overexpressed from a *lacI* or *lacI<sup>q</sup>* gene on the vector or host strain. However, there is a leakiness associated with the synthetic promoters which means that there will be expression of the foreign gene without IPTG induction. This is a concern when the foreign protein is toxic to the host cell.

Prokaryotic expression vectors have also been designed to produce fusion proteins with the foreign protein which allows for ease of purification using affinity chromatography. These fusion partners include maltose-binding protein (MBP), thioredoxin, Protein A and glutathione S-transferase. Affinity resins are commercially available for the purification of all of these fusion proteins together with the enzymes to excise the foreign protein from the fusion partner. Vectors containing hexahistidine tags instead of fusion proteins have also been developed for purification using nickel-chelate chromatography.

#### **4.1.2 Foreign gene expression using prokaryotic expression systems**

Prokaryotic expression systems have been used successfully for the expression of many proteins including PDE enzymes. In most cases, the foreign proteins have been expressed either as fusion proteins, or directly but containing a polyhistidine tag. In both cases, the fusion partner or the polyhistidine tag has been used to aid purification. Table 4.1 gives an overview of some of the proteins expressed using *E. coli* as the host cell.

**Table 4.1** Foreign genes expressed using *E. coli* as the host.

Foreign protein	Fusion partner	Vector	Reference
<i>P. gingivalis</i> cysteine protease	His <sub>6</sub> -tag	pET	Margetts <i>et al.</i> , 2000
Mouse phosphofructokinase	His <sub>6</sub> -tag	pET20b	Gunasekera and Kemp, 1999
Human leptin	His <sub>6</sub> -tag	pET	Varnerin <i>et al.</i> , 1998
Rat connexin 32	Thioredoxin	pTrxFus	Mambetisaeva <i>et al.</i> , 1997
GluR2 receptor	His <sub>6</sub> -tag	pETGQ	Chen and Gouaux, 1997
Bovine mitochondrial translation initiation factor 2	His <sub>6</sub> -tag	pQE	Ma and Spremulli, 1996
Thyroid hormone receptor	GST	pGEX-KG	Ball <i>et al.</i> , 1995
Human glutathione S-transferase	His <sub>6</sub> -tag	pET-15b	Chang <i>et al.</i> , 1999
<i>Plasmodium falciparum</i> Ag63, Ag361	GST	pGEX-3X	Smith and Johnson, 1988
<b>PDEs:</b>			
PDE7A	C-terminal His-tagged	pET21-C	Richter <i>et al.</i> , 2002
HSPDE4A	C-terminal His-tagged	pET	Richter <i>et al.</i> , 2000
RNPDE4D1	GST	pGEX-KG	Kovala <i>et al.</i> , 1997
PDE3	N-terminal His-tagged	pQE-30	Tang <i>et al.</i> , 1997

Despite the success of using prokaryotic expression systems, there are some well-known problems associated with the use of bacterial expression systems especially when the protein of interest is a eukaryotic protein requiring complex post-translational modifications, such as glycosylation, which cannot be carried out by the *E. coli*. Additionally, overproduction of heterologous proteins in *E. coli* often results in their misfolding and segregation into insoluble aggregates called inclusion bodies (Prouty *et al.*, 1975; Williams *et al.*, 1982). A large range of recombinant proteins have been shown to be accumulated in inclusion bodies and includes proteins that were expressed as fusion proteins, such as myoglobin, bovine and human growth hormones,  $\alpha_1$ -antitrypsin, as well as proteins that were expressed directly (interleukin-2, bovine and human growth hormones, calf prochymosin) (Marston, 1986). It should be noted that it is not just the foreign proteins that the host segregates into inclusion bodies but also normal *E. coli* proteins synthesised to high levels using recombinant DNA technology (Marston, 1986).

There have been many strategies employed to overcome the accumulation of recombinant proteins in inclusion bodies. This has included the co-expression of molecular chaperones

which aid the proper folding of proteins but are not themselves part of the final product (Baneyx, 1999; Hannig and Makrides, 1998). The expression of foreign proteins at room temperature (Kovala *et al.*, 1997; Ball *et al.*, 1995) and 30°C (Gunasekera and Kemp, 1999) as opposed to 37°C has also been used successfully. The supplementation of the bacterial medium with agents such as sorbitol which do not permeate through the cell membrane have also been used successfully (Blackwell and Horgan, 1991; Gunasekera and Kemp, 1999).

The redox state of the *E. coli* cytoplasm has also been said to play a role in the aggregation of recombinant proteins. The cytoplasmic environment is reducing with at least five bacterial proteins involved in the reduction of disulphide bridges. This is also thought to be a factor in the misfolding of proteins (Baneyx, 1999). *E. coli* mutants lacking genes for the thioredoxins and glutaredoxins (*trxA*, *trxC*, *grxA*, *grxB* or *grxC* genes) have been used for the expression of foreign proteins which do not form aggregates (Schneider *et al.*, 1997).

The fusion protein systems developed for the purpose of purification and detection of the expressed fusion protein have been shown to facilitate protein folding. The presence of the fusion partner is thought to help in the correct folding of the foreign protein, improving solubility as well as providing protection from proteolytic cleavage. Smith and Johnson (1988) developed the pGEX vector system which expressed foreign proteins with a *Schistosoma japonicum* glutathione S-transferase (GST) protein as a fusion partner. These were successful in generating soluble fusion proteins (Smith and Johnson, 1988). Other fusion partners used have included maltose-binding protein which is thought to directly interact with the recombinant protein thereby acting as an 'intramolecular' chaperone but the MBP has to be synthesised first because if the fusion order is reversed, proteins become insoluble (Sachdev and Chirgwin, 1998; Baneyx, 1999; Kapust *et al.*, 1999).

Recombinant proteins are also prone to proteolytic degradation especially if they are misfolded. This is carried out by at least five ATP-dependent proteases which includes the protease La, a *lon* gene product and HflB, a *hflB* gene product (Baneyx, 1999; Gottesman, 1996). The protease La, a serine protease, has been shown to catalyse the degradation of many proteins and *lon*<sup>-</sup> mutants allow the accumulation of foreign proteins without

proteolysis occurring (Mizusawa and Gottesman, 1983). The concentration of La protease also increases when cells accumulate large amount of foreign proteins, especially at high temperatures, which is followed by proteolysis of the foreign proteins by La (Goff *et al.*, 1984). The protease HflB has a zinc protease motif and the *in vivo* activity can be modulated by zinc ions. This protease is thought to be an essential *E. coli* protease involved in the proteolysis of both cytoplasmic and membrane protein. Protease-deficient strains of *E. coli* have been developed to overcome proteolytic degradation of recombinant proteins but these mutant strains show reduced cell growth rates and also compromised strain fitness (Chin *et al.*, 1988; Baneyx, 1999).

Recombinant proteins destined for *E. coli* periplasm has also been explored. The periplasm provides an oxidizing environment that contains enzymes catalyzing the formation of disulphide bonds so is an attractive target of eukaryotic protein disulphide bond formation. This has been successfully used to express the cysteine-rich recombinant protein, human tissue plasminogen activator (Baneyx, 1999; Qiu *et al.*, 1998), and also the glutamate receptor (Arvola and Keinänen, 1996). Unfortunately, only small amounts (100µg/L) of the proteins have been produced by this method. Also, although there is no periplasmic ATP pool, proteolytic degradation does occur but via energy-independent proteases. Secretion of polypeptides to the extracellular medium is another desirable strategy but information regarding the secretion of proteins from the host cell remains scant and also may not be possible for large proteins (Baneyx, 1999).

Codon usage between prokaryotes and eukaryotes can also have an impact on foreign gene expression in *E. coli* (Hannig and Makrides, 1998; Baneyz, 1999). Heterologous genes containing codons that are rarely used in *E. coli* may be poorly expressed. Moreover, the occurrence of rare codons (e.g. AGA, AGG) in the heterologous gene is associated with a low level of their tRNA species. However, this can be overcome by using site-directed mutagenesis to replace the rare codons with *E. coli*-preferred codons (e.g. CGC) (Zahn, 1996; Baneyx, 1999)

Although many strategies have been developed to overcome inclusion body formation when recombinant genes are expressed in *E. coli*, the fact that foreign proteins are sequestered into inclusion bodies can be used to advantage in the purification of the foreign proteins.

Inclusion bodies generally contain large amounts of the desired protein and they can be relatively easily isolated from the remaining cellular components. The foreign proteins can then be retrieved from these inclusion bodies using the denaturants, urea (8M) or guanidine (6M), and then allowed to gently refold into their native state following dilution or dialysis of the denaturant. The refolding process can be very slow and the conditions have to be empirically determined. Many proteins have been extracted from inclusion bodies and refolded to yield biologically active proteins including PDE enzymes (Richter *et al.*, 2000, 2002). In most cases, the conditions for the refolding of the recombinant proteins are individually optimised. Richter and co-workers (2000) expressed PDE4A in *E. coli* as a histidine tagged protein and purified the recombinant protein from inclusion bodies to yield a biologically active protein. Patra and co-workers (2000) successfully extracted recombinant human growth hormone from *E. coli* inclusion bodies using a range of pH buffers (pH 3-13), with and without urea, for the solubilisation of the inclusion bodies. Chen and Gouaux (1997) used an extensive folding screen involving changes in twelve different factors ranging from different protein concentrations for the starting material, buffer pH, divalent ions, temperature, presence and absence of chaotrope as well addition of additives such as arginine and ethylene glycol. These conditions were investigated for the refolding of the glutamate receptor (GluR2) ligand binding domain (~40 kDA) extracted from *E. coli* inclusion bodies (Chen and Gouaux, 1997). Their experiments revealed that the pH (pH 8.5), temperature (4°C) and presence of divalent metal ions ( $Mg^{2+}$ ,  $Ca^{2+}$ ) were the most important factors for the optimal refolding of GluR2 receptor protein. It is therefore apparent that purification from inclusion bodies requires lengthy investigation into finding the optimum refolding conditions and this is generally made more difficult if the target protein is very large. Additionally, the inclusion bodies themselves are not free from certain proteases which can adsorb onto the surface of the inclusion bodies and may actually degrade the desired protein while it is being refolded. This includes the protease ompT protease, which adsorbs to the inclusion bodies, as well as an inner membrane protease FtsH which is also active under denaturing conditions (Gottesman, 1996; Baneyx, 1999).

## **4.2 Background and aims of the present study using the bacterial expression system for the cloning and expression of dog heart PDE1A1**

### **4.2.1 Overview**

The full-length dog heart PDE1A1 cDNA was produced by Clapham and Wilderspin (2001) as already discussed in Chapter 1 (1.8). This cDNA, which had been cloned into the cloning vector pCR-Script (Clapham and Wilderspin, 2001), was used as the starting point of the present work.

As outlined in section 1.9.1, one of the three expression systems to be explored in the present study was the bacterial expression system. The dog heart PDE1A1 cDNA was cloned into two different prokaryotic expression vectors: pGEX-3X and pTrcHisA. The constructs (pGEX-3X-PDE1A1 or pTrcHisA-PDE1A1<sub>N-trunc</sub>) were then used to transform *E. coli* cells and expression studies carried out on these. The effect of temperature, IPTG and media composition were explored during the expression studies. The purpose of these investigations was to discover optimum conditions for the expression of soluble recombinant protein. The cloning strategies are discussed below (4.2.2).

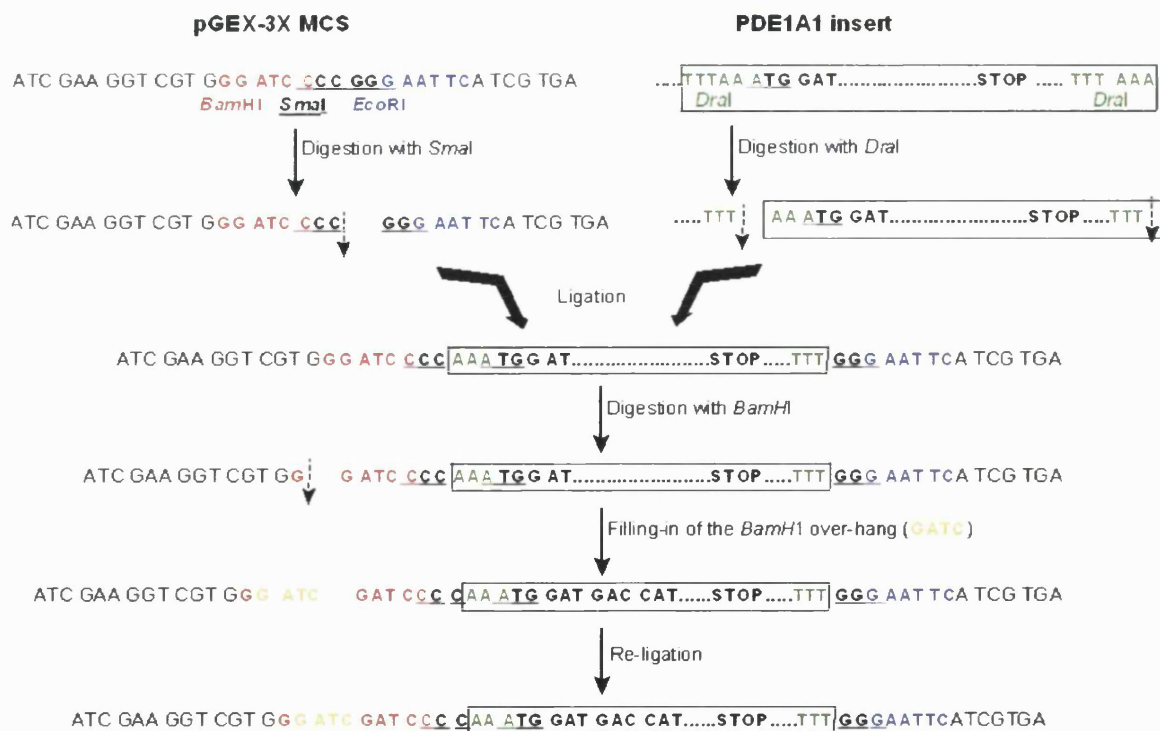
### **4.2.2 Cloning the full-length and N-terminal truncated PDE1A1 into prokaryotic expression vectors**

#### **4.2.2.1 pGEX-3X expression vector**

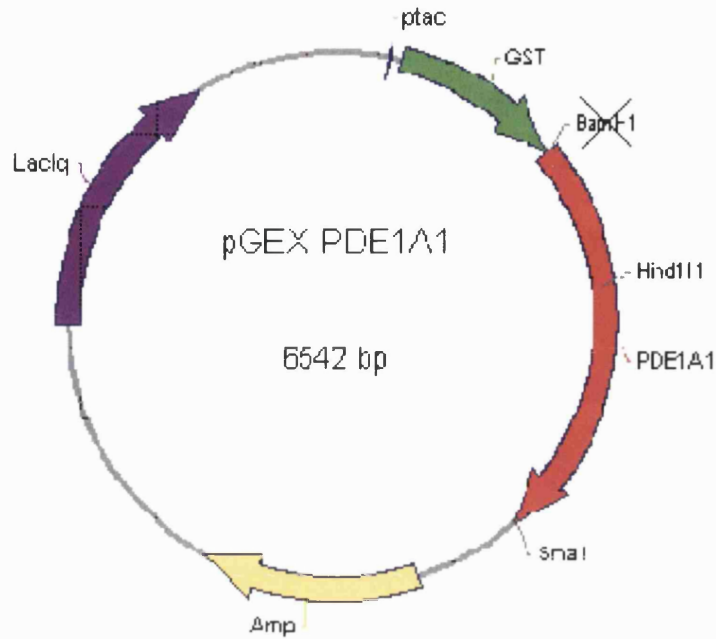
The full-length PDE1A1 cDNA (~1.6 kb) was cloned into the vector pGEX-3X for the expression of the recombinant protein as a fusion protein with glutathione-S-transferase. The GST is derived from the helminth parasite *Schistosoma japonicum* (Sj26) and serves as an affinity tag for the purification of the fusion protein as well as identification of the expressed fusion protein using commercially available anti-GST antibody by Western blotting techniques. The vector also contains a strong *taq* promoter for the induction of expression using IPTG as well as an internal *lacI<sup>q</sup>* gene for the overexpression of repressor protein to maintain a tight regulation of expression in an uninduced state. The GST gene precedes the recognition sequence for Factor Xa protease, used for the separation of the

target protein from the fusion partner, followed by the multiple cloning site (MCS) where the gene of interest is cloned (Smith and Johnson, 1988).

The full-length PDE1A1 cDNA fragment was first extracted from pCR-Script-PDE1A1 using the restriction enzyme *DraI* followed by agarose gel electrophoresis of the resulting DNA fragments which included the full-length PDE1A1 fragment. The required fragment was purified from the agarose gel and then cloned into the *SmaI* restriction site within the MCS of the vector. This produced a frame-shift in the PDE1A1 open reading frame (ORF) so to bring the ORF back into frame, the construct was cut with the enzyme *BamHI* and a filling-in reaction carried out to add four additional bases (**GATC**). The vector was then re-ligated to give the final in-frame construct. Figure 4.1 gives a summary of this cloning strategy and Figure 4.2 shows a schematic map of the resulting pGEX-3X-PDE1A1 construct. The addition of the four extra bases meant that the *BamHI* restriction site was destroyed. This was used as a basis for selecting constructs in the correct reading frame.



**Figure 4.1** Cloning strategy for the full-length PDE1A1 in pGEX-3X. This figure shows the multiple cloning site (MCS) of the vector with the three enzyme restriction sites indicated in color and underlined. The PDE1A1 ORF (boxed) is shown with the *DraI* restriction sites flanking the ORF together with the first codon to be translated in the ORF shown underlined (ATG).



**Figure 4.2** Schematic map of the pGEX-3X-PDE1A1 construct. The map marks the position of the ORF (shown in red) together with the restriction enzymes used to screen transformant colonies (*Bam*HI, *Hind*III and *Sma*I). It also shows the positions of the ampicillin resistance gene (*Amp*; shown in yellow), the *lacI<sup>q</sup>* gene (shown in purple), as well as the GST gene (shown in green).

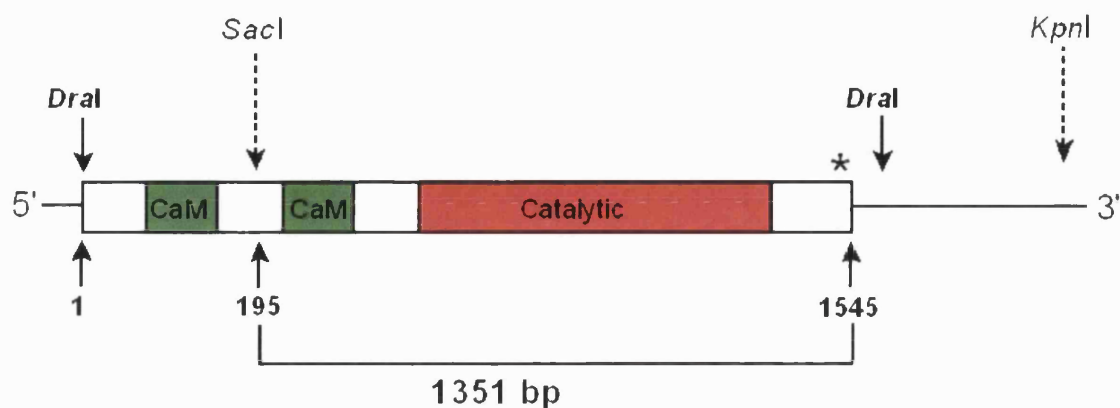
#### 4.2.2.2 pTrcHisA expression vector

The pTrcHisA vector allowed expression of PDE1A1 as an N-terminally hexahistidine tagged protein. The pTrcHis vectors contain an ampicillin resistance gene, a *trc* promoter together a copy of the *lacI<sup>q</sup>* gene coding for the *lac* repressor protein which allows for the efficient repression of expression in the uninduced state just as it does in the pGEX-3X vector. The gene of interest is cloned downstream and in-frame with the N-terminal peptide which codes for an initiation codon, six histidine residues in series, Anti-Xpress antibody epitope and an EK cleavage recognition sequence. This is followed by the multiple cloning site where the gene of interest is cloned.

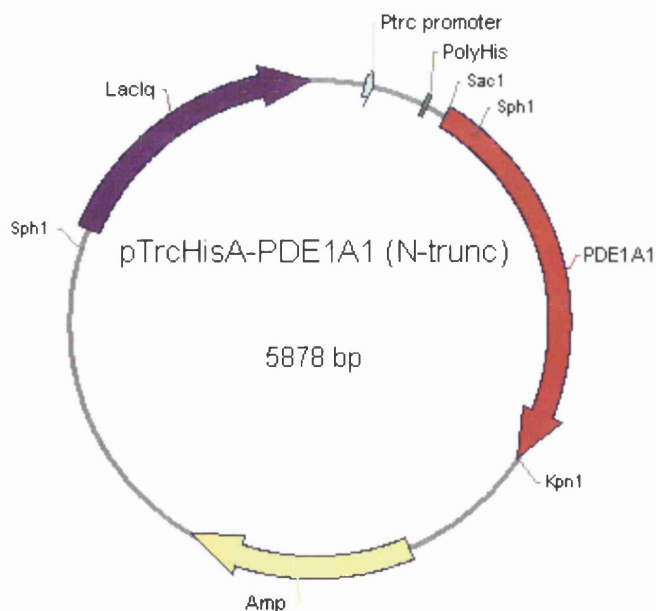
The pCR-Script-PDE1A1 construct was digested with two restriction enzymes, *Sac*I and *Kpn*I, which produced a PDE1A1 coding sequence encoding an N-terminal truncated PDE1A1 enzyme. The enzyme digestion products were analysed by agarose gel electrophoresis and the required PDE1A1 fragment extracted and purified from the agarose



gel. This fragment was then cloned into a similarly digested pTrcHisA vector to give the final construct: pTrcHisA-PDE1A1<sub>N-trunc</sub>. Figure 4.3 shows the *SacI* and *KpnI* restriction sites on the PDE1A1 ORF while Figure 4.4 shows a schematic map of the construct.



**Figure 4.3** Schematic showing the coding sequence for the full-length dog heart PDE1A1 cDNA. The position of the *DraI* restriction sites flanking the ORF (used for cloning in pGEX-3X) are shown together with the restriction sites *SacI* and *KpnI* used for cloning the truncated PDE1A1 fragment in pTrcHisA. The asterisk indicates the position of the stop codon while the numbers indicate base pairs comprising the ORF.



**Figure 4.4** Schematic map of the pTrcHisA-PDE1A1<sub>N-trunc</sub> construct. The map marks the position of the ORF (shown in red) together with the restriction enzymes used for the cloning (*SacI* and *KpnI*) and the enzyme used to screen transformant colonies (*SphI*).

### 4.2.3 Aims

- ▶ Cloning PDE1A1 cDNA into two prokaryotic expression vectors, pGEX-3X and pTrcHisA for subsequent expression studies.
- ▶ Determine optimum conditions for the expression of soluble recombinant enzyme for the two constructs, pGEX-3X-PDE1A1 and pTrcHisA-PDE1A1<sub>N-trunc</sub>.
- ▶ Scale-up of protein expression for purification and biochemical analysis of the recombinant proteins, and subsequent structural studies.

### 4.3 Materials

Most of the reagents used for this part of the work have already been described in Chapter 2 so this section will only list reagents not so described. All manipulations involving DNA and bacteria were carried out using sterile tips and reagents. Milli Q water was used to prepare all stock solutions and reagents. These were sterilised by autoclaving for 20 minutes 15 Psi at 121°C. Heat-labile reagents such as antibiotics were sterilised by filtration using 0.2µm sterile filters.

The DNA reagents included Ultrapure dNTPs and DNA polymerase from Pharmacia. T4 DNA ligase and the Klenow fragment (DNA polymerase 1) were from United States Biochemical (USB). The restriction enzyme *SphI* was from GibcoBRL.

Select Yeast Extract and Select Peptone 140 for the preparation of 2xYT media were purchased from Gibco BRL. Sorbitol for supplementing bacterial media was from Sigma. The expression vectors pGEX-3X and pTrcHisA were from Amersham Pharmacia Biotech and Invitrogen respectively. Nickel resin (in 20% ethanol) for affinity chromatography was from Invitrogen.

## 4.4 Methods

### 4.4.1 Cloning of the full length PDE1A1 ORF into pGEX-3X

#### 4.4.1.1 PDE1A1 ORF purification from pCR-Script-PDE1A1

The PDE1A1 ORF was excised from the vector pCR-Script-PDE1A1 using the restriction enzyme *DraI* in a reaction mixture consisting of 1 µl of 10x Multicore reaction buffer, 2 µl of pCR-Script-PDE1 DNA (~1.4 µg DNA), 1 µl (10 units) of *DraI* and 6 µl of water. This was carried out in quadruplicate and the mixtures incubated at 37°C for one hour. Gel loading buffer was added to the samples, loaded onto 1% agarose gel and electrophoresed as described in 2.2.8. The ORF in the vector was flanked with *DraI* restriction sites resulting in the release of the ORF from the vector. The vector also had two *DraI* restriction sites quite close to each other as well as a third site. Digestion with this enzyme therefore was expected to yield five DNA fragments of the sizes: 1.6 kb (required ORF), 1.2 kb, 1.1 kb, 0.7 kb and one <0.5 kb. The fragments were visualised on a UV Transilluminator very briefly so as to locate the 1.6 kb fragment and excise the bands from the gel (2.2.9).

#### 4.4.1.2 Cloning purified PDE1A1 ORF into pGEX-3X

An overview of the cloning strategy has already been discussed in section 4.2.2.1 with Figure 4.1 showed a schematic of this strategy.

The vector pGEX-3X was cut with restriction enzyme *SmaI* (see 2.2.7) followed by a clean-up step using the Wizard DNA Clean-up kit according to the manufacturers instructions (see 2.2.9). Ligation of the ORF with the vector was carried out in a mixture containing 1 µl of 10x ligase buffer, 4 µl each of the purified ORF and the vector, and 0.5 µl of the enzyme T4 DNA ligase (1.5 units). The mixture was incubated at 15°C for 16 hours followed by incubation at 4°C for at least 24 hours. The ligated products were used to transform calcium chloride-competent *E. coli* JM109(DE3) cells as described in section 2.2.4.

#### **4.4.1.3 Screening transformant colonies using *Bam*HI**

Transformant colonies were selected and small scale plasmid purification (2.2.5.1) carried out to screen for the correct construct using *Bam*HI and analysing the resulting DNA fragments on agarose gel electrophoresis (2.2.8). Constructs with the PDE1A1 insert were then selected for large-scale plasmid DNA purification (2.2.5.2) and this DNA used for the insertion of four additional bases to bring the ORF back into the correct reading frame.

#### **4.4.1.4 Filling-in the *Bam*HI overhang in pGEX-3X-PDE1A1 constructs**

The correctly identified construct (6.5 kb) was cut using *Bam*HI and then the overhang filled in a reaction mixture containing ~2µg construct DNA, 10mM each of the dNTPs and DNA polymerase (Klenow fragment). The mixture was incubated at 22°C for 15 minutes followed by incubation at 75°C for 10 minutes. This was then cleaned using the Wizard DNA Clean-up kit as before (2.2.9). The cleaned product was re-ligated in a reaction mixture containing ligase buffer and T4 DNA ligase as before (4.4.1.2). The ligated products were used to transform calcium chloride-competent *E. coli* JM109(DE3) cells as described in section 2.2.4.

#### **4.4.1.5 Screening transformant colonies using *Bam*HI and *Hind*III**

Small scale DNA purification of 20 transformant colonies was carried out followed by enzyme restriction analysis using *Bam*HI alone as well as a combination of *Bam*HI and *Hind*III. As already stated before (4.2.2.1), the addition of four bases (filling-in the *Bam*HI overhang) destroyed the *Bam*HI restriction site. This was therefore used as a basis for screening for the desired clones. Large scale plasmid purification was carried out on correctly identified constructs (pGEX-3X-PDE1A1). Automated DNA sequence analysis (see section 2.2.10) was used to further confirm the identity of the clones 12 and 17 (c12 and c17) identified from the screening studies.

#### **4.4.2 Expression studies on pGEX-PDE1A1 (clone 12, c12) in *E. coli* JM109(DE3)**

Small-scale expression studies were carried out to ascertain the optimum conditions for the

expression of soluble, active recombinant enzyme. The main criteria for these experiments were expression temperature following induction with IPTG, the induction time before harvesting cells, and composition of growth media. Expression was also carried out without the addition of IPTG.

#### **4.4.2.1 The effect of temperature on recombinant protein expression**

##### **4.4.2.1.1 Protein expression at 37°C**

40% glycerol stocks for c12 and pGEX-3X were used to inoculate 10ml LB media with ampicillin (100µg/ml) for growth overnight at 37°C. 500µl of these were used to inoculate 50ml of LB media containing ampicillin (1 in 100 dilution) and allowed to grow at 37°C to an OD<sub>600</sub> of ~0.7 - 0.8 before inducing with 1mM IPTG. These cultures were then allowed to grow further at 37°C for 3 hours before harvesting the cells (see section 4.4.3.2). A second set of cultures for c12 and the empty vector were also allowed to continue growth at 37°C for 3 hours without the addition of IPTG. These samples were designated as c12N and PGN for “non-induced” samples. PDE activity assays were carried out on the harvested cells in the presence and absence of Ca<sup>2+</sup>/CaM (100µM and 10 units per assay respectively) and vinpocetine (100µM) as described in section 2.2.11.

##### **4.4.2.1.2 Protein expression at 24°C**

Protein expression was carried out for both c12 and the empty vector as before in the presence and absence of IPTG (4.4.2.1.1) except that the temperature was dropped to 24°C for the expression period. Also, expression was continued for up to 6 hours. Protein expression was monitored by removing 1ml samples of the cultures at the times 0, 2, 4 and 6 hours following the addition of IPTG. These cells were resuspended in 2x SDS loading buffer (4.4.3.1) and analysed on SDS PAGE. Western blotting was also carried out on these samples using anti-GST as the primary antibody (2.2.14).

##### **4.4.2.2 Protein expression in media supplemented with sorbitol**

LB media was supplemented with 0.5M sorbitol (designated LBS) and protein expression

carried out at 30°C using c12. As a comparison, c12 was also grown and expressed in LB media under the same conditions. Protein expression was continued for up to 48 hours and expression was monitored by SDS PAGE. This experiment showed the presence of the GST-PDE1A1 fusion protein for up to 48 hours so further expression experiments were carried out by allowing cultures to grow up to 24 hours and harvesting the cells. Cells harvested at 24 hours were analysed by PDE activity assays in the presence and absence of Ca<sup>2+</sup>/CaM and vinpocetine (4.4.3.2) as well as carrying out Western blot analysis using GST as the antibody.

#### **4.4.3 Processing bacterial cells following protein expression**

##### **4.4.3.1 Timed bacterial samples**

The absorbance at the wavelength of 600nm (OD<sub>600</sub>) was measured for the 1ml samples of bacterial cultures removed at the designated time points for monitoring protein expression. This reading was then used in the formula “42.21/OD<sub>600</sub> x 2” to give a value for the volume of culture to be used so that the cells processed at each time point were kept constant. Cultures were centrifuged in 1.5ml eppendorf tube at maximum speed for 2 minutes in a bench top centrifuge. The supernatant was discarded and the cell pellet resuspended in 40µl of 2x SDS gel loading buffer. These were stored at -20°C until analysed on SDS PAGE or Western blot analysis.

##### **4.4.3.2 Bacterial cultures grown to the end of the expression period**

Cultures grown for the duration of the time for protein expression were centrifuged in pre-weighed falcon tubes at 2,400g, 4°C for 20 minutes. The supernatant was discarded and the cell pellet stored at either -20°C or -70°C if not processed straight away. These were then allowed to thaw and the cell pellet resuspended in lysis buffer 2, containing protease inhibitors (see section 2.2.16), at 3ml/g wet pellet weight (Sambrook *et al.*, 1989). The resuspended cells were sonicated at setting 3 for four 10 second bursts, with cooling on ice for 1 - 2 minutes between the sonications, using a Sanyo Soniprep 150 sonicator. Sonicated samples were then centrifuged as before. The supernatant sample was separated from the particulate fraction and both retained for analysis. Both the supernatant and particulate

fraction were analysed on SDS PAGE and Western blots using anti-GST as the primary antibody. Supernatant samples were also analysed for PDE activity in the presence and absence of  $\text{Ca}^{2+}$ /CaM (100 $\mu\text{M}$  and 10 units per assay respectively) and vinpocetine (100 $\mu\text{M}$ ).

#### **4.4.4 Washing and refolding of GST-PDE1A1 (c12) from inclusion bodies**

##### **4.4.4.1 Washing of the inclusion bodies**

The insoluble material containing the inclusion bodies, from the expression studies carried out on c12, was used for the purification of the recombinant enzyme using the denaturant urea. The inclusion bodies were washed by resuspending the inclusion bodies at 15ml/g wet pellet weight in TEN buffer (50mM Tris pH 8.0, 1mM EDTA, 50mM NaCl) containing 0.5% v/v Triton X-100. Samples were vortex-mixed and lysozyme added to a final concentration of 200 $\mu\text{g/ml}$ . The mixture was vortex-mixed again, homogenised for about 5 minutes and then centrifuged at 20,000 rpm, 4°C for 30 minutes. The supernatant was discarded and the wash step repeated four more times.

##### **4.4.4.2 Denaturing inclusion bodies for extraction of the recombinant protein**

Washed inclusion bodies were resuspended in denaturation buffer (50mM Tris pH 8.0, 5mM EDTA, 50mM NaCl, 8M urea) at 20mg inclusion bodies per 1ml buffer. The inclusion bodies were homogenised in this buffer for 5 minutes and then incubated at room temperature for up to one hour to allow complete denaturation of the inclusion bodies.

##### **4.4.4.3 Renaturation of the recombinant protein**

The denatured inclusion bodies, containing the recombinant protein, were renatured slowly by adding the denatured mixture into a five-fold volume of renaturation buffer (20mM Tris pH 7.0, 1mM EDTA, 100mM NaCl). Proteins were allowed to refold slowly at 37°C overnight. The mixture was then centrifuged at 20,000rpm, 4°C for 30 minutes to remove any insoluble material remaining. The final refolded sample was concentrated using a Centriprep 10 Concentrator unit with a 10 kDa cut-off membrane. This was used to



concentrate the sample from ~40ml down to ~4ml. 1ml aliquots were dialysed twice in ~200ml of 50mM Tris pH 8.0 buffer to reduce the urea. The dialysed sample was centrifuged at maximum speed (14,000 rpm) in a benchtop centrifuge for 5 minutes after the first dialysis step and a small aliquot of the centrifuged sample retained for analysis together with any precipitated protein. The sample was centrifuged again after the second dialysis step and as before, samples retained for analysis. Both the supernatant and any pellet formed were analysed on SDS PAGE. PDE activity assays were carried out on the supernatant samples.

#### **4.4.5 Cloning of the PDE1A1 ORF into pTrcHisA**

Initial results using the pGEX-3X vector did not show the presence of any soluble, active PDE1A1 protein. There have been a number of reports of this expression vector yielding insoluble recombinant protein so an alternative vector, pTrcHis, was chosen for the expression of PDE1A1. Restriction enzymes selected for the cloning meant that the protein would be truncated at the N-terminal such that it would lack the first of the two calmodulin-binding domains (Figure 4.3).

##### **4.4.5.1 PDE1A1 purification from pCR-Script-PDE1A1**

pCR-Script vector containing the PDE1A1 ORF was digested with the restriction enzymes *SacI* and *KpnI* in a reaction mixture consisting of 1µl 10x Multicore reaction buffer, 4µl of DNA (~2.8µg), 1µl each of the enzymes (10 units each) and 3µl of water. The reaction was carried out in quadruplicate and incubated at 37°C for ~1 hour. All four samples were loaded onto a 1% agarose gel for electrophoresis (2.2.8). Ethidium bromide visualisation showed the presence of the expected two DNA fragments corresponding to the ~1.4 kb PDE1 fragment together with vector containing part of the PDE1 ORF (~3 kb). The four PDE1 fragments were excised from the gel and the Wizard DNA Clean-up kit for the purification of the DNA fragments for cloning (2.2.9).

##### **4.4.5.2 Cloning the purified truncated PDE1A1 into pTrcHisA**

The vector pTrcHisA was digested with *SacI* and *KpnI* in a reaction mixture containing 2µl

of pTrcHisA vector (50ng), 10 $\mu$ l 10x restriction enzyme buffer, 2 $\mu$ l each of *SacI* and *KpnI* (20 units each) and 84 $\mu$ l of water. This was incubated at 37°C for ~1 hour followed by incubation at 65°C to inactivate the enzymes before proceeding to the next step. The digested vector was dephosphorylated in a reaction mixture containing 90 $\mu$ l of the digested vector (45ng), 13 $\mu$ l of phosphatase buffer, 4 $\mu$ l (4 units) of Calf Intestinal Alkaline Phosphatase and 23 $\mu$ l of water. This was incubated at 37°C for 15 minutes followed by incubation at 56°C for another 15 minutes. The mixture was cleaned using the Wizard DNA Clean-up kit as described in section 2.2.9.

Ligation reactions were set up in a mixture containing approximate vector:insert ratios of between 1:3 and 1:12. These were estimated from the intensities of the DNA bands on agarose gels. The mixtures were incubated at 4°C for 8 hours followed by incubation at 15°C for at least 24 hours. The ligated products were used to transform calcium chloride competent *E. coli* JM109 cells as described in section 2.2.4.

#### **4.4.5.3 Screening transformant colonies**

Transformant colonies were selected and inoculated into 5ml LB with ampicillin and allowed to grow overnight in a 37°C shaking incubator (200 rpm). Small scale plasmid DNA purification was carried out on these samples (2.2.5.1) followed by enzyme restriction analysis using *SphI*. There are two *SphI* restriction sites within the construct: one in the PDE1A1 ORF and the second in the vector (see Figure 4.4). Constructs containing more than one insert (multimers) would be differentiated from the constructs containing a single insert by the presence of a third fragment following *SphI* digestion. This enzyme was therefore used to screen the DNA from the small scale purification. Correctly identified clones were grown for large scale plasmid DNA purification, and *SphI* digestion carried out on these to further confirm the identity of the clone. Automated DNA sequence analysis was also carried out on the clone identified (clone 1) by the screening studies. The method for the DNA sequence analysis has already been described in section 2.2.10.

#### **4.4.6 Expression studies on pTrcHisA-PDE1A1<sub>N-trunc</sub> clone 1 (c1)**

##### **4.4.6.1 Small-scale expression studies on pTrcHisA-PDE1A1<sub>N-trunc</sub> clone 1 (c1)**

###### **4.4.6.1.1 Expression of pTrcHisA and pTrcHisA-PDE1A1<sub>N-trunc</sub> in *E. coli* JM109**

Protein expression was carried out for both c1 and c3 in LB media with ampicillin for up to 17 hours at 30°C in the presence of IPTG as before (4.4.2). 1ml samples of the cultures were removed at the times of 0, 3 and 17 hours following the addition of IPTG. These samples were analysed by SDS PAGE as well as Western blot analysis using CaM-PDE antibody to monitor protein expression. The vector, pTrcHisA, was used as a control for background PDE activity. PDE activity assays in the presence and absence of Ca<sup>2+</sup>/CaM and vinpocetine were also carried out.

###### **4.4.6.1.2 Expression of pTrcHisA and pTrcHisA-PDE1A1<sub>N-trunc</sub> (c1) in *E. coli* JM109(DE3)**

Expression of c1 and the vector was also carried out using in *E. coli* JM109(DE3) strain of cells under the same expression conditions as for JM109 (4.4.6.1.1) but using both LB media and LB media supplemented with sorbitol. These were allowed to grow for up to 22 hours and 1ml samples were removed at the times 0, 1, 3, 4 and 22 hours after the addition of IPTG for analysis on SDS PAGE and Western blot using CaM-PDE antibody. PDE activity assays in the presence and absence of Ca<sup>2+</sup>/CaM and vinpocetine were also carried out.

#### **4.4.6.2 Large-scale expression and purification of pTrcHisA-PDE1A<sub>1N-trunc</sub> clone 1**

Large scale expression of c1 was carried out in order to produce enough recombinant protein for purification using nickel chelate affinity chromatography.

##### **4.4.6.2.1 Expression of pTrcHisA-PDE1A<sub>1N-trunc</sub> (c1) in *E. coli* JM109 using a 10-litre fermenter vessel**

An overnight culture of the construct, c1, was started by inoculating 100µl of a 40% glycerol stock of the construct into 100ml of LB (ampicillin). This was used to inoculate 10 litres of LB in a fermenter vessel supplemented with 100µg/ml ampicillin. The culture was allowed to grow for approximately 3 hours and then IPTG added to a final concentration of 1mM. This was then grown for a further 4 hours before harvesting the cells. 500ml volumes of the cultures were centrifuged at 3,600g, 4°C for 25 minutes which were then washed once with PBS. Washed cells were collected into pre-weighed 50ml-falcon tubes and stored at -70°C until required. The 10-litre bacterial culture was divided into seven pre-weighed falcon tubes. Each contained a pellet of approximately 3.5g. For analysis, one of the falcon tubes containing the cells was freeze-thawed twice, resuspended in Lysis Buffer 2 (Table 2.3) containing protease inhibitors. Cells were then sonicated at setting 3 with three 10 second bursts separated by cooling of the cells on ice for about 30 seconds. The lysed cells were centrifuged at 40,000g and the supernatant sample analysed for PDE activity while SDS PAGE and Western blot analysis were carried out both the supernatant and the particulate samples.

##### **4.4.6.2.2 Purification of pTrcHisA-PDE1<sub>1N-trunc</sub> clone 1 expressed in *E. coli* JM109**

The Xpress Protein Purification system (Invitrogen) protocol was followed for purification of the histidine-tagged recombinant protein from the large-scale expression. SDS PAGE as well as Western blot analysis had indicated that the recombinant protein was sequestered into inclusion bodies so the protein was extracted from these inclusion bodies under denaturing conditions. The procedure was carried out at 4°C with buffers also equilibrated to 4°C (pH of the buffers adjusted at 4°C).

#### 4.4.6.2.2.1 Denaturing and Elution Buffers

Guanidinium Lysis Buffer    6M Guanidine Hydrochloride  
   20mM Sodium Phosphate  
   500mM Sodium Chloride  
   pH 7.8

Denaturing Binding Buffer    8M Urea  
   20mM Sodium Phosphate  
   500mM Sodium Chloride  
   pH 7.8

Denaturing Wash Buffer       8M Urea  
pH 6.0                               20mM Sodium Phosphate  
   500mM Sodium Chloride  
   pH 6.0

Denaturing Wash Buffer       8M Urea  
pH 5.3                               20mM Sodium Phosphate  
   500mM Sodium Chloride  
   pH 5.3

Denaturing Elution Buffer    8M Urea  
   20mM Sodium Phosphate  
   500mM Sodium Chloride  
   pH 4.0

#### 4.4.6.2.2.2 Equilibration of the nickel resin

2ml of the resuspended nickel resin were poured into a plastic 20ml column and allowed to settle by gravity. The buffer containing preservatives was allowed to drain through and the resin washed twice with 10ml of sterile, distilled water. Resin was then washed twice with 10ml of Denaturing Binding Buffer and kept in this buffer until sample application.

#### **4.4.6.2.2.3 Sample preparation**

An aliquot of the cell pellet (~1.5g) from the 10 litre fermenter culture was allowed to thaw completely and 25ml of guanidinium lysis buffer used to resuspend the cells thoroughly. The cells were left on a rocking platform at room temperature for approximately 30 minutes then sonicated for 10 seconds up to five times with cooling on ice between the pulses. The sample was then centrifuged at 10,000g for 30 minutes to clear the lysate which was separated from the particulate fraction and divided into two. Half was processed straightaway and the other half stored at -20°C for use later.

#### **4.4.6.2.2.4 Sample application and elution**

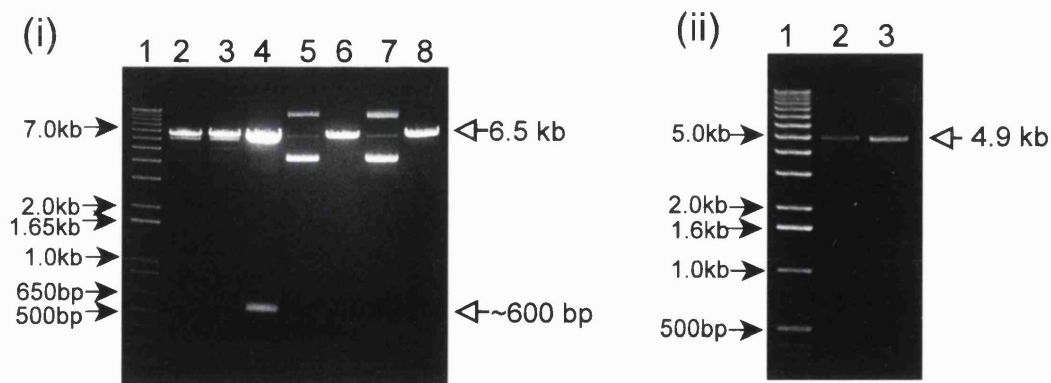
The cleared cell lysate was applied to the pre-equilibrated nickel resin and allowed to flow through the resin by gravity. The flow-through was reapplied to the resin twice more. The resin was then washed twice with 5ml of Denaturing Binding Buffer followed by two 5ml washes of each of the Denaturing Wash Buffer pH 6.0 and Denaturing Wash Buffer pH 5.3. Protein was eluted using 25ml of the Denaturing Elution Buffer (pH 4.0) which allowed elution of the recombinant protein from the resin through a drop in pH. 1ml elution fractions were collected and the presence of protein detected by measuring the absorbance at wavelength 280nm. Fractions containing protein were pooled and dialysed overnight at 4°C against buffer (10mM Tris, pH 8.0, 0.1% Triton X-100, PMSF) containing 1M urea followed by dialysis against 400ml of buffer containing no urea. The dialysed sample was concentrated ten-fold and analysed on SDS PAGE and by Western blotting using CaM-PDE antibody. PDE bioassays were also performed on the sample as described in section 2.2.11.

## 4.5 Results and Discussion

### 4.5.1 Cloning of PDE1A1 in pGEX-3X

#### 4.5.1.1 Screening transformant *E. coli* colonies

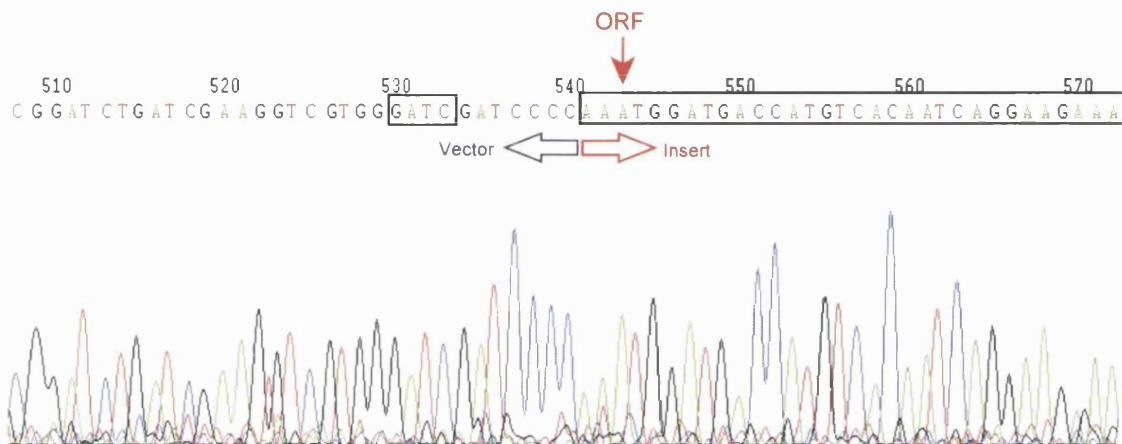
Plasmid DNA purified from *E. coli* cells, transformed with the construct pGEX-3X-PDE1A1, was analysed using a combination of the restriction enzymes *Bam*HI and *Hind*III as well as *Bam*HI alone. As already discussed (section 4.2.2.1), cloning of the PDE1A1 ORF in pGEX-3X caused a frame-shift which was overcome by carrying out a filling-in reaction to add four extra bases (see cloning strategy Figure 4.1) which in turn destroyed a *Bam*HI restriction site. This was used as the basis for selecting constructs in the correct reading frame. Figure 4.5.1 shows the results for the two constructs (clones 12 and 17) positively identified by enzyme restriction analysis using *Bam*HI and *Hind*III enzymes which gave single bands equivalent to 6.5 kb arising from a single cut at the *Hind*III site since the in-frame constructs no longer have the *Bam*HI restriction site (Lanes 2 and 3). It also shows the results for constructs digested with *Bam*HI to confirm that the *Bam*HI site had indeed been destroyed (lanes 5 and 7).



**Figure 4.5.1** Agarose gel analysis of pGEX-3X-PDE1A1 constructs showing clones 12 and 17 (i) and the vector pGEX-3X (ii). Figure (i) Lane 1 = 1 kb<sup>+</sup> DNA ladder with sizes indicated on the left; Lanes 2 and 3 = *Bam*HI+*Hind*III digested clones 12 and 17 showing a single linearised fragment (6.5 kb); Lane 4 = out-of-frame pGEX-3X-PDE1A1 construct digested with *Bam*HI+*Hind*III giving two fragments of 5.9 kb and 0.6 kb sizes; Lanes 5 and 7 = *Bam*HI digested clones 12 and 17; Lanes 6 and 8 = *Hind*III digested clones 12 and 17. Figure (ii) Lane 1 = 1 kb DNA ladder; Lanes 2 and 3 = empty vector pGEX-3X digested with *Bam*HI (4.9 kb).

### 4.5.1.2 Automated DNA sequence analysis

DNA sequence analysis was carried out to further confirm the in-frame cloning of the PDE1A1 ORF in pGEX-3X for both clones 12 and 17. Figure 4.5.2 shows a portion of the sequenced DNA for clone 12 at the junction of the insert and the vector. This showed the successful insertion of the four additional bases upstream of the ORF (GATC) used to bring the ORF back into the correct reading frame.



**Figure 4.5.2** DNA sequence analysis of the construct pGEX-3X-PDE1A1 (c12). The PDE1A1 insert is indicated by the open box which also marks the position of the first codon translated (red arrow). The four extra bases (GATC) added to the construct to bring the ORF back in-frame are indicated by the closed box.

Expression studies were carried out on c12 and the empty vector as the control for background PDE activity. Parameters investigated for the recombinant protein expression were temperature of protein expression, presence and absence of IPTG as well as the addition of sorbitol to the expression media.

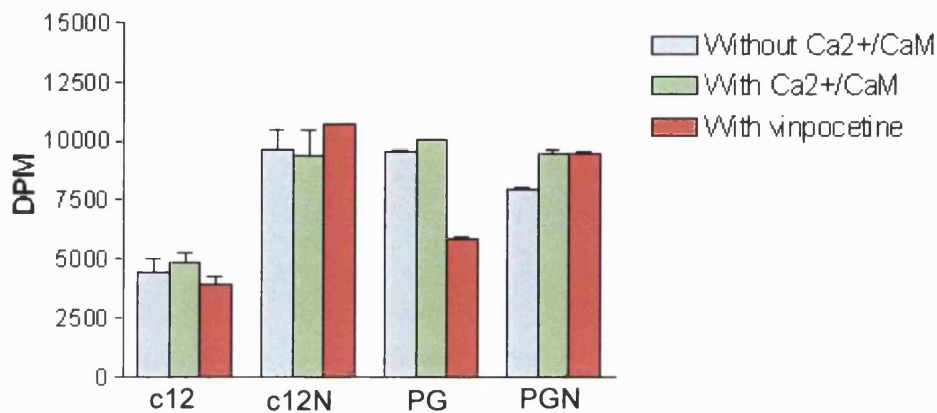
## 4.5.2 Expression studies on pGEX-3X-PDE1A1 (c12)

### 4.5.2.1 Effect of temperature on protein expression

Expression was first carried out at 37°C in LB media (with ampicillin) in the presence and absence of IPTG, and samples allowed to grow for three hours. PDE activity assays were performed at the end of this time on cleared total cell lysate samples (supernatants) for c12



as well as the vector only (PG). Figure 4.6 shows the PDE activity results for this expression study.

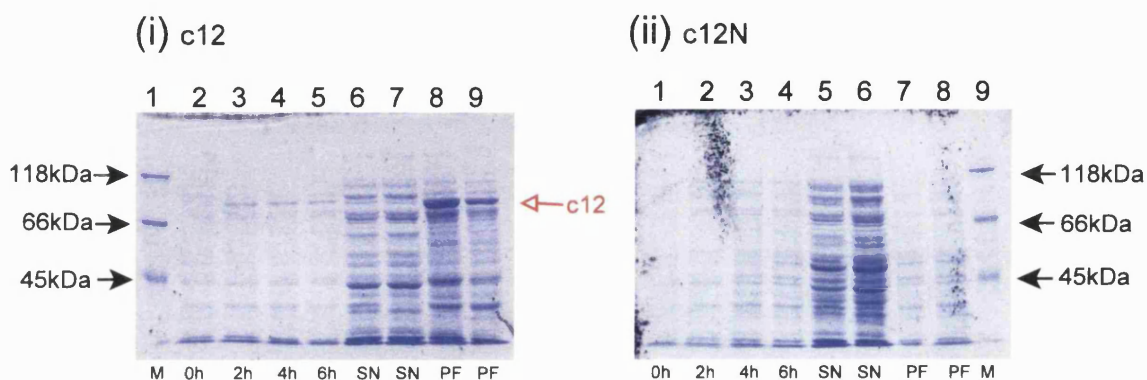


**Figure 4.6** Effect of IPTG on recombinant protein expression carried out at 37°C. PDE activity assays were carried out on cleared total cell lysate samples using cAMP as the substrate in the presence and absence of Ca<sup>2+</sup>/CaM (100µM and 10units per assay respectively) and vinpocetine (100µM). c12 and PG represent samples that were induced with IPTG while c12N and PGN represent samples that were left uninduced.

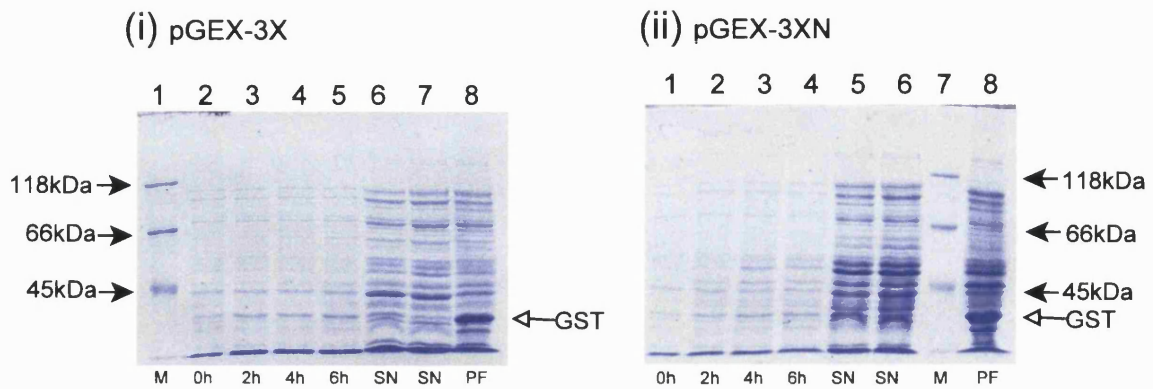
The expression carried out at 37°C did not show significant PDE activity in c12 above the background activity detected in the empty vector (Figure 4.6). In fact, PDE activity in the vector was slightly higher than for c12. When IPTG was omitted for c12, levels of PDE activity were similar to the empty vector. These results indicated that there was insignificant soluble recombinant PDE activity present in the supernatant samples and that the PDE activity detected in c12 was background activity. The fact that the recombinant PDE activity was lower in c12 compared to the empty vector may be because the presence of the recombinant enzyme following IPTG resulted in the initial over-expression of the recombinant enzyme which was possibly followed by the proteolytic cleavage of the recombinant protein as well as the endogenous PDE. This was likely to be the case since omission of IPTG in c12 gave similar activity results as the empty vector.

In order to improve recombinant protein expression, the expression temperature was lowered to 24°C. Growth at lower temperatures has been thought to facilitate the correct folding of proteins (Georgio and Valax, 1996), and has been used successfully for PDE4 proteins (Kovala *et al.*, 1997). However, in the present study, PDE activity analysis on cleared total cell lysate samples of c12 expressed at a lower temperature again did not show

significant activity above background (data not shown). Total cell lysate samples (from 0 - 6 hours post-induction) as well as cleared lysate samples (supernatant samples, SN) were analysed by SDS PAGE and by Western blotting using GST antibody as well as CaM-PDE antibody. Figures 4.7.1a and 4.7.1b show c12 and the empty vector respectively analysed by SDS PAGE while Figures 4.7.2 (i) and 4.7.2 (ii) shows the Western blot analysis carried out on these samples using GST and CaM-PDE antibodies.

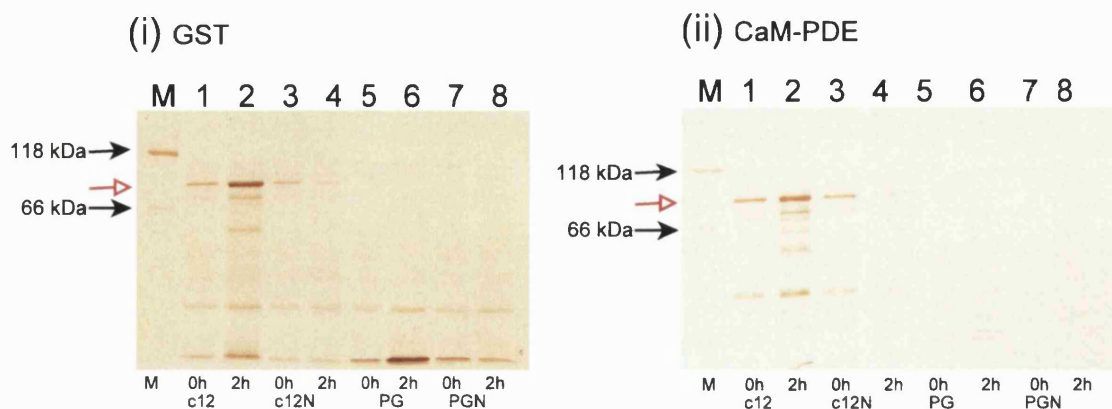


**Figure 4.7.1a** SDS PAGE analysis of c12 expressed at 24°C in the presence and absence of IPTG. (i) Lanes 2 - 5 represent c12 timed samples removed for analysis at time 0, 2, 4 and 6 hours post-induction; (ii) Lanes 2 - 5 represents samples removed at the same time points for uninduced c12 samples. Time points are indicated below the lanes which also indicate the supernatant (SN) and the particulate fraction (PF) samples, in duplicate, harvested at 6 hours post-induction together with the marker lanes. The position of the fusion protein (GST-PDE1A1) is indicated on the first gel (i) by the red arrow (~83 kDa size).



**Figure 4.7.1b** SDS PAGE analysis on pGEX-3X expressed at 24°C in the presence and absence of IPTG. (i) shows the results for the induced pGEX-3X samples removed at the time points 0, 2, 4 and 6 hours post-induction (Lanes 2 - 5) together with the supernatant (SN) and particulate fraction (PF) samples of cells harvested at the end of the induction period (6 hours). (ii) shows the samples removed at the same time points (0 - 6 hours; Lanes 1 - 4) but were allowed to grow without the addition of IPTG (PGN). The position of the GST protein is indicated by the open arrow on both gels (~26 kDa).

SDS PAGE analysis for total cell lysate samples of c12 and the empty vector following expression at 24°C revealed the presence of a protein band in c12 corresponding to the fusion protein, GST-PDE1A1 (~83 kDa), which was absent in the samples for the empty vector (Figure 4.7.1a). The vector showed the presence of a band at ~26 kDa which corresponded to the GST protein (Figure 4.7.1b). However, GST-PDE1A1 protein was only present in the total cell lysate and particulate fraction samples with no corresponding protein band seen in the supernatant samples (see Figure 4.7.1a). PDE activity analysis on supernatant samples of c12 and the vector gave similar results as for expression at 37°C (data not shown).



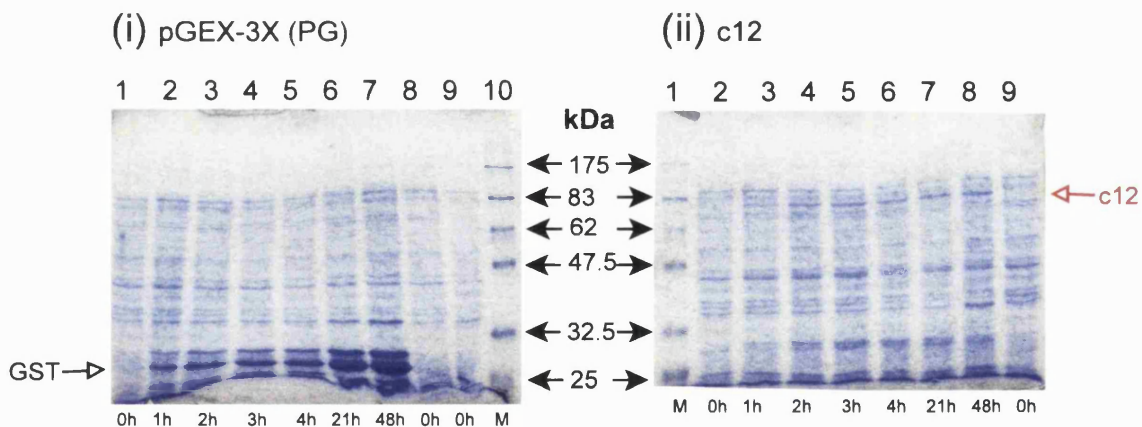
**Figure 4.7.2** Western blot analysis on c12 and the vector using GST and CaM-PDE antibodies for expression carried out at 24°C. (i) represents results for the GST Western blot carried out on both c12 and pGEX-3X (PG) in the presence and absence of IPTG. Lanes 1 and 3 = c12 at time 0 hours in the presence (c12) and absence (c12N) of IPTG respectively; Lane 2 and 4 = c12 at time 2 hours in the presence and absence of IPTG respectively; Lanes 5 and 7 = pGEX-3X at time 0 hours in the presence (PG) and absence (PGN) of IPTG; Lanes 6 and 8 = PG and PGN respectively at 2 hours post-induction. (ii) represents the results for the CaM-PDE Western blot for these samples with samples loaded in the same order. The marker lane represents the in-house marker mixture which included  $\beta$ -Galactosidase (118 kDa), BSA (66 kDa) and ovalbumin (45 kDa). Position of the markers are indicated on the left of both gels. The position of the fusion protein, GST-PDE1A1 (~83 kDa), is indicated by the red arrow.

The Western blot analysis carried out on c12 total cell lysate samples, using GST as well as CaM-PDE antibody, did confirm the successful expression of GST-PDE1A1 (Figure 4.7.2). However, the Western blot analysis carried out on c12 supernatant samples did not show a positive signal which meant that the fusion protein was not being expressed in a soluble form (data not shown), which was confirmed by the lack of PDE activity in these samples. The presence of GST-PDE1A1 in the total cell lysate and particulate fraction samples only suggested that the protein was probably not being folded correctly so was being sequestered into insoluble inclusion bodies. This occurred despite the drop in the expression temperature. Fusion proteins with a GST fusion partner have been expressed successfully as soluble proteins by Kovala and co-workers (1997). These workers initially expressed GST-PDE4 at 37°C and found that most of the fusion protein was being formed into insoluble inclusion bodies. However, a drop in the expression temperature from 37°C to 24°C was successful in the generation of soluble protein which could subsequently be purified from cleared total cell lysate samples to yield an active protein. Since a drop in

expression temperature was not successful in the present study, supplementing the culture media for the expression of soluble PDE1A1 was explored.

#### 4.5.2.2 Protein expression in media supplemented with sorbitol

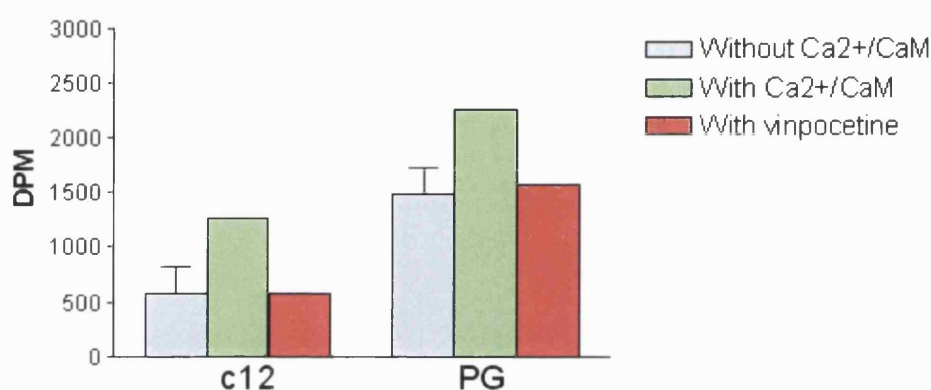
Supplementing culture media with sorbitol for the expression of soluble recombinant protein in *E. coli* has been used successfully for proteins such as mouse phosphofructo-1-kinase (Gunasekera and Kemp, 1999; Blackwell and Horgan, 1991). In the present study, LB media as well as LB media supplemented with 0.5M sorbitol (designated LBS) was used for expression studies on c12 and the vector as described in section 4.4.2.2. Cultures were allowed to grow for up to 48 hours. Figure 4.8 shows the SDS PAGE analysis carried out on total cell lysate samples. These revealed the presence of GST-PDE1A1 as well as GST protein from 1 hour after the addition of IPTG with the strongest signals seen between 21 and 48 hours post-induction in the total cell lysate samples.



**Figure 4.8** SDS PAGE analysis of c12 and the vector for expression carried out at 30°C with media supplemented with sorbitol. (i) vector showing expression of GST: Lanes 1 - 7 = 0 - 48 hours post-induction. GST protein is indicated by the open arrow on the left. (ii) c12 showing expression of the fusion protein (c12; ~83 kDa; indicated by the red arrow): Lanes 2 - 8 = 0 - 48h post-induction.

A second expression experiment was set up using identical conditions but cells were allowed to grow for up to 24 hours following the addition of IPTG. This was carried out for both c12 and the vector as before. Cleared total cell lysate samples at the end of the expression period were analysed for PDE activity and these results are shown in Figure

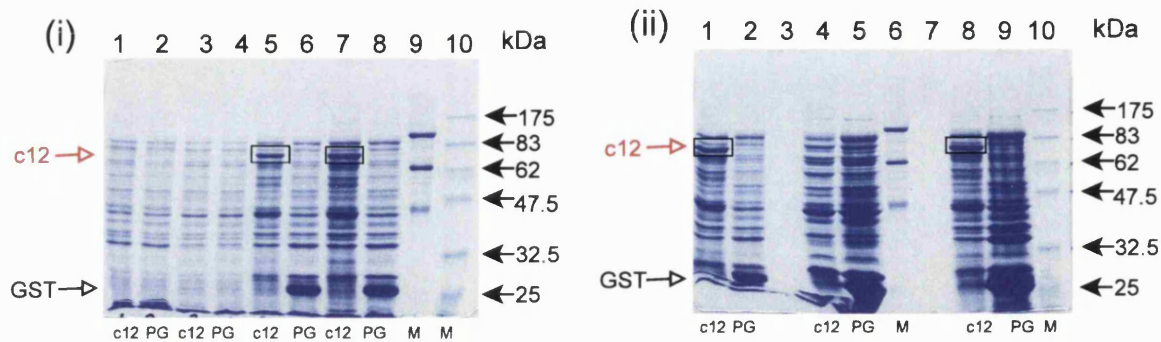
4.9.1. The PDE assays were carried out in the presence and absence of  $\text{Ca}^{2+}/\text{CaM}$  and vinpocetine. The activity results for c12 did show the presence of PDE activity which was stimulated in the presence of  $\text{Ca}^{2+}/\text{CaM}$  and inhibited by vinpocetine but the vector also showed similar results indicating that the activity detected in c12 supernatant samples was background PDE activity. In fact, just as with the GST-PDE1A1 protein expressed at 37°C and 24°C using LB media, the background activity in the vector was higher than that detected in c12.



**Figure 4.9.1** PDE activity analysis of c12 and pGEX-3X cleared total cell lysate samples for expression carried out at 30°C with media supplemented with sorbitol.

PDE activity assays were carried out using cAMP as the substrate in the presence and absence of  $\text{Ca}^{2+}/\text{CaM}$  and vinpocetine.

Figure 4.9.2 (i) shows the SDS PAGE analysis of total cell lysate samples of c12 and the empty vector while Figure 4.9.2 (ii) shows the cleared lysate samples as well as particulate fraction samples for c12 and the empty vector. The latter figure (ii) showed the presence of the recombinant protein in the total cell lysate and the particulate fraction samples only, and not in the cleared lysate sample (also shown in Figure 4.10.1). These results were confirmed by the Western blot analysis (Figure 4.10.2) which showed that most of the recombinant protein was present as insoluble inclusion bodies. However, the blot did show a very weak signal in the cleared total cell lysate sample so it was possible that there was some soluble recombinant protein but that it was not active.



**Figure 4.9.2** SDS PAGE analysis of c12 and pGEX-3X samples expressed at 30°C in media supplemented with sorbitol. Order of samples is shown in the keys below.

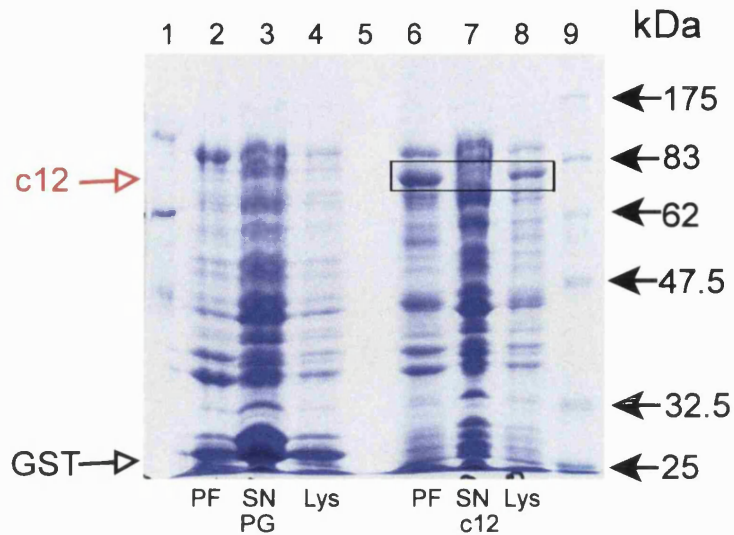
**Key to Figure 4.9.2 (i):**

Lane	1	2	3	4	5	6	7	8	9	10
Sample	c12	PG	c12	PG	c12	PG	c12	PG	M	M
			Lys	Lys	Lys	Lys	Lys	Lys		
Post-IPTG	ON	ON	0	0	24	24	24	24		
Time (hours)										

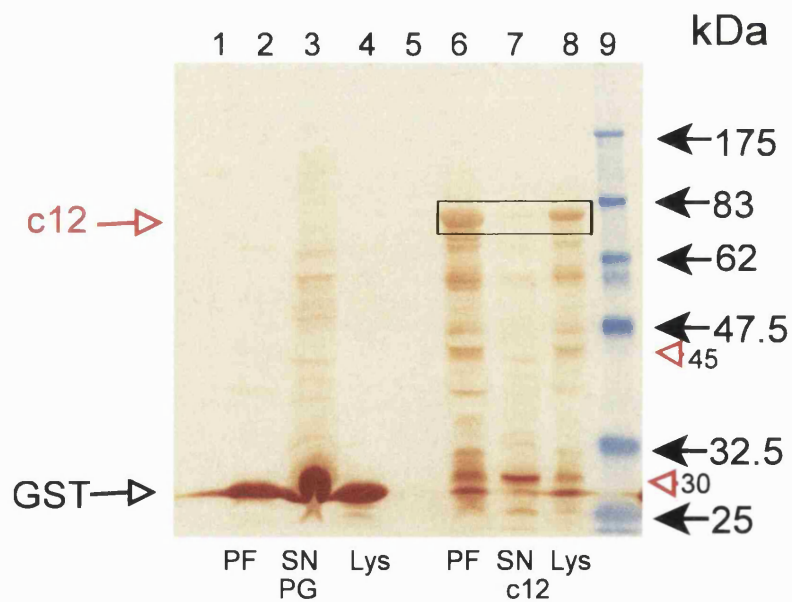
**Key to Figure 4.9.2 (ii):**

Lane	1	2	3	4	5	6	7	8	9	10
Sample	c12	PG	-	c12	PG	M	-	c12	PG	M
	Lys	Lys	-	SN	SN		-	PF	PF	
Post-IPTG	24	24	-	24	24		-	24	24	
Time (hours)										

Abbreviations: Lys = Total cell lysate sample  
 SN = cleared total cell lysate following sonication  
 PF = particulate fraction  
 c12 = clone 12 (pGEX-3X-PDE1A1)  
 PG = vector (pGEX-3X)  
 M = pre-stained protein markers



**Figure 4.10.1** SDS PAGE analysis of clone 12 and the vector for expression carried out at 30°C in media supplemented with sorbitol. Lanes 2, 3 and 4 = 24h PG post-sonication particulate fraction (PF), supernatant and lysate samples respectively; Lanes 6, 7 and 8 = 24h c12 post-sonication PF, supernatant and lysate samples respectively; Lane 1 = in-house protein marker mixture; Lane 9 = pre-stained protein marker mixture with sizes indicated on the right. The closed box shows the position of the recombinant protein which is also marked by the red arrow.



**Figure 4.10.2** Western blot analysis of clone 12 and the vector for expression carried out at 30°C in media supplemented with sorbitol. Order of sample loading is as for Figure 4.10.1. The closed box shows the position of the recombinant protein which is also marked by the red arrow on the left of the blot.

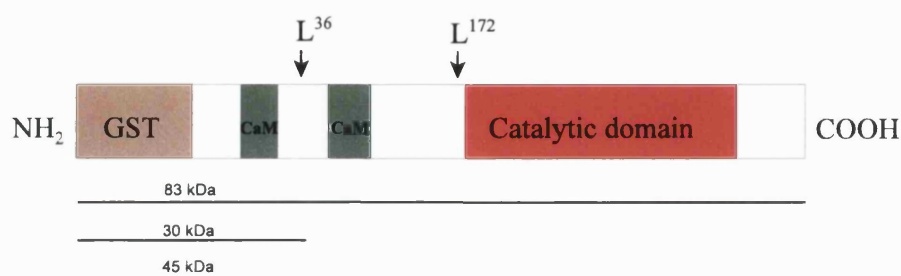
Abbreviations: Lys = Total cell lysate sample; SN = cleared total cell lysate following sonication; PF = particulate fraction; c12 = clone 12 (pGEX-3X-PDE1A1); PG = vector (pGEX-3X).



The Western blot results for c12 (Figure 4.10.2) showed that there was extensive proteolysis of GST-PDE1A1 protein in the particulate fraction sample which contained the insoluble inclusion bodies. The supernatant sample did show a strong signal for a proteolytic fragment of ~28-30 kDa in the Western blot (Figure 4.10.2; Lane 7, indicated by the arrowhead). Since the Western blot analysis was carried out using anti-GST antibody, the c12 cleavage product was likely to be the GST protein (26 kDa) plus a small portion of the PDE1A1 protein (~4 kDa). Kovala and co-workers (1997) found that the GST-PDE4D1 protein (73 kDa) they expressed was also being cleaved (50 kDa fragment) so they carried out N-terminal amino acid sequencing of the blotted full-length as well as the cleaved protein. They were able to match nine internal residues (XL<sup>210</sup>KTFKIPVD) for the cleaved protein starting at leucine 210 (L<sup>210</sup>) suggesting that cleavage had occurred at L<sup>210</sup>. An examination of the dog heart PDE1A1 amino acid sequence used in the present study (see Figure 1.19.1) did reveal the presence of two possible proteolytic cleavage sites at the N-terminal region of the enzyme, and cleavage at one of these sites (L<sup>36</sup>) would yield a fragment matching the 30 kDa signal seen on the Western blot (Figure 4.10.2). Table 4.2 shows the possible sites for proteolytic cleavage in GST-PDE1A1 together with the predicted fragment sizes of 30 kDa and 45 kDa while the panel below the table marks the position of these sites on GST-PDE1A1 protein. As already stated, the 30kDa fragment can be matched to the strong signal on the Western blot for c12 supernatant as well as particulate fraction samples (Figure 4.10.2) while the 45 kDa signal can be seen in the particulate fraction samples but is not so obvious in the supernatant samples. Proteolytic fragments identified are indicated by the arrowheads on the Western blot (Figure 4.10.2). Since there were more than just two proteolytic products, a number of additional cleavage sites must be present in the fusion protein. N-terminal amino acid sequencing of the blotted 30 kDa and 45 kDa proteolytic fragments would confirm the position of the cleavage site(s) in the GST-PDE1A1 protein.

**Table 4.2** GST-PDE1A1 fragments predicted following proteolytic cleavage.

Protein	Cleavage sequence	Fragment size (kDa)
PDE4D	X~L <sup>216</sup> KTFKIPVD	50
GST-PDE1A1	GST-X~L <sup>36</sup> KKNI	30
GST-PDE1A1	GST-X~L <sup>172</sup> INRFKIPVS	45



As already discussed in section 4.1.2, *E. coli* contains many proteases which are present in the cytosol as well as the cell membrane. The proteolytic degradation of recombinant proteins is a common problem of the prokaryotic expression systems. PDE enzymes expressed as GST fusion proteins (Kovala *et al.*, 1997) or as polyhistidine tagged protein (Richter *et al.*, 2000) have also been shown to be proteolytically cleaved when expressed in *E. coli*. The other major drawback of the prokaryotic expression system is the generation of inclusion bodies during heterologous protein expression. Despite modulation in the growth temperature or growth media, most of the foreign proteins are frequently expressed as insoluble proteins, as was the case in the present study. This however, can be advantageous since the inclusion bodies contain large amounts of the foreign protein. This was certainly the case in the present study for GST-PDE1A1 protein as indicated by the SDS PAGE and Western blot analysis on the particulate fraction samples which contained the insoluble inclusion bodies. Richter and co-workers (2000, 2002) have successfully refolded and purified PDE proteins (PDE4A and PDE7A) from inclusion bodies as active proteins so refolding of GST-PDE1A1 from inclusion bodies was carried out as the next step in the present study.

#### 4.5.3 Refolding of GST-PDE1A1 from inclusion bodies

Since protein expression studies on c12 had resulted in the production of GST-PDE1A1 as insoluble inclusion bodies, refolding of the fusion protein from these inclusion bodies was

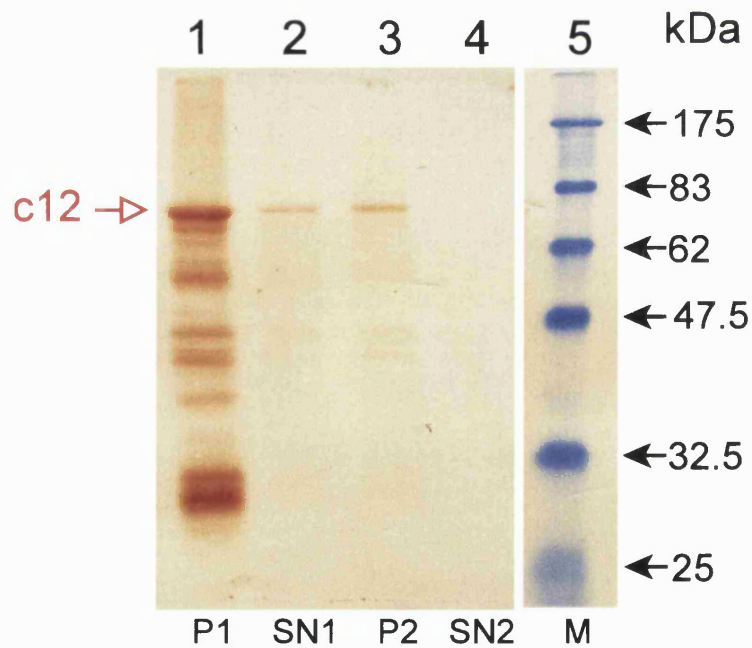
carried out as described in section 4.4.4. The refolded proteins were dialysed in two steps in order to remove the denaturant as described in section 4.4.4.3. Dialysed samples were analysed by SDS PAGE analysis and Figure 4.11 shows the silver stained SDS PAGE gel for c12 samples following the first dialysis step. These results revealed the presence of GST-PDE1A1 protein (~83 kDa) in the refolded, concentrated sample (Figure 4.11; Lane 1, C1) as well as the dialysed lysate sample (Figure 4.11; Lane 2, L1). However, when the dialysed lysate sample was centrifuged, there was no protein detected in the resulting supernatant sample (Figure 4.11; Lane 3, SN1) but analysis on the resultant pellet sample showed the presence of GST-PDE1A1 protein (Figure 4.11; Lane 4, P1) indicating that the fusion protein was precipitating out of solution following dialysis. It was possible that the fusion protein was being refolded incorrectly so tending to precipitate out of solution. Western blot analysis using GST antibody was carried out on the dialysed c12 supernatant and pellet samples from the two dialysis steps (Figure 4.12). These, firstly, confirmed the presence of GST-PDE1A1 in the refolded, dialysed sample from the first dialysis step (Figure 4.12; Lane 2) and, secondly, confirmed the loss of soluble refolded protein following the second dialysis step (Figure 4.12; Lane 4). It was possible that while some of the GST-PDE1A1 protein may be folding correctly, there may have been some misfolded GST-PDE1A1 protein which was aggregating and thereby resulting in the aggregation of the rest of the proteins present. Also, there may have been *E. coli* contaminating proteins present in the inclusion bodies, which were insoluble, and may have caused aggregation of the recombinant protein. The silver-stained gel (Figure 4.11) does show the presence of many proteins, some of which were likely to be *E. coli* proteins since the Western blot revealed much fewer proteins, corresponding to the full-length GST-PDE1A1 as well as the proteolytically cleaved fragments (Figure 4.12). This proteolysis may have occurred following over-expression in *E. coli* before segregation of the fusion protein into inclusion bodies, or during the refolding stages as some of the *E. coli* proteases are active under denaturing conditions with some adsorbing onto the inclusion body surface (Baneyx, 1999). The use of GST-affinity chromatography in the purification of the fusion protein from inclusion bodies may have been useful in separating the fusion protein from contaminating proteins and host proteases but this was not investigated in the present study.

PDE analysis was also carried out on the dialysed c12 supernatant samples and these did not show any PDE activity (data not shown). The Western blot on both supernatant

samples did show the presence of GST-PDE1A1 in the sample following the first dialysis step (Figure 4.12; Lane 2) but PDE activity analysis revealed that this protein was not an active protein. Although soluble, the protein may not have folded correctly for activity. PDE proteins have been successfully refolded from inclusion bodies by Richter and co-workers for PDE4A (2000) and the catalytic fragment for PDE7A (2002). In the case of PDE7A (Richter *et al.*, 2002), refolding of the protein was found to be enhanced by the presence of high concentrations of arginine (1M), ethylene glycol (50%) and magnesium chloride (200mM). These workers also found that the addition of protease inhibitors, especially PMSF, actually decreased refolding efficiency. In the present study, PMSF was only added to the bacterial cells resuspended in lysis buffer 2, together with a mixture of protease inhibitors (see section 2.2.16), during the disruption of the cells by sonication as described in section 4.4.3.2. Protease inhibitors were not added during the refolding or dialysis procedures but only added to the final dialysed sample of refolded GST-PDE1A1 (TPCK, TLCK, leupeptin, chymostatin and pepstatin but no PMSF). Richter and co-workers used affinity chromatography to further purify their refolded PDE4A (Richter *et al.*, 2000) and PDE7A (Richter *et al.*, 2002) proteins. The refolded GST-PDE1A1 protein in the present study was not purified further since the dialysis of the refolded recombinant protein had resulted in the precipitation of the protein, and hence loss of the soluble protein. Another factor to consider was that of the fusion partner. In the refolding and purification studies carried out by Richter and co-workers (2000, 2002), the PDE proteins were polyhistidine (His<sub>6</sub>)-tagged proteins. It was possible that the presence of the large GST fusion partner used in the present study was having a detrimental effect on the solubility of the PDE1A1 protein despite the fact that fusion partners are thought to help form soluble proteins (Smith and Johnson, 1988; Sachdev and Chirgwin, 1998; Kapust and Waugh, 1999).



**Figure 4.11** Analysis of c12 proteins refolded from inclusion bodies. Lane 1 = purified centriprep-10 c12 concentrate (C1); Lane 2 = purified c12 lysate following dialysis (L1); Lane 3 = dialysed c12, supernatant sample (SN1); Lane 4 = dialysed c12, pellet sample (P1); Lane 6 = pre-stained protein marker mixture with the sizes indicated on the right. The position of the fusion protein, GST-PDE1A1 (c12), is shown in red (~83 kDa).



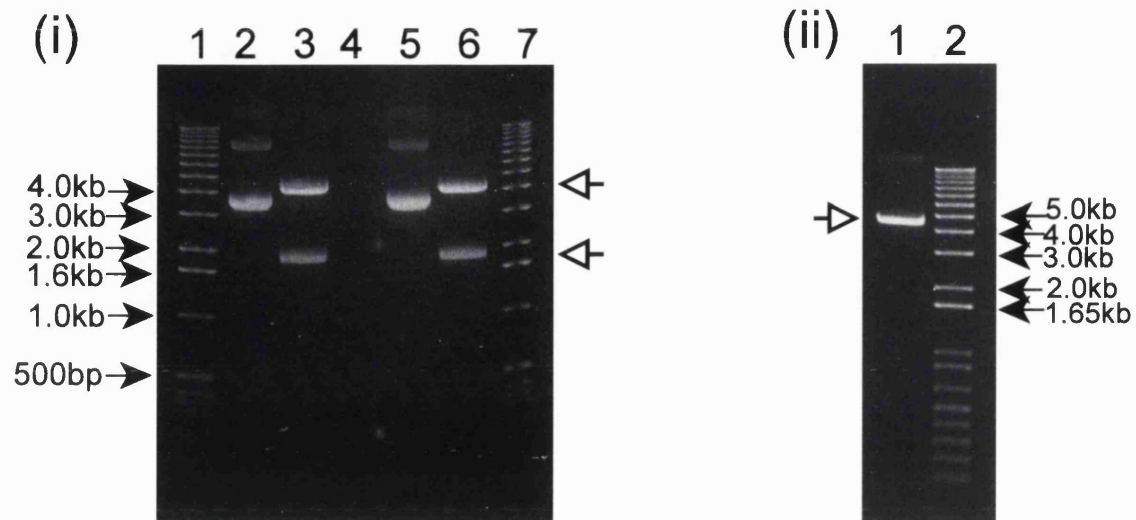
**Figure 4.12** Western blot analysis of c12 proteins purified from inclusion bodies. Lanes 1 and 2 = c12 pellet (P1) and supernatant (SN1; dialysed to ~8mM urea) samples respectively; Lanes 3 and 4 = c12 P2 and SN2 (dialysed to ~40 $\mu$ M urea) samples respectively; Lane 5 = pre-stained protein marker mixture with sizes indicated on the right.

Since initial attempts at producing soluble protein produced insoluble protein using the pGEX expression vector, no further expression studies were carried out with this vector. Also, initial purification of the recombinant protein from inclusion bodies indicated extensive proteolysis of the fusion protein and this together with the fact that the recombinant protein was being precipitated out of solution following dialysis indicated that the purified protein was not being refolded correctly. Optimisation of the refolding conditions would be required in this case exploring buffer composition, pH as well as additives such as arginine as described by Richter and co-workers (2002) and also by Chen and Gouaux (1997). These parameters do vary between the proteins being refolded so extensive screening was necessary to optimise the refolding conditions for GST-PDE1A1 in the present study. However, this was not pursued for GST-PDE1A1 but an alternative vector, pTrcHis, was used for further studies on the expression of soluble PDE1A1 in *E. coli*. This vector was chosen since it added just six histidine residues to the PDE1A1 protein and presented an alternative to the large GST fusion partner used so far. Also, the PDE proteins purified from inclusion bodies by Richter and co-workers (2000, 2002) were His<sub>6</sub>-tagged as already stated.

#### **4.5.4 Cloning of the N-terminal truncated PDE1A1 in pTrcHisA**

##### **4.5.4.1 Screening transformant *E. coli* colonies**

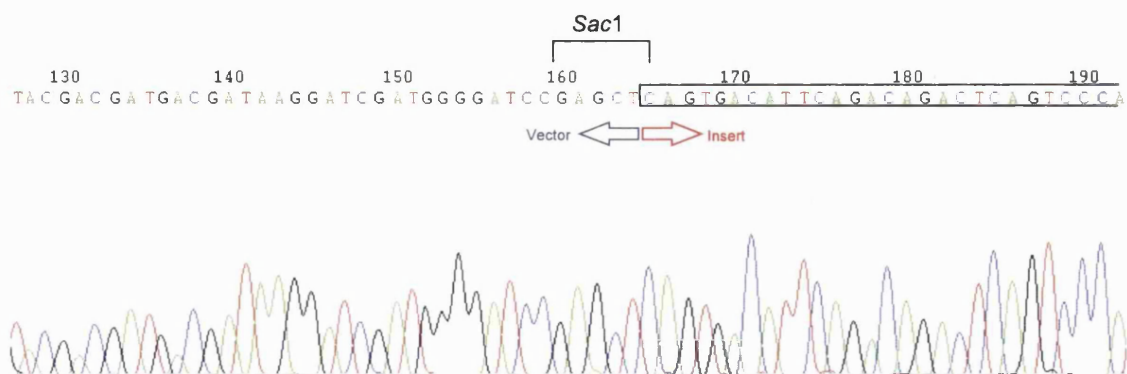
Plasmid DNA purified from *E. coli* cells transformed with pTrcHisA-PDE1A1<sub>N-trunc</sub> was analysed by restriction enzyme digestion using *Sph*I. Two clones were positively identified, c1 and c3. Figure 4.13.1 (i) shows the results of the two clones digested with *Sph*I. Similarly digested empty vector, pTrcHisA, is shown in Figure 4.13.1 (ii).



**Figure 4.13.1** Agarose gel analysis of pTrcHisA-PDE1A1<sub>N-trunc</sub> clones 1 and 3. Gel (i): Lanes 2 and 5 = uncut c1 and c3; Lanes 3 and 6 = *Sph*I-digested c1 and c3 showing the expected ~2.0 kb and ~4.0 kb fragments (indicated by the open arrows); Lanes 1 and 7 = 1kb DNA ladder with sizes indicated on the left. Gel (ii) Lane 1 = *Sph*I-digested vector, pTrcHisA, showing a single linearised fragment of ~4.4 kb; Lane 2 = 1kb+ DNA ladder.

#### 4.5.4.2 Automated DNA sequence analysis

DNA sequence analysis was carried out on the two clones, c1 and c3, to further confirm the cloning of PDE1A1<sub>N-trunc</sub> into pTrcHisA vector. Figure 4.13.2 shows a portion of the DNA sequence for c1 corresponding to the cloning of the insert in the multiple cloning site of the vector. The ORF had been successfully inserted into the *Sac*I (GAGCT↓C) cloning site of the vector as indicated by the sequence shown in Figure 4.13.2. The clone c1 was selected for expression studies.



**Figure 4.13.2** DNA sequence analysis for construct pTrcHisA-PDE1A1<sub>N-trunc</sub> c1. The sequence is shown at the site of the cloning of the insert into the *Sac*I restriction site located in the multiple cloning site.

#### 4.5.5 Small-scale expression of pTrcHisA-PDE1A1<sub>N-trunc</sub> in *E. coli*

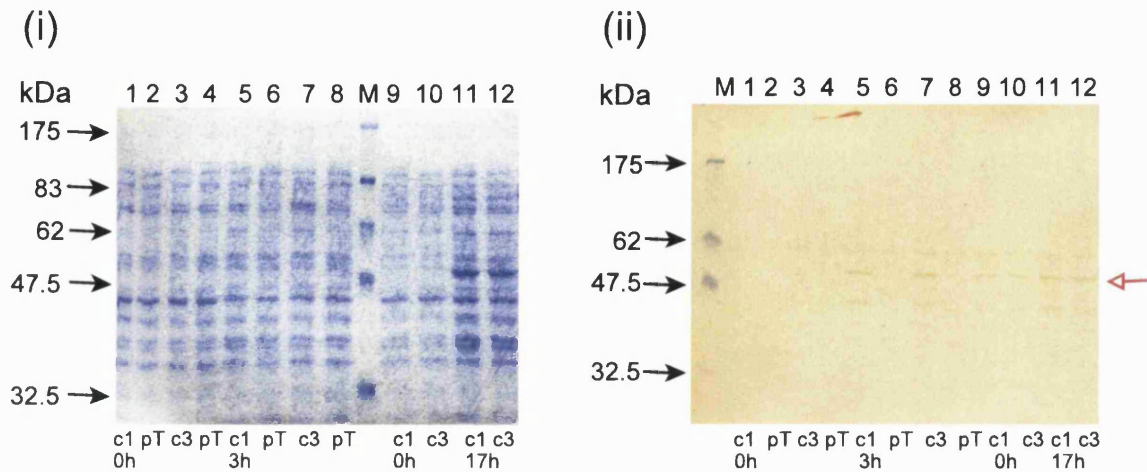
##### 4.5.5.1 pTrcHisA-PDE1A1<sub>N-trunc</sub> (c1 and c3) in *E. coli* JM109 cells

Initial expression studies were carried out in *E. coli* JM109 cells using the expression conditions described in section 4.4.2.2. which were for expression carried out at 30°C in the presence of IPTG using LB media supplemented with sorbitol. Figure 4.14.1 shows the total cell lysates for c1, c3 and the vector (pTrcHisA; PTA or pT) analysed by SDS PAGE and Western blot analysis. There was no obvious recombinant protein band visible on the Coomassie-stained gel but a signal for the recombinant protein was detected on the Western blot carried out using CaM-PDE antibody. Cells (c1) harvested at 3 hours post-induction were analysed for PDE activity and these results are shown in Figure 4.14.2.

The PDE activity analysis carried out for c1 and the empty vector (PTA) from the initial expression studies using *E. coli* JM109 cells did show the presence of PDE activity in c12 which was slightly above the background seen for the empty vector (Figure 4.14.2). This activity was inhibited by vinpocetine while the background was not. Based on these results, as well as the Western blot analysis (Figure 4.14.1), large scale protein expression in a fermenter was carried out for the production of sufficient protein for the purposes of purification which is described in section 4.5.6. However, small scale purification was also carried out using a different strain of *E. coli* cells, JM109(DE3) cells which is described in

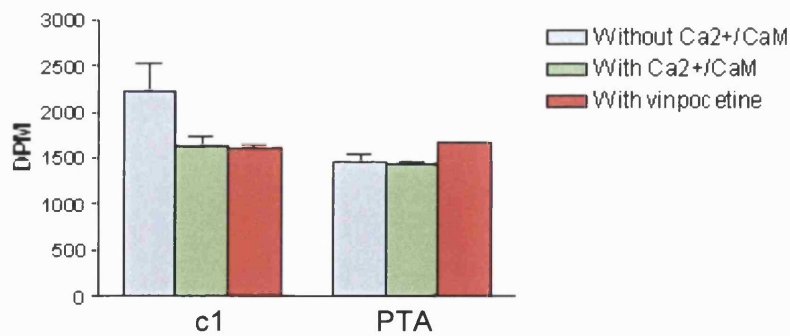


the next section (4.5.5.2).



**Figure 4.14.1** SDS PAGE and Western blot analysis of c1 and c3 expressed in *E. coli*

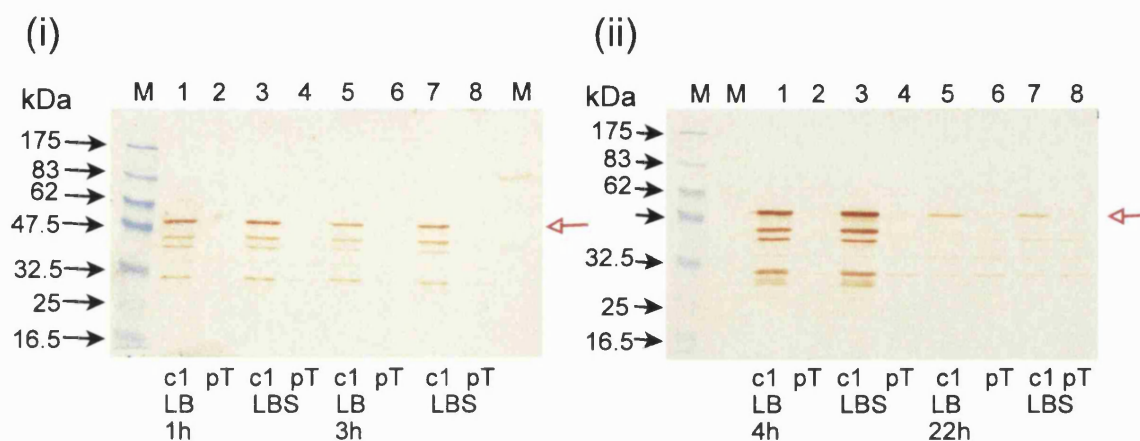
JM109 cells. (i) Lanes 1 and 3 = c1 and c3 respectively at 0 hours post-induction; Lanes 2 and 4 = empty vector (pT) at 0 hours post-induction; Lanes 5 and 7 = c1 and c3 respectively at 3 hours post-induction; Lanes 6 and 8 = empty vector at 3 hours post-induction; Lanes 9 and 10 = c1 and c3 respectively at 0 hours post-induction; Lanes 11 and 12 = c1 and c3 respectively at 17 hours post-induction. Marker lane is indicated (M) and sizes are shown in the left. (ii) Western blot analysis was carried out using CaM-PDE antibody with samples loaded in the same order as (i). The red arrow marks the position of the His<sub>6</sub>-PDE1A1<sub>N-trunc</sub> protein (~54 kDa).



**Figure 4.14.2** PDE activity analysis of c1 and PTA supernatant samples harvested at 3 hours post-induction. Assays were carried out in the presence of Ca<sup>2+</sup>/CaM and vinpocetine with cAMP as the substrate.

#### 4.5.5.2 pTrcHisA-PDE1A1<sub>N-trunc</sub> (c1) in *E. coli* JM109(DE3) cells

Small-scale expression studies were carried out in *E. coli* JM109 (DE3) cells for c1 which was expressed for up to 22 hours at 30°C in the presence of IPTG using both LB and LB media supplemented with sorbitol. Samples were removed at 1, 3, 4 and 22 hours post-induction for SDS PAGE, Western blot and PDE activity analysis. Figure 4.15.1 shows the Western blot results for total cell lysates. These showed the presence of the recombinant protein (His<sub>6</sub>-PDE1A1<sub>N-trunc</sub>) from one hour and for up to four hours after the addition of IPTG. The signal for the recombinant protein was markedly reduced at 22 hours post-IPTG (Figure 4.15.1(ii)). There was also no noticeable difference in the recombinant protein expressed in LB media or LB media supplemented with sorbitol. As with recombinant protein expression using the pGEX expression system, the recombinant protein expressed using the pTrcHis expression vector showed partial proteolysis of the recombinant protein (Figure 4.15.1). The Western blot for His<sub>6</sub>-PDE1A1<sub>N-trunc</sub> gave a relatively strong signal for the full-length protein as well as the proteolytic fragments so N-terminal amino acid sequencing would provide valuable insights into the cleavage sites present in the PDE1A1 protein. However, this was not carried out in the present study but could form part of the follow-up work on both GST-PDE1A1 and His<sub>6</sub>-PDE1A1<sub>N-trunc</sub> proteins. Potential proteolytic sites could then be mutated using the method of site-direction mutagenesis to prevent proteolysis of the protein.



**Figure 4.15.1** Western blot analysis of total cell lysates of c1 and the empty vector using CaM-PDE antibody for the expression carried out in *E. coli* JM109 (DE3) cells. The order of the samples is given in the key below. The position of pre-stained protein marker mixture is indicated (M) with sizes given on the left of the blots. Position of the recombinant protein is indicated by the open red arrows.

**Key to Figure 4.15.1(i):**

Lane	1	2	3	4	5	6	7	8
Sample	c1	pT	c1	pT	c1	pT	c1	pT
Media	LB	LB	LBS	LBS	LB	LB	LBS	LBS
Post-IPTG	1	1	1	1	3	3	3	3
Time (hours)								

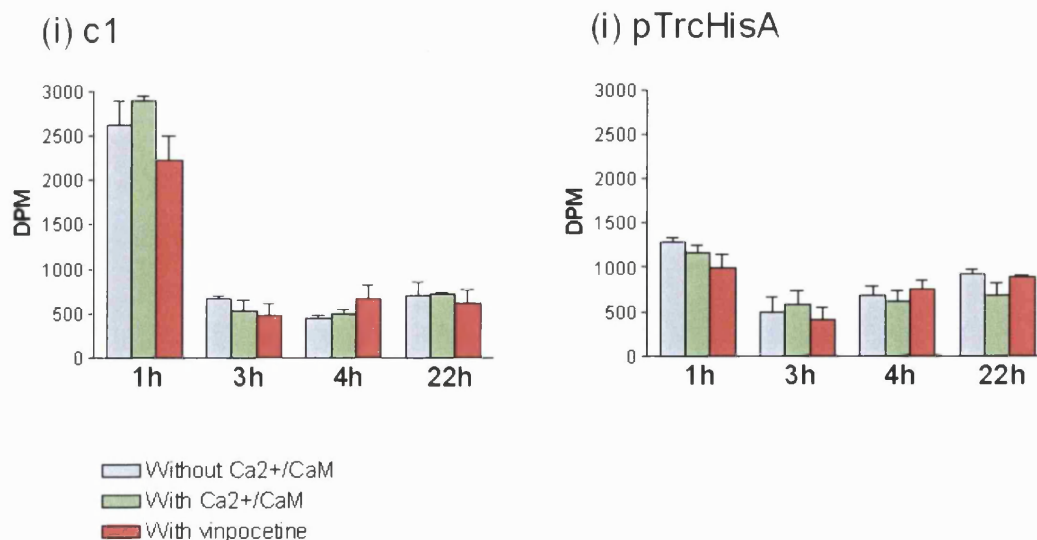
**Key to Figure 4.15.1 (ii):**

Lane	1	2	3	4	5	6	7	8
Sample	c1	pT	c1	pT	c1	pT	c1	pT
Media	LB	LB	LBS	LBS	LB	LB	LBS	LBS
Post-IPTG	4	4	4	4	22	22	22	22
Time (hours)								

Abbreviations: c1 = construct pTrcHisA-PDE1A1<sub>N-trunc</sub> pT = vector pTrcHisA  
 LB = Luria Broth LBS = Luria Broth supplemented with sorbitol

PDE activity assays were also carried out on the cleared sonicated total cell lysate samples for c1 and the vector expressed in LB media. Figure 4.15.2 shows the results for the PDE assay carried out in the presence and absence of Ca<sup>2+</sup>/CaM and vinpocetine. These showed that there was significant PDE activity above the background for c1 for samples at one hour post-induction. However, PDE activity was markedly reduced for samples analysed at three

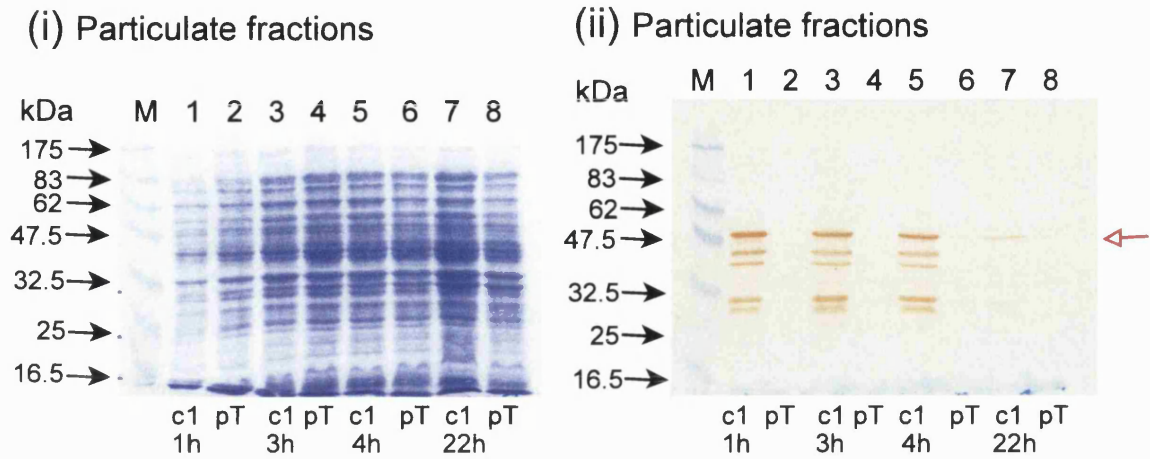
to twenty two hours post-IPTG (Figure 4.15.2). The activity for c1 was not stimulated in the presence of  $\text{Ca}^{2+}/\text{CaM}$  but was inhibited by vinpocetine. However, this inhibition by vinpocetine ( $100\mu\text{M}$ ) was not remarkable. This may have been due to the presence of other proteins (*E.coli* proteins) present in the sample which may be binding the inhibitor. The other point to note about the activity results for c1 is that of the lack of stimulation of the activity in the presence of  $\text{Ca}^{2+}/\text{CaM}$ . Although the construct His<sub>6</sub>-PDE1A1<sub>N-trunc</sub> was truncated at the N-terminal region, the second calmodulin-binding domain was still present in the construct (see Figure 4.3). The removal of the first calmodulin-binding domain in PDE1A1 and PDE1A2 enzymes was shown to produce enzymes that were still stimulated in the presence of  $\text{Ca}^{2+}/\text{CaM}$  (Sonnenburg *et al.*, 1995). Therefore, the PDE activity detected in the present study for His<sub>6</sub>-PDE1A1<sub>N-trunc</sub> was expected to be stimulated in the presence of  $\text{Ca}^{2+}/\text{CaM}$ . Sonnenburg and co-workers (1995) also identified a region of 11 amino acid residues located between the two calmodulin-binding domains as being important for retaining the enzymes in a less active state. This segment of inhibitory amino acids was still present in the His<sub>6</sub>-PDE1A1<sub>N-trunc</sub> construct used in the present study. It was possible that this segment was retaining the His<sub>6</sub>-PDE1A1<sub>N-trunc</sub> construct in a permanently less active state and that despite the addition of  $\text{Ca}^{2+}/\text{CaM}$ , the enzyme was not being stimulated. It was also possible that the presence of host proteins that may be binding  $\text{Ca}^{2+}/\text{CaM}$  were preventing access of the His<sub>6</sub>-PDE1A1<sub>N-trunc</sub> construct to  $\text{Ca}^{2+}/\text{CaM}$ .



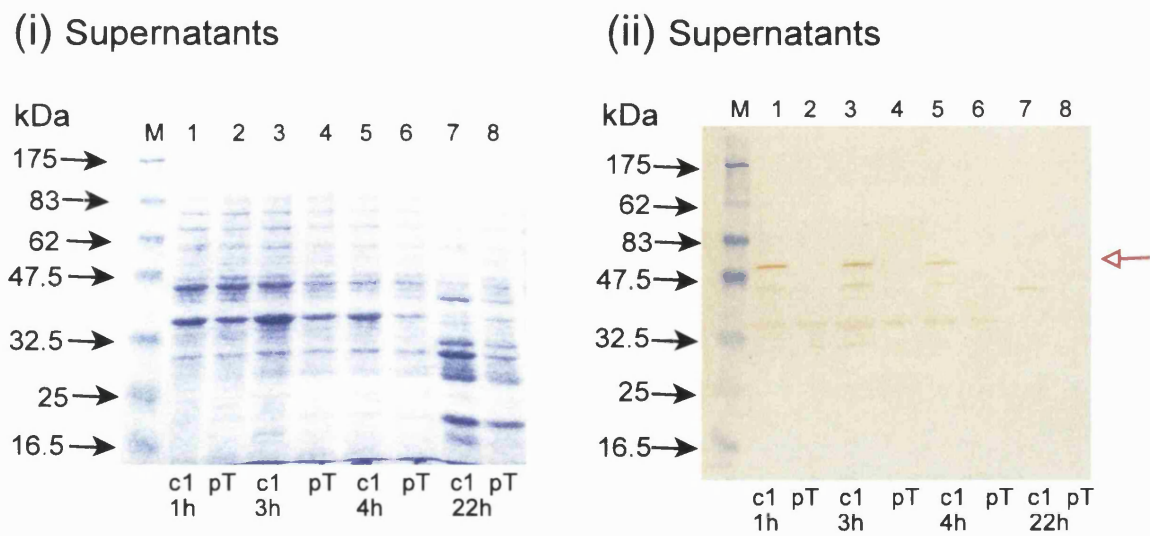
**Figure 4.15.2** PDE activity analysis of c1 and PTA supernatant samples. Assays were carried out in the presence of  $\text{Ca}^{2+}/\text{CaM}$  and vinpocetine with cAMP as the substrate.

The cleared lysate samples and the particulate fraction for c1 and the empty vector were further analysed by SDS PAGE and Western blot analysis using CaM-PDE antibody to see if the recombinant protein was mainly in inclusion bodies, as was the case with the pGEX vectors. Figure 4.16.1 shows the Coomassie-stained gel (i) and the Western blot (ii) for the particulate fraction samples for c1 and the empty vector. The Coomassie-stained gels did not show any obvious band corresponding to the recombinant protein (~54 kDa) but the Western blot does show the presence of the recombinant protein which also revealed that partial proteolysis of the recombinant protein had occurred. The fact that the recombinant protein was present in the particulate fraction samples indicated that a large amount of the recombinant protein was being sequestered into insoluble inclusion bodies.

Figure 4.16.2 shows the Coomassie-stained (i) and the Western blot (ii) for the cleared lysate samples (supernatants) of c1 and the empty vector. The Western blot for the supernatants clearly showed a signal for the recombinant protein indicating the presence of soluble PDE1A1. As with the recombinant protein signal detected in the particulate fraction samples, the signal for the recombinant protein in supernatant samples diminished by 22 hours post-IPTG which just showed the presence of a soluble proteolytic fragment (~40 - 45 kDa) (Figure 4.16.2 (ii), Lane 7). A slightly larger proteolytic fragment (~45 - 47 kDa) was present in the earlier samples of 1 - 4 hours post-IPTG (Figure 4.16.2 (ii), Lanes 1, 3 and 5). The Western blot results for c1 do reflect the PDE activity results in that the activity diminished after the first hour of protein expression (Figure 4.15.2) and the Western blot signal for the recombinant protein does diminish in intensity after the first hour (Figure 4.16.2). The reason for this may be that the recombinant protein was being proteolytically cleaved after the first hour of expression. Also, as the recombinant protein accumulated in the host cell, the host will probably sequester the foreign protein into inclusion bodies, firstly, because it was toxic to the host, and secondly, the foreign protein may not all be folding correctly. The majority of the recombinant protein was detected in the particulate fraction samples which contained the inclusion bodies (Figure 4.16.1). Nevertheless, the PDE activity results for c1 (Figure 4.15.2) together with the Western blot analysis of the supernatant samples (4.16.2) do confirm the successful expression of soluble, active recombinant protein using the pTrcHis expression vector in *E. coli* JM109(DE3) cells.



**Figure 4.16.1** SDS PAGE and Western blot analysis of c1 and PTA particulate fractions. Results are shown for Coomassie-stained gels (i), and Western blots (ii). Lanes 1 and 2 = c1 and the vector (pTrcHisA, pT) respectively at 1h post-induction; Lanes 3 and 4 = c1 and pT respectively at 3h post-induction; Lanes 5 and 6 = c1 and pT respectively at 4h post-induction; Lanes 7 and 8 = c1 and pT respectively at 22h post-induction. Marker (M) lanes are indicated with sizes on the left. Position of the His<sub>6</sub>-PDE1A1<sub>N-trunc</sub> (c1) is indicated by the red arrow (~54 kDa).



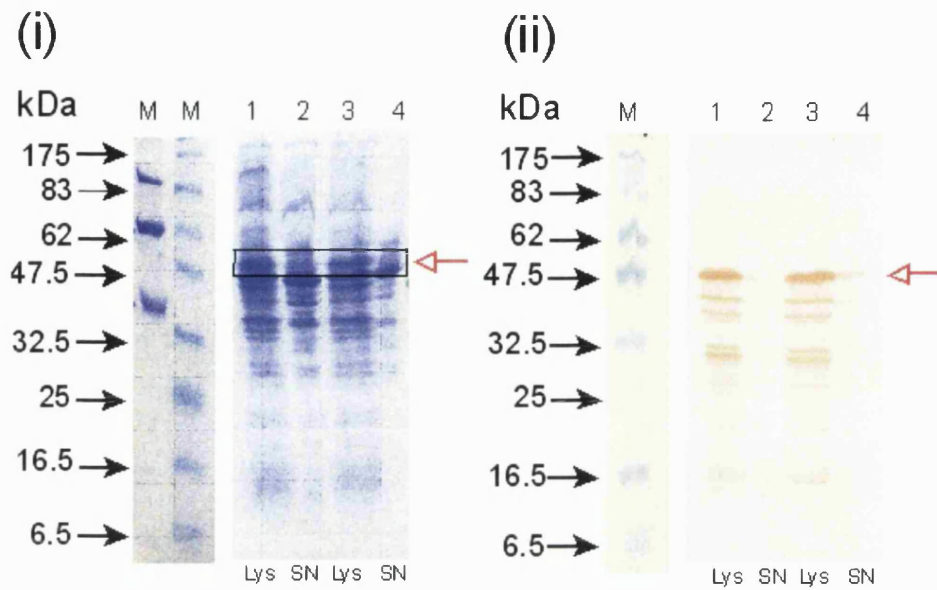
**Figure 4.16.2** SDS PAGE and Western blot analysis of c1 and PTA supernatant samples. Results are shown for Coomassie-stained gels (i) and Western blots (ii). The order of the samples is as for Figure 4.16.1. Marker lanes are indicated with sizes shown on the left. The red arrow indicates the position of the His<sub>6</sub>-PDE1A1<sub>N-trunc</sub> (c1) protein.

Initial expression studies with the construct pTrcHisA-PDE1A1<sub>N-trunc</sub> were carried out at small-scale using *E. coli* JM109 strain of cells. Since these studies gave early promising results, large-scale protein expression was carried out with this strain of cells. Small-scale expression studies using *E. coli* JM109(DE3) strain of cells did give soluble, active recombinant PDE1A1 as already discussed, but scale-up and subsequent purification was not pursued as large-scale expression using a 10L fermenter vessel had already been carried out using c1 in *E. coli* JM109 cells. Therefore, purification of His<sub>6</sub>-PDE1A1<sub>N-trunc</sub> from inclusion bodies from the large-scale protein expression was carried out and is described in section 4.5.7.

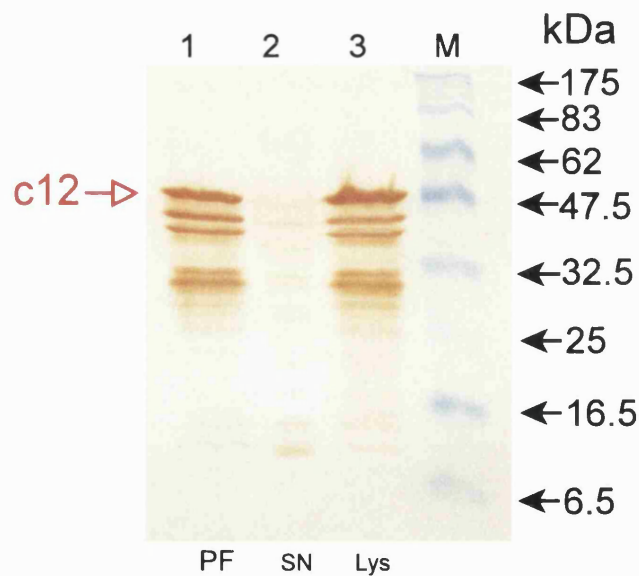
#### **4.5.6 Large-scale expression of pTrcHisA-PDE1A1<sub>N-trunc</sub> in *E. coli* JM109 cells**

Large scale expression of c1 was carried out in *E. coli* JM109 cells using LB media since the initial expression studies in this strain of cells had shown promising early results in terms of PDE activity (see section 4.5.5.1 and Figure 4.14.2). Figure 4.17.1 shows the Coomassie-stained SDS PAGE gels as well as the Western blot analysis carried out using CaM-PDE antibody on total cell lysate and cleared lysate samples (supernatant samples). The Coomassie-stained gel (i) showed the presence of the recombinant protein in the total cell lysates (indicated by the red arrow) but not in the supernatant samples. Western blot analysis (ii) confirmed the presence of the recombinant protein in total cell lysate sample. The presence of the smaller protein fragments seen in the Western blot indicated that the recombinant protein was prone to hydrolysis.

Further Western blots were carried out on the cleared cell lysates (supernatants) and the particulate fraction samples (Figure 4.17.2) from the large-scale protein expression of c1. These showed that most of the recombinant protein was present in the particulate fraction samples suggesting presence of the protein as insoluble inclusion bodies. There was a weak signal detected in the supernatant samples. PDE activity analysis on the supernatant sample is shown in Figure 4.17.3.

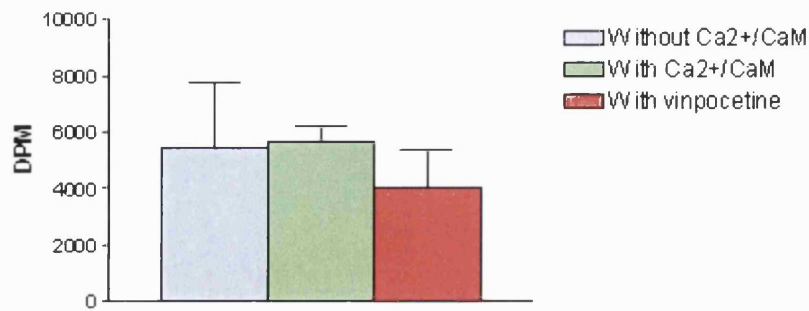


**Figure 4.17.1** SDS PAGE and Western blot analysis of c1 from large-scale protein expression. (i) Coomassie-stained gel and (ii) Western blot analysis carried out using CaM-PDE antibody. Lanes 1 and 3 = whole cell lysate samples (Lys) in duplicate; Lanes 2 and 4 = supernatant samples (SN) in duplicate. Marker lanes (M) are indicated with the sizes on the left. The box in (i) show the position of the recombinant protein (His<sub>6</sub>-PDE1A1<sub>N-trunc</sub>) while the red arrow marks the position of the recombinant protein.



**Figure 4.17.2** Western blot analysis on c1 from large-scale protein expression. Lane 1 = particulate fraction (PF); Lane 2 = supernatant sample (SN); Lane 3 = total cell lysate sample (Lys). Pre-stained protein marker mixture is indicated (M) with sizes shown on the right.





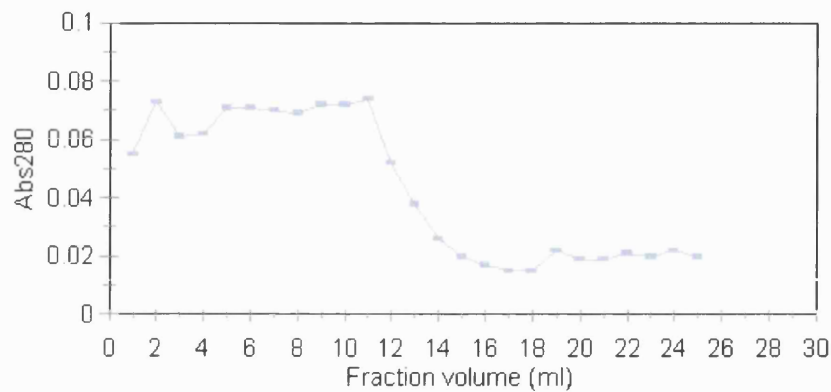
**Figure 4.17.3** PDE activity results for the supernatant sample from the large-scale expression of pTrcHisA-PDE1A1<sub>N-trunc</sub> (c1). Activity assays were carried out in the presence and absence of Ca<sup>2+</sup>/CaM and vinpocetine using cAMP as the substrate.

The expression studies carried out on c1 (pTrcHis-PDE1A1<sub>N-trunc</sub>) vectors had shown that the recombinant protein was mainly being expressed in an insoluble form as inclusion bodies. Small amounts of the recombinant protein were detected in the supernatant samples as shown by the Western blots (Figure 4.16.2) as well as by PDE activity analysis (Figure 4.15.2) when *E. coli* JM109(DE3) strain of cells was used. But the majority of the recombinant protein was still found as insoluble inclusion bodies (Figure 4.16.1). The c1 samples from the large-scale expression were therefore used for purification of the recombinant protein from inclusion bodies using nickel chelate affinity chromatography.

#### 4.5.7 Purification of His<sub>6</sub>-PDE1A1<sub>N-trunc</sub> using nickel chelate affinity chromatography

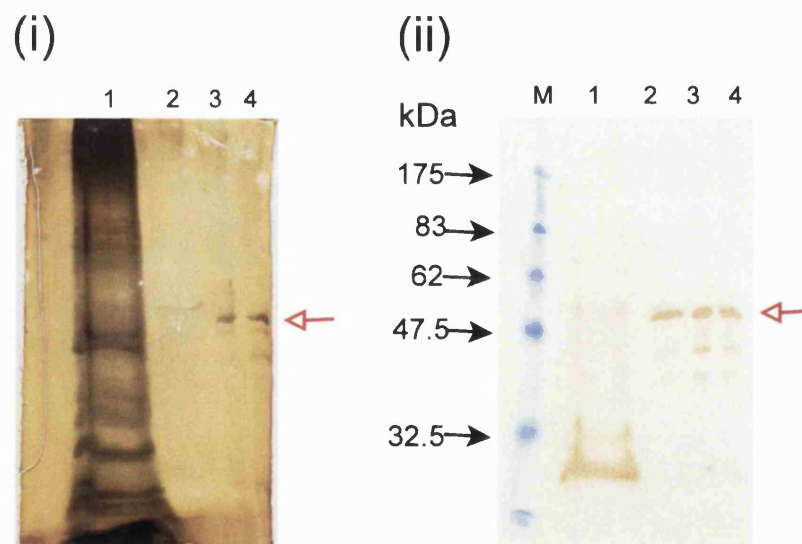
The recombinant protein, His<sub>6</sub>-PDE1A1<sub>N-trunc</sub>, was purified from inclusion bodies using nickel chelate chromatography under denaturing conditions as described in section 4.4.6.2.2. The absorbance of the eluted samples was measured at 280nm wavelength using a UV/Vis spectrophotometer for the detection of protein in the fractions collected (Figure 4.18.1). Protein was shown to be present in the first 12 fractions and so fractions 1 - 12 were pooled for further analysis. The pooled fractions were dialysed in two steps of 400ml buffer to reduce the urea from 8M to ~3mM as described in section 4.4.6.2.2.4. Figure 4.18.2 shows the results of the fractions analysed (fractions 1 - 12 pooled fractions) using 12% SDS PAGE and Western blot analysis using CaM-PDE antibody respectively. Silver-stained gels showed the presence of the recombinant protein (~54 kDa), and the Western blot confirmed the identity of the recombinant protein. The Western blot did show up to

three smaller protein fragments suggesting proteolysis of the protein had occurred. Protein concentration was also measured using Bradford assays and found to be 0.1mg/ml. This value, coupled with the intensity of the 54 kDa-recombinant protein band on the Western blot, was used to estimate the recombinant protein concentration for the PDE1A1 expressed using the Semliki Forest virus expression system (Chapters 5 and 6).



**Figure 4.18.1** Analysis of the c1 fractions following nickel chelate affinity purification.

The absorbance (Abs<sub>280</sub>) of the 1ml fractions collected is shown plotted against the fraction volume. Fractions 1 - 12 were pooled for analysis.



**Figure 4.18.2** SDS PAGE and Western blot analysis on purified His<sub>6</sub>-PDE1A1<sub>N-trunc</sub> (c1)

protein. Lane 1 = total cell lysate in denaturing buffer; Lane 2 = pooled fractions showing the presence of protein (ii); Lane 3 = fraction dialysed to ~1.0M urea; Lane 4 = fraction dialysed to ~3mM urea. Marker lane is indicated (M) with sizes on the left and the position of the recombinant protein is shown by the red arrow.

Purification of His<sub>6</sub>-PDE1A1<sub>N-trunc</sub> protein was therefore successfully carried out using nickel chelate affinity chromatography as shown by the Western blot analysis on the pooled fractions from the affinity chromatography (Figure 4.18.2). However, the purified protein had undergone partial proteolysis as the Western blot revealed at least three smaller protein fragments but the majority of the purified protein was intact. Also, PDE activity assays carried out on the purified protein sample did not show any PDE activity (results not shown) which suggested that the purified protein had not folded correctly. Moreover, it was possible that the recombinant protein was not active because it lacked the post-translational modifications that most eukaryotic proteins require for activity. These modifications are not usually carried out by prokaryotic cells.

Refolding and purification from inclusion bodies generally requires an optimisation of the refolding parameters. These include the pH of the buffer used where a high pH (up to pH 12) has been favourable to the efficiency of protein refolding (Chen and Gouaux, 1997). The addition of additives such as arginine (0.5M to 1M) has also been beneficial for the refolding process (Li *et al.*, 1999b; Richter *et al.*, 2002). Richter and co-workers (2002) observed a synergistic effect on PDE7 refolding when arginine (1M) and ethylene glycol (50%) were used. Other factors that supported PDE7 refolding included the addition of reducing agents such as DTT and  $\beta$ -mercaptoethanol, as well as ions such as Mg<sup>2+</sup> or Mn<sup>2+</sup> (Richter *et al.*, 2002). The position of the histidine-tag has also been shown to have an influence on the purification and the proteolytic degradation of PDE4 proteins (Richter *et al.*, 2000). PDE4 proteins that were C-terminally His-tagged were found to be stable against proteolysis compared to the N-terminally His-tagged constructs (Richter *et al.*, 2000).

#### 4.7 Conclusion

The primary aim of the work described in this chapter was the cloning of the PDE1A1 cDNA into prokaryotic expression vectors for subsequent expression studies. Cloning into two prokaryotic expression vectors, pGEX-3X and pTrcHisA, was successfully carried out. Expression conditions for the expression of soluble recombinant proteins were investigated and this was also successful for the His<sub>6</sub>-PDE1A1<sub>N-trunc</sub> protein. However, most of this protein, as well as the GST-PDE1A1 protein, was still present as insoluble inclusion

bodies.

Table 4.3 summarises the results of the expression experiments for both GST-PDE1A1 and His<sub>6</sub>-PDE1A1<sub>N-trunc</sub> proteins.

**Table 4.3** Summary of PDE1A1 expression using the pGEX-3X and pTrcHisA expression vectors in *E. coli*.

Expression vector		Recombinant protein
<b>pGEX-3X (GST-PDE1A1)</b>		
Culture media	Expression conditions	
LB	37°C (+/- IPTG)	Insoluble inclusion bodies
LB	24°C (+/- IPTG)	Insoluble inclusion bodies
LBS	30°C (+/- IPTG)	Insoluble inclusion bodies
Refolding from inclusion bodies	-	GST-PDE1A1 not active; protein precipitating due to incorrect folding
<b>pTrcHisA (His<sub>6</sub>-PDE1A1<sub>N-trunc</sub>)</b>		
Culture media	Expression conditions	
LB	30°C (+ IPTG) ( <i>E. coli</i> JM109)	Insoluble inclusion bodies
LB (large-scale)	30°C (+ IPTG) ( <i>E. coli</i> JM109)	Insoluble inclusion bodies
LB (+/- S)	30°C (+ IPTG) ( <i>E. coli</i> JM109(DE3))	Soluble His <sub>6</sub> -PDE1A1 <sub>N-trunc</sub> ; low levels
Refolding from inclusion bodies	-	His <sub>6</sub> -PDE1A1 <sub>N-trunc</sub> purified but not active

Abbreviations: LB = Luria Broth LBS = LB + sorbitol

As is apparent from this summary, the recombinant proteins were being sequestered into inclusion bodies which is a common problem with prokaryotic expression vectors as already discussed in section 4.1.2. Strategies to explore the optimisation conditions for the refolding of the recombinant proteins from inclusion bodies (GST-PDE1A1 and His<sub>6</sub>-PDE1A1<sub>N-trunc</sub>) produced in the present work were not fully explored. Initial refolding of GST-PDE1A1 from inclusion bodies had resulted in the precipitation of the refolded protein, while refolding and purification of His<sub>6</sub>-PDE1A1<sub>N-trunc</sub> had produced a purified protein, but this protein was not active. While prokaryotic expression systems have been used successfully to either produce soluble, active PDE proteins (Kovala *et al.*, 1997) or active PDE proteins following purification from inclusion bodies (Richter *et al.*, 2000,

2002), the prokaryotic expression system was not pursued further. However, future work on the two constructs produced in the present work (pGEX-3X-PDE1A1 and pTrcHisA-PDE1A1<sub>N-trunc</sub>) can be used to explore refolding conditions as well as purification using affinity chromatography (GST-PDE1A1). Another factor that can be explored is the position of the histidine-tag on the recombinant protein as Richter and co-workers (2000) found C-terminal His-tagged PDE4 to be more stable to proteolytic degradation than the N-terminal tagged protein. However, these factors were not explored in the present work but expression studies continued using the Semliki Forest virus expression system (Chapter 5).

## Chapter Five

### 5 Semliki Forest virus for the cloning and expression of full-length and truncated PDE1A1

This chapter will give a background to the eukaryotic expression systems used for the expression of heterologous proteins. The Semliki Forest virus expression system will be discussed in detail since it was used in the present study. The experimental work will include the generation and cloning of the full-length and truncated PDE1A1 enzymes as well as characterisation studies on the recombinant enzymes for substrate specificity. Small-scale purification of the recombinant enzymes is also described. Biochemical characterisation is described in the next chapter (Chapter 6).

#### 5.1 Introduction

Eukaryotic expression systems based on viral vectors have been widely used for the expression of heterologous proteins in insect cells as well as mammalian cells. The viral vector expression systems provide high levels of protein expression as well as allowing the generation of high-titre virus stocks. The advantage of using eukaryotic systems is that the expressed protein will be processed correctly in terms of post-translational modifications as well as the correct folding of the protein, both of which are required for a biologically active protein. Virus vectors that have been used include the baculovirus, *Vaccinia* virus, Adenovirus and the Alphavirus vectors. These are discussed briefly below with an emphasis on the Semliki Forest virus (Alphavirus) which was the vector used for the expression of dog heart PDE1A1 in the present study and forms the subject of this chapter.

#### 5.1.2 Virus vectors for heterologous protein expression

##### 5.1.2.1 Insect cells for the expression for heterologous proteins

Baculoviruses have been isolated primarily from insect cells and are not known to be infectious to vertebrates. They are broadly classified into two groups: nucleopolyhedroviruses (NPV) and granuloviruses. It is the NPV group of viruses that are

mainly used as expression vectors. The viruses are named after the species of insect from which they are isolated (Merrington *et al.*, 1999). The virus *Autographa californica* NPV (AcMNPV), isolated from the larva of the alfalfa looper (*A. californica*), is the prototype baculovirus used for expression studies. Cell lines commonly used for the propagation of baculovirus include the IPLB-Sf-21 and ATCC-Sf-9 as well as cell lines derived from *Trichoplusia ni* TN-368 and BTI-TN-5B1-4 (High 5). AcMNPV is propagated in cell lines derived from the pupal ovaries of the worm *Spodoptera frugiperda* (Sf) (Merrington *et al.*, 1999).

Baculovirus expression systems offer many advantages over prokaryotic expression systems which include the ability to correctly process and fold the recombinant protein as well as produce antigenically authentic proteins. Baculovirus have been used for the investigation of HTLV II viral polyprotein processing (Takahashi *et al.*, 1999), as well as for the production of vaccines based on the generation of virus-like particles (VLPs) for the development of HIV vaccines (Rasmussen *et al.*, 1990; Ross *et al.*, 1991; Kang *et al.*, 1999), and a multistage *Plasmodium falciparum* vaccine (Shi *et al.*, 1999). Conventional recombinant antigens expressed in the baculovirus system have been used for the development of a vaccine for the influenza A virus (Johansson, 1999).

There are some drawbacks to the baculovirus expression system. Firstly, only insect cells can be used for the propagation of baculovirus; secondly, there is a tendency for the formation of large aggregates of the recombinant proteins which can be detrimental to the functional activity of the expressed protein; and thirdly, insect cells are also thought to over-glycosylate heterologous proteins which may have an effect on the biological properties of recombinant enzymes. However, the baculovirus expression system has been used successfully for the expression of heterologous protein including PDE enzymes. The purified PDE4B2B used for the recent elucidation of the crystal structure of the catalytic domain was expressed in Sf9 cells using the baculovirus expression system (Rocque *et al.*, 1997a; Xu *et al.*, 2000). Baculovirus expression systems have also been used for PDE4 mutagenesis studies (Herman *et al.*, 2000), as well as studying phosphorylation of PDE4, MAP kinase and PKA (Lenhard *et al.*, 1996; Sette and Conti, 1996).

### **5.1.2.2 Mammalian cells for the expression of heterologous proteins**

#### **5.1.2.2.1 *Vaccinia* virus vectors**

The *Vaccinia* viruses are dsDNA enveloped viruses belonging to the Poxviridae family. They are unique in that they have the ability to replicate within the cytoplasm of the host cell rather than the nucleus. They have been widely used as a means for expressing proteins in eukaryotic cells (Moss *et al.*, 1991). The virus is relatively easy to handle but does require strict safety precautions which includes vaccination against small pox for all personnel working with the virus. The *Vaccinia* virus was originally developed for use as a vaccine against smallpox as part of the Intensified Smallpox Eradication Programme by the World Health Organisation which was implemented in 1967 and ended with the eradication of Smallpox in 1988 (Fenner *et al.*, 1988). Following this period, several highly attenuated strains of the virus were developed for use in the laboratory as expression vectors. One of these was the modified *Vaccinia* Ankara (MVA) strain which was shown to be very effective as a vector for the expression of foreign proteins using human and other mammalian cell lines (Sutter and Moss, 1992). It has been successfully used for the large scale production of proteins such as human prothrombin protein (Falkner *et al.*, 1992).

#### **5.1.2.2.2 Adenovirus vectors**

The Adenoviruses are dsDNA viruses of the Adenoviridae family and unlike the *Vaccinia* virus, the Adenovirus DNA is transcribed within the host cell nucleus. For the purposes of expression of heterologous protein and for biosafety reasons, the virus vector has been constructed so that the gene of interest is cloned into a viral vector lacking the structural genes for the packaging of the virus. Target cells are co-transfected with this vector together with a helper vector containing the structural genes.

#### **5.1.2.2.3 Alphavirus vectors**

The Alphaviruses are members of the Togaviridae family. They are enveloped viruses containing a positive ssRNA genome (Strauss and Strauss, 1994). Vectors based on alphaviruses have several features making them attractive as expression vectors. Their



positive polarity RNA genome means that the naked genomic RNA is able to initiate an infection when introduced into the host cell. The RNA is self-replicating since it codes for its own replicase, and replication is extremely efficient producing over  $10^5$  RNA molecules per cell (Liljestrom, 1994). Replication takes place in the cell cytoplasm and leads to the rapid inhibition of the host cell protein synthesis. The Alphaviruses have a very broad host range and are able to infect virtually all animal cell types which is a distinct advantage over the baculovirus vectors which only infect insect cells.

The two most well studied members of alphaviruses are the Sindbis and the Semliki Forest viruses (Strauss and Strauss, 1994). Both of these are of low pathogenicity to humans, infecting mainly animal species which include rodents and birds. However, there are still safety concerns regarding the use of these viruses as vectors due to a fatality resulting from the use of Semliki Forest virus (Willems *et al.*, 1979). Strategies have therefore been developed whereby the structural proteins for the viruses are removed from the genome and are contained on a separate helper vector. The structural proteins are required for the packaging of the viral particles for infection. For the Semliki Forest virus, this has been taken a step further in that the infective virus has been made conditionally-infective so that it requires the *in vitro* cleavage of a surface structural protein (virus spike proteins) for activation of the virus. This system has not proved to be so effective for the Sindbis virus as it has been for the Semliki Forest virus (Liljestrom, 1994). The Semliki Forest virus expression vector is discussed in detail in the next section.

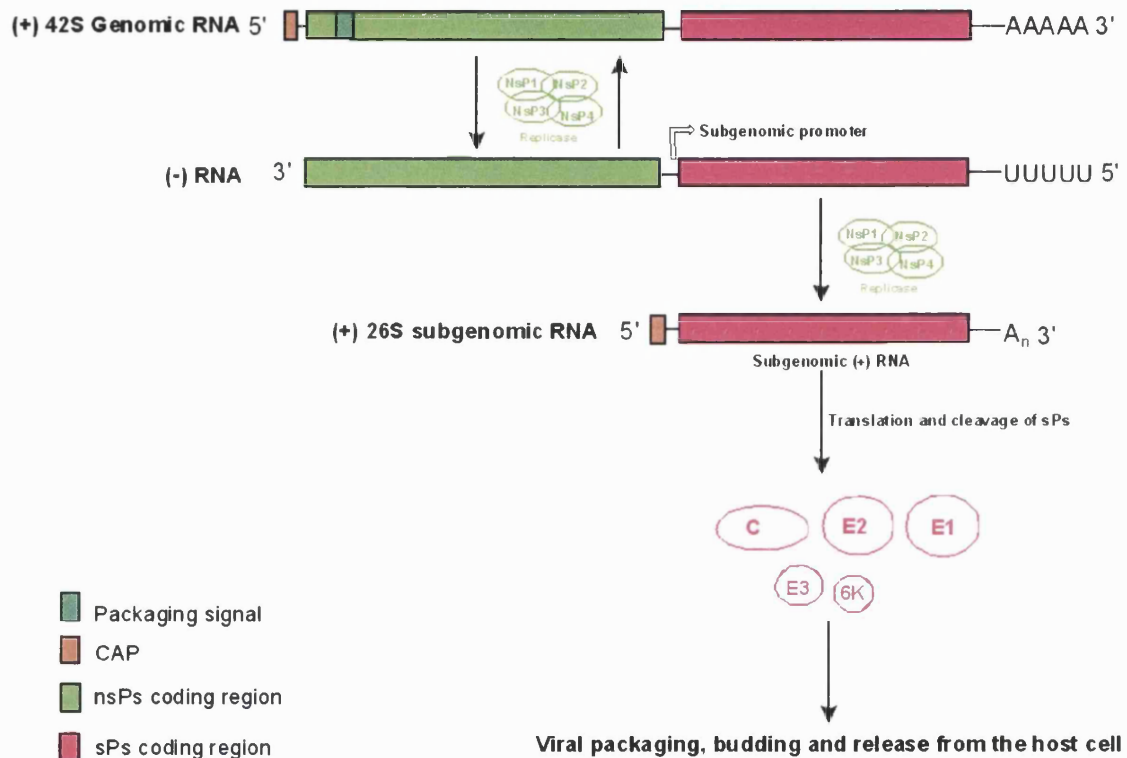
## **5.2 Semliki Forest virus**

### **5.2.1 Lifecycle of the Semliki Forest virus**

The Semliki Forest virus is a mosquito-transmitted pathogen of rodents such as mice. The virus was first isolated in 1944 from mosquitoes (*Aedes abnormalis*) caught from the Semliki Forest in Western Uganda (Smithburn and Haddow, 1944). Several strains of the virus are known to exist with some strains (SFV4 and strain L10) causing lethal encephalitis in mice of all ages leading to death within a few days while other strains cause axonal demyelination but infected mice remain asymptomatic.

The Semliki Forest virus genome consists of a positive strand RNA molecule of ~12 kb. This genomic RNA is complexed with basic capsid protein (C), surrounded by a lipid bilayer containing the envelope E1E2 (spike protein) glycoprotein heterodimers. The virus enters the host cell via a receptor-mediated endocytosis involving more than one receptor recognition on the host cell. When the pH in the endosome drops, the transmembrane spike glycoprotein of the virus catalyses fusion between the viral and endosomal membranes thereby delivering the nucleocapsid into the host cytoplasm. This is followed by the translation of the genomic RNA for the generation of the nonstructural proteins (nsPs) which are required for the initiation of the viral RNA amplification. The 5' two-thirds of the genomic RNA is directly translated to produce the viral replicase which comprises of four subunits (nsP1, nsP2, nsP3 and nsP4; nsP1-4) and is also thought to contain the packaging signal since only the positive-sense RNA is packaged (White *et al.*, 1998). The nsPs are generated as a polyprotein which is self-cleaved by nsP2 and then assemble to form the replicase enzyme. This enzyme copies the genome to form negative strands which serve as the template for the production of new positive strand 42S genomic RNA. Once the negative strand is available, replicase binds to a subgenomic promoter located in the 3'-terminal third of the genomic RNA to produce the positive-sense 26S RNA. This codes for the structural proteins (sPs) which comprise the capsid (C), E3, E2, 6K and E1 proteins. The structural proteins are translated as a polyprotein (NH<sub>2</sub> - C-p62(E3-E2)-6K-E1 - COOH) which is then cleaved at the C-E3 junction by the chymotrypsin-like activity located at the carboxy-terminal portion of the capsid (C) protein. E3 and E2 themselves are initially produced as a precursor (p62 or PE2) before being processed during the release of the virus from the host cell. Once the capsid is cleaved from the polyprotein, the remaining peptide is transported to the endoplasmic reticulum where a host signal peptidase (signalase) cleaves it into p62, 6K and E1 proteins. p62 and E1 dimerise and are directed to the host cell surface during which the p62 is cleaved by a host cell protease to generate the mature E2 protein. Post-translational processing also occurs at the endoplasmic reticulum and includes glycosylation and palmitoylation of the sPs. This is necessary for the proper folding of the proteins before they leave the endoplasmic reticulum. Proteins that do not fold correctly are not transported from here and are slowly degraded in the endoplasmic reticulum. The processed p62-E1 dimer is then transported to the Golgi apparatus and ultimately to the cell surface. During this transport, the p62-E1 complex is cleaved by a host cell proteinase to release E2 and E3 with cleavage occurring after the

motif **RHRR**. Three E1-E2 dimers form the spikes (spike proteins) on the virus surface and these spike proteins are a prerequisite for infectivity. E3 remains associated with 6K and is thought to be important for virus assembly and release from the host cell. The SFV has previously been used in model systems to study membrane fusion (Strauss and Strauss, 1994; Liljestrom *et al.*, 1991). Figure 5.1 summarises the replication cycle of the Semliki Forest virus.



**Figure 5.1** Overview of the Semliki Forest virus replication cycle.

Abbreviations used: nsP = non-structural proteins (nsP1 - 4); sPs = structural proteins (C, E1, E2, E3, 6K). See text (5.2.1) for explanatory notes.

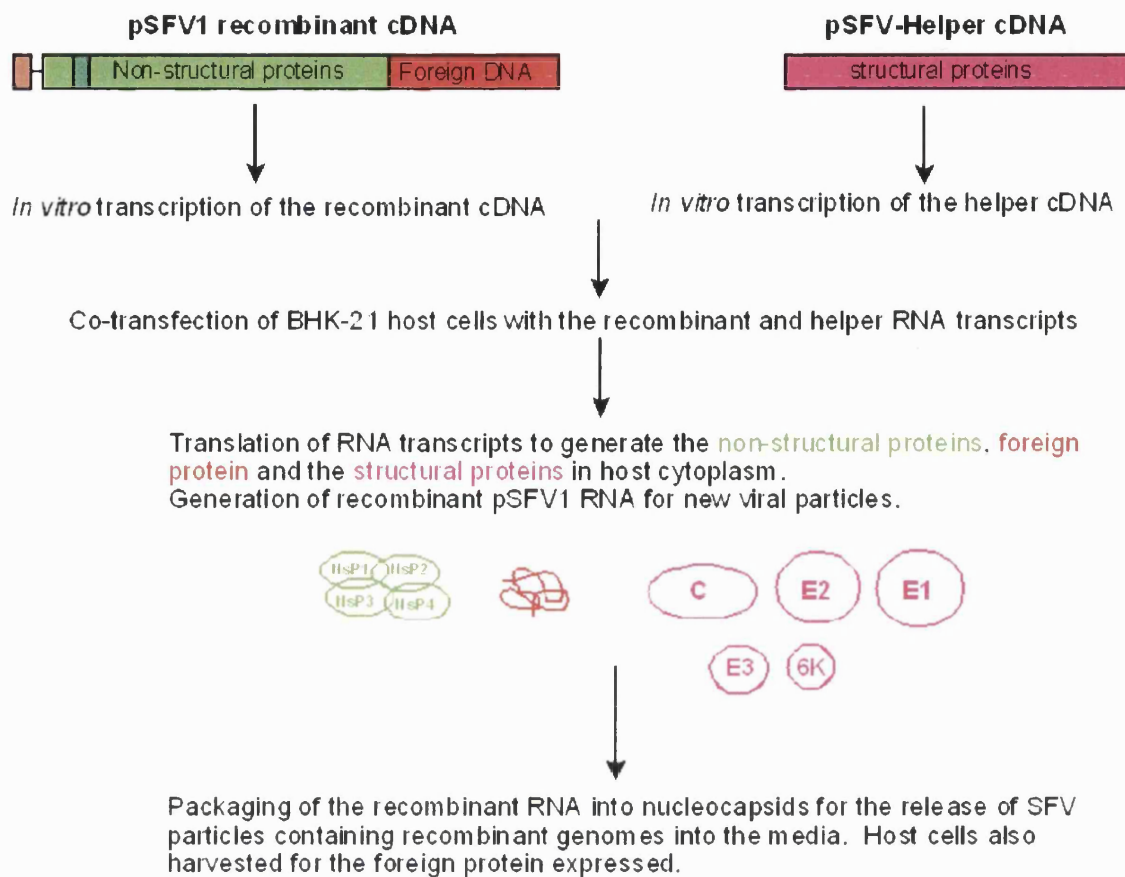
Diagram adapted from Strauss and Strauss, 1994; Berglund *et al.*, 1996.

## 5.2.2 Semliki Forest virus expression vectors

### 5.2.2.1 Background to the construction of the Semliki Forest virus vectors

The Semliki Forest virus (SFV) was developed as a vector for protein expression in mammalian cells by Liljestrom and Garoff (1991). The SFV expression system was developed by inserting the genomic SFV cDNA into a SP6 promoter plasmid to create

pSP6-SFV4 cDNA. The subgenomic coding region for the structural proteins was deleted and a *Bam*HI-*Xma*I-*Sma*I polylinker sequence inserted downstream of the 26S promoter site to allow insertion of foreign DNA into this vector. These vectors were called pSFV1, pSFV2 and pSFV3 vectors; differing by just a few base pairs in the polylinker site (Liljestrom and Garoff, 1991). The polylinker sites of the vectors pSFV2 and pSFV3 contain the Kozak sequence necessary for the efficient translation of mRNA (Kozak, 1989). The vector pSFV1 does not contain this sequence so genes cloned into this vector must contain a signal for the initiation of translation together with the codon AUG. Liljestrom and Garoff (1991) cloned the mouse dihydrofolate reductase, human transferrin receptor and chicken lysozyme genes into pSFV1 to show efficiency of protein expression using the Semliki Forest virus system. *In vitro* RNA generated from these were used to transfect host BHK-21 cells. The system proved to be highly efficient in expressing the foreign proteins with there being a substantial decrease in the production of host protein synthesis. To allow packaging of recombinant RNA into infectious SFV particles, Liljestrom and Garoff (1991) also constructed a helper plasmid, pSFV-Helper 1 (pSFV-H1). This helper vector had the 5' and 3' signals necessary for RNA replication as well as the complete structural region including its promoter. However, it lacked the region at the end of nsP1 which is required to package SFV RNA into complete viral particles. Co-transfection of BHK-21 cells with both the recombinant pSFV1 containing the foreign gene and pSFV-H1 meant that only the recombinant genome would be packaged and the resulting virus stock could be used for one round of infection to express the foreign gene. This again was shown to be a very efficient for the expression of the foreign genes. Figure 5.2 gives an overview of the replication events occurring when pSFV1 and pSFV-H1 are used for the production of foreign protein.



**Figure 5.2** Recombinant pSFV1 and pSFV-Helper for the production of foreign proteins. Abbreviations used: nsP = non-structural proteins (nsP1 - 4); sPs = structural proteins (C, E1, E2, E3, 6K). See Figure 5.1 for key to the figure.

Figure adapted from Strauss and Strauss, 1994; Liljestrom and Garoff, 1991.

Liljestrom and Garoff (1991) also cloned the *Escherichia coli*  $\beta$ -galactosidase ( $\beta$ -gal) protein, *lacZ*, into the *Bam*HI site of pSFV3 to give pSFV3*lacZ*. The *in vitro* generated pSFV3*lacZ* and pSFV-H1 RNA were used to co-transfect BHK-21 cells and the resulting virus stock used to infect further BHK-21 cells. Protein expression was monitored by sampling infected cells at 24, 48 and 72 hours post-infection and the cell lysates analysed on SDS PAGE gels. These results showed the presence of the  $\beta$ -gal protein at all time points with 48 and 72 hours showing the most intense bands of protein (Liljestrom and Garoff, 1991).

Berglund and co-workers (1993) carried out a further modification to the pSFV-H1 expression system developed by Liljestrom and Garoff (1991). In the first system, it was

assumed that since the pSFV-H1 lacked the packaging signal, there would only be selective packaging of the recombinant RNA into SFV particles. However, there was still the possibility of the wild type virus arising from *in vivo* packaging. The Sindbis virus, which is closely related to the SFV, was shown to undergo recombination through strand-switching which could result in replication-proficient virus (Geigenmuller-Gnirke *et al.*, 1991). Because of the biosafety concerns, a cleavage-deficient variant of the pSFV-H1 was developed and called pSFV-H2. Cleavage of the precursor spike protein p62 is necessary for infectivity of the viral particles and occurs via a host cell proteinase before packaging and budding of the virus from the host cell (see section 5.2.1). This cleavage occurs after the motif **RHRR** located at the junction of E3 and E2 which form the precursor p62. Berglund and co-workers (1993) showed that the p62 cleavage could be abolished without affecting virus maturation and budding, and the virus produced was largely noninfectious. This mutated virus was denoted “mL” to represent mutation of the arginine (R) to leucine (L) (RHRR → RHRL). However, this variant was still shown to have some residual infectivity which was postulated as being due to cleavage occurring via residual trypsin in the culture media and was indeed proven to be the case when the residual infectivity was abolished using protease inhibitors. A second variant (denoted SQL then pSFV-Helper 2; pSFV-H2) was created whereby three amino acid residues were altered in the RHRR motif instead of the single mutation carried out for the first variant. Figure 5.3 shows the amino acids involved in these variants together with the altered amino acids.

	E3		E2
Wild type	NGT <b>RHRR</b>	~	SVSQHFN
mL variant	NGT <b>RHRL</b>	~	SVSQHFN
SQL variant (H2)	NGT <b>SHQL</b>	~	SVSQHFN

**Figure 5.3** Wild type and variant amino acid sequences surrounding the p62 cleavage site in the SFV Helper virus. Bold amino acid residues represent the motif for endoprotease cleavage of the precursor p62 protein to release E2 from E3. Residues shown in red represent the mutated residues in the two SFV Helper virus variants.

Figure adapted from Berglund *et al.*, 1993.

The pSFV-H2 and pSFV3*lacZ* RNA were co-transfected into BHK cells as before to generate virus stocks. Virus stock activated with chymotrypsin as well as unactivated virus stocks were used to infect BHK cells. The activated virus stock was shown to be very efficient in the expression of β-gal. However, there was still some residual infectivity with

the unactivated virus and the reason for this is unknown. Berglund and co-workers (1993) then carried out experiments to check for pathogenicity of these viral particles by injecting mice (intracerebral and intranasal route) with both activated and unactivated pSFV3*lacZ* particles and found them to be non-pathogenic. Virus stocks generated using pSFV-H1, on the other hand, caused the death of at least half the mice infected by the intracerebral route. But when the same virus stock was introduced into the mice by the intranasal route, all the mice survived. These experiments demonstrated a worst-case scenario and confirmed an improvement in the relative biosafety of using the Helper-2 virus for the generation of virus stocks.

#### **5.2.2.2 Semliki Forest virus vectors for the production of foreign protein**

The Semliki Forest virus vectors have been proven to be efficient for the production of more than 50 recombinant proteins at small scale level with some proteins expressed at large scale level. Examples of proteins expressed using the SFV system are given in Table 5.1. Most of these proteins were expressed using BHK-21 as host cells although some proteins were also expressed using CHO-K1 and COS-7 cells (Liljestrom, 1994).

Recombinant proteins using the SFV system have been successfully expressed at large scale levels to provide biologically functional proteins. Blasey and co-workers (1997) used 1L spinner flasks (21-Bellco spinners) for the expression of human cyclooxygenase-2. Scale up to a bioreactor using a 11.5L volume has also been carried out to express the mouse serotonin 5-HT<sub>3</sub> receptor protein (Blasey *et al.*, 2000). Large scale expression of these proteins has provided the starting material for structural studies to be carried out. The fact that the SFV system can be successfully scaled up is an important feature since one of the aims of the present work was to produce sufficient recombinant enzyme (dog heart PDE1A1) for subsequent structural studies.

**Table 5.1** Proteins expressed using the SFV expression system.

<b>Recombinant Protein</b>	<b>Reference</b>
<b>Enzymes</b>	
$\beta$ -galactosidase	Blasey <i>et al.</i> , 1997; Ciccarone <i>et al.</i> , 1993
Dihydrofolate reductase	Liljestrom and Garoff, 1991
Lysozyme	Liljestrom and Garoff, 1991
<b>Receptors</b>	
5-HT <sub>1D<math>\alpha</math></sub> Serotonin receptor	Stables <i>et al.</i> , 1997
Human Neurokinin 1 receptor	Lundstrom <i>et al.</i> , 1995
Transferrin receptor	Liljestrom and Garoff, 1991
<b>Viral proteins</b>	
Human Cytomegalovirus (CMV)	McCue and Anders, 1998
Murine Leukemia Virus envelope proteins	Lebedeva <i>et al.</i> , 1997
Human Dopamine D <sub>3</sub> receptor	Lundstrom and Turpin, 1996
Human Papillomavirus 16 Capsid proteins	Heino <i>et al.</i> , 1995

### **5.2.3 Background and aims of the present study using the Semliki Forest virus expression system**

#### **5.2.3.1 Semliki Forest virus vectors used in the present study**

The SFV vectors used for the present study for the cloning and expression of full-length as well as amino- and/or carboxy-terminal truncated dog heart PDE1A1 enzymes are discussed briefly in this section. This includes the pSFV3*lacZ* vector which was used to monitor the transfection of BHK-21 cells and protein expression efficiencies.

##### **5.2.3.1.1 pSFV3*lacZ* vector**

The pSFV3*lacZ* plasmid contains the *E. coli*  $\beta$ -gal gene, *lacZ*, as already stated. This vector was used to monitor protein expression in BHK-21 cells following electroporation of these cells. *In vitro* RNA transcripts for pSFV3*lacZ* were generated for transfection of BHK-21 cells and the cells stained using the substrate 5-bromo-4-chloro-3-indolyl- $\beta$ -D-galactoside (X-gal). X-gal was hydrolysed to form galactose plus a blue insoluble indolyl





pGEX-3X (see Chapter 4), was used as a template in the present study for generating copies of the cDNA using PCR. Forward and reverse primers for the PDE1A1 ORF were designed in order to introduce enzyme restriction sites together with a Kozak sequence into the ORF using PCR. The Kozak sequence (GCCGCC(A/G)CCATGG) was important for the efficient production of mRNA transcripts (Kozak, 1989). The restriction sites *Bam*HI and *Sma*I were used for directional cloning of the ORF into the pSFV1 multiple cloning site (polylinker site) (Figure 5.4). Four primers were designed: two forward (F1 and F2) and two reverse (R1 and R2). F1 and R1 were designed to give the full-length PDE1A1 ORF while F2 and R2 would give a truncated construct comprising mainly the catalytic domain of the enzyme. Combinations of the primers were used to provide N- or C-terminal truncated constructs as well. Table 5.2 shows the four PDE1A1 constructs generated for the present study. This table also indicates the DNA fragment sizes together the predicted protein size. Figure 1.19.1 (Chapter 1) shows the position of the four primers on the full-length dog heart PDE1A1 cDNA used as the template and Figure 1.19.2 shows a schematic of the four PDE1A1 fragments generated using the two forward and two reverse primers.

**Table 5.2** PCR primer combinations used for the generation of full-length and truncated PDE1A1 constructs for the present study.

<b>Primer combination</b>	<b>DNA fragment size (kb)</b>	<b>Amino acids</b>	<b>Protein size (kDa)</b>	<b>Construct name and amino acid residues present (designated name of clone in the present study)</b>
PDE1F1/PDE1R1	1.6	515	57	Full length protein: PDE1 <sup>1-515</sup> (FL4, FL28)
PDE1F1/PDE1R2	1.4	476	53	C-terminal truncated: PDE1 <sup>1-476</sup> (G2)
PDE1F2/PDE1R1	1.2	398	44	N-terminal truncated: PDE1 <sup>118-515</sup> (End6)
PDE1F2/PDE1R2	1.1	359	40	Catalytic fragment : PDE1 <sup>118-476</sup> (Cat9)

### 5.2.3.3 Expression of full-length and truncated dog heart PDE1A1

*In vitro* RNA transcripts were generated for the four pSFV1-PDE1A1 constructs. These were co-transfected with pSFV-H2 RNA into BHK-21 cells for small scale protein expression studies. Recombinant virus particles were harvested and activated using  $\alpha$ -chymotrypsin for infecting further BHK-21 cells. Infected cells were allowed to grow for up to 72 hours. These were harvested at 24, 48 and 72 hours post-infection to ascertain the

optimum time for protein expression which was monitored using PDE activity assays.

Recombinant PDE1A1 enzymes (full-length and truncated) were characterised using a range of PDE inhibitors as well as measurement of the  $K_m$  and  $V_{max}$  values. These results were compared with the full-length native dog heart PDE1A enzyme (Clapham and Wilderspin, 2001) as well as published results for PDE1 enzymes isolated from bovine or rodent species.

#### **5.2.4 Aims**

- ▶ Generation of full-length and truncated PDE1A1 cDNA for cloning into pSFV1.
- ▶ Production and optimisation of recombinant virus stocks for infection of BHK-21 cells for the subsequent expression of recombinant PDE1A1 enzymes.
- ▶ Scale-up of the expression system for purification of the recombinant enzymes.
- ▶ Biochemical characterisation of the recombinant enzymes and comparison with the full-length native dog heart PDE1A.

### 5.3 Materials

The reagents and materials described in this section cover those unique to the SFV expression work while those in common with the other expression systems have already been described in Chapter 2 (2.1). All the materials used for this part of the work were sterilised by autoclaving or filter sterilisation using 2µm filters and included all the reagents, tips and tubes used. Autoclaved Milli Q water was used for all procedures and DEPC-treated sterile Milli-Q water was used for all procedures involving the synthesis and use of *in vitro* RNA.

#### 5.3.1 Chemical reagents

Phenol/chloroform, sodium acetate, propan-2-ol (isopropanol), gluteraldehyde, methanol, chloroform and ethanol were from BDH. Phosphate Buffered Saline tablets were from ICN Biomedicals. X-gal was from Melfords.  $K_3Fe(CN)_6$  and  $K_4Fe(CN)_6 \cdot 3H_2O$  were from Sigma.

#### 5.3.2 Vectors

pSFV1 and pSFV3*lacZ* were purchased from GibcoBRL. pSFV1 was used to clone the PDE1A1 ORF while pSFV3*lacZ* was used to monitor the transfection procedures. Both of these vectors contain the gene for ampicillin resistance to allow for selection of transformant colonies when grown on media containing ampicillin.

pGEX-3X expression vector was purchased from Promega and was used to clone the full-length dog heart PDE1A1 cDNA for the bacterial expression studies (Chapter 4). The construct pGEX-3X-PDE1A1 was used as a template for the generation of full-length and truncated PDE1A1 using PCR for subsequent cloning of the fragments into pSFV1.

#### 5.3.3 Bacteria strains

*Escherichia coli* DH5α strain was used for the propagation of pSFV1, pSFV3*lacZ* plasmids as well as the pSFV1-PDE1A1 recombinant constructs for small scale and large scale DNA

purification. The bacterial media and reagents have already been described in Chapter 2.

#### 5.3.4 DNA reagents

In addition to the DNA reagents described in Chapter 2, *SpeI* (10 units/ $\mu$ l) for linearisation of recombinant pSFV1-PDE1A1 and pSFV-H2 prior to *in vitro* RNA synthesis was purchased from Amersham Life Science. *Taq* polymerase (5 unit/ $\mu$ l), *Pfu* (1 unit/ $\mu$ l) and dATP, dTTP, dGTP, dCTP were also from Amersham Life Science. 25 $\mu$ l each of dATP, dTTP, dGTP and dCTP were mixed to give a working solution of 100mM for the dNTP mixture used in the PCR reaction. PCR primers were synthesised by GibcoBRL and were supplied freeze-dried. T4 DNA ligase (3 units/ $\mu$ l) was purchased from Promega. Calf Intestinal Alkaline Phosphatase (CIAP) was from Boehringer.

#### 5.3.5 RNA reagents

RNasin Ribonuclease Inhibitor, SP6 RNA Polymerase (20 units/ $\mu$ l) and rNTPs (ATP, CTP, GTP, UTP) were purchased from Promega. RNA Capping Analog (m<sup>7</sup>G(5')ppp(5')G) was purchased from GibcoBRL. Diethyl pyrocarbonate (DEPC) was from Sigma.

#### 5.3.6 Tissue culture reagents

Glasgow Minimum Essential Medium (GMEM) with NaHCO<sub>3</sub> and without L-glutamine was purchased from Sigma and stored at 4°C. Trypsin (0.25%)-EDTA (1mM), stored at -20°C, and Foetal Bovine Serum, stored in 50ml aliquots at -70°C, were from GibcoBRL. Tryptose Phosphate Broth was also purchased from GibcoBRL but was stored at 4°C. 200mM L-Glutamine was from Imperial while the antibiotic Penicillin-Streptomycin (100ml; 5000 units penicillin and 5mg/ml streptomycin) solution was from Sigma. Both of these solutions were stored at -20°C.

BHK-21 cells were purchased from the European collection of Cell Cultures (ECCC). These were received frozen and resuscitated as described in section 5.4.6. Following resuscitation and propagation, samples were prepared for storage in liquid nitrogen for further use (section 5.4.6). Electroporation cuvettes (4mm) were from Equibio.

### **5.3.7 Protein reagents**

Triton X-100, Nonidet-40,  $\alpha$ -chymostatin, TPCK, TLCK, Leupeptin, pepstatin, Dimethylsulfoxide (DMSO) and Dimethylformamide (DMF) were from Sigma. Centricon 10/30 and Centriprep 10 concentrating units were from Amicon.

### **5.3.8 Protein purification resins and columns**

Q Sepharose Fast Flow and Sephadex G100 gel filtration resins were from Amersham Life Science. Vivaspin Q ion exchange columns were trial columns kindly provided by Vivascience. Calmodulin-agarose resin was purchased from Sigma.

## 5.4 Methods

### 5.4.1 Polymerase Chain Reaction

#### 5.4.1.1 Primer design and preparation

There were a number of factors to be taken into consideration for the designing of primers and the preferred values were as follow:

1. Optimal primer length of 15 - 25 nucleotides.
2. GC percentages of 40 - 60% (G+C).
3. The two bases at the 3' end to be G or C.
4. Melting temperature of between 55-65°C.
5. Self-complementarity (ability to form 2° structures such as hairpins) should be avoided. Annealing of the forward and reverse primers should also be avoided.
6. Runs of three or more Gs or Cs should be avoided as these may promote mis-priming at these sites.

(Innis and Gelfand, 1990)

Forward and reverse primers for the PDE1A1 ORF were designed in order to introduce enzyme restriction sites together with a Kozak sequence into the ORF using the technique of PCR. The Kozak sequence (GCCGCC(A/G)CCATGG) was important for the efficient production of mRNA transcripts (Kozak, 1989) while the restriction sites, *Bam*HI and *Sma*I, were used for cloning the ORF into the pSFV1 vector. The four primers designed are shown in Table 5.3.



**Table 5.3** Sequences of the PCR primers designed for the generation of full-length and truncated PDE1A1 enzymes.

<b>Primer name</b>	<b>Primer sequence</b>
<b>Forward primers:</b>	
PDE1F1	5'-ATATAGGATCC <sup>Ctaa</sup> <u>GCCGCCACCATGGATGACCATGTCACAATC</u> -3'
PDE1F2	5'-ATATAGGATCC <sup>Ctaa</sup> <u>GCCGCCACCATGTACAGAAAAGTCCTATCAC</u> -3'
<b>Reverse primers:</b>	
PDE1R1	5'-ATATGAATTCCCGGG <sup>tca</sup> TCAAACCTATGAATGTGTATC-3'
PDE1R2	5'-ATATGAATTCCCGGG <sup>tca</sup> GTCCACCAGGTTGTTTTTGAAGC-3'

The forward primers included a *Bam*HI (GGATCC) restriction site (italicised), STOP codon (lower case), Kozak sequence (shown underlined and includes the start codon of the PDE1A1 ORF) followed by a stretch of sequence corresponding to the 5' end of the ORF (bold). Reverse primers included *Eco*RI (GAATTC) and *Sma*I (CCCGGG) restriction sites (italicised) followed by a STOP codon (lower case) then a small stretch of sequence corresponding to the 3' end of the ORF (bold). Combinations of forward and reverse primers were used to generate different fragments of the ORF. These are shown in Table 5.2 while Figure 1.19.2 (Chapter 1) shows the position of the primers on the PDE1A1 ORF.

Primers were received freeze-dried and were briefly centrifuged before being reconstituted with 500µl of sterile Milli Q water. These were further diluted to provide a working concentrations of 100ng/µl.

#### **5.4.1.2 DNA template used for the generation of full-length and truncated PDE1A1 fragments by PCR**

The *Dra*I-cut PDE1A1 fragment from the vector pCRScript-PDE1A1 had already been cloned into the vector pGEX-3X (see Chapter 4) and the insertion confirmed by DNA sequence analysis in the two recombinant constructs identified (pGEX-3X-PDE1A1 clones 12 and 17). Clone 12 was used as the template for the PCR described in this section of the present work.

### 5.4.1.3 Optimisation of the PCR

*Taq* polymerase and the proof-reading enzyme *Pfu* were used for the PCR procedure for which the ‘hot start’ method was followed whereby all the reagents, except the *Taq* (G2) or *Pfu* (FL4, End6, Cat9) enzyme, were mixed and heated at 95°C for five minutes after which the enzyme was added and the PCR reaction allowed to proceed. Factors investigated for the optimisation included altering concentrations of primers, dNTPs and the DNA template. The composition of the PCR reaction mixture found to give the best results comprised of 200µM dNTP mixture, 400ng each of the forward and reverse primers, 5ng template DNA and 1 unit of *Pfu* enzyme together with the *Pfu* enzyme buffer in a final volume of 100µl. Sterile Milli Q water was used to bring the PCR reaction volume up to 100µl. The other factor found to be important in the PCR was the length of annealing time required to produce the full-length and truncated PDE1A1 fragments. Table 5.4 shows the optimised PCR conditions for the different fragments.

**Table 5.4** Optimised PCR conditions for the generation of full-length and truncated PDE1A1 fragments.

Step	F1R1 (1.6 kb)	F2R2 (1.1 kb)	F1R2 (1.4 kb) and F2R1 (1.2 kb)	Cycles
1: Initial denaturation	94°C 5 minutes	94°C 5 minutes	94°C 5 minutes	1
2: Denaturation	94°C 45 secs	94°C 45 secs	94°C 45 secs	30
3: Annealing	57°C 45 secs*	57°C 45 secs*	55°C 45 secs*	
4: Elongation	72°C 255 secs**	72°C 192 secs**	72°C 255 secs**	
5: Final elongation	72°C 10 minutes	72°C 10 minutes	72°C 10 minutes	1
6	4°C ∞	4°C ∞	4°C ∞	

F1R1 correspond to the forward and reverse primers used to generate the full-length PDE1A1 fragment (1.6 kb); F2R2 primers generated the PDE1A1 catalytic fragment (1.1 kb); and F1R2 and F2R1 produced the C-terminal and N-terminal truncated PDE1A1 enzymes respectively. \*/\*\* denote cycling parameters optimised.

Reactions were set up in 0.5ml eppendorf tubes. A sample (5-7µl) of the PCR product was analysed on 0.6% agarose (section 2.2.8) to confirm that the expected fragments had been obtained. The remaining PCR product was either used straight away for cloning into pSFV1 or stored at -20°C for use later.

## **5.4.2 Cloning the PDE1A1 PCR products into pSFV1**

### **5.4.2.1 *Bam*HI and *Sma*I restriction digestion of the PCR product**

A mixture of 45µl of the PCR product, 10µl of 10x Multicore Reaction Buffer, 2µl (20 units) of each of the restriction enzymes and 41µl of dH<sub>2</sub>O was prepared in a 0.5ml eppendorf and incubated at 30°C for 2 hours followed by incubation at 37°C for a further 2 hours. The mixture was then cleaned using the Wizard DNA Clean-up kit according to manufacturers instructions to remove the restriction enzymes and buffers before proceeding to the next stage of ligating the digested fragments into pSFV1.

### **5.4.2.2 *Bam*HI and *Sma*I restriction digestion of pSFV1**

Approximately 2.8µg of pSFV1 were digested in a mixture comprising of 2µl pSFV1 (1.4µg/µl stock), 10µl of 10x Multicore Reaction Buffer, 2µl each of the restriction enzymes (20 units each) and 84µl of dH<sub>2</sub>O. The mixture was incubated at 30°C for 2 hours followed by incubation at 37°C then cleaned using the Wizard DNA Clean-up kit as before (section 2.2.9).

### **5.4.2.3 Dephosphorylation of pSFV1**

Dephosphorylation of the vector was carried out in order to minimise re-ligation of the vector occurring without the insert. 100µl (~2.8µg) of the digested and cleaned vector were mixed with 20µl of 10x CIAP buffer, 2µl of CIAP enzyme (2 units) and 78µl of H<sub>2</sub>O. The mixture was incubated at 37°C for 1 hour followed by incubation at 65°C for 10 minutes to inactivate the enzyme. The dephosphorylated vector was cleaned using the Wizard DNA Clean-up kit as before (2.2.9).

### **5.4.2.4 Ligation of digested PDE1A1 PCR fragments and pSFV1**

Before carrying out the ligation reactions, samples (5µl from total volume of 50µl) of the digested and cleaned insert and vector were analysed on a 0.6% agarose (section 2.2.8). An estimate of the relative amounts of DNA for the insert and vector was made from the

ethidium bromide visualisation of the samples. These were estimated as having ~1 µg insert DNA in 5 µl of sample and the vector estimated to have ~2 µg of DNA in 5 µl.

Different vector to insert ratios (0.5:1 to 1:20), based on the DNA estimations from ethidium bromide-visualised gels, were then used in a mixture comprising of 10x ligase buffer, vector, insert, T4 ligase (3 units), 8mM ATP in a final volume of 10 µl. More insert DNA was used because when more vector DNA was used, all the transformant colonies analysed contained just vector DNA (religated vector). Controls were also included where the insert was omitted from the mixture. The ligation mixtures were left at 4°C for 8 hours followed by incubation at 15°C for at least 24 hours. At the end of this period, the complete ligation mixture was used to transform *E. coli* DH5α competent cells.

#### **5.4.3 Transformation of *E. coli* DH5α competent cells with ligation mixtures**

The method used has been described in section 2.2.4.

#### **5.4.4 Screening transformant colonies for the correct construct**

##### **5.4.4.1 DNA purification for screening of transformant colonies**

Transformant colonies were selected for inoculation into LB media supplemented with ampicillin and incubated in a shaking, 37°C incubator overnight. 1ml of each of the cultures was used for small scale DNA purification as described in section 2.2.5. Purified DNA was then subjected to restriction enzyme analysis to identify the required construct as described in section 2.2.7. Large scale DNA purification of the required clone(s) was carried out as described in section 2.2.5. Positive recombinant clones were further confirmed by carrying out Automated DNA Sequence Analysis (section 2.2.10).

##### **5.4.4.2 *Bam*HI, *Sma*I and *Eco*RV Enzyme Restriction Analysis for selection of constructs**

A combination of *Bam*HI, *Sma*I and *Eco*RV restriction enzymes were used to screen for the required recombinant constructs. Confirmation of the recombinant construct was carried

out using *Bam*HI and *Eco*RV together as well as single enzyme restriction analysis to linearise the construct. Purified DNA was digested with these enzyme(s) and analysed on 0.6 - 1.0% agarose gels as described in section 2.2.7 and 2.2.8.

#### **5.4.5 *In vitro* RNA synthesis**

All reagents used in these procedures were prepared using RNase-free water or were RNase-free. RNase-free sterile tips were also purchased from Molecular Bioproducts.

##### **5.4.5.1 Linearisation of the construct**

pSFV1 has a unique *Spe*I site (absent in PDE1A1 ORF) which was used to linearise the construct prior to RNA synthesis. This was carried out in a 100µl total reaction mixture comprising of 60µg of construct DNA, 30 units of *Spe*I enzyme, 10x Reaction Buffer and sterile Milli Q water to make up the total volume. The mixture was incubated at 37°C overnight. A further 30 units of the enzyme were added to the mixture the following day and incubated for 1 - 2 hours at 37°C to ensure complete linearisation of the DNA. *Spe*I linearisation was also carried out on pSFV3*lacZ* and Helper-2 virus DNA and these processed in exactly the same way as the construct for the *in vitro* RNA synthesis.

##### **5.4.5.2 Phenol/Chloroform Clean-up of linearised construct, pSFV3*lacZ* and pSFV-H2 DNA**

The linearised DNA was subjected to a phenol/chloroform clean-up to remove the restriction enzymes and buffers. The construct was mixed with an equal volume of the phenol/chloroform and centrifuged in a benchtop centrifuge for 1 minute at maximum speed. The upper aqueous layer was transferred into a fresh tube and an equal volume of 100% chloroform was added to this, mixed and centrifuged for 1 minute. The chloroform extract was removed and retained. The process was repeated twice more using 100µl of DEPC-treated water to extract any remaining DNA from the phenol/chloroform mixture as well as from the chloroform solution. All extracts were pooled for the salt/ethanol precipitation of the DNA.

#### **5.4.5.3 Salt/ethanol precipitation**

The chloroform extracted sample was now subjected to a salt/ethanol precipitation. The volume of sample was estimated and 1/10th of this volume of 3M sodium acetate pH 5.2 plus 2-volumes of ice cold 100% ethanol were added to the sample. This was mixed and chilled at -20°C overnight. The sample was then centrifuged at maximum speed in a bench top centrifuge for 15 minutes at 4°C. The supernatant was discarded, and twice the volume of 70% ethanol added to the pellet and centrifuged as before. The ethanol was discarded and the pellet allowed to air dry for approximately 1 hour. The dried pellet was resuspended in 50% of the original sample volume of RNase-free water and a UV/Vis spectrophotometric scan was performed on a 1 in 100 dilution of the sample. The sample was aliquoted into volumes corresponding to 5µg of DNA and stored at -70°C until needed.

#### **5.4.5.4 *In vitro* RNA synthesis**

An rNTP mixture (2.5mM ATP, 2.5mM CTP, 2.5mM UTP and 1.25mM GTP) was prepared in DEPC-treated water. Linearised, phenol/chloroform cleaned samples of the construct DNA, pSFV3*lacZ* and Helper-2 virus were used to synthesise RNA transcripts. These were prepared in 50µl reaction mixtures containing 5x SP6 Reaction Buffer, 20µl of rNTP mixture, 5µg DNA, 1mM Capping Analog, 80 units RNasin (an RNase inhibitor), 38 units SP6 RNA Polymerase, 10mM DTT and DEPC-treated H<sub>2</sub>O to make up the volume to 50µl. The mixture was incubated at 42°C for 3 hours. 1-2µl of the product were removed for analysis on 0.4% agarose gel electrophoresis (section 2.2.8). The remainder of the RNA sample was either used the same day for electroporation of BHK-21 cells or aliquoted into 10µl volumes and stored at -70°C until needed. Note that RNA aliquots were not subjected to repeated freeze-thaw cycles as this would have reduced the quality of the RNA. RNA samples were only thawed once and used straight away.

#### **5.4.5.5 Analysis of RNA transcripts**

The 1-2µl of the RNA sample removed for analysis were mixed with 8µl of DEPC-treated water and 2µl of gel loading buffer and analysed on 0.4 - 0.6 % agarose gels. The 0.4 - 0.6% agarose gels were prepared as described in section 2.2.8.

#### 5.4.6 Growth and maintenance of Baby Hamster Kidney-21 cells (BHK-21)

All manipulations involving BHK-21 cells were carried out in a Class II tissue culture cabinet (Laminar flow biological safety cabinet). All items taken into the cabinet were sterile and pre-sprayed with 70% ethanol.

##### 5.4.6.1 Preparation of Complete Media used for the maintenance of BHK-21 cells

Complete Media (CM) was routinely used for the growth and maintenance of BHK-21 cells. Table 5.5 gives the composition of this CM which was prepared and stored at 4°C for up to two weeks only.

**Table 5.5** Composition of the Complete Media used for BHK-21 cells.

<b>Reagent</b>	<b>Volume (ml)</b>
GMEM	500
Foetal Calf Serum	50
Tryptose Phosphate Broth	25
L-Glutamine	5
Penicillin-Streptomycin	5

##### 5.4.6.2 Resuscitation of BHK-21 cells

The frozen BHK-21 cells received from ECCC were thawed quickly by agitating the cells gently in a 37°C waterbath for two minutes. Cells were mixed gently and transferred into 10ml of pre-warmed (37°C) GMEM Complete Media (CM). The cells were centrifuged at 400g, 18°C for three minutes to remove the storage or Freezing Solution (see section 5.4.6.4). The supernatant was discarded and the cells resuspended in 30ml of fresh, warm CM. The mixture was divided into two 75cm<sup>2</sup> flasks and the cells incubated at 37°C, 5% CO<sub>2</sub> and 100% humidity. Cells were passaged on the third day at a dilution of 1/5 - 1/10 depending on the confluency of the cells (section 5.4.6.3). This was continued until passage 30 - 40 depending on the growth and morphology of the cells when they were discarded and a lower passage of cells resuscitated.

### **5.4.6.3 BHK-21 Cell Passage**

This was carried out on cells every third day when the cells were 90-100% confluent. Cells were washed twice using 10ml PBS. 1ml of trypsin (0.25%) was added to the cells ensuring all the cells were covered with the trypsin. Cells were incubated at 37°C, 5% CO<sub>2</sub> and 100% humidity for three minutes. The flask was tapped on the bench firmly to separate the aggregated cells then between 4 - 9ml of CM media added for 1/5 and 1/10 dilution respectively. Cells were resuspended thoroughly and 1ml of cells transferred into 14ml of fresh warm CM in a 75cm<sup>2</sup> flask and incubated as before.

### **5.4.6.4 Freezing BHK-21 cells**

100% confluent cells from a 75cm<sup>2</sup> flask were treated with trypsin (Section 5.4.6.3) and 5ml of warm (37°C) CM added to the cells. Cells were centrifuged at 400g, 18°C for three minutes. The supernatant was discarded and the cells resuspended in the Freezing Solution (GMEM with 27% Foetal Calf Serum, 7mM Glutamine and 10% DMSO). These were transferred into a Cryo tube and frozen slowly in an isopropanol cryo chamber at -70°C overnight then transferred into liquid nitrogen for long-term storage.

## **5.4.7 Direct transfection of BHK-21 cells with pSFV3*lacZ* RNA transcripts**

pSFV3*lacZ* plasmid contains the gene for the expression of the enzyme β-galactosidase. Cells transfected with this RNA transcript were stained for the enzyme using X-Gal solution. This was used as an indicator of the electroporation conditions subsequently used for the transfection of BHK-21 cells with recombinant pSFV1-PDE1A1 RNA transcripts.

### **5.4.7.1 BHK-21 cell preparation and electroporation**

Cells at 50-60% confluency were washed as before using PBS (section 5.4.6.3) and treated with 2ml of warm (37°C) diluted trypsin (1/5) and incubated at 37°C, 5% CO<sub>2</sub> for three minutes. 4ml of warm CM were added to the treated cells and a pipette used to gently resuspend the cells in the media. Resuspended cells were transferred into a sterile 20ml universal and the cells centrifuged at 400g, 18°C for three minutes. The supernatant was



discarded and 4ml of warm GMEM media containing 2mM Glutamine (no other additives) used to resuspend the cells before being centrifuged again. The supernatant was discarded and the cells resuspended in 1ml of ice cold PBS. A 40 $\mu$ l sample of the resuspended cells were removed for an estimation of cells per ml. A further 3ml of ice cold PBS were added to the washed cells and these centrifuged as before. Cells were counted using a haemocytometer to obtain a count for cells per ml and 0.75ml of the resuspended cells ( $1 \times 10^6$  cells) were mixed with 10 $\mu$ l of pSFV3*lacZ* RNA in an eppendorf tube before being transferred into a 4mm electroporation cuvette. Electroporation was carried out using the parameters: 350V, 1500 $\mu$ F and 99 $\Omega$  (Liljestrom and Garoff, 1991). Electroporated cells were transferred immediately into 5ml warm CM, mixed gently then poured into a 25cm<sup>2</sup> flask for incubation at 37°C, 5% CO<sub>2</sub> for 18 - 24 hours. Cells were then stained for the detection of  $\beta$ -galactosidase (pSFV3*lacZ*). Control reactions were also carried out using 10 $\mu$ l of PBS instead of RNA transcripts to determine the effect on electroporated empty BHK-21 cells.

#### **5.4.7.2 In-situ $\beta$ -Galactosidase ( $\beta$ -Gal) staining with X-Gal**

Staining of the BHK-21 cells transfected with pSFV3*lacZ* RNA was carried out in order to assess the efficiency of the electroporation procedure. This was to be used as a direct indication of the efficiency of the cells transfected with the pSFV1-PDE1A construct RNA as the same conditions were used for both procedures.

Cells were washed twice with 1ml PBS then fixed using 2ml 0.25% glutaraldehyde by rocking gently at room temperature for 15 minutes. The glutaraldehyde was then removed and the cells washed thoroughly three times with 1ml PBS. Cells were then covered with 0.2% X-gal solution (2mM MgCl<sub>2</sub>, 5mM K<sub>3</sub>Fe(CN)<sub>6</sub>, 5mM K<sub>3</sub>Fe(CN)<sub>6</sub>.3H<sub>2</sub>O, 0.2% X-gal) and incubated at 37°C for one hour. Flasks were rocked gently every fifteen minutes during this time. At the end of the hour, cells were counted to obtain transfection efficiency (%) by counting the total number of cells in a designated area of the flask then counting the blue-stained cells in the same area and using the formula below to obtain a value for percentage of stained cells: Total Blue-stained cells/Total cells x 100 = % Stained cells.

#### **5.4.8 Direct transfection of BHK-21 cells with pSFV1-PDE1A1 RNA transcripts**

The method for the direct transfection of BHK-21 cells with pSFV3*lacZ* RNA was repeated for the direct transfection of pSFV1-PDE1A1 RNA transcripts (section 5.4.7) except that the transfected cells were not stained for  $\beta$ -Gal but harvested for the soluble recombinant PDE1A1 enzyme (see section 5.4.13). *In vitro* RNA transcripts were also generated for the empty vector pSFV1 and used to transfect BHK-21 cells in the same way. These were used as controls for background PDE activity in transfected BHK-21 cells.

#### **5.4.9 Co-transfection of BHK-21 cells with pSFV1-PDE1A1/ pSFV3*lacZ* RNA and Helper-2 virus RNA**

This method was essentially the same as that described in section 5.4.7 except that BHK-21 cells were mixed with 10 $\mu$ l each of pSFV3*lacZ* RNA or pSFV1-PDE1A1 RNA together with 10 $\mu$ l of pSFV-H2 virus RNA for electroporation. Media was harvested for the virus for both pSFV3*lacZ* and pSFV1-PDE1A1 (section 5.4.10). BHK-21 cells transfected with pSFV3*lacZ*/pSFV-H2 were stained for the presence of  $\beta$ -gal (5.4.7.2) while cells transfected with pSFV1-PDE1A1/pSFV-H2 were harvested for the presence of PDE (section 5.4.13).

#### **5.4.10 Harvesting recombinant virus**

Culture media containing the recombinant virus particles was removed approximately 18-24 hours following electroporation (pSFV3*lacZ*/pSFV-H2 or pSFV1-PDE1A1/pSFV-H2 RNA) and collected into 20ml-sterile universal bottles and centrifuged at 2000g, 4°C for 10 minutes. The supernatant containing the virus was separated from the cells and aliquoted into 200 $\mu$ l volumes for storage at -70°C until needed. The pSFV1-PDE1A1/pSFV-H2 cells remaining were harvested (5.4.13) and processed further for PDE assays (section 2.2.11) and Western blotting (section 2.2.14).

## **5.4.11 Infection of BHK-21 cells with recombinant virus particles**

### **5.4.11.1 BHK-21 cell preparation for infection with recombinant virus**

Confluent cells from a 75cm<sup>2</sup> flask were treated with trypsin as usual (section 5.4.6.3), 4ml of CM added and the cells centrifuged at 400g, 18°C for three minutes. Cells were then resuspended in 1ml of CM, and 20µl removed for counting, using the haemocytometer, for cells per ml. Approximately 1x10<sup>5</sup> and 1x10<sup>6</sup> cells were routinely seeded for infection for small-scale (25cm<sup>2</sup>) and large-scale (75cm<sup>2</sup>) infections respectively. These cells were incubated at 37°C, 5% CO<sub>2</sub> and 100% humidity for 24 hours before being infected with the recombinant virus.

### **5.4.11.2 Recombinant virus activation**

A 200µl aliquot of virus stock was thawed and α-chymotrypsin added to the virus at a concentration of 0.4mg/ml. This was incubated at room temperature for 45 minutes then protease activity stopped using 0.6mg/ml of aprotinin and incubated for a further 5-10 minutes at room temperature. 1ml of CM was added to 2 - 5 1.5ml eppendorf tubes and a range (25µl - 100µl) of activated virus added to these. A range of virus volumes was used in order to assess the efficiency of the virus stocks for subsequent infections.

### **5.4.11.3 Determination of transfection efficiency and virus titer**

Transfection efficiency and the virus titer were determined using the method described by DiCiommo and co-workers (1998).

#### **5.4.11.3.1 Infection of BHK-21 cells with pSFV3lacZ virus stocks**

Prepared cells (section 5.4.11.1) were washed twice using 1ml PBS. Activated virus (section 5.4.11.2) in the 1ml CM was poured onto the washed cells and the flask rocked gently so that there was an even distribution of the virus on the cells. Cells were incubated with the virus for exactly 45 minutes at 37°C, 5% CO<sub>2</sub> and 100% humidity. The media was then poured into a disinfectant container for disposal and 5ml fresh, warm CM was poured

onto the infected cells. These were incubated for a further 24 hours after which they were stained for  $\beta$ -Galactosidase (section 5.4.7.2). Staining of the pSFV3*lacZ* virus-infected cells was carried out in order to assess infection-efficiency of the virus stocks for an indirect correlation to the pSFV1-PDE1A1 virus infection efficiency which was generated under the same conditions.

#### **5.4.11.3.2 Transfection efficiency and viral titer determination**

To determine transfection efficiency, cells infected with pSFV3*lacZ* virus and stained for  $\beta$ -Galactosidase were counted under a microscope at 40x magnification. An eyepiece with a template was used to count cells. The area of this template field was 0.13cm<sup>2</sup>. Total number of cells and cells stained blue were counted in this field and a percentage calculated for stained cells which was equivalent to transfection efficiency according to the formula below:

$$(\text{Blue cells}) \div (\text{Total cells}) \times 100 = \% \text{ Transfection Efficiency}$$

The titer of the virus was calculated according to the formula below:

$$(\text{Area of plate} \div \text{Area of field}) \times (\% \text{ Transfection efficiency}) \times (\text{Dilution factor}) \\ = \text{Infectious units/ml (Equivalent to the virus titer)}$$

This was used as an indirect indication of the virus titre for the recombinant PDE1A1 virus as this was produced under the same conditions (DiCiommo and Bremner, 1998).

#### **5.4.11.4 Infection of BHK-21 cells with the recombinant pSFV1-PDE1A1 virus stocks**

Results for the *in situ*  $\beta$ -Galactosidase staining of BHK-21 cells transfected with pSFV3*lacZ* virus indicated that 100 $\mu$ l of the virus stock was needed for 91% staining of the cells, and hence infection of the cells with the virus for cells grown up to 24 hours. Therefore, 100 $\mu$ l of the recombinant pSFV1-PDE1A1 virus were treated with  $\alpha$ -chymotrypsin followed by treatment with aprotinin as before (section 5.4.11.2). Prepared BHK-21 cells were infected using the activated virus in exactly the same way as for

pSFV3*lacZ* virus (5.4.11.3) and the cells incubated for 24 hours before harvesting for the soluble recombinant PDE1A1 enzyme (5.4.13).

#### **5.4.12 Optimisation of the conditions for the expression of recombinant enzyme following pSFV1-PDE1A1 virus infection**

These were carried out to evaluate the use of smaller volumes of the recombinant virus stock so as to allow scale-up of the infection from 25cm<sup>2</sup> flasks to 75cm<sup>2</sup> flasks more readily. The range of virus stock used was from 25µl up to 200µl of the recombinant pSFV1-PDE1A1 virus and prepared cells in 25cm<sup>2</sup> flasks were infected as before. Infected cells were grown for up to 72 hours and cells harvested at 24, 48 and 72 hours for PDE activity in order to ascertain the optimum time required for recombinant protein expression. PDE activity assays were carried out on the cleared total cell lysate samples (supernatants) of the harvested cells. These results indicated that using 25µl of the virus and harvesting the infected cells at 48 hours gave the best results for recombinant enzyme expression. These parameters were subsequently used for scale-up to 75cm<sup>2</sup> flasks to produce sufficient recombinant enzyme for kinetic analysis and purification studies.

#### **5.4.13 Harvesting BHK-21 cells following direct transfection with pSFV1-PDE1A1 RNA transcripts or co-transfection with pSFV1-PDE1A1 and pSFV-H2 RNA transcripts**

##### **5.4.13.1 BHK-21 cell harvesting following direct transfection with pSFV1-PDE1A1 RNA transcripts**

Cells from the direct transfection of BHK-21 cells with the recombinant pSFV1-PDE1A1 RNA were processed further to analyse the cell lysates for PDE activity. The media was removed from the cells and centrifuged at 2000g, 4°C for 10 minutes. The media was then discarded leaving any cells containing recombinant protein that may have become detached from the flasks. These cells were washed using 2ml of PBS by centrifuging as before. These were then resuspended in 1ml of ice cold lysis buffer 2 or lysis buffer 3 (see Table 2.3 for buffer composition) with protease inhibitors (20µM TLCK, 0.1mM TPCK, 20µM chymostatin, 8µg/ml leupeptin, 8µg/ml pepstatin) and a detergent (NP-40). Meanwhile,

the cells in the flask were washed twice using 2ml PBS. The washed cell pellet resuspended in the lysis buffer was poured over the washed cells in the flask and rocked gently at room temperature for 10 minutes. Cells were then scraped from the flask surface into the lysis buffer. Lysis buffer containing the released cells was transferred into a 1.5ml eppendorf tube and centrifuged in a benchtop centrifuge at maximum speed (14,000rpm), 4°C for 2 minutes. The supernatant containing the recombinant PDE1A1 protein was separated from the cell debris and analysed for PDE activity (section 2.2.11). Both the cell debris and the supernatant samples were also analysed using Western blot (section 2.2.14). The cell debris was resuspended in 100-200µl of lysis buffer, vortex mixed then assayed for PDE activity. Protein concentration was measured using the Bradford assay (section 2.2.15). In some cases, the supernatant samples were subjected to methanol/chloroform concentration (section 5.4.14.1) before Western blot analysis in order to concentrate the recombinant protein. Both the cell debris and supernatant samples were stored at -20°C.

#### **5.4.13.2 BHK-21 cell harvesting following co-transfection of pSFV1-PDE1A1 and pSFV-H2 RNA transcripts**

BHK-21 cells co-transfected with the recombinant pSFV1-PDE1A1 plus pSFV-H2 RNA transcripts, were processed further to analyse the cell lysates for PDE activity. The cells remaining in the flask once the media containing the virus had been harvested, were washed twice with 2ml of PBS. 1ml of ice cold lysis buffer 2 or 3 containing protease inhibitors and NP-40 as before (5.4.13.1) was added directly onto the washed cells. These were now treated in exactly the same way as before (5.4.13.1) to harvest the supernatant containing the recombinant PDE1A1 enzyme. The harvested recombinant protein was used for the purification process (5.4.17) and for the biochemical characterisation of the recombinant protein (Chapter 6).

#### **5.4.14 Concentration of samples**

##### **5.4.14.1 Methanol/chloroform concentration of samples**

Supernatant samples collected following cell harvesting (section 5.4.13) were concentrated ten fold for analysis on SDS PAGE and Western blotting using the methanol/chloroform

method. Briefly, 150µl of the sample were added to 600µl of methanol, vortex mixed, and 150µl of chloroform added. The mixture was vortex mixed again and 450µl of water added. The sample was then centrifuged for 3 minutes at maximum speed. The upper layer was discarded without disturbing the pellet at the interface and a further 150µl of methanol added. This was centrifuged for 3 minutes at maximum speed and the supernatant discarded. The resulting protein pellet was air-dried for about half an hour then resuspended in 15µl of lysis buffer 2 or 3 with protease inhibitors but not containing any detergent and left on ice for about an hour to allow complete dissolution of the protein pellet. 3µl of 6x SDS gel loading buffer together with 1.8µl of 1M DTT were added to the sample and analysed on SDS PAGE and Western blot analysis the same day.

#### **5.4.14.2 Centricon 10/30 concentration of samples**

Eluates collected from the Q Sepharose purification procedure (section 5.4.17) showing PDE activity were pooled and concentrated using either Centricon 10 or Centricon 30. Manufacturers instructions were followed for the procedure. Briefly, the column was first washed with 2 - 3ml of water to remove preservatives from the membrane. The Centricon columns were centrifuged at 5000 - 7000rpm for 10 - 20 minutes using a Beckman JA20 rotor and the 5ml samples concentrated down to approximately 500 - 700µl. Concentrated samples were tested for PDE activity and also analysed on SDS PAGE followed by Western blot analysis.

#### **5.4.15 Stability studies on the full-length PDE1A1 enzyme**

These were carried out to ascertain the stability of the recombinant PDE activity at 4°C as samples were to be stored at this temperature during the kinetic analysis. Also investigated were the effect of glycerol on recombinant PDE activity following storage at -70°C. The effect of pH on recombinant PDE activity was another factor that was investigated.

##### **5.4.15.1 Storage of FL4 at 4°C**

PDE activity assays using cAMP in the presence and absence of Ca<sup>2+</sup>/CaM were carried out on crude supernatant samples of FL4 stored at 4°C for up to a week.

#### **5.4.15.2 Effect of pH on FL4 PDE activity**

The buffers used for this study were as follows:

1. Sodium acetate pH 4.5
2. Sodium acetate pH 5.2
3. MES pH 6.5
4. Hepes pH 7.5
5. Tris-HCl pH 8.0
6. Tris-HCl pH 8.5
7. Bicine pH 9.0

All buffers were used at 50mM concentration. Crude FL4 supernatant sample was diluted 1 in 4 in the appropriate buffer and PDE assays carried out the same day (Day 0) using cAMP as the substrate. Samples were then stored at 4°C for up to a week and assayed for PDE activity at Day 1 through to Day 4.

#### **5.4.15.3 Effect of glycerol on FL4 and End6 PDE activity**

Glycerol is commonly added to protein samples requiring repeated freeze-thawing in order to minimise the detrimental effect of this process on the recombinant protein. FL4 and End6 supernatant samples were diluted 1 in 4 in lysis buffer 3 containing a range of glycerol concentrations (v/v) ranging from 0% to 40%. This was investigated, firstly, because samples of the recombinant enzymes were to be stored for up to six months at -70°C in buffers containing glycerol; and, secondly, some of the lysis and purification buffers used for the present work contained up to 40% glycerol. The prepared samples were analysed the same day then stored at -70°C for approximately eight weeks after which they were thawed and analysed for PDE activity again.



## **5.4.16 Studies to determine the native state of the recombinant PDE1A1 enzyme (FL4 and End6 constructs)**

### **5.4.16.1 Cross-linking studies on End6**

The cross-linker Suberic acid bis (N-hydroxysuccinimide ester) (Disuccinimidyl suberate: DSS) was used to study the cross-linking of the recombinant End6 (N-terminal truncated) enzyme. These studies were carried out on End6 only and not on FL4 as the detection of the end product of the cross-linking reaction by Western blot analysis was more straightforward for End6 than for FL4; the latter had a very weak signal on the Western blot. PDE activity assays following cross-linking reactions were not carried out due to time constraints. Also, the cross-linking reactions are said to inactivate enzymes.

#### **5.4.16.1.1 DSS stock preparation**

10mg of DSS were dissolved in 525 $\mu$ l of DMSO to provide a stock concentration of 50mM.

#### **5.4.16.1.2 Cross-linking reaction using DSS**

End6 sample harvested using lysis buffer 3 was used (Table 2.3; HEPES-containing buffer) for the cross-linking experiments. Tris-containing buffers were unsuitable as the primary amines present in these buffers form covalent amide bonds with the DSS ester thereby quenching the reaction.

50mM stock DSS was added to the End6 protein sample to give final DSS concentrations of 0.25, 0.5, 1.0, 2.0 and 5.0mM. Control reactions using DMSO alone were also included. The mixtures were incubated at room temperature for 30, 60 and 120 minutes. Aliquots of samples were removed at these time points and the reactions quenched using Tris buffer pH8.0 buffer at a final concentration of 50mM. Samples were mixed with 6x SDS gel loading buffer for Western blot analysis using CaM-PDE antibody (section 2.2.14).

#### **5.4.16.2 Sephadex G100 size exclusion chromatography on FL4**

The Western blot signal for the full-length PDE1A (FL4) enzyme was quite weak compared to the N-terminal truncated enzyme (End6) so it was not practical to carry out the cross-linking experiment on FL4. Size exclusion chromatography (gel filtration) was therefore carried out on FL4 in order to provide information on the native state of the full-length enzyme.

##### **5.4.16.2.1 Sephadex G100 resin equilibration**

4g of dry Sephadex G100 powder were slowly added to 100ml of gel filtration buffer 1 (see Table 2.3) in a 250ml conical flask and allowed to swell fully overnight at room temperature. Buffer 1 was then decanted carefully so as not to disturb the swollen resin, but removing the fines, and 100ml of gel filtration buffer 2 (Table 2.3) added to the resin and mixed. The resin was then degassed for approximately five minutes before allowing it to settle again. The clear buffer was decanted off as before and fresh gel filtration buffer 2 added to resin which was degassed a second time. The resin was left to equilibrate at 4°C overnight. The following day, as much as possible of the buffer was decanted, together with any remaining fines, and the slurry mixed gently and poured into a vertically positioned glass column. One smooth movement was used to pour the resin so as not to have any breaks in the pouring motion and to avoid trapped air. The resin was allowed to settle overnight. Gel filtration buffer 3 (Table 2.3) was then used to equilibrate the column before loading the samples. Standards and samples were run using gel filtration buffer 3.

##### **5.4.16.2.2 Standards for Sephadex G100 gel filtration chromatography**

Three proteins were used as standards for gel filtration. Amounts of individual proteins used are shown in Table 5.6.

**Table 5.6** Standards used for Sephadex G100 gel filtration chromatography

<b>Protein</b>	<b>Size (kDa)</b>	<b>μg</b>
β-Amylase (Sweet Potato)	~200	600
Bovine Serum Albumin	66	1500
Carbonic Anhydrase	29	600

The proteins were premixed before loading on to the column. They were allowed to enter the resin completely before adding 4-5ml of gel filtration buffer 3 on top of the resin very carefully so as not to disturb the resin. An Amersham Pharmacia LKB pump set at 10ml/h was used for the duration of the run. Approximately one hundred 0.5ml fractions were collected using a Pharmacia LKB fraction collector. The absorbance at 280nm was measured for all the fractions for the detection of protein.

#### **5.4.16.2.3 Preparation and loading of the FL4 sample for gel filtration**

20ml of Full-length (FL4) recombinant enzyme from a large scale infection (ten 75cm<sup>2</sup> flasks) were concentrated down to approximately 2ml using the 20ml-Vivapure-Q ion exchange spin columns (see section 5.4.17.2). Elution of the bound protein was carried out with two 1ml steps of purification buffer 2 (Table 2.3) containing 0.2M NaCl. The two eluates were pooled and loaded onto the gel filtration column in the same way as the standards. The column was run using gel filtration buffer 3. Buffer was allowed to flow through the resin at 10ml/h setting and 0.5ml fractions were collected. These fractions were assayed for PDE activity using cGMP as the substrate. A small amount of the pooled 0.2M eluate was retained for PDE activity analysis which was also carried out on all the fractions collected from the ion exchange chromatography. 12% SDS PAGE was carried out on all the fractions.

## **5.4.17 PDE1A1 purification**

### **5.4.17.1 Q Sepharose Fast Flow ion exchange chromatography**

#### **5.4.17.1.1 Column packing and equilibration**

2ml of the resuspended Q Sepharose resin (in 20% ethanol) were degassed and poured into a tapered plastic 5ml column. This was allowed to settle overnight then the liquid drained through almost completely before washing and equilibrating the settled resin with approximately 20ml of purification buffer 1 (Table 2.3) or purification buffer 2 at a flow rate of 25ml/hr. Note that all steps were carried out at 4°C with reagents equilibrated at 4°C.

#### **5.4.17.1.2 Protein binding and elution**

To bind the protein of interest, the purification buffer in the column was allowed to drain through until the meniscus had reached the top of the resin. The samples used for the purification were supernatant samples obtained from the infection of BHK-21 cells with the recombinant End6 virus particles. Supernatant samples (~4ml) containing the active PDE1A1 protein were allowed to flow through the resin at a rate of 10ml/hr and the flow-through collected. This flow-through (unbound protein) sample was reapplied to the resin to ensure binding of all the protein in the sample. The final flow-through sample was retained for analysis. The resin was then washed twice with 5ml of the purification buffer 1 or 2 and the wash samples retained (Wash 1 and Wash 2). Elution was carried out in a step-wise manner using 5ml of purification buffer 1 or 2 containing 0.1M to 1.0M NaCl. The column was then washed twice with purification buffer 1 or 2 (End wash1 and End wash 2). All the retained fractions were analysed for PDE activity and subjected to SDS PAGE analysis (see sections 2.2.11 and 2.2.12 respectively). The End6 fraction containing peak PDE activity was also concentrated using the Centricon 30 (see section 5.4.14.2) and the fraction volume reduced from 5ml down to ~700µl. The concentrated sample was analysed for PDE activity as well as SDS PAGE analysis.

#### **5.4.17.2 Vivapure-Q Spin Columns for ion exchange chromatography**

Vivapure-Q Spin Columns were single-use filter-based 0.5ml and 20ml capacity spin columns for anion exchange chromatography. The base matrix of the ion exchange membrane was regenerated cellulose and the ionizable groups were quaternary ammonium ions. These units were used as they allowed concentration of the protein sample for gel filtration chromatography (5.4.16.2). A large volume of the recombinant enzyme sample could be bound to these ion exchange filters and a small volume of elution buffer could then be used to elute the protein. This was very useful when samples needed to be in a small, concentrated volume as for gel filtration chromatography.

##### **5.4.17.2.1 Equilibration of the Vivapure-Q Spin Columns**

The columns were first washed twice with either 0.5ml or 20ml of water. The units were centrifuged either in a fixed-angle benchtop centrifuge at 14,000rpm for 1 minute for the 0.5ml units or in a Sigma swing-out bucket rotor at 800g for 2 minutes for the 20ml units. The filters were then primed using either purification buffer 1 or 2 (Table 2.3) and used straightaway.

##### **5.4.17.2.2 Sample application and elution from the Q Spin Columns**

Sample application, elution and washing was carried out by centrifuging the units as before. Supernatant samples of FL4 were applied to the columns at least twice before washing with purification buffer followed by step elution with either 0.5ml (0.5ml units) or 1.0ml (20ml units) purification buffer 1 or 2 containing 0.1M to 1.0M NaCl. All washes and eluted fractions were analysed for PDE activity as well as SDS PAGE analysis. Western blot analysis was carried out on fractions showing peak PDE activity. For the FL4 fraction containing peak activity, this fraction was used for further purification using calmodulin-agarose affinity chromatography (5.4.17.3).

### **5.4.17.3 Calmodulin-agarose affinity chromatography on pSFV1-PDE1A1 (FL4)**

#### **5.4.17.3.1 Calmodulin-agarose resin equilibration**

0.25ml of the resuspended calmodulin-agarose resin were transferred into a 1.5ml eppendorf tube. This was centrifuged in a bench top centrifuge at 10,000rpm for 2 minutes and the preservative solution discarded. The resin was washed twice in water then twice purification buffer 1. Purification buffer 1 containing 100 $\mu$ M Ca<sup>2+</sup> was used to equilibrate the resin by washing the resin twice in this buffer.

#### **5.4.17.3.2 Sample application and elution**

Crude FL4 supernatant samples were not applied directly to the calmodulin-agarose resin as it was possible that the crude sample may have contained calmodulin-binding proteins such as calcineurin which would interfere with the binding of the recombinant protein. The crude sample (0.5ml from direct transfection) was therefore first applied to the Vivaspin-Q spin columns and the enzyme eluted with two 1ml steps of purification buffer 1 containing 0.2M NaCl (5.4.17.2.2). These two eluates were applied separately to the calmodulin agarose resin, after the addition of calcium chloride to a final concentration of 100 $\mu$ M Ca<sup>2+</sup>. The samples were mixed with the resin and this gently rocked for 20-30 minutes to allow complete binding of the protein. The resin was then centrifuged as before and the two 'flow-through' samples containing the unbound material, removed and retained for analysis (FT1 and FT2). Resin was then washed once with purification buffer 1 containing 100 $\mu$ M Ca<sup>2+</sup> then once with purification buffer 1 alone. Elution of the bound protein was carried out using 1ml of purification buffer 1 containing 2mM EGTA. The elution buffer was mixed with the resin and rocked gently for 20-30 minutes before centrifuging as before. Eluted protein was separated from the resin and retained for analysis. The resin was washed further with purification buffer 1 twice then buffer with 1M NaCl. All the fractions were analysed for PDE activity.

#### **5.4.18 Preliminary PDE assays on the full-length (FL4) and N-terminal truncated (End6) enzymes**

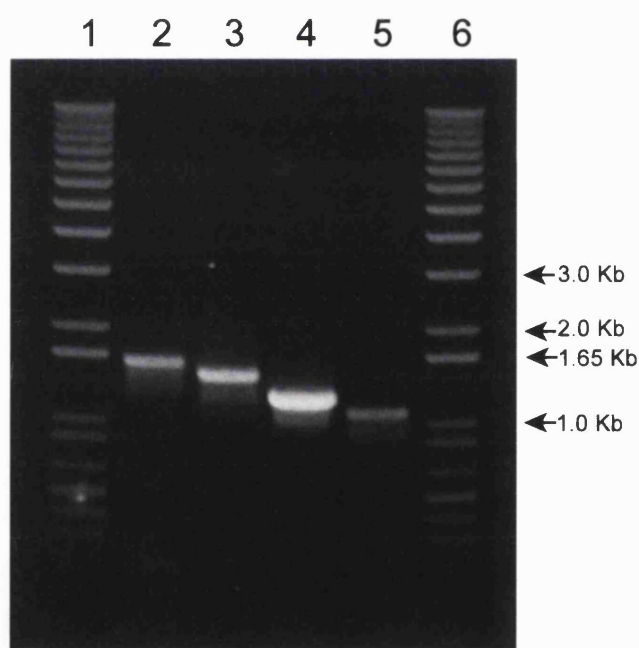
PDE assays using cAMP and cGMP as substrates, were carried out on neat as well as diluted samples of both FL4 and End6 to ascertain substrate specificity as described in section 2.2.11. A range of sample dilutions ( 1/2 - 1/100) were made using 50mM Hepes pH 7.5 buffer with protease inhibitors. PDE assays were also carried out to determine the Ca<sup>2+</sup>/CaM stimulation of FL4. 100μM Ca<sup>2+</sup> and 10 units calmodulin were used per reaction.

## 5.5 Results

### 5.5.1 Generation of Full-length and truncated PDE1A1 for cloning in pSFV1

#### 5.5.1.1 PCR products

PCR was used to generate the four PDE1A1 fragments corresponding to the Full-length, N-terminal truncated, C-terminal truncated and both N- and C-terminal truncated PDE1A1. A combination of two forward (F1, F2) and two reverse primers (R1, R2) (see Table 5.3) were used under the conditions described in Table 5.4. The expected fragments for all four combination of primers were generated successfully and are shown in Figure 5.5. Table 5.2 showed a summary of the PCR fragment sizes generated using different combination of the primers.



**Figure 5.5** Analysis of the PDE1A1 PCR products generated using the full-length dog heart PDE1A1 cDNA. Lanes 1 and 6 correspond to the 1 kb plus DNA marker with some of the marker sizes indicated on the right. Lane 2 = Full-length PDE1A1 fragment (1.6 kb), Lane 3 = C-terminal truncated fragment (1.4 kb), Lane 3 = N-terminal truncated fragment (1.2 kb) and Lane 5 = catalytic fragment (1.1 kb).



### 5.5.1.2 pSFV1-PDE1A1 constructs

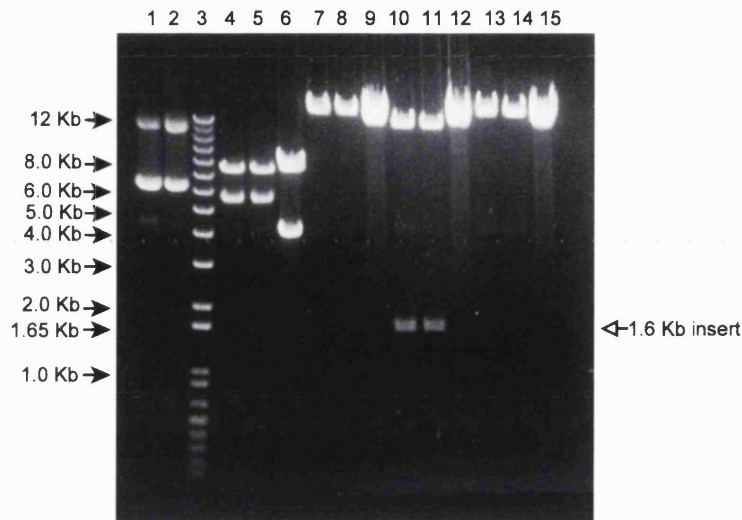
The PCR products were subjected to *Bam*HI and *Sma*I digestion and then cloned into a similarly digested pSFV1 vector. Constructs were successfully identified. These corresponded to the full-length and three truncated PDE1A1 clones and were as follows:

1. Five clones for the full-length pSFV1-PDE1A1 (FL4, 8, 28, 29 and 31)
2. One clone for the C-terminal truncated pSFV1-PDE1A1 (G2)
3. Four clones for the N-terminal truncated fragment pSFV1-PDE1A1 (End3, 4, 5 and 6)
4. Two clones for the catalytic fragment pSFV1-PDE1A1 (Cat2 and Cat9)

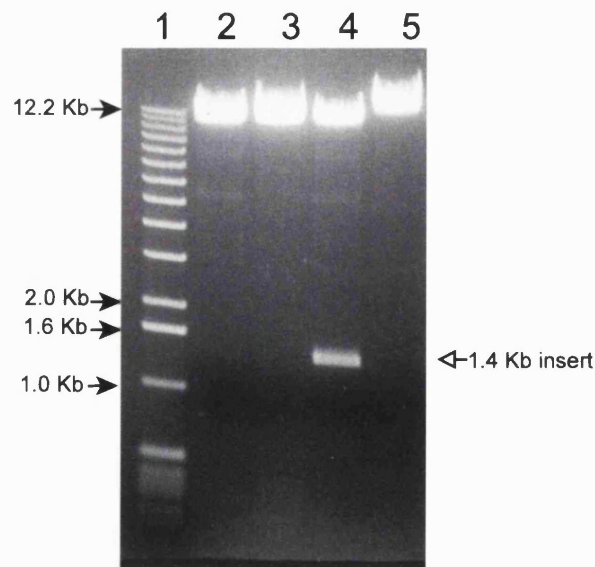
Four constructs were selected for expression studies: FL4, G2, End6 and Cat9. All except the C-terminal truncated clone (G2) were products of *Pfu* PCR; G2 was a *Taq* PCR product. Figures 5.6 and 5.7 show the results of the *Bam*HI, *Sma*I and *Eco*RV enzyme restriction analysis carried out on the Full-length and truncated constructs together with the pSFV1 vector for comparison. Table 5.7 summarises the DNA fragments expected following enzyme restriction analysis of the four constructs analysed.

**Table 5.7** pSFV1-PDE1A1 DNA fragments following digestion with *Bam*HI, *Eco*RV and *Sma*I restriction enzymes.

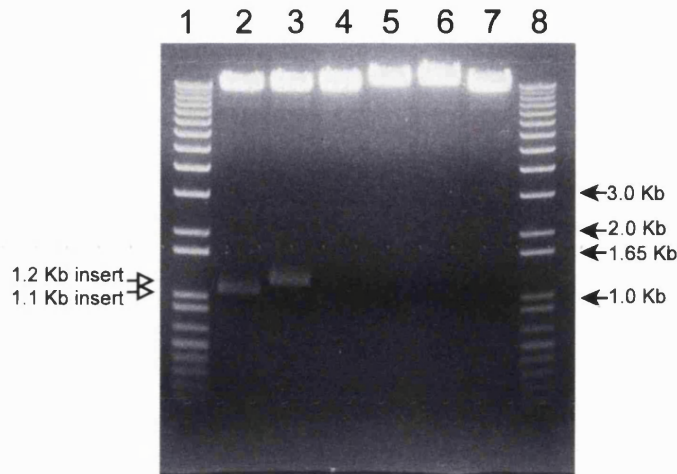
pSFV1-PDE1A1 Constructs	DNA fragment sizes for restriction enzyme(s) used (kb)		
	<i>Bam</i> HI+ <i>Sma</i> I	<i>Sma</i> I or <i>Bam</i> HI	<i>Bam</i> HI+ <i>Eco</i> RV
Full-length PDE1A (FL4)	11 + 1.6	12.6	7.1 + 5.5
C-terminal truncated (G2)	11 + 1.4	12.4	7.1 + 5.3
N-terminal truncated (End6)	11 + 1.2	12.2	7.1 + 5.1
N- and C-terminal truncated (Cat9)	11 + 1.1	12.1	7.1 + 5.0
pSFV1 only	11	11	7.1 + 3.9



**Figure 5.6** Analysis of the full-length pSFV1-PDE1A1 constructs (FL4 and FL28) following *Bam*HI, *Sma*I and *Eco*RV restriction analysis. Lane 3 represents the 1 kb Plus DNA marker with some of the marker sizes indicated on the left. Lanes 1 and 2 = Undigested FL4 and FL28 constructs showing the supercoiled DNA; Lanes 4, 5 and 6 = *Bam*HI+*Eco*RV digestion of FL4, FL28 and pSFV1 respectively; Lanes 7, 8 and 9 = *Bam*HI digestion of FL4, FL28 and pSFV1 respectively; Lanes 10, 11 and 12 = *Bam*HI+*Sma*I digestion of FL4, FL28 and pSFV1 respectively; and Lanes 13, 14 and 15 = *Sma*I digestion of FL4, FL28 and pSFV1 respectively. See Table 5.7 for the sizes of DNA fragments following enzyme digestion.



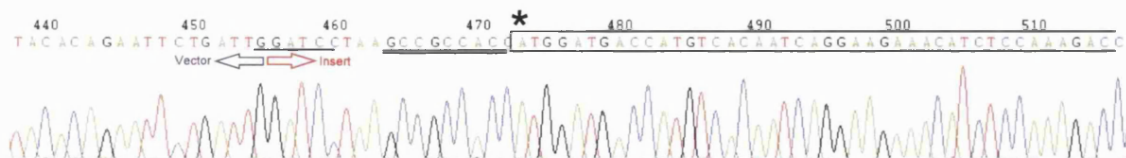
**Figure 5.7.1** Analysis of the C-terminal truncated pSFV1-PDE1A1 (G2) construct following *Bam*HI and *Sma*I restriction analysis. Lane 1 = 1 kb DNA marker; Lanes 2 and 3 = *Bam*HI+*Sma*I and *Bam*HI only digestion of pSFV1 respectively; Lane 4 = *Bam*HI+*Sma*I digestion of construct G2; Lane 5 = *Bam*HI digestion of construct G2.



**Figure 5.7.2** Analysis of the N-terminal truncated (End6) and the catalytic (Cat9) pSFV1-PDE1A1 constructs following *Bam*HI and *Sma*I digestion. Lanes 1 and 8 = 1 kb Plus DNA marker; Lane 2 = *Bam*HI+*Sma*I digestion of construct Cat9; Lane 3 = *Bam*HI+*Sma*I digestion of construct End6; Lane 4 = *Bam*HI+*Sma*I digestion of pSFV1; Lanes 5, 6 and 7 = *Bam*HI digestion of constructs Cat9, End6 and the vector pSFV1 respectively.

### 5.5.2 Automated DNA sequence analysis

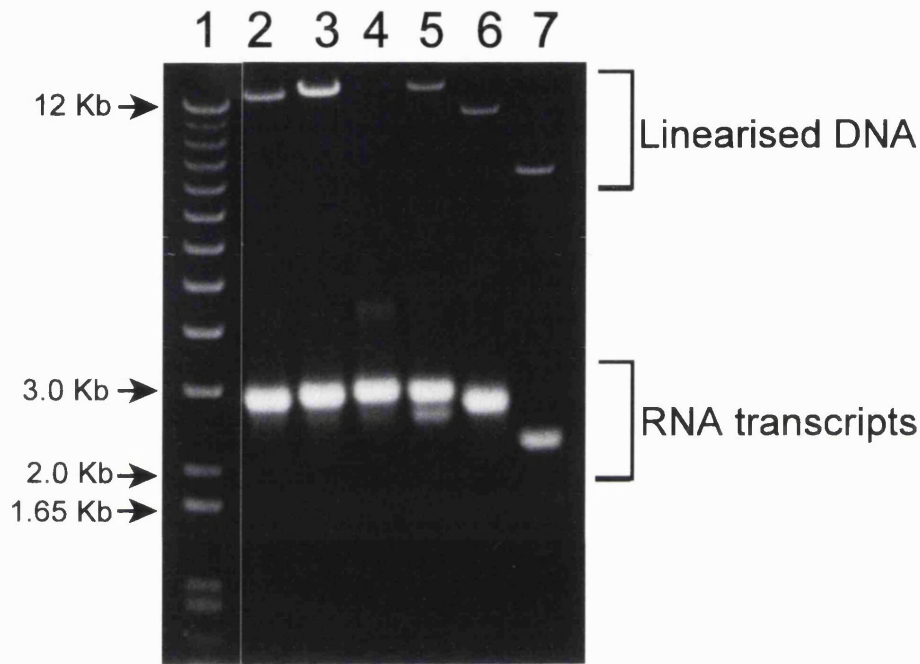
Automated DNA sequence analysis carried out on the selected constructs (FL4, G2, End6 and Cat9) confirmed the successful cloning of the full-length and truncated PDE1A1 constructs. The sequenced constructs showed no deviation from the original dog heart PDE1A cDNA produced by Clapham and Wilderspin (2001). Figure 5.8 shows a portion of the sequence for the Full-length construct (FL4) sequenced using the reverse PDE1 primer, L11.



**Figure 5.8** DNA sequence analysis of FL4. Sequence is shown for the pSFV1 polylinker site with the full-length PDE1A1 cloned into the *Bam*HI site (shown underlined) and the *Sma*I site (not shown on sequence). The Kozak sequence is shown double underlined and the start codon marking the ORF (shown as an open box) is indicated by the asterisk.

### 5.5.3 *In vitro* RNA synthesis of the four recombinant pSFV1-PDE1A1 constructs

The RNA transcripts generated for the constructs (FL4, G2, End6 and Cat9) together with the RNA transcripts for the empty vector pSFV1 and pSFV-H2 are shown in Figure 5.9. These results indicated that *in vitro* RNA synthesis was successfully carried out and that there was very little DNA template present in these samples relative to the RNA.



**Figure 5.9** Analysis of the RNA transcripts for all four PDE1A1 constructs. Lane 1 = 1 kb Plus DNA ladder; Lane 2 = Cat9 RNA transcript; Lane 3 = End6 RNA transcript; Lane 4 = FL4 RNA transcript; Lane 5 = G2 RNA transcript; Lane 6 = pSFV1 RNA transcript; Lane 7 = pSFV-H2 RNA transcript.

### 5.5.4 BHK-21 cells transfected by electroporation directly with pSFV3*lacZ* RNA or pSFV1-PDE1A1 construct RNA

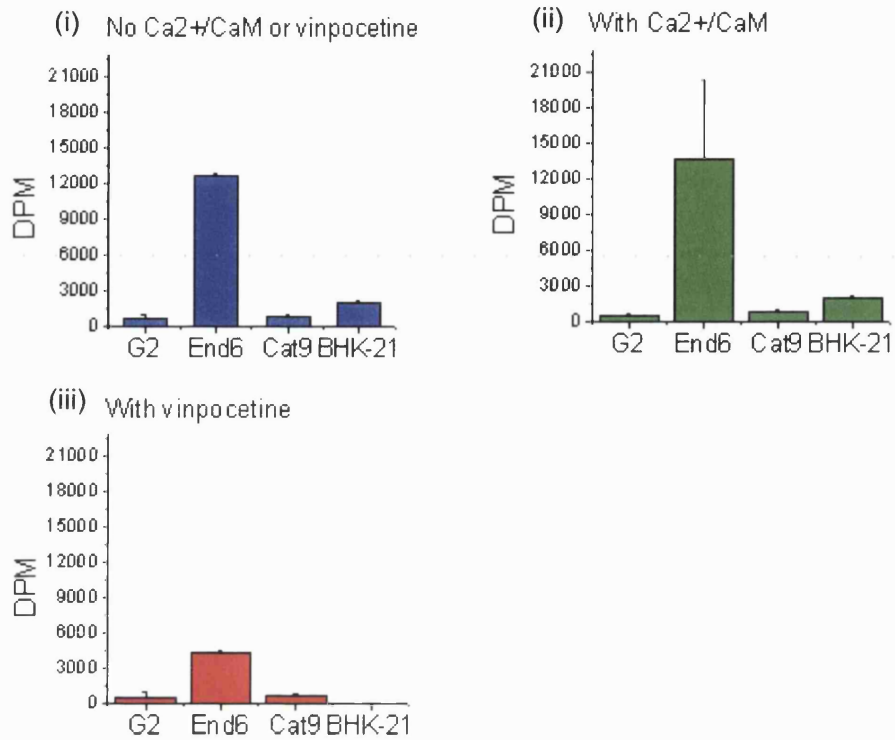
The PDE assay results presented in this chapter represent initial screening assays carried out to test samples and controls for the presence of any PDE activity as well identifying the activity of the recombinant PDE1 using  $\text{Ca}^{2+}/\text{CaM}$  and vinpocetine. Detailed kinetic analysis was carried out on these samples and forms the subject of the next chapter (Chapter 6).

#### **5.5.4.1 *In-situ* $\beta$ -galactosidase staining of BHK-21 cells transfected with pSFV3*lacZ* RNA**

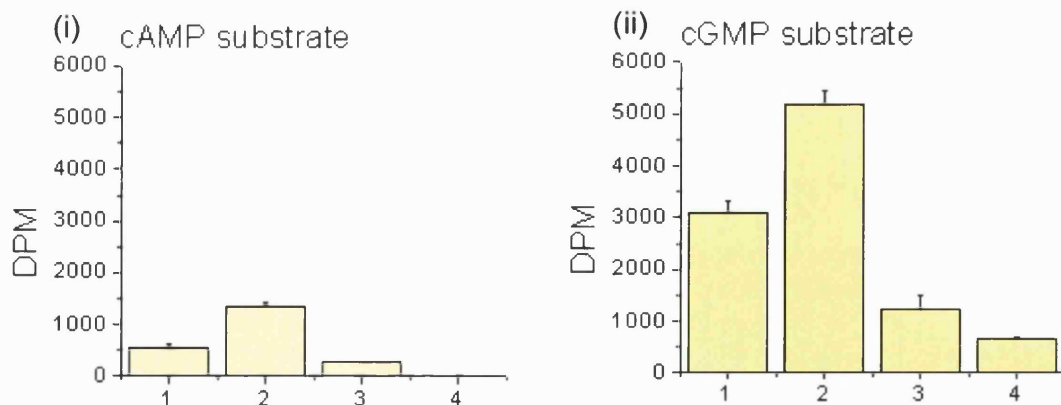
Cells transfected with pSFV3*lacZ* RNA were stained using X-gal as described in section 5.4.7.2. All the cells were found to be stained blue (i.e. 100% transfection efficiency achieved) indicating that the electroporation parameters used for transfection were optimal. This was used as a direct indication for transfection efficiency for the subsequent transfection of cells with pSFV1-PDE1A1 construct RNA.

#### **5.5.4.2 PDE assay results for cells harvested following direct transfection with pSFV1-PDE1A1 RNA**

PDE activity assays using cAMP as the substrate were carried out on cleared total cell lysate samples (supernatants) for all four PDE1A1 constructs (FL4, G2, End6 and Cat9). These results showed that only the cells transfected with RNA encoding the full-length enzyme (FL4) and the N-terminal truncated enzyme (End6) had significant PDE activity above background PDE activity. Figure 5.10 shows the PDE activity results for the constructs G2, End6, Cat9 as well as BHK-21 cells, harvested as a control for background PDE activity, in the presence and absence of calcium ions (100 $\mu$ M) and calmodulin (10 units per reaction) and vinpocetine (50 $\mu$ M). These assays were carried out on neat, undiluted samples. However, the full-length construct, FL4, was diluted a hundred fold so that the activity counts were within the range of the assay limits. Diluted FL4 samples were analysed using both cAMP and cGMP in the presence and absence of Ca<sup>2+</sup>/CaM and vinpocetine as before. These results are shown in Figure 5.11. The PDE activity results were adjusted for the blank (DPM - Blank DPM; blank-adjusted) and where these results are represented graphically, they have been blank-adjusted.

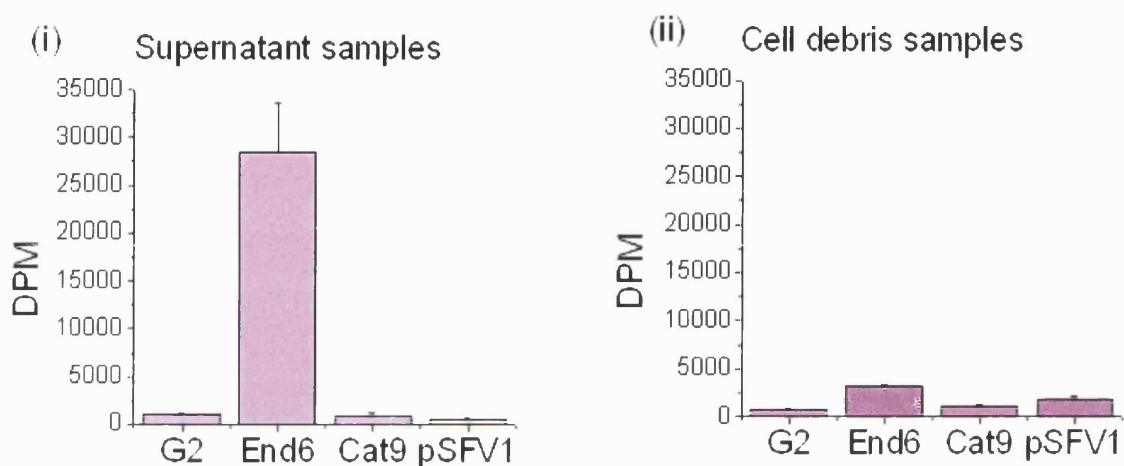


**Figure 5.10** PDE activity analysis of truncated PDE1A1 constructs (G2, End6 and Cat9) as well as BHK-21 cells for background PDE activity. These assays were carried out on supernatant samples with cAMP as the substrate without the presence of Ca<sup>2+</sup>/CaM or vinpocetine (i); in the presence of Ca<sup>2+</sup>/CaM (ii); and, in the presence of vinpocetine (iii). Results are means  $\pm$  S.E. of two determinations in a single experiment.



**Figure 5.11** PDE activity analysis of the full-length construct (FL4) diluted a hundred fold. cAMP (i) and cGMP (ii) were used as substrates and the assays carried out in the presence and absence of Ca<sup>2+</sup>/CaM and vinpocetine on supernatant samples of FL4. FL4 cAMP-hydrolysing activity was completely inhibited in the presence of 50 $\mu$ M vinpocetine. 1=Without Ca<sup>2+</sup>/CaM or vinpocetine; 2=With Ca<sup>2+</sup>/CaM; 3=Ca<sup>2+</sup>/CaM and vinpocetine; 4=With vinpocetine. Results are means  $\pm$  S.E. of two determinations in a single experiment.

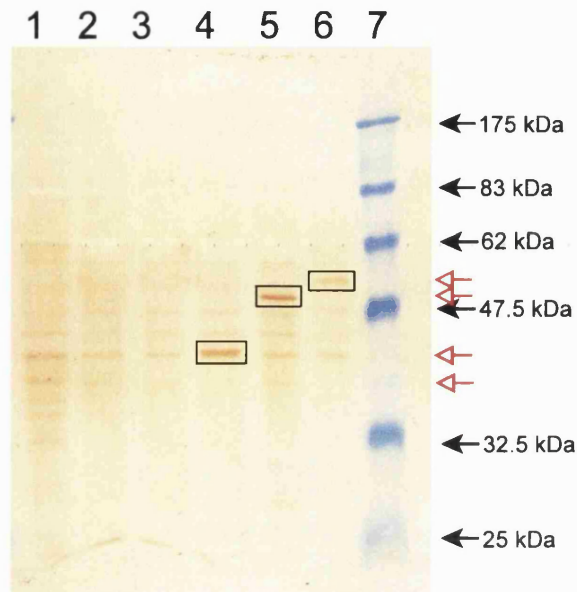
The cell debris samples for G2, End6 and Cat9 constructs, resuspended in buffer, were also analysed for cAMP-hydrolysing PDE activity. None of these samples showed any significant PDE activity (Figure 5.12). BHK-21 cells transfected with the empty vector, pSFV1, were also analysed for background PDE activity. Figure 5.12 shows the results for both the cleared supernatant and the remaining cell debris samples analysed for PDE activity.



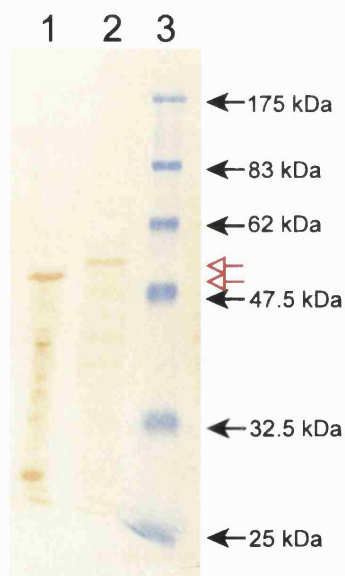
**Figure 5.12** PDE activity analysis of the supernatant and cell debris samples for G2, End6, Cat9 and pSFV1. Assays were carried out on the supernatant samples (i) and the cell debris samples (ii) using cAMP as the substrate. Results are means  $\pm$  S.E. of two determinations in a single experiment.

#### 5.5.4.3 SDS PAGE and Western blot analysis of cells harvested following direct transfection with pSFV1-PDE1A1 RNA

Coomassie stained SDS PAGE gels for all four constructs did not reveal any distinct recombinant protein band against the background protein expression seen with just BHK-21 cells or cells transfected with the vector pSFV1. However, Western blot analysis using CaM-PDE antibody did give a signal for all four constructs (Figure 5.13). Figure 5.14 and 5.15 show the Western blot results for samples concentrated ten fold.

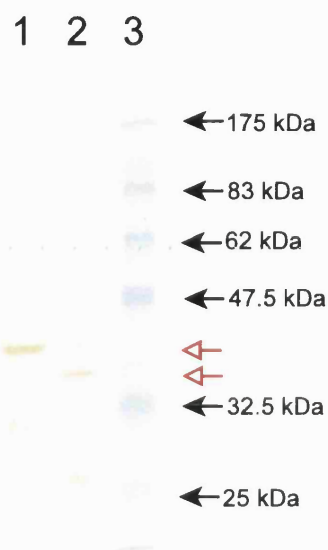


**Figure 5.13** Western blot analysis of full-length and truncated PDE1A1 constructs together with the pSFV1 vector and no-vector-BHK-21 cells. Lane 1 = BHK-21 cell control; Lane 2 = pSFV1 control; Lane 3 = Cat9 construct (40 kDa protein; signal too weak to be seen); Lane 4 = End6 construct (44 kDa protein); Lane 5 = G2 construct (53 kDa protein); Lane 6 = FL4 construct (57 kDa protein; seen as a weak signal); Lane 7 = Pre-stained Protein Marker with sizes indicated on the right. The red arrows mark the position of the recombinant proteins while the boxes on the blot indicate recombinant protein signals.



**Figure 5.14** Western blot analysis of FL4 and G2 enzymes concentrated ten fold. Lane 1 = G2 construct (53 kDa protein); Lane 2 = FL4 construct (57 kDa); Lane 3 = Pre-stained Protein Marker with sizes indicated on the right. The red arrows mark the position of the two recombinant proteins.





**Figure 5.15** Western blot analysis of End6 and Cat9 enzymes concentrated ten fold. Lane 1 = End6 (44 kDa protein); Lane 2 = Cat9 (40 kDa protein); Lane 3 = Pre-stained Protein Marker with sizes indicated on the right. The red arrows mark the position of the two recombinant proteins.

### 5.5.5 Virus titer determination and optimisation of BHK-21 cell infection with recombinant FL4 virus

#### 5.5.5.1 Transfection efficiency and virus titer determination

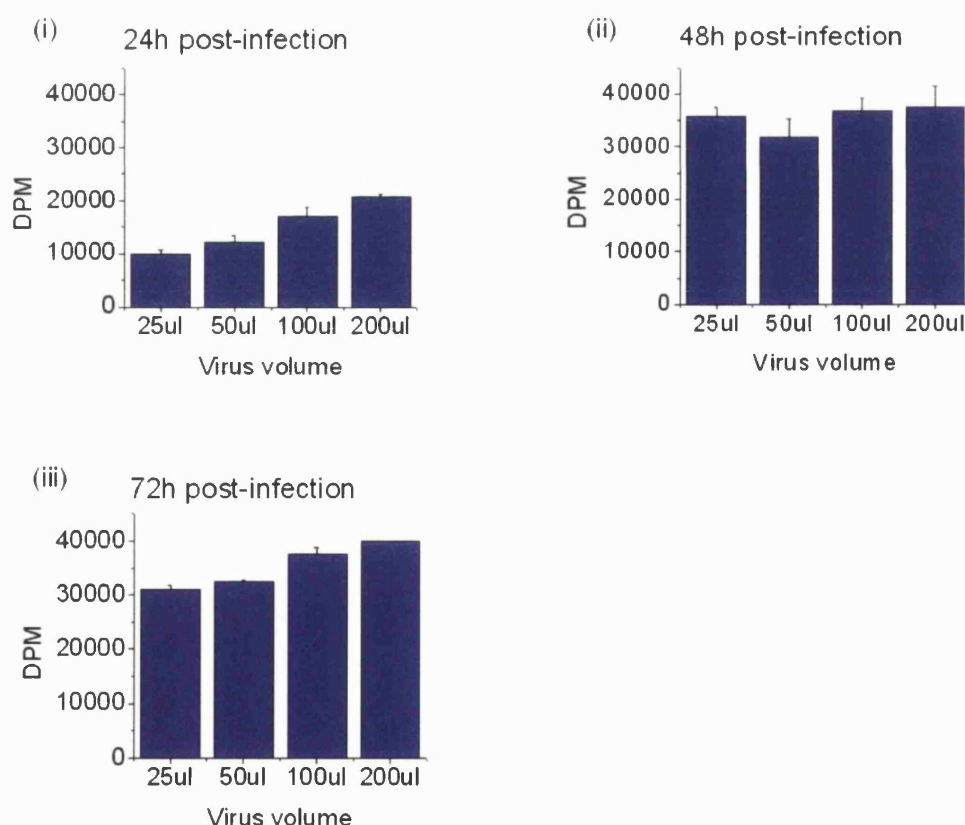
BHK-21 cells were infected with 25 $\mu$ l, 50 $\mu$ l and 100 $\mu$ l of pSFV3*lacZ* virus as described in section 5.4.11 and stained for  $\beta$ -galactosidase using X-gal (5.4.7.2). Transfection efficiency and the virus titer were calculated as described in section 5.4.11.3.2 and are shown in Table 5.8. This was used as a direct indication of the titer for the recombinant FL4 virus which was produced under the same conditions.

**Table 5.8** Transfection efficiency and virus titer for pSFV3*lacZ* virus particles.

Virus volume ( $\mu$ l)	% Transfection efficiency	Virus Titer (Infectious units/ml)
25	31	2.4 x 10 <sup>5</sup>
50	64	2.5 x 10 <sup>5</sup>
100	91	1.8 x 10 <sup>5</sup>

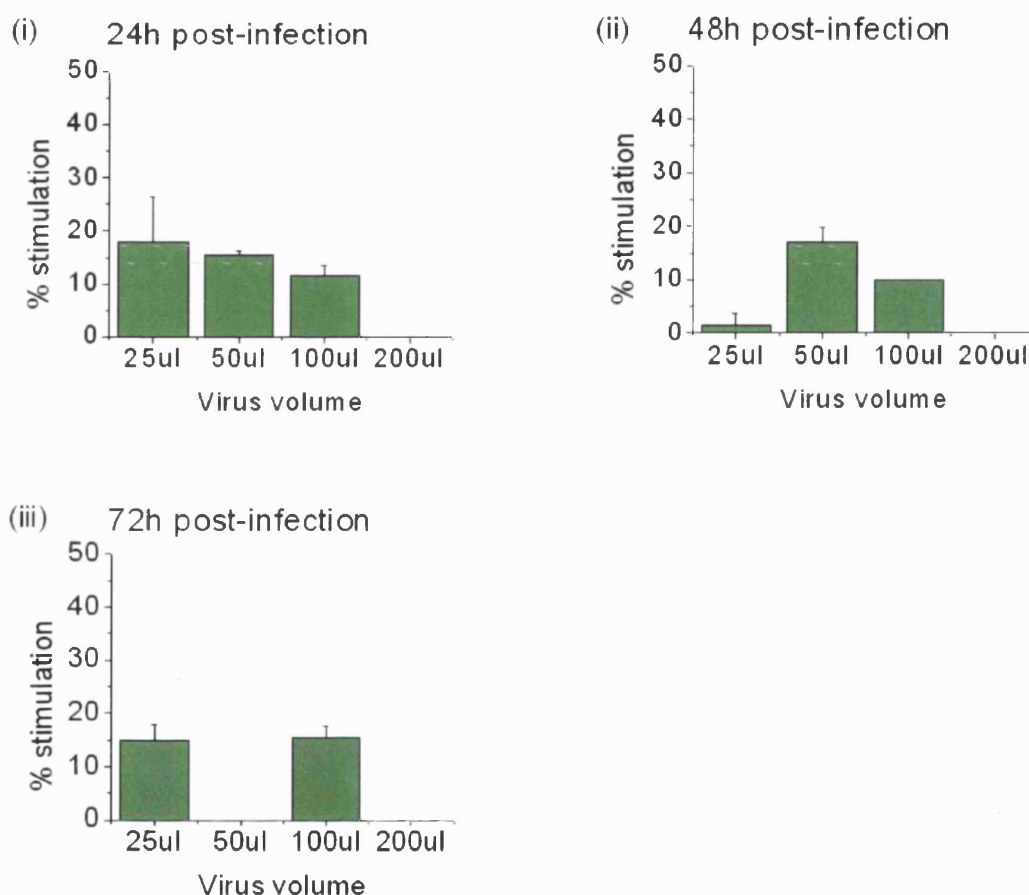
### 5.5.5.2 Optimisation of the conditions for the infection of BHK-21 cells with pSFV1-PDE1A1 virus particles

The parameters investigated for assessing recombinant protein expression were optimum infection ratio for virus to cells and the length of time the infected cells were incubated before harvesting the cells for the recombinant enzyme. PDE activity assays were used to analyse cleared total cell lysates (supernatants) from harvested cells and these results used as an indication of the optimal conditions for recombinant protein expression. This approach guided scale-up from 25cm<sup>2</sup> flasks to 75cm<sup>2</sup> flasks for cell growth. Figure 5.16 shows the results of the optimisation experiments for PDE activity using recombinant FL4 virus. Figure 5.16.1 shows the results for basal PDE activity while 5.16.2 shows the Ca<sup>2+</sup>/CaM-stimulated activity. Figure 5.17 shows the results for the total protein in the supernatant samples, measured using the Bradford assay.



**Figure 5.16.1** Optimisation of the infection of BHK-21 cells with recombinant FL4 virus. Basal PDE activity is shown as DPM plotted against the volume (μl) of recombinant virus added with cells analysed at 24h (i), 48h (ii) and 72h (iii) post-infection. Results are means ± S.E. of two determinations in a single experiment.

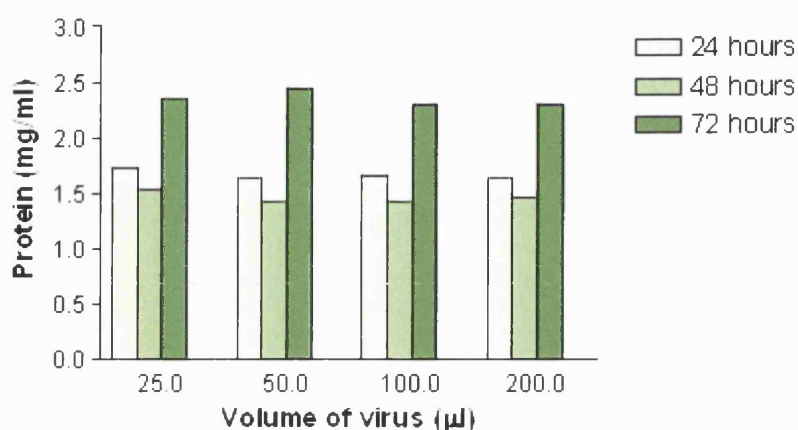
PDE activity analysis of the supernatant samples revealed optimum PDE activity at 48 hours post-infection with 25 $\mu$ l of recombinant virus. Using more virus did not give a significant increase in PDE activity. PDE activity assays on cells harvested at 72 hours again did not show a significantly higher activity compared to cells harvested at 48 hours. In fact, infected cells left for 72 hours showed changes in cell morphology indicating cells may be dying.



**Figure 5.16.2** PDE activity analysis for the optimisation of the infection of BHK-21 cells with recombinant FL4 virus carried out in the presence of  $Ca^{2+}$ /CaM. The results are represented as percentage stimulation above basal PDE activity for cells harvested at 24h (i), 48h (ii) and 72h (iii) post-infection. Results are means  $\pm$  S.E. of two determinations from 3 - 4 separate experiments.

PDE activity assays carried out in the presence of  $Ca^{2+}$ /CaM on cleared total cell lysate samples of FL4 (Figure 5.16.2) did show stimulation of up to 25% above basal PDE activity. However, this stimulation was not consistent between the experiments which were carried out as four separate experiments with samples stored at 4 $^{\circ}$ C, and not frozen until

the completion of all of the experiments. It was possible that proteolysis of the full-length enzyme was occurring, releasing the N-terminal calmodulin-binding domain (s), such that the enzyme was in a fully-active state. This was an early indication that the full-length enzyme may be undergoing cleavage. Another possibility was that the N-terminal portion was folded into a state that could not be reversed by the addition of  $\text{Ca}^{2+}/\text{CaM}$ .

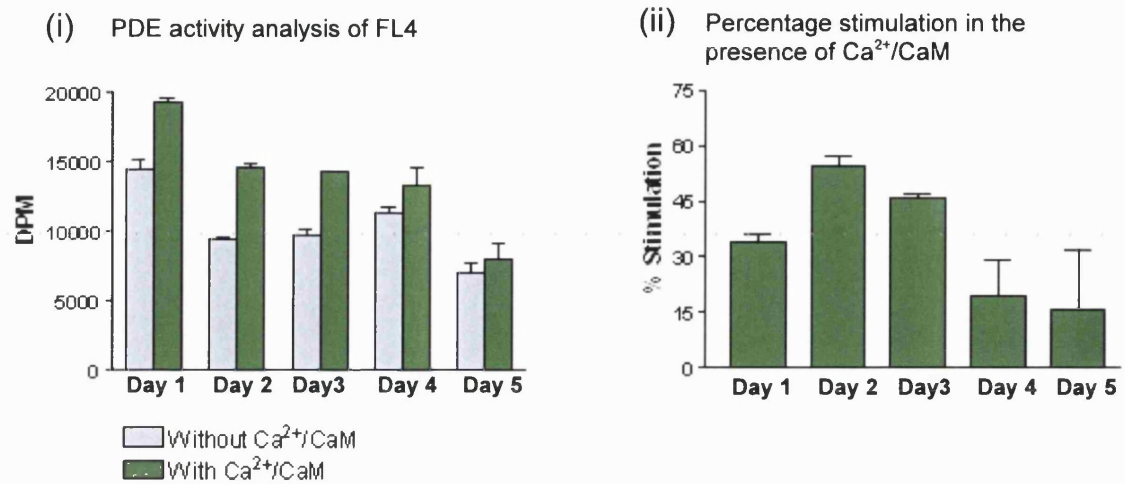


**Figure 5.17** Total protein concentration for BHK-21 cells infected with the recombinant FL4 virus. Protein concentration was measured for cleared total cell lysate samples for infected cells harvested at 24, 48 and 72 hours post-infection.

## 5.5.6 Stability studies on FL4

### 5.5.6.1 Storage of FL4 at 4°C

Figure 5.18 shows the PDE activity results for FL4 supernatant sample (from the direct transfection of BHK-21 cells with recombinant RNA) stored at 4°C up to five days. Samples were analysed during this period to monitor stability of the basal as well as  $\text{Ca}^{2+}/\text{CaM}$  stimulated PDE activity as samples were routinely stored at 4°C during the kinetic analysis (Chapter 6).

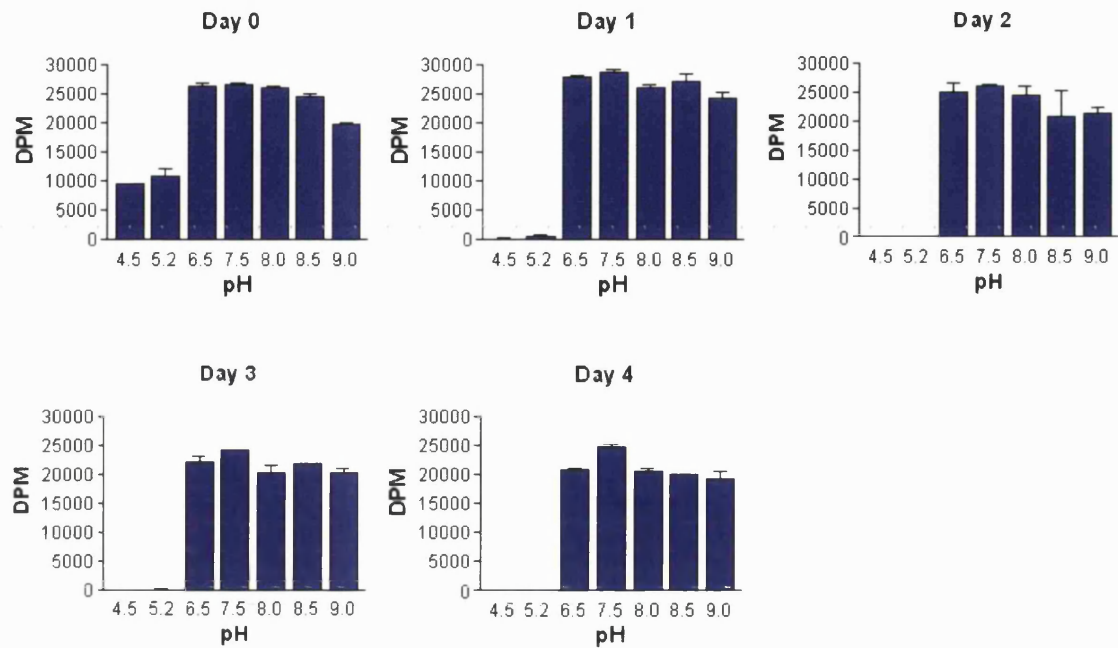


**Figure 5.18** PDE activity analysis of FL4 stored at 4°C for up to five days. Assays were carried out using cAMP as the substrate in the absence and presence of Ca<sup>2+</sup>/CaM (i). Percentage stimulation is shown in (ii). Results are means ± S.E. of two determinations in a single experiment.

Storage of cleared total cell lysate samples at 4°C revealed that there was some loss of basal PDE activity following storage of the enzyme for up to five days. The Ca<sup>2+</sup>/CaM stimulation was also reduced during this period. As such, samples were stored for no longer than 4 - 5 days at 4°C during the kinetic analysis.

### 5.5.6.2 Effect of pH on FL4 PDE activity

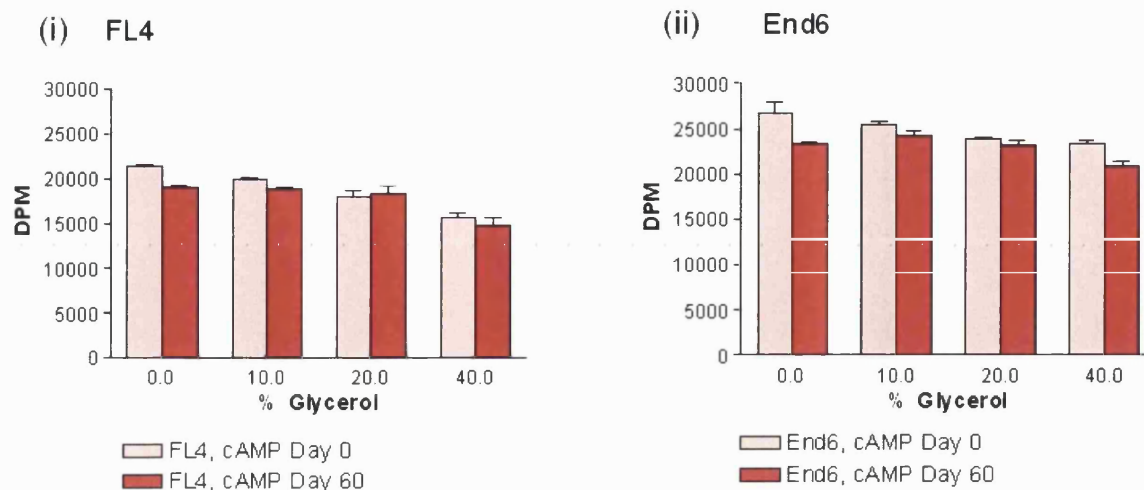
FL4 supernatant sample was diluted in a range of pH buffers (pH 4.5 - 9.0) then analysed for PDE activity the same day and then for up to four days of storage at 4°C (Figure 5.19). These studies revealed that the recombinant PDE activity was significantly reduced at pH of pH 4.5 and pH 5.2 shortly after being diluted in these buffers and it was undetectable after storage for one day at these pH. PDE activity was retained above pH 6.5. Buffer pH 7.5 was found to be marginally better at retaining the recombinant PDE activity so this pH was used throughout for storage and dilution of recombinant samples.



**Figure 5.19** PDE activity analysis of FL4 stored in different pH buffers at 4°C for up to four days. Assays were carried out using cAMP as the substrate at day 0, day 1, day 2, day 3 and day 4 following storage at 4°C in the appropriate pH buffer. Results are means  $\pm$  S.E. of two determinations in a single experiment.

### 5.5.6.3 The effect of glycerol on basal FL4 PDE activity

FL4 and End6 supernatant samples were diluted in lysis buffer 3 containing glycerol over the range 0% to 40%. These samples were analysed for PDE activity to determine the effect, if any, the presence of glycerol would have on this activity. The analysis was carried out the same day as well as after storage at -70°C (designated Day 60) using cAMP as the substrate (Figure 5.20). This study showed that the presence of increasing amounts of glycerol did not have a significant effect on the PDE activity for FL4 or End6. Also to note was that there was not a significant reduction in PDE activity when the samples were thawed for analysis at day 60, regardless of the presence or absence of glycerol. Therefore, PDE activity was stable following one freeze-thaw cycle in the presence or absence of glycerol.



**Figure 5.20** The effect of glycerol on FL4 and End6 PDE activity. PDE assays were carried out using cAMP as the substrate at Day 0 (same day samples diluted in lysis buffer 3 containing 0% - 40% glycerol) then after storage at  $-70^{\circ}\text{C}$  (Day 60). Results are means  $\pm$  S.E. of two determinations in a single experiment.

## 5.5.7 Determination of the native state of the recombinant enzymes End6 and FL4

### 5.5.7.1 DSS cross-linking studies on End6

Figure 5.21 shows the Western blot results of the DSS cross-linking reaction carried out on the N-terminal truncated PDE1A1 enzyme (End6). The figure shows the results spread across two separate blots. However, these blots were processed in parallel starting from the SDS PAGE analysis followed by Western blot transfer to the development of the blots. The Western blot revealed that the truncated enzyme, End6, appeared to have formed tetramers as indicated by the position of the signal on the blot. End6 shows a signal at the position of 44 kDa in the absence of the cross-linker, equivalent to the monomer unit. However, in the presence of increasing concentrations of the cross-linker, this signal begins to disappear but a signal was seen at an approximate position of 175 kDa in these samples. End6 monomers assembling as tetrameric units would give a signal at 176 kDa position.



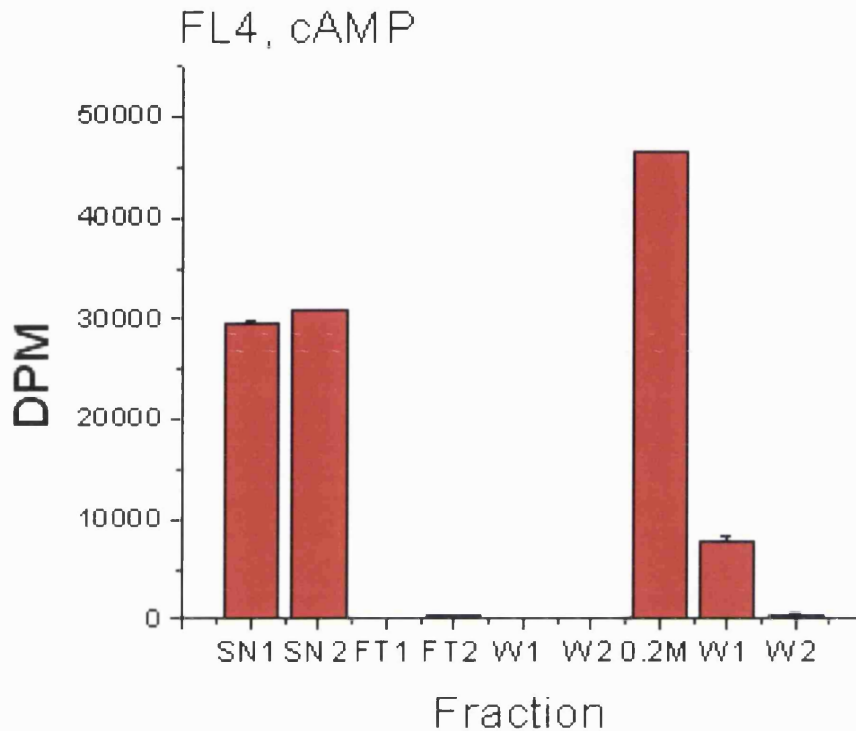
**Figure 5.21** Western blot analysis of the DSS cross-linking of End6 (N-terminal truncated) enzyme. Lanes 1 and 16 = Pre-stained protein marker with sizes indicated on the right; Lanes 2, 3 and 4 = 0mM DSS, sampled at time points of 30, 60 and 120 minutes respectively. The DSS-End6 mixtures were all sampled at 30, 60 and 120 minutes at each of the DSS concentrations. Lanes 5, 6 and 7 = 0.25mM DSS; Lanes 8, 9 and 10 = 0.5mM DSS; Lanes 11, 12 and 13 = 1.0mM DSS; Lane 14 = unprocessed, neat End6 supernatant sample; Lane 15 = unprocessed, neat FL4 supernatant sample (FL4 protein very faint on the blot); Lanes 17, 18 and 19 = 2.0mM DSS; Lanes 20, 21 and 22 = 5.0mM DSS. The open red arrow indicates the position of the monomer End6 protein (44 kDa) while the solid red arrow indicates the position of the cross-linked End6 samples ( $\geq 175$  kDa).

#### 5.5.7.2 Gel filtration chromatography on FL4

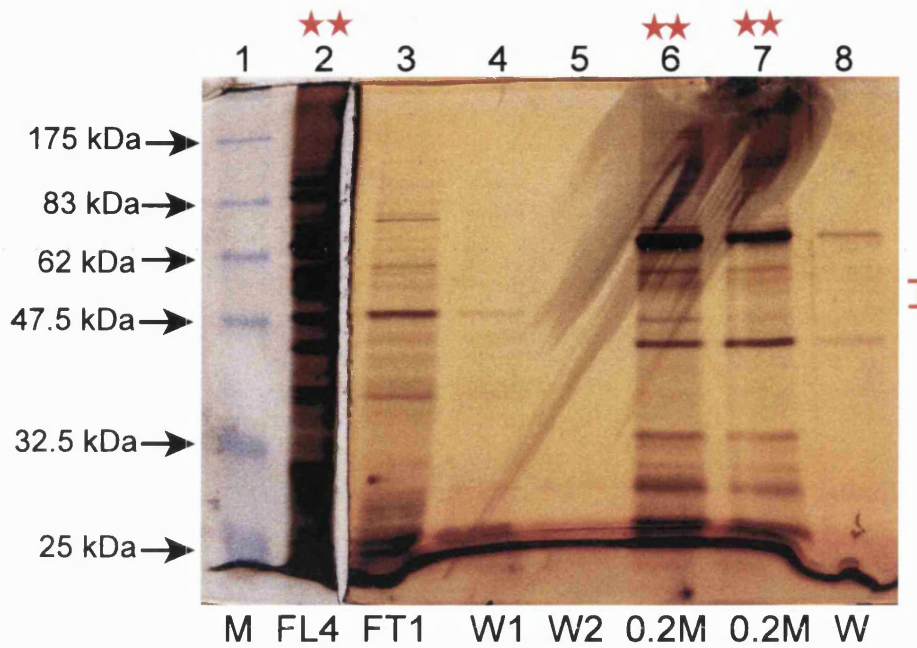
Gel filtration chromatography was carried out on FL4 to determine the native state of the full-length enzyme. 20ml of cleared total cell lysate FL4 (supernatant) from a large-scale infection (ten 75cm<sup>2</sup> flasks) was first concentrated, and semi-purified, using the Vivaspin Q ion exchange units as described in section 5.4.17.2. Peak PDE activity was determined as being in the 0.2M NaCl fraction (see Figure 5.25.1). Once all protein had been allowed to bind to the ion exchange units, protein was eluted with two 1ml steps of 0.2M NaCl elution buffer. Figure 5.22.1 shows the PDE activity results of this purification. These samples were also analysed using 12% SDS PAGE and these results are shown in Figure 5.22.2. Fractions containing peak PDE activity are indicated with red stars on the gel. The two 0.2M fractions were pooled and loaded onto the gel filtration column as described in section 5.4.16.2.3. Figure 5.23.1 shows the absorbance (280nm) profile for the fractions collected for the gel filtration standards while Figure 5.23.2 shows the PDE activity results



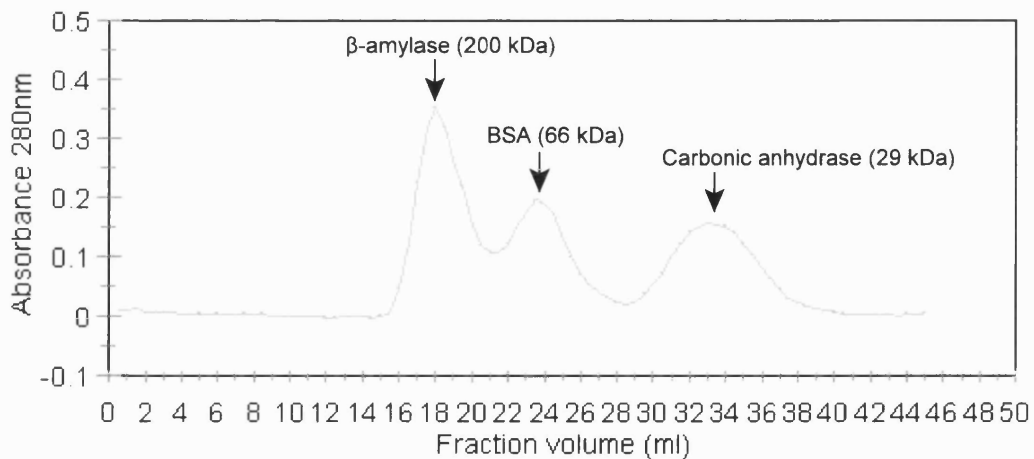
for the FL4 fractions collected following gel filtration chromatography of FL4. This graph (5.23.2) also indicates the position of the standards  $\beta$ -amylase and bovine serum albumin (BSA) together with the void volume.



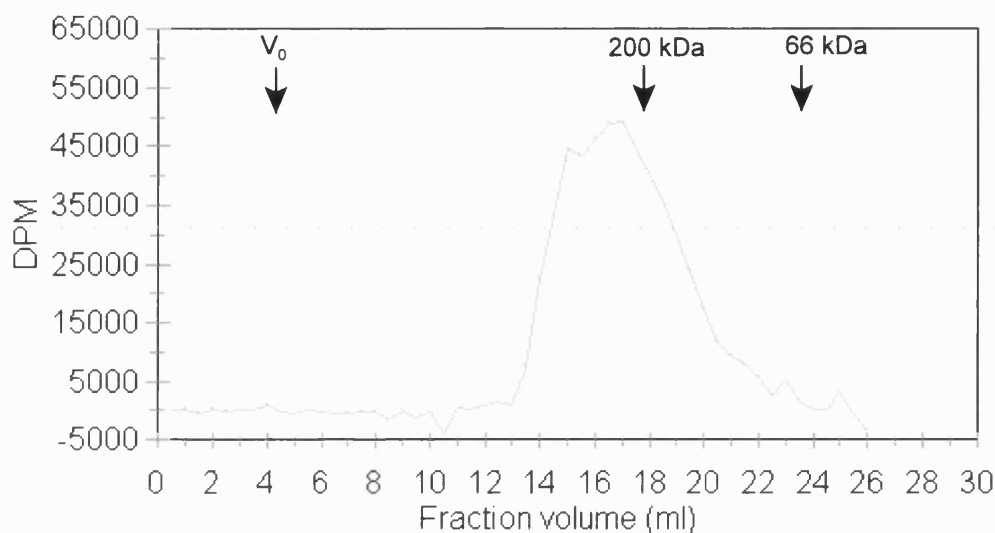
**Figure 5.22.1** PDE activity analysis of FL4 purified using Vivaspin Q ion exchange chromatography. Activity assays were carried out using cAMP as the substrate and are shown as DPM for the fractions analysed. The two 0.2M fractions from the Vivaspin Q units were pooled and activity in the above graph represents results for the pooled fractions. Results are means  $\pm$  S.E. of two determinations in a single experiment.



**Figure 5.22.2** SDS PAGE analysis of FL4 purified following Vivaspin Q ion exchange chromatography. Lane 1 = pre-stained protein marker; Lane 2 = FL4 supernatant sample; Lane 3 = flow-through fraction (FT; unbound protein); Lanes 4 and 5 = wash fractions (W1 and W2); Lanes 6 and 7 = 0.2M NaCl Vivaspin Q fractions, pooled and used for analysis on gel filtration chromatography; Lane 8 = end-wash fraction (W). The open red box on the right of the gel marks the position of the FL4 protein (not visualised on the gel).



**Figure 5.23.1** Absorbance ( $A_{280}$ ) profile for the gel filtration standards. The absorbance of the 0.5ml fractions collected was measured at 280nm and is shown plotted against the fraction volume.

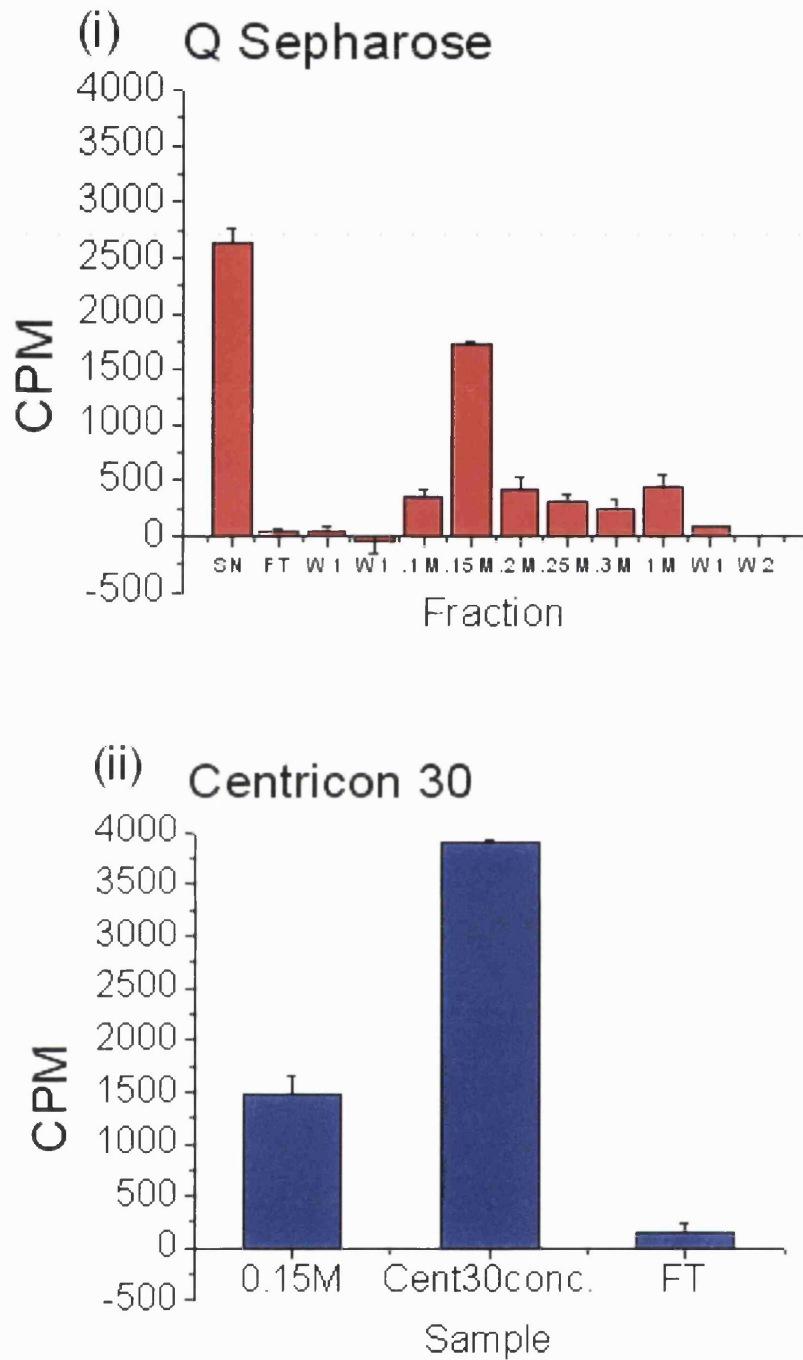


**Figure 5.23.2** PDE activity (DPM) profile for FL4 sample analysed by gel filtration chromatography. The cGMP-hydrolysing activity of the 0.5ml fractions collected was measured and is shown plotted against the fraction volume. The position of the 200 kDa and 66 kDa standards is also indicated on this graph together with the void volume ( $V_0$ ).

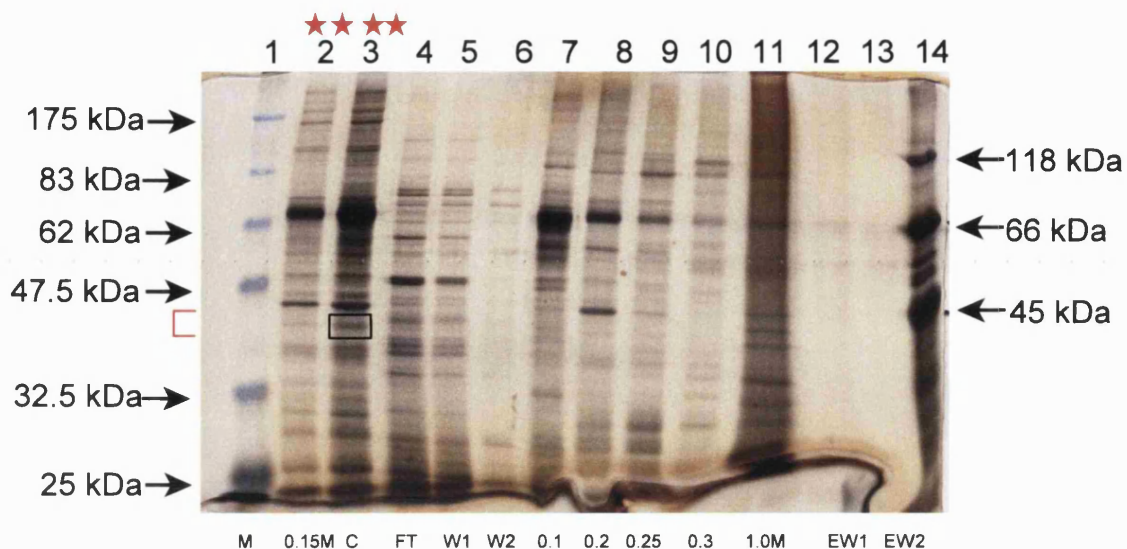
## 5.5.8 PDE1A1 purification

### 5.5.8.1 Q Sepharose ion exchange chromatography on End6

Figure 5.24.1 shows the PDE activity measured in the fractions collected from the Q Sepharose ion exchange chromatography on ~4ml of End6 cleared total cell lysate samples (supernatants). The step elution of the recombinant protein was carried out using purification buffer 2 (Table 2.3) containing 0.1M - 1.0M NaCl. Peak PDE activity was seen in eluate 0.15M NaCl and this fraction was concentrated seven-fold using Centricon30 concentration units as described in section 5.4.14.2. All the fractions (Figure 5.24.1 (i)), including the concentrated 0.15m eluate (Figure 5.24.1 (ii)), were analysed for PDE activity as well as by SDS PAGE analysis (Figure 5.24.2). SDS PAGE gels were silver-stained to visualise the proteins which showed the presence of End6 protein in the concentrated 0.15M eluate fraction (Figure 5.24.2; Lane 3, shown boxed on the gel).



**Figure 5.24.1** PDE activity analysis of End6 purified using Q Sepharose ion exchange chromatography. The results are represented as blank-adjusted counts per minute (CPM) plotted against the fraction using cAMP as the substrate for the fractions (i) as well as the 0.15M fraction concentrated 7-fold (ii). Abbreviations used: SN = supernatant sample; FT = flow-through fraction (unbound protein); W = wash fraction; EW = end wash fractions. Results are means  $\pm$  S.E. of two determinations in a single experiment.

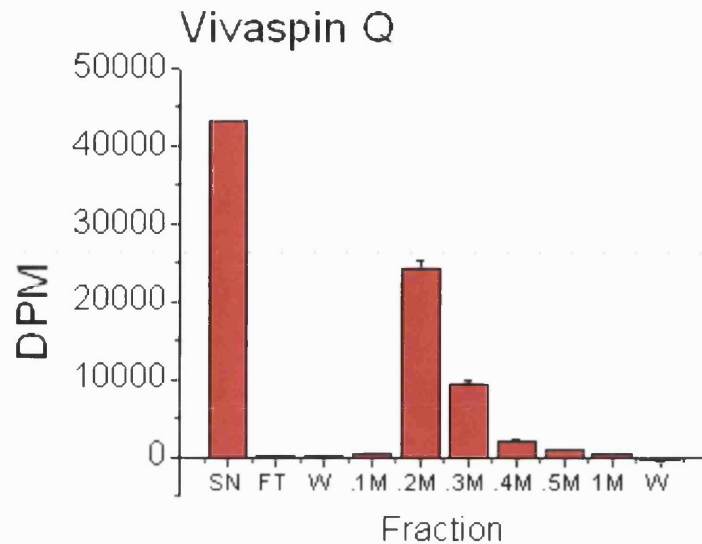


**Figure 5.24.2** SDS PAGE analysis of End6 purified using Q Sepharose ion exchange chromatography. Lane 1 = Pre-stained protein marker (sizes indicated on the left of the gel); Lane 2 = 0.15M eluate; Lane 3 = 0.15M eluate concentrated seven fold (location of End6 protein, 44 kDa, indicated by the closed box); Lane 4 = flow through sample (unbound protein); Lanes 5 and 6 = washes 1 and 2, respectively; Lane 7 = 0.1M NaCl eluate; Lane 8 = 0.2M eluate; Lane 9 = 0.25M eluate; Lane 10 = 0.3M eluate; Lane 11 = 1.0M eluate; Lanes 12 and 13 = end washes 1 and 2, respectively; Lane 14 = in-house protein marker mix ( $\beta$ -gal, BSA and ovalbumin proteins; sizes indicated on the right). The open red box marks the region of the expected End6 protein band. The stars (Lanes 2 and 3) represent the fractions showing peak PDE activity.

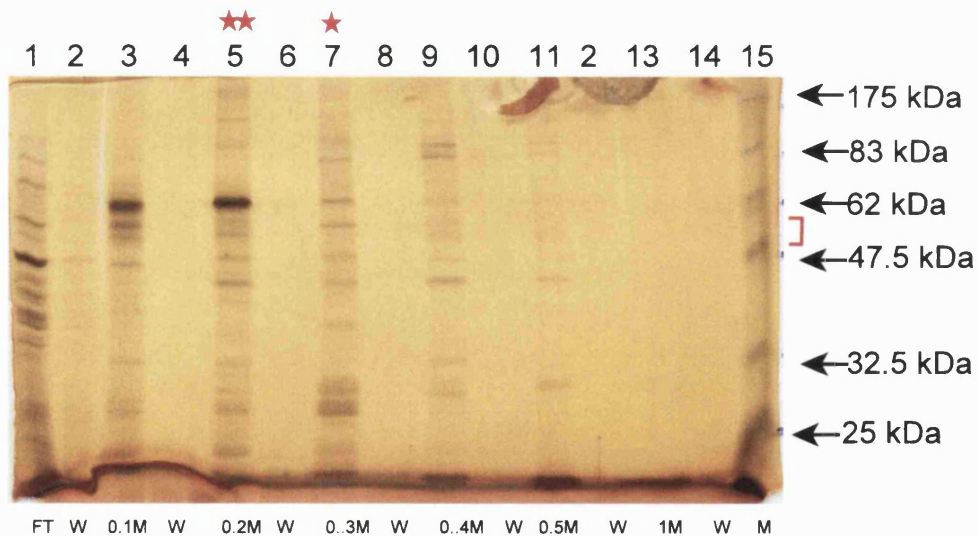
### 5.5.8.2 Vivaspin-Q ion exchange chromatography on FL4

Vivaspin Q ion exchange units were used to ascertain the elution profile of the recombinant FL4 enzyme as described in section 5.4.17.2. Ion exchange chromatography of FL4 was also used to concentrate the cleared total cell lysates (supernatants) from the large scale infection procedure from a total volume of 20ml down to 2ml as described in section 5.4.16.2.3. This sample was then used for further analysis on gel filtration chromatography for determination of the native state of FL4 as discussed in section 5.5.7.2.

Figure 5.25.1 shows the PDE activity profile for the FL4 fractions collected from the Vivaspin Q ion exchange units. Peak activity was seen in the 0.2M NaCl eluate. The fractions were also analysed on 12% SDS PAGE and gels were silver stained (Figure 5.25.2).



**Figure 5.25.1** PDE activity profile for FL4 fractions obtained from the Vivaspin Q ion exchange units. Results are shown as DPM plotted against fractions (wash, W; 0.1M - 1.0M NaCl eluates; end wash, EW) together with results for the FL4 supernatant (FL4 SN) applied to the Vivaspin Q unit. Assays were carried out using cAMP as the substrate. Results are means  $\pm$  S.E. of two determinations in a single experiment.



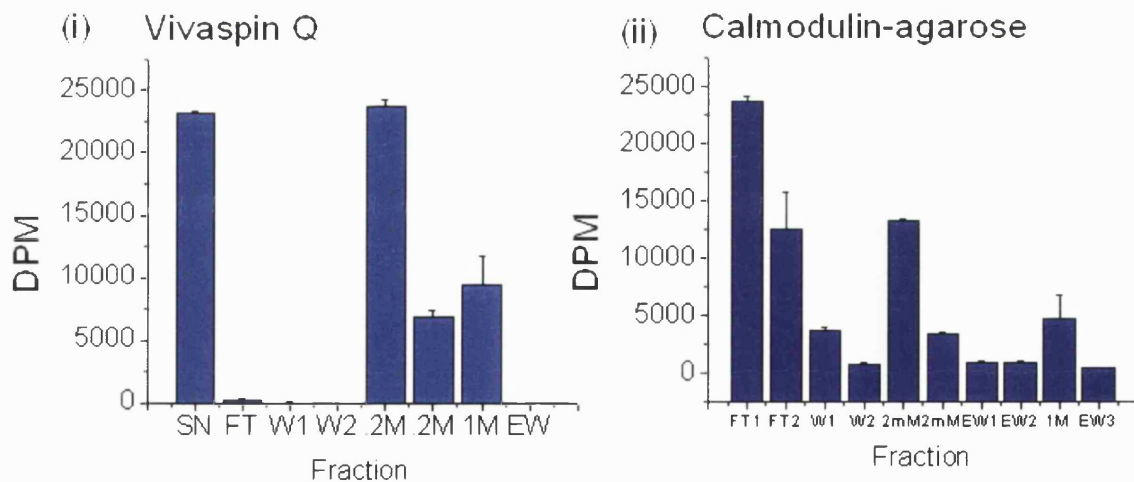
**Figure 5.25.2** SDS PAGE analysis of FL4 purified using Vivaspin Q ion exchange units.

Lane 1 = flow-through sample (FT; unbound protein); Lane 3 = 0.1M eluate; Lane 5 = 0.2M eluate (peak PDE activity marked with a double star); Lane 7 = 0.3M eluate; Lane 9 = 0.4M eluate; Lane 11 = 0.5M eluate; Lane 13 = 1.0M eluate. Lane 15 = pre-stained protein marker. Lanes 2, 4, 6, 8, 10, 12 and 14 represent the washes carried out between the NaCl step elutions. The open red box on the right of the gel marks the expected position of FL4 protein (not visualised on the silver-stained gel).

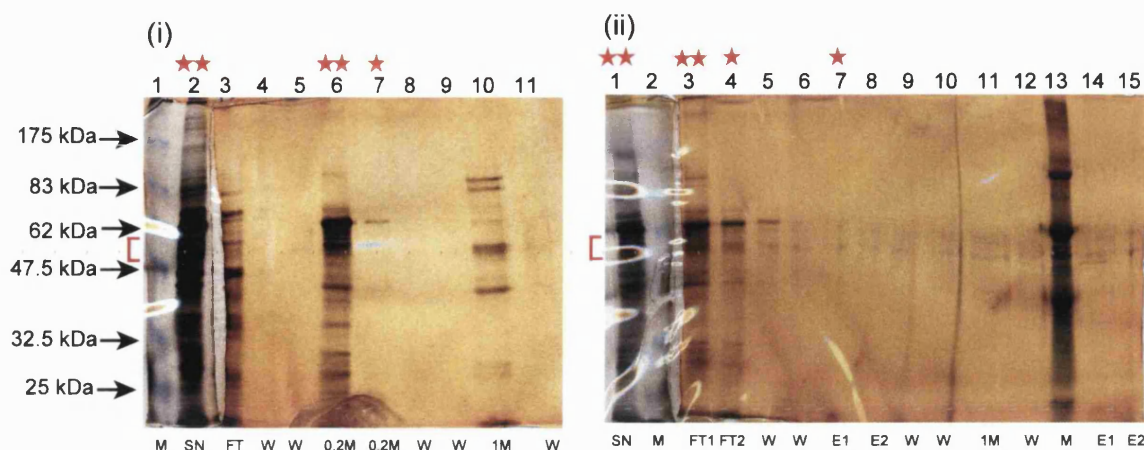
### 5.5.8.3 Calmodulin-agarose affinity chromatography on FL4

Cleared total cell lysates (supernatants) from cells expressing FL4 were first applied to Vivaspin Q ion exchange units to semi-purify the sample and to remove calmodulin-binding protein as described in section 5.4.17.3.2. Step-elution of the recombinant protein was carried out with two 1ml steps of 0.2M NaCl. The two 0.2M eluates were then applied to the calmodulin-agarose resin as described in section 5.4.17.3.2. Recombinant protein was eluted from the calmodulin-agarose resin using 1ml of purification buffer 1 containing 2mM EGTA.

Figure 5.26.1(i) shows the elution profile, represented as PDE activity, for FL4 purified using Vivaspin Q ion exchange units while Figure 5.26.1 (ii) shows the PDE activity profile of the fractions collected following calmodulin agarose affinity chromatography of the 0.2M NaCl fractions. Figure 5.26.2 shows silver stained SDS PAGE gels carried out on the Vivaspin Q and calmodulin agarose chromatography fractions.



**Figure 5.26.1** Purification profile of FL4 purified by Vivaspin Q ion exchange chromatography followed by calmodulin-agarose chromatography. (i) shows the PDE activity profile of the FL4 fractions from Vivaspin Q units while (ii) shows the PDE activity profile of the fractions collected from the calmodulin-agarose resin for the semi-purified FL4. Results are means  $\pm$  S.E. of two determinations in a single experiment.



**Figure 5.26.2** SDS PAGE analysis of FL4 purified using Vivaspin Q ion exchange chromatography followed by calmodulin agarose affinity chromatography. Gel (i) represents FL4 samples from the Vivaspin Q ion exchange chromatography, and gel (ii) represents the fractions collected following calmodulin agarose affinity chromatography of the two 0.2M ion exchange eluates. Stars above the lanes represent peak PDE activity using cAMP as the substrate.

(i) Lane 1 = pre-stained protein marker with sizes indicated on the left; Lane 2 = FL4 supernatant sample used for the ion exchange chromatography (SN); Lane 3 = flow-through sample (FT); Lanes 4 and 5 = wash samples (W); Lanes 6 and 7 = 0.2M elution samples; Lanes 8 and 9 = wash samples; Lane 10 = 1.0M eluate; Lane 11 = wash sample.

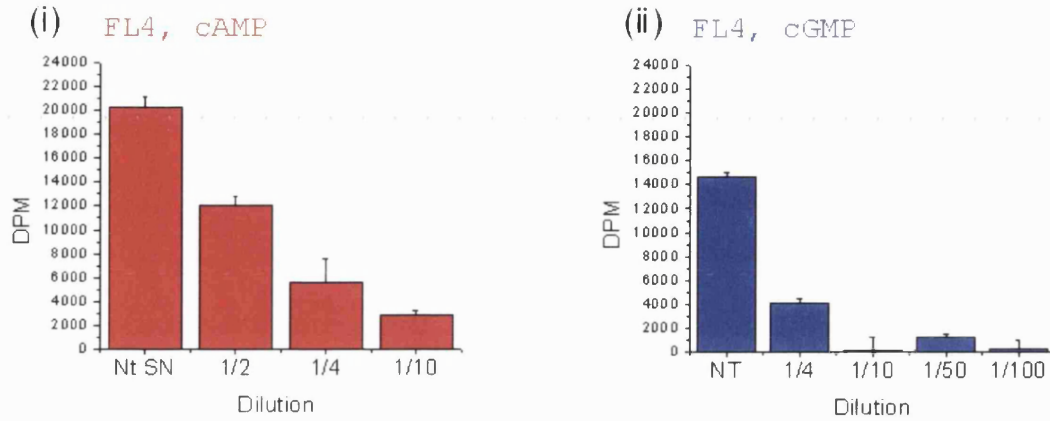
(ii) Lane 1 = FL4 supernatant sample used for ion exchange chromatography; Lane 2 = pre-stained protein marker; Lanes 3 and 4 = two flow-through samples (FT1, FT2); Lanes 5 and 6 = wash fractions; Lanes 7 and 8 = 2mM EGTA eluates; Lanes 9 and 10 = wash fractions; Lane 11 = 1.0M eluate; Lane 12 = wash fraction; Lane 13 = in-house protein marker mixture ( $\beta$ -gal, BSA and ovalbumin); Lanes 14 and 15 = 2mM EGTA eluates (E1, E2) concentrated ten fold. The open red boxes on the left of both gels marks the position of the 57 kDa FL4 protein (not visualised on the gel).

### 5.5.9 Preliminary kinetic analysis on FL4 and End6

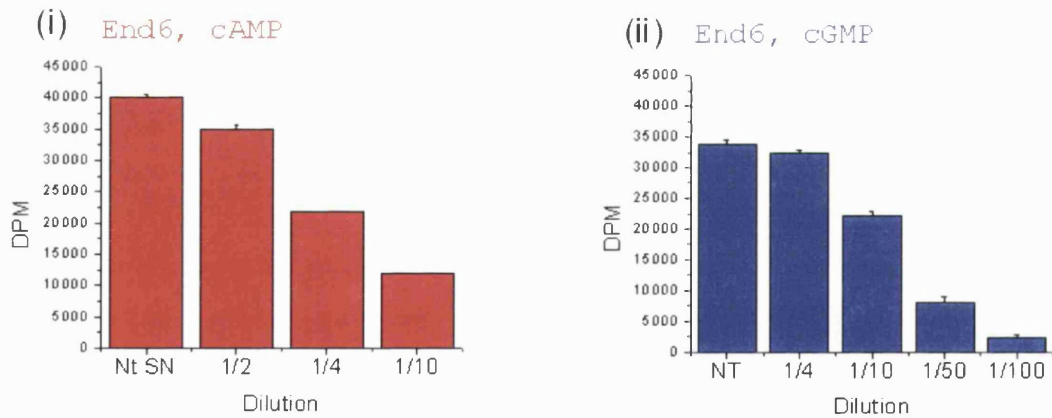
Preliminary kinetic analysis was carried out on FL4 and End6 cleared total cell lysate samples (supernatants) in order to determine substrate specificity, while  $K_m$  and  $V_{max}$  values were determined in the next chapter (Chapter 6). A range of dilutions (up to a hundred-fold) were made using 50mM Hepes pH 7.5 buffer and PDE activity assays carried out on these as described in section 5.4.18. Figure 5.27 shows the results for the PDE activity results for these samples. These were used as a guide for diluting FL4 and End6 samples



for subsequent kinetic analysis (Chapter 6) so that the activity counts could be reliably measured.

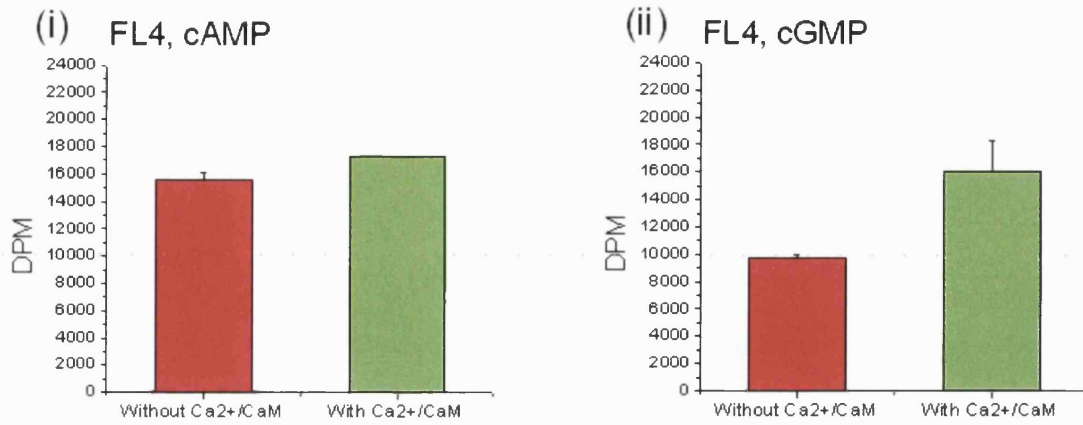


**Figure 5.27.1** Cyclic nucleotide substrate specificity of FL4. FL4 supernatant samples were diluted up to ten-fold and PDE activity assays carried out using both cAMP (i) and cGMP (ii) as substrates. Results are means  $\pm$  S.E. of two determinations from 3 - 4 separate experiments.

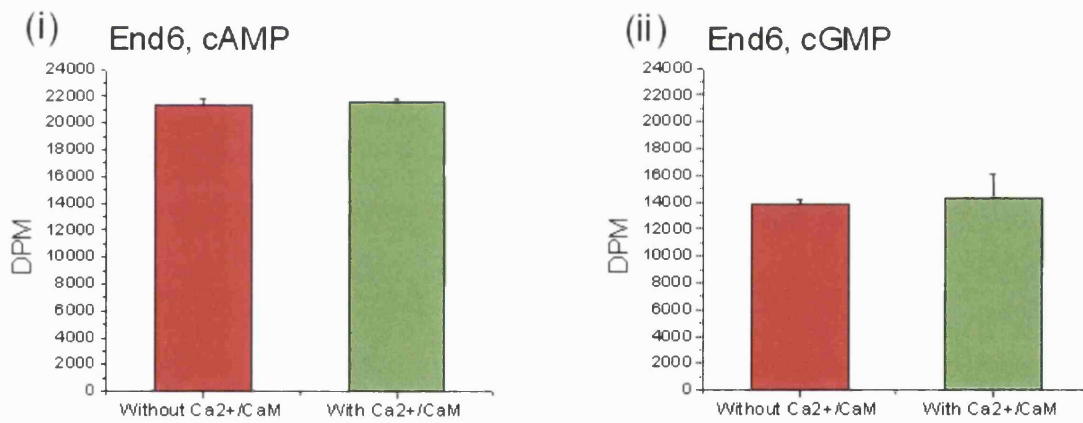


**Figure 5.27.2** Cyclic nucleotide substrate specificity of End6. End6 supernatant samples were diluted up to ten-fold and PDE activity assays carried out using both cAMP (i) and cGMP (ii) as substrates. Results are means  $\pm$  S.E. of two determinations from 3 - 4 separate experiments.

PDE activity assays to determine  $\text{Ca}^{2+}/\text{CaM}$  stimulation were also carried out on both FL4 and End6 supernatant samples as described in section 5.4.18. Figure 5.28 shows the PDE activity results for FL4 (5.28.1) and End6 (5.28.2) carried out in the presence and absence of  $\text{Ca}^{2+}/\text{CaM}$  using both cAMP and cGMP as substrates.



**Figure 5.28.1** Response of FL4 to  $\text{Ca}^{2+}/\text{CaM}$  using cAMP and cGMP as substrates. Results are shown as blank-adjusted DPM values. Results are means  $\pm$  S.E. of two determinations from 3 - 4 separate experiments.



**Figure 5.28.2** Response of End6 to  $\text{Ca}^{2+}/\text{CaM}$  using cAMP and cGMP as substrates. Results are means  $\pm$  S.E. of two determinations from 3 - 4 separate experiments.

## 5.6 Discussion

The principal aims of the work described in this chapter were two-fold. Firstly, full-length and truncated PDE1A1 fragments were to be generated by PCR for subsequent cloning and expression in the Semliki Forest virus system. Secondly, the recombinant constructs, together with the helper virus, were to be used for the transfection of BHK-21 cells for the production of recombinant virus to generate sufficient recombinant enzyme for the purification and biochemical characterisation of the recombinant enzymes. This included optimisation of the recombinant virus infection of BHK-21 cells with the intention of scaling-up the expression system. Preliminary biochemical characterisation of the recombinant enzymes was carried out in this chapter with detailed characterisation described in the next chapter (Chapter six).

### 5.6.1 Cloning and expression of the full-length and truncated PDE1A1 in pSFV1

The four PDE1A1 fragments (full-length and the N- and/or C-terminal truncated) were successfully generated by PCR as shown by the agarose gel analysis on the PCR products in Figure 5.5. These were then cloned into pSFV1 as described in section 5.5.1. Enzyme restriction analysis identified at least one clone for each of the constructs (Figure 5.6 and 5.7). Selected clones were then used for subsequent expression in the Semliki Forest virus system. The constructs were also analysed by Automated DNA sequence analysis for further confirmation and Figure 5.8 shows a portion of the sequence for the full-length clone (FL4), selected for expression studies, at the junction of the *Bam*HI cloning site in the vector. The sequences analysed did not deviate from the original sequence obtained by Clapham and Wilderspin (2001) shown in Figure 1.19.1.

Transfection efficiency of the recombinant virus was determined indirectly by using pSFV3*lacZ* virus particles as described in section 5.4.11.3. This virus was generated under the same conditions as the recombinant PDE1A1 virus particles so was used as an indication of the recombinant virus efficiency. The pSFV3*lacZ*-infected BHK-21 cells were stained for  $\beta$ -galactosidase to obtain a value for the transfection efficiency which was used to calculate the viral titer or infectious virus units per millilitre. This was found to be between  $1.8 \times 10^5$  to  $2.5 \times 10^5$  infectious units/ml. For the infection of cells with PDE1A1

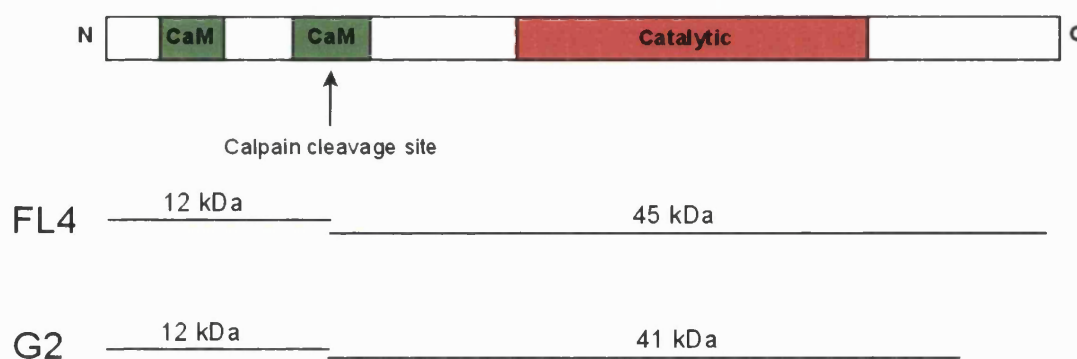
recombinant virus stock (FL4), a range of virus volumes, from 25µl to 200µl, were used to infect approximately  $1 \times 10^5$  cells for small-scale expression studies. Infected cells were allowed to grow for up to 72 hours. PDE activity assays carried out on cells harvested at 24, 48 and 72 hours revealed that optimum PDE activity was present when infected cells were harvested after 48 hours. Activity results for 25µl virus volume were very similar to the PDE activity results obtained for cells infected with a larger volume of virus (Figure 5.16.1). For the large-scale infection studies, between 75µl and 100µl of the virus stock was used to infect approximately  $1 \times 10^6$  cells routinely.

### **5.6.2 Preliminary PDE activity analysis of the full-length and truncated PDE1A1 enzymes**

Direct transfection of BHK-21 cells, with the *in vitro* generated RNA transcripts, was carried out as described in section 5.4.5. Cleared total cell lysate samples (supernatants) for all four constructs (FL4, G2, End6 and Cat9), together with the uninfected cells, were analysed for PDE activity. These revealed that of the four constructs analysed, only the full-length (FL4) and the N-terminal truncated (End6) constructs had significant PDE activity above the background (Figures 5.10 and 5.11). This activity was inhibited by vinpocetine, and for the full-length construct, the PDE activity was stimulated at least two-fold by the presence of  $\text{Ca}^{2+}/\text{CaM}$  (Figure 5.11). Activity assays were also carried out on cell debris samples of the C-terminal truncated (G2) and the N- and C-terminal truncated (Cat9) constructs (Figure 5.12). As with the supernatant samples, G2 and Cat9 cell debris samples did not show significant PDE activity above the background.

Western blot analysis carried out on all four constructs, using CaM-PDE antibody, showed the presence of the recombinant protein in all four supernatant samples analysed, including samples, G2 and Cat9, which showed no significant PDE activity above the background. Figure 5.13 shows the results for neat supernatant samples which gave an indication of the relative amounts of the recombinant protein present. G2 and End6 gave the strongest signal on the Western blot followed by a weaker signal for FL4 and a very much weaker signal for Cat9. These samples were concentrated ten-fold and the Western blot carried out on the concentrated samples. Figure 5.14 shows the results for FL4 and G2 while Figure 5.15 shows the results for End6 and Cat9 concentrated samples. These revealed the presence of

at least one proteolytic fragment in all four constructs despite the inclusion of protease inhibitors in all the buffers. The PDE1 family of enzymes are thought to contain calpain cleavage sites located at the N-terminal regions of the enzymes as discussed in Chapter one (section 1.7.3.2). The dog heart PDE1A enzyme used in the present study does contain a consensus sequence for such proteolysis as discussed in section 1.8.2.2. If cleavage did occur at the predicted cleavage point, then the presence of the smaller fragments detected in the Western blots for FL4 and G2 could be accounted for. Figure 5.29 shows a schematic of the PDE1A1 enzyme together with the possible fragments generated following cleavage at the calpain cleavage site. The 45 kDa and 41 kDa fragments for FL4 and G2, respectively, predicted following cleavage at the calpain cleavage site can be identified on the Western blot of these two samples, as shown in Figure 5.14. There was also at least one more smaller fragment visible in the Western blot with an approximate size of 25 - 30 kDa which denoted the presence of other proteolytic cleavage sites.



**Figure 5.29** Schematic showing possible PDE1A1 fragments generated following proteolysis. The full-length enzyme is represented in the upper panel in which the arrow marks the calpain cleavage site. The lengths of the predicted cleavage products are shown for the FL4 and G2 enzymes.

The proteolysis of the CaM-PDE enzymes by trypsin and chymotrypsin has been studied by several workers (Charbonneau *et al.*, 1991; Yuan *et al.*, 1999). These studies have generally revealed that limited proteolysis with trypsin resulted in a catalytically active,  $\text{Ca}^{2+}$ /CaM-independent, fragment lacking a portion of the N-terminal and the C-terminal regions of the enzyme. The chymotryptic fragment produced a similarly active fragment but lacking just the N-terminal region of the enzyme. The cleavage products have all been shown to be 2 - 3 fold more active than the full-length enzymes. These studies were carried

out to identify the conserved catalytic domain in the PDE1 enzymes. There have been very few reports of PDE activity studies on truncated PDE1 constructs to examine the effect of the removal of N- and/or C-terminal domain amino acids on enzyme activity. In the studies carried out by Sonnenburg and co-workers (1995) on N-terminal truncated PDE1A1 mutants, the principal aim was to identify a second calmodulin-binding domain in the PDE1A enzymes, which was indeed identified. Also to note was that their N-terminal truncated constructs were all active mutants which is in agreement with the results obtained in the present study where the N-terminal truncated construct, End6, was an active mutant.

There have been a number of studies examining the effect of truncations on PDE activity, as well as effects on the tertiary structure of the enzymes, following N- and/or C-terminal truncations of PDE2, PDE3 and PDE4 enzymes (Rocque *et al.*, 1997b; Kovala *et al.*, 1997; Jacobitz *et al.*, 1996; Jin *et al.*, 1992). Studies on full-length (1 - 564 amino acids) and truncated PDE4 enzymes by Rocque and co-workers (1997) did give similar results to the ones obtained in the present study. These workers constructed N- and C-terminal truncated PDE4B2B constructs (Table 5.9) and found that the N-terminal truncated constructs retained the PDE activity while the C-terminal truncated constructs showed a very much reduced activity. Both the active and inactive constructs in their studies were detected by Western blot analysis. These workers reasoned that the critical amino acid residues, necessary for catalytic activity, resided at the C-terminal region of the enzymes. Other workers studying full-length and truncated PDE enzymes (PDE3 and PDE4) have also had similar results (Kovala *et al.*, 1997; Jacobitz *et al.*, 1996; Jin *et al.*, 1992). Generally, these studies have indicated that truncations at the C-terminal regions of the enzymes resulted in enzymes with dramatically reduced activity, or no activity, while deletions at the N-terminal regions of the enzymes have tended to give dramatic increases in the  $V_{\max}$  values of the enzymes while having little or no effect on the  $K_m$ . It is possible that the constructs generated in the present study that were lacking the complete C-terminal portion (G2 and Cat9) were catalytically inactive because critical C-terminal amino acid residues were not present. Further work is required to confirm the involvement of the C-terminal residues in PDE1A1 by constructing a series of deletion mutants lacking different number of amino acid residues at the C-terminal portion of the enzyme. Another possibility to consider as an explanation for the lack of activity in G2 and Cat9 is the factor of incorrect protein folding which would affect the catalytic activity of the enzymes. The C-terminal

portion has been said to play a role in the formation of multimeric units consisting of dimers or tetramers (Kovala *et al.*, 1997; Rocque *et al.*, 1997). It may be possible that PDE1A1 needs to be associated as dimeric - tetrameric complexes for the catalytic process and therefore, those constructs lacking the C-terminal region in the present study (G2 and Cat9) were unable to form these associations so were catalytically inactive. Table 5.9 summarises the PDE activity results for constructs in the present study together with the activity results for full-length and truncated PDE enzymes by other workers (Kovala *et al.*, 1997; Rocque *et al.*, 1997; Tang *et al.*, 1997).

**Table 5.9** Summary of the PDE activity results for the full-length and truncated constructs in the present study.

Study	PDE construct: Active or inactive			
	Full-length	C-terminal truncated	N-terminal truncated*	N- and C-terminal truncated
Present study	PDE1A1 (1-515): Active (FL4)	PDE1A1 (1-476): Inactive (G2) (+WB)	PDE1A1 (118-515): Active (End6)	PDE1A1 (118-476): Inactive (Cat9) (+WB)
Sonnenburg <i>et al.</i> , 1995	PDE1A1 (1-514): Active	-	$\Delta$ M5-PDE1A (91-514): Active	-
Tang <i>et al.</i> , 1997	PDE3: Active	-	PDE3 $\Delta$ 2: Active	-
Kovala <i>et al.</i> , 1997	PDE4D1 (1-584): Active	PDE4D1 (1-482; 1-510): $\pm$ activity (+WB)	PDE4D1 (121-584): Active	-
Rocque <i>et al.</i> , 1997	PDE4B2B (1-564): Active	-	PDE4B2B (81-564): Active	PDE4B2B (152-528; 152-505): Active
Rocque <i>et al.</i> , 1997	-	-	-	PDE4B2B (152-478): Inactive (+WB)
Fink <i>et al.</i> , 1999	PDE5 (1-865): Active	-	PDE5 (508-865): Active	-

\* Activity in the N-terminal constructs generally resulted in an increase in the  $V_{max}$  values of these enzymes relative to the full-length enzymes. +WB denotes the detection of the protein by Western blot analysis. Proteins showing PDE activity were all detected on Western blots. Catalytic domain amino acids: PDE1A1 in the present study 178-431.  
PDE4D1 (Kovala *et al.*, 1997) 213-480.  
PDE4B2B (Rocque *et al.*, 1997) 152-528.  
PDE5 (Fink *et al.*, 1999): 578-812.

Initial kinetic analysis on FL4 and End6 samples was also carried out to determine substrate specificity as well as response to  $Ca^{2+}$ /CaM. FL4 and End6 both hydrolysed cAMP as well

as cGMP (Figure 5.27). PDE activity results obtained for the range of sample dilutions analysed were used as a guide for the kinetic analysis carried out in the next chapter (Chapter 6). Samples were diluted so that the activity counts were in the range of approximately 10,000 to 40,000 DPM for an accurate measurement of PDE activity counts for the determination of  $K_m$  and  $IC_{50}$  values.

The response of FL4 and End6 to the presence of  $Ca^{2+}/CaM$  was also measured using both cAMP and cGMP as substrates (Figure 5.28). End6 (N-terminal truncated) showed no stimulation which was as expected since the truncated enzyme does not contain the calmodulin-binding domains (Figure 5.28.2). FL4 did show some stimulation in the presence of  $Ca^{2+}/CaM$  with cAMP as substrate (10% stimulation) and cGMP as substrate (38% stimulation). However, this stimulation was not reproducible between the experiments carried out. There are a number of reasons why this may have been the case. Firstly, the enzyme being analysed was not a pure preparation so contained a number of proteins, any of which may be binding to the extraneous  $Ca^{2+}/CaM$ . The addition of up to 1mM  $Ca^{2+}$  and 50 units of calmodulin had little or no effect on the FL4 stimulation (data not shown). The full-length protein may also have undergone proteolysis, despite the presence of protease inhibitors, releasing the N-terminal calmodulin-binding domain (s), thus rendering the enzyme fully active and not responsive to the addition of  $Ca^{2+}/CaM$ . The second factor to consider is that the enzyme may have been folded into a state which was not readily reversible by the presence of  $Ca^{2+}$ ; or access to these domains was restricted because of the tertiary state of the enzyme. It was also possible that there were protein(s) present in the crude mixture which were tightly bound to the calmodulin-binding domains of FL4 which in turn restricted access to these domains. Calmodulin itself has been shown to be tightly associated with bovine lung PDE1A as a stable complex,  $CaM \cdot PDE$ , by Sharma and Wang (1986b), which was not dissociated through successive chromatography purification stages; but the purified complex was activated by  $Ca^{2+}$ . However, the addition of up to 1mM  $Ca^{2+}$  did not show significant activation of FL4 in the present study. But the fact that the FL4 enzyme was not a pure preparation, and the effect of the presence of other proteins in the preparation which may be  $Ca^{2+}$  and /or CaM-binding proteins, cannot be ruled out. The third factor to consider in the non-responsiveness of FL4 to  $Ca^{2+}/CaM$  is that of the phosphorylation state of FL4. As already discussed in section 1.7.3, phosphorylation of PDE1 enzymes results in a reduced affinity of the enzymes for calmodulin (Sharma *et*



*al.*, 1980; Sharma and Wang, 1985, 1986; Sharma, 1991; Florio *et al.*, 1994). Phosphorylation of calmodulin has also been shown to reduce the binding affinity of calmodulin with its target proteins through changes in the conformation of the phosphorylated calmodulin (Leclerc *et al.*, 1999; Corti *et al.*, 1999). Based on the results obtained for Ca<sup>2+</sup>/CaM stimulation of FL4, the kinetic analysis carried out on FL4 in the next chapter (Chapter 6) does not include analysis involving Ca<sup>2+</sup>/CaM.

### 5.6.3 Stability studies on FL4

The parameters investigated for the stability studies on FL4 were basal and stimulated enzyme activity following storage of the sample at 4°C, effect of pH and the presence of glycerol on basal FL4 activity. These were explored since samples were to be stored at 4°C during the kinetic analysis (Chapter 6) as well as in glycerol for long term storage at -70°C.

FL4 supernatant samples were stored at 4°C in Lysis buffer 2 or 3 (Table 2.3) in the presence of protease inhibitor for up to five days. PDE activity assays carried out on these samples indicated that there was a small loss of basal PDE activity following storage at 4°C for up to five days (Figure 5.18). Percentage stimulation by Ca<sup>2+</sup>/CaM over this period was also reduced from approximately 30 - 60% down to approximately 15 - 20% (Figure 5.18 (ii)). This loss in stimulation may be associated with loss of the calmodulin-binding domain of FL4 due to proteolysis, or due to changes in the enzyme conformation during the storage period. Kincaid and co-workers (1981a) also noted a time-dependent loss in Ca<sup>2+</sup>/CaM stimulation of the bovine brain PDE1 when this enzyme was stored at 4°C for up to eight days. Studies were then carried out by the same workers (Kincaid *et al.*, 1981b) on the relationship of the subunit structure of bovine brain PDE1 and Ca<sup>2+</sup>/CaM stimulation. These workers proposed the existence of PDE as interconvertible monomers and oligomers which differed in their catalytic activity in that the monomers were fully active in the absence of Ca<sup>2+</sup>/CaM, while dimers were inactive under the same conditions and required the presence of Ca<sup>2+</sup>/CaM for full activity. It is possible that storage of FL4 at 4°C in the present study created FL4 species that were unresponsive to Ca<sup>2+</sup>/CaM due to the conformation adopted by the enzyme.

FL4 samples stored in different pH buffers, over the range pH 4.5 to pH 9.0, revealed that

the PDE activity was stable between the pH 6.5 to pH 9.0 (Figure 5.19). There was complete loss of activity by Day 2 in samples stored in acid buffers (pH 4.5 to pH 5.2) with insignificant affect on activity in alkali buffers. Samples were routinely stored at either pH 7.5 or pH 8.0 for up to five days only during the kinetic analysis (Chapter 6).

FL4 and End6 supernatant samples were stored at  $-70^{\circ}\text{C}$ , in the absence and presence of glycerol (up to 40%), and thawed once for PDE activity analysis. The presence of increasing amounts of glycerol did not have a significant affect of the basal PDE activity fo the two enzymes (Figure 5.20). Also, thawing the samples did not show a significant loss of PDE activity regardless of the presence or absence of glycerol in the samples. Therefore, basal PDE activity was stable for at least one freeze-thaw cycle. Samples used for the kinetic analysis (Chapter 6) were stored in small volumes (without glycerol) and only thawed once for the kinetic work.

#### **5.6.4 Determination of the native state of the recombinant enzymes**

Two methods were employed for the determination of the native state of the recombinant enzymes, FL4 and End6. Firstly, a cross-linking method employing the cross-linker DSS as described in section 5.4.16.1 followed by Western blot analysis to detect the cross-linked product. This method was used for End6 since the Western blot signal for this enzyme was readily detected. The second method used was gel filtration or size exclusion chromatography as described in section 5.4.16.2 which was carried out on FL4 since this protein was not readily detected on Western blots. Fractions collected from the gel filtration experiment were analysed for PDE activity. Figure 5.21 shows the Western blot analysis on the cross-linked samples of End6 which also included control End6 samples not containing any cross-linker. These results showed the 44 kDa End6 protein as expected in the control samples not containing the cross-linker and the gradual disappearance of this signal as samples were incubated with the cross-linker for up to 2 hours. There was the appearance of a larger protein in these samples at an approximate position of 175 kDa. There were no other protein bands visible on the Western blot apart from this large protein and a fainter protein at the monomer position of 44 kDa. These results strongly suggested the presence of End6 protein as tetrameric units which would give a signal at 175 kDa position.

FL4 fractions collected following gel filtration chromatography showed an elution profile for FL4 suggestive of the protein being associated as tetrameric units as well (Figure 5.23.2). PDE activity profile of these fractions showed peak activity between fractions 15 - 18 mls. The largest protein marker used ( $\beta$ -amylase; 200 kDa) eluted between the volumes 17 - 19mls. This would be consistent with FL4 eluting as a tetramer of 228 kDa size. The size of the purified native dog heart PDE1A, however, was found to be consistent with the full-length protein being associated as dimeric proteins (Clapham and Wilderspin, 2001).

PDE enzymes are thought to exist as dimeric proteins but larger species (larger than dimeric) are also thought to exist. Sonnenburg and co-workers (1995) showed that the full-length (1-514 amino acids) and N-terminal truncated PDE1A1 constructs they had produced (91-514 amino acids) had a native molecular weight corresponding to a dimeric protein indicating that residues at the amino terminal portion were not directly involved in the quaternary state of the enzymes. Kovala and co-workers (1997) found that full-length PDE4D1 tended to form aggregates which were equivalent to tetrameric units or larger when analysed by gel filtration chromatography. However, PDE4D1 constructs lacking the C-terminal region behaved as monomeric enzymes. These workers also found that the PDE4D1 constructs just lacking the N-terminal region tended to be associated as dimers thus suggesting a role for the N-terminal region in the formation of multimers. Rocque and co-workers (1997) found that their full-length PDE4B2B appeared to exist as a large multimeric protein (larger than a tetramer) but that the N-, and the N- and/or C-terminal, truncated proteins were no larger than tetramers when analysed by gel filtration chromatography. In general, these studies implicate the involvement of C-terminal regions in the formation of dimers, and the requirement of both N- and C-terminal regions in the formation of larger multimers such as tetramers. Table 5.10 summarises the results obtained in the present study for the native state of the recombinant enzymes, FL4 and End6, together with the results obtained by other workers (Kovala *et al.*, 1997; Rocque *et al.*, 1997).

**Table 5.10** Summary of results for the native state of FL4 and End6.

Study	PDE construct: Tertiary state			
	Full-length	C-terminal truncated	N-terminal truncated	N- and C-terminal truncated
Present study	PDE1A1 (1-515): Tetramer (FL4)	-	PDE1A1 (118-515): Tetramer (End6)	-
Clapham and Wilderspin, 2001	PDE1A (1-515): Dimer	-	-	-
Sonnenburg <i>et al.</i> , 1995	PDE1A1 (1-514): Dimer	-	ΔM5-PDE1A (91-514): Dimer	-
Kovala <i>et al.</i> , 1997	PDE4D1 (1-584): Tetramer	PDE4D1 (1-482; 1-510): Monomers	PDE4D1 (121-584): Dimer	-
Rocque <i>et al.</i> , 1997	PDE4B2B (1-564): Multimers	-	PDE4B2B (81-564): Dimer	PDE4B2B (152-528; 152-505): Dimers - Tetramers
Richter <i>et al.</i> , 2000	PDE4A (1-886): Tetramer	-	PDE4A (201-886; 342-886): Tetramer	PDE4A (342-704): Dimer

Catalytic domain amino acids: PDE1A1 in the present study 178-431.  
PDE4D1 (Kovala *et al.*, 1997) 213-480.  
PDE4B2B (Rocque *et al.*, 1997) 152-528.  
PDE4A (Richter *et al.*, 2000): 352-681.

### 5.6.5 Purification studies on FL4 and End6

Ion exchange chromatography using anion exchange resin or filter units was carried out on FL4 and End6 as described in section 5.4.17. Q-Sepharose fast flow ion exchange resin was initially used for the purification of End6. Step elution with NaCl (0 - 1M) was used to elute the bound protein which was found to elute between 0.15 - 0.2M NaCl, as shown by the PDE activity analysis on the fractions (Figure 5.24.1). The 0.15M fraction was concentrated 7-fold as described in section 5.4.17.1 and this together with the fractions collected from the Q-Sepharose resin were analysed by SDS PAGE. These revealed the presence of a protein band at ~44 kDa position in the concentrated sample, corresponding to the End6 protein (Figure 5.24.2). SDS PAGE analysis also revealed many co-purifying proteins.

Vivaspin-Q ion exchange chromatography units were used for the purification of FL4 as

described in section 5.4.17.2. These were used as they allowed samples to be purified much quicker (approximately 20 minutes) than by Q-Sepharose fast flow resin (1 - 2 hours). Step elution with NaCl revealed peak PDE activity in the 0.2M NaCl fraction (Figure 5.25.1). SDS PAGE analysis of the fractions revealed co-purification of a number of proteins, just as for End6. The elution of End6 and FL4 at low salt concentrations (0.15 - 0.2M NaCl) was consistent with the results obtained for the native dog heart PDE1A (Clapham and Wilderspin, 2001).

The 0.2M NaCl fraction for FL4 was processed further by loading the fraction onto a calmodulin-agarose resin column as described in section 5.4.17.3. This was carried out in order to further purify FL4. Calmodulin-agarose affinity chromatography has been used successfully to purify the native dog heart PDE1A following the application of the Mono-Q peak fraction (Clapham and Wilderspin, 2001). However, PDE activity analysis on the FL4 fractions from the calmodulin-agarose resin in the present study showed that most of the protein was not being bound to the resin (Figure 5.26.1). SDS PAGE analysis on the fractions did reveal that most of the proteins co-purifying with FL4 using ion exchange chromatography were not retained by the calmodulin resin (Figure 5.26.2). One of the reasons for FL4 protein not binding to the calmodulin resin may have been that the calmodulin-binding region on the protein was inaccessible due to the conformation of the protein. Another reason may have been the presence of the 0.2M NaCl, present in the FL4 sample, in conjunction with the calmodulin resin used in the present study. The calmodulin resin had been prepared from native sources (bought from Sigma) and calmodulin-binding proteins can be eluted from this resin using EGTA containing 0.15M NaCl (Vaillancourt *et al.*, 2000). An alternative calmodulin resin prepared from a recombinant calmodulin protein is available (Stratagene), binding to which is not affected by the presence of low salt concentrations. In fact, EGTA containing 1M NaCl is used to elute proteins from this resin. So this is an alternative that can be used for the purification of FL4 in future work on the enzyme.

The purification of End6 and FL4 enzymes to homogeneity was not completed due to time constraints and the requirement for larger amounts of the crude recombinant enzymes. Instead kinetic analysis was carried out on the crude samples of the enzymes since PDE activity assays had already indicated that there was insignificant background PDE activity

in cells transfected with the vector only (Figures 5.10 and 5.12).

### 5.6.6 Summary of the preliminary analysis of full-length and truncated PDE1A1 proteins

Table 5.11 summaries the results of the analysis carried out on the full-length and truncated PDE1A1 enzymes produced in the present study.

**Table 5.11** Summary of the analysis of the full-length and truncated PDE1A1 recombinant enzymes.

	<b>Full-length: FL4</b>	<b>C-terminal truncated: G2</b>	<b>N-terminal truncated: End6</b>	<b>N- and C-terminal truncated: Cat9</b>
<b>PDE activity</b>	Active	Inactive	Active	Inactive
<b>Substrate preference</b>	cAMP > cGMP	-	cGMP > cAMP	-
<b>Ca<sup>2+</sup>/CaM stimulation</b>	± but inconsistent	-	0%	-
<b>Monomer size</b>	57 kDa	53 kDa	44 kDa	40 kDa
<b>Native size</b>	~228 kDa	-	~176 kDa	-
<b>Tertiary state</b>	Tetramer	-	Tetramer	-
<b>Elution from Q-sepharose resin</b>	Low salt: 0.2M NaCl	-	Low salt: 0.2M NaCl	-

## 5.7 Conclusion

The successful expression of PDE1A1 enzyme in the present study represents the first report of the expression of PDE1 enzymes using the Semliki Forest virus expression system. The primary aims of the work described in this chapter were the generation of full-length and truncated PDE1A1 fragments for cloning into the Semliki Forest virus vector, pSFV1, followed by the expression and characterisation of the recombinant enzymes. As discussed in section 5.6, both of these were successfully carried out. Optimisation of the expression system using the full-length construct, FL4, was also carried out to allow scale-up of the system from 25cm<sup>2</sup> flasks to 75cm<sup>2</sup> flasks which were used to produce sufficient recombinant FL4 and End6 enzymes for the kinetic analysis described in the next chapter. The conditions used for the expression of the recombinant enzymes can be further adapted

to produce the enzymes using a 1 L spinner flask or a  $\geq 10$  L bioreactor for the larger-scale production of the recombinant enzymes for purification and subsequent structural analysis.

## Chapter Six

### 6 Biochemical analysis of the recombinant full-length (FL4) and N-terminal truncated (End6) PDE1A1 enzymes

This chapter will describe the biochemical analysis carried out on the recombinant full-length (FL4) and N-terminal truncated (End6) PDE1A1 enzymes produced using the Semliki Forest virus system as described in Chapter 5.

#### 6.1 Introduction

##### 6.1.1 Cyclic nucleotide specificity for PDE1 family members

Members of the PDE1 family demonstrate a broad substrate specificity for cAMP and cGMP as indicated by the wide variation in  $K_m$  values. The  $K_m$  value, or the Michaelis-Menten constant, refers to the substrate concentration at which the enzyme velocity is at half-maximal ( $\frac{1}{2} V_{max}$ ). It is used as an indicator for the affinity of the enzyme for the substrate such that a low  $K_m$  value means that the enzyme has a high substrate affinity while a high  $K_m$  value indicates the converse. Table 6.1 shows the  $K_m$  values for some of the PDE1 isoenzymes and includes enzymes that have been purified from mammalian tissues as well as recombinant enzymes expressed using yeast (*S. cerevisiae*), mammalian expression (COS-7 cells) or insect cell (Sf9 cells) systems. The variation in  $K_m$  values seen within the PDE1 family may be because of the method used to purify the enzymes which may mean that more than one PDE1 isoform was present or that there were other PDEs present. The variation may also reflect differences between PDE1 enzymes isolated from tissues or animals. However, there is a relative difference between the PDE1A, PDE1B and PDE1C families in terms of substrate affinities. In general, PDE1A and PDE1B families have a preference for cGMP over cAMP while the PDE1C family has an equal affinity for both substrates.



**Table 6.1**  $K_m$  values for PDE1 isoenzymes.

Enzyme source	$K_m$ values ( $\mu\text{M}$ )		Reference
	cAMP	cGMP	
<i>Purified from mammalian tissues:</i>			
Dog heart PDE1A	1.2	0.53	Clapham and Wilderspin, 2001
Dog heart PDE1A	2.82 <sup>†</sup>	2.05 <sup>†</sup>	Clapham and Wilderspin, 2001
60-kDa Bovine brain PDE (PDE1A2)	35 <sup>†</sup>	2.7 <sup>†</sup>	Sharma and Kalra, 1994
63-kDa Bovine brain PDE (PDE1B1)	12 <sup>†</sup>	1.2 <sup>†</sup>	Sharma and Kalra, 1994
Bovine lung PDE (PDE1A)	42 <sup>†</sup>	2.8 <sup>†</sup>	Sharma and Kalra, 1994
Guinea pig left ventricle	0.8	0.9	Reeves <i>et al.</i> , 1987
Human cardiac ventricle	0.75	1.0	Reeves <i>et al.</i> , 1987
Bovine Heart (PDE1A)	215	9	Ho <i>et al.</i> , 1976
<i>Crude recombinant enzymes:</i>			
Human PDE1A1	72.7 $\pm$ 2.9 <sup>††</sup>	2.62 $\pm$ 0.18 <sup>††</sup>	Snyder, 1999
Human PDE1A2/5	93.1 $\pm$ 6.2 <sup>††</sup>	2.20 $\pm$ 0.13 <sup>††</sup>	Snyder, 1999
Human PDE1A3/6	101 $\pm$ 22 <sup>††</sup>	3.15 $\pm$ 0.11 <sup>††</sup>	Snyder, 1999
Human PDE1A4	124 $\pm$ 13 <sup>††</sup>	3.51 $\pm$ 0.52 <sup>††</sup>	Snyder, 1999
Bovine PDE1A1	-	3.5 $\pm$ 0.5 <sup>††</sup>	Sonnenburg <i>et al.</i> , 1995
Bovine PDE1A2	-	5.1 $\pm$ 0.7 <sup>††</sup>	Sonnenburg <i>et al.</i> , 1995
Bovine PDE1A2	112.7 $\pm$ 7.9	5.1 $\pm$ 0.6	Yan <i>et al.</i> , 1996
Bovine PDE1B1	24.3 $\pm$ 2.9	2.7 $\pm$ 0.2	Yan <i>et al.</i> , 1996
Mouse PDE1C1	3.5 $\pm$ 0.3	2.2 $\pm$ 0.1	Yan <i>et al.</i> , 1996
Rat PDE1C2	1.2 $\pm$ 0.1	1.1 $\pm$ 0.2	Yan <i>et al.</i> , 1996
Mouse PDE1C4/5	1.1 $\pm$ 0.0	1.0 $\pm$ 0.1	Yan <i>et al.</i> , 1996
<i>Gel filtration (S300) purified recombinant enzyme:</i>			
Human PDE1B1 (yeast expression system)	19.4 $\pm$ 4.1	3.3 $\pm$ 2.1	Yu <i>et al.</i> , 1997

Assays carried out in the presence of  $\text{Ca}^{2+}/\text{CaM}$  (100 $\mu\text{M}/5\text{nM}$ )<sup>†</sup>;  $\text{Ca}^{2+}/\text{CaM}$  (100 $\mu\text{M}/60\text{ng/ml}$ )<sup>††</sup>;  $\text{Ca}^{2+}/\text{CaM}$  (10mM/30 $\mu\text{g/ml}$ )<sup>†††</sup>;  $\text{Ca}^{2+}/\text{CaM}$  (200 $\mu\text{M}/240\text{nM}$ )<sup>††††</sup>.

### 6.1.2 Inhibition of PDE1 enzymes by PDE inhibitors

Traditionally, a range of different PDE inhibitors have been used to characterise the PDE families. These have included inhibitors that were specific for particular PDE families such as rolipram which is widely accepted as a specific inhibitor for the PDE4 family of enzymes or zaprinast which is a PDE1-, PDE5- and PDE6-specific inhibitor. Non-specific inhibitors

have included IBMX. Table 6.2 summarises the inhibition profiles for the PDE1 family while Table 6.3 shows some of the  $IC_{50}$  values for the rest of the PDE families. Results are shown as either  $IC_{50}$  values or percentage inhibition at 100 $\mu$ M inhibitor for cAMP and cGMP as substrates. The  $IC_{50}$  value is the inhibitor concentration where the enzyme activity is at half-maximal activity.

**Table 6.2** IC<sub>50</sub> values for PDE1 isoenzymes.

Enzyme source	IC <sub>50</sub> (μM) using cAMP [IC <sub>50</sub> using cGMP as substrate] or % inhibition at 100μM inhibitor				Reference
	IBMX	Vinpocetine	Zaprinast	Rolipram	
<i>Purified from mammalian tissues:</i>					
Dog heart PDE1A	16.37	1.38	1.93	3%	Clapham and Wilderspin, 2001
Bovine brain PDE1	7	36	14	NT	Yu <i>et al.</i> , 1997
<i>Crude recombinant enzymes:</i>					
Bovine PDE1A1	[1.76 ± 0.022] <sup>†</sup>	[9.7]; [9.49 ± 1.9] <sup>†</sup>	NT	NT	Yan <i>et al.</i> , 1996; <sup>†</sup> Snyder <i>et al.</i> , 1999 (human PDE1A1)
Bovine PDE1A2	3.0	8.1; [10.9] <sup>†</sup>	10.1	180	Loughney <i>et al.</i> , 1996; <sup>†</sup> Yan <i>et al.</i> , 1996
Bovine PDE1B1	NT	[9.8 ± 0.9]	NT	NT	Yan <i>et al.</i> , 1996
Mouse PDE1C1	NT	[39.5 ± 3.5]	NT	NT	Yan <i>et al.</i> , 1996
Rat PDE1C2	NT	[32.4 ± 3.9]	NT	NT	Yan <i>et al.</i> , 1996
Mouse PDE1C	7.5 ± 2	>100	4.5 ± 2	>100	Han <i>et al.</i> , 1999
Human PDE1C3	5.1	50	3.5	160	Loughney <i>et al.</i> , 1996
Mouse PDE1C4/5	NT	[42.4 ± 2.6]	NT	NT	Yan <i>et al.</i> , 1996
Pancreatic PDE1C	NT	>100	4.5	>100	Yan <i>et al.</i> , 1999
<i>Gel filtration (S300) purified recombinant enzyme:</i>					
Human PDE1B1	14 ± 1	22 ± 1	24 ± 2	143 ± 14	Yan <i>et al.</i> , 1996 Yu <i>et al.</i> , 1997

NT = Not Tested

**Table 6.3** IC<sub>50</sub> values for PDE2 through to PDE11 families.

PDE Family	IC <sub>50</sub> (μM) or % inhibition at 100μM inhibitor using cAMP [cGMP] as substrate							Reference
	IBMX	Vinpocetine	Zaprinast	Amrinone	Rolipram	EHNA	Dipyridamole	
PDE2	62	20%	20%	16%	8%	1.4 <sup>†</sup>	29.2	Clapham and Wilderspin, 2001; <sup>†</sup> Dickinson <i>et al.</i> , 1997
PDE3	4	32%	13%; 0% <sup>‡</sup>	5.18	5%; 5% <sup>‡</sup> ; 100 <sup>††</sup>	6% <sup>‡</sup> ; 5% <sup>†</sup>	27%	Clapham and Wilderspin, 2001; <sup>††</sup> Reeves <i>et al.</i> , 1987
PDE4	9.65; 32.2 <sup>††</sup>	92; 34% <sup>††</sup>	28.72; 29% <sup>††</sup>	25%	1.39; 3 <sup>††</sup> ; 0.18 <sup>††</sup>	12% <sup>††</sup>	1.12	Clapham and Wilderspin, 2001; <sup>††</sup> Richter <i>et al.</i> , 2001a
PDE5	8; 22 <sup>†</sup>	NT	[0.3]; 0.8 <sup>†</sup>	NT	480	5% <sup>†</sup>	0.9 <sup>°</sup>	Turko <i>et al.</i> , 1998b; Thomas <i>et al.</i> , 1990a; <sup>†</sup> Turko <i>et al.</i> , 1996; <sup>°</sup> Soderling <i>et al.</i> , 1998
PDE6	NT	NT	0.15	NT	NT	NT	0.38	Soderling <i>et al.</i> , 1998
PDE7	3.81 (7A); 7.37 (7B)	NT	>100	>100	>100	>100	42 (7A); 9 (7B)	Gardner <i>et al.</i> , 2000; Hetman <i>et al.</i> , 2000
PDE8	>200 <sup>°</sup>	>100	>100 <sup>°</sup>	NT	>200 <sup>°</sup>	>100 <sup>°</sup>	4.5 <sup>°</sup>	<sup>°</sup> Soderling <i>et al.</i> , 1998; Fisher <i>et al.</i> , 1998
PDE9	>100	>100	35	NT	>100	>100	>38	Fisher <i>et al.</i> , 1998b; Soderling <i>et al.</i> , 1998
PDE10	17 [11]	77 [73]	22 [14]	NT	>100 [>100]	>100 [>100]	1.2 [0.45]	Fujishige <i>et al.</i> , 1999
PDE11	50	NT	12	NT	>100	NT	0.37	Fawcett <i>et al.</i> , 2000

<sup>‡</sup> % inhibition of cAMP hydrolysis in the presence of 10-20μM inhibitors (Tang *et al.*, 1997). NT = Not Tested

## 6.2 Background and aims of the present work

### 6.2.1 Background

The soluble recombinant enzyme expressed using the bacterial expression system did not yield measurable activity (Chapter 4). The majority of the enzyme was sequestered into inclusion bodies and purification of this insoluble form of the enzyme required denaturing conditions (8M urea) resulting in the loss of any PDE activity. The Semliki Forest virus expression system, on the other hand, did yield a soluble, active recombinant PDE1A1 enzyme (Chapter 5). As already discussed in Chapter 5, two of the PDE1A1 constructs showed cAMP and cGMP hydrolysing activity: the full-length PDE1A1 (FL4) and the N-terminal truncated PDE1A1 (End6) enzymes. Kinetic analysis was therefore carried out on both these constructs. Crude samples (cleared total cell lysates) of both enzymes were used and these were diluted four-fold for kinetic analysis using cAMP and cGMP as the substrates. These dilutions were used following initial studies on cyclic nucleotide specificity as described in Chapter 5 (section 5.5.9; Figure 5.27). At these dilutions, background PDE in BHK-21 cells, transfected with just the vector, was undetectable. Kinetic analysis for the determination of  $K_m$  and  $V_{max}$  for both FL4 and End6 was carried out using cAMP and cGMP over the range 0.1 - 10 $\mu$ M. The experiments were performed at least twice with samples run in duplicate for each experiment.

Inhibitor studies for the present work were carried out on FL4 and End6 using both cAMP and cGMP. Substrate concentration was kept constant at 0.25 $\mu$ M for both substrates. The experiments were carried out at least twice for each inhibitor with the samples run in duplicate in each experiment. The inhibitors used for this study were Vinpocetine, Zaprinast, EHNA, Amrinone, Rolipram and IBMX. These were reconstituted using DMSO to give a stock concentration of 20mM for Vinpocetine and Zaprinast, and 10 mM for the remaining inhibitors. These were further diluted in DMSO or 50mM HEPES pH 7.5 buffer as required for the assays. The range of inhibitors used was from 0 $\mu$ M - 400 $\mu$ M final concentration.

## 6.2.2 Aims

- ▶ Kinetic analysis of FL4 and End6 enzymes.
- ▶ Exploration of the effect of the N-terminal truncation on substrate affinity and specificity.
- ▶ Exploration of the effect of the N-terminal truncation on inhibitor sensitivity.
- ▶ Exploration of the unexpected FL4 and End6 sensitivity to rolipram.

### **6.3 Materials**

The PDE assay reagents together with the PDE inhibitors have already been described in Chapter 2.

### **6.4 Methods**

#### **6.4.1 Determination of the linear range of reaction of cAMP and cGMP hydrolysis by FL4 and End6**

PDE activity assays were carried out for both FL4 and End6 enzymes over the incubation period of 5 minutes to 30 minutes to examine the cAMP and cGMP hydrolysis by the recombinant enzymes. Assays were carried out as described in section 2.2.11 but were stopped after 5, 10, 15, 20 and 30 minutes of incubation at 30°C. The velocity (V) was calculated in moles/min/assay and plotted against time using GraphPad Prism program to determine the linear range of the reaction.

#### **6.4.2 Determination of the kinetic parameters of FL4 and End6**

PDE activity assays for the determination of the kinetic parameters for FL4 and End6 were carried out on the enzymes produced from a single infection of BHK-21 cells with the recombinant virus from a large-scale expression (75cm<sup>2</sup> flasks) as described in section 5.4.11. The  $K_m$  and  $V_{max}$  values were calculated from data obtained from the PDE assays carried out for FL4 and End6 using a range of substrate concentrations. Both cAMP and cGMP master mixtures were prepared as described in section 2.2.11, containing the labelled tritiated substrates (<sup>3</sup>H-cAMP or <sup>3</sup>H-cGMP), but not containing the unlabelled substrate. The unlabelled substrate was added to reaction tubes to give a range of final, total, substrate concentration of between 0.1μM - 10μM. The labelled substrate was therefore kept constant. Assays were carried out at least twice with samples analysed in duplicate in each assay. The initial velocity (V), or rate, was calculated for the samples as moles/minute/mg protein and plotted against the substrate concentration (μM) for a direct linear plot using the SigmaPlot software program which was a dedicated enzyme kinetic analysis computer program. This software was also used to plot reciprocals of the velocity (1/V) against

substrate concentration ( $1/S$ ) for a Lineweaver-Burk plot to determine the  $K_m$  and  $V_{max}$  values for FL4 and End6 using both cAMP and cGMP. The protein concentration of the samples was estimated as described in section 6.4.3 and these values used for the calculation of the initial velocity,  $V$ , in nmol/min/mg protein.

For the measurement of  $IC_{50}$  values, cAMP and cGMP master mixtures were prepared containing a constant, total, substrate concentration of  $0.25\mu\text{M}$  (included both the labelled and unlabelled substrates) as described in section 2.2.11. Individual PDE inhibitors were added to reaction tubes for the assay. The range of inhibitor concentrations used was from 0 -  $800\mu\text{M}$ . All of the assays were carried out at least three times with samples analysed in duplicate in each assay. To examine the effect of DMSO on recombinant PDE activity, assays were also carried out using up to 2.5% DMSO in the reaction mixture. DMSO was used to prepare the stock PDE inhibitors and these were used for the inhibitor study at final DMSO percentages of 1% or below in the reaction mixture.

#### **6.4.3 Estimation of PDE1A1 protein concentration in total cell lysate samples**

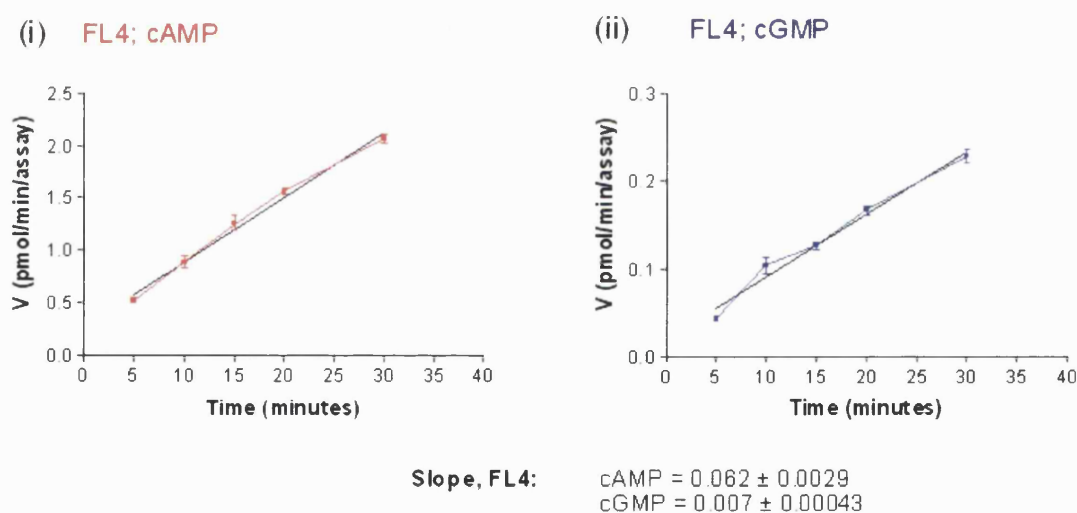
An estimation of the PDE protein concentration for the two crude recombinant enzymes, FL4 and End6, was made from comparisons of the Western blot signals for these enzymes using the Western blot signal obtained for suitably diluted purified bacterial recombinant enzyme His<sub>6</sub>-PDE1A1<sub>N-trunc</sub> (Chapter 4). The protein concentration of this purified enzyme was measured using the Bradford assay and found to be  $0.1\text{mg/ml}$  (see section 2.2.14).  $10\mu\text{l}$  of each of the enzymes were analysed by SDS PAGE analysis for staining with Coomassie stain as well as Western blot analysis using polyclonal calmodulin-PDE as the primary antibody (section 2.2.12 and 2.2.14 respectively). The estimated protein concentrations of PDE1A1 in FL4 and End6 samples were used to determine  $V_{max}$  values relative to the recombinant enzymes produced in the present work.



## 6.5 Results

### 6.5.1 Time-course study on FL4 and End6

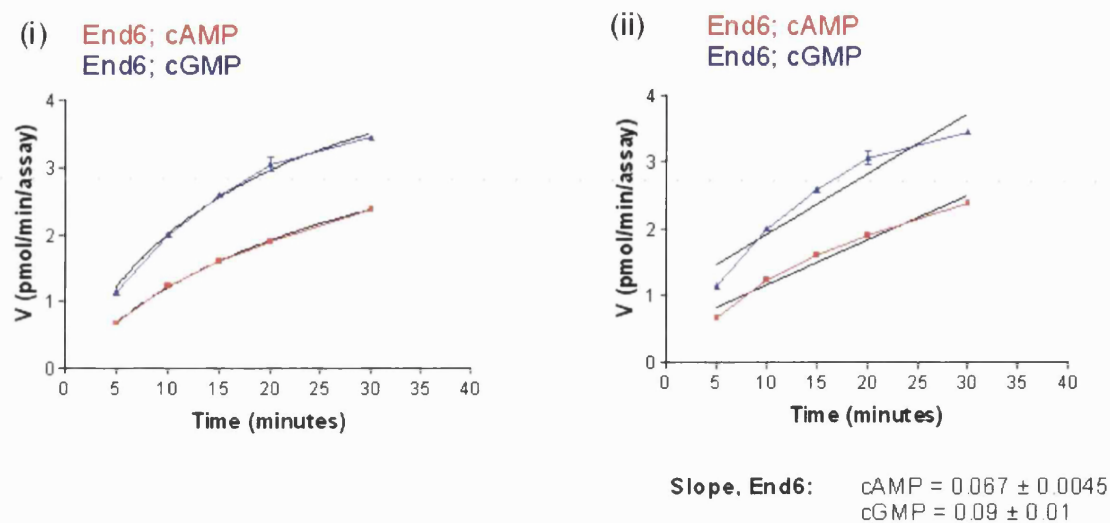
Hydrolysis of cAMP and cGMP by FL4 and End6 was determined for up to 30 minutes of incubation of the recombinant enzymes with the substrate as described in section 6.4.1. The GraphPad Prism program was used to plot the velocity (V; pmol/min/assay) against time. Linear regression analysis was used to determine the slope of the hydrolysis reactions as a guide to the rate of hydrolysis of cAMP and cGMP by FL4 and End6. Figure 6.1.1 shows the results for the cAMP and cGMP hydrolysis by FL4. These indicated that at 0.25 $\mu$ M substrate concentration, FL4 had a very much slower rate of hydrolysis of cGMP (0.007pmol/min/assay) compared to cAMP (0.062pmol/min/assay) as indicated by the slopes of the graphs in Figure 6.1.1.



**Figure 6.1.1** Time course study on FL4. PDE activity assays carried out for cleared total cell lysate FL4 samples in duplicate using cAMP (i) and cGMP (ii) as substrates. Reactions were stopped after 5, 10, 15, 20 and thirty minutes. The solid black lines represent Linear regression analysis carried out using the GraphPad Prism program.

Figure 6.1.2 shows the results for the hydrolysis of cAMP and cGMP by End6 for up to 30 minutes. Figure 6.1.2 (i) represents the velocity plotted against time for both substrates, while Figure 6.1.2 (ii) shows these results together with the linear regression analysis (black line) carried out using GraphPad Prism to obtain a result for the slope. These showed that End6 hydrolysed cGMP at a higher rate (0.09pmol/min/assay) compared to cAMP (0.067

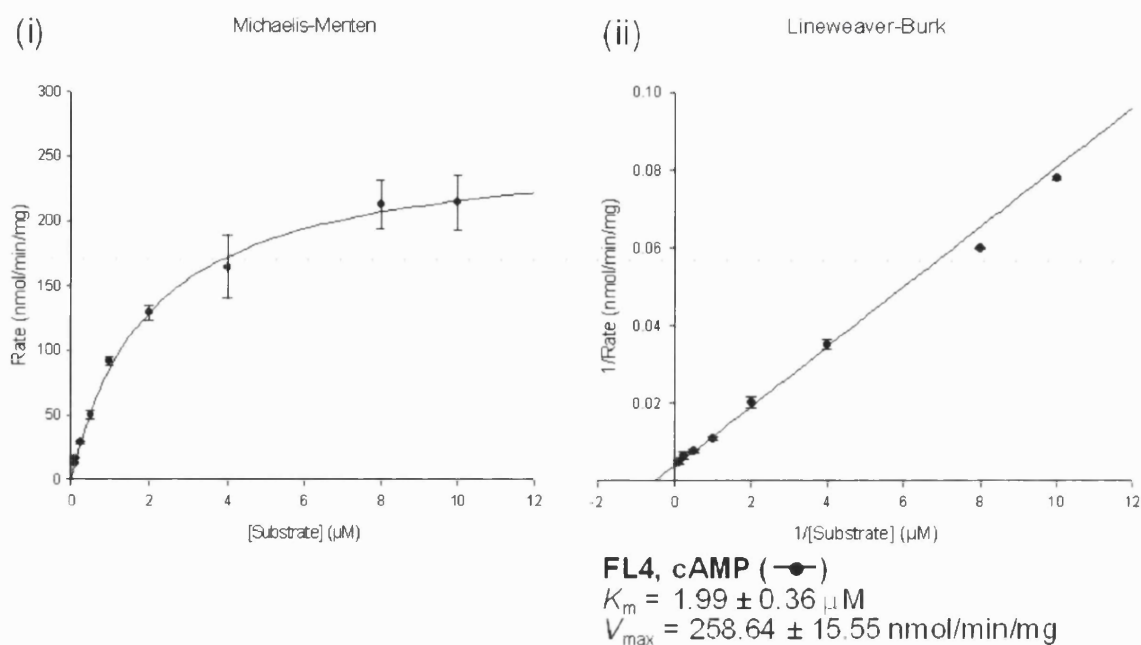
pmol/min/assay); converse was true for FL4.



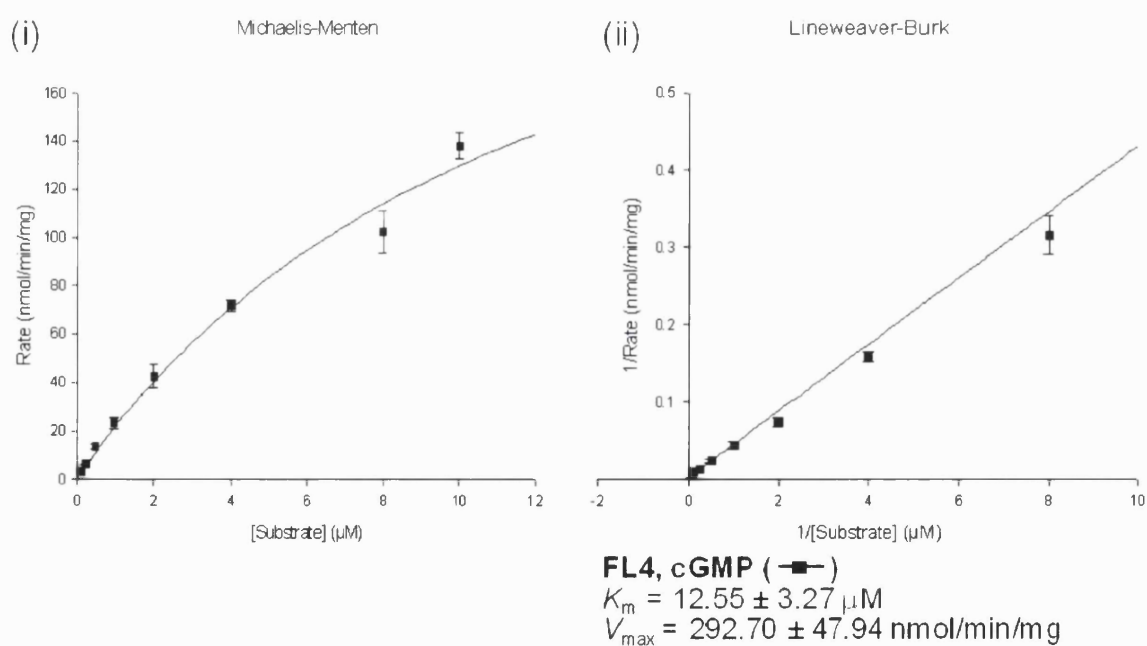
**Figure 6.1.2** Time course study on End6. PDE activity assays carried out for cleared total cell lysate End6 samples in duplicate using cAMP and cGMP as substrates. Reactions were stopped after 5, 10, 15, 20 and thirty minutes. (i) represents results for End6 using cAMP (red) and cGMP (blue) analysed using GraphPad Prism program for the best-fit curve. (ii) represents linear regression analysis results (solid black lines) carried out using the GraphPad Prism program which was used to calculate the slopes of the results.

### 6.5.2 Determination of the $K_m$ and $V_{max}$ values for the full-length (FL4) and N-terminal truncated (End6) enzymes

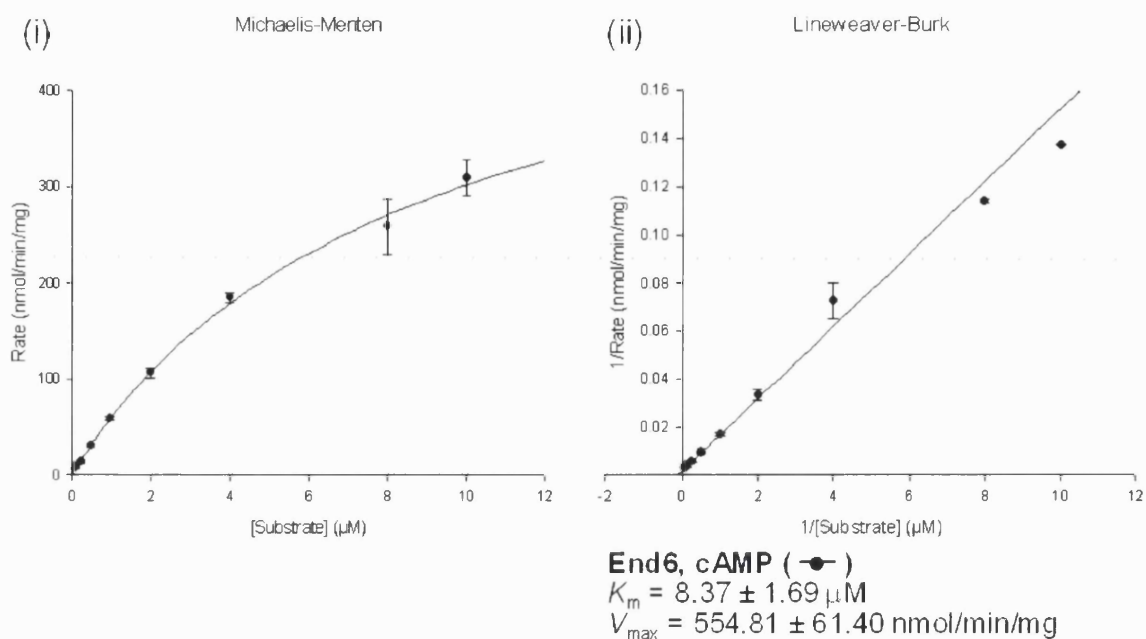
The velocity ( $V$ ), or rate, for both FL4 and End6 was calculated as moles per minute per milligram protein and plotted against substrate concentration ( $S$ ;  $\mu\text{M}$ ). Figure 6.2.1(i) shows the direct linear plot (Michaelis-Menten) for FL4 using cAMP while Figure 6.2.1 (ii) shows the reciprocal of velocity, or rate, against substrate concentration to represent Lineweaver-Burk plots. Figure 6.2.2 shows the results for FL4 using cGMP as the substrate as a direct linear plot (i) as well as a Lineweaver-Burk plot (ii). Figure 6.3.1 and 6.3.2 shows the direct linear (i) and reciprocal (ii) plots for End6. The  $K_m$  values for both enzymes, using cAMP and cGMP as substrates, are indicated on these graphs.  $V_{max}$  was calculated as nmol/min/mg protein using estimates of the concentration of the recombinant enzyme as described in section 6.4.3. Concentration of FL4 was estimated as 0.0125mg/ml and that for End6 as 0.025mg/ml. Table 6.4.1 summarises the  $K_m$  and  $V_{max}$  values obtained for FL4 and End6 while Table 6.4.2 shows the values obtained for the native full-length dog heart PDE1A by Clapham and Wilderspin (2001).



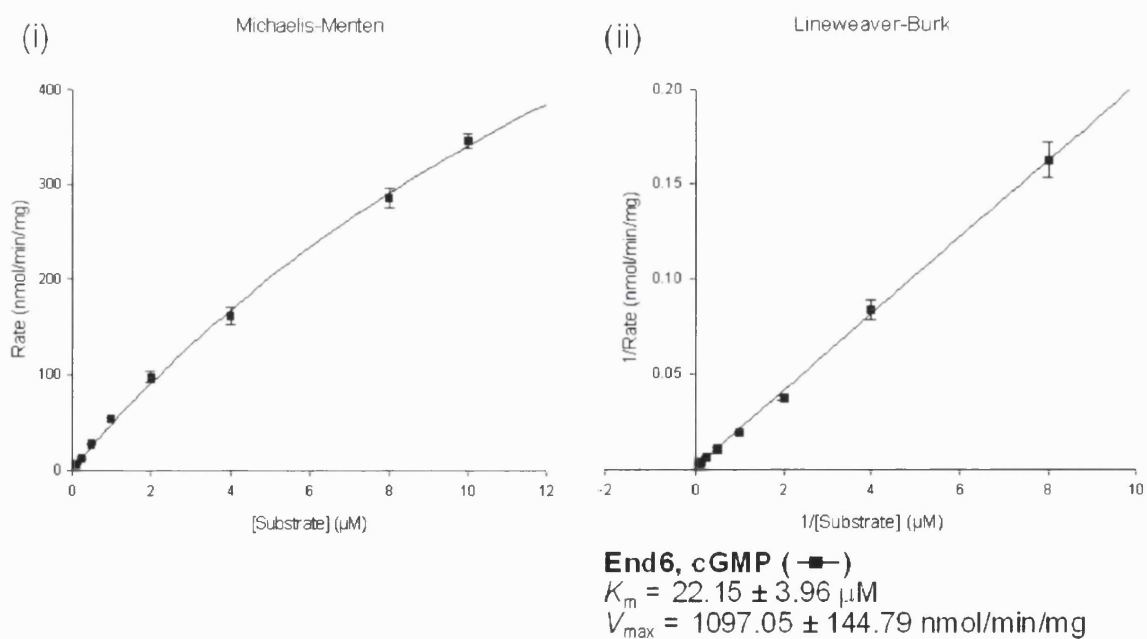
**Figure 6.2.1** Determination of  $K_m$  value for FL4 using cAMP as the substrate. Data was analysed using the SigmaPlot enzyme kinetic analysis software for the determination of  $K_m$  and  $V_{\text{max}}$  values as described in section 6.5.2. Results represent means of at least two experiments with samples analysed in duplicate in each experiment.



**Figure 6.2.2** Determination of  $K_m$  value for FL4 using cGMP as the substrate. Data was analysed using the SigmaPlot enzyme kinetic analysis software for the determination of  $K_m$  and  $V_{\text{max}}$  values as described in section 6.5.2. Results represent means of at least two experiments with samples analysed in duplicate in each experiment.



**Figure 6.3.1** Determination of  $K_m$  value for End6 using cAMP as the substrate. Data was analysed using the SigmaPlot enzyme kinetic analysis software for the determination of  $K_m$  and  $V_{\text{max}}$  values as described in section 6.5.2. Results represent means of at least two experiments with samples analysed in duplicate in each experiment.



**Figure 6.3.2** Determination of  $K_m$  value for End6 using cGMP as the substrate. Data was analysed using the SigmaPlot enzyme kinetic analysis software for the determination of  $K_m$  and  $V_{\text{max}}$  values as described in section 6.5.2. Results represent means of at least two experiments with samples analysed in duplicate in each experiment.

**Table 6.4.1** Summary of the  $K_m$  and  $V_{max}$  values for the full-length (FL4) and N-terminal truncated (End6) PDE1A1 enzymes obtained in the present study.

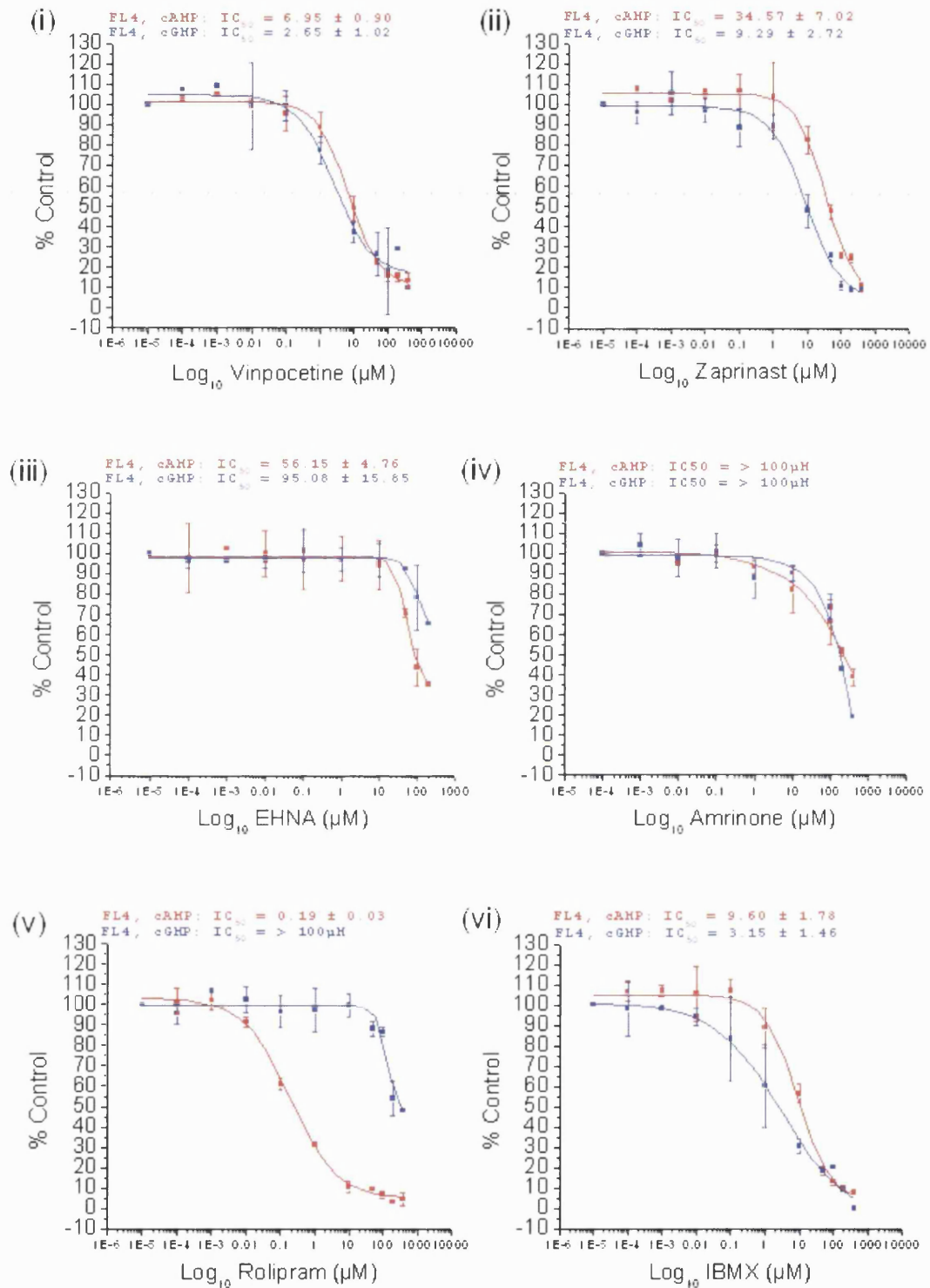
Construct	cAMP		cGMP	
	$K_m$ ( $\mu\text{M}$ )	$V_{max}$ (nmol/min/mg)	$K_m$ ( $\mu\text{M}$ )	$V_{max}$ (nmol/min/mg)
FL4	1.99 $\pm$ 0.36	259 $\pm$ 16	12.55 $\pm$ 3.27	293 $\pm$ 48
End6	8.37 $\pm$ 1.69	555 $\pm$ 61	22.15 $\pm$ 3.96	1097 $\pm$ 145

**Table 6.4.2**  $K_m$  and  $V_{max}$  values for the full-length native dog heart PDE1A obtained by Clapham and Wilderpsin (2001).

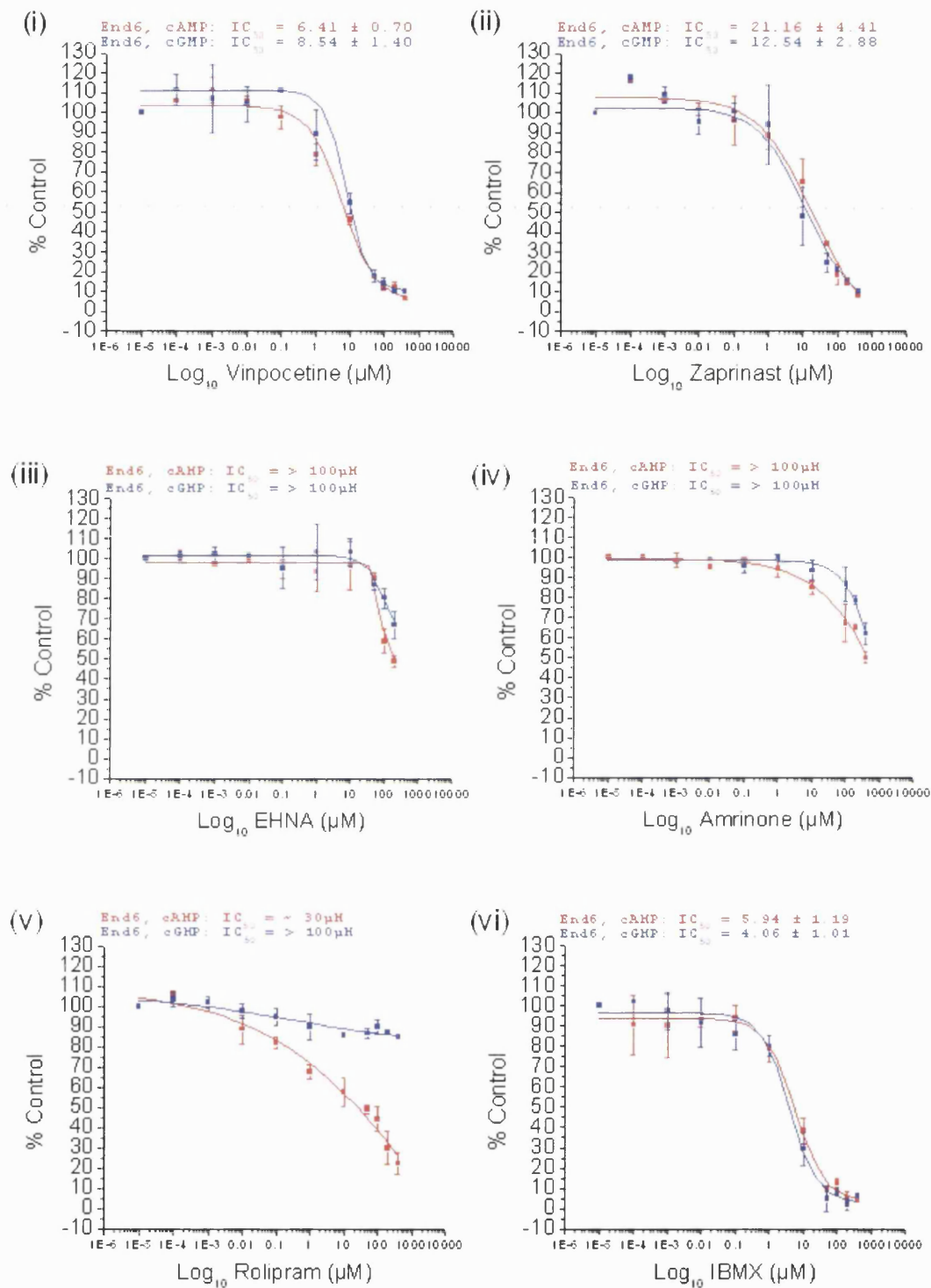
Enzyme	cAMP		cGMP	
	$K_m$ ( $\mu\text{M}$ )	$V_{max}$ (nmol/min/mg)	$K_m$ ( $\mu\text{M}$ )	$V_{max}$ (nmol/min/mg)
Full-length native dog heart PDE1A	1.2	283	0.53	146

### 6.5.3 Inhibitor studies on the full-length (FL4) and N-terminal truncated (End6) enzymes

Inhibitor study results are represented as a percentage of the total PDE activity for each PDE inhibitor used, for both cAMP and cGMP substrates. Figure 6.4 (i - vi) shows the results for the effect of inhibitors on FL4 activity using cAMP and cGMP as substrates. The graphs also indicate the  $IC_{50}$  value for each inhibitor. Figure 6.5 (i - vi) shows the effect of inhibitors on End6 activity. Again, both cAMP and cGMP were used as substrates (0.25 $\mu\text{M}$ ) and the  $IC_{50}$  values are indicated on these graphs. Table 6.5.1 summarises the  $IC_{50}$  values for FL4 and End6. Table 6.5.2 summarises the  $IC_{50}$  values obtained for the full-length native dog heart PDE1A for comparison with the recombinant PDE1A1 enzymes (FL4 and End6) analysed in the present work.



**Figure 6.4** The effect of inhibitors on FL4 activity using cAMP and cGMP as substrates. PDE activity results are shown as a percentage of the basal (uninhibited) activity. Data represents the mean of at least two experiments with samples analysed in duplicate in each experiment.



**Figure 6.5** The effect of inhibitors on End6 activity using cAMP and cGMP as substrates. PDE activity results are shown as a percentage of the basal (uninhibited) activity. Data represents the mean of at least two experiments with samples analysed in duplicate in each experiment.

The results of the inhibitor study are summarised in Table 6.5.1 while results for the native dog heart PDE1A are shown in Table 6.5.2 for comparison. Both FL4 and End6 enzymes showed a similar inhibitor sensitivity profile to the native dog heart PDE1A with one notable exception. Both recombinant enzymes displayed an unexpected and unusual sensitivity to the PDE4-specific inhibitor rolipram. This finding was explored further in section 6.5.4. The full-length recombinant enzyme, FL4, also showed a reduced sensitivity to the PDE1-specific inhibitor vinpocetine, and also to the PDE1/5-specific inhibitor zaprinast relative to the native enzyme.

**Table 6.5.1** Summary of the IC<sub>50</sub> values for the full-length (FL4) and N-terminal truncated (End6) PDE1A1 enzymes.

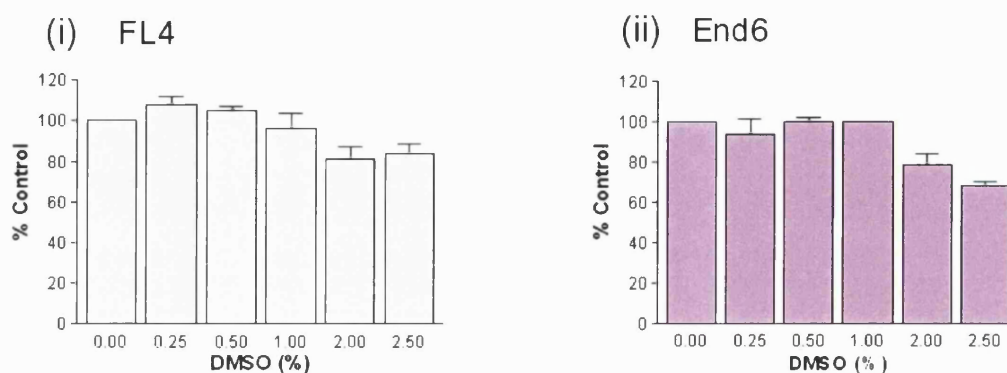
Inhibitor	IC <sub>50</sub> for FL4 (μM)		IC <sub>50</sub> for End6 (μM)	
	cAMP	cGMP	cAMP	cGMP
Vinpocetine	6.95 ± 0.90	2.65 ± 1.02	6.41 ± 0.70	8.54 ± 1.40
Zaprinast	34.57 ± 7.02	9.29 ± 2.72	21.16 ± 4.41	12.54 ± 2.88
EHNA	56.15 ± 4.76	95.08 ± 15.85	>100	>100
Amrinone	>100	>100	>100	>100
Rolipram	0.19 ± 0.03	>100	~30	>100
IBMX	9.6 ± 1.78	3.15 ± 1.46	5.94 ± 1.19	4.06 ± 1.01

**Table 6.5.2** IC<sub>50</sub> values obtained for the native dog heart PDE1A by Clapham and Wilderspin (2001).

Inhibitor	IC <sub>50</sub> (μM) for full-length native PDE1A using cAMP as the substrate
Vinpocetine	1.38
Zaprinast	1.93
Amrinone	>100
Rolipram	>100
IBMX	16.37



PDE activity assays were also carried out to examine the effect of DMSO on recombinant PDE activity as DMSO was used to prepare the stock PDE inhibitors used in the inhibitor studies. The presence of DMSO up to 2.5% in reaction mixtures for FL4 and End6 was examined and Figure 6.6 shows the results for these.



**Figure 6.6** Effect of DMSO on recombinant PDE activity. Assays were carried out using cAMP as the substrate. Results are shown as a percentage of the control (no DMSO) plotted against the percentage of DMSO in reaction mixtures for FL4 (i) and End6 (ii).

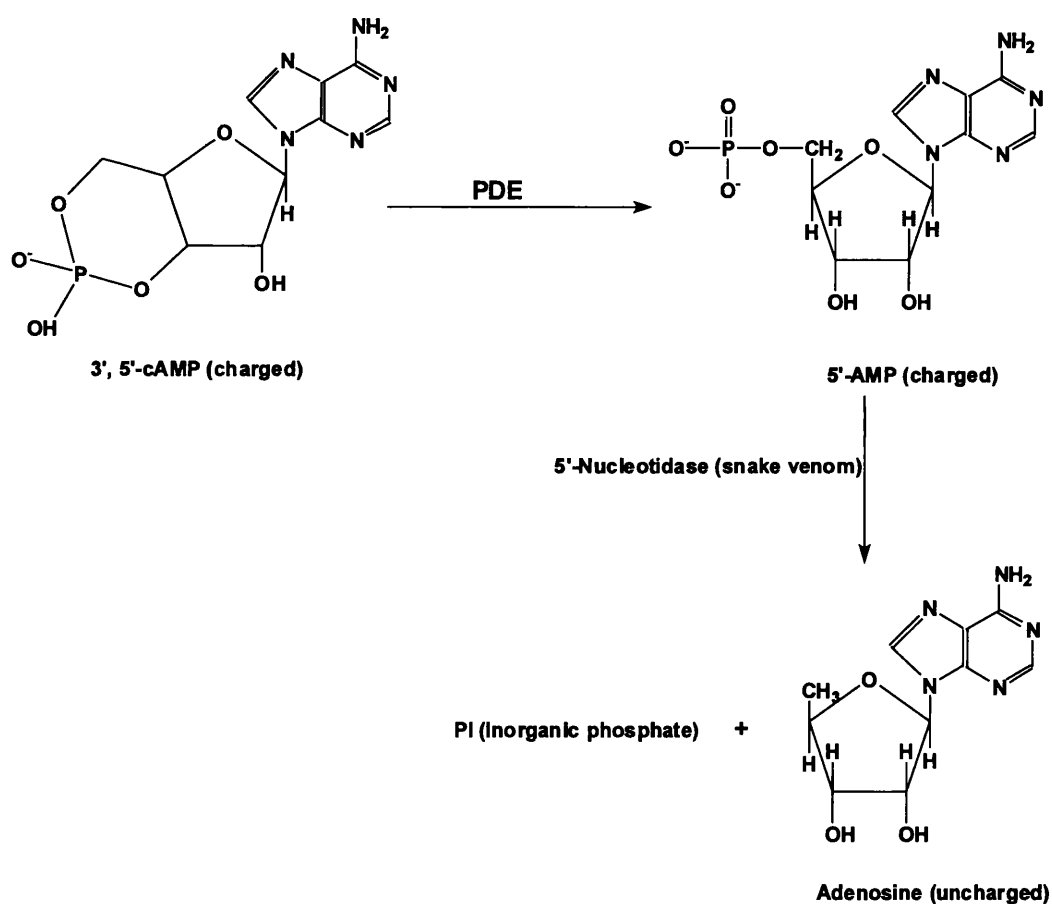
The presence of DMSO in up to 1% had little or no effect on the recombinant PDE activity but there was a reduction in PDE activity when DMSO of 2% or higher was present. However, for the present work, DMSO was present in the assay mixture for up to a maximum of 1% only.

#### 6.5.4 Focus on the FL4 and End6 sensitivity to rolipram

##### 6.5.4.1 PDE activity assays

The full-length (FL4) and N-terminal truncated (End6) enzymes produced in the present study displayed unexpected sensitivity to rolipram when assayed using cAMP as the substrate as described in section 6.5.3. The PDE activity assay was repeated at least three times for both recombinant enzymes for the inhibitor experiments using rolipram with both cAMP and cGMP as substrates. These all confirmed the results already obtained. Also, freshly bought rolipram was used to rule out contamination of the rolipram stock and these again confirmed results already obtained.

The two-step PDE activity assay was then carried out for the rolipram inhibitor study to rule out the possibility of any artefact-interference from the snake venom in the assay mixture. In the one-step assay, which was used throughout in the present work, the assay mixture contained the 5'-nucleotidase (snake venom) which converted the charged product of the PDE hydrolysis, 5'-AMP, into an uncharged adenosine moiety plus inorganic phosphate. The charged product (5'-AMP), as well as the charged, non-hydrolysed, substrate, cAMP, were removed by the anion exchange resin, Dowex, in the assay procedure as described in section 2.2.11. Figure 6.7 shows a schematic of the PDE assay steps involved in the one-step assay procedure.

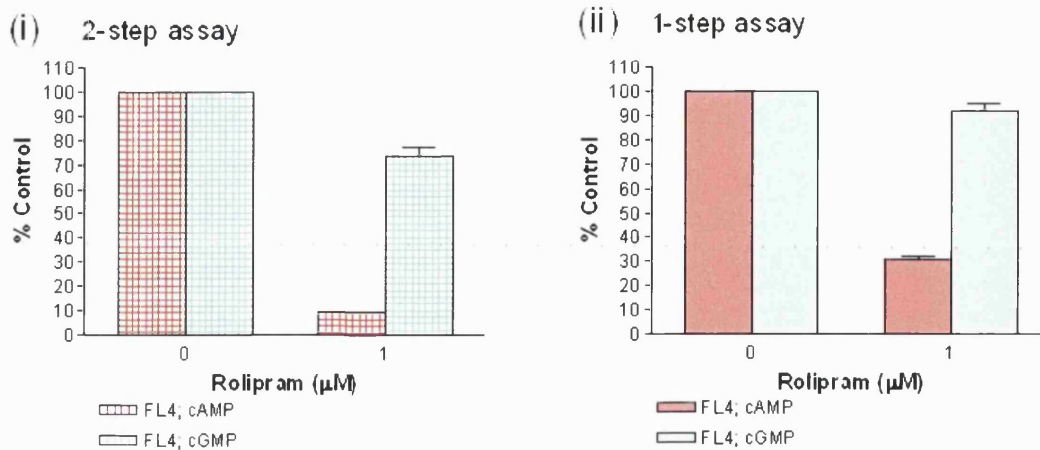


**Figure 6.7** Schematic of the one-step PDE assay.

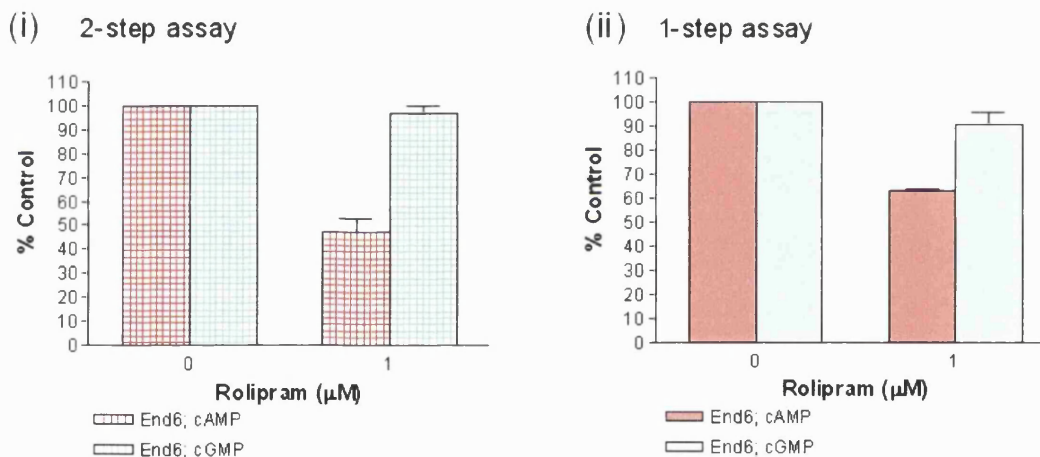
The two-step (2-step) PDE assay involved incubation of the substrate, enzyme and the inhibitor in a reaction mixture without the 5'-nucleotidase. The reaction in this first step was then stopped by boiling the mixture for five minutes followed by the addition of snake venom containing the 5'-nucleotidase (0.01mg). This was incubated for a further 15 minutes at 30°C and the reaction from this second step stopped with 20µl 10% SDS as

usual (see section 2.2.11). The 2-step assay was carried in the absence and presence ( $1\mu\text{M}$ ) of rolipram for both FL4 and End6 using cAMP as well as cGMP as substrates, both at  $0.25\mu\text{M}$  concentration.

Figures 6.8.1 and 6.8.2 show the results of the two-step assay for FL4 and End6 respectively, together with the results obtained using the one-step assay (section 6.5.3). These results showed that rolipram inhibition of FL4 in the presence of cAMP was accentuated for FL4 in the 2-step assay (90% inhibition) (Figure 6.8.1 (i); hatched bars shown in pink) compared to inhibition exhibited in the 1-step assay (70%) (Figure 6.8.1 (ii); solid bars shown in pink). The inhibition observed for FL4 when cGMP was used as the substrate again showed a similar increase in sensitivity to rolipram in the 2-step assay (25% inhibition) (Figure 6.8.1 (i); hatched bars shown in blue) compared to the 1-step assay (10%) (Figure 6.8.1 (ii); solid bars shown in blue). The fact that there was a difference in inhibition between the 2-step and 1-step assay suggests that some of the rolipram in the 1-step assay may be bound to proteins in the snake venom and was therefore unavailable during the 1-step assay. If this was the case, then the results for End6 rolipram-inhibition in the 2-step assay would also have been expected to show similar to FL4. Indeed the rolipram inhibition of End6 in the 2-step assay did show a small increase in the inhibition for the 2-step assay (50% inhibition) (Figure 6.8.2 (i); hatched bars shown in pink) compared to the inhibition seen in the 1-step assay (40%) (Figure 6.8.1 (i); solid bars shown in pink) with cAMP as the substrate. The inhibition of End6 by rolipram when cGMP was used as the substrate does not show a significant difference in rolipram sensitivity between the 2-step and the 1-step assay (Figure 6.8.2; blue bars). Also, as Figure 6.5 (v) showed, the inhibition of End6 activity in the presence of increasing concentrations of rolipram showed a gradual inhibition of the enzyme as opposed to the steeper drop in activity, as observed for FL4 (Figure 6.4 (v)), for both cAMP and cGMP substrates. The 2-step assay for both FL4 and End6 can be explored further using higher concentrations of rolipram (up to  $400\mu\text{M}$ ) in future work on these constructs.



**Figure 6.8.1** Rolipram inhibition of FL4 using the two-step PDE assay. Assays were carried out using both cAMP and cGMP in the absence and presence (1 μM) of rolipram. Results for the 1-step PDE assay are also shown (ii) for comparison.

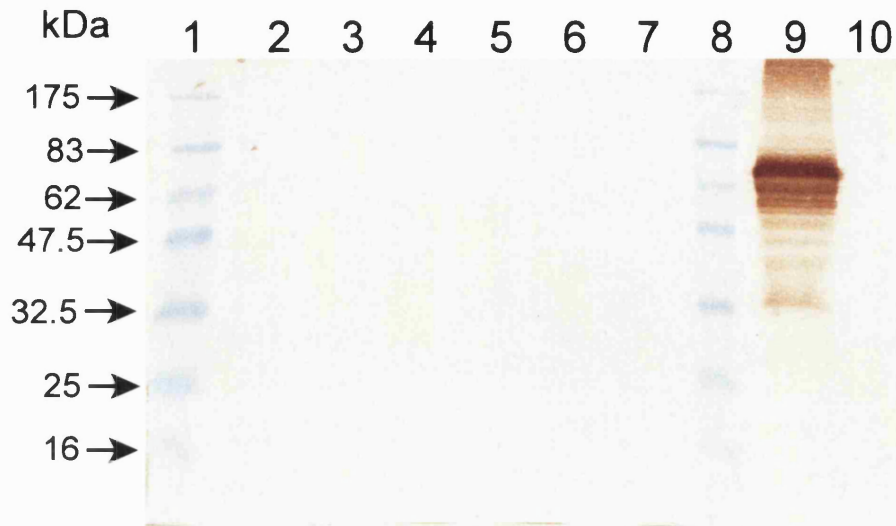


**Figure 6.8.2** Rolipram inhibition of End6 using the two-step PDE assay. Assays were carried out using both cAMP and cGMP in the absence and presence (1 μM) of rolipram. Results for the 1-step PDE assay are also shown (ii) for comparison.

#### 6.5.4.2 Immunoblot to demonstrate the absence of PDE4 in FL4 and End6 samples

Western blot analysis of FL4 and End6 was carried out using polyclonal PDE4 antibody to demonstrate the presence, if any, of endogenous or contaminating PDE4 enzyme as described in section 2.2.14. If there was background PDE4 present in either the uninfected BHK-21 cells or cells transfected with the empty vector, it may have been possible that the PDE4 was forming associations (dimers or tetramers) with the recombinant FL4 and End6 in cells infected with the recombinant virus. Studies to determine the native state of these

enzymes had already shown that both recombinant enzymes tended to form tetrameric units (see section 5.5.7). Figure 6.9.1 shows the results for the Western blot analysis carried out using PDE4 antibody, while Figure 6.9.2 shows the same samples run in parallel but analysed using CaM-PDE antibody. Samples analysed using PDE4 antibody (Figure 6.9.1) did not show a positive signal for the presence of any PDE4 in the four PDE1A1 constructs (FL4, G2, End6, Cat9) analysed nor in the controls for BHK-21 cells infected with the empty vector, and the uninfected BHK-21 cells. It does show a positive signal for the PDE4 enzyme as expected (Figure 6.9.1; Lane 9). Figure 6.9.2 shows the expected signals for FL4 (57 kDa), G2 (53 kDa), End6 (44 kDa) and a very faint signal for Cat9 (40 kDa) and no signal for PDE4 protein (Lane 9). These results therefore rule out the possibility of contamination of FL4 and End6 enzymes by PDE4 enzymes.



**Figure 6.9.1** Western blot analysis of FL4 and End6 using polyclonal PDE4 antibody.

Analysis was carried out on cleared total cell lysate samples. Lanes 1 and 8 = pre-stained protein marker mixture; Lane 2 = FL4 (full-length enzyme); Lane 3 = G2 (C-terminal truncated construct); Lane 4 = End6 (N-terminal truncated enzyme); Lane 5 = Cat9 (N- and C-terminal truncated construct); Lane 6 = vector, pSFV1; Lane 7 = uninfected BHK-21 cells; lane 9 = PDE4 enzyme as the positive control.



**Figure 6.9.2** Western blot analysis of FL4 and End6 using polyclonal CaM-PDE antibody.

Lane 1 = pre-stained protein marker mixture; Lane 2 = FL4; Lane 3 = G2 (C-terminal truncated construct); Lane 4 = End6; Lane 5 = Cat9 (N- and C-terminal truncated construct); Lane 6 = vector, pSFV1; Lane 7 = uninfected BHK-21 cells; Lane 8 = in-house protein marker mixture ( $\beta$ -gal, BSA, ovalbumin); lane 9 = PDE4 enzyme.

## 6.6 Discussion

### 6.6.1 Kinetic analysis of FL4 and End6 for the determination of $K_m$ and $V_{max}$

Kinetic analysis to determine the  $K_m$  and  $V_{max}$  values for FL4 and End6 enzymes was carried out using both cAMP and cGMP as substrates as described in section 6.4.2. Table 6.4.1 shows the summary of these values while Table 6.4.2 represents the values obtained for the purified native dog heart PDE1A by Clapham and Wilderspin (2001). FL4 (full-length) enzyme in the present study, gave a  $K_m$  value ( $1.99\mu\text{M}$ ) which was comparable to the native dog heart enzyme ( $1.2\mu\text{M}$ ) for cAMP as the substrate. The  $K_m$  value obtained for cGMP as the substrate was, however, higher for FL4 ( $12.55\mu\text{M}$ ) than for the native enzyme ( $0.53\mu\text{M}$ ). The reason for this variation may be due to the fact that FL4 was not a pure preparation so the presence of other cyclic nucleotide binding proteins may have contributed to this difference by modifying the effective cAMP or cGMP concentration in the assay. The N-terminal truncated construct, End6, showed increased values for  $K_m$  for both cAMP ( $8.37\mu\text{M}$ ) and cGMP ( $22.15\mu\text{M}$ ) compared to the full-length enzyme, FL4.

There are a number of studies on PDE3 and PDE4 truncated mutants which have indicated that most N-terminal truncations demonstrate dramatic increases in the  $V_{max}$  values of the mutant enzymes (see Table 6.6). This was certainly the case in the present study where End6 displayed higher  $V_{max}$  values for the hydrolysis of both cAMP ( $555\text{ nmol/min/mg}$ ) and cGMP ( $1097\text{ nmol/min/mg}$ ) compared to FL4 ( $259$  and  $293\text{ nmol/min/mg}$  for cAMP and cGMP respectively). End6 also hydrolysed cGMP preferentially over cAMP. Tang and co-workers (1997) produced N-terminal truncated PDE2 mutants and found that the mutants hydrolysed cGMP preferentially over cAMP ( $V_{max}(\text{cGMP})/V_{max}(\text{cAMP}) = 0.49$ ) compared to the full-length PDE2 ( $V_{max}(\text{cGMP})/V_{max}(\text{cAMP}) = 0.16$ ). Limited proteolysis studies of PDE1A2 enzyme using trypsin or chymotrypsin have also given catalytically active fragments which displayed a 2-3 fold higher activity than the  $\text{Ca}^{2+}/\text{CaM}$ -stimulated full-length enzyme (Charbonneau *et al.*, 1991; Yuan *et al.*, 1999). The results of the present study do indicate that the N-terminal mutant hydrolysed cGMP preferentially over cAMP ( $V_{max}(\text{cGMP})/V_{max}(\text{cAMP}) = 1.98$ ) compared to the full-length enzyme ( $V_{max}(\text{cGMP})/V_{max}(\text{cAMP}) = 1.13$ ).

**Table 6.6** Comparison of the kinetic parameters of PDE enzymes.

Study	cAMP or cGMP $V_{max}$ (nmol/min/mg) for construct: [ $K_m$ ( $\mu$ M)]			
	Full-length	C-terminal truncated	N-terminal truncated	N- and C-terminal truncated
Present study (PDE1A1)	cAMP: 259 [1.99] cGMP: 293 [12.55]	-	cAMP: 555 [8.37] cGMP: 1097 [22.15]	-
Clapham and Wilderspin, 2001 (PDE1A)	cAMP: 283 [1.2] cGMP: 146 [0.53]	-	-	-
Sonnenburg <i>et al.</i> , 1995 (PDE1A1)*	cGMP: 216 [3.5]	-	$\Delta$ M1 mutant: 320 [5.2] $\Delta$ M5 mutant: 201 [3.7]	-
Jin <i>et al.</i> , 1992 (PDE3)	cAMP: 0.36 [2.84]	cAMP: 0.24 [3.73]	cAMP: 1.04 [2.36]	-
Kovala <i>et al.</i> , 1997 (PDE4D1)	cAMP: 318 [5.2]	cAMP: 146 [3.2]	cAMP: 1325 [2.8]	cAMP: 1360 [1.8]
Jacobitz <i>et al.</i> , 1996 (PDE4A)	cAMP: 2.9 [10]	-	cAMP: 6.3 [3.0]	cAMP: 2.8 [6.0]
Richter <i>et al.</i> , 2000 (PDE4A)	cAMP: 5610 [3.09]	-	cAMP: 6170 [5.16]	cAMP: 9430 [4.28]

\*  $\Delta$ M1 mutant = PDE1A1 lacking the first of the two calmodulin-binding domains while  $\Delta$ M5 mutant = PDE1A1 lacking the first calmodulin-binding domain as well as the stretch of inhibitory amino acids said to be important in retaining the enzymes in a less active state (Sonnenburg *et al.*, 1995).

The increased hydrolysis of cAMP, and especially cGMP, observed for the N-truncated enzyme, End6, in the present study is not without precedent as indicated by N-terminal truncation studies on PDE3 (Jin *et al.*, 1992), PDE4D (Kovala *et al.*, 1997) and PDE4A (Jacobitz *et al.*, 1996) which all showed a two- to three-fold increase in  $V_{max}$  in the mutant enzymes (see Table 6.6). Furthermore, Kovala and co-workers (1997) reported a four-fold increase in the  $V_{max}$  for their N-terminal truncated PDE4D1. End6 in the present study showed a similar fold increase for the  $V_{max}$  for cGMP.

Amino-terminal truncations will tend to remove the regulatory regions of the enzymes (see Figure 1.9). In the case of the PDE1 enzymes, the deletion of the amino terminal residues removes the calmodulin-binding domains which are thought to be present in a conformation which prevents complete activation of the full-length enzymes. There is a short sequence of amino acids identified by Sonnenburg and co-workers (1995), located between the two calmodulin-binding domains, which is said to be important for retaining the PDE1A enzymes in a less active state in the absence of  $Ca^{2+}$ /CaM (see Figure 1.19.1). The presence of  $Ca^{2+}$ /CaM usually causes an activation of the enzyme through binding of the calmodulin



to the amino terminal domains in the presence of calcium ions. In the truncation studies carried out by Sonnenburg and co-workers (1995) on PDE1A2 enzymes, their N-terminal construct, lacking the amino acid residues 4-46 (encompassing the first of the two calmodulin-binding domains), produced a mutant which was still stimulated in the presence of  $\text{Ca}^{2+}/\text{CaM}$ . This mutant still had the stretch of amino acids at the amino terminal, which were identified by the same workers (1995) as being important in maintaining the enzymes in a less active state, as well as the second calmodulin-binding domain also identified in their study.  $\text{Ca}^{2+}/\text{CaM}$ -independent activity was only seen in the constructs lacking the first calmodulin-binding domain as well as the stretch of inhibitory amino acids located between the two calmodulin-binding domains. Constructs containing just the second calmodulin-binding domain were therefore not stimulated in the presence of  $\text{Ca}^{2+}/\text{CaM}$ . This would suggest that both calmodulin-binding domains are not necessary for retaining the enzymes in a less active state but that the presence of at least the second domain together with inhibitory amino acids is important in the less active state of the enzymes.

The N-terminal truncated construct, End6, produced in the present study does not contain the two calmodulin-binding domains nor the stretch of inhibitory amino acids, so this construct would be predicted to display  $\text{Ca}^{2+}/\text{CaM}$ -independent activity, which was indeed found in the present study (see Figure 5.28.2). The construct also displayed a higher catalytic activity for cGMP hydrolysis (see Table 6.6) which is in contrast to the results obtained by Sonnenburg and co-workers (1995) with their N-terminal truncated PDE1A1 enzymes but in agreement with other workers where cyclic nucleotide hydrolysis was increased in the truncated enzymes (see Table 6.6). However, the PDE1A1 mutants produced by Sonnenburg and co-workers (1995) still had the second calmodulin-binding domain so although this gave  $\text{Ca}^{2+}/\text{CaM}$ -independent enzyme activity, the presence of the calmodulin-binding domain may have had an effect on the conformation of the enzyme and hence the cGMP hydrolytic activity.

The results of the present study indicate that the amino terminal residues are directly involved in the hydrolysis of both substrates, cAMP and cGMP, as denoted by the increased hydrolysis of both substrates for the N-terminal truncated construct, End6. This increase was more notable for cGMP compared to cAMP, as indicated by the  $V_{\max}$  values (see Table 6.4.1), suggesting an important role for the N-terminal residues in the hydrolysis of cGMP.

Further mutagenesis studies are necessary in order to identify amino acid residues involved in this catalytic process. Also, further truncation and mutagenesis studies need to be carried out to determine why the C-terminal truncated and the N- and C-terminal truncated constructs, G2 and Cat9 respectively, did not show any PDE activity despite the detection of the protein by Western blot analysis (see Figures 5.14 and 5.15). Similar truncations carried out on PDE3 and PDE4 enzymes by several workers showed the mutant enzymes to retain PDE activity (see Table 6.6). It was possible that for the PDE1 enzymes, the presence of all or some of the carboxy-terminal residues was important for enzymatic activity since it was the constructs lacking these residues which did not show enzymatic activity.

### **6.6.2 Inhibitor studies on FL4 and End6**

Inhibitor studies were carried out on FL4 and End6 for both cAMP and cGMP substrates as described in section 6.4.2. Table 6.5.1 summarises these results while Table 6.5.2 summarises the results obtained for the purified native dog heart PDE1A for comparison. The inhibitor studies on recombinant FL4 and End6 showed that the enzymes were sensitive to the PDE1- and PDE5-specific inhibitors vinpocetine and zaprinast respectively as well as the non-specific inhibitor IBMX. Both enzymes showed little or no inhibition by the PDE2 and PDE3 inhibitors EHNA and amrinone, respectively, for up to 100 $\mu$ M inhibitors. These results were consistent with the inhibitor sensitivity profile obtained for the native dog heart PDE1A. However, both FL4 and End6 displayed unusual sensitivity to the PDE4-specific inhibitor rolipram when analysed using both cAMP and cGMP as the substrates (see Figures 6.4 (v) and 6.5 (v) for FL4 and End6 respectively). This phenomenon was explored further as described in section 6.5.4. Repeating the rolipram inhibition studies using the same and a fresh batch of the stock inhibitor produced the same results. In addition, variation in the method for the PDE bioassay from the one-step, routinely adopted throughout, to a two-step assay again produced inhibition by rolipram for both enzymes (Figure 6.8); but as already discussed in section 6.5.4.1, the inhibition of FL4 by rolipram was more marked in the 2-step assay compared to the 1-step assay. Western blot analysis on the recombinant enzymes using polyclonal PDE4 antibody confirmed the absence of any contaminating PDE4 enzyme (Figure 6.9.1).

The rolipram sensitivity of FL4 was particularly marked ( $IC_{50} = 0.19\mu\text{M}$ ) when cAMP was used as the substrate but not when cGMP was used as the substrate ( $IC_{50} \geq 100\mu\text{M}$ ), as shown in Figure 6.4 (v). The full-length construct also showed a reduced sensitivity to the PDE1-specific inhibitor vinpocetine and the PDE1/5-specific inhibitor zaprinast compared to the native enzyme (see Table 6.5.2).

End6 also displayed the unusual rolipram inhibition profile when cAMP was the substrate ( $IC_{50} \sim 30\mu\text{M}$ ), while displaying minimal inhibition when cGMP was the substrate, as shown in Figure 6.5 (v). There have been several studies which have examined the effect of N- and/or C-terminal truncations of PDE enzymes on the inhibitor specificity of these enzymes. Table 6.7 summarises some of these studies which were carried out on PDE3, PDE4 and PDE5 enzymes exploring the PDE-specific inhibitor sensitivity on the full-length and truncated constructs. The N-terminal truncation of PDE1A1 in the present study (End6 construct) did not have a significant effect on the vinpocetine sensitivity when cAMP was used as the substrate, but the sensitivity was reduced when cGMP was used as the substrate (see Table 6.7). The same was also true for zaprinast with cGMP as the substrate. Similar results for changes in the inhibitor sensitivities following N-terminal truncations of PDE enzymes have been observed by several workers (see Table 6.7) with reduced inhibitor sensitivity seen for PDE3 (Jin *et al.*, 1992) and PDE4A (Richter *et al.*, 2000; Jacobitz *et al.*, 1996) enzymes. In general, N-terminal truncations reduce the sensitivity to specific inhibitors while C-terminal truncations increase the sensitivity to specific inhibitors. The results of the present study are in agreement with these observations.

**Table 6.7** PDE inhibitor sensitivity of full-length and truncated PDE enzymes.

Study	IC <sub>50</sub> (μM) for cAMP (cGMP)			
	Full-length	C-terminal truncated	N-terminal truncated	N- and C-terminal truncated
Present study (PDE1A1)	Vinpocetine: 6.95 (2.65) Zaprinast: 34.57 (9.29)	-	Vinpocetine: 6.41 (8.54) Zaprinast: 21.16 (12.54)	-
Tang <i>et al.</i> , 1997 (PDE3)	Lixazinone: 53 Milrinone: 474	-	Lixazinone: 165 Milrinone: 1207	-
Jin <i>et al.</i> , 1992 (PDE3)	Milrinone: 7.73	Milrinone: 3.1	Milrinone: 10.9	-
Richter <i>et al.</i> , 2000 (PDE4A)	Rolipram: 0.495	Rolipram: 0.408	Rolipram: 1.272	Rolipram: 1.906
Jacobitz <i>et al.</i> , 1996 (PDE4A)	Rolipram: 325	-	Rolipram: 2050	Rolipram: 1800
Fink <i>et al.</i> , 1999 (PDE5)	IBMX: (20) Sildenafil: (0.0039)	-	-	IBMX: (20) Sildenafil: (0.0040)

The mechanism(s) involved in the inhibition of PDE enzymes by selective inhibitors has not been fully elucidated for the PDE enzymes. Most of the studies on the mechanism of selective-inhibitor binding have been carried out on PDE4 enzymes. Rocque and co-workers (1997) working on full-length and truncated PDE4B enzymes showed that the full-length (1-564) and the N-terminal truncated (81-564) enzymes contained a low- as well as a high-affinity rolipram-binding site within the enzyme. The N- and C-terminal truncated PDE4B (81-528) still displayed high-affinity rolipram-binding, but the construct PDE4B (152-528; catalytic domain only), on the other hand, showed low-affinity rolipram-binding only. These results indicate the involvement of both the N-terminal region and the catalytic domain in the high-affinity rolipram-binding whereas residues in the catalytic domain alone are sufficient for the low-affinity binding. Binding studies using <sup>3</sup>H-Rolipram on full-length and truncated PDE4 enzymes have denoted the presence of a high-affinity rolipram-binding site located at the N-terminal region of the enzymes and a low-affinity rolipram-binding site located within the catalytic domain (Jacobitz *et al.*, 1996). Sette and Conti (1996) obtained rolipram-inhibition results for PDE4D3 which displayed a biphasic curve, with a high-affinity inhibition at 10<sup>-9</sup> M rolipram and a low-affinity inhibition at 10<sup>-6</sup> M rolipram which again was consistent with results of other workers for rolipram-binding

(Rocque *et al.*, 1997b; Jacobitz *et al.*, 1996).

There have been other studies which have looked at the effect of specific amino acid mutations on both substrate affinity and inhibitor sensitivity (Pillai *et al.*, 1993; Atienza *et al.*, 1999; Herman *et al.*, 2000). Pillai and co-workers (1993) introduced single amino acid mutations within the catalytic region of PDE4B1 (Asp,D239Asn,N; Thr,T405Ala,A) and found that the T405A mutant had an increased  $k_m$  but a very much lower  $V_{max}$ , while the mutant D239N had an increased  $V_{max}$ . Both mutants, however, showed an approximately 300-400-fold decrease in rolipram affinity. It is notable that the asparagine residue 239 in PDE4B1 follows the first of two metal-binding motifs which are conserved in all the PDE enzymes (D241 in HSPDE4B2, and D210 in CFPDE1A1; Figure 1.14.2). The equivalent residue was also mutated in studies carried out by Herman and co-workers (2000). In these studies, the mutant D333N in PDE4D3 was, firstly, able to hydrolyse cGMP, and secondly, this mutant was about 10-fold less sensitive to inhibition by rolipram. Interestingly, this mutant showed an increased sensitivity to the PDE3 inhibitor cilostamide ( $IC_{50} > 100\mu M \rightarrow 58.9\mu M$ ) and the PDE1/5 inhibitor zaprinast ( $IC_{50} 72.4\mu M \rightarrow 27.7\mu M$ ). Therefore, it is obvious from these studies that individual amino acids can have a dramatic effect on both substrate affinity and inhibitor sensitivity. In the present study, an examination of the DNA sequence analysis carried out on both FL4 and End6 did not reveal any deviations from the published dog heart derived sequence (AF252536) so the rolipram sensitivity of these two enzymes noted in the present study cannot be attributed to inadvertent mutations in the sequence.

The involvement of metal ions has also been said to play an important role in the inhibition of PDE enzymes by specific inhibitors. Laliberte and co-workers (2000) used a fluorescence resonance energy transfer (FRET)-based equilibrium binding assay to show a conformational difference between the PDE4 apoenzyme, which contains no bound metal ion, and the PDE4 holoenzyme which has a bound metal ion ( $Mg^{2+}$ ). They showed that the inhibitor rolipram exhibited a conformation-dependent sensitivity to the PDE4 enzyme such that rolipram bound with high affinity (5nM) to the holoenzyme but showed low affinity (300nM) binding to the apoenzyme. The substrate cAMP was also shown to bind with high affinity ( $K_d \sim 2\mu M$ ) to the holoenzyme complex compared to the low affinity binding ( $K_d \sim 170\mu M$ ) seen with the apoenzyme. The association of the  $Mg^{2+}$  with the enzyme is

thought to act as a 'switch' to 'activate' the PDE4 enzyme and allow for the high affinity substrate and inhibitor binding. It is possible that the presence of  $Mg^{2+}$  played a role in the sensitivity of FL4 and End6 enzymes to the inhibitor rolipram in the present study whereby the conformation adopted by the recombinant enzymes in the presence of  $Mg^{2+}$  (added to the PDE assay buffer) allowed inhibition by rolipram. The other metal ion that is important for the activity of PDE enzymes is  $Zn^{2+}$ .  $Zn^{2+}$  was not included in any of the buffers used in the preparation and analysis of the recombinant enzymes in the present study. This metal may also play a role in the PDE sensitivity to inhibitors such as vinpocetine and zaprinast. In the present study, the sensitivity of the recombinant enzymes to both these inhibitors was reduced compared to the native enzyme (Tables 6.5.1 and 6.5.2). Further analysis is necessary to determine whether the addition of  $Zn^{2+}$  would restore the vinpocetine and zaprinast sensitivity of the recombinant enzymes.

## 6.7 Conclusion

The primary aim of the work described in the present chapter was the biochemical characterisation of the recombinant enzymes FL4 and End6. The kinetic properties of the full-length recombinant enzyme, FL4, were established as discussed in section 6.6 and were compared with the native dog heart PDE1A. The effect of the N-terminal truncation on the  $K_m$  and  $V_{max}$  values was also established and found to be consistent with studies carried out by other workers as discussed in section 6.6. Both  $K_m$  and  $V_{max}$  values were increased for the N-terminal truncated enzyme. Inhibitor sensitivity was also reduced in the truncated construct when cGMP was used as the substrate, an observation noted for other PDE N-terminal truncated enzymes (see Table 6.7).

Inhibitor studies on FL4 were also comparable to the native enzyme with the notable exception of the sensitivity of FL4 to rolipram. This sensitivity to rolipram was an unexpected finding for the PDE1A1 enzyme used in the present study and was also present in the N-terminal truncated construct, End6. Currently, sensitivity to rolipram inhibition is the key determining feature of the PDE4 family of enzymes. However, data obtained in the present study indicates that rolipram is not as selective as first reported. Furthermore, interpretation of experiments involving recombinant PDE1 enzymes may need to be reassessed.

## Chapter Seven

### 7 General discussion

#### 7.1 Introduction

The intracellular messengers cAMP and cGMP are key molecules in the intracellular signal transduction pathways. PDEs are key enzymes in these pathways since they are the sole enzymes hydrolysing the cyclic nucleotides to their corresponding inactive monophosphates, and hence terminating the intracellular signal. This termination is important for the proper functioning of the cells as discussed in Chapter 1.

The therapeutic potential of PDE inhibitors is now well established with the introduction of the PDE5 inhibitor, sildenafil, in the treatment of erectile dysfunction (Boolell *et al.*, 1996) and the promising clinical data obtained for the PDE4 inhibitor roflumilast (Bundschuh *et al.*, 2001). An understanding of the mechanisms involved in the substrate and inhibitor recognition sites on the PDEs is important for the design of potential PDE family-specific inhibitors, and also PDE isoform-specific inhibitors. The latter have a potential for specific targeting of tissues since it is obvious from the earlier discussion on the tissue distribution of the PDE enzymes (section 1.7.5), that different isoforms exhibit subcellular localisation as well as tissue specificity.

The information provided by the elucidation of the atomic structure of the catalytic domain of PDE4B2B, a short PDE4 isoform, resolved to 1.77 Å resolution (Xu *et al.*, 2000) has been invaluable in the understanding of the regions involved in substrate and inhibitor binding. However, regions outside of the catalytic domain are also important in cyclic nucleotide hydrolysis and inhibitor affinity so the elucidation of a full-length PDE would provide further invaluable information on the regions and residues important for modulation of catalytic activity. This is an important consideration as most of the PDE families have been shown to contain amino terminal regulatory domains which influence and regulate catalytic activity (see Figure 1.9). In the case of PDE4 enzymes, these are the N-terminal regulatory domains, UCR1 and/or UCR2, which regulate enzyme activity as well as being involved in enzyme dimerisation (Richter and Conti, 2002), while PDE1

enzymes contain calmodulin-binding domains which modulate activity of the PDE1 enzymes. Several studies involving N-terminal truncations of PDE enzymes have shown that these truncations cause an increase in substrate hydrolysis (see Table 6.6) and indeed this was the case in the present study where the N-terminal truncated construct showed increased substrate hydrolysis. The binding of rolipram to PDE4 enzymes is also thought to involve regions outside of the catalytic domain with the presence of a low affinity rolipram-binding site and a high affinity rolipram-binding site, located within the catalytic domain and the amino-terminal region of the enzyme respectively. Furthermore, the binding of PDE4 inhibitors to the high affinity binding site has been associated with the major side effect of emesis seen in this class of drugs. However, second generation PDE4 inhibitors such as roflumilast (Bundschuh *et al.*, 2001; see Figure 1.15.2) have been shown to be better tolerated (up to 500µg per day) with emesis only seen at higher doses ( $\geq 1$  mg per day). Clinical trial data on roflumilast has shown it to provide clinically relevant improvement in asthma control (Bundschuh *et al.*, 2001).

Atomic structure information on other members of the PDE family has not been reported to date. Structure information is available on a cyclic phosphodiesterase (CPDase) enzyme involved in the tRNA processing pathway in *Saccharomyces cerevisiae* (Culver *et al.*, 1993, 1994), *Arabidopsis thaliana* (Hofmann *et al.*, 2000), and is thought to be present in other eukaryotes as well since the splicing enzymes are highly conserved. The CPDase enzyme hydrolyses ADP-ribose 1',2'-cyclic phosphate, a product of the tRNA splicing reaction, to ADP-ribose 1'-phosphate (Culver *et al.*, 1994) - analogous to the 3',5'-cyclic AMP hydrolysis to 5'-AMP by PDE enzymes. The crystal structure of CPDase from *Arabidopsis thaliana* was determined to 2.5 Å resolution by Hofmann and co-workers (2000). The molecular assembly of CPDase is different from the PDE4B2B catalytic domain structure, comprising of a mixture of  $\alpha$ -helices and antiparallel  $\beta$ -sheets. Despite this difference, the CPDase does contain two metal-binding motifs (**HXT/SX**; <sup>42</sup>**HVTV** and <sup>119</sup>**HLSL**) within its catalytic site with the histidine residues participating in the catalytic process. PDE enzymes also contain two metal-binding motifs (**HX<sub>3</sub>HXE**; <sup>234</sup>**HNSLH** and <sup>374</sup>**HDVDH** in PDE4B2B; Figure 1.14.2) where the histidine residues co-ordinate with metal ions ( $Zn^{2+}$  and  $Mg^{2+}$ ) in the catalytic process as discussed in section 1.4.7.4. The fact that these metal-binding motifs are present in enzymes involved in tRNA processing and cyclic nucleotide hydrolysis suggests an evolutionary link between these enzymes. It also



emphasises the importance of the presence of the metal-binding motifs in the catalytic domains of the enzymes since the motif is highly conserved in these enzymes. Metal-binding motifs have also been shown to be present in other enzymes such as carboxypeptidases, thermolysins, and carbonic anhydrases (Vallee and Auld, 1990a, 1990b). However, these enzymes only contain a single metal-binding motif.

The cGMP-binding region(s) (GAF domains) present at the N-terminal regions of PDE2, PDE5 and PDE6 have been shown to have similarities with the GAF domain of *Saccharomyces cerevisiae* YKG9. Motifs homologous to the GAF domains of PDEs have been found in a large number of proteins involved in regulatory and signalling pathways in yeasts (*Saccharomyces cerevisiae*, *Candida albicans*), bacteria (*E. coli*, *Streptomyces coelicolor*) as well as in plants (*Pelargonium spp.*) (Aravind and Ponting, 1997). The crystal structure of the *S. cerevisiae* YKG9 GAF domain protein has been determined to 1.9 Å resolution by Ho and co-workers (2000). The protein was found to consist of six-stranded β-sheets and four α-helices. Ho and co-workers (2000) used this model as a template to model the structure of the first GAF domain (GAF<sub>a</sub>) in PDE5 and thus provide information on the binding of cGMP to these domains. The YKG9 protein also revealed unexpected similarity to the PAS domain which is present in the PDE8 enzyme as well as the photoactive yellow protein (PYP) which consists entirely of a single PAS domain and is a cytosolic photoreceptor in bacteria (*Ectothiorhodospira halophila*). The crystal structure of the PYP has been determined to 1.4 Å resolution by Borgstahl and co-workers (1995) and is characterised by a central, twisted, 6-stranded, anti-parallel β-sheet which is flanked on both sides by loops and α-helices. PYP was found to be closely superimposable over the YKG9 protein (Ho *et al.*, 2000) which in turn was shown to be superimposable on the GAF<sub>b</sub> domain of PDE2A (Martinez *et al.*, 2002). The crystal structure of the two GAF (a and b) domains present in PDE2A has recently been resolved to 2.9 Å by Martinez and co-workers (2002) who cloned and expressed the N-terminal regulatory domain of mouse PDE2A. These workers showed that GAF a domain functions as a dimerisation locus while GAF b domain displayed a new cGMP-binding motif which is shown in Figure 7.1. This motif contained an important aspartic acid residue (Asp<sup>439</sup>, D<sup>439</sup>, shown in red in Figure 7.1, lower panel) making contact with the guanine moiety of cGMP. The presence of this residue has been suggested to provide a positive determinant for cGMP specificity and is present in the GAF-containing enzymes PDE2, PDE5 and PDE6. Furthermore, Muradov

and co-workers (2003) constructed a series of chimeric proteins between PDE6 $\alpha\beta$  and PDE5 which contained the N-terminal GAF $\alpha$ /GAF $\beta$  domains of the rod enzymes and showed that the GAF $\alpha$  domains of rod cGMP-phosphodiesterase 6 (PDE6) are also involved in the dimerisation of the enzyme.

**Conserved cGMP motif:**  $SX_{13-18}FDX_{18-22}IAX_{21}[Y/N]X_2VDX_2TX_{19}[E/Q]$

**cGMP motif in PDE2A Gaf  $\beta$ :**  $^{424}SX_{13}FD^{439}X_{18}IAX_{21}YX_2VDX_2TX_{19}E^{512}$

**Figure 7.1** Conserved cGMP-binding motif. The upper panel shows the cGMP-binding motif shown to be present in PDE2, PDE5 and PDE6 enzymes while the lower panel shows the motif present in the mouse PDE2A enzyme. The bold residues represent residues making contacts with cGMP through side chains or through water molecules while 'X' represents any amino acid. The presence of the conserved aspartic acid ( $D^{439}$ ) is a strong positive determinant for cGMP specificity. Figure adapted from Martinez *et al.*, 2002.

The GAF domains of PDE2A comprise of a mixture of  $\alpha$ -helices and anti-parallel  $\beta$ -sheets. The overall fold of the GAF domains, YKG9 protein and the PYP domain is very similar which suggests an evolutionary relationship between these proteins. Figure 7.2 shows the structure of these proteins represented as ribbon diagrams.

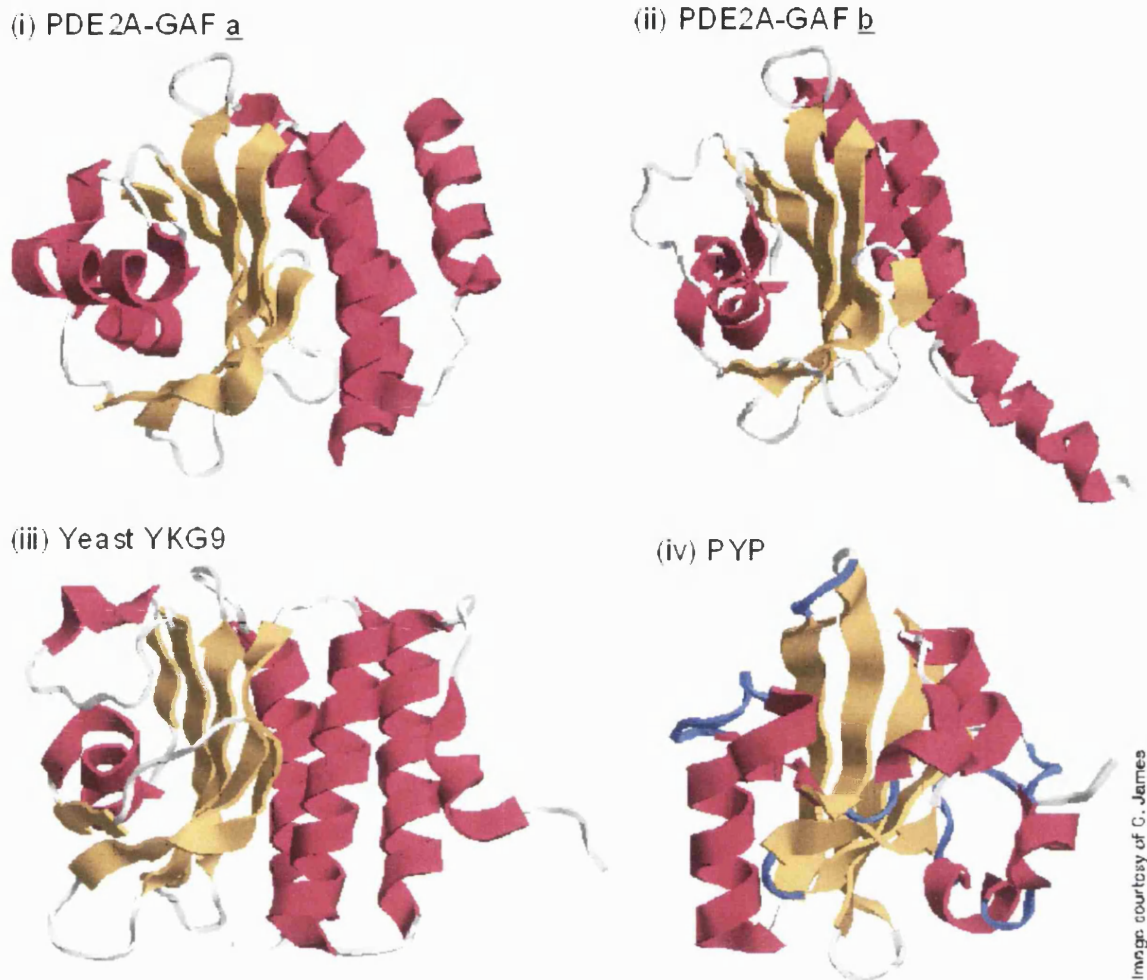


Image courtesy of C. James

**Figure 7.2** Structure of the PDE2A GAF domains (a and b), YKG9 and PYP proteins. Ribbon diagrams to show structural similarities between the GAF domains present in PDE2A, yeast YKG9 and the Photoactive Yellow Protein (PYP).  $\alpha$ -helices are shown in pink while the  $\beta$ -sheets are shown in mustard colour. Figure adapted from Martinez *et al.*, 2002; Ho *et al.*, 2000; Borgstahl *et al.*, 1995.

Atomic structure information can therefore provide vital information regarding the regulation of enzymes. Since PDE enzymes contain regulatory domains which influence the binding of substrate/inhibitors, structure information on the full-length enzymes would be invaluable. For the PDE I enzymes, the calmodulin-binding domains serve as important modulators for this class of enzymes since calmodulin (CaM) is a small, ubiquitous and a highly conserved molecule involved in a wide range of  $\text{Ca}^{2+}$ /CaM signalling pathways. The crystal structure of calmodulin protein has been elucidated to 3.0 Å resolution by Babu and co-workers (1985) and found to resemble a dumbbell with two lobes (N- and C-terminal lobes) connected by an eight-turn  $\alpha$ -helix with no direct contacts between the two lobes. The lobes each contain two  $\text{Ca}^{2+}$ -binding regions, and binding of  $\text{Ca}^{2+}$  to these regions

elicits a conformational change in the molecule, exposing hydrophobic regions on the molecule. The activated calmodulin then binds to target proteins inducing a conformational change in these target proteins which in most instances leads to the stimulation of the target, as is the case for PDE1 enzymes. Target proteins include CaM-PDE enzymes, CaM-dependant adenylyl cyclases (see section 1.2.2), CaM-dependant kinases (see section 1.7.3) as well as venoms from bees and wasps (Crivici and Ikura, 1995). However, there is no single consensus sequence for CaM recognition but the CaM-binding domain is usually limited to a short region of 14 - 26 residues and which is also able to adopt a helical state (Crivici and Ikura, 1995). Structure information on the complex formed between the CaM protein and the target proteins is limited as the target proteins are usually large and multimeric. Much of the structural information, therefore, has been obtained from studies of CaM complexed with small peptide molecules or just the calmodulin-binding domains of target proteins. These include proteins such as melittin which is a 26 amino acid helical protein binding calmodulin and found in the venom of the honey bee *Apis mellifera*. The CaM complexed with the calmodulin-binding regions of the enzymes myosin light chain kinase from striated muscle (Ikura *et al.*, 1992) and from smooth muscle (Meador *et al.*, 1992) have also been studied. The calmodulin-binding domains of the myosin light chain kinases complexed with calmodulin showed that the two lobes of calmodulin enfolded the  $\alpha$ -helical structure of the target proteins. The structure of a  $\text{Ca}^{2+}$ -activated  $\text{K}^+$  channel calmodulin-binding domain complexed with CaM protein has also been elucidated to 1.6 Å resolution by Schumacher and co-workers (2001). The calmodulin-binding domain of the channel was found to comprise of  $\alpha$ -helices with loops connecting the helices.

Structure information on the PDE1 enzymes with and without the presence of the calmodulin protein would thus provide valuable information on the calmodulin-PDE1 interactions at the molecular level, as well as provide structural information on the structure of the catalytic domain for comparison with the PDE4B2B catalytic domain structure elucidated by Xu and co-workers (2000). Milligram quantities of the pure enzyme are usually needed for the purposes of structural studies. These enzymes are usually obtained through over-expression in either prokaryotic or eukaryotic expression systems. The prokaryotic expression systems have the advantage of ease of manipulation, the short time required for expression, and scale-up with relative ease to a 10 L fermenter volume. Eukaryotic expression systems on the other hand, offer the advantage of proper protein

processing which is not usually carried out in prokaryotic systems. Indeed the PDE4B2B protein used for the elucidation of the crystal structure of the catalytic domain was expressed and purified from a eukaryotic expression system employing the baculovirus system using Sf9 insect cells (Rocque *et al.*, 1997a). In the present study, both prokaryotic and eukaryotic expression systems were explored for the expression of the dog heart PDE1A1 enzyme.

## 7.2 Expression of dog heart PDE1A1

The main achievement of the present study was the expression of a novel dog heart PDE1A1 recombinant enzyme in a soluble, active form in an expression system not reported to have been used for the production of PDE1 enzymes. This was achieved using the eukaryotic expression system employing the Semliki Forest virus (SFV) system as described in Chapter 5. Although the yeast system using the *Pichia pastoris* expression system was also explored, this did not yield any recombinant enzyme (Chapter 3). The prokaryotic expression system was also explored using two different expression vectors and these produced the recombinant enzyme mainly as insoluble inclusion bodies as described in Chapter 4. PDE enzymes expressed using prokaryotic systems have invariably resulted in the production of insoluble inclusion bodies, necessitating the employment of complex strategies for refolding the enzymes from the inclusion bodies (Richter *et al.*, 2000, 2002) as discussed in Chapter 4. The two bacterial constructs produced in the present study, GST-PDE1A1 and His<sub>6</sub>-PDE1A1<sub>N-trunc</sub>, can be used to further explore the refolding conditions necessary to produce active enzymes from inclusion bodies using recently reported strategies on the folding of PDE7A from inclusion bodies (Richter *et al.*, 2002).

There have been no reports on the expression of PDE1 enzymes using the SFV system so the work described in the present study represents the first such report. As discussed earlier (section 1.8), sequence alignment studies of the translated putative polypeptide amino acid sequence of the dog heart PDE1A cDNA (Clapham and Wilderspin, 2001) with the bovine and human PDE1A1 proteins showed a strong sequence homology suggesting that the dog heart PDE1A cDNA encoded for a functional gene. The results of the present study on the recombinant dog heart PDE1A1 do indeed confirm that the cDNA encoded for a functional protein.

The expression studies using the SFV expression system were initially carried out in 25cm<sup>2</sup> flasks, then subsequently scaled up to 75cm<sup>2</sup> flasks. This produced sufficient enzyme for biochemical analysis of the crude recombinant enzyme but was not enough for full purification studies. The system, however, has the potential to be scaled up to 1 L spinner flasks or ≥ 10 L bioreactor level to produce sufficient recombinant enzyme for purification and subsequent structural studies. Large scale expression of proteins using the SFV system have been reported for human neurokinin-1 receptor protein (Lundstrom *et al.*, 1994) as well as for β-galactosidase and human cyclooxygenase-2 proteins (Blasey *et al.*, 1997).

For studies involving crystal structure elucidation, milligram quantities of the pure enzyme are required as already stated. This has often proven to be difficult since the full-length enzymes tend to be prone to hydrolysis so it has been more practical to produce truncated forms of the enzyme - as was the case for the PDE4B2B (Rocque *et al.*, 1997a). For the present work, both full-length and N- and/or C-terminal truncated PDE1A1 were produced with the intention of producing sufficient pure enzyme(s) for exploring structure-activity relationship as well as for crystallisation purposes for the elucidation of the crystal structure of the expressed enzymes. The results of the present study revealed that only the full-length and the N-terminal truncated PDE1A1 enzymes were active proteins, as described in Chapter 5. Since PDE1 enzymes are known to contain calmodulin-binding regions at the amino terminal portions of the enzymes, the effect of the removal of these domains on the conformation of the enzyme would be an interesting area to explore at the molecular level. The results of the present study have provided the basis for the initiation of a large-scale expression system, either 1 L spinner flasks or ≥ 10 L bioreactor, for the production of the full-length and the N-terminal truncated dog heart PDE1A1 proteins for subsequent purification and structural analysis.

### **7.3 Biochemical characterisation of dog heart PDE1A1**

Biochemical characterisation was carried out on the two active constructs: the full-length and the N-terminal truncated PDE1A1 enzymes as described in Chapter 6. As discussed in Chapter 5, the C-terminal and the N- and C-terminal truncated constructs were not catalytically active. The reason for this is unclear since the expression of similarly truncated PDE3 and PDE4 enzymes did produce active mutants (see Table 6.6). The

PDE4B2B enzyme used for the elucidation of the crystal structure also encompassed just the catalytic domain (Xu *et al.*, 2000). Furthermore, truncation studies on the bovine PDE1A1 enzyme removing the N-terminal domain also produced an active enzyme (Sonnenburg *et al.*, 1995).

The kinetic parameters of the full-length dog heart PDE1A1 protein produced in the present study were compared to the native enzyme produced by Clapham and Wilderspin (2001). As described in Chapter 6 (Tables 6.4.1 and 6.4.2), the  $K_m$  and  $V_{max}$  of the recombinant and native enzymes were comparable except that the  $K_m$  for cGMP hydrolysis for the recombinant enzyme was much higher. The inhibitor studies carried out using non-selective PDE inhibitors also revealed comparable results (Tables 6.5.1 and 6.5.2) for the recombinant and native full-length PDE1A1 enzymes. However, inhibitor sensitivity of the recombinant enzyme was reduced for the selective inhibitors, vinpocetine and zaprinast, relative to the native enzyme. Kinetic analysis of the N-terminal truncated enzyme produced in the present study showed an increased  $V_{max}$  compared to the full-length enzymes which was in agreement with other N-terminal truncated PDE enzymes (see Table 6.6).

An intriguing finding of the biochemical characterisation of the full-length and N-terminal truncated PDE1A1 enzymes in the present work was that of the unexpected, potent sensitivity of the recombinant enzymes to the archetypical PDE4 inhibitor rolipram. This finding is described and explored in Chapter 6. This sensitivity was pronounced in the full-length PDE1A1 enzyme which showed an  $IC_{50}$  of  $0.2\mu\text{M}$  when cAMP was used as the substrate (see Table 6.5.1). The N-terminal truncated PDE1A1 showed a similar sensitivity profile to inhibition by rolipram (see Figure 6.5 (v) and Table 6.5.1). It is apparent from the data presented in Chapter 6, that further investigation into this unusual rolipram-sensitivity is necessary and would form the key focus of future work on these constructs.

PDE1 and PDE4 enzymes do show similar tissue distribution patterns with both being found in the brain as well as the lungs. PDE1 is also present in the B lymphocytes and macrophages which also contain PDE4 enzymes (Dent *et al.*, 1998; Schudt *et al.*, 1999). Pharmacological *in vivo* studies evaluating the use of potential PDE inhibitors in diseases such as asthma and cardiovascular disease use small mammals such as the mouse, rat or

ferrets, but dogs have also been used for the evaluation of PDE inhibitors. Studies on dogs using PDE4 -selective inhibitors based on the rolipram structure may need to be reassessed in the light of the findings of the present work. It is possible that the rolipram-sensitivity of the PDE1A1 constructs in the present work might provide some clues to the major side effect of emesis seen with PDE4-selective inhibitors being evaluated for clinical use.



## References

- Andrews R, Cowley AJ (1993). Phosphodiesterase Inhibitors. *Drug Safety* **9**:404-409.
- Andrin C, Corbett EF, Johnson S, Dabrowska M, Campbell ID, Eggleton P, Opas M, Michalak, M (2000). Expression and purification of mammalian calreticulin in *Pichia pastoris*. *Protein Expr. Purif.* **20**:207-215.
- Anhold RRH, Rivers AM (1990). Olfactory Transduction: Cross-Talk between Second-Messenger Systems. *Biochemistry* **29**:4049-4054.
- Appelbaum ER, Shatzman AR (1999). Prokaryotic *in vivo* expression systems. In *Protein Expression A Practical Approach* (Higgins SJ, Hames BD, eds.), pp169-200. Oxford University Press, England.
- Aravind L, Ponting CP (1997). The GAF domain: an evolutionary link between diverse phototransducing proteins. *Trends Biochem. Sci.* **22**:458-459.
- Arvola M, Keinänen K (1996). Characterisation of the Ligand-binding Domains of Glutamate Receptor (GluR)-B and GluR-D Subunits Expressed in *Escherichia coli* as Periplasmic Proteins. *J. Biol. Chem.* **271**:15527-15532.
- Atienza JM, Susanto D, Huang C, McCarty AS, Colicelli J (1999). Identification of Inhibitor Specificity Determinants in a Mammalian Phosphodiesterase. *J. Biol. Chem.* **274** :4839-4847.
- Babu YS, Sack JS, Greenhough TJ, Bugg CE, Means AR, Cook WJ (1985). Three-dimensional structure of calmodulin. *Nature* **315**:37-40.
- Ball EH, Shephard LB, Gill GN (1995). Purification and Properties of Thyroid Hormone Receptor b1 Expressed in *Escherichia coli* as a Fusion Protein. *Protein Expr. Purif.* **6**:33-38.
- Baneyz F (1999). Recombinant protein expression in *Escherichia coli*. *Curr. Opin. Biotechnol.* **10**:411-421.
- Beard MB, O'Connell JC, Bolger GB, Houslay MD (1999). The unique N-terminal domain of the cAMP phosphodiesterase PDE4D4 allows for interaction with specific SH3 domains. *FEBS Lett.* **460**:173-177.
- Beard MB, Olsen AE, Jones RE, Erdogan S, Houslay MD, Bolger GB (2000). UCR1 and UCR2 Domains Unique to the cAMP-specific Phosphodiesterase Family Form a Discrete Module via Electrostatic Interactions. *J. Biol. Chem.* **275**:10349-10358.
- Beavo JA (1995). Cyclic Nucleotide Phosphodiesterases: Functional Implications of Multiple Isoforms. *Physiol. Rev.* **75**:725-748.
- Beavo JA, Conti M, Heaslip RJ (1994). Multiple Cyclic Nucleotide Phosphodiesterases. *Mol. Pharmacol.* **46**:399-405.
- Beavo JA, Reifsnyder DH (1990). Primary sequence of cyclic nucleotide phosphodiesterase isozymes and the design of selective inhibitors. *Trends Pharmacol. Sci.* **11**:150-155.
- Beltman J, Becker DE, Butt E, Jensen GS, Rybalkin SD, Jastorff B, Beavo JA (1995). Characterization of Cyclic Nucleotide Phosphodiesterases with Cyclic GMP Analogs: Topology of the Catalytic Domains. *Mol. Pharmacol.* **47**:330-339.
- Bentley JK, Beavo JA (1992). Regulation and function of cyclic nucleotides. *Curr. Opin. Cell Biol.* **4**:233-240.
- Berglund P, Sjöberg M, Garoff H, Atkins GJ, Sheahan BJ, Liljeström P (1993). Semliki Forest Virus Expression System: Production of Conditionally Infectious Recombinant Particles. *Bio/Technology* **11**:916-920.
- Berglund P, Tubulekas I, Liljeström P (1996). Alphaviruses as vectors for gene delivery. *Trends Biotechnol.*

14:130-134.

Beynon RJ, Salvesen G (1996). Commercially available protease inhibitors. In *Proteolytic Enzymes A Practical Approach* (Beynon RJ, Bond JS, eds.), pp241-249. IRL press by Oxford University Press, New York.

Blackwell JR, Horgan R (1991). A novel strategy for production of a highly expressed recombinant protein in an active form. *FEBS*. **295**:10-12.

Blasey HD, Brethon B, Hovius R, Vogel H H, Tairi AP, Lundström K, Rey L, Bernard, AR (2000). Large scale transient 5-HT<sub>3</sub> receptor production with the Semliki Forest Virus Expression System. *Cytotechnology* **32**:199-208.

Blasey HD, Lundström K, Tate S, Bernard AR (1997). Recombinant protein production using the Semliki Forest Virus expression system. *Cytotechnology* **24**:65-72.

Bloom TJ, Beavo JA (1996). Identification and tissue-specific expression of PDE7 phosphodiesterase splice variants. *Proc. Natl. Acad. Sci. USA* **93**:14188-14192.

Bofill-Cardona E, Kudlacek O, Yang Q, Ahorns H, Freissmuth M, Nanoff C (2000). Binding of Calmodulin to the D<sub>2</sub>-Dopamine Receptor Reduces Receptor Signaling by Arresting the G Protein Activation Switch. *J. Biol. Chem.* **42**:32672-32680.

Bolger GB (1994). Molecular biology of the cyclic AMP-specific cyclic nucleotide phosphodiesterase: A diverse family of regulatory enzymes. *Cell. Signal.* **6**:851-859.

Bolger GB, Erdogan S, Jones RE, Loughney K, Scotland G, Hoffman R, Wilkinson I, Farrell C, Houslay, MD (1997). Characterization of five different proteins produced by alternatively spliced mRNAs from the human cAMP-specific phosphodiesterase PDE4D gene. *Biochem. J.* **328**:539-548.

Bolger GB, McPhee I, Houslay MD (1996). Alternative Splicing of cAMP-specific Phosphodiesterase mRNA Transcripts. *J. Biol. Chem.* **271**:1065-1071.

Bolger G, Michaeli T, Martins T, St. John T, Steiner B, Rodgers L, Riggs M, Wigler M, Ferguson K (1993). A family of human phosphodiesterases homologous to the dunce learning and memory gene product of *Drosophila melanogaster* are potential targets for antidepressant drugs. *Mol. Cell. Biol.* **13**:6558-6571.

Boolell M, Allen MJ, Ballard SA, Gepi-Attee S, Muirhead GJ, Naylor AM, Osterloh IH, Gingell C (1996). Sildenafil: an orally active type 5 cyclic GMP-specific phosphodiesterase inhibitor for the treatment of penile erectile dysfunction. *Int. J. Impot. Res.* **8**:47-52.

Borgstahl GEO, Williams DR, Getzoff ED (1995). 1.4 Å Structure of Photoactive Yellow Protein, a Cytosolic Photoreceptor Unusual Fold, Active Site, and Chromophore. *Biochemistry* **34**:6278-6287.

Bradford MM (1976). A rapid and sensitive method for the quantitation of microgram quantities of protein utilizing the principle of protein-dye binding. *Anal. Biochem.* **72**:248-254.

Brake AJ, Merryweather JP, Coit DG, Heberlein UA, Masiarz RR, Mullenbach GT, Urdea MS, Valenzuela P, Barr PJ (1984).  $\alpha$ -Factor- directed synthesis and secretion of mature foreign proteins in *Saccharomyces cerevisiae*. *Proc. Natl. Acad. Sci. USA* **81**: 4642-4646.

Braun T, Dods RF (1975). Development of a Mn<sup>2+</sup>-Sensitive "Soluble" Adenylate Cyclase in Rat Testis. *Proc. Natl. Acad. Sci. USA* **72**:1097-1101.

Brostrom CO, Brostrom MA, Wolff DJ (1977). Calcium-dependent Adenylate Cyclase from Rat Cerebral Cortex. *J. Biol. Chem.* **252**:5677-5685.

Buck J, Sinclair ML, Schapal L, Cann MJ, Levin LR (1999). Cytosolic adenylyl cyclase defines a unique signaling molecule in mammals. *Proc. Natl. Acad. Sci. USA* **96**:79-84.

- Buckholz RG, Gleeson MA (1991). Yeast systems for the commercial production of heterologous proteins. *Bio/Technology* **9**: 1067-1073.
- Bundschuh DS, Eltze M, Barsig J, Wollin L, Hatzelmann A, Beume R (2001). *In Vivo* Efficacy in Airway Disease Models of Roflumilast, a Novel Orally Active PDE4 Inhibitor. *J. Pharmacol. Exp. Ther.* **297**:280-290.
- Burnette WN (1981). "Western Blotting": Electrophoretic transfer of Proteins from Sodium Dodecyl Sulfate-Polyacrylamide Gels to Unmodified Nitrocellulose and Radiographic Detection with Antibody and Radioiodinated Protein A. *Analytical Biochem.* **112**:195-203.
- Burns F, Zhao AZ, Beavo JA (1996). Cyclic Nucleotide Phosphodiesterases: Gene Complexity, Regulation by Phosphorylation, and Physiological Implications. *Adv. Pharmacol.* **36**:29-48.
- Butcher RW, Sutherland EW (1962). Adenosine 3',5'-Phosphate in Biological Materials. *J. Biol. Chem.* **237**:1244-1250.
- Butt E, Beltman J, Becker DE, Jensen GS, Rybalkin SD, Jastorff B, Beavo JA (1995). Characterization of Cyclic Nucleotide Phosphodiesterases with Cyclic GMP Analogs: Topology of the Catalytic Sites and Comparison with Other Cyclic AMP-Binding Proteins. *Mol. Pharmacol.* **47**:340-347.
- Byers D, Davis RL, Kiger JA Jr. (1981). Defect in cyclic AMP phosphodiesterase due to the dunce mutation of learning in *Drosophila melanogaster*. *Nature* **289**:79-81.
- Carafoli E, Molinari M (1998). Calpain: A Protease in Search of a Function? *Biochem. Biophys. Res. Commun.* **247**:193-203.
- Carter BD, Kaltschmidt C, Kaltschmidt B, Offenauser N, Bohm-Matthaei, Baeuerle PA, Barde YA (1996). Selective activation of NF- $\kappa$ B by nerve growth factor through the neurotrophin receptor p75. *Science* **272**:542-545.
- Chang M, Bolton JL, Blond SY (1999). Expression and Purification of Hexahistidine-Tagged Human Glutathione S-Transferase P1-1 in *Escherichia coli*. *Protein Expr. Purif.* **17**:443-448.
- Chang BY, Conroy KB, Machleder EM, Cartwright CA (1998). RACK1, a Receptor for Activated C Kinase and a Homolog of the  $\beta$  Subunit of G Proteins, Inhibits Activity of Src Tyrosine Kinases and Growth of NIH 3T3 Cells. *Mol. Cell Biol.* **18**:3245-3256.
- Charbonneau H, Beier N, Walsh KA, Beavo JA (1986). Identification of a conserved domain among cyclic nucleotide phosphodiesterases from diverse species. *Proc. Natl. Acad. Sci. USA* **83**:9308-9312.
- Charbonneau H, Kumar S, Novack JP, Blumenthal DK, Griffin PR, Shabanowitz J, Hunt DF, Beavo JA, Walsh KA (1991). Evidence for Domain Organization within the 61-kDa Calmodulin-Dependent Cyclic Nucleotide Phosphodiesterase from Bovine Brain. *Biochemistry* **30**:7931-7940.
- Chen Y, Cann MJ, Litvin TN, Iourgenko V, Sinclair ML, Levin LR, Buck J (2000). Soluble Adenylyl Cyclase as an Evolutionary Conserved Bicarbonate Sensor. *Science* **289**:625-628.
- Chen C-N, Denome S, Davis RL (1986). Molecular analysis of cDNA clones and the corresponding genomic coding sequences of the *Drosophila* dunce<sup>+</sup> gene, the structural gene for cAMP phosphodiesterase. *Proc. Natl. Acad. Sci. USA* **83**:9313-9317.
- Chen G-Q, Gouaux E (1997). Overexpression of a glutamate receptor (GluR2) ligand binding domain in *Escherichia coli*: Application of a novel protein folding screen. *Proc. Natl. Acad. Sci. USA* **94**:13431-13436.
- Cheung WY (1967). Cyclic 3',5'-Nucleotide Phosphodiesterase: Pronounced stimulation by snake venom. *Biochem. Biophys. Res. Commun.* **29**:478-482.
- Cheung WY (1970). Cyclic 3',5'-Nucleotide Phosphodiesterase: Demonstration of an Activator. *Biochem.*

*Biophys. Res. Commun.* **30**:533-538.

Cheung WY (1971). Cyclic 3',5'-Nucleotide Phosphodiesterase: Evidence for and properties of a protein activator. *J. Biol. Chem.* **246**:2859-2869.

Cheung PP, Xu H, McLaughlin MM, Ghazaleh FA, Livi GP, Colman RW (1996). Human Platelet cGI-PDE: Expression in Yeast and Localization of the Catalytic Domain by Deletion Mutagenesis. *Blood* **88**:1321-1329.

Chin DT, Goff SA, Webster T, Smith T, Goldberg AL (1988). Sequence of the *lon* Gene in *Escherichia coli*. *J. Biol. Chem.* **263**:11718-11728.

Chinkers M, Garbers DL, Chang MS, Lowe DG, Chin H, Goeddel DV, Schulz S (1989). A membrane form of guanylate cyclase is an atrial natriuretic peptide receptor. *Nature* **338**: 78-83.

Chinkers M, Singh S, Garbers DL (1991). Adenine Nucleotides Are Required of Rat Atrial Natriuretic Peptide Receptor/Guanylyl Cyclase Expressed in a Baculovirus System. *J. Biol. Chem.* **266**:4088-4093.

Ciccarone V, Jessee J, Berglund P, Liljeström P (1993). pSFV1 Eukaryotic Expression Vector: A Novel Protein Expression System. *Focus* **15**:103-105.

Cik M, Chazot PL, Stephenson FA (1993). Optimal expression of cloned NMDAR1/NMDAR2A heteromeric glutamate receptors: a biochemical characterisation. *Biochem J.* **296**:877-883.

Clapham JC, Wilderspin AF (2001). Cloning of dog heart PDE1A - a first detailed characterization at the molecular level in this species. *Gene* **268**:165-171.

Clare JJ, Rayment RB, Ballantine SP, Sreekrishna K, Romanos MA (1991). High-level expression of tetanus toxin fragment C in *Pichia pastoris* strains containing multiple tandem integrations of the gene. *Bio/Technology* **9**:455-457.

Compton CH, Gubb J, Nieman R, Edelson J, Amit O, Bakst A, Ayres JG, Creemers JPH, Schultze-Werninghaus G, Brambilla C, Barnes NC (2001). Cilomilast, a selective phosphodiesterase-4 inhibitor for treatment of patients with chronic obstructive pulmonary disease: a randomised, dose-ranging study. *Lancet* **358**:265-270.

Conti M (2000). Phosphodiesterases and Cyclic Nucleotide Signaling in Endocrine cells. *Mol. Endocrinol.* **14**:1317-1327.

Conti M, Jin S-LC (1999). The Molecular Biology of Cyclic Nucleotide Phosphodiesterases. *Nucl. Acid Res. Mol. Biol.* **63**:1-38.

Corbin JD, Turko IV, Beasley A, Francis SH (2000). Phosphorylation of phosphodiesterase-5 by cyclic nucleotide-dependent protein kinase alters its catalytic and allosteric cGMP-binding activities. *Eur. J. Biochem.* **267**:2760-2767.

Corti C, L'Hostis EL, Quadroni M, Schmid H, Durussel I, Cox J, Hatt PD, James P, Carafoli E (1999). Tyrosine phosphorylation modulates the interaction of calmodulin with its target proteins. *Eur. J. Biochem.* **262**:790-802.

Cregg JM, Higgins, DR (1995). Production of foreign proteins in the yeast *Pichia pastoris*. *Can. J. Bot.* **73**(1):S891-S897.

Cregg JA, Madden KR, Barringer KJ, Thill GP, Stillman CA (1989). Functional characterization of the Two Alcohol Oxidase Genes from the Yeast *Pichia pastoris*. *Mol. Cell. Biol.* **9**(3):1316-1323.

Cregg JM, Tschopp JF, Stillman C, Siegel R, Akong SM, Craig WS, Buckholz RG, Madden KR, Kellaris PA, Davis GR, Smiley BL, Cruze J, Torregrossa R, Velicelebi G, Thill, GP (1987). High-level expression and efficient assembly of Hepatitis B surface antigen in the methylotrophic yeast, *Pichia pastoris*. *Bio/Technology*

5:479-485.

Cregg JM, Vedvick TS, Raschke WD (1993). Recent Advances in the Expression of Foreign Genes in *Pichia pastoris*. *Bio/Technology* **11**:905-910.

Crivici A, Ikura M (1995). Molecular and structural basis of target recognition by calmodulin. *Annu. Rev. Biophys. Biomol. Struct.* **24**:85-116

Croall DE, Demartino GN (1991). Calcium-Activated Neutral Protease (Calpain) System: Structure, Function, and Regulation. *Physiol. Rev.* **71**:813-843.

Culver GM, Consaul SA, Tycowski KT, Filipowicz W, Phizicky EM (1994). tRNA Splicing in Yeast and Wheat Germ. *J. Biol. Chem.* **269**:24928-24934.

Culver GM, McCraith SM, Zillmann M, Kierzek R, Michaud N, La-Reau RD, Turner DH, Phizicky EM (1993). An NAD derivative produced during transfer RNA splicing: ADP-ribose 1"-2" cyclic phosphate. *Science* **261**:206-208.

Cunningham AM, Ryugo DK, Sharp AH, Reed RR, Snyder SH, Ronnett GV (1993). Neuronal inositol 1,4,5-Triphosphate receptor localised to the plasma membrane of olfactory cilia. *Neuroscience* **57**:339-352.

Daniel PB, Walker WH, Habener JF (1998). Cyclic AMP signalling and gene regulation. *Annu. Rev. Nutr.* **18**:353-383.

Davis RL, Takayasu H, Eberwine M, Myres J (1989). Cloning and characterisation of mammalian homologs of the *Drosophila dunce+* gene. *Proc. Natl. Acad. Sci. USA* **86**:3604-3608.

De Nobel JG, Barnett JA (1991). Passage of Molecules Through Yeast Cell Walls: a Brief Essay-Review. *Yeast* **7**:313-723.

Dent G, White SR, Tenor H, Bodtke K, Schudt C, Leff AR, Magnussen H, Rabe KF (1998). Cyclic Nucleotide Phosphodiesterase in Human Bronchial Epithelial Cells: Characterization of Isozymes and Functional Effects of PDE Inhibitors. *Pul. Pharmacol. Ther.* **11**:47-56.

Degerman E, Belfrage P, Manganiello VC (1997). Structure, Localization, and Regulation of cGMP-inhibited Phosphodiesterase (PDE3). *J. Biol. Chem.* **272**:6823-6826.

Deterre P, Bigay J, Forquet F, Robert M, Chabre M (1988). cGMP phosphodiesterase of retinal rods is regulated by two inhibitory subunits. *Proc. Natl. Acad. Sci. USA* **85**:2424-2428.

DiCiommo DP, Bremner R (1998). Rapid, High Level Protein Production Using DNA-based Semliki Forest Virus Vectors. *J. Biol. Chem.* **273**:18060-18066.

Dickinson NT, Jang EK, Haslam RJ (1997). Activation of cGMP-stimulated phosphodiesterase by nitroprusside limits cAMP accumulation in human platelets: effects on platelet aggregation. *Biochem. J.* **325**:371-377.

Dizhoor AM, Ray S, Kumar S, Niemi G, Spencer M, Brolley D, Walsh KA, Philipov PP, Hurley JB, Stryer L (1991). Recoverin: A Calcium Sensitive Activator of Retinal Rod Guanylate Cyclase. *Science* **251**:915-918.

Dodge KL, Khouangsathiene S, Kapiloff MS, Mouton R, Hill EV, Houslay MD, Langeberg KL, Scott JD (2001). mAKAP assembles a protein kinase A/PDE4 phosphodiesterase cAMP signaling module. *EMBO J.* **20**:1921-1930.

Dudai Y (1983). Mutations affect storage and use of memory differentially in *Drosophila*. *Proc. Natl. Acad. Sci. USA* **80**:5445-5448.

Dudai Y, Jan YN, Byers D, Quinn WG, Benzer S (1976). *dunce*, a mutant of *Drosophila* deficient in

- learning. *Proc. Natl. Acad. Sci. USA* **73**:1684-1668.
- Duntze W, Mackay V, Manney TR (1970). *Saccharomyces cerevisiae*: a diffusible sex factor. *Science* **168**:1472-1473.
- Dwarki VJ, Montminy M, Verma IM (1990). Both the basic region and the 'leucine zipper' domain of the cyclic AMP response element binding (CREB) protein are essential for transcriptional activation. *EMBO J.* **9**:225-232.
- Esmon PC, Esmon BE, Schauer IE, Taylor A, Schekman R (1987). Structure, assembly, and secretion of octomeric invertase. *J. Biol. Chem.* **262**:4387-4394.
- Faber KN, Harder W, AB G, Veenhuis M (1995). Review: Methylophilic Yeasts as Factories for the Production of Foreign Proteins. *Yeast* **11**:1331-1344.
- Falkner FG, Turecek PL, MacGillivray RTA, Bodemer W, Scheiflinger F, Kandels S, Mitterer A, Kistner O, Barrett N, Eibl J, Dorner F (1992). High level Expression of Active Human Prothrombin in a Vaccinia Virus Expression System. *Thromb. Haemost.* **68**:119-124.
- Fawcett L, Baxendale R, Stacey P, McGrouther C, Harrow I, Soderling S, Hetman J, Beavo JA, Phillips SC (2000). Molecular cloning and characterization of a distinct human phosphodiesterase gene family: PDE11A. *Proc. Natl. Acad. Sci. USA* **97**:3702-3707.
- Fenner F, Henderson DA, Arita I, Jezek Z, Ladnyi ID (1988). Smallpox and Its Eradication. *WHO* 216-227.
- Fidock M, Miller M, Lanfear J (2002). Isolation and differential tissue distribution of two human cDNAs encoding PDE1 splice variants. *Cell. Signal.* **14**:53-60.
- Fink TL, Francis SH, Beasley A, Grimes KA, Corbin JD (1999). Expression of an Active, Monomeric Catalytic Domain of the cGMP-binding cGMP-specific Phosphodiesterase (PDE5). *J. Biol. Chem.* **274**:34613-4620.
- Firestein S, Darrow B, Shepherd GM (1991). Activation of the Sensory Current in Salamander Olfactory Receptor Neurons Depends on a G Protein-Mediated cAMP Second Messenger System. *Neuron* **6**:825-835.
- Fischer EH, Krebs EG (1955). Conversion of phosphorylase *b* to phosphorylase *a* in muscle extracts. *J. Biol. Chem.* **216**:121-132.
- Fisher DA, Smith JF, Pillar JS, St. Denis SH, Cheng JB (1998b). Isolation and Characterization of PDE9A, a Novel Human cAMP-Specific Phosphodiesterase. *J. Biol. Chem.* **273**:15559-15564.
- Fisher DA, Smith JF, Pillar JS, St. Denis SH, Cheng JB (1998a). Isolation and Characterization of PDE8A, a Novel Human cAMP-Specific Phosphodiesterase. *Biochem. Biophys. Res. Commun.* **246**:570-577.
- Fliegel L, Walsh MP, Singh D, Wong C, Barr A (1992). Phosphorylation of the C-terminal domain of the Na<sup>+</sup>/H<sup>+</sup> exchanger by Ca<sup>2+</sup>/calmodulin-dependent protein kinase II. *Biochem. J.* **282**:139-145.
- Florio SK, Prusti RK, Beavo JA (1996). Solubilization of Membrane-bound Rod Phosphodiesterase by the Rod Phosphodiesterase Recombinant  $\delta$  Subunit. *J. Biol. Chem.* **271**:24036-24047.
- Florio VA, Sonnenburg WK, Johnson R, Kwak KS, Jensen GS, Walsh KA, Beavo JA (1994). Phosphorylation of the 61-kDa Calmodulin-Stimulated Cyclic Nucleotide Phosphodiesterase at Serine 120 Reduces Its Affinity for Calmodulin. *Biochemistry* **33**:8948-8954.
- Forte LR, Bylund DB, Zahler WL (1983). Forskolin Does Not Activate Sperm Adenylate Cyclase. *Mol. Pharmacol.* **24**:42-47.
- Francis SH, Colbran JL, McAllister-Lucas LM, Corbin JD (1994). Zinc Interactions and Conserved Motifs of the cGMP-binding cGMP-specific Phosphodiesterase Suggest That It is A Zinc Hydrolase. *J. Biol. Chem.*

269(36):22477-22480.

Francis SH, Corbin JD (1988). Purification of cGMP-Binding Protein Phosphodiesterase from Rat Lung. *Methods Enzymol.* **159**:722-729.

Francis SH, Turko IV, Corbin JD (2000a). Cyclic Nucleotide Phosphodiesterases: Relating Structure and Function. *Prog. Nucleic Acid Res. Mol. Biol.* **65**:1-52.

Francis SH, Turko IV, Grimes KA, Corbin JD (2000b). Histidine-607 and Histidine-643 Provide Important Interactions for Metal Support of Catalysis in Phosphodiesterase-5. *Biochemistry* **39**:9591-9596.

Fujishige K, Kotera J, Michibata H, Yuasa K, Takebayashi S, Okumura K, Omari K (1999). Cloning and Characterization of a Novel Human Phosphodiesterase that Hydrolyzes both cAMP and cGMP (PDE10A). *J. Biol. Chem.* **274**(26):18438-18445.

Garbers DL (1989). Guanylate Cyclase, a Cell Surface Receptor. *J. Biol. Chem.* **264**(16):9103-9106.

Garbers DL, Tubb JD, Hyne RV (1982). A requirement of Bicarbonate for Ca<sup>2+</sup>-induced Elevations of Cyclic AMP in Guinea Pig Spermatozoa. *J. Biol. Chem.* **257**(15):8980-8984.

Gardner C, Robas N, Cawkill D, Fidock M (2000). Cloning and Characterization of the Human and Mouse PDE7B, a Novel cAMP-Specific Cyclic Nucleotide Phosphodiesterase. *Biochem. Biophys. Res. Commun.* **272**:186-192.

Garty NB, Salomon Y (1987). Stimulation of partially purified adenylate cyclase from bull sperm by bicarbonate. *FEBS Lett.* **218**:148-152.

Geigenmüller-Gnirke U, Weiss B, Wright R, Schlesinger S (1991). Complementation between Sindbis viral RNAs produces infectious particles with a bipartite genome. *Proc. Natl. Acad. Sci. USA* **88**:3253-3257.

Georgiou G, Valax P (1996). Expression of correctly folded proteins in *Escherichia coli*. *Curr. Opin. Biotechnol.* **9**:190-197.

Gillespie PG, Beavo JA (1988). Characterization of a Bovine Cone Photoreceptor Phosphodiesterase Purified by Cyclic GMP-Sepharose Chromatography. *J. Biol. Chem.* **263**(17):8133-8141.

Glavas NA, Ostenson C, Schaefer JB, Vasta V, Beavo JA (2001). T cell activation up-regulates cyclic nucleotide phosphodiesterases 8A1 and 7A3. *Proc. Natl. Acad. Sci. USA* **98**:6319-6324.

Goff SA, Casson LP, Goldberg AL (1984). Heat shock regulatory gene *htpR* influences rates of protein degradation and expression of the *lon* gene in *Escherichia coli*. *Proc. Natl. Acad. Sci. USA* **81**:6647-6651.

Goren EN, Rosen OM (1970). Purification and Properties of a Cyclic Nucleotide Phosphodiesterase from Bovine Heart. *Arch. Biochem. Biophys.* **153**:384-397.

Gottesman S (1996). Proteases and their targets in *Escherichia coli*. *Ann. Rev. Genet.* **30**:465-506.

Gunasekera D, Kemp RG (1999). Cloning, Sequencing, Expression, and Purification of the C Isozyme of Mouse Phosphofructokinase. *Protein Expr. Purif.* **16**:448-453.

Hagenson MJS (1991). Production of Recombinant Proteins in the Methylotrophic Yeast *Pichia pastoris*. In *Purification and Analysis of Recombinant Proteins* (Seetharam R, Sharma SK, eds), pp193-212. Dekker, New York.

Hagiwara M, Endo T, Hidaka H (1984). Effects Of Vinpocetine On Cyclic Nucleotide Metabolism In Vascular Smooth Muscle. *Biochem. Pharmacol.* **33**:453-457.

Han P, Zhu X, Michaeli T (1997). Alternative Splicing of the High Affinity cAMP-Specific Phosphodiesterase (*PDE7A*) mRNA in Human Skeletal Muscle and Heart. *J. Biol. Chem.* **272**:16152-16157.

- Hannig G, Makrides SC (1998). Strategies for optimizing heterologous protein expression in *Escherichia coli*. *Trends Biotechnol.* **16**:54-60.
- Hardman JG, Davis JW, Sutherland EW (1966). Measurement of Guanosine 3',5'-Monophosphate and Other Cyclic Nucleotides. *J. Biol. Chem.* **241**:4812-4815.
- Hardman JG, Davis JW, Sutherland EW (1969). Effects of Some Hormonal and Other Factors on the Excretion of Guanosine 3',5'-Monophosphate and Adenosine 3',5'-Monophosphate in Rat Urine. *J. Biol. Chem.* **244**:6354-6362.
- Hardman JG, Sutherland EW (1969). Guanyl Cyclase, an Enzyme Catalyzing the Formation of Guanosine 3',5'-Monophosphate from Guanosine Triphosphate. *J. Biol. Chem.* **244**:6363-6370.
- Hashimoto Y, Sharma RK, Soderling TR (1989). Regulation of Ca<sup>2+</sup>/Calmodulin-dependent Cyclic Nucleotide Phosphodiesterase by the Autophosphorylated Form of Ca<sup>2+</sup>/Calmodulin-dependent protein Kinase II. *J. Biol. Chem.* **264**:10884-10887.
- Hayashi N, Matsushima K, Ohashi H, Tsunoda H, Murase S, Kawarada Y, Tanaka T (1988). Molecular cloning and characterization of human PDE8B, a novel thyroid-specific isozyme of 3',5'-cyclic nucleotide phosphodiesterase. *Biochem. Biophys. Res. Commun.* **250**:751-756.
- Head JF (1992). A better grip on Calmodulin. *Curr. Biol.* **2**:609-611.
- Heino P, Dillner J, Schwartz S (1995). Human Papillomavirus Type 16 Capsid Proteins Produced from Recombinant Semliki Forest Virus Assemble into Virus-like Particles. *Virology* **214**:349-359.
- Herman SB, Juilfs DM, Fauman EB, Juneau P, Menetski JP (2000). Analysis of a Mutation in Phosphodiesterase Type 4 that alters Both Inhibitor Activity and Nucleotide Selectivity. *Mol. Pharmacol.* **57**:991-999.
- Hetman JM, Soderling SH, Glavas NA, Beavo JA (2000). Cloning and characterization of PDE7B, a cAMP-specific phosphodiesterase. *Proc. Natl. Acad. Sci. USA* **97**:472-476.
- Higgins DR, Cregg JM (1998). Introduction to *Pichia pastoris*. In *Pichia* Protocols (Higgins DR, Cregg JM, eds.), pp15. Humana Press, Totowa, New Jersey.
- Hirai S, Kawasaki H, Yaniv M, Suzuki K (1991). Degradation of transcription factors, c-Jun and c-Fos, by calpain. *FEBS Lett.* **287**:57-61.
- Hitzeman RA, Hagie FE, Levine HL, Goeddel DV, Ammerer G, Hall BD (1981). Expression of a human gene for interferon in yeast. *Nature* **293**:717-722.
- Ho YS, Burden LM, Hurley JH (2000). Structure of the GAF domain, a ubiquitous signaling motif and a new class of cyclic GMP receptor. *EMBO J.* **19**:5288-5299.
- Ho C, Teo TS, Desai R, Wang JH (1976). Catalytic and regulatory properties of two forms of bovine heart cyclic nucleotide phosphodiesterase. *Biochim. Biophys. Acta* **8**:461-473.
- Ho HC, Wirch E, Stevens FC, Wang JH (1977). Purification of a Ca<sup>2+</sup>-activatable Cyclic Nucleotide Phosphodiesterase from Bovine Heart by Specific Interaction with its Ca<sup>2+</sup>-dependant Modulator Protein. *J. Biol. Chem.* **252**:43-50.
- Hoffmann R, Baillie GS, MacKenzie SJ, Yarwood SJ, Houslay MD (1999). The MAP kinase ERK2 inhibits the cyclic AMP-specific phosphodiesterase HSPDE4D3 by phosphorylating it at Ser579. *EMBO J.* **18**:893-903.
- Hofmann A, Zdanov A, Genschik P, Ruvinov S, Filipowicz W, Wlodawer A (2000). Structure and mechanism of activity of the cyclic phosphodiesterase of Appr>p, a product of the tRNA splicing reaction. *EMBO J.* **19**:6207-6217.



- Houslay MD (2001). PDE4 cAMP-Specific Phosphodiesterases. *Prog. Nucleic Acid Res.* **69**:249-315.
- Houslay MD, Sullivan M, Bolger GB (1998). The Multienzyme PDE4 Cyclic Adenosine Monophosphate-Specific Phosphodiesterase Family: Intracellular Targeting, Regulation, and Selective Inhibition by Compounds Exerting Anti-inflammatory and Antidepressant Actions. *Adv. Pharmacol.* **44**:225-342.
- Huang ZJ, Edery I, Rosbash M (1993). PAS is a dimerisation domain common to *Drosophila* Period and several transcription factors. *Nature* **364**:259-262.
- Huston E, Beard M, McCallum F, Pyne NJ, Vandenabeele P, Scotland G, Houslay MD (2000). The cAMP-specific Phosphodiesterase PDE4A5 Is Cleaved Downstream of its SH3 Interaction Domain by Caspase-3. *J. Biol. Chem.* **275**:28063-28074.
- Ignarro LJ (1989). Endothelium-derived nitric oxide: actions and properties. *FASEB J.* **3**:31-36.
- Ignarro LJ, Wood KS, Ballot B, Wolin MS (1984). Guanylate cyclase from bovine lung. *J. Biol. Chem.* **259**(9):5923-5931.
- Ignarro LJ, Wood KS, Ballot B, Wolin MS (1989). Guanylate Cyclase from Bovine Lung. *J. Biol. Chem.* **259**: 5923-5931.
- Ikura M, Clore GM, Gronenborn AM, Zhu G, Klee CB, Bax A (1992). Solution structure of a calmodulin-target peptide complex by multidimensional NMR. *Science* **256**:632-38.
- Innis MA, Gelfand DH (1990). Optimisation of PCRs. In *PCR Protocols* (Innis MA, Gelfand DH, Sninsky JJ, White TJ, eds), pp3-12. Academic Press, New York.
- Ishikawa E, Ishikawa S, Davis JW, Sutherland EW (1969). Determination of Guanosine 3',5'-Monophosphate in Tissues and of Guanyl Cyclase in Rat Intestine. *J. Biol. Chem.* **244**:6371-6376.
- Jacobitz S, McLaughlin MM, Livi GP, Burman M, Torphy TJ (1996). Mapping the Functional Domains of Human Recombinant Phosphodiesterase 4A: Structural Requirements for Catalytic Activity and Rolipram Binding. *Mol. Pharmacol.* **50**:891-899.
- Jaiswal BJ, Conti M (2001). Identification and Functional Analysis of Splice Variants of the Germ Cell Soluble Adenylyl Cyclase. *J. Biol. Chem.* **276**:31698-31708.
- Jiang S, Li J, Paskind M, Epstein PM (1996). Inhibition of calmodulin-dependent phosphodiesterase induces apoptosis in human leukemic cell. *Proc. Natl. Acad. Sci. USA* **93**:11236-11241.
- Jin S-LC, Bushnik T, Lan L, Conti M (1998). Subcellular Localization of Rolipram-sensitive, cAMP-specific Phosphodiesterases. (Differential Targeting And Activation Of The Splicing Variants Derived From The *PDE4D* Gene). *J. Biol. Chem.* **273**:19672-19678
- Jin S-LC, Richard F, Kuo W-P, D'Ercole, Conti M (1999). Impaired growth and fertility of cAMP-specific phosphodiesterase PDE4D-deficient mice. *Proc. Natl. Acad. Sci. USA* **96**:11998-12003.
- Jin S-LC, Swinnen JV, Conti M (1992). Characterization of the Structure of a Low  $K_m$  Rolipram-sensitive cAMP Phosphodiesterase.(Mapping Of The Catalytic Domain). *J. Biol. Chem.* **267**:18929-18939.
- Johansson BE (1999). Immunisation with influenza A virus hemagglutinin and neuraminidase produced in recombinant baculovirus results in a balanced and broadened immune response superior to conventional vaccine. *Vaccine* **17**:2073-2080.
- Julius D, Blair L, Brake A, Sprague G, Thorner J (1983). Yeast  $\alpha$  Factor Is Processed from a Larger Precursor Polypeptide: The Essential Role of a Membrane-bound Dipeptidyl Aminopeptidase. *Cell* **32**:839-852.
- Julius D, Schekman R, Thorner J (1984). Glycosylation and Processing of Prepro- $\alpha$ -Factor through the Yeast

Secretory Pathway. *Cell* **36**:309-318.

Kakiuchi S, Yamazaki R (1970). Calcium dependent phosphodiesterase activity and its activating factor (PAF) from brain: Studies on Cyclic 3',5'-Nucleotide Phosphodiesterase (III). *Biochem. Biophys. Res. Commun.* **41**:1104-1110.

Kakkar R, Raju RVS, Sharma RK (1998). *In Vitro* Generation of an Active Calmodulin-Independent Phosphodiesterase from Brain Calmodulin-Dependent Phosphodiesterase (PDE1A2) by m-calpain. *Arch. Biochem. Biophys.* **358**:320-328.

Kakkar R, Raju RVS, Sharma RK (1999). Calmodulin-dependent cyclic nucleotide phosphodiesterase (PDE1). *Cell. Mol. Life Sci.* **55**:1164-1186.

Kakkar R, Seitz DP, Kanthan R, Rajala RVS, Radhi JM, Wang X, Pasha MK, Wang R, Sharma RK (2002). Calmodulin-dependent cyclic nucleotide phosphodiesterase in an experimental rat model of cardiac ischemia-reperfusion. *Can. J. Physiol. Pharmacol.* **80**:59-66.

Kang YC, Luo L, Wainberg MA, Li Y (1999). Development of HIV/AIDS Vaccine Using Chimeric gag-env Virus-Like Particles. *Biol. Chem.* **380**:353-364.

Kapust RB, Waugh DS (1999). *Escherichia coli* maltose-binding protein is uncommonly effective at promoting the solubility of polypeptides to which it is fused. *Protein. Sci.* **8**:1668-1674.

Kasahara M, Unno T, Yashiro K, Ohmori M (2001). CyaG, a novel cyanobacterial adenylyl cyclase and a possible ancestor of mammalian guanylyl cyclases. *J. Biol. Chem.* **276**:10564-10569.

Kincaid RL, Kempner E, Manganiello VC, Osborne Jr. JC, Vaughan M (1981b). Calmodulin- activated Cyclic Nucleotide Phosphodiesterase from Brain. (Relationship Of Subunit Structure To Activity Assessed By Radiation Inactivation). *J. Biol. Chem.* **256**:11351-11355.

Kincaid RL, Manganiello VC, Ody CE, Osborne Jr JC, Stith-Coleman IE, Danello MA, Vaughan M (1984). Purification and Properties of Calmodulin-stimulated Phosphodiesterase from Mammalian Brain. *J. Biol. Chem.* **259**:5158-5166.

Kincaid RL, Manganiello VC, Vaughan M (1981a). Calmodulin-activated Cyclic Nucleotide Phosphodiesterase from Brain. (Changes In Molecular Size Assessed By Gel Filtration And Electrophoresis). *J. Biol. Chem.* **256**:11345-11350.

Kincaid RL, Stith-Coleman IE, Vaughan M (1985). Proteolytic Activation of Calmodulin-dependent Cyclic Nucleotide Phosphodiesterase. *J. Biol. Chem.* **260**:9009-9015.

King DJ, Walton EF, Yarranton GT (1989). The production of proteins and peptides from *Saccharomyces cerevisiae*. In *Molecular And Cell Biology of Yeasts* (Walton EF, Yarranton GT, eds. ), pp107-133, Blackie, Glasgow.

Kitamura T, Kitamura Y, Kuroda S, Hino Y, Ando M, Kotani K, Konishi H, Matsuzaki H, Kikkawa U, Ogawa W, Kasuga M (1999). Insulin-Induced Phosphorylation and Activation of Cyclic Nucleotide Phosphodiesterase 3B by the Serine-Threonine Kinase Akt. *Mol. Cell Biol.* **19**:6286-6296.

Klee CB, Crouch TH, Krinks MH (1979). Subunit Structure and Catalytic Properties of Bovine Brain Ca<sup>2+</sup>-Dependent Cyclic Nucleotide Phosphodiesterase. *Biochemistry* **18**:722-729.

Koch K-W (1991). Purification and identification of Photoreceptor Guanylate Cyclase. *J. Biol. Chem.* **266**:8634-8637.

Koch K-W, Stryer L (1988). Highly cooperative feedback control of retinal rod guanylate cyclase by calcium ions. *Nature* **334**:64-71.

Kotera J, Fujishige K, Akatsuka H, Imai Y, Yanaka N, Omori K (1998). Novel Alternative Splice Variants

of cGMP-binding cGMP-specific Phosphodiesterase. *J. Biol. Chem.* **273**:26982-26990.

Kotera J, Fujishige K, Imai Y, Kawai E, Michibata H, Akatsuka H, Noriyuki Y, Omori K (1999). Genomic origin and transcriptional regulation of two variants of cGMP-binding cGMP-specific phosphodiesterases. *Eur. J. Biochem.* **262**:866-872.

Kotera J, Yanaka N, Fujishige K, Imai Y, Akatsuka H, Ishizuka T, Kawashima K, Omori K (1997). Expression of rat cGMP-specific phosphodiesterase mRNA in Purkinje cell layers during postnatal development. *Eur. J. Biochem.* **249**:434-442.

Kovala T, Sanwal BD, Ball EH (1997). Recombinant Expression of a Type IV, cAMP-Specific Phosphodiesterase: Characterization and Structure-Function Studies of Deletion Mutants. *Biochemistry* **36**:2968-2976.

Koyanagi M, Suga H, Hoshiyama D, Ono K, Iwabe N, Kuma K, Miyata T (1998). Ancient gene duplication and domain shuffling in the animal cyclic nucleotide phosphodiesterase family. *FEBS Lett.* **436**:323-328.

Kozak M (1989). The Scanning Model for Translation: An Update. *J. Cell Biol.* **108**:229-241.

Krebs EG, Fischer EH (1956). The phosphorylase *b* to *a* converting enzyme of rabbit skeletal muscle. *J. Biol. Chem.* **20**:150-157.

Kurjan J, Herskowitz I (1982). Structure of a Yeast Pheromone Gene (*Mf $\alpha$* ): A Putative  $\alpha$ -Factor Precursor Contains Four Tandem Copies of Mature  $\alpha$ -Factor. *Cell* **30**:933-943.

Laemmli UK (1970). Cleavage of Structural Proteins during the Assembly of the Head of Bacteriophage T4. *Nature* **227**:680-685.

Laliberte F, Han Y, Govindarajan A, Giroux A, Liu S, Bobechko B, Lario P, Bartlett A, Gorseth E, Gresser M, Huang Z (2000). Conformational Difference between PDE4 Apoenzyme and Holoenzyme. *Biochemistry* **39**:6449-6458.

Laroy W, Contreras R (2000). Cloning of *Trypanosoma cruzi* trans-Sialidase and Expression in *Pichia pastoris*. *Protein Expr. Purif.* **20**:389-393.

Lebedeva I, Fujita K, Nihrane A, Silver J (1997). Infectious Particles Derived from Semliki Forest Virus Vectors Encoding Murine Leukemia Virus Envelopes. *J. Virol.* **71**:7061-7067.

Leclerc E, Corti C, Schmid H, Vetter S, James P, Carafoli E (1999). Serine/threonine phosphorylation of calmodulin modulates its interaction with the binding domains of target enzymes. *Biochem. J.* **344**:403-411.

Lenhard JM, Kassel DB, Rocque WJ, Hamacher L, Holmes WD, Patel I, Hoffman C, Luther M (1996). Phosphorylation of a cAMP-specific phosphodiesterase (HSPDE4B2B) by mitogen-activated protein kinase. *Biochem. J.* **316**:751-758.

LeRoy M-J, Degerman E, Taira M, Murata T, Wang LH, Movsesian MA, Meacci E, Manganiello VC (1996). Characterisation of Two Recombinant PDE3 (cGMP-Inhibited Cyclic Nucleotide Phosphodiesterase) Isoforms, RcGIP1 and HcGIP2, Expressed in NIH 3006 Murine Fibroblasts and Sf9 Insect Cells. *Biochemistry* **35**:10194-10202.

Li N, Qu L-J, Liu Y, Li Q, Gu H, Chen Z (1999b). The Refolding, Purification, and Activity Analysis of a Rice Bowman Birk Inhibitor Expressed in *Escherichia coli*. *Protein Expr. Purif.* **15**:99-104.

Li T, Volpp K, Applebury ML (1990). Bovine cone photoreceptor cGMP phosphodiesterase structure deduced from a cDNA clone. *Proc. Natl. Acad. Sci. USA* **87**:293-297.

Li L, Yee C, Beavo JA (1999a). CD3- and CD28-Dependent Induction of PDE7 Required for T Cell Activation. *Science* **283**:848-851.

- Liljeström P (1994). Alphavirus expression systems. *Curr. Opin. Biotechnol.* **5**:495-500.
- Liljeström P, Garoff H (1991). A New Generation Of Animal Cell Expression Vectors Based On The Semliki Forest Virus Replicon. *Bio/Technology* **9**:1356-1361.
- Lim J, Pahlke G, Conti M (1999). Activation of the cAMP-specific Phosphodiesterase PDE4D3 by Phosphorylation.(Identification And Function Of An Inhibitory Domain). *J. Biol. Chem.* **274**:19677-19685.
- Lipkin VM, Khramtsov NV, Vasilevskaya IA, Atabekova NV, Muradov KG, Gubanov VV, Li T, Johnston JP, Volpp KJ, Applebury ML (1990).  $\beta$ -Subunit of Bovine Rod Photoreceptor cGMP Phosphodiesterase. *J. Biol. Chem.* **265**:12955-12959.
- Liu H, Maurice DH (1999). Expression of cyclic GMP-inhibited phosphodiesterases 3A and 3B (PDE3A and PDE3B) in rat tissues; Differential subcellular localisation and regulated expression by cyclic AMP. *Br. J. Pharmacol.* **125**:1501-1510.
- Liu H, Palmer D, Jimmo SL, Tilley DG, Dunkerley HA, Pang SC, Maurice DH (2000). Expression of Phosphodiesterase 4D (*PDE4D*) is Regulated by Both the Cyclic AMP-dependent Protein Kinase and Mitogen-activated Protein Kinase Signaling Pathways (A Potential Mechanism Allowing For The Co-ordinated Regulation Of *PDE4D* Activity And Expression In Cells). *J. Biol. Chem.* **275**:26615-26624.
- Londesborough J (1985). Evidence that the peripheral cyclic AMP phosphodiesterase of rat liver plasma membranes is a metalloenzyme. *Biochem. J.* **225**:143-147.
- Loughney K, Hill TR, Florio VA, Uher L, Rosman GY, Wolda SL, Jones BA, Howard ML, McAllister-Lucas LM, Sonnenburg WK, Francis SH, Corbin JD, Beavo JA, Ferguson K (1998). Isolation and characterisation of cDNAs encoding PDE5A, a human cGMP-binding, cGMP-specific 3',5'-cyclic nucleotide phosphodiesterase. *Gene* **216**:139-147.
- Loughney K, Martins TJ, Harris EAS, Sadhu K, Hicks JB, Sonnenburg WK, Beavo JA, Ferguson K (1996). Isolation and Characterization of cDNAs Corresponding to Two Human Calcium, Calmodulin-regulated, 3',5'-Cyclic Nucleotide Phosphodiesterases. *J. Biol. Chem.* **271**:796-806.
- Lundström K, Mills A, Buell G, Allet E, Adami N, Liljeström P (1994). High-level expression of the human neurokinin-1 receptor in mammalian cell lines using the Semliki Forest virus expression system. *Eur. J. Biochem.* **224**:917-921.
- Lundström K, Turpin MP (1996). Proposed Schizophrenia-Related Gene Polymorphism: Expression of the Ser9Gly Mutant Human Dopamine D<sub>3</sub> with the Semliki Forest Virus System. *Biochem. Biophys. Res. Commun.* **225**:1068-1072.
- Lundström K, Vargas A, Allet B (1995). Functional Activity Of A Biotinylated Human Neurokinin 1 Receptor Fusion Expressed In The Semliki Forest Virus System. *Biochem. Biophys. Res. Commun.* **208**:260-266.
- Ma J, Spremulli LL (1996). Expression, Purification, and Mechanistic Studies of Bovine Mitochondrial Translational Initiation Factor 2. *J. Biol. Chem.* **271**:5805-5811.
- MacFarland TR, Zelus BD, Beavo JA (1991). High Concentrations of a cGMP-stimulated Phosphodiesterase Mediate ANP-induced Decreases in cAMP and Steroidogenesis in Adrenal Glomerulosa Cells. *J. Biol. Chem.* **266**:136-142.
- MacKenzie SJ, Baillie GS, McPhee I, Bolger GB, Houslay MD (2000). ERK2 Mitogen-activated Protein Kinase Binding, Phosphorylation, and Regulation of the PDE4D cAMP-specific Phosphodiesterases. *J. Biol. Chem.* **275**:16609-16617.
- Maggi M, Filippi S, Ledda F, Magini A, Forti G (2000). Erectile dysfunction: from biochemical pharmacology to advances in medical therapy. *Eur. J. Endocrinol.* **143**:143-154.

- Mambetisaeva ET, Martin PEM, Evans WH (1997). Expression of Three Functional Domains of Connexin 32 as Thioredoxin Fusion Proteins in *Escherichia coli* and Generation of Antibodies. *Protein Expr. Purif.* **11**:26-34.
- Manganiello V, Murata T, Taira M, Belfrage P, Degerman E (1995). Diversity in Cyclic Nucleotide Phosphodiesterase Isoenzyme Families. *Arch. Biochem. Biophys.* **322**:1-13.
- Margetts MB, Barr IG, Webb EA (2000). Overexpression, Purification, and Refolding of a *Porphyromonas gingivalis* Cysteine Protease from *Escherichia coli*. *Protein Expr. Purif.* **18**:262-268.
- Marston FAO (1986). The purification of eukaryotic polypeptides synthesized in *Escherichia coli*. *Biochem. J.* **240**:1-12.
- Martinez SE, WU AY, Glavas NA, Tang X-B, Turley S, Hol WGL, Beavo JA (2002). The two GAF domains in phosphodiesterase 2A have distinct roles in dimerization and in cGMP binding. *Proc. Natl. Acad. Sci. USA* **99**:13260-13265.
- Mathews CK, Van Holde KE (1990). Carbohydrate Metabolism 1: Anaerobic Processes in Generating Metabolic Energy. In *Biochemistry*, pp433-466. The Benjamin/Cummings Publishing Company Inc. California.
- Mayer B, Klatt P, Bohme E, Schmidt K (1992). Regulation of Neuronal Nitric Oxide and Cyclic GMP Formation by Ca<sup>2+</sup>. *J. Neurochem.* **59**:2024-2029.
- McAllister-Lucas LM, Haik TL, Colbran JL, Sonnenburg WK, Seger D, Turko IV, Beavo JA, Francis SH, Corbin JD (1995). An Essential Aspartic Acid at Each of Two Allosteric cGMP-binding Sites of a cGMP-specific Phosphodiesterase. *J. Biol. Chem.* **270**:30671-30679.
- McAllister-Lucas LM, Sonnenburg WK, Hadlecek A, Seger D, Trong HL, Colbran JL, Colbran JL, Thomas MK, Walsh KA, Francis SH, Corbin JD, Beavo JA (1993). The Structure of a Bovine Lung cGMP-binding, cGMP-specific Phosphodiesterase Deduced from a cDNA Clone. *J. Biol. Chem.* **268**:22863-22873.
- McCue LA, Anders DG (1998). Soluble Expression and Complex Formation of Proteins Required for HCMV DNA Replication Using the SFV Expression System. *Protein Exp. Purif.* **13**:301-312.
- McPhee I, Yarwood SJ, Scotland G, Huston E, Beard MB, Ross AH, Houslay ES, Houslay MD (1999). Association with the SRC Family Tyrosyl Kinase LYN Triggers a Conformational Change in the Catalytic Region of Human cAMP-specific Phosphodiesterase HSPDE4A4B. *J. Biol. Chem.* **274**:11796-11810.
- Meacci E, Taira M, Moos Jr. M, Smith CJ, Movsesian MA, Degerman, Belfrage P, Manganiello V (1992). Molecular cloning and expression of human myocardial cGMP-inhibited cAMP phosphodiesterase. *Proc. Natl. Acad. Sci. USA* **89**:3721-3725.
- Meador WE, Means AR, Quioco FA (1992). Target enzyme recognition by calmodulin: 2.4Å structure of a calmodulin-peptide complex. *Science* **257**:1251-1255.
- Merrington CL, King LA, Possee RD (1999). Baculovirus expression systems. In *Protein Expression A Practical Approach* (Higgins SJ, Hames BD, eds.), pp101-125. Oxford University Press, England.
- Michaeli T, Bloom TJ, Martins T, Loughney K, Ferguson K, Riggs M, Rodgers L, Beavo JA, Wigler M (1993). Isolation and Characterization of a previously Undetected Human cAMP Phosphodiesterase by Complementation of cAMP Phosphodiesterase-deficient *Saccharomyces cerevisiae*. *J. Biol. Chem.* **268**:12925-12932.
- Michibata H, Yanaka N, Kanoh Y, Okumura K, Omori K (2001). Human Ca<sup>2+</sup>/calmodulin-dependent phosphodiesterase PDE1A: novel splice variants, their specific expression, genomic organization, and chromosomal localization. *Biochim. Biophys. Acta.* **1517**:278-287.
- Mizusawa S, Gottesman S (1983). Protein degradation in *Escherichia coli*: The *lon* gene controls the stability

- of sulA protein. *Proc. Natl. Acad. Sci. USA* **80**:358-362.
- Molinari M, Anagli J, Carafoli E (1995). PEST Sequences Do Not Influence Substrate Susceptibility to Calpain Proteolysis. *J. Biol. Chem.* **270**:2032-2035.
- Monsalve RI, Lu G, King TP (1999). Expressions of Recombinant Venom Allergen, Antigen 5 of Yellowjacket (*Vespula vulgaris*) and Paper Wasp (*Polistes annularis*), in Bacteria or Yeast. *Protein Expr. Purif.* **16**:410-416.
- Morrill ME, Thompson ST, Stellwagen E (1979). Purification of a Cyclic Nucleotide Phosphodiesterase from Bovine Brain Using Blue Dextran-Sepharose Chromatography. *J. Biol. Chem.* **254**:4371-4374.
- Moss B (1991). *Vaccinia* Virus: A Tool for Research and Vaccine Development. *Science* **252**:1662-1667.
- Movsesian MVD (1999). Beta-Adrenergic Receptor Agonists and Cyclic Nucleotide Phosphodiesterase Inhibitors: Shifting the Focus From Inotropy to Cyclic Adenosine Monophosphate. *J. Am. Coll. Cardiol.* **34**:318-324.
- Murachi T (1983). Calpain and calpastatin. *Trends Biochem. Sci.* **8**:167-169.
- Muradov KG, Boyd KK, Martinez SE, Beavo JA, Artemyev NO (2003). The GAFa domains of rod cGMP-phosphodiesterase 6 determine the selectivity of the enzyme dimerisation. *J. Biol. Chem.* In press.
- Murakami K, Whiteley MK, Routtenberg A (1987). Regulation of Protein Kinase C Activity by Cooperative Interaction of Zn<sup>2+</sup> and Ca<sup>2+</sup>. *J. Biol. Chem.* **262**:13902-13906.
- Mykles DL, Skinner DM (1986). Four Ca<sup>2+</sup>-dependent Proteinase Activities Isolated from Crustacean Muscle Differ in Size, Net Charge, and Sensitivity to Ca<sup>2+</sup> and Inhibitors. *J. Biol. Chem.* **261**:9865-9871.
- Nakamura T, Gold GH (1987). A cyclic nucleotide-gated conductance in olfactory receptor cilia. *Nature* **325**:442-444.
- Nigg EA (1997). Nucleocytoplasmic transport: signals, mechanisms and regulation. *Nature* **386**:779-787.
- Nishi A, Snyder GL, Greengard P (1997). Bidirectional Regulation of DARPP-32 Phosphorylation by Dopamine. *J. Neurosci.* **17**:8147-8155.
- Novack JP, Charbonneau H, Bentley JK, Walsh KA, Beavo JA (1991). Sequence Comparison of the 63-, 61-, and 59-kDa Calmodulin-Dependent Cyclic Nucleotide Phosphodiesterases. *Biochemistry* **30**:7940-7947.
- O'Connell JC, McCallum JF, McPhee I, Wakefield J, Houslay ES, Wishart W, Bolger G, Frame M, Houslay MD (1996). The SH3 domain of Src tyrosyl protein kinase interacts with the N-terminal splice region of the PDE4A cAMP-specific phosphodiesterase RPDE-6 (RNPDE4A5). *Biochem. J.* **318**:255-262.
- Ogata K, Nishikawa H, Ohsugi M (1969). A Yeast Capable of Utilizing Methanol. *Agr. Biol. Chem.* **33**(10):1519-1520.
- Ogawa R, Streiff MB, Bugayenko A, Kato G (2002). Inhibition of PDE4 phosphodiesterase activity induces growth suppression, apoptosis, glucocorticoid sensitivity, p53, and p21<sup>WAF1/CIP1</sup> proteins in human acute lymphoblastic leukemia cells. *Blood* **99**:3390-3397.
- Ohno S (1997). The Reason for as Well as the Consequence of the Cambrian Explosion in Animal Evolution. *J. Mol. Evol.* **44**:S23-S27.
- Okamura N, Onoe S, Sugita Y, Paquignon M, Dacheux F, Dacheux JL (1991). Water insoluble fraction of egg yolk maintains porcine sperm motility by activating adenylate cyclase. *Mol. Reprod. Dev.* **28**:136-142.
- Okamura N, Tajima Y, Soejima A, Masuda H, Sugita Y (1985). Sodium Bicarbonate in Seminal Plasma Stimulates the Motility of Mammalian Spermatozoa through Direct Activation of Adenylate Cyclase. *J. Biol.*

*Chem.* **260**:9699-9705.

Ollivier V, Parry GC, Cobb RR, de Prost D, Mackman N (1996). Elevated cyclic AMP inhibits NF-kappaB-mediated transcription in human monocytic cells and endothelial cells. *J. Biol. Chem.* **271**:20828-20835.

Pace U, Hanski E, Salomon Y, Lancet D (1985). Odorant-sensitive adenylate cyclase may mediate olfactory reception. *Nature* **316**:255-259.

Packer M, Carver JR, Rodeheffer RJ, Ivanhoe RJ, DiBianco R, Zeldis SM, Hendrix GH, Bommer WJ, Elkayam U, Kukin ML, Mallis GI, Sollano JA, Shannon J, Tandon PK, DeMets DL (1991). Effect of oral milrinone on mortality in severe chronic heart failure. *New Engl. J. Med.* **325**:1468-1475.

Palmer D, Maurice DH (2000). Dual Expression and Differential Regulation of Phosphodiesterase 3A and Phosphodiesterase 3B in Human Vascular Smooth Muscle: Implications for Phosphodiesterase 3 Inhibition in Human Cardiovascular Tissues. *Mol. Pharmacol.* **58**:247-252.

Patra AK, Mukhopadhyay R, Mukhija R, Krishnan A, Garg LC, Panda AK (2000). Optimization of Inclusion Body Solubilization and Renaturation of Recombinant Human Growth Hormone from *Escherichia coli*. *Protein Expr. Purif.* **18**:182-192.

Pawson T, Scott JD (1997). Signaling Through Scaffold, Anchoring, and Adaptor Proteins. *Science* **278**:2075-2080.

Payne ME, Schworer CM, Soderling TR (1983). Purification and Characterisation of Rabbit Liver Calmodulin-dependent Glycogen Synthase Kinase. *J. Biol. Chem.* **258**:2376-2382.

Pearson RB, Woodgett JR, Cohen P, Kemp BE (1985). Substrate Specificity of a Multifunctional Calmodulin-dependent Protein Kinase. *J. Biol. Chem.* **260**:14471-14476.

Pfeuffer T, Metzger H (1982). 7-O-Hemisuccinyl-deacetyl forskolin-Sepharose: a novel affinity support for purification of adenylate cyclase. *FEBS Lett.* **146**:369-375.

Pillai R, Kytte K, Reyes A, Colicelli J (1993). Use of a yeast expression system for the isolation and analysis of drug-resistant mutants of a mammalian phosphodiesterase. *Proc. Natl. Acad. Sci. USA* **90**:11970-11974.

Prouty WF, Karnovsky MJ, Goldberg AL (1975). Degradation of Abnormal Proteins in *Escherichia coli*. *J. Biol. Chem.* **250**:1112-1122.

Purvis K, Rui H (1988). High-affinity, calmodulin-dependent isoforms of cyclic nucleotide phosphodiesterase in rat testis. *Methods Enzymol.* **159**:675-685.

Qiu J, Swartz JR, Georgiou G (1998). Expression of Active Human Tissue-Type Plasminogen Activator in *Escherichia coli*. *Appl. Environ. Microbiol.* **64**:4891-4896.

Quadroni M, L'Hostis EL, Corti C, Myagkikh I, Durussel I, Cos J, James P, Carafoli E (1998). Phosphorylation of Calmodulin Alters Its Potency as an Activator of Target Enzymes. *Biochemistry* **37**:6523-6532.

Rajamohan F, Doumbia SO, Engstrom CR, Pendergras SL, Maher DL, Uckun FM (2000). Expression of Biologically Active Recombinant Pokeweed Antiviral Protein in Methylotrophic Yeast *Pichia pastoris*. *Proc. Natl. Acad. Sci. USA* **18**:193-201.

Rall TW, Sutherland EW (1958). Formation Of A Cyclic Adenine Ribonucleotide By Tissue Particles. *J. Biol. Chem.* **232**:1065-1076.

Rall TW, Sutherland EW, Berthet J (1957). The relationship of epinephrine and glucagon to liver phosphorylase. *J. Biol. Chem.* **224**:463475.

Rasmussen L, Battles JK, Ennis WH, Nagashima K, Gonda MA (1990). Characterisation of virus-like

particles produced by a recombinant baculovirus containing the *gag* gene of the bovine immunodeficiency-like virus. *Virology* **178**:435-451.

Reeves ML, Leigh BK, England PJ (1987). The identification of a new cyclic nucleotide phosphodiesterase activity in human and guinea-pig cardiac ventricle.(Implications for the mechanism of action of selective phosphodiesterase inhibitors.). *Biochem. J.* **241**:535-541.

Reinhardt RR, Chin E, Zhou J, Taira M, Manganiello VC, Bondy CA (1995). Distinctive Anatomical Patterns of Gene Expression for cGMP-inhibited Cyclic Nucleotide Phosphodiesterases. *J. Clin. Invest.* **95**:1528-1538.

Reiser J, Glumoff V, Kalin M, Ochsner U (1990). Transfer and Expression of Heterologous Genes in Yeasts Other Than *Saccharomyces cerevisiae*. In *Advances in Biochemical Engineering/Biotechnology* (Fiechter A, ed), pp75-102. Springer-Verlag, Berlin, Heidelberg.

Repaske DR, Corbin JG, Conti M, Goy MF (1993). A cyclic GMP-stimulated cyclic nucleotide phosphodiesterase gene is highly expressed in the limbic system of the rat brain. *Neuroscience* **56**:673-686.

Repaske DR, Swinnen JV, Jin S-LC, Van Wyk JJ, Conti M (1992). A Polymerase Chain Reaction Strategy to Identify and Clone Cyclic Nucleotide Phosphodiesterase cDNAs. *J. Biol. Chem.* **267**:18683-18688.

Restrepo D, Miyamoto T, Bryant BP, Teeter JH (1990). Odor Stimuli Trigger Influx of Calcium into Olfactory Neurons of the Channel Catfish. *Science* **249**:1166-1168.

Richter W, Conti M (2002). Dimerisation of the Type 4 cAMP-specific Phosphodiesterase Is Mediated by the Upstream Conserved Regions (UCRs). *J. Biol. Chem.* **277**:40212-40221.

Richter W, Hermsdorf T, Kronbach T, Dettmer D (2002). Refolding and Purification of Recombinant Human PDE7A Expressed in *Escherichia coli* as inclusion Bodies. *Protein Expr. Purif.* **25**:138-148.

Richter W, Hermsdorf T, Lilie H, Egerland U, Rudolph R, Kronbach T, Dettmer D (2000). Refolding, Purification, and Characterization of Human Recombinant PDE4A Constructs Expressed in *Escherichia coli*. *Protein Expr. Purif.* **19**:375-383.

Richter W, Unciuleac L, Hermsdorf T, Kronbach T, Dettmer D (2001a). Identification of substrate specificity determinants in human cAMP-specific phosphodiesterase 4A by single-point mutagenesis. *Cell. Signal.* **13**:159-167.

Richter W, Unciuleac L, Hermsdorf T, Kronbach T, Dettmer D (2001b). Identification of inhibitor binding sites of the cAMP-specific phosphodiesterase 4. *Cell. Signal.* **13**:287-297.

Rocque WJ, Holmes WD, Patel IR, Dougherty RW, Ittoop O, Overton L, Hoffman CR, Wisely GB, Willard DH, Luther MA (1997a). Detailed Characterization of a Purified Type 4 Phosphodiesterase, HSPDE4B2B: Differentiation of High- and Low-Affinity (*R*)-Rolipram Binding. *Protein Expr. Purif.* **9**:191-202.

Rocque WJ, Tian G, Wiseman JS, Holmes WD, Zajac-Thompson I, Willard DH, Patel IR, Wisely GB, Clay WC, Kadwell SH, Hoffman CR, Luther MA (1997b). Human Recombinant Phosphodiesterase 4B2B Binds (*R*)-Rolipram at a Single Site with Two Affinities. *Biochemistry* **36**:14250-14261.

Rogelj B, Strukelj B, Bosch D, Jongsma MA (2000). Expression, Purification, and Characterisation of Equistatin in *Pichia pastoris*. *Protein Expr. Purif.* **19**:329-334.

Rogers S, Wells R, Rechsteiner M (1986). Amino Acid Sequences Common to Rapidly Degraded Proteins: The PEST Hypothesis. *Science* **234**:364-368.

Romanos MA, Scorer CA, Clare JJ (1992). Foreign Gene Expression in Yeast: a Review. *Yeast* **8**:423-488.

Rosenberg GB, Storm DR (1987). Immunological Distinction between Calmodulin-sensitive and Calmodulin-insensitive Adenylate Cyclases. *J. Biol. Chem.* **262**:7623-7628.



- Rosman GJ, Martins TJ, Sonnenburg WK, Beavo JA, Ferguson K, Loughney K (1997). Isolation and characterisation of human cDNAs encoding a cGMP-stimulated 3',5'-cyclic nucleotide phosphodiesterase. *Gene* **191**:89-95.
- Ross EK, Fuerst TR, Orenstein JM, O'Neill JM, Martin T, Venkatesan S (1991). Maturation of human immunodeficiency virus particles assembled from the gag precursor protein required in situ processing by gag-pol protease. *AIDS Res. Hum. Retroviruses* **7**:475-483.
- Rossi P, Giorgi M, Geremia R (1988). Testis-specific Calmodulin-dependent phosphodiesterase. *J. Biol. Chem.* **263**:15521-15527.
- Sachdev D, Chirgwin JM (1998). Order of Fusions between Bacterial and Mammalian Proteins Can Determine Solubility in *Eschericia coli*. *Biochem. Biophys. Res. Commun.* **244**:933-937.
- Sambrook J, Fritsch EF, Maniatis T (eds) (1989). *Molecular cloning: A laboratory manual*. Cold Spring Harbour Laboratory Press. New York.
- Sasaki T, Kotera J, Yuasa K, Omori K (2000). Identification of Human PDE7B, a cAMP-Specific Phosphodiesterase. *Biochem. Biophys. Res. Commun.* **271**:575-583.
- Sass P, Field J, Nikawa J, Toda T, Wigler M (1986). Cloning and characterisation of the high-affinity cAMP phosphodiesterase of *Saccharomyces cerevisiae*. *Proc. Natl. Acad. Sci. USA* **83**:9303-9307.
- Schneider EL, Thomas GJ, Bassuk JA, Sage EH, Baneyz F (1997). Manipulating the aggregation and oxidation of human SPARC in the cytoplasm of *Eschericia coli*. *Nature Biotechnol.* **15**:581-585.
- Schudt C, Gantner F, Tenors H, Hatzelmann A (1999). Therapeutic Potential of Selective PDE Inhibitors in Asthma. *Pulm. Pharmacol. Ther.* **12**:123-129.
- Schulz S, Chinkers M, Garbers DL (1989). The guanylate cyclase/receptor family of proteins. *FASEB J.* **3**:2026-2035.
- Schumacher MA, Rivard AF, Bächinger HP, Adelman JP (2001). Structure of the gating-domain of a Ca<sup>2+</sup>-activated K<sup>+</sup> channel complexed with Ca<sup>2+</sup>/calmodulin. *Nature* **410**:1120-1124.
- Schwabe U, Miyake M, Ohga Y, Daly JW (1976). 4-(3-Cyclopentyloxy-4-methoxyphenyl)-2-pyrrolidone (ZK 62711): a Potent Inhibitor of Adenosine Cyclic 3',5'-Monophosphate Phosphodiesterase in Homogenates and Tissue Slices from Rat Brain. *Mol. Pharmacol.* **12**:900-910.
- Seamon KB, Padgett W, Daly JW (1981). Forskolin: Unique diterpene activator of adenylate cyclase in membranes and in intact cells. *Proc. Natl. Acad. Sci. USA* **78**:3363-3367.
- Seidah NG, Lazure C, Chretien M, Thibault G, Garcia R, Cantin M, Genest J, Nutt RF, Brady SF, Lyle TA, Paleveda WJ, Colton CD, Ciccarone TM, Veber DF (1984). Amino acid sequence of homologous rat atrial peptides: Natriuretic activity of native and synthetic forms. *Proc. Natl. Acad. Sci. USA* **81**:2640-2644.
- Sette C, Conti M (1996). Phosphorylation and Activation of a cAMP-specific Phosphodiesterase by the cAMP-dependent Protein Kinase. (Involvement Of Serine 54 In The Enzyme Activation). *J. Biol. Chem.* **271**:16526-16534.
- Shakur Y, Takeda K, Kenan Y, Yu Z-X, Rena G, Brandt D, Houslay MD, Degerman E, Ferrans VJ, Manganiello VC (2000). Membrane Localization of Cyclic Nucleotide Phosphodiesterase 3 (PDE3). *J. Biol. Chem.* **275**:38749-38761.
- Shabb JB, Corbin JD (1992). Cyclic Nucleotide-binding Domains in Proteins Having Diverse Functions. *J. Biol. Chem.* **267**:5723-5726.
- Sharma RK (1991). Phosphorylation and Characterisation of Bovine Heart Calmodulin-Dependent Phosphodiesterase. *Biochemistry* **30**:5963-5968.

- Sharma RK, Adachi A-M, Adachi K, Wang JH (1984). Demonstration of Bovine Brain Calmodulin-dependent Cyclic Nucleotide Phosphodiesterase Isozymes by Monoclonal Antibodies. *J. Biol. Chem.* **259**:9248-9254.
- Sharma RK, Kalra J (1994). Characterisation of calmodulin-dependent cyclic nucleotide phosphodiesterase isoenzymes. *Biochem. J.* **299**:97-100.
- Sharma RK, Wang JH (1985). Differential regulation of bovine brain calmodulin-dependent cyclic nucleotide phosphodiesterase isoenzymes by cyclic AMP-dependent protein kinase and calmodulin-dependent phosphatase. *Proc. Natl. Acad. Sci. USA* **82**:2603-2607.
- Sharma RK, Wang JH (1986a). Calmodulin and Ca<sup>2+</sup>-dependent Phosphorylation and Dephosphorylation of 63-kDa Subunit-containing Bovine Brain Calmodulin-stimulated Cyclic Nucleotide Phosphodiesterase Isozyme. *J. Biol. Chem.* **261**:1322-1328.
- Sharma RK, Wang JH (1986b). Purification and Characterization of Bovine Lung Calmodulin-dependent Cyclic Nucleotide Phosphodiesterase. *J. Biol. Chem.* **261**:14160-14166.
- Sharma RK, Wang TH, Wirch E, Wang JH (1980). Purification and Properties of Bovine Brain Calmodulin-dependent Cyclic Nucleotide Phosphodiesterase. *J. Biol. Chem.* **255**:5916-5923.
- Sharma RK, Wirch E (1979). Ca<sup>2+</sup>-dependent cyclic nucleotide phosphodiesterase from rabbit lung. *Biochem. Biophys. Res. Commun.* **91**:338-344.
- Shenolikar S, Thompson WJ, Strada SJ (1985). Characterisation of a Ca<sup>2+</sup>-Calmodulin-Stimulated Cyclic GMP Phosphodiesterase from Bovine Brain. *Biochemistry* **24**:672-678.
- Shi YP, Hasnain SE, Sacci JB, Holloway BP, Fujioka H, Kumar N, Wohlhueter R, Hoffman SL, Collins WE, Lal AA (1999). Immunogenicity and *in vitro* protective efficacy of a recombinant multistage *Plasmodium falciparum* candidate vaccine. *Proc. Natl. Acad. Sci. USA* **96**:1615-1620.
- Singh S, Lowe DG, Thorpe DS, Rodriguez H, Kuang W-J, Dangott LJ, Chinker M, Goeddel DV, Garbers DL (1988). Membrane guanylate cyclase is a cell-surface receptor with homology to protein kinases. *Nature* **334**:708-715.
- Sklar PB, Anholt RRH, Snyder SH (1986). The Odorant-sensitive Adenylate Cyclase of Olfactory Receptor Cells. *J. Biol. Chem.* **261**:15538-15543.
- Smigel MD (1986). Purification of the Catalyst of Adenylate Cyclase. *J. Biol. Chem.* **264**:1976-1986.
- Smith DB, Johnson KS (1988). Single-step purification of polypeptides expressed in *Escherichia coli* as fusions with glutathione S-transferase. *Gene* **67**:31-40.
- Smith KJ, Scotland G, Beattie J, Trayer IP, Houslay MD (1996). Determination of the Structure of the N-terminal Splice Region of the Cyclic AMP-specific Phosphodiesterase RD1 (RNPDE4A1) by <sup>1</sup>H NMR and Identification of the Membrane Association Domain Using Chimeric Constructs. *J. Biol. Chem.* **271**:16703-16711.
- Smithburn KC, Haddow AJ (1944). Semliki Forest Virus: I. Isolation and Pathogenic Properties. *J. Immunol.* **49**:141-157.
- Snyder PB, Florio VA, Ferguson K, Loughney K (1999). Isolation, Expression and Analysis of Splice Variants of a Human Ca<sup>2+</sup>/Calmodulin-Stimulated Phosphodiesterase (PDE1A). *Cell. Signal.* **11**:535-544.
- Soderling SH, Bayuga SJ, Beavo JA (1998). Cloning and characterization of a cAMP-specific cyclic nucleotide phosphodiesterase. *Proc. Natl. Acad. Sci. USA* **95**:8991-8996.
- Soderling SH, Bayuga SJ, Beavo JA (1999). Isolation and characterization of a dual-substrate

- phosphodiesterase gene family: PDE10A. *Proc. Natl. Acad. Sci. USA* **96**:7071-7076.
- Soderling SH, Beavo JA (2000). Regulation of cAMP and cGMP signaling: new phosphodiesterases and new functions. *Curr. Opin. Cell Biol.* **12**:174-179.
- Soderling TR, Schworer CM, Payne ME, Jett MF, Porter DK, Atkinson JL, Richtand NM (1986). Calcium (calmodulin)-dependent protein kinase 11. In *Hormones and Cell Regulation* (Nunez J, Dumont JE, King RJB, eds), pp141-157. John Libbey Eurotext Ltd.
- Sonnenburg WK, Mullaney PJ, Beavo JA (1991). Molecular Cloning of a Cyclic GMP-stimulated Cyclic Nucleotide Phosphodiesterase cDNA. *J. Biol. Chem.* **266**:17655-17661.
- Sonnenburg WK, Rybalkin SD, Bornfeldt KE, Kwak KS, Rybalkina IG, Beavo JA (1998). Identification, Quantitation, and Cellular Localization of PDE1 Calmodulin-Stimulated Cyclic Nucleotide Phosphodiesterases. *Methods Companion Methods Enzymol* **14**:3-19.
- Sonnenburg WK, Seger D, Kwak KS, Huang J, Charbonneau H, Beavo JA (1995). Identification of Inhibitory and Calmodulin-binding Domains of the PDE1A1 and PDE1A2 Calmodulin-stimulated Cyclic Nucleotide Phosphodiesterases. *J. Biol. Chem.* **270**:30989-31000.
- Sorimachi H, Ishiura S, Suzuki K (1997). Structure and physiological function of calpains. *Biochem. J.* **328**:721-732.
- Sreekrishna K, Potenz RHB, Cruze JA, McCombie WR, Parker KA, Nelles L, Mazzaferro PK, Holden KA, Harrison RG, Wood PJ, Phelps DA, Hubbard CE, Fuke M (1988). High level expression of heterologous proteins in methylotrophic yeast *Pichia pastoris*. *J. Basic Microbiol.* **28**:265-278.
- Stables J, Rees S, Lundstrom K, Livingstone D, Lee MG (1997). High Level Expression of the Human 5-HT<sub>1D</sub> Serotonin Receptor Using the Semliki Forest Virus Expression System. *Ann. N. Y. Acad. Sci.* **812**:229-230.
- Stone JR, Marletta MA (1995). Heme Stoichiometry of Heterodimeric Soluble Guanylate Cyclase. *Biochemistry* **34**:14668-14674.
- Strada SJ, Martins, MW, Thompson WJ (1984). Nomenclature recommendations. *Adv. Cyclic nucleotide Protein Phosphorylation Res.* **16**:13-29.
- Strauss JH, Strauss EG (1994). The Alphaviruses: Gene Expression, Replication, and Evolution. *Microbiol. Rev.* **58**:491-562.
- Sutherland EW, Rall TW (1958). Fractionation And Characterization Of A Cyclic Adenine Ribonucleotide Formed By Tissue Particles. *J. Biol. Chem.* **232**:1077-1091.
- Sutter G, Moss B (1992). Nonreplicating *Vaccinia* vector efficiently expresses recombinant genes. *Proc. Natl. Acad. Sci. USA* **89**:10847-10851.
- Takahashi RH, Nagashima K, Kurata T, Takahashi H (1999). Analysis of Human Lymphotropic T-Cell Virus Type 11-like Particle Production by Recombinant Baculovirus-infected Insect Cells. *Virology* **256**:371-380.
- Tang KM, Jang EK, Haslam RJ (1997). Expression and Mutagenesis of the catalytic domain of cGMP-inhibited phosphodiesterase (PDE3) cloned from human platelets. *Biochem. J.* **323**:217-224.
- Tasken KA, Collas P, Kemmner WA, Witczak O, Conti M, Tasken K (2001). Phosphodiesterase 4D and Protein Kinase A Type II Constitute a Signaling Unit in the Centrosomal Area. *J. Biol. Chem.* **276**:21999-22002.
- Taussig R, Gilman AG (1995). Mammalian Membrane-bound Adenylyl cyclases. *J. Biol. Chem.* **270**:1-4.
- Tempel BL, Bonini N, Dawson DR, Quinn WG (1983). Reward learning in normal and mutant *Drosophila*.

*Proc. Natl. Acad. Sci. USA* **80**:1482-1486.

Teo TS, Wang TH, Wang JH (1973). Purification and Properties of the Protein Activator of Bovine Heart Cyclic Adenosine 3',5'-Monophosphate Phosphodiesterase. *J. Biol. Chem.* **248**:588-595.

Thomas MK, Francis SH, Corbin JD (1990a). Characterisation of a Purified Bovine Lung cGMP-binding cGMP Phosphodiesterase. *J. Biol. Chem.* **265**:14964-14970.

Thomas MK, Francis SH, Corbin JD (1990b). Substrate- and Kinase-directed Regulation of Phosphorylation of a cGMP-binding Phosphodiesterase by cGMP. *J. Biol. Chem.* **265**:14971-14978.

Thompson WJ, Appleman MM (1971). Multiple Cyclic Nucleotide Phosphodiesterase Activities from Rat Brain. *Biochemistry* **10**:311-316.

Trong HL, Beier N, Sonnenburg WK, Stroop SD, Walsh KA, Beavo JA, Charbonneau H (1990). Amino Acid Sequence of the cyclic GMP Stimulated Cyclic Nucleotide Phosphodiesterase from Bovine Heart. *Biochemistry* **29**:10280-10288.

Tschopp JF, Brust PF, Cregg JM, Stillman CA, Gingeras TR (1987a). Expression of the *lacZ* gene from two methanol-regulated promoters in *Pichia pastoris*. *Nucl. Acids Res.* **15**:3859-3877.

Tschopp JF, Sverlow G, Kosson R, Craig W, Grinna L (1987b). High-level expression of glycosylated invertase in the methylotrophic yeast, *Pichia pastoris*. *Bio/Technology* **5**:1305-1308.

Tucker MM, Robinson Jr. JB, Stellwagen E (1981). The Effect of Proteolysis on the Calmodulin Activation of Cyclic Nucleotide Phosphodiesterase. *J. Biol. Chem.* **256**:9051-9058.

Turko IV, Francis SH, Corbin JD (1998a). Potential Roles of Conserved Amino Acids in the Catalytic Domain of the cGMP-binding cGMP-specific Phosphodiesterase (PDE5). *J. Biol. Chem.* **273**:6460-6466.

Turko IV, Francis SH, Corbin JD (1998b). Binding of cGMP to both allosteric sites of cGMP-binding cGMP-specific phosphodiesterase (PDE5) is required for its phosphorylation. *Biochem. J.* **329**:505-510.

Turko IV, Haik TL, McAllister-Lucas LM, Burns F, Francis SH, Corbin JD (1996). Identification of Key Amino Acids in a Conserved cGMP-binding Site of cGMP-binding Phosphodiesterases. *J. Biol. Chem.* **271**:22240-22244.

Vaillancourt P, Zheng C-F, Hoang DQ, Breister L (2000). Affinity Purification of Recombinant Proteins Fused to Calmodulin or to Calmodulin-Binding Peptides. *Methods Enzymol.* **326**:340-362.

Valenzuela P, Medina A, Rutter WJ (1982). Synthesis and assembly of hepatitis B virus surface antigen particles in yeast. *Nature* **298**:347-350.

Vallee BL, Auld DS (1990a). Active-site zinc ligands and activated H<sub>2</sub>O of zinc enzymes. *Proc. Natl. Acad. Sci. USA* **87**:220-224.

Vallee BL, Auld DS (1990b). Zinc Coordination, Function, and Structure of Zinc Enzymes and Other Proteins. *Biochemistry* **29**:5647-5659.

Varnerin JP, Smith T, Rosenblum CI, Vongs A, Murphy BA, Nunes C, Mellin TN, King JJ, Burgess BW, Junker B, Chou M, Hey P, Frazier E, MacIntyre DE, Van der Ploeg LHT, Tota MR (1998). Production of Leptin in *Escherichia coli*: A Comparison of Methods. *Protein Expr. Purif.* **14**:335-342.

Verde I, Pahlke G, Salanova M, Zhang G, Wang S, Coletti D, Onuffer J, Jin S-LJ, Conti M (2001). Myomegalin Is a Novel Protein of the Golgi/Centrosome That Interacts with a Cyclic Nucleotide Phosphodiesterase. *J. Biol. Chem.* **276**:11189-11198.

Waisman D, Stevens FC, Wang JH (1975). The distribution of the Ca<sup>2+</sup>-dependent protein activator of cyclic nucleotide phosphodiesterase in invertebrates. *Biochem. Biophys. Res. Commun.* **65**:975-982.

- Waldman SA, Rapoport RM, Murad F (1984). Atrial Natriuretic Factor Selectively Activates Particulate Guanylate Cyclase and Elevates Cyclic GMP in Rat Tissues. *J. Biol. Chem.* **259**:14332-14334.
- Wang J, Cooper MD (1993). Histidine residue in the zinc-binding motif of aminopeptidase A is critical for enzymatic activity. *Proc. Natl. Acad. Sci. USA* **90**:1222-1226.
- Wang P, Wu P, Egan RW, Billah MB (2000). Cloning, Characterization, and Tissue Distribution of Mouse Phosphodiesterase 7A1. *Biochem. Biophys. Res. Commun.* **276**:1271-1277.
- Wegner GH (1990). Emerging applications of the methylotrophic yeasts. *Microbiol. Rev.* **87**:279-284.
- Weishaar RE, Burrows SD, Kobylarz DC, Quade MM, Evans DB (1986). Multiple molecular forms of cyclic nucleotide phosphodiesterase in cardiac and smooth muscle and in platelets. *Biochem. Pharmacol.* **35**:787-900.
- Westcott KR, La Porte DC, Storm DR (1979). Resolution of adenylate cyclase sensitive and insensitive to  $Ca^{2+}$  and calcium-dependent regulatory protein (CDR) by CDR-Sepharose affinity chromatography. *Proc. Natl. Acad. Sci. USA* **76**:204-208.
- White DW, Tartaglia LA (1996). Leptin and OB-R: Body Weight Regulation by a Cytokine Receptor. *Cytokine Growth Factor Rev.* **7**:303-309.
- White CL, Thomson M, Dimmock NJ (1998). Deletion Analysis of a Defective Interfering Semliki Forest Virus RNA Genome Defines a Region in the nsP2 Sequence That Is Required for Efficient Packaging of the Genome into Virus Particles. *J. Virol.* **72**:4320-4326.
- Wijkander J, Host LS, Rahn T, Resjo S, Castan I, Manganiello V, Belfrage P, Degerman E (1997). Regulation of Protein Kinase B in Rat Adipocytes by Insulin, Vanadate, and Peroxovanadate. *J. Biol. Chem.* **272**:21520-21526.
- Willems WR, Kaluza G, Boschek CB, Bauer H, Hager H, Schutz H-J, Feistner H (1979). Semliki Forest Virus: Cause of a Fatal Case of Human Encephalitis. *Science* **203**:1127-1129.
- Williams DC, Van Frank RM, Muth WL, Burnett JP (1982). Cytoplasmic Inclusion Bodies in *Escherichia coli* Producing Biosynthetic Human Insulin Proteins. *Science* **215**:687-689.
- Winqvist RJ, Faison EP, Waldman SA, Schwartz K, Murad F, Rapoport RM (1984). Atrial natriuretic factor elicits an endothelium-independent relaxation and activates particulate guanylate cyclase in vascular smooth muscle. *Proc. Natl. Acad. Sci. USA* **81**:7661-7664.
- Wuttke MS, Buck J, Levin LR (2001). Bicarbonate-Regulated Soluble Adenylyl Cyclase. *J. Pancreas* **2**:154-158.
- Xu RX, Hassell AM, Vanderwall D, Lambert MH, Holmes WD, Luther MA, Rocque WJ, Milburn MV, Zhao Y, Ke H, Nolte RT (2000). Atomic Structure of PDE4: Insights into Phosphodiesterase Mechanism and Specificity. *Science* **288**:1822-1825.
- Yan C, Bentley JK, Sonnenburg, Beavo JA (1994). Differential Expression of the 61 kDa and 63 kDa Calmodulin-Dependent Phosphodiesterase in the Mouse Brain. *J. Neurosci.* **14**:973-984.
- Yan C, Zhao AZ, Bentley JK, Beavo JA (1996). The Calmodulin-dependent Phosphodiesterase Gene *PDE1C* Encodes Several Functionally Different Splice Variants in a Tissue-specific Manner. *J. Biol. Chem.* **271**:25699-25706.
- Yan C, Zhao AZ, Bentley JK, Loughney K, Ferguson K, Beavo JA (1995). Molecular cloning and characterization of a calmodulin-dependent phosphodiesterase enriched in olfactory sensory neurons. *Proc. Natl. Acad. Sci. USA* **92**:9677-9681.
- Yarwood SJ, Steele MR, Scotland G, Houslay MD, Bolger GB (1999). The RACK1 Signaling Scaffold

Protein Selectively Interacts with the cAMP-specific Phosphodiesterase PDE4D5 Isoform. *J. Biol. Chem.* **274**:14909-14917.

Yu J, Wolda SL, Frazier ALB, Florio VA, Martins TJ, Snyder PB, Harris EAS, McCaw KN, Farrell CA, Steiner B, Bentley KJ, Beavo JA, Ferguson K, Gelin R (1997). Identification and Characterisation of a Human Calmodulin-Stimulated Phosphodiesterase PDE1B1. *Cell. Signal.* **9**:519-529.

Yuan T, Walsh MP, Sutherland C, Fabian H, Vogel HJ (1999). Calcium-Dependent and -Independent Interactions of the Calmodulin-Binding Domain of Cyclic Nucleotide Phosphodiesterase with Calmodulin. *Biochemistry* **38**:1446-1455.

Yuasa K, Kanoh Y, Okumura K, Omori K (2001). Genomic organisation of the human phosphodiesterase PDE11A gene. *Eur. J. Biochem.* **268**:168-178.

Yuasa K, Kotera J, Fujishige K, Michibata H, Sasaki T, Omori K (2000). Characterisation and Characterisation of Two Novel Phosphodiesterase PDE11A Variants Showing Unique Structure and Tissue-specific Expression. *J. Biol. Chem.* **275**:31469-31479.

Zahn K (1996). Overexpression of an mRNA Dependent on Rare Codons Inhibits Protein synthesis and Cell Growth. *J. Bacteriol.* **178**:2926-2933.

Zhao AZ, Shinohara MM, Huang D, Shimizu M, Eldar-Finkelman H, Krebs EG, Beavo JA, Bornfeldt KE (2000). Leptin Induces Insulin-like Signaling that Antagonizes cAMP Elevation by glucagon in Hepatocytes. *J. Biol. Chem.* **275**:11348-11354.

Zsebo KM, Lu H-S, Fieschko JC, Goldstein L, Davis J, Duker K, Suggs SV, Lai P-H, Bitter GA (1986). Protein Secretion from *Saccharomyces cerevisiae* Directed by the Prepro- $\alpha$ -factor Leader Region. *J. Biol. Chem.* **261**:5858-5865.